# NOVEL CONCEPTS IN USING BROADLY NEUTRALIZING ANTIBODIES FOR HIV-1 TREATMENT AND PREVENTION

EDITED BY: Philipp Schommers, Harry Gristick, Marit J. Van Gils and Kshitij Wagh

PUBLISHED IN: Frontiers in Immunology

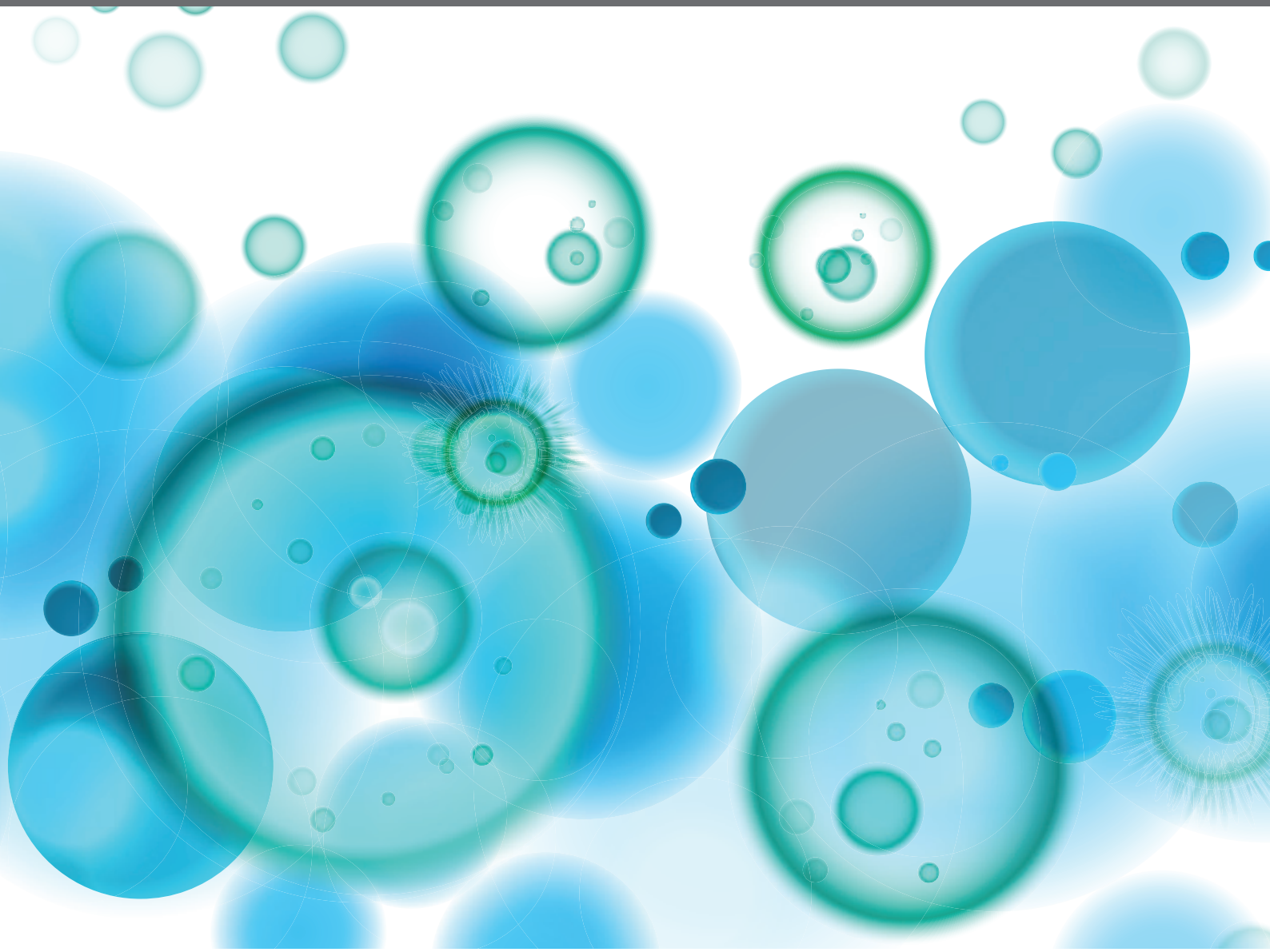

frontiers Research Topics

frontiers



ISSN 1664-8714
ISBN 978-2-88974-305-6
DOI 10.3389/978-2-88974-305-6

## About Frontiers

Frontiers is more than just an open-access publisher of scholarly articles: it is a pioneering approach to the world of academia, radically improving the way scholarly research is managed. The grand vision of Frontiers is a world where all people have an equal opportunity to seek, share and generate knowledge. Frontiers provides immediate and permanent online open access to all its publications, but this alone is not enough to realize our grand goals.

## Frontiers Journal Series

The Frontiers Journal Series is a multi-tier and interdisciplinary set of open-access, online journals, promising a paradigm shift from the current review, selection and dissemination processes in academic publishing. All Frontiers journals are driven by researchers for researchers; therefore, they constitute a service to the scholarly community. At the same time, the Frontiers Journal Series operates on a revolutionary invention, the tiered publishing system, initially addressing specific communities of scholars, and gradually climbing up to broader public understanding, thus serving the interests of the lay society, too.

## Dedication to Quality

Each Frontiers article is a landmark of the highest quality, thanks to genuinely collaborative interactions between authors and review editors, who include some of the world's best academicians. Research must be certified by peers before entering a stream of knowledge that may eventually reach the public - and shape society; therefore, Frontiers only applies the most rigorous and unbiased reviews.
Frontiers revolutionizes research publishing by freely delivering the most outstanding research, evaluated with no bias from both the academic and social point of view. By applying the most advanced information technologies, Frontiers is catapulting scholarly publishing into a new generation.

## What are Frontiers Research Topics?

Frontiers Research Topics are very popular trademarks of the Frontiers Journals Series: they are collections of at least ten articles, all centered on a particular subject. With their unique mix of varied contributions from Original Research to Review Articles, Frontiers Research Topics unify the most influential researchers, the latest key findings and historical advances in a hot research area! Find out more on how to host your own Frontiers Research Topic or contribute to one as an author by contacting the Frontiers Editorial Office: frontiersin.org/about/contact

# NOVEL CONCEPTS IN USING BROADLY NEUTRALIZING ANTIBODIES FOR HIV-1 TREATMENT AND PREVENTION

Topic Editors:
**Philipp Schommers,** University of Cologne, Germany
**Harry Gristick,** California Institute of Technology, United States
**Marit J. Van Gils,** Academic Medical Center, Netherlands
**Kshitij Wagh,** Los Alamos National Laboratory (DOE), United States

**Citation:** Schommers, P., Gristick, H., Van Gils, M. J., Wagh, K., eds. (2022). Novel Concepts in Using Broadly Neutralizing Antibodies for HIV-1 Treatment and Prevention. Lausanne: Frontiers Media SA. doi: 10.3389/978-2-88974-305-6

# Table of Contents

frontiers in Immunology

EDITORIAL
published: 21 December 2021
doi: 10.3389/fimmu.2021.823576

# Editorial: Novel Concepts in Using Broadly Neutralizing Antibodies for HIV-1 Treatment and Prevention

*Kshitij Wagh*[1†], *Marit J. van Gils*[2†], *Harry Gristick*[3] *and Philipp Schommers*[4,5,6*]

[1] Theoretical Biology and Biophysics, Los Alamos National Laboratory, Los Alamos, NM, United States, [2] Department of Medical Microbiology and Infection Prevention, Amsterdam Institute for Infection and Immunity, Amsterdam University Medical Centers (UMC), University of Amsterdam, Amsterdam, Netherlands, [3] Division of Biology and Biological Engineering, California Institute of Technology, Pasadena, CA, United States, [4] Department of Internal Medicine, Faculty of Medicine and University Hospital Cologne, University of Cologne, Cologne, Germany, [5] German Center for Infection Research, Partner Site Bonn-Cologne, Cologne, Germany, [6] Laboratory of Experimental Immunology, Institute of Virology, Faculty of Medicine and University Hospital Cologne, University of Cologne, Cologne, Germany



**Edited and reviewed by:**
Denise L. Doolan,
James Cook University, Australia

***Correspondence:**
Philipp Schommers
philipp.schommers@uk-koeln.de

[†]These authors have contributed equally to this work

**Specialty section:**
This article was submitted to Vaccines and Molecular Therapeutics, a section of the journal Frontiers in Immunology

**Received:** 27 November 2021
**Accepted:** 07 December 2021
**Published:** 21 December 2021

**Citation:**
Wagh K, van Gils MJ, Gristick H and Schommers P (2021) Editorial: Novel Concepts in Using Broadly Neutralizing Antibodies for HIV-1 Treatment and Prevention. Front. Immunol. 12:823576. doi: 10.3389/fimmu.2021.823576

**Keywords: HIV, antibodies, acquired immunodeficiency syndrome (AIDS), Neutralization, bNAbs**

**Editorial on the Research Topic**

**Novel Concepts in Using Broadly Neutralizing Antibodies for HIV-1 Treatment and Prevention**

## INTRODUCTION

Despite the success of antiretroviral therapy (ART) in suppressing HIV-1 replication and preventing disease progression, the high costs, the burden of daily medication, toxicity and the development of resistance underscore the need for new therapeutic approaches.

Over the past decade, broadly HIV-1 neutralizing antibodies (bNAbs) were discovered that are up to a 1000-fold more potent than HIV-1-reactive antibodies previously described. About 10 years after the first identification of these broadly neutralizing antibodies, bNAbs that effectively target multiple HIV-1 variants with a high potency have been found for most of the immunological important epitopes on the HIV-1 envelope-trimer like the CD4 binding site, the V1/V2 loop, the V3-glycan, the membrane-proximal external region (MPER), the interface region with the fusion peptide and the so called 'silent face'. Some of these bNAbs have been demonstrated to safely suppress viremia and delay viral rebound after interruption of antiretroviral therapy (ART) in HIV-1-infected individuals. Moreover, bNAbs have been demonstrated to prevent infection in animal models and prevention studies where bNAbs are tested for their effectivity as passive immunization in humans are currently ongoing. Thus, bNAbs represent a promising novel approach for effective HIV-1 immunotherapy and prevention. However, infusions of single

bNAbs drive the emergence of viral escape mutations and some patients harbor pre-existing resistance in their proviral or circulating HIV-1 quasispecies. Furthermore, the recently completed proof-of-concept Antibody Mediated Prevention (AMP) phase 2b trials showed that much higher bNAb titers or more potent and broader bNAbs, especially for single bNAbs, would be required for HIV-1 prevention in real-world settings. Thus, in order to restrict HIV-1 escape mechanisms and for improved antibody-mediated HIV-1 prevention, future regimens will require novel antibodies, antibody combinations or novel concepts like e.g. bi- or trispecific antibodies.

In this Research Topic, we aim to bring together new studies and comprehensive reviews that advance the field of bNAbs and their future clinical use for treatment and prevention of HIV-1.

## *IN VIVO*/CLINICAL STUDIES

### Modeling HIV-1 Within-Host Dynamics After Passive Infusion of the Broadly Neutralizing Antibody VRC01

A better understanding of the effect of antibody treatment on viral loads will guide future antibody dosing strategies as well as gain insights on the mechanisms of viral clearance by the antibody. Cardozo-Ojeda and Perelson have used different mathematical models to explain the observed viral load dynamics in the VRC01 phase 1 clinical trial. A model containing reversible bNAb binding to virions and clearance of virus-antibody complexes by a two-step process explains best the observed viral loads. First, VRC01 induces an enhancement of virus clearance by a phagocytic mechanism, but due to saturation this process slows down and the long-term viral decline is due to neutralization. However, selection pressure may lead to the outgrowth of a less-susceptible virus population to VRC01 which is reflected in the viral load final rebound.

### Validation of a Triplex Pharmacokinetic Assay for Simultaneous Quantitation of HIV-1 Broadly Neutralizing Antibodies PGT121, PGDM1400, and VRC07-523-LS

An important clinical trial outcome is the accurate measurement of the passively infused bnAbs to determine effective doses for therapy and/or prevention. Wesley et al. describe an assay to simultaneously quantify the respective physiological concentrations of passively infused bnAb cocktails in human serum to ultimately define the threshold needed for protection from HIV-1 infection.

### Anti-Drug Antibodies in Pigtailed Macaques Receiving HIV Broadly Neutralising Antibody PGT121

Non-human primate models of passively transferred bNAbs for SHIV/SIV prevention and therapy have been critical for evaluating the *in vivo* bNAb activity. Nonetheless, the delivery of human-derived IgG in heterologous species such as rhesus macaques can limit their success due the animals developing antidrug antibodies (ADA) to human IgG. Such ADA responses restrict the number, frequency and doses of bNAbs given to non-human primates. Lee et al. extend these observations to the pigtailed macaque model. They show that such ADA responses were positively correlated with the number of doses and target the constant region of therapeutic bNAb, and not the variable region, resulting in cross-reactivity with either human control IgG1 antibody as well as another bNAb not delivered to the animals. Most notably, stronger ADA responses correlated with more precipitous decline of plasma bNAb concentrations and were significantly associated with worse control of simian HIV (SHIV). This study therefore outlines the caution that should be exercised in future studies of bNAb activity in pigtail macaques, and by extending the ADA observations to pigtail macaques, suggest that similar mechanisms could restrict study of bNAbs in other immunocompetent animal models.

### Characterizing the Relationship Between Neutralization Sensitivity and env Gene Diversity During ART Suppression

The diversity of replication competent HIV-1 latent proviruses and their susceptibility to therapeutic bNAbs are critical to successful bNAb-mediated HIV-1 therapy. Most HIV-1 infected induce robust autologous neutralizing antibodies (aNAbs) that drive viral Env escape, and this raises the following interesting questions: how do such autologous antibodies impact the composition of the latent reservoir, and how does escape from such autologous antibodies impact resistance to therapeutic bNAbs? Wilson et al. present compelling data present compelling data addressing these questions. They show that the latent reservoir can harbor aNAb resistant viruses and the latent viral Env diversity, presumably created by escape from aNAbs, can lead to resistance to certain therapeutic bNAbs, but not others. Clinical studies such as this can thus begin to address the key question of how many and which bNAbs will be needed to prevent viral breakthrough in analytical treatment interruption (ATI) studies and to ultimately succeed in HIV-1 therapy.

## *IN VITRO* STUDIES

### Combinations of Single Chain Variable Fragments from HIV Broadly Neutralizing Antibodies demonstrate High Potency and Breadth

Single chain variable fragments (scFv) antibodies comprise of heavy and light chain variable fragments connected by glycine linkers in the same gene construct. Their smaller size as compared to full-length IgG can provide substantial advantages such as improved penetration of tissue, especially mucosa, and practical considerations such as expression by nucleic acids and viral vectors. However, the lack of Fc regions results in lower half-lives for scFv versus IgG and in the absence of antibody effector functions. The scFv molecules also lose some neutralization potency and breadth as compared to IgG due to loss of bivalent binding and/or subtly different paratope

structures, albeit scFvs were shown to retain substantial activity of the parental antibodies. In this study, (van Dorsten et al.) explored whether combinations of scFvs targeting different HIV-1 Env epitopes can improve the breadth and potency against HIV-1 isolates. They show using experimental and theoretical approaches that combinations of scFv can significantly enhance breadth and potency over individual scFvs and that combinations of 2-3 scFvs could cover majority of viruses tested with high potency. By demonstrating that combinations of scFvs have favorably broad and potent *in vitro* neutralization profiles, this study lays the groundwork for further *in vivo* testing and development of scFv combinations as promising novel antibody-based prophylactics and therapeutics against HIV-1.

## HIV Broadly Neutralizing Antibodies Expressed as IgG3 Preserve Neutralization Potency and Show Improved Fc Effector Function

Richardson et al. describe the change in Fc-effector function profiles of HIV-1 bNAbs when expressed as IgG3 isotypes. Some HIV-1 reactive bnAbs expressed as IgG3 demonstrated enhanced binding to Fc receptors and improved FC-mediated effector functions while maintaining their neutralization activity. Thus, the antiviral effect of already very broad and potent bNAbs can even be enhanced by manipulations of the constant regions. These insights are important for the field given the current focus on using HIV-1 bNAbs for passive immunization strategies.

## Elimination of SHIV Infected Cells by Combinations of Bispecific HIVxCD3 DART® Molecules

A potential future role of dual-affinity re-targeting Antibodies (DART) for treatment of HIV-1 is elegantly shown by Tuyishime et al. They investigated the effect of HIVxCD3 DART® Molecules that have broadly-neutralizing and non-neutralizing activities on SHIV infected cells and found that these molecules effectively eliminated SHIV infected cells. Thus, these findings can be crucial for futures HIV-1 cure strategies since it is here shown that HIVxCD3 DART® Molecules can leverage the host immune system for treatment of HIV-1 infection.

# REVIEWS

This Research Topic hosts articles that review currently available bNAbs and their potential future use. While Griffith and McCoy provide a comprehensive overview of the most promising currently available bNAbs, Hsu et al., Phelps and Balazs, and Umotoy and de Taeye review and outline the use of these bNAbs in future HIV-1 cure, treatment and prevention approaches.

## To bnAb or Not to bnAb: Defining Broadly Neutralising Antibodies Against HIV-1

Griffith and McCoy describe a possible definition of antibody features that are required by a specific antibody to be classified as "broadly neutralizing". To this end they review and compare the neutralizing profiles, mutations, genetic features and the targeted epitopes of an array of currently known neutralizing antibodies. Through this effort the authors provide a comprehensive and unbiased overview of the currently available bNAbs of which several are or will be tested in clinical studies.

## Can Broadly Neutralizing HIV-1 Antibodies Help Achieve an ART-Free Remission?

In this review Hsu et al. concisely and yet thoroughly review the potential role of HIV bNAbs in strategies to achieve long term virologic control in the absence of ART. The authors comprehensively review this complicated area of research with clinical studies from many different groups. They discuss a plethora of preclinical and clinical studies that aim to determine if bNAbs can act alone, in combination, and/or together with other drugs to control HIV infection and eliminate or decrease the viral reservoir.

## Contribution to HIV Prevention and Treatment by Antibody- Mediated Effector Function and Advances in Broadly Neutralizing Antibody Delivery by Vectored Immunoprophylaxis

While neutralization is a crucial component of therapeutic efficacy, numerous studies have demonstrated that bNAbs can also mediate effector functions. Phelps and Balazs review key concepts of effector functions mediated by bNAbs and the potential for vectored immunoprophylaxis as a means of producing bNAbs in patients to overcome the need for constant re-administration in order to maintain steady-state bNAb concentrations.

## Antibody Conjugates for Targeted Therapy Against HIV-1 as an Emerging Tool for HIV-1 Cure

By reading the review of Umotoy and de Taeye readers will get a thorough and historical perspective on the use antibody conjugates (ACs) in HIV research. The authors describe the concept of an antibody-based carrier of anti-HIV-molecules and why specifically bNAbs could be the ideal carrier. The anti-HIV-molecules include toxins fused to the antibody, antibodies conjugated by radionuclides (radioimmunotherapy) and small drugs or oligonucleotides conjugated to antibodies. In contrast to anticancer treatment, for which several constructs are already FDA-approved, no AC is currently approved for treatment of viral infections. However, with new potent bNAbs available ACs have a huge potential for future HIV-1 cure strategies which is discussed in detail by the authors.

## Broadly Neutralizing Antibodies for HIV-1 Prevention

The current status of clinical studies evaluating bNAbs for HIV-1 prevention is reviewed by Walsh and Seaman. To this end, the authors summarize key clinical trials like the recently published AMP-trial, based on their advantage and how they contributed to the field. Besides recent clinical studies, the authors also discuss

strategies that will lead to an improved breadth, potency and durability of antiviral protection in future clinical trials.

## CONCLUSION AND OUTLOOK

Altogether, bNAbs show promise for successful HIV-1 prevention, therapeutic control and potential towards HIV-1 cure, especially when they are further tailored to improve breadth, potency, bioavailability and increased killing of infected cells through protein engineering. For future evaluation of bNAb prophylaxis and therapy in clinical trials it is crucial to have well validated quantitative assays with well-predicting antibody distribution and viral load models.

## AUTHOR CONTRIBUTIONS

All authors listed have made a substantial, direct, and intellectual contribution to the work and approved it for publication.

## FUNDING

KW was supported by the Comprehensive Antibody Vaccine Immune Monitoring Consortium (CAVIMC) (Grant: OPP1032144 from the Bill & Melinda Gates Foundation.

**Conflict of Interest:** The authors declare that the research was conducted in the absence of any commercial or financial relationships that could be construed as a potential conflict of interest.

frontiers in Immunology

REVIEW
published: 01 July 2021
doi: 10.3389/fimmu.2021.708806

# Antibody Conjugates for Targeted Therapy Against HIV-1 as an Emerging Tool for HIV-1 Cure

*Jeffrey C. Umotoy* * *and Steven W. de Taeye* *

*Laboratory of Experimental Virology, Department of Medical Microbiology, Amsterdam University Medical Center (UMC), Amsterdam Infection and Immunity Institute, University of Amsterdam, Amsterdam, Netherlands*

Although advances in antiretroviral therapy (ART) have significantly improved the life expectancy of people living with HIV-1 (PLWH) by suppressing HIV-1 replication, a cure for HIV/AIDS remains elusive. Recent findings of the emergence of drug resistance against various ART have resulted in an increased number of treatment failures, thus the development of novel strategies for HIV-1 cure is of immediate need. Antibody-based therapy is a well-established tool in the treatment of various diseases and the engineering of new antibody derivatives is expanding the realms of its application. An antibody-based carrier of anti-HIV-1 molecules, or antibody conjugates (ACs), could address the limitations of current HIV-1 ART by decreasing possible off-target effects, reduce toxicity, increasing the therapeutic index, and lowering production costs. Broadly neutralizing antibodies (bNAbs) with exceptional breadth and potency against HIV-1 are currently being explored to prevent or treat HIV-1 infection in the clinic. Moreover, bNAbs can be engineered to deliver cytotoxic or immune regulating molecules as ACs, further increasing its therapeutic potential for HIV-1 cure. ACs are currently an important component of anticancer treatment with several FDA-approved constructs, however, to date, no ACs are approved to treat viral infections. This review aims to outline the development of AC for HIV-1 cure, examine the variety of carriers and payloads used, and discuss the potential of ACs in the current HIV-1 cure landscape.

**Keywords: antibody conjugates, immunoconjugates, HIV-1 cure, ADC, HIV-1 antibody conjugates, HIV-1 ADC**

OPEN ACCESS

***Edited by:***
*Philipp Schommers, University of Cologne, Germany*

***Reviewed by:***
*Rebecca M. Lynch, George Washington University, United States*
*Matthew Gardner, Emory University, United States*

***Correspondence:**
*Jeffrey C. Umotoy*
*j.c.umotoy@amsterdamumc.nl*
*Steven W. de Taeye*
*s.w.detaeye@amsterdamumc.nl*

***Specialty section:***
*This article was submitted to Vaccines and Molecular Therapeutics, a section of the journal Frontiers in Immunology*

***Received:*** *12 May 2021*
***Accepted:*** *18 June 2021*
***Published:*** *01 July 2021*

***Citation:***
*Umotoy JC and de Taeye SW (2021) Antibody Conjugates for Targeted Therapy Against HIV-1 as an Emerging Tool for HIV-1 Cure. Front. Immunol. 12:708806. doi: 10.3389/fimmu.2021.708806*

## INTRODUCTION

Decades after the discovery of HIV-1 as the causative agent for AIDS, no vaccine or curative treatment is available against HIV-1 infection. Although the advent of antiretroviral therapy (ART) has significantly improved the disease outcome of people living with HIV-1 (PLWH) from a disease with high morbidity and mortality to a manageable chronic disease, HIV-1 remains incurable. In 2019, an estimated 67% of HIV-1 infected individuals were undergoing ART out of the estimated 38 million people infected with HIV-1 globally. The effectiveness of ART regimen is unequivocal in keeping viral loads to undetectable levels, reduction of transmissions, and the overall impact on the life expectancy of PLWH, however, life-long ART is linked to new sets of challenges. Accessibility remains an issue with an estimated 12 million people without access to ART in 2019, as well as the

issue of adherence to daily drug intake for people undergoing treatment (UNAIDS data 2020). More alarming is the increasing evidence of drug resistance in the current ART, which could undermine the advances achieved thus far. Therefore, an innovative therapeutic approach for a functional or total cure is needed to fully end the AIDS epidemic. One such focus is the engineering of a highly targeted delivery system of molecular payload for HIV-1 to target host cells acutely or latently infected with HIV.

Antibody conjugates (ACs) are engineered therapeutics designed with a targeting "carrier" moiety, such as monoclonal antibodies (mAb), conjugated to a cytotoxic or immune regulating molecular "payload" connected *via* a linker (**Figure 1**). In cancer immunotherapy, the targeting molecule is directed against a specific disease-related antigen expressed on cells to which the cytotoxic drug payload is delivered inducing cell death. The main goal of targeted drug delivery is to optimize a payload's therapeutic index by localizing its pharmacological activity only to sites expressing the antigen target. The conjugation of the carrier and payload subunits are mutually beneficial: improved cytocidal effect for the antibody carrier, while increased systemic half-life, and reduced off-target toxicities for the payload. The cancer immunotherapy field is dominating the AC landscape with 12 FDA-approved ACs used for the treatment of various cancers (antibodysociety.org).

To date, no ACs for antiviral use are approved for therapy. Although advances and challenges in the design of AC for cancer immunotherapy can, in theory, be applied to ACs for antiviral use, a different set of challenges must be overcome for HIV-1. Some challenges in ACs for HIV-1 that are unique from cancers are (a) high variability of viral antigen expressed on infected cells, (b) release of cell-free virions, (c) persistence of infected cells in the blood and lymphoid tissues, (d) infection of anatomic "sanctuary sites", and (f) the persistence of latently infected cells which are void of any viral surface protein expression until after reactivation.

This review will focus on the diverse AC constructs designed for HIV-1 cure including the variety of carrier molecules, effector payloads, and the choice of viral or host antigen targets (**Table 1**). This review will not focus on the broader AC landscape such as conjugation chemistries, linker design, and biodistribution, which has been reviewed extensively elsewhere (1–5). Instead,

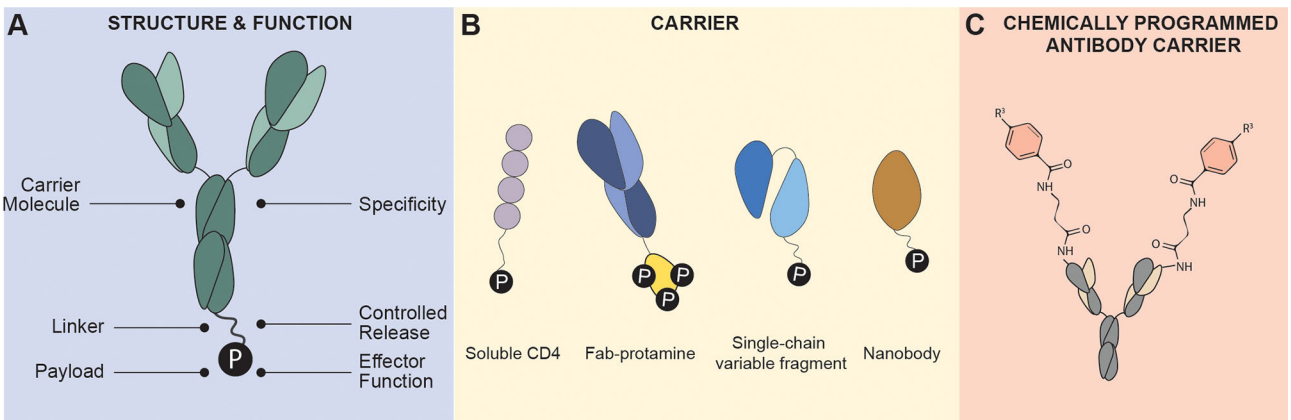


**FIGURE 1** | Antibody Conjugate Structure. **(A)** Antibody conjugates are characterized by a fusion of a carrier molecule specific to an antigen for specificity, a linker that connects the carrier and payload providing flexibility and controlled release of payload, and the effector molecule "payload" that can induce cytotoxicity or immune modulation. **(B)** Carrier molecules are typically monoclonal antibodies (such as IgG1), soluble ligands such as cytokines or receptors), Fab fragment, single-chain variable fragment, and nanobodies. **(C)** Chemically programmed antibody containing a reactive residue on its binding pocket that can react to derivatives of small molecules. Targeting is conferred by the conjugated small molecules instead of the antibody.

**TABLE 1** | Antibody conjugate categories.

| Antibody Conjugate | Payload | Description |
|---|---|---|
| Antibody-toxin conjugates | Toxin | Commonly referred to as immunotoxin in the cancer immunotherapy field, ATC is characterized by the conjugation of toxins usually derived from plants or bacteria. |
| Antibody-radionuclide conjugates | Radionuclide | Antibody-radionuclide conjugate is the conjugation of a radionuclide to an antibody carrier |
| Antibody-drug conjugates | Small molecule or compounds | Antibody-drug conjugate is the conjugation of small molecule drugs to antibodies. |
| Antibody-oligonucleotide conjugates | Oligonucleotides such as siRNA | Conjugation of oligonucleotide-based payloads such as siRNA |
| Antibody-photosensitizer | Photosensitizers | Antibody-photosensitizer conjugates, also known as photoimmunotherapy (PIT), is a targeted photodynamic therapy designed with a conjugated photosensitizer to a mAb. |

this review will provide insights into the development of the next-generation ACs for HIV-1 cure based on the use of novel antibody carriers such as broadly neutralizing antibodies (bNAbs) and their subunit derivatives (**Figure 1B**), combination ART and AC treatment, and how the AC landscape can advance to human clinical trials for HIV-1 cure.

## HIV LATENCY

HIV-1 persists in all subsets of memory CD4+ T cells as well as a subset of functional T cells, such as T follicular helper cells, T regulatory cells, Th1 cells, and Th17 cells (6). Besides these cellular reservoirs, HIV-1 can persist latently in tissue reservoirs throughout the body (7, 8). Latency is characterized by the presence of integrated but transcriptionally silent HIV-1 DNA, undetectability from immune surveillance, and resistance to ART (9–12). Current ART interferes at various stages of the HIV-1 replication cycle and has been shown to effectively control viral loads to undetectable levels (13). However, ART fails to eliminate or reduce the viral reservoir of latently infected cells, and upon ART cessation, a rapid viral rebound is observed (14). Therefore, major efforts in the HIV-1 cure field aims at eliminating the viral reservoir of latently infected cells. The two main curative approaches for HIV-1 cure include the shock-and-kill and block-and-lock approach.

The shock-and-kill approach aims to reactivate or "shock" the transcriptionally silent host-integrated HIV-1 DNA in latently infected cells *via* latency-reversing agents (LRAs). Upon reactivation, the "kill" stage occurs either through host cytopathic effects or *via* induction of immune-mediated clearance (15). Concurrent ART simultaneously addresses the suppression of infection. A variety of LRAs has been described to reactivate latently infected cells. The most studied LRAs either activate the NF-κb signaling pathway or inhibit the epigenetic writers, but a plethora of LRAs belonging to various functional categories are growing (16). The shock-and-kill approach, therefore, relies heavily on the induction of *de novo* HIV-1 protein expression upon latency reversal with LRAs, permitting immune recognition and killing. In initial clinical trials, an increase in cellular HIV-1 RNA after LRA treatment was observed indicating latency reversal, however, no decrease in the overall reservoir size was observed (17, 18). The failure to reduce the reservoir size, therefore, indicates that latency reversal must be combined with therapies that can augment antiviral immune responses. To boost the "killing" phase of shock-and-kill, various therapeutic approaches are currently under consideration, such as immunomodulatory therapies, CAR-T/NK therapy, therapeutic HIV-1 vaccinations, and various antibody-based strategies (19, 20).

The failure to eradicate the viral reservoir size through the shock-and-kill approach encouraged the re-evaluation of the definition of HIV cure. The total cure strategy (also referred to as sterilizing cure), centered around the eradication of all latently infected cells, proved to be challenging and a more feasible "functional cure" is proposed, which is characterized by a long-term HIV-1 remission (21). One such approach is the block-and-lock strategy that aims to prevent viral reactivation in latently infected cells for a prolonged drug-free remission (22, 23). This approach targets either HIV-1 or host-specific factors to induce a state of deep or permanent latency in the absence of ART. As a counterpart to LRAs, the block-and-lock approach uses latency-promoting agents (LPAs) to promote "blocking" of virus transcription and "locking" the virus promoter in a deep latent state *via* repressive epigenetic modifications (24–26).

The quest to finding an HIV-1 cure, either a total or functional cure, continues. It is likely that monotherapy will not be sufficient to address the complexities of HIV-1 infection, and a multi-pronged approach involving combination ART, LRAs/LPAs, and immunotherapies are needed.

## TARGET OF HIV-1 SPECIFIC ANTIBODY CONJUGATES

To deliver cytotoxic or immune-modulating molecules to HIV-1 infected cells, the specificity of the antibody carrier molecule to its antigenic target is of extreme importance. In cancer immunotherapy, malignant cells often overexpress receptors belonging to the epidermal growth factor receptor (EGFR) family that is required for cell growth and survival (27). These are ideal antigen targets for ACs on malignant cells, which require high specificity and affinity to enable efficient payload delivery (28, 29). Conversely, latently infected cells are void of such antigenic markers which makes targeting them challenging. In this section, we will summarize the main targets of ACs on acutely and latently infected cells and discuss the advantages and disadvantages of each target. These targets include the HIV-1 envelope glycoprotein, HIV-1 coreceptors, and host membrane proteins (**Figure 2**).

### Envelope Glycoprotein

The HIV-1 envelope glycoprotein (Env) is the sole viral protein expressed on the membrane of viral particles as well as on HIV-1 infected cells with active viral replication and is, therefore, the primary target of antibody-based therapies (30). HIV-1 Env protein is expressed as a precursor gp160 molecule which is cleaved by furin into its gp41 and gp120 subunits. Three gp120 and gp41 subunits together form the HIV-1 Env trimer. Following CD4 receptor engagement, the metastable Env trimer undergoes conformational changes to orchestrate co-receptor binding and activation of the fusion machinery. Besides the expression of functional HIV-1 Env trimeric proteins on HIV-1 infected cells, other forms of Env are presented including uncleaved gp160, gp41 stumps, and aberrant trimers (30). The conformational plasticity and heterogeneity of HIV-1 Env can elicit antibody responses that are classified into three groups: binding but non-neutralizing, neutralizing but strain-specific, and bNAbs (31). The optimal carrier antibody for ACs, however, is not solely based on the broadest and most potent antibody that can neutralize most of the HIV-1 global strains. An efficient antibody carrier for ACs

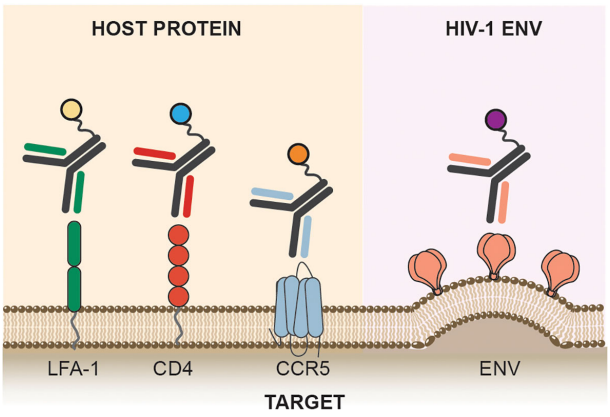


**FIGURE 2** | Targets. Antibody conjugates can target host receptors required for viral entry, CD4, and coreceptor such as CCR5. Host factors such as LFA-1, an integrin protein expressed on lymphocytes are also targeted by antibody conjugates. HIV-1 Env, the sole viral protein expressed on infected cells is also the targets of antibody conjugates.

depends on the effector mechanism of its payload, the rate of internalization of the AC, and the subsequent intracellular routing of the carrier and payload. Because high antibody affinity and potency to HIV-1 Env does not guarantee antibodies to be the best AC carriers, the use of soluble CD4, non-neutralizing antibodies, and bNAbs were all explored as carriers for HIV-1 cure ACs (**Table 2**).

## gp41

Early exploration of ACs for HIV-1 cure argued that gp41 might be a more suitable target than gp120 as gp120 exhibits significant heterogeneity and variability amongst various isolates of HIV (53). Moreover, gp120 shedding from the Env trimer releasing free monomeric gp120 could potentially bind anti-gp120 antibodies, further reducing the efficacy of gp120-directed antibodies (54). Gp41, besides acting as an anchor for gp120 contains highly conserved regions and is known to have a fusogenic potential, thus catalyzing membrane fusion (55). Furthermore, surface expression of the N-terminal half of gp41 on both the virion and infected cells render their susceptibility to immune surveillance (56). For these reasons, some of the earliest AC used mAb targeting gp41.

The rapid advances in mAb isolation and epitope mapping resulted in a family of anti-gp41 mAbs with defined epitopes (57). These anti-gp41 mAb directed towards the extracellular disulfide loop domain and heptad repeat region conjugated to toxins showed efficacy in killing infected T cell lines and monocytes (58, 59), and superior efficacy in both *in vitro* and *in vivo* mouse model compared to gp120-targeted ACs (39, 41). Moreover, the efficiency of gp41-directed ACs was further improved *via* the addition of soluble CD4 and virtually eliminated p24 production in a mouse model of infection, compared to a gp120-directed carrier requiring 15-times higher dosage with marginal effect (39).

The promising result with gp41-directed ACs also encouraged the construct of antibody-radionuclide conjugate directed towards gp41. Moreover, an important work by Tsukrov and colleagues showed that the low-level residual expression of gp41 on PBMCs isolated from ART-treated HIV-1 infected individuals is sufficient for antibody-radionuclide conjugate to deliver cytocidal radiation to infected cells making this epitope an attractive target for ACs (60).

## CD4-Binding Site

To facilitate entry of HIV-1, the trimeric HIV-1 Env binds receptor CD4 found on host cells. The CD4-binding site (CD4bs) found on HIV-1 gp120 is highly conserved and has a low degree of glycan masking (61) making it an attractive target for mAb-based therapy.

Early *in vitro* data demonstrated significant neutralization of HIV-1 infection in T-cell lines with recombinant soluble CD4 (sCD4), prompting the field to explore the potential of sCD4 for HIV-1 therapy (62). Consequently, sCD4 was explored as the first-ever cytotoxic carrier molecule for *Pseudomonas* exotoxin A (PE) to kill HIV-1 infected cells, which will be further discussed in a later section. Furthermore, the isolation and identification of CD4bs-directed bNAbs from HIV-1 infected individuals offered a variety of possible carriers for ACs. A more stable, affinity-matured, and broader 3B3 single-chain variable fragment (scFv) derivative of b12, a CD4bs-directed bNAb, was generated and exhibited enhanced activity as a carrier molecule for PE. The 3B3 (Fv)-PE AC, solved the challenges faced by sCD4 as a carrier, such as toxicities and apparent enhancement of infection at a low sCD4 concentration (63). The availability of various bNAbs targeting this epitope, as well as the retained functionality of IgG subunits as a carrier makes this epitope a highly attractive target for ACs.

## Host Cellular Proteins

Alternatively, ACs can be designed to target host cellular markers of infection-susceptible cells, receptor and coreceptors used by HIV-1, and biomarkers expressed on latently infected cells (**Table 3**). AC strategies that rely on host factor targeting are not dependent on LRAs to reverse latency and induce viral protein expression, which is a major advantage compared to HIV-1 Env targeting strategies. This section will focus on various host factors targeted by ACs for HIV-1 cure (**Figure 2**).

Reasonably, the first host factor targeted by ACs is the HIV-1 entry receptor, CD4. CD4 is expressed on the surface of T cells, monocytes, macrophages, and dendritic cells (76). An anti-CD4 mAb conjugated with toxin exhibited selectivity and efficacy in eliminating HIV-1 production in activated CD4+ T cells from an infected individual *in vitro*. Since HIV-1 mainly infects CD4+ T cells, additional T cell markers were also targeted by the conjugation of toxins and small-interfering RNA (siRNAs) to anti-CD5 and anti-CD7 mAb (43, 65, 77). Additionally, markers of T cell activation such as IL2 receptor, CD25 (or IL-2 receptor α-chain), and CD45RO, were also the target of several ACs, which aims at targeting only activated T cells, while sparing quiescent T cells (43, 65).

**TABLE 2** | Virus-directed antibody conjugates.

| Antibody Conjugate | Target | Carrier | Payload | Payload Type | Reference |
|---|---|---|---|---|---|
| 7B2-PIT | gp41 | 7B2 mAb | Porphyrin, IR700 | Photosensitizer | (32) |
| rCD4-dgA | gp120 | CD4 Receptor | Ricin A chain | Toxin | (33) |
| CD4 (178)-PE40 | gp120 | CD4 Receptor | Pseudomonas exotoxin | Toxin | (34) |
| 907-RAC | gp120 | 907mAb | Ricin A chain | Toxin | (35) |
| 0.5β-RAC | gp120 | 0.5β mAb | Ricin A chain | Toxin | (36) |
| 0.5β-PE | gp120 | 0.5β mAb | Pseudomonas exotoxin | Toxin | (36) |
| DAB389-CD4 | gp120 | CD4 Receptor | Diptheria toxin | Toxin | (37) |
| 3B3(Fv)-PE38 | gp120 | 3B3 scFv | Pseudomonas exotoxin | Toxin | (38) |
| 924-RAC | gp120 | 924mAb | Ricin A chain | Toxin | (39) |
| 924-PAC | gp120 | 924mAb | Pulchellin A chain | Toxin | (40) |
| Anti-gp160-RAC | gp160 | Anti-gp160 mAb | Ricin A chain | Toxin | (41) |
| 7B2-RAC | gp41 | 7B2 mAb | Ricin A chain | Toxin | (39) |
| 41.1-RAC | gp41 | 41.1 mAb | Ricin A chain | Toxin | (39) |
| 7B2-PAC | gp41 | 7B2 mAb | Pulchellin A chain | Toxin | (40) |
| F105-P-*gag* | gp120 | F105 Fab | *gag*-siRNA | siRNA | (42) |
| scFvCD7-9R-*vif* | *Vif* | Anti-CD7 scFv | *vif*-siRNA | siRNA | (43) |
| scFvCD7-9R-*tat* | *Tat* | Anti-CD7 scFv | *tat*-siRNA | siRNA | (43) |
| 188-Re-246-D | gp41 | 246-D mAb | 188-Re | Radionuclide | (44) |
| 213-Bi-246-D | gp41 | 246-D mAb | 213-Bi | Radionuclide | (44) |
| 213-Bi-2556 | gp41 | 2556 mAb | 213-Bi | Radionuclide | (45) |
| 225-Ac-2556 | gp41 | 2556 mAb | 225-Ac | Radionuclide | (46) |
| 177-Lu-2556 | gp41 | 2556 mAb | 177-Lu | Radionuclide | (46) |
| Dox-P4/D10 | gp120 | P4/D10 mAb | Doxorubicin | Drug | (47) |
| e10-1074 | V3-glycan | 10-1074 bNAb | CCR5mim6 | Inhibitor | (48) |
| ePGT121 | V3-glycan | PGT121 bNAb | CCR5mim6 | Inhibitor | (48) |
| ePGT122 | V3-glycan | PGT122 bNAb | CCR5mim6 | Inhibitor | (48) |
| ePGT128 | V3-glycan | PGT128 bNAb | CCR5mim6 | Inhibitor | (48) |
| e3BNC117 | CD4bs | 3BNC117 | CCR5mim6 | Inhibitor | (48) |
| ePGDM1400 | V2-apex | PGDM1400 | CCR5mim6 | Inhibitor | (48) |
| ePGT151 | gp120-gp41 interface | PGT151 bNAb | CCR5mim6 | Inhibitor | (48) |
| e10E8 | MPER | 10E8 bNAb | CCR5mim6 | Inhibitor | (48) |
| eE51 | CD4i | E51 bNAb | CCR5mim6 | Inhibitor | (48) |
| 50-69-RAC | gp41 | 50-69 mAb | Ricin A chain | Toxin | (49) |
| gp120-brefeldin A | gp120 | Anti-gp120 Polyclonal Ab | Brefeldin A | Drug | (50) |
| 2F5-Cholesterol | gp120/membrane | 2F5 bNAb | Cholesterol | Lipid | (51) |
| eCD4-Ig | gp120 | Anti-CCR5 mAb | CCR5mim1 | Small drug | (52) |

Coreceptor targeting emerged as a central theme of subsequent ACs for HIV-1 cure. CCR5 and CXCR4 are the coreceptors required for HIV-1 viral entry and are widely expressed on immune cells including CD4+ T-cells. The choice of coreceptor generally determines viral tropism with CCR5, and CXCR4 usage for R5, and X4 viruses, respectively (64, 66–68, 78). CXCR4 constitutes a highly attractive target for ACs because this receptor is efficiently and rapidly internalized after interaction with its natural ligand, SDF-1α (79). CXCR4 is therefore an ideal target for ACs with payloads requiring internalization to function. However, to date, only one AC construct targeted this receptor for the delivery of an anti-*tat* siRNA conjugated to a CXCR4 nanobody (70, 80).

Coreceptor targeting favored CCR5 over CXCR4 mainly because R5 tropic viruses are predominantly involved in the early viral transmission of infection, predominate in the asymptomatic stage of infection, and persist throughout all stages of the disease (81, 82). In comparison, the emergence of X4 tropic or dual tropic R5X4 viruses tends to occur at a later stage of infection to only about 50% of progressing patients (83, 84). The predominance of R5 tropic viruses during infection explains the preference of targeting the CCR5 coreceptor by ACs. Furthermore, the availability of structural data of CCR5-Env interaction further fueled the development of many CCR5-targeting small molecules and mAbs (85–88). One class of CCR5-targeting molecules is CCR5 sulfopeptide mimetics that simulate CCR5-Env interaction (71, 89–91). These mimetic peptides were later used by several ACs discussed in a later section. Overall, the targeting of HIV-1 coreceptors is an attractive host factor target for ACs as they are implicated in viral entry and transmission.

Lastly, lymphocyte function-associated antigen-1 (LFA-1) was also the target of an AC aiming at preventing the cell-cell spread of HIV-1. LFA-1 is an integrin expressed on all lymphocytes and is involved in emigration and adhesion processes (69). Additionally, LFA-1 expression increases during HIV-1 infection and is also implicated in the formation of virological synapse for HIV-1 propagation (92). It was therefore hypothesized that an anti-LFA-1 mAb could be used therapeutically against HIV-1 infection. Early studies indeed showed that an anti-LFA-1 mAb could reduce HIV-1 RNA in HIV-1 infected individuals (93), and more recently it was found to inhibit the cell-cell spread of infection (94). Cell-cell transmission of HIV-1 plays an important role in the

**TABLE 3** | Host-directed antibody conjugates.

| Antibody Conjugate | Target | Carrier | Payload | Payload Type | Reference |
|---|---|---|---|---|---|
| Anti-CD25-RAC | CD25 | Anti-CD25 mAb | Ricin A chain | Toxin | (64) |
| Anti-CD4-PAP | CD4 | Anti-CD4 mAb | Pokeweed antiviral protein | Toxin | (65) |
| Anti-CD45RO IT | CD45RO | Anti-CD45RO mAb | Ricin A chain | Toxin | (66) |
| Anti-CD5-PAP | CD5 | Anti-CD5 mAb | Pokeweed antiviral protein | Toxin | (65) |
| Anti-CD7-PAP | CD7 | Anti-CD7 mAb | Pokeweed antiviral protein | Toxin | (65) |
| DAB486-IL2 | IL2R | IL2 | Diphtheria toxin | Toxin | (67) |
| DAB389-IL-2 | IL2R | IL2 | Diphtheria toxin | Toxin | (68) |
| AL-57-PF-CCR5 | LFA-1 | AL-57 scFv | CCR5-siRNA | siRNA | (69) |
| CD7-9R-CD4-siRNA | CD4 | Anti-CD7 scFv | CD4-siRNA | siRNA | (43) |
| CD7-9R-CCR5-siRNA | CCR5 | Anti-CD7 | CCR5-siRNA | siRNA | (43) |
| 4M5.3-3X4 | CXCR4 | Anti-CXCR4 scFv | *tat-siRNA* | siRNA | (70) |
| CCR5mAb-FI | CCR5 | Anti-CCR5 mAb | T-2635 | Small drug | (71) |
| 38C2-Apalviroc | CCR5 | 38C2 cpAb | Aplaviroc | Small drug | (72) |
| cP4/D10-T20 | gp120 | P4/D10 mAb | Enfuvirtide | Small drug | (73) |
| 38C2-BMS-488043 | CCR5 | 38C2 cpAb | BMS-488043 | Small drug | (74) |
| 38C2-Maraviroc | CCR5 | 38C2 cpAb | Maraviroc | Small drug | (75) |

propagation of infection in addition to cell-free infection of target cells, with some reporting that cell-cell infection could be the main route of HIV-1 infection (95–97). Although the efficiency of cell-cell *vs* cell-free propagation of HIV-1 is still under debate, the availability of mAb that can inhibit cell-cell spread could be an attractive carrier for ACs. Therefore, host factors such as LFA-1 that are involved in the formation of virological synapse and cell-cell propagation are another important target for HIV-1 cure ACs.

Ultimately, the most convenient host factor targets for HIV-1 ACs are latency surface biomarkers only expressed on infected cells. The discovery of such latency biomarkers is an active area of research. Enrichment of certain surface markers such as CD2, CD20, CD30 and immune checkpoint inhibitors on latently infected cells are currently being explored as potential host biomarkers of latency (98, 99). To further highlight the substantial challenge of finding such biomarker, the discovery of CD32a as a marker of latency associated with enrichment of HIV DNA (100), has been challenged by subsequent studies (101–103). However, while the discovery of such biomarkers is underway, ACs can overcome this limitation by designing constructs with which the payload confers the selectivity against viral factors while remaining inert in uninfected cells. Therefore, host-targeting ACs could be an attractive method for conjugation with oligonucleotide or small drugs that are highly HIV-1 genome-specific.

## ANTIBODY CONJUGATES FOR HIV-1 CURE

The approval of zidovudine in 1987 as the first drug for HIV-1 ART revealed the apparent need for an alternative curative agent to address the inability of ART to fully eradicate HIV-1. ACs are an attractive complement to ART because of their high selectivity and targeted delivery of cytotoxic and immune regulating payload. Some of the advantages of ACs over their unconjugated components are increased therapeutic index of the payload, reduction in off-target toxicities, increased circulation half-life, and selectivity accomplished by the carrier molecule to its antigen. Furthermore, once a certain threshold of binding is achieved, the use of high-affinity antibodies is not as crucial for efficacy as unconjugated antibodies (104). ACs can be further modified for internalization capacity, intracellular routing, controlled payload release, drug-to-antibody ratio, and linker chemistries, which is beyond the scope of this review.

In this section, the diversity of ACs for HIV-1 cure is explored. Special attention is given to mAb-based carriers for molecular payload; therefore, this review excludes other targeted approaches such as immunoliposomes, nanoparticles, dendrimers, aptamers, etc. Although not a mAb carrier, the use of sCD4 as a carrier of a cytotoxic payload is also discussed in this review as the use of this construct marked the origination of a highly targeted therapeutic approach for HIV-1 cure.

Currently, the AC landscape for HIV-1 cure is diverse and depending on the payload used the naming conventions are not standardized. This naming convention phenomenon mainly occurred because of the asynchronous development of ACs in cancer immunotherapy. In this review, a naming convention focusing on the payload is used (**Table 1**). This aims to consolidate the field of using antibodies as the primary carrier of cytotoxic and immune regulating payload. Therefore, antibody conjugation of toxins herein referred to as antibody-toxin conjugates; antibody conjugation of radionuclide, herein referred to as antibody-radionuclide conjugates; antibody conjugation of drugs/small molecules, herein referred to as antibody-drug conjugates; antibody conjugation of an oligonucleotide, herein referred to as antibody-oligonucleotide conjugates, and other novel payloads discussed herein will follow a similar naming convention.

Overall, this section aims to describe each AC type focusing on their unique structure, mode of action (**Figure 3**), potential therapeutic use, as well as challenges in the bigger HIV-1 cure landscape.

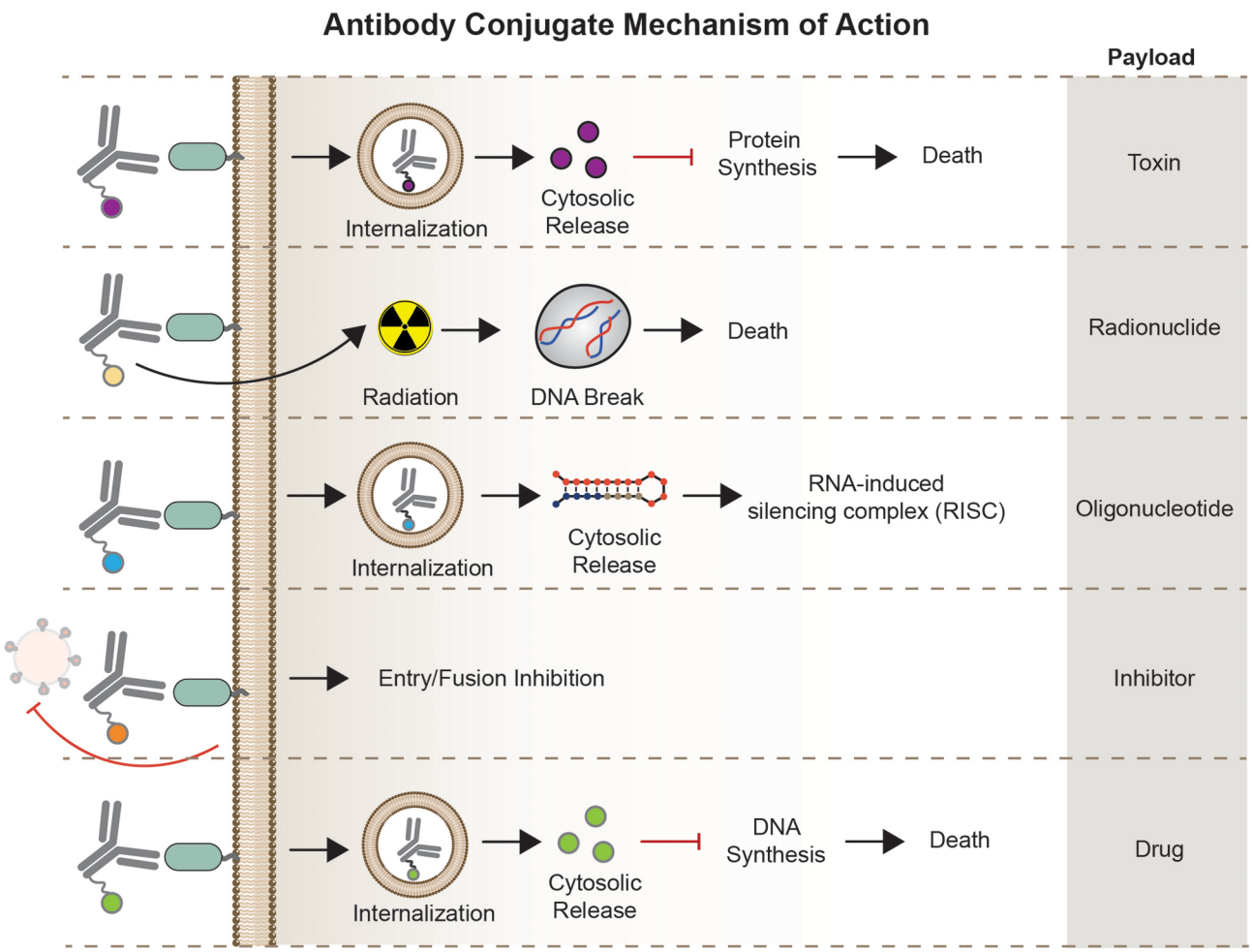


**FIGURE 3** | Mechanism of Action. Antibody conjugates execute different mechanism of action depending on the carrier molecule, antigen, internalization requirement, and effector function of the payload. Antibody-toxin binds to target epitopes, internalized, followed by escape of toxin to the cytosol to halt protein synthesis. Antibody-radionuclide binds to the receptor to deliver ionizing radiation to the cell inducing DNA breaks. Antibody-oligonucleotide binds to its receptor, internalized, and bind complementary sequences in the cytosol for gene silencing. Antibody-drugs can act either internally or non-internally depending on the effector molecule – fusion inhibitor binds to a receptor or viral particle to inhibit entry, some classes of cytotoxic compounds act by intercalating to cell's DNA inducing DNA/RNA synthesis.

## Toxins

The antibody-toxin conjugate is the fusion of toxin payload to a carrier antibody molecule. Antibody-toxin is more commonly known in the field of cancer immunotherapy as an immunotoxin. However, immunotoxins can be characterized as the fusion of toxins to other carrier molecules such as growth factors, cytokines, or soluble ligands. For this review, antibody-toxin is used when the carrier molecule is an antibody.

Typically, a toxin contains a cell-binding domain, a translocation domain, and a catalytic effector domain responsible for cell death. An antibody-toxin replaces the cell-binding domain of toxins with a mAb carrier to provide selectivity, retaining the translocation and catalytic effector domains for functionality. To be effective, antibody-toxins must bind to their antigen, rapidly internalize, and translocated to the cytosol where it can catalytically disrupt protein synthesis leading to cell death. Toxins used in HIV-1 ACs are derived from bacteria such as PE, Diphtheria toxin (DT), and anthrax toxin, and plants such as pokeweed, and ricin. These toxins are an ideal payload for ACs due to the ease of recombination, high expression and yields, potency, and relatively low toxicity compared to other toxins (105).

The first-generation toxin conjugates for HIV-1 were developed in the late 1980s. Soluble CD4 was the first carrier molecule for PE, and ricin A chain (RAC) producing CD4-PE40 and rCD4-dgA constructs, respectively. These toxin conjugates showed high efficacy in targeting gp120-expressing cells and inhibiting HIV-1 protein synthesis in both acute and chronic HIV-1 T cell line models (34, 58). PE and RAC, upon internalization, interrupt HIV-1 protein synthesis by ADP-

ribosylation and the inactivation of the 60S ribosomal subunit, respectively. Toxin DT conjugated to sCD4, DAB389CD4, also exhibited highly efficient killing of HIV-infected cell lines *in vitro*, as well PBMCs from HIV-seropositive patients, and displayed no apparent toxicity. However, in both HIV-infected cell lines and PBMCs, DAB389CD4 resistant strains emerged (37, 106). DT conjugation to IL-2 (DAB486-IL2) also exhibited potency in eliminating HIV-1 infected cells in a mixed culture of infected and uninfected T cells detected by the inhibition of HIV-1 protein and RNA production (67).

The early efficacy in *in vitro* characterization of CD4-PE40 in cell line models pushed the field to extensively evaluate this toxin conjugate. The construct exhibited favorable potency with half-maximal inhibitory concentration ($IC_{50}$) <0.1 nM in cell culture, efficacy in monocytes and macrophages, little toxicity against uninfected cells, and efficacy in primary isolates of HIV-1 (107, 108). Additionally, CD4-PE40 demonstrated synergy when combined with ART (109), and was well tolerated in rhesus macaques (110). However, in a human phase I clinical study, a single low dose of CD4-PE40 at 15 μg/kg resulted in hepatic toxicity with no apparent antiviral activity (110). The same results were attained in a human phase III multi- and dose-escalating treatment (111). Both human trials resulted in dose-related toxicities, induction of anti-drug antibodies (ADA), and limited circulation half-life of only 3 hours.

The discouraging results of the first-generation toxin conjugates based on CD4 carriers prompted the exploration of new carriers that could offer increased circulation half-life, reduced hepatotoxicity, and prevents potential involvement of sCD4 in the release of gp120 on the virion or cell surface (39, 112). The use of mAb carriers could address the shortcomings of CD4 as toxin carriers, which led to the development of the second-generation toxin conjugates to mAb targeting HIV-1 Env. The chemical conjugation of RAC to 50-69 and 907 mAbs, both targeting gp41 showed efficacy in infected cell lines with $IC_{50}$ in the nM range (35, 58). Furthermore, 924-RAC, targeting gp41, exhibited superior efficacy and addressed most of the shortcomings of CD4-PE40 and showed increased potency when combined with CD4-Ig in an *in vivo* mouse model of infection, and decreased susceptibility to blocking effects from anti-HIV antibodies found in the serum of HIV-infected patients (39, 113). Therefore, the use of antibodies as carriers for toxins showed a more favorable outcome both in potency and pharmacokinetics of the construct in comparison to sCD4.

Antibody-toxin conjugates based on PAP conjugated onto antibodies targeting CD4, CD5, and CD7 showed pM efficacy in the inhibition of HIV-1 replication in primary CD4+ T cells (65). Moreover, anti-CD4-PAP was found effective at inhibiting HIV-1 production for several weeks in an *ex vivo* samples of activated replicating CD4+ T cells, as well as in clinical HIV-1 isolates *in vitro* and demonstrated superior anti-HIV-1 activity compared to zidovudine treatment, and also exhibited efficacy against zidovudine-resistant viruses (65, 114). Subsequently, attempts were made to specifically target the latent reservoirs *via* antibody-toxin conjugates. Antibody-toxin directed to CD25 and CD45RO aims at targeting activated and latent cells, respectively. These antibody-toxins proved to be effective in eliminating replication-competent HIV-1 infected PBMCs as well as *ex vivo* treatment of CD4+ T cells from HIV-infected individuals (64, 66, 115).

Currently, antibody-toxins are taking advantage of the recent advancement in bNAb discovery, antibody engineering, and ART complementation to further increase their therapeutic value. A mAb carrier based on b12 bNAb subunit, 3B3 scFv, fused to PE38 (a truncated version of PE40), exhibited enhanced therapeutic attributes than the previous generation of toxin conjugates. 3B3(Fv)-PE38 retained broad reactivity against HIV-1 isolates, enhanced cytotoxicity in transfected cell line models compared to CD4-PE40, and suppressed viral load in an *in vivo* mouse model. Further characterization of 3B3(Fv)PE38 also showed the ability to block primary HIV-1 isolates in both PBMCs and monocyte-derived macrophages, and encouragingly, showed no apparent *in vivo* hepatotoxicity in rhesus macaques that were previously observed with CD4-PE40 (38, 116–118).

In the context of HIV-1 treatment, antibody-toxins are likely to be most effective when combined with ART. This has already been indicated in several studies showing that antibody-toxin in combination with ART, is more effective in blocking infection than when used alone *in vitro* and *in vivo*, as well as a sustained delay in viral rebound than combination ART treatment alone after cessation (109, 116, 119).

Despite decades of antibody-toxin conjugate research for HIV-1 cure, no such constructs are approved therapeutically. ART and antibody-toxins were developed side-by-side in the early days of the AIDS epidemic with ART significantly changing the course of the disease. Antibody-toxins for HIV-1 cure, therefore, warrants a second look because of the following advantages that they offer; 1) antibody-toxin can target actively and latently infected cells where current ART is ineffective, 2) antibody-toxin have reduced toxicities and improved half-life compared to CD4-PE40, 3) a variety of antibodies can be used as next-generation carriers with broad reactivity against HIV-1 strains, and finally, 4) antibody-conjugates are proven safe and effective in the field of cancer immunotherapy.

## Radionuclides

Antibody-radionuclide is the conjugation of radioisotopes to a carrier mAb to deliver lethal doses of ionizing radiation to cells. In the field of cancer immunotherapy, antibody-radionuclide is also referred to as radioimmunotherapy. The main mode of action of antibody-radionuclide is the radiation-induced cell death *via* double-stranded DNA breaks or the formation of reactive oxygen species (ROS) upon engagement with its antigen. The FDA approval of Ibritumomab tiuxetan (Zevalin) for the treatment of non-Hodgkin's lymphoma in 2002 marked the first clinical use of RIT. Zevalin uses an anti-CD20 mAb carrying a radioactive $^{90}$Yttrium and is administered as a single dose.

Dadachova and colleagues reported the first proof-of-concept construct of antibody-radionuclide for HIV-1 with the conjugation of bismuth 213 ($^{213}$Bi) and rhenium 188 ($^{188}$Re) to anti-gp120 and anti-gp41 antibodies. These antibody-radionuclides selectively killed chronically HIV-1 infected cells

and acutely infected PBMCs *in vitro*. The degree of cytotoxicity depends on the energy and half-life of the conjugated radionuclide. Gp41-$^{188}$Re exhibited superior potency in an *in vivo* mouse model due to the longer physical half-life of $^{188}$Re ($t_{1/2}$ = 16.9 h), enabling adequately access to infected cells in the circulation in comparison to $^{213}$Bi ($_{t1/2}$ = 46 m) which loses its radioactivity at a relatively shorter time (44).

To further elucidate the contribution of the radionuclide's physical properties for its efficacy, different radionuclides were conjugated to the same antibody carrier. Garg and colleagues conjugated an anti-gp41 mAb 2556 with $^{213}$Bi ($_{t1/2}$ = 46 min, alpha radionuclide), and two radionuclides with a much longer half-life, $^{225}$Actinium ($^{225}$Ac, $_{t1/2}$ = 9.9 days, alpha radionuclide), and a beta emitter $^{177}$Lutetium ($^{77}$Lu, $_{t1/2}$ = 6.7 days). Three days post-treatment, both $^{213}$Bi, and $^{177}$Lu antibody-radionuclides significantly killed PBMCs infected with HIV-$1_{p49.5}$ *in vitro*, while $^{225}$Ac antibody-radionuclide exhibited minimal potency. However, at 7 days post-treatment, all three antibody-radionuclides showed a significant reduction of p24 levels compared to an anti-RSV mAb control (46). Similar results were observed in the infected $CD14^+CD16^+$ monocyte, which is known to play a role in HIV-1 neuropathogenesis.

Antibody-radionuclides were observed to be more potent in killing monocytes than other cell populations. This led McFarrren and colleagues to test their efficacy in targeting HIV-1 reservoirs in the central nervous system (CNS). Using an *in vitro* blood-brain barrier (BBB) model the group added 2556-$^{213}$Bi AC in PBMCs and monocytes that transmigrated across the BBB. This AC induced increased apoptosis with 30% of infected PBMCs and 60% of infected monocytes killed. However, a high level of nonspecific apoptosis of uninfected monocytes was observed, in some conditions reaching up to 80% bystander killing. This could be due to the high concentration of radiation in the sample, or cell crowding in the BBB *in vitro* model causing the crossfire effect (45).

Finally, the efficacy of antibody-radionuclide complemented with ART was evaluated by Tsukrov and colleagues. Both in an *ex vivo* infection model and ART-treated PBMCs from HIV-1 infected individuals, the treatment with 2556-$^{213}$Bi demonstrated no negative effect and exhibited similar potency as ART-naïve PBMCs (60).

Antibody-radionuclide conjugates are a valuable addition to cancer immunotherapy, for HIV-1 cure, however, a different set of challenges must be overcome. Both approved antibody-radionuclide conjugates for cancer immunotherapy are not used as first-line treatment and are most widely applied to most radiosensitive tumors, such as leukemias and lymphomas. Therefore, the utility of antibody-radionuclide conjugates as a therapeutic intervention in the context of HIV-1 infection must be further explored. As with antibody-toxin conjugates, antibody-radionuclide conjugates are more likely to be effective in combination treatment with ART, therefore the optimal timing of treatment in acute *vs* chronic HIV-1 infection, as well as its effect during the immunocompromised status of infection must be investigated. Next, the sensitivity and dosimetry profiles of actively and latently infected cells for radiation, as well as HIV-1 sanctuary sites must be established. Finally, since HIV-1 persistence in macaque models might not recapitulate HIV-1 infection in humans, efficacy studies will be best performed in humans, which could add more complexities in testing its efficacy and safety in humans.

## Small Drugs

Antibody-drug conjugate is a targeted drug delivery approach characterized by the fusion of a small molecule drug to a carrier mAb. In the cancer immunotherapy field, antibody-drug conjugates, or ADCs, are commonly designed with the conjugation of a potent cytotoxic agent that can induce cell death. However, antibody-drug conjugates for HIV-1, as described in this review, also include conjugation of small molecules and peptides that can block infection and are not apoptotic agents.

Repurposing of approved drugs proved to be beneficial in the field of HIV-1 cure. Zidovudine, originally intended for cancer treatment, was repurposed for HIV-1 treatment and approved by the FDA as the first-ever treatment available for HIV-1. Hence, the pioneering antibody-drugs for HIV-1 conjugated doxorubicin, a cancer drug, to a murine anti-gp120 mAb, P4/D10. The P4/D10-doxorubicin conjugate exhibited protection in mice after challenge with an 8-fold less concentration compared to the unconjugated mAb (47). This construct was further optimized using a humanized P4/D10 mAb conjugated to approved HIV-1 drug enfuvirtide to reduce potential immunogenicity of the murine P4/D10. The hP4/D10-enfuvirtide conjugate exhibited improved potency in both pseudovirus and cell-spread assays (73).

These studies demonstrated that conjugation of drugs with different modes of actions can be effective when designed as ACs. Doxorubicin and enfuvirtide are two small drugs that inhibit nucleic acid synthesis, and viral entry, respectively. Additionally, another intracellularly-acting payload, brefeldin A, inhibiting ER-Golgi protein trafficking, was also shown to be an effective payload for ACs (50).

ACs with small drugs later focused on increasing potency by blocking cell entry and fusion. Particularly, CCR5 antagonism was favored. A promising early study by Ji and colleagues showed synergistic potential *in vitro* when an anti-CCR5 mAb was combined with a CCR5 small molecule antagonist targeting non-overlapping epitopes (88). Encouraged by this result, Kopetzi and colleagues designed a bifunctional AC consisting of an anti-CCR5 mAb covalently linked to T-2635, a fusion inhibitor. This construct exhibited efficient blocking of HIV-1 Env-mediated fusion but showed viral tropism dependency with its inability to prevent X4-tropic infection in PBMCs (71).

Alternatively, several groups explored the conjugation of CCR5 antagonist to a chemically programmed antibody (cpAb) 38C2 (120). However, this construct is different than the traditional AC since the CCR5 antagonist itself provides the targeting and effector function, while the antibody carrier mainly functions to extend the pharmacokinetic profile of CCR5 antagonists (**Figure 1C**). The 38C2 cpAb can form a site-selective conjugation with *N-acyl-β*-lactam derivatives of drugs

and small molecules. Explored here includes $\beta$-lactam derivatives of BMS-378806, BMS-488043, Apalviroc, and Maraviroc (72, 74, 75). This conjugation technique dramatically extended the pharmacokinetic profiles of the attached molecule which increased serum stability compared to its unconjugated counterpart, however, this technique only exhibited minimal improvement in neutralization potency compared to the parental molecule.

Improvement in potency was later observed when Gardner and colleagues designed eCD4-Ig, which is a fusion of a CCR5 mimetic peptide, mim1, to CD4-Ig. This construct can simultaneously bind to CD4- and coreceptor-binding site on HIV-1 Env, and was found to have an increased breadth and similar potencies as bNAbs (48, 52). Subsequent variants of eCD4-Ig were designed with improved versions of mim1. These eCD4-Ig variants exhibited cooperative avidity to Env, improved potency and breadth compared to bNAbs tested, ability to neutralize neutralization-resistant strain of HIV-1, and showed protection in rhesus macaques after viral challenge (52, 121, 122). These encouraging results prompted the conjugation of the CCR5 mimetic to bNAbs belonging to different classes. When conjugated to the C-terminus of bNAbs, mim6, exhibited improved potency of all classes of bNAbs against HIV-1 isolates. However, this is only true to HIV-1 isolates that were previously sensitive to mim6, suggesting possible bNAb epitope dependency. Indeed, the importance of bNAb carriers to potentiate improved potency of conjugated mim6 was exhibited by its conjugation to V3-targeting bNAbs. V3-targeting bNAbs conjugated with mim6 displayed a 2-fold increase in potency even against mim6-resistant HIV-1 isolates tested (48).

Antibody-drug development for HIV-1 cure is slow, in comparison to cancer immunotherapy, and more preclinical data is needed to evaluate its potential as a therapy for HIV-1. To date, only one study showed the possible cooperative potential of antibody-drug as a complement to ART, which was investigated in the late 1990s. An anti-gp120 mAb-brefeldin A conjugate exhibited efficacy in a chronic cell line model of infection as well as infected PBMCs when used alone. However, antibody-brefeldin A combined with zidovudine resulted in a remarkable 90% reduction of virus production in an $IC_{50}$ in the nM range, potency in zidovudine-resistant virus strain, and low toxicity against uninfected cells (50).

In a recent patent application, the repurposing of commonly used anti-cancer payloads in cancer antibody-drug was outlined. An HIV-1 antibody-drug was designed with the conjugation of a bNAb to monomethyl auristatin E (MMAE), a synthetic antineoplastic agent commonly used in cancer antibody-drug conjugates. The AC vc-MMAE-NIH45-46 G54W, which is the conjugation of NHI45-46 G54W bNAb to MMAE, could be further explored and highlights the potential application of various cytotoxic drugs not originally intended for HIV-1 cure as a payload for HIV-1 AC (123).

Overall, the success of antibody-drug conjugates in cancer immunotherapy can potentially be mirrored and translated for an HIV-1 cure. The early preclinical successes in the conjugation of HIV-1 drugs, small drugs, and peptide inhibitors to mAbs described herein display a great deal of promise. To move forward, future development of antibody-drugs for HIV-1 should also explore the potential efficacy of conjugating other HIV-1 inhibitors blocking various stages of the viral replication cycle besides entry and fusion inhibition. More importantly, future antibody-drugs should explore drug-drug interaction under current ART and establish its cooperative tendencies to ART, effectiveness alongside LRA, and finally, monitor any potential development of resistance to the drug or AC itself.

## Oligonucleotide

The conjugation of an oligonucleotide to a mAb herein referred to as antibody-oligonucleotide conjugate, describes the use of mAb as the carrier molecule to RNA, DNA, or synthetic oligonucleotide that often exerts a variety of functions. A variety of engineered oligonucleotides based on their functionality has been described. This includes oligonucleotide involved in targeting (aptamers), gene expression regulation (miRNA), gene silencing (antisense oligonucleotide or ASO, and siRNA) (124).

Twenty years ago, Elbashir and colleagues published the hallmark proof-of-principle experiment demonstrating the use of siRNA to knockdown a specific gene in a mammalian system (125). This discovery led to an increased interest in RNA interference (RNAi)-based technologies leading to the first siRNA-based drug approved by the FDA in 2018, Onpattro, to treat polyneuropathy in people with hereditary transthyretin-mediated amyloidosis (126).

RNAi technology uses 19-23 base pair (bp) RNA duplexes that intervene post-translationally triggering cellular degradation of cognate messenger RNA (mRNA). RNAi can silence a gene with high specificity and can virtually target any gene. The potential of RNAi is challenged by stability, biodistribution, delivery to target cells, and *in vivo* delivery across the cell membrane to the cytoplasm where the mRNA is located (127).

In 2002, hallmark papers showed the capacity of RNAi technology to silence HIV-1 replication and production *via* the use of synthetic siRNA. Researchers showed the efficacy of siRNA to target both the pre- and post-integration RNA of the HIV replication cycle by targeting HIV genes [*vif, nef, tat, rev, p24*, and long terminal repeat (LTR)] (128, 129). Additional studies by Novina and colleagues showed the potential use of siRNA in targeting host cellular factors by designing siRNA specific for human CD4, which exhibited a reduction of viral entry and viral production, as well as siRNA targeting HIV-1 coreceptors CXCR4 and CCR5 (130).

Various methods are actively being developed to solve the delivery problem with oligonucleotides including chemical modifications, and conjugation of siRNA to targeting moiety. However, issues of rapid clearance (siRNA-peptide conjugation), potential immunogenicity (liposome, PEGylation), and increased off-targeting and toxicity (high dosage) remain a problem (127, 131). The use of mAb as a siRNA carrier could

address such limitations by enabling a cell-targeted approach, reduction of siRNA payload, limiting nonspecific silencing, and minimizing related toxicities. In this section, the current state of antibody-oligonucleotide for HIV-1 cure is detailed.

The first proof-of-principle antibody-oligonucleotide conjugate for HIV-1 cure was designed by Song and colleagues with an anti-*gag* siRNA fused to the F105 Fab antibody fragment. The AC was engineered from a bicistronic plasmid encoding the Fab fragments of the F105 heavy- and light-chains with protamine fused at the C-terminus (**Figure 1B**). Protamine can form a complex with oligonucleotides, which bypasses the need for covalent coupling. F105-P *gag* siRNA induced gene silencing of targeted cells and inhibition of HIV replication in HIV-infected primary T cells, as well as in an *in vivo* mouse model (42).

Subsequently, antibody-oligonucleotide conjugates displayed efficacy when tested in an *in vivo* humanized mouse model. Using an scFv targeting CD7, a pan-T cell receptor, anti-CCR5 siRNA, and a combination of siRNAs targeting viral genes *vif* and *tat* were conjugated *via* the addition of nine arginine residues (9R) to scFv which facilitated the conjugation of siRNA through charge interaction. Intravenous injection of scFvCD7-9R siRNA halted CD4+ T cell decline and reduced viral loads in comparison to controls in a humanized mouse model (43). Using another host-expressed protein as a target, Peer and colleagues designed AL-57-PF-CCR5, an scFv targeting LFA-1 conjugated with an anti-CCR5 siRNA. This construct showed effective reduction of mRNA expression in memory T cells expressing LFA-1, attenuating CCR5 expression in activated T cells (69).

It took over a decade for the next antibody-oligonucleotide construct to be published. Using a nanobody against CXCR4, an anti-*tat* siRNA was conjugated. The construct 4M5.3X4 efficiently delivered anti-*tat* siRNA to CXCR4+ cell lines as well as human primary T cells, and abolished Tat-driven HIV transcription (70). This construct also marked the first time a nanobody was used as a carrier for HIV-1 AC (**Figure 4**).

The field of antibody-oligonucleotide conjugates for HIV-1 cure is at the early phases of exploration. Although siRNA must escape to the cytoplasm to exert its gene-silencing function, the trafficking pathway of the constructs described herein remains to be understood. Additionally, for antibody-oligonucleotide conjugates to be effective, timing and durability are crucial. It is still not known whether transient treatment with antibody-oligonucleotide conjugates could offer sustained silencing of targets that is therapeutic in HIV-1 infected individuals. Furthermore, more preclinical data is needed to determine whether endogenous siRNA could potentially interfere with antibody-oligonucleotide, or whether off-target effects will be an issue.

## Novel Payloads

Innovative conjugation techniques are enabling the development of novel payloads for ACs. One such example is the conjugation of photosensitizers (PS) to antibodies. Antibody-photosensitizer conjugates, also known as photoimmunotherapy (PIT), is a targeted photodynamic therapy designed with a conjugated PS to a mAb. PIT is proposed to be minimally invasive and safer than conjugated toxins or radionuclide, reducing possible immunogenicity and crossfire effects, respectively. Conventional PS treatment using light called photodynamic therapy (PDT), destroys cells nonspecifically when exposed to light through the production of ROS. The inclusion of mAb as the targeting molecule thus provides selectivity. Sadraeian and colleagues showed the first proof-of-principle use of antibody-photosensitizer conjugate for HIV-1. Using 7B2 anti-gp41 carrier antibody, a cationic porphyrin and anionic IR700 PS were conjugated and tested for cytotoxicity in an Env-transfected cell line. The addition of both porphyrin- and IR700-conjugated 7B2 exhibited an increase in ROS levels after irradiation compared to untransfected controls. Following the increase in ROS level, cell death was observed. Although the adaptation of PDT to HIV-1 described in this study is preliminary, this approach is a welcomed addition to the increasing lineup of ACs for HIV-1 cure. Further studies are warranted to fully elucidate the potential of antibody-photosensitizer in the field of HIV-1 cure, especially its effectiveness in non-solid tumors, such as HIV-1, considering that the main restriction of this approach is the constraint of light penetration.

The conjugation of cholesterol to mAb was also explored. When cholesterol was conjugated outside the paratope of the membrane-proximal external region (MPER)-class of bNAbs, Lacek and colleagues found that the neutralization activity of the bNAbs was dramatically increased. This antiviral potentiation is due to the increased interaction between cholesterol and the lipid raft domains on the membrane. The antibody-cholesterol conjugate was also shown to rescue the activity of a mutated version of an MPER bNAb with abolished interaction to the viral membrane, with the cholesterol moiety mimicking the interaction. Therefore, cholesterol conjugation can be a valuable tool in increasing the antiviral activity of bNAbs. Since the conjugation can be made at several positions on the mAb and occurs outside the antibody paratope, it can complement various affinity maturation strategies (51)

Lastly, in recent years there has been an interest in the use of Toll-like receptor (TLR) agonists in the context of HIV-1 cure. The engagement of TLRs and their ligands can lead to activation of the innate immune response and priming of the adaptive immune system. Therefore, TLR agonists can play a dual role in HIV-1 by acting as an LRA and an immune regulator (132). In the HIV-1 cure context, Borducchi and colleagues showed that a combination treatment of a TLR7 agonist (GS-9620) and PGT121 delayed viral rebound following ART interruption in rhesus macaques. Moreover, 5/11 treated animals did not result in a viral rebound following ART interruption (133). These results, therefore, provide a good rationale for conjugating TLR agonists to mAb. An antibody-TLR agonist conjugate can directly target immune activation to latently infected cells, activate effector cells, and potentiate bNAb function by immediate recognition of reactivated cells. The conjugation of TLR agonists to mAb is already being explored in cancer (134).

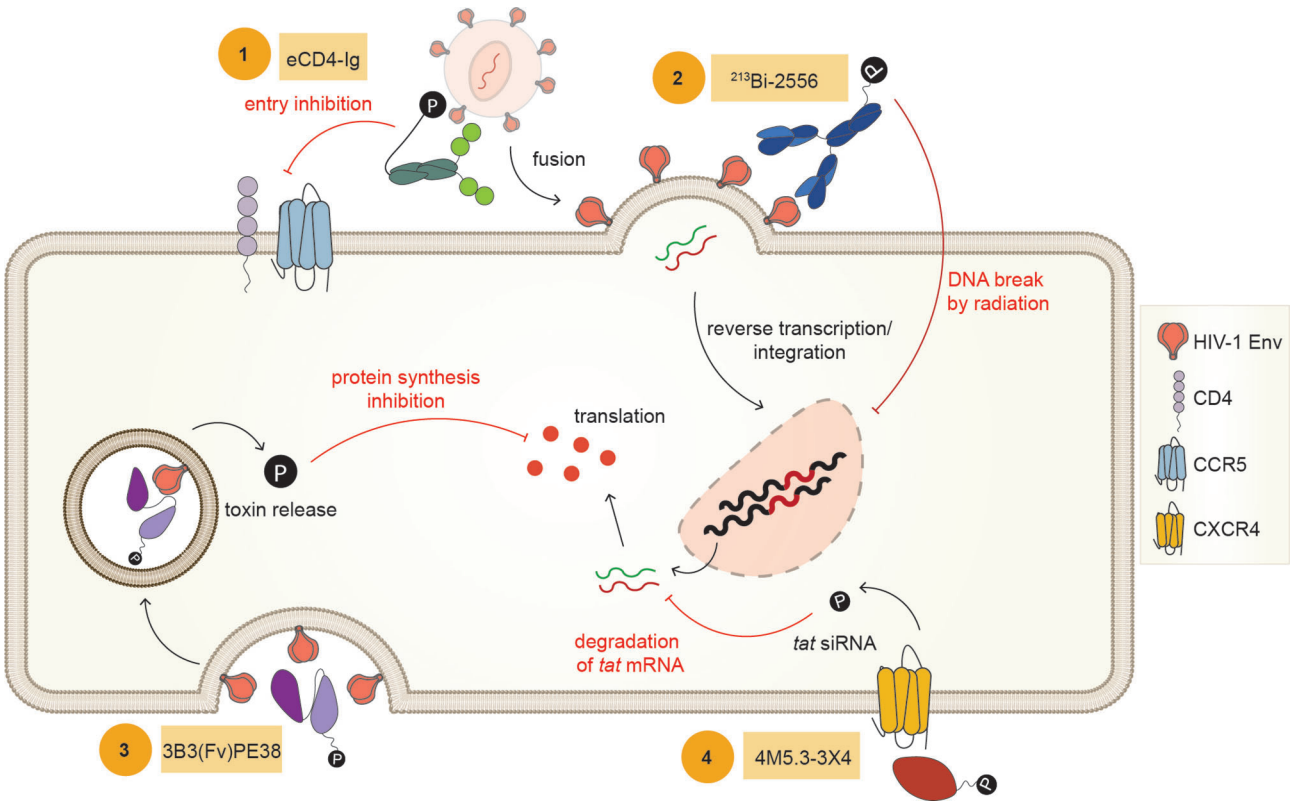


**FIGURE 4** | Example of Antibody Conjugates. Representative antibody conjugates described in this review (1) eCD4-Ig is the conjugation of CD4 to a CCR5 mimetic peptide inhibiting viral fusion and entry, (2) $^{213}$Bi-2556 is an antibody-radionuclide with $^{213}$Bi fused to an antibody targeting gp41, this conjugate delivers cytocidal radiation upon binding inducing DNA break, (3) 3B3(Fv)PE-38 is an antibody-toxin constructed with the scFv subunit of b12 bNAb conjugated to PE toxin and functions by inhibiting protein synthesis upon internalization, (4) 4M5.3-3X4 is an antibody-oligonucleotide designed with a nanobody targeting CXCR4 conjugated with an anti-*tat* siRNA, inhibiting Tat-driven transcription.

## ANTIGEN BINDING AND INTERNALIZATION

Another essential factor in the efficacy of ACs, besides antigen specificity and payload efficacy, is the internalization requirement of ACs (**Figure 5**). ACs described herein showed different requirements for cellular uptake, internalization, and intracellular routing. While radionuclides were functional upon mere binding to its antigen, certain payloads require internalization, effective linker cleavage, and lysosomal escape to be functional such as toxins, oligonucleotide, and small drugs. In cancer immunotherapy, alongside antigen density, the varying rate of internalization after AC engagement is directly linked to its efficacy (135). It is therefore not a surprise that payloads that act intracellularly were most effective when conjugated with a rapidly internalized receptor, and antibodies binding to a more proximal epitope to the plasma membrane (136), which is the case of siRNAs and toxins, respectively (59, 70).

The internalization kinetics, therefore, must be considered when designing the next-generation ACs. This parameter has not been fully exploited by ACs described herein. For example, an internalized radionuclide in combination with a radionuclide having a shorter range of radiation could decrease the potential crossfire effect. Additionally, a combination of a small drug payload targeting intracellular viral proteins (reverse transcriptase, integrase, protease) could be effective when endocytosed and released into the cytoplasm.

## SAFETY AND IMMUNOGENICITY

The disappointing termination of CD4-PE40 in human clinical trials, the only AC for HIV-1 cure to date, because of safety concerns highlights the need to improve both the efficacy and safety in future AC development. The diversity of ACs for HIV-1, including its choice of antigen, carrier molecule, types of payloads, mode of action, and linker chemistries, complicates the generalization of the safety profile of each AC category described in this review. In this section, the safety and immunogenicity parameters involved in each AC category are discussed.

The result of CD4-PE40 clinical trials for HIV-1 cure exhibited unfavorable hepatotoxicity and the development of ADA with no apparent therapeutic benefits. Early speculation behind the observed hepatotoxicity of CD4-PE40 focused on the CD4 carrier moiety

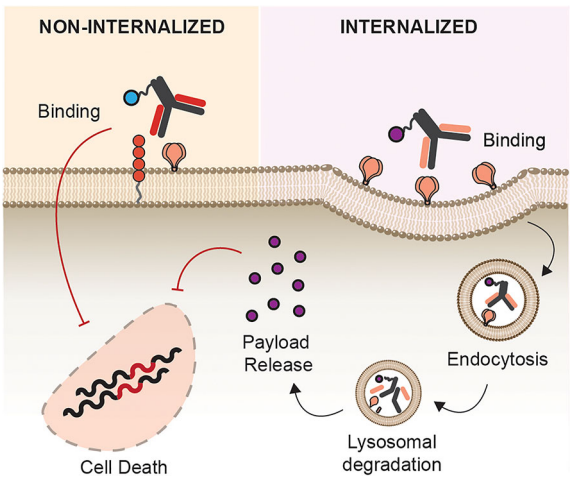


**FIGURE 5** | Site of Action. Antibody conjugates can act either intracellularly or intercellularly upon antigen binding. Toxins, siRNA, and inhibitors of DNA synthesis require internalization as they are only functional upon cytosolic release. Payloads such radionuclide, entry inhibitors, and photosensitizers are functional without internalization.

binding to free gp120 in the circulation leading to nonspecific uptake by hepatocyte (63), however, this was later refuted. Onda and colleagues found that the isoelectric point (pI) of the carrier molecule is positively associated with hepatotoxicity, and lowering the carrier molecule's pI decreases the potential for hepatotoxicity (137). The high pI of CD4 (pI=8.86) could therefore explain the hepatotoxicity observed in animal studies and human trials. This was later addressed by the design of 3B3-PE38 with a carrier moiety exhibiting a much lower pI leading to no *in vivo* hepatotoxicity in rhesus macaques (118).

The issue of immunogenicity, especially for toxins, was later addressed by several strategies. This led to the truncation of the toxin (PE40 to a less immunogenic PE38), co-treatment with immune-modulating drugs, identification and manipulation of B and T cell epitopes, and other various recombinant modifications (138). Mutagenic deimmunization was also applied to DT, as well as deglycosylation of RAC to minimize interaction with hepatocytes (49, 139).

The development of ADA which could arise against the payload, linker, and the entire AC itself, is another major safety concern. The elicitation of ADAs could augment immune-related adverse events, anaphylactic reaction, and decreased potency of ACs. Ramachandran and colleagues observed the development of ADA against the carrier and payload for CD4-PE40, as well as the elicitation of antibodies neutralizing the construct (111). To track the development of ADAs, constant monitoring using highly sensitive assays are being used in cancer immunotherapy, which could then help inform the course of treatment, and therefore should be a crucial part of preclinical development for HIV-1 cure.

Antibody-radionuclide comes with a different set of safety considerations. The issue of the crossfire effect, notably to all constructs described herein, is a major concern. Current approved antibody-radionuclides, Zevalin and Bexxar, both FDA approved to treat non-Hodgkin's lymphomas, contain beta-emitters and are both non-internalized. Beta particle-emitting radionuclides are characterized by the emission of high energy, sparsely ionizing, with ranges of up to a few millimeters. Due to this wider range of effects, beta emitters can induce a crossfire effect to neighboring, non-targeted cells. In contrast to a beta emitter, an alpha emitter radionuclide offers a much shorter range of radioactive decay, only traversing a few cells which are ideal for non-solid tumor-like targets. Alpha emitter radionuclide, as well as Auger radionuclide, both having shorter range, could therefore be an attractive choice to reducing crossfire effect. Furthermore, the *in vitro* characterization described in these studies observed cell crowding at the bottom of the cell culture plate, which could have potentiated the crossfire observed (45). Therefore, it is crucial to design new *in vitro* assays for crossfire determination.

The use of mAb subunits or nanobodies can also address concerns reading AC half-life. An intact IgG exhibits a longer circulation half-life which, depending on the conjugated payload, not be desirable (140). For radionuclide, for example, longer circulation half-life can promote undesirable radiation-absorbed doses to organs and blood which leads to myelotoxicity (141). Therefore, the availability of mAb subunits and nanobodies can be used to tailor a carrier of ACs depending on the intended circulation half-life requirements of a specific AC.

Antibody-oligonucleotide is a relatively new strategy and data on safety and immunogenicity is limited. The delivery of oligonucleotides has traditionally been the major limitation of its clinical applications. Strategies and modification of oligonucleotide for improved pharmacokinetics, pharmacodynamics, and biodistribution are an active area of research beyond the scope of this review (142). Two conjugation strategies were explored by AC for HIV-1, antibody-protamine fusion, and antibody-oligo-9-arginine peptide, both of which showed no toxicity in *in vitro* assay and *in vivo* mouse model (43, 143). An additional concern with oligonucleotide therapy is the possible off-target activation of intracellular TLRs, leading to an unwanted immune response. In mouse models, no TLR activation was observed, though careful monitoring in future studies is important (43, 69).

## NEXT-GENERATION AC FOR HIV-1

### Broadly Neutralizing Antibodies as Next-Generation Carrier

Most antibody carriers explored in the HIV-1 ACs employed murine, polyclonal, non-neutralizing, and/or first-generation neutralizing antibodies. However, the last decade saw increased innovation in the isolation and discovery of bNAbs with increased breadth and potency. BNAbs can be placed in a distinct category than ART because they directly target circulating virus, recognize Env-expressing infected cells, and can directly engage host antiviral responses such as ADCC.

Several of these bNAbs have already entered various phases of human clinical trials for prevention, ART interruption, and therapeutic studies (144). Moreover, bNAbs are an attractive next-generation "armed" antibody for the delivery of molecular payloads for HIV-1 cure. The fundamental characteristics of bNAbs recognizing conserved epitopes across various clades and strains of HIV-1 remain of utmost importance providing selectivity as well as breadth, but additionally, the whole gamut of isolated bNAbs could offer increased flexibility, adaptability, and customization depending on the payload of choice.

The interest in bNAbs for clinical applications is indisputable, however, evidence reveals that not all bNAbs are created equal. Beyond their physical characteristics and binding specificities, bNAbs are diverse in terms of their function, and effectiveness in the context of therapeutic application. The requirement for neutralization of cell-free virions differs from those of cell-expressed viral proteins for effective ADCC. This can be explained by the various conformation of Env depending on the stage of infection, as well as the extensive viral heterogeneity that exists in the latent reservoir. The discovery and functional analysis of bNAbs for therapy is reviewed elsewhere (144, 145).

The functional variabilities of bNAbs make them an attractive carrier for ACs. As discussed throughout this review, the various mode of action of the payloads must be complemented by an appropriate mAb carrier moiety for optimal efficacy. Evidence provided that for toxins, carrier mAb targeting epitopes near the membrane is most effective (39, 136). However, these first-generation antibodies require sCD4 to be effective. In an indirect assay to screen bNAbs that make the best carriers of toxin, Pincus and colleagues found that bNAbs targeting CD4bs, V3 loops of gp120, and the gp41 HR/loop region to be effective as toxin carriers. Interestingly, not all gp41-targeting bNAbs showed efficacy as carriers with bNAbs targeting the MPER showed little to no efficacy as toxin carriers (59). This study therefore suggests that further characterization of bNAbs is required to elucidate the optimal carrier for ACs and that bNAbs targeting the CD4bs, V3 loops, and gp120-gp41 interface would be an interesting candidate for carriers of ACs.

For some ACs, rapid internalization is crucial for functionality. Therefore, antibodies that are readily internalized upon binding to their antigen are preferred. It has been reported that bNAbs targeting the Env "closed" conformation are readily internalized upon antigen-antibody ligation, in comparison to non-neutralizing anti-HIV-1 antibodies (146). The rapid internalization of Env in the closed conformation upon bNAb binding is a known evasion mechanism also seen in other viruses such as respiratory syncytial virus (RSV) and feline coronavirus infection (147, 148). This rapid antibody-Env internalization decreases the exposure time of bNAbs on the surface of infected cells, impairing host surveillance, and thus decreases the Fc-effector function of bNAbs. However, since ADCC is not the primary effector objective of ACs, this bNAb limitation for therapeutic use is not going to affect their efficacy as carrier molecules of ACs. Therefore, payloads such as toxins, oligonucleotide, and small drugs can be conjugated to bNAbs binding to the closed Env epitopes for rapid internalization. Meanwhile, non-neutralizing antibodies could be used for payloads with less dependence on internalization.

Several human trials have been conducted to test the safety and efficacy of bNAbs for therapy. In these clinical trials, bNAb infusion is deemed safe and well-tolerated without evidence of dose-limiting toxicity or adverse effect (149–152). Tested bNAbs were found to exhibit circulation half-life in the range of 9-13 days for HIV-1 infected individuals and 12-24 days for healthy subjects (144). The circulation half-life of bNAbs is an important factor for their efficacy as sufficient levels of bNAbs are needed to be maintained in the circulation to effectively neutralize and kill HIV-1infected cells. Moreover, certain mutations have been shown to further increase the half-life of bNAbs, without detrimental effect to its binding site and Fc-effector functions (153). BNAbs are also shown to have longer half-lives than receptor-targeting antibodies (144) which further makes them more advantageous than other carriers described herein. The safety and favorable pharmacokinetic profiles of bNAbs make them highly attractive carriers of ACs for HIV-1. This ensures increased circulation duration for ACs to reach their target sites. In case longer circulation half-life is not favored, bNAb subunits or nanobodies can be used.

## AC for HIV-1 Therapy

Evidence points to a multipronged approach for an effective cure for HIV-1. ACs could be a vital component in all stages of the HIV-1 treatment regimen. Although efficacies of bNAb monotherapy, bNAb in combination with ART and ART interruption studies, and bNAb in combination with LRAs are showing limited results in early human trials, the fact that these various combination treatments alongside bNAbs are all being tested for clinical efficacy could increase interest in ACs (144, 154, 155). In all these trials, bNAb infusion proved to be safe and well-tolerated which further highlights the advantage of mAb-based therapy over drug intensification approach for HIV-1 cure.

The modification of bNAbs as AC could further increase bNAb's antiviral activity such as (1) neutralization of virus, (2) Fc-mediated effector function, (3) activation of endogenous host antiviral responses, with (4) directly delivering cytotoxic and immune-regulating payloads to infected cells.

ACs, like bNAbs, are likely to be transiently active limited by the pharmacokinetics and therapeutic window of their subunits. Therefore, ACs will require multiple infusions until all infected cells are purged. An active area of research focuses on a durable long-term expression of anti-HIV-1 antibodies *via* viral vector delivery or gene editing technologies (156). Additionally, the role ACs against cell-free virions remains to be established. In theory, during the acute phase of infection characterized by highly productive release of virions, the released virions can act as an antigen sink, decreasing potential AC-infected cell interaction (59).

Therapeutically, ACs could have the greatest efficacy for treatment during the acute infection phase of HIV-1 in complement with ART. After exposure, patients can undergo ART treatment immediately combined with ACs. This treatment strategy can simultaneously inhibit viral replication through the action of ART and eliminate infected cells through ACs. Clinicians can use information gathered from laboratory testing used to monitor ART responses such as plasma HIV-1 RNA and CD4+ T cell count to determine the appropriate carrier mAb and payload that may offer the best efficacy. In cancer immunotherapy, immunocompromised patients exhibited lower immunogenicity and adverse effect against antibody-toxins (157). If the same applies in the context of acute HIV-1 infection, it is worth exploring whether antibody-toxin is safe and effective during an active high-viremic HIV-1 infection in combination with ART. A lock-out approach *via* antibody-oligonucleotide could also be explored during acute infection by silencing host factors hijacked by HIV-1 such as the ESCRT machinery, coreceptors CCR5, and CXCR4, and HIV-1 genes preventing integration and viral maturation (158). Finally, a tandem antibody-based acute infection therapy could be explored by replacing ART entirely. As mentioned earlier, ACs role in neutralization of cell-free virion remains to be tested, however, unconjugated bNAbs in combination with conjugated bNAbs as ACs could potentially target both cell-free virions and infected cells, preventing the establishment and spread of viral reservoirs, respectively. This can be done by careful selection of bNAbs with high neutralization potency, and ACs with higher affinity to infected cells, both targeting non-overlapping epitopes on HIV-1 Env.

Since the involvement of cytotoxic effector cells are not primarily involved in the clearance of infected cells *via* ACs, during the chronic phase, LRA administration or ART interruption can be then followed by ACs. AC treatment can therefore act immediately after reactivation of latently infected cells, potentiating the "kill" in the shock-and-kill strategy. Antibody-TLR agonist conjugates would be an ideal construct during chronic HIV-1 infection as they can dually function as an LRA and engage Fc-effector function for the killing of reactivated cells. A lock-out AC construct with siRNA that can deliver epigenetic silencing can also be explored at during chronic infection (26). An example of such siRNA, developed by Suzuki and colleagues, targets the NF-κB sites in the HIV-1 promoter to induce potent transcriptional gene silencing (158). Lastly, ACs could be explored during virological blips observed in some patients. Blips are characterized by a sudden increase in viral RNA during suppressive ART. A recent study showed that endocervical endothelial cells release endogenous signals that can reactivate the latent reservoir (159). Therefore, passive administration of ACs during suppressive ART could potentially act immediately during virological blips, potentially decreasing the size of the viral reservoir.

To experimentally test the utility of ACs as a curative approach, preliminary *in vitro* cell line models of latency can be used. Cell lines such as U1 and ACH-2 are widely used HIV latency models and are suitable with reactivation by LRAs. However, these cell line models are limited in truly recapitulating the mechanism behind the actual HIV-1 reservoir in PLWH (160), therefore the best model would likely require *ex vivo* samples isolated from PLWH over established cell line models of infection and latency. Confounding differences in the Env conformation of various cell line models, integration site and method of establishing latency in latent cell lines, and the variability of Env expressed on released virions *versus* Env expressed on infected cell lines could obscure characterization results of ACs. Additionally, *ex vivo* isolated PBMCs can be isolated during acute phase of infection, upon ART treatment, ART naïve patients, and elite controllers to further elucidate the efficacy of ACs in various stages of infection. *Ex vivo* isolated PBMCs from PLWH can be further used to determine the optimal bNAb carrier that exhibits superior activity. The utility of ACs must overcome the safety and immunogenicity challenge of the first-generation ACs, and thus an appropriate safety, tolerability, and immunogenicity studies must be performed in a non-human primate model (NHP) model such as rhesus macaques. The established rhesus macaque persistence model can be adapted to determine the potency of ACs (161), either treated concurrently with ART, or during ART interruption or latency reversal.

## DISCUSSION

As of the writing of this review, 14 new ACs are undergoing late phase clinical trials to test their efficacy against various cancer forms. These new ACs are employing the use of IgG carriers, as well as scFv, and bispecific antibodies. Additionally, these ACs are conjugating diverse payloads such as cytokines, toxins, inhibitors, and photosensitizers (antibodysociety.org). However, no HIV-1 ACs are being tested in human trials.

The high modularity of ACs for HIV-1 cure that was explored here is a double-edged sword. Although in theory, this makes ACs highly adaptable and customizable depending on the context of infection, this also makes them harder to characterize and investigate as a distinct therapeutic modality. This suggests that preclinical development, assay design, and validation will be different in each ACs.

The maximum potential of ACs for HIV-1 cure is currently untapped. Since the initial AC trials for HIV-1 three decades ago, the HIV landscape has significantly improved with dozens of approved ART, various preventative modalities, as well as increased diagnostics and surveillance. These advancement warrants a renewed interest in AC as a possible HIV-1 cure strategy that can address the limitations of ART. Furthermore, the HIV-1 AC field, though lacking relevant human trials experience, could piggyback in the thriving AC landscape in cancer immunotherapy, as well as the current enthusiasm for bNAbs in human trials. Therefore, it can be argued that an HIV-1 cure approach based on ACs will play a major role in the development of new HIV-1 cure therapies.

## AUTHOR CONTRIBUTIONS

JU proposed the topic. JU created the tables and figures with input from ST. JU and ST structured the content, wrote, edited, and reviewed the manuscript. All authors contributed to the article and approved the submitted version.

## FUNDING

JU is supported by TKI-PPP grants Target2Cure by Health Holland/Aids Fund (LSHM19101-SGF) and Innovation Exchange Amsterdam (2019-1167). ST is supported by Young investigator grant P-53301 Aids fonds.

## REFERENCES

1. Leung D, Wurst JM, Liu T, Martinez RM, Datta-Mannan A, Feng Y. Antibody Conjugates-Recent Advances and Future Innovations. *Antibodies* (2020) 9(1):2. doi: 10.3390/antib9010002
2. Han AQ, Olson WC. Next-Generation Antibody-Drug Conjugate Technologies. In: *Antibody-Drug Conjugates*. Hoboken, NJ, USA: John Wiley & Sons, Inc (2016). p. 473–503. doi: 10.1002/9781119060727.ch18
3. Tsuchikama K, An Z. Antibody-Drug Conjugates: Recent Advances in Conjugation and Linker Chemistries. *Protein Cell* (2018) 9(1):33–46. doi: 10.1007/s13238-016-0323-0
4. Dennler P, Fischer E, Schibli R. Antibody Conjugates: From Heterogeneous Populations to Defined Reagents. *Antibodies* (2015) 4(3):197–224. doi: 10.3390/antib4030197
5. Birrer MJ, Moore KN, Betella I, Bates RC. Antibody-Drug Conjugate-Based Therapeutics: State of the Science. *J Natl Cancer Inst* (2019) 111(6):538–49. doi: 10.1093/jnci/djz035
6. Pegu A, Asokan M, Wu L, Wang K, Hataye J, Casazza JP, et al. Activation and Lysis of Human CD4 Cells Latently Infected With HIV-1. *Nat Commun* (2015) 6(1):8447. doi: 10.1038/ncomms9447
7. Banga R, Procopio FA, Perreau M. Current Approaches to Assess HIV-1 Persistence. *Curr Opin HIV AIDS* (2016) 11(4):424–31. doi: 10.1097/COH.0000000000000282
8. Yukl SA, Gianella S, Sinclair E, Epling L, Li Q, Duan L, et al. Differences in HIV Burden and Immune Activation Within the Gut of HIV-Positive Patients Receiving Suppressive Antiretroviral Therapy. *J Infect Dis* (2010) 202(10):1553–61. doi: 10.1086/656722
9. Chun T, Carruth L, Finzi D, Shen X, DiGiuseppe JA, Taylor H, et al. Quantification of Latent Tissue Reservoirs and Total Body Viral Load in HIV-1 Infection. *Nature* (1997) 387(6629):183–8. doi: 10.1038/387183a0
10. Finzi D, Blankson J, Siliciano JD, Margolick JB, Chadwick K, Pierson T, et al. Latent Infection of CD4+ T Cells Provides a Mechanism for Lifelong Persistence of HIV-1, Even in Patients on Effective Combination Therapy. *Nat Med* (1999) 5(5):512–7. doi: 10.1038/8394
11. Hermankova M, Siliciano JD, Zhou Y, Monie D, Chadwick K, Margolick JB, et al. Analysis of Human Immunodeficiency Virus Type 1 Gene Expression in Latently Infected Resting CD4+ T Lymphocytes In Vivo. *J Virol* (2003) 77 (13):7383–92. doi: 10.1128/JVI.77.13.7383-7392.2003
12. Siliciano JD, Kajdas J, Finzi D, Quinn TC, Chadwick K, Margolick JB, et al. Long-Term Follow-Up Studies Confirm the Stability of the Latent Reservoir for HIV-1 in Resting CD4+ T Cells. *Nat Med* (2003) 9(6):727–8. doi: 10.1038/nm880
13. Pau AK, George JM. Antiretroviral Therapy. *Infect Dis Clin North Am* (2014) 28(3):371–402. doi: 10.1016/j.idc.2014.06.001
14. De Jong MD, De Boer RJ, De Wolf F, Foudraine NA, Boucher CAB, Goudsmit J, et al. Overshoot of HIV-1 Viraemia After Early Discontinuation of Antiretroviral Treatment. *Aids* (1997) 11(11):79–84. doi: 10.1097/00002030-199711000-00002
15. Hamer DH, Bocklandt S, McHugh L, Chun T-W, Blumberg PM, Sigano DM, et al. Rational Design of Drugs That Induce Human Immunodeficiency Virus Replication. *J Virol* (2003) 77(19):10227–36. doi: 10.1128/JVI.77.19.10227-10236.2003
16. Abner E, Jordan A. HIV "Shock and Kill" Therapy: In Need of Revision. *Antiviral Res* (2019) 166(March):19–34. doi: 10.1016/j.antiviral.2019.03.008
17. Spivak AM, Planelles V. HIV-1 Eradication: Early Trials (and Tribulations). *Trends Mol Med* (2016) 22(1):10–27. doi: 10.1016/j.molmed.2015.11.004
18. Thorlund K, Horwitz MS, Fife BT, Lester R, Cameron DW. Landscape Review of Current HIV "Kick and Kill" Cure Research - Some Kicking, Not Enough Killing. *BMC Infect Dis* (2017) 17(1):1–12. doi: 10.1186/s12879-017-2683-3
19. Perreau M, Banga R, Pantaleo G. Targeted Immune Interventions for an HIV-1 Cure. *Trends Mol Med* (2017) 23(10):945–61. doi: 10.1016/j.molmed.2017.08.006
20. Desimio MG, Covino DA, Doria M. Potential of the NKG2D/NKG2DL Axis in NK Cell-Mediated Clearance of the HIV-1 Reservoir. *Int J Mol Sci* (2019) 20(18):4490. doi: 10.3390/ijms20184490
21. International AIDS Society Scientific Working Group on HIV Cure. Towards an HIV Cure: A Global Scientific Strategy. *Nat Rev Immunol* (2012) 12(8):607–14. doi: 10.1038/nri3262
22. Katlama C, Deeks SG, Autran B, Martinez-Picado J, Van Lunzen J, Rouzioux C, et al. Barriers to a Cure for HIV: New Ways to Target and Eradicate HIV-1 Reservoirs. *Lancet* (2013) 381(9883):2109–17. doi: 10.1016/S0140-6736(13)60104-X
23. Liu C, Ma X, Liu B, Chen C, Zhang H. HIV-1 Functional Cure: Will the Dream Come True? *BMC Med* (2015) 13(1):1–12. doi: 10.1186/s12916-015-0517-y
24. Vansant G, Bruggemans A, Janssens J, Debyser Z. Block-And-Lock Strategies to Cure HIV Infection. *Viruses* (2020) 12(1):1–17. doi: 10.3390/v12010084
25. Moranguinho I, Valente ST. Block-And-Lock: New Horizons for a Cure for HIV-1. *Viruses* (2020) 12(12):1443. doi: 10.3390/v12121443
26. Ahlenstiel CL, Symonds G, Kent SJ, Kelleher AD. Block and Lock HIV Cure Strategies to Control the Latent Reservoir. *Front Cell Infect Microbiol* (2020) 10(August):1–13. doi: 10.3389/fcimb.2020.00424
27. Moasser MM. The Oncogene HER2: Its Signaling and Transforming Functions and its Role in Human Cancer Pathogenesis. *Oncogene* (2007) 26(45):6469–87. doi: 10.1038/sj.onc.1210477
28. Rinnerthaler G, Gampenrieder SP, Greil R. HER2 Directed Antibody-Drug-Conjugates Beyond T-DM1 in Breast Cancer. *Int J Mol Sci* (2019) 20(5):1–17. doi: 10.3390/ijms20051115
29. Maennling AE, Tur MK, Niebert M, Klockenbring T, Zeppernick F, Gattenlöhner S, et al. Molecular Targeting Therapy Against Egfr Family in Breast Cancer: Progress and Future Potentials. *Cancers (Basel)* (2019) 11 (12):1826. doi: 10.3390/cancers11121826
30. Ward AB, Wilson IA. The HIV-1 Envelope Glycoprotein Structure: Nailing Down a Moving Target. *Immunol Rev* (2017) 275(1):21–32. doi: 10.1111/imr.12507
31. Burton DR, Mascola JR. Antibody Responses to Envelope Glycoproteins in HIV-1 Infection. *Nat Immunol* (2015) 16(6):571–6. doi: 10.1038/ni.3158
32. Sadraeian M, Bahou C, da Cruz EF, Janini LMR, Diaz RS, Boyle RW, et al. Photoimmunotherapy Using Cationic and Anionic Photosensitizer-Antibody Conjugates Against Hiv Env-Expressing Cells. *Int J Mol Sci* (2020) 21(23):1–16. doi: 10.3390/ijms21239151
33. Till MA, Ghetie V, Gregory T, Patzer EJ, Porter JP, Uhr JW, et al. HIV-Infected Cells are Killed by Rcd4-Ricin A Chain. *Sci (80-)* (1988) 242 (4882):1166–8. doi: 10.1126/science.2847316
34. Chaudhary VK, Mizukamit T, Fuerstt TR, Fitzgerald DJ, Mosst B, Pastan I, et al. Selective Killing of HIV -Infected Cells by Recombinant Human CD4-Pseudomonas Exotoxin Hybrid Protein. *Nature* (1988) 335((6188):369–72. doi: 10.1038/335369a0
35. Pincus SH, Wehrly K, Chesebro B. Treatment of HIV Tissue Culture Infection With Monoclonal Antibody-Ricin A Chain Conjugates. *J Immunol* (1989) 142(9):3070–5.

36. Matsushita S, Koito A, Maeda Y, Hattori T, Takatsuki K. Killing of HIV-Infected Cells by Anti-Gpl20 Immunotoxins. *AIDS Res Hum Retroviruses* (1990) 6(2):193–204. doi: 10.1089/aid.1990.6.193
37. Aullo P, Alcami J, Popoff MR, Klatzmann DR, Murphy JR, Boquet P. A Recombinant Diphtheria Toxin Related Human CD4 Fusion Protein Specifically Kills HIV Infected Cells Which Express Gp120 But Selects Fusion Toxin Resistant Cells Which Carry HIV. *EMBO J* (1992) 11 (2):575–83. doi: 10.1002/j.1460-2075.1992.tb05089.x
38. Bera TK, Kennedy PE, Berger EA, Barbas CF, Pastan I. Specific Killing of HIV-Infected Lymphocytes by a Recombinant Immunotoxin Directed Against the HIV-1 Envelope Glycoprotein. *Mol Med* (1998) 4(6):384–91. doi: 10.1007/BF03401745
39. Pincus SH, Fang H, Wilkinson RA, Marcotte TK, Robinson JE, Olson WC. *In Vivo* Efficacy of Anti-Glycoprotein 41, But Not Anti-Glycoprotein 120, Immunotoxins in a Mouse Model of HIV Infection. *J Immunol* (2003) 170 (4):2236–41. doi: 10.4049/jimmunol.170.4.2236
40. Sadraeian M, Guimarães FEG, Araújo APU, Worthylake DK, Lecour LJ, Pincus SH. Selective Cytotoxicity of a Novel Immunotoxin Based on Pulchellin A Chain for Cells Expressing HIV Envelope. *Sci Rep* (2017) 7 (1):1–12. doi: 10.1038/s41598-017-08037-3
41. Pincus SH, Wehrly K, Cole R, Fang H, Lewis GK, McClure J, et al. *In Vitro* Effects of Anti-HIV Immunotoxins Directed Against Multiple Epitopes on HIV Type 1 Envelope Glycoprotein 160. *AIDS Res Hum Retroviruses* (1996) 12(11):1041–51. doi: 10.1089/aid.1996.12.1041
42. Song E, Zhu P, Lee S-K, Chowdhury D, Kussman S, Dykxhoorn DM, et al. Antibody Mediated *In Vivo* Delivery of Small Interfering RNAs *via* Cell-Surface Receptors. *Nat Biotechnol* (2005) 23(6):709–17. doi: 10.1038/nbt1101
43. Kumar P, Ban H-S, Kim S-S, Wu H, Pearson T, Greiner DL, et al. T Cell-Specific siRNA Delivery Suppresses HIV-1 Infection in Humanized Mice. *Cell* (2008) 134(4):577–86. doi: 10.1016/j.cell.2008.06.034
44. Dadachova E, Patel MC, Toussi S, Apostolidis C, Morgenstern A, Brechbiel MW, et al. Targeted Killing of Virally Infected Cells by Radiolabeled Antibodies to Viral Proteins. *PloS Med* (2006) 3(11):2094–103. doi: 10.1371/journal.pmed.0030427
45. McFarren A, Lopez L, Williams DW, Veenstra M, Bryan RA, Goldsmith A, et al. A Fully Human Antibody to Gp41 Selectively Eliminates HIV-Infected Cells That Transmigrated Across a Model Human Blood Brain Barrier. *Aids* (2016) 30(4):563–71. doi: 10.1097/QAD.0000000000000968
46. Garg R, Mills K, Allen KJH, Causey P, Perron RW, Gendron D, et al. Comparison of Various Radioactive Payloads for a Human Monoclonal Antibody to Glycoprotein 41 for Elimination of HIV-Infected Cells. *Nucl Med Biol* (2020) 82–83:80–8. doi: 10.1016/j.nucmedbio.2020.02.009
47. Johansson S, Goldenberg DM, Griffiths GL, Wahren B, Hinkula J. Elimination of HIV-1 Infection by Treatment With a Doxorubicin-Conjugated Anti-Envelope Antibody. *AIDS* (2006) 20(15):1911–5. doi: 10.1097/01.aids.0000247111.58961.60
48. Fetzer I, Davis-Gardner ME, Gardner MR, Alfant B, Weber JA, Prasad NR, et al. A Coreceptor-Mimetic Peptide Enhances the Potency of V3-Glycan Antibodies. *J Virol* (2019) 93(5):1–16. doi: 10.1128/JVI.01653-18
49. Till M, Ghetie V, Gregory T, Patzer EJ, Porter JP, Uhr JW, et al. HIV-Infected Cells Are Killed by Rcd4-Ricin A Chain M. *Sci (80-)* (1989) 242 (4):2–5. doi: 10.1126/science.2847316
50. Paulik M, Grieco P, Kim C, Maxeiner HG, Grunert HP, Zeichhardt H, et al. Drug-Antibody Conjugates With Anti-HIV Activity. *Biochem Pharmacol* (1999) 58(11):1781–90. doi: 10.1016/S0006-2952(99)00272-5
51. Lacek K, Urbanowicz RA, Troise F, De Lorenzo C, Severino V, Di Maro A, et al. Dramatic Potentiation of the Antiviral Activity of HIV Antibodies by Cholesterol Conjugation. *J Biol Chem* (2014) 289(50):35015–28. doi: 10.1074/jbc.M114.591826
52. Gardner MR, Kattenhorn LM, Kondur HR, Von Schaewen M, Dorfman T, Chiang JJ, et al. AAV-Expressed Ecd4-Ig Provides Durable Protection From Multiple SHIV Challenges. *Nature* (2015) 519(7541):87–91. doi: 10.1038/nature14264
53. Modrow S, Hahn BH, Shaw GM, Gallo RC, Wong-Staal F, Wolf H. Computer-Assisted Analysis of Envelope Protein Sequences of Seven Human Immunodeficiency Virus Isolates: Prediction of Antigenic Epitopes in Conserved and Variable Regions. *J Virol* (1987) 61(2):570–8. doi: 10.1128/jvi.61.2.570-578.1987
54. Schneider J, Kaaden O, Copeland TD, Oroszlan S, Hunsmann G. Shedding and Interspecies Type Sero-Reactivity of the Envelope Glycopolypeptide Gp120 of the Human Immunodeficiency Virus. *J Gen Virol* (1986) 67 (11):2533–8. doi: 10.1099/0022-1317-67-11-2533
55. Chen B. Molecular Mechanism of HIV-1 Entry. *Trends Microbiol* (2019) 27 (10):878–91. doi: 10.1016/j.tim.2019.06.002
56. Neurath AR, Strick N, Taylor P, Rubinstein P, Stevens CE. Search for Epitope-Specific Antibody Responses to the Human Immunodeficiency Virus (HIV-1) Envelope Glycoproteins Signifying Resistance to Disease Development. *AIDS Res Hum Retroviruses* (1990) 6(10):1183–92. doi: 10.1089/aid.1990.6.1183
57. Xu JY, Gorny MK, Palker T, Karwowska S, Zolla-Pazner S. Epitope Mapping of Two Immunodominant Domains of Gp41, the Transmembrane Protein of Human Immunodeficiency Virus Type 1, Using Ten Human Monoclonal Antibodies. *J Virol* (1991) 65(9):4832–8. doi: 10.1128/JVI.65.9.4832-4838.1991
58. Till MA, Zolla-Pazner S, Gorny MK, Patton JS, Uhr JW, Vitetta ES. Human Immunodeficiency Virus-Infected T Cells and Monocytes are Killed by Monoclonal Human Anti-Gp41 Antibodies Coupled to Ricin A Chain. *Proc Natl Acad Sci U.S.A.* (1989) 86(6):1987–91. doi: 10.1073/pnas.86.6.1987
59. Pincus SH, Song K, Maresh GA, Frank A, Worthylake D, Chung H-K, et al. Identification of Human Anti-HIV Gp160 Monoclonal Antibodies That Make Effective Immunotoxins. *J Virol* (2017) 91(3):1–17. doi: 10.1128/JVI.01360-16
60. Tsukrov D, McFarren A, Morgenstern A, Bruchertseifer F, Dolce E, Gorny MK, et al. Combination of Antiretroviral Drugs and Radioimmunotherapy Specifically Kills Infected Cells From HIV-Infected Individuals. *Front Med* (2016) 3(SEP):1–12. doi: 10.3389/fmed.2016.00041
61. Cheng HD, Grimm SK, Gilman MS, Gwom LC, Sok D, Sundling C, et al. Fine Epitope Signature of Antibody Neutralization Breadth at the HIV-1 Envelope CD4-Binding Site. *JCI Insight* (2018) 3(5):1–14. doi: 10.1172/jci.insight.97018
62. Daar ES, Li XL, Moudgil T, Ho DD. High Concentrations of Recombinant Soluble CD4 are Required to Neutralize Primary Human Immunodeficiency Virus Type 1 Isolates. *Proc Natl Acad Sci U.S.A.* (1990) 87(17):6574–8. doi: 10.1073/pnas.87.17.6574
63. Berger EA, Pastan I. Immunotoxin Complementation of HAART to Deplete Persisting HIV-Infected Cell Reservoirs. *PloS Pathog* (2010) 6(6):1–6. doi: 10.1371/journal.ppat.1000803
64. Bell KD, Ramilo O, Vitetta ES. Combined Use of an Immunotoxin and Cyclosporine to Prevent Both Activated and Quiescent Peripheral Blood T Cells From Producing Type 1 Human Immunodeficiency Virus. *Proc Natl Acad Sci U.S.A.* (1993) 90(4):1411–5. doi: 10.1073/pnas.90.4.1411
65. Zarling JM, Moran PA, Haffar O, Sias J, Richman DD, Spina CA, et al. Inhibition of HIV Replication by Pokeweed Antiviral Protein Targeted to CD4+ Cells by Monoclonal Antibodies. *Nature* (1990) 347(6288):92–5. doi: 10.1038/347092a0
66. McCoig C, Van Dyke G, Chou CS, Picker LJ, Ramilo O, Vitetta ES. An Anti-CD45RO Immunotoxin Eliminates T Cells Latently Infected With HIV-1 *In Vitro*. *Proc Natl Acad Sci U.S.A.* (1999) 96(20):11482–5. doi: 10.1073/pnas.96.20.11482
67. Finberg RW, Wahl SM, Allen JB, Soman G, Strom TB, Murphy JR, et al. Selective Elimination of HIV-1-Infected Cells With an Interleukin-2 Receptor-Specific Cytotoxin. *Sci (80-)* (1991) 252(5013):1703–5. doi: 10.1126/science.1904628
68. Zhang L, Waters C, Nichols J, Crumpacker C. Inhibition of HIV-1 RNA Production by the Diphtheria Toxin-Related IL-2 Fusion Proteins DAB486IL-2 and DAB389IL-2. *J Acquir Immune Defic Syndr* (1992) 5 (12):1181–7. doi: 10.1097/00126334-199212000-00001
69. Peer D, Zhu P, Carman CV, Lieberman J, Shimaoka M. Selective Gene Silencing in Activated Leukocytes by Targeting siRNAs to the Integrin Lymphocyte Function-Associated Antigen-1. *Proc Natl Acad Sci U S A* (2007) 104(10):4095–100. doi: 10.1073/pnas.0608491104
70. Cunha-Santos C, Perdigao PRL, Martin F, Oliveira JG, Cardoso M, Manuel A, et al. Inhibition of HIV Replication Through siRNA Carried by CXCR4-

Targeted Chimeric Nanobody. *Cell Mol Life Sci* (2020) 77(14):2859–70. doi: 10.1007/s00018-019-03334-8
71. Kopetzki E, Jekle A, Ji C, Rao E, Zhang J, Fischer S, et al. Closing Two Doors of Viral Entry: Intramolecular Combination of a Coreceptor- and Fusion Inhibitor of HIV-1. *Virol J* (2008) 5:1–10. doi: 10.1186/1743-422X-5-56
72. Gavrilyuk J, Uehara H, Otsubo N, Hessell A, Burton DR, Barbas CF. Potent Inhibition of HIV-1 Entry With a Chemically Programmed Antibody Aided by an Efficient Organocatalytic Synthesis. *ChemBioChem* (2010) 11 (15):2113–8. doi: 10.1002/cbic.201000432
73. Chang CH, Hinkula J, Loo M, Falkeborn T, Li R, Cardillo TM, et al. A Novel Class of Anti-HIV Agents With Multiple Copies of Enfuvirtide Enhances Inhibition of Viral Replication and Cellular Transmission *In Vitro*. *PloS One* (2012) 7(7):1–8. doi: 10.1371/journal.pone.0041235
74. Sato S, Inokuma T, Otsubo N, Burton DR, Barbas CF. Chemically Programmed Antibodies as HIV-1 Attachment Inhibitors. *ACS Med Chem Lett* (2013) 4(5):460–5. doi: 10.1021/ml400097z
75. Asano S, Gavrilyuk J, Burton DR, Barbas CF. Preparation and Activities of Macromolecule Conjugates of the CCR5 Antagonist Maraviroc. *ACS Med Chem Lett* (2014) 5(2):133–7. doi: 10.1021/ml400370w
76. Cohn LB, Chomont N, Deeks SG. The Biology of the HIV-1 Latent Reservoir and Implications for Cure Strategies. *Cell Host Microbe* (2020) 27(4):519–30. doi: 10.1016/j.chom.2020.03.014
77. Sweet RW, Truneh A, Hendrickson WA. CD4: Its Structure, Role in Immune Function and AIDS Pathogenesis, and Potential as a Pharmacological Target. *Curr Opin Biotechnol* (1991) 2(4):622–33. doi: 10.1016/0958-1669(91)90089-N
78. Hermiston ML, Xu Z, Weiss A. CD45: A Critical Regulator of Signaling Thresholds in Immune Cells. *Annu Rev Immunol* (2003) 21:107–37. doi: 10.1146/annurev.immunol.21.120601.140946
79. Berger EA, Murphy PM, Farber JM. Chemokine Receptors as HIV-1 Coreceptors: Roles in Viral Entry, Tropism, and Disease. *Annu Rev Immunol* (1999) 17:657–700. doi: 10.1146/annurev.immunol.17.1.657
80. Amara A, Le Gall S, Schwartz O, Salamero J, Montes M, Loetscher P, et al. HIV Coreceptor Downregulation as Antiviral Principle: SDF-1α-Dependent Internalization of the Chemokine Receptor CXCR4 Contributes to Inhibition of HIV Replication. *J Exp Med* (1997) 186(1):139–46. doi: 10.1084/jem.186.1.139
81. Westby M, Lewis M, Whitcomb J, Youle M, Pozniak AL, James IT, et al. Emergence of CXCR4-Using Human Immunodeficiency Virus Type 1 (HIV-1) Variants in a Minority of HIV-1-Infected Patients Following Treatment With the CCR5 Antagonist Maraviroc Is From a Pretreatment CXCR4-Using Virus Reservoir. *J Virol* (2006) 80(10):4909–20. doi: 10.1128/JVI.80.10.4909-4920.2006
82. Mild M, Kvist A, Esbjörnsson J, Karlsson I, Fenyö EM, Medstrand Patrik P. Differences in Molecular Evolution Between Switch (R5 to R5X4/X4-Tropic) and non-Switch (R5-Tropic Only) HIV-1 Populations During Infection. *Infect Genet Evol* (2010) 10(3):356–64. doi: 10.1016/j.meegid.2009.05.003
83. Philpott S. HIV-1 Coreceptor Usage, Transmission, and Disease Progression. *Curr HIV Res* (2005) 1(2):217–27. doi: 10.2174/1570162033485357
84. Connor RI, Sheridan KE, Ceradini D, Choe S, Landau NR. Change in Coreceptor Use Correlates With Disease Progression in HIV-1–Infected Individuals. *J Exp Med* (1997) 185(4):621–8. doi: 10.1084/jem.185.4.621
85. Palani A, Shapiro S, Josien H, Bara T, Clader JW, Greenlee WJ, et al. Synthesis, SAR, and Biological Evaluation of Oximino-Piperidino-Piperidine Amides. 1. Orally Bioavailable CCR5 Receptor Antagonists With Potent Anti-HIV Activity. *J Med Chem* (2002) 45(14):3143–60. doi: 10.1021/jm0200815
86. Maeda K, Nakata H, Koh Y, Miyakawa T, Ogata H, Takaoka Y, et al. Spirodiketopiperazine-Based CCR5 Inhibitor Which Preserves CC-Chemokine/CCR5 Interactions and Exerts Potent Activity Against R5 Human Immunodeficiency Virus Type 1 *In Vitro*. *J Virol* (2004) 78 (16):8654–62. doi: 10.1128/JVI.78.16.8654-8662.2004
87. Watson C, Jenkinson S, Kazmierski W, Kenakin T. The CCR5 Receptor-Based Mechanism of Action of 873140, a Potent Allosteric Noncompetitive HIV Entry Inhibitor. *Mol Pharmacol* (2005) 67(4):1268–82. doi: 10.1124/mol.104.008565
88. Ji C, Zhang J, Dioszegi M, Chiu S, Rao E, DeRosier A, et al. CCR5 Small-Molecule Antagonists and Monoclonal Antibodies Exert Potent Synergistic Antiviral Effects by Cobinding to the Receptor. *Mol Pharmacol* (2007) 72 (1):18–28. doi: 10.1124/mol.107.035055
89. Gulick RM, Lalezari J, Goodrich J, Clumeck N, DeJesus E, Horban A, et al. Maraviroc for Previously Treated Patients With R5 HIV-1 Infection. *N Engl J Med* (2008) 359(14):1429–41. doi: 10.1056/NEJMoa0803152
90. Moore JP, Kuritzkes DR. A Pièce De Resistance: How HIV-1 Escapes Small Molecule CCR5 Inhibitors. *Curr Opin HIV AIDS* (2009) 4(2):118–24. doi: 10.1097/COH.0b013e3283223d46
91. Olson WC, Jacobson JM. CCR5 Monoclonal Antibodies for HIV-1 Therapy. *Curr Opin HIV AIDS* (2009) 4(2):104–11. doi: 10.1097/COH.0b013e3283224015
92. Springer TA. Traffic Signals on Endothelium for Lymphocyte Recirculation and Leukocyte Emigration. *Annu Rev Physiol* (1995) 57:827–72. doi: 10.1146/annurev.ph.57.030195.004143
93. Allen AD, Hart DN, Hechinger MK, Slattery MJ, Chesson CV, Vidikan P. Leukocyte Adhesion Molecules as a Cofactor in AIDS: Basic Science and Pilot Study. *Med Hypotheses* (1995) 45(2):164–8. doi: 10.1016/0306-9877(95)90065-9
94. Rychert J, Jones L, McGrath G, Bazner S, Rosenberg ES. A Monoclonal Antibody Against Lymphocyte Function-Associated Antigen-1 Decreases HIV-1 Replication by Inducing the Secretion of an Antiviral Soluble Factor. *Virol J* (2013) 10:1–10. doi: 10.1186/1743-422X-10-120
95. Bracq L, Xie M, Benichou S, Bouchet J. Mechanisms for Cell-to-Cell Transmission of HIV-1. *Front Immunol* (2018) 9(FEB):1–14. doi: 10.3389/fimmu.2018.00260
96. Zhong P, Agosto LM, Munro JB, Mothes W. Cell-To-Cell Transmission of Viruses. *Curr Opin Virol* (2013) 3(1):44–50. doi: 10.1016/j.coviro.2012.11.004
97. Sourisseau M, Sol-Foulon N, Porrot F, Blanchet F, Schwartz O. Inefficient Human Immunodeficiency Virus Replication in Mobile Lymphocytes. *J Virol* (2007) 81(2):1000–12. doi: 10.1128/JVI.01629-06
98. Hioe CE, Tuen M, Vasiliver-Shamis G, Alvarez Y, Prins KC, Banerjee S, et al. HIV Envelope Gp120 Activates LFA-1 on CD4 T-Lymphocytes and Increases Cell Susceptibility to LFA-1-Targeting Leukotoxin (LtxA). *PloS One* (2011) 6(8):1–11. doi: 10.1371/journal.pone.0023202
99. Darcis G, Berkhout B, Pasternak AO. The Quest for Cellular Markers of HIV Reservoirs: Any Color You Like. *Front Immunol* (2019) 10(September):1–9. doi: 10.3389/fimmu.2019.02251
100. Descours B, Petitjean G, López-Zaragoza JL, Bruel T, Raffel R, Psomas C, et al. CD32a is a Marker of a CD4 T-Cell HIV Reservoir Harbouring Replication-Competent Proviruses. *Nature* (2017) 543(7646):564–7. doi: 10.1038/nature21710
101. Pérez L, Anderson J, Chipman J, Thorkelson A, Chun TW, Moir S, et al. Conflicting Evidence for HIV Enrichment in CD32+ CD4 T Cells. *Nature* (2018) 561(7723):E9–16. doi: 10.1038/s41586-018-0493-4
102. Bruel T, Schwartz O. Markers of the HIV-1 Reservoir: Facts and Controversies. *Curr Opin HIV AIDS* (2018) 13(5):383–8. doi: 10.1097/COH.0000000000000482
103. Osuna CE, Lim SY, Kublin JL, Apps R, Chen E, Mota TM, et al. Evidence That CD32a Does Not Mark the HIV-1 Latent Reservoir. *Nature* (2018) 561 (7723):E20–8. doi: 10.1038/s41586-018-0495-2
104. Fujimori K, Covell DG, Weinstein JN, Fletcher JE. Modeling Analysis of the Global and Microscopic Distribution of Immunoglobulin G, F(ab′)2, and Fab in Tumors. *Cancer Res* (1989) 49(20):5656–63.
105. Antignani A, FitzGerald D. Immunotoxins: The Role of the Toxin. *Toxins (Basel)* (2013) 5(8):1486–502. doi: 10.3390/toxins5081486
106. Martín-Serrano J, Folgueira L, Laín De Lera T, Pedraza MA, Lemichez E, Sánchez-Palomino S, et al. *In Vitro* Selective Elimination of HIV-Infected Cells From Peripheral Blood in AIDS Patients by the Immunotoxin DAB389CD4. *Aids* (1998) 12(8):859–63. doi: 10.1097/00002030-199808000-00007
107. Ashorn P, Moss B, Berger EA. Therapeutic Strategies Employing CD4, the HIV Receptor. *Adv Exp Med Biol* (1992) 312:71–81. doi: 10.1007/978-1-4615-3462-4_6
108. Kennedy PE, Moss B, Berger EA. Primary HIV-1 Isolates Refractory to Neutralization by Soluble CD4 are Potently Inhibited by CD4-Pseudomonas Exotoxin. *Virology* (1993) 192(1):375–9. doi: 10.1006/viro.1993.1047

109. Ashorn P, Moss B, Weinstein JN, Chaudhary VK, FitzGerald DJ, Pastan I, et al. Elimination of Infectious Human Immunodeficiency Virus From Human T-Cell Cultures by Synergistic Action of CD4-Pseudomonas Exotoxin and Reverse Transcriptase Inhibitors. *Proc Natl Acad Sci U S A* (1990) 87(22):8889–93. doi: 10.1073/pnas.87.22.8889
110. Davey RT, Boenning CM, Herpin BR, Batts DH, Metcalf JA, Wathen L, et al. Use of Recombinant Soluble CD4 Pseudomonas Exotoxin, a Novel Immunotoxin, for Treatment of Persons Infected With Human Immunodeficiency Virus. *J Infect Dis* (1994) 170(5):1180–8. doi: 10.1093/infdis/170.5.1180
111. Ramachandran RV, Katzenstein DA, Wood R, Batts DH, Merigan TC. Failure of Short-Term CD4-PE40 Infusions to Reduce Virus Load in Human Immunodeficiency Virus-Infected Persons. *J Infect Dis* (1994) 170 (4):1009–13. doi: 10.1093/infdis/170.4.1009
112. Kirsh R, Ellens H, Miller J, Hart TK, Bugelski PJ, Petteway SA, et al. Morphometric Analysis of Recombinant Soluble CD4-Mediated Release of the Envelope Glycoprotein Gp120 From HIV-1. *AIDS Res Hum Retroviruses* (1990) 6(10):1209–12. doi: 10.1089/aid.1990.6.1209
113. Pincus SH, McClure J. Soluble CD4 Enhances the Efficacy of Immunotoxins Directed Against Gp41 of the Human Immunodeficiency Virus. *Proc Natl Acad Sci U.S.A.* (1993) 90(1):332–6. doi: 10.1073/pnas.90.1.332
114. Erice A, Balfour HH, Myers DE, Leske VL, Sannerud KJ, Kuebelbeck V, et al. Anti-Human Immunodeficiency Virus Type 1 Activity of an Anti-CD4 Immunoconjugate Containing Pokeweed Antiviral Protein. *Antimicrob Agents Chemother* (1993) 37(4):835–8. doi: 10.1128/AAC.37.4.835
115. Saavedra-Lozano J, McCoig C, Xu J, Cao Y, Keiser P, Ghetie V, et al. An Anti-CD45RO Immunotoxin Kills Latently Infected Human Immunodeficiency Virus (HIV) CD4 T Cells in the Blood of HIV-Positive Persons. *J Infect Dis* (2002) 185(3):306–14. doi: 10.1086/338565
116. Goldstein H, Pettoello-Mantovani M, Bera TK, Pastan IH, Berger EA. Chimeric Toxins Targeted to the Human Immunodeficiency Virus Type 1 Envelope Glycoprotein Augment the *In Vivo* Activity of Combination Antiretroviral Therapy in Thy/Liv-SCID-Hu Mice. *J Infect Dis* (2000) 181 (3):921–6. doi: 10.1086/315351
117. McHugh L, Hu S, Lee BK, Santora K, Kennedy PE, Berger EA, et al. Increased Affinity and Stability of an Anti-HIV-1 Envelope Immunotoxin by Structure-Based Mutagenesis. *J Biol Chem* (2002) 277(37):34383–90. doi: 10.1074/jbc.M205456200
118. Kennedy PE, Bera TK, Wang Q-C, Gallo M, Wagner W, Lewis MG, et al. Anti-HIV-1 Immunotoxin 3B3(Fv)-PE38: Enhanced Potency Against Clinical Isolates in Human PBMCs and Macrophages, and Negligible Hepatotoxicity in Macaques. *J Leukoc Biol* (2006) 80(5):1175–82. doi: 10.1189/jlb.0306139
119. Denton PW, Long JM, Wietgrefe SW, Sykes C, Spagnuolo RA, Snyder OD, et al. Targeted Cytotoxic Therapy Kills Persisting HIV Infected Cells During ART. *PloS Pathog* (2014) 10(1):e1003872. doi: 10.1371/journal.ppat.1003872
120. Wagner J, Lerner RA, Barbas CF. Efficient Aldolase Catalytic Antibodies That Use the Enamine Mechanism of Natural Enzymes. *Sci (80-)* (1995) 270 (5243):1797. doi: 10.1126/science.270.5243.1797
121. Fetzer I, Gardner MR, Davis-Gardner ME, Prasad NR, Alfant B, Weber JA, et al. Ecd4-Ig Variants That More Potently Neutralize HIV-1. *J Virol* (2018) 92(12):1–13. doi: 10.1128/JVI.02011-17
122. Gardner MR, Fellinger CH, Kattenhorn LM, Davis-Gardner ME, Weber JA, Alfant B, et al. AAV-Delivered Ecd4-Ig Protects Rhesus Macaques From High-Dose SIVmac239 Challenges. *Sci Transl Med* (2019) 11(502):1–13. doi: 10.1126/scitranslmed.aau5409
123. Debnath AK, Zhang H. Antibody Drug Conjugates for Reducing the Latent HIV Reservoir. *WO 2016/133927 Al* (2016).
124. Dovgan I, Koniev O, Kolodych S, Wagner A. Antibody-Oligonucleotide Conjugates as Therapeutic, Imaging, and Detection Agents. *Bioconjug Chem* (2019) 30(10):2483–501. doi: 10.1021/acs.bioconjchem.9b00306
125. Elbashir SM, Martinez J, Patkaniowska A, Lendeckel W, Tuschl T. Functional Anatomy of siRNAs for Mediating Efficient RNAi in Drosophila Melanogaster Embryo Lysate. *EMBO J* (2001) 20(23):6877–88. doi: 10.1093/emboj/20.23.6877
126. Hoy SM. Patisiran: First Global Approval. *Drugs* (2018) 78(15):1625–31. doi: 10.1007/s40265-018-0983-6
127. Hu B, Zhong L, Weng Y, Peng L, Huang Y, Zhao Y, et al. Therapeutic siRNA: State of the Art. *Signal Transduct Target Ther* (2020) 5(1):101. doi: 10.1038/s41392-020-0207-x
128. Coburn GA, Cullen BR. Potent and Specific Inhibition of Human Immunodeficiency Virus Type 1 Replication by RNA Interference. *J Virol* (2002) 76(18):9225–31. doi: 10.1128/JVI.76.18.9225-9231.2002
129. Martínez MA, Clotet B, Esté JA. RNA Interference of HIV Replication. *Trends Immunol* (2002) 23(12):559–61. doi: 10.1016/S1471-4906(02)02328-1
130. Novina CD, Murray MF, Dykxhoorn DM, Beresford PJ, Riess J, Lee S-K, et al. siRNA-Directed Inhibition of HIV-1 Infection. *Nat Med* (2002) 8 (7):681–6. doi: 10.1038/nm725
131. Dugal-Tessier J, Thirumalairajan S, Jain N. Antibody-Oligonucleotide Conjugates: A Twist to Antibody-Drug Conjugates. *J Clin Med* (2021) 10 (4):838. doi: 10.3390/jcm10040838
132. Martinsen JT, Gunst JD, Højen JF, Tolstrup M, Søgaard OS. The Use of Toll-Like Receptor Agonists in HIV-1 Cure Strategies. *Front Immunol* (2020) 11 (June):1–13. doi: 10.3389/fimmu.2020.01112
133. Borducchi EN, Liu J, Nkolola JP, Cadena AM, Yu WH, Fischinger S, et al. Antibody and TLR7 Agonist Delay Viral Rebound in SHIV-Infected Monkeys. *Nature* (2018) 563(7731):360–4. doi: 10.1038/s41586-018-0600-6
134. Gadd AJR, Greco F, Cobb AJA, Edwards AD. Targeted Activation of Toll-Like Receptors: Conjugation of a Toll-Like Receptor 7 Agonist to a Monoclonal Antibody Maintains Antigen Binding and Specificity. *Bioconjug Chem* (2015) 26 (8):1743–52. doi: 10.1021/acs.bioconjchem.5b00302
135. Polson AG, Ho WY, Ramakrishnan V. Investigational Antibody-Drug Conjugates for Hematological Malignancies. *Expert Opin Investig Drugs* (2011) 20(1):75–85. doi: 10.1517/13543784.2011.539557
136. May RD, Finkelman FD, Wheeler HT, Uhr JW, Vitetta ES. Evaluation of Ricin A Chain-Containing Immunotoxins Directed Against Different Epitopes on the δ-Chain of Cell Surface-Associated IgD on Murine B Cells. *J Immunol* (1990) 144(9):3637–42.
137. Onda M, Nagata S, Tsutsumi Y, Vincent JJ, Wang Qc, Kreitman RJ, et al. Lowering the Isoelectric Point of the Fv Portion of Recombinant Immunotoxins Leads to Decreased Nonspecific Animal Toxicity Without Affecting Antitumor Activity. *Cancer Res* (2001) 61(13):5070–7.
138. Mazor R, Pastan I. Immunogenicity of Immunotoxins Containing Pseudomonas Exotoxin A: Causes, Consequences, and Mitigation. *Front Immunol* (2020) 11:1261. doi: 10.3389/fimmu.2020.01261
139. Schmohl JU, Todhunter D, Oh S, Vallera DA. Mutagenic Deimmunization of Diphtheria Toxin for Use in Biologic Drug Development. *Toxins (Basel)* (2015) 7(10):4067–82. doi: 10.3390/toxins7104067
140. Booth BJ, Ramakrishnan B, Narayan K, Wollacott AM, Babcock GJ, Shriver Z, et al. Extending Human IgG Half-Life Using Structure-Guided Design. *MAbs* (2018) 10(7):1098–110. doi: 10.1080/19420862.2018.1490119
141. Jurcic JG, Wong JYC, Knox SJ, Wahl DR, Rosenblat TL, Meredith RF. Targeted Radionuclide Therapy. In: *Clinical Radiation Oncology, 4th ed.* Elsevier Inc (2015). p. 399–418.e14. doi: 10.1016/B978-0-323-24098-7.00022-8
142. Roberts TC, Langer R, Wood MJA. Advances in Oligonucleotide Drug Delivery. *Nat Rev Drug Discov* (2020) 19(10):673–94. doi: 10.1038/s41573-020-0075-7
143. Bäumer S, Bäumer N, Appel N, Terheyden L, Fremerey J, Schelhaas S, et al. Antibody-Mediated Delivery of Anti-KRAS-siRNA *In Vivo* Overcomes Therapy Resistance in Colon Cancer. *Clin Cancer Res* (2015) 21(6):1383–94. doi: 10.1158/1078-0432.CCR-13-2017
144. Promsote W, DeMouth ME, Almasri CG, Pegu A. Anti-HIV-1 Antibodies: An Update. *BioDrugs* (2020) 34(2):121–32. doi: 10.1007/s40259-020-00413-2
145. Hua CK, Ackerman ME. Engineering Broadly Neutralizing Antibodies for HIV Prevention and Therapy. *Adv Drug Delivery Rev* (2016) 103:157–73. doi: 10.1016/j.addr.2016.01.013
146. Anand SP, Grover JR, Tolbert WD, Prévost J, Richard J, Ding S, et al. Antibody-Induced Internalization of HIV-1 Env Proteins Limits Surface Expression of the Closed Conformation of Env. *J Virol* (2019) 93(11):1–14. doi: 10.1128/JVI.00293-19
147. Dewerchin HL, Cornelissen E, Nauwynck HJ. Feline Infectious Peritonitis Virus-Infected Monocytes Internalize Viral Membrane-Bound Proteins Upon Antibody Addition. *J Gen Virol* (2006) 87(6):1685–90. doi: 10.1099/vir.0.81692-0

148. Leemans A, De Schryver M, van der Gucht W, Heykers A, Pintelon I, Hotard AL, et al. Antibody-Induced Internalization of the Human Respiratory Syncytial Virus Fusion Protein. *J Virol* (2017) 91(14):1–15. doi: 10.1128/JVI.00184-17
149. Ledgerwood JE, Coates EE, Yamshchikov G, Saunders JG, Holman L, Enama ME, et al. Safety, Pharmacokinetics and Neutralization of the Broadly Neutralizing HIV-1 Human Monoclonal Antibody VRC01 in Healthy Adults. *Clin Exp Immunol* (2015) 182(3):289–301. doi: 10.1111/cei.12692
150. Lynch RM, Boritz E, Coates EE, DeZure A, Madden P, Costner P, et al. Virologic Effects of Broadly Neutralizing Antibody VRC01 Administration During Chronic HIV-1 Infection. *Sci Transl Med* (2015) 7(319):319. doi: 10.1126/scitranslmed.aad5752
151. Crowell TA, Colby DJ, Pinyakorn S, Sacdalan C, Pagliuzza A, Intasan J. VRC01 in Acutely Treated HIV-Infected Adults: A Randomised, Double-Blind, Placebo-Controlled Trial. *Lancet HIV* (2019) 6(5):139–48. doi: 10.1016/S2352-3018(19)30053-0.VRC01
152. Caskey M, Klein F, Lorenzi JCC, Seaman MS, West AP, Buckley N, et al. Viraemia Suppressed in HIV-1-Infected Humans by Broadly Neutralizing Antibody 3BNC117. *Nature* (2015) 522(7557):487–91. doi: 10.1038/nature14411
153. Zalevsky J, Chamberlain AK, Horton HM, Karki S, Leung IWL, Sproule TJ, et al. Enhanced Antibody Half-Life Improves *In Vivo* Activity. *Nat Biotechnol* (2010) 28(2):157–9. doi: 10.1038/nbt.1601
154. Halper-Stromberg A, Lu CL, Klein F, Horwitz JA, Bournazos S, Nogueira L, et al. Broadly Neutralizing Antibodies and Viral Inducers Decrease Rebound From HIV-1 Latent Reservoirs in Humanized Mice. *Cell* (2014) 158(5):989–99. doi: 10.1016/j.cell.2014.07.043
155. Gunst JD, Højen JF, Søgaard OS. Broadly Neutralizing Antibodies Combined With Latency-Reversing Agents or Immune Modulators as Strategy for HIV-1 Remission. *Curr Opin HIV AIDS* (2020) 15(5):309–15. doi: 10.1097/COH.0000000000000641
156. Deal CE, Balazs AB. Vectored Antibody Gene Delivery for the Prevention or Treatment of HIV Infection. *Curr Opin HIV AIDS* (2015) 10(3):190–7. doi: 10.1097/COH.0000000000000145
157. Mazor R, Onda M, Pastan I. Immunogenicity of Therapeutic Recombinant Immunotoxins. *Immunol Rev* (2016) 270(1):152–64. doi: 10.1111/imr.12390
158. Suzuki K, Shijuuku T, Fukamachi T, Zaunders J, Guillemin G, Cooper D, et al. Prolonged Transcriptional Silencing and CpG Methylation Induced by siRNAs Targeted to the HIV-1 Promoter Region. *J RNAi Gene Silencing* (2005) 1(2):66–78.
159. Ananworanich J, Dubé K, Chomont N. How Does the Timing of Antiretroviral Therapy Initiation in Acute Infection Affect HIV Reservoirs? *Curr Opin HIV AIDS* (2015) 10(1):18–28. doi: 10.1097/COH.0000000000000122
160. Fujinaga K, Cary DC. Experimental Systems for Measuring HIV Latency and Reactivation. *Viruses* (2020) 12(11):1–21. doi: 10.3390/v12111279
161. Kumar N, Chahroudi A, Silvestri G. Animal Models to Achieve an HIV Cure. *Curr Opin HIV AIDS* (2016) 11(4):432–41. doi: 10.1097/COH.0000000000000290

**Conflict of Interest:** The authors declare that the research was conducted in the absence of any commercial or financial relationships that could be construed as a potential conflict of interest.

frontiers in Immunology

REVIEW
published: 12 July 2021
doi: 10.3389/fimmu.2021.710044

# Can Broadly Neutralizing HIV-1 Antibodies Help Achieve an ART-Free Remission?

*Denise C. Hsu*[1,2], *John W. Mellors*[3] *and Sandhya Vasan*[1,2*]

[1] U.S. Military HIV Research Program, Walter Reed Army Institute of Research, Silver Spring, MD, United States, [2] Henry M. Jackson Foundation for the Advancement of Military Medicine, Bethesda, MD, United States, [3] Division of Infectious Diseases, Department of Medicine, University of Pittsburgh, Pittsburgh, PA, United States

OPEN ACCESS

**Edited by:**
Philipp Schommers,
University of Cologne, Germany

**Reviewed by:**
Anthony DeVico,
University of Maryland, United States
Marina Caskey,
The Rockefeller University, United States
Susan Zolla-Pazner,
Icahn School of Medicine at Mount Sinai, United States

***Correspondence:**
Sandhya Vasan
SVasan@hivresearch.org

**Specialty section:**
This article was submitted to Vaccines and Molecular Therapeutics, a section of the journal Frontiers in Immunology

**Received:** 15 May 2021
**Accepted:** 25 June 2021
**Published:** 12 July 2021

**Citation:**
Hsu DC, Mellors JW and Vasan S (2021) Can Broadly Neutralizing HIV-1 Antibodies Help Achieve an ART-Free Remission? Front. Immunol. 12:710044. doi: 10.3389/fimmu.2021.710044

Many broadly neutralizing antibodies (bnAbs) targeting the HIV-1 envelope glycoprotein are being assessed in clinical trials as strategies for HIV-1 prevention, treatment, and antiretroviral-free remission. BnAbs can neutralize HIV-1 and target infected cells for elimination. Concerns about HIV-1 resistance to single bnAbs have led to studies of bnAb combinations with non-overlapping resistance profiles. This review focuses on the potential for bnAbs to induce HIV-1 remission, either alone or in combination with latency reversing agents, therapeutic vaccines or other novel therapeutics. Key topics include preliminary activity of bnAbs in preclinical models and in human studies of HIV-1 remission, clinical trial designs, and antibody design strategies to optimize pharmacokinetics, coverage of rebound-competent virus, and enhancement of cellular immune functions.

**Keywords: broadly neutralizing HIV-1 antibody, HIV remission, HIV cure, HIV immunotherapy, HIV therapeutics**

## INTRODUCTION

Antiretroviral therapy (ART) has dramatically reduced the morbidity and mortality associated with human immunodeficiency virus type-1 (HIV-1) infection by suppressing viral replication (1, 2) but ART does not cure HIV-1 because of long-lived cells carrying replication-competent (intact) proviruses (3–5). Viral rebound occurs within weeks in most people with HIV-1 (PWH) who discontinue ART, including those who initiate ART early during acute infection with long-term successful suppression of plasma viremia measured as HIV-1 RNA (6, 7). Additionally, there are barriers to universal ART uptake that include toxicities, stigma, and the need for lifelong adherence (8–10). Therefore, alternative ART-free strategies that confer durable viral suppression, prevent disease progression, and avoid drug resistance are highly desirable (11, 12). Proposed minimal target profiles for these strategies include the ability to maintain plasma HIV-1 RNA below the level at which transmission occurs, for at least 2 years, and be generally safe and tolerated (13).

Broadly neutralizing antibodies target specific vulnerable sites on the HIV-1 envelope, mediate neutralization and target infected cells for elimination. In this review, we will focus on the potential for bnAbs to induce antiretroviral-free HIV-1 control, either alone or in combination with latency reversing agents, immune activating agents, therapeutic vaccines or other novel therapeutics.

## BROADLY NEUTRALIZING ANTIBODIES IN CLINICAL DEVELOPMENT

Multiple bnAbs that exhibit breath and potency against epitopes on the HIV-1 envelope trimer are currently being assessed in clinical trials for HIV-1 prevention, treatment as well as remission induction. The targeted areas on HIV-1 envelope (see **Figure 1**) include the CD4-binding site (CD4bs) on gp120 [VRC01 (14); VRC01-LS (15), 3BNC117 (16), 3BNC117-LS (17), VRC07-523LS (18) and N6LS (19)]; the glycan-dependent epitopes on V1/V2 (PGDM1400 (20) and CAP256V2LS (21) as well as V3 loops (10-1074 (22), 10-1074-LS (17), PGT121 (23) and PGT121.414.LS); the linear epitopes in the membrane-proximal external region (MPER) on gp41 [10E8VLS (24, 25)]. Other bnAbs with high potency and breadth that have not yet entered clinical trials include antibodies targeting the gp120-gp41 interface (26) and the N49 lineage of CD4bs bnAbs (27, 28).

A number of clinical trials have shown that bnAbs (including VRC01, 3BNC117, 10-1074, VRC01-LS, VRC07-523LS, PGT121 and N6LS) are safe and well tolerated (29–38). Serious adverse events are rare but have been reported. A phase 1 study evaluating the subcutaneous administration of 10E8VLS alone or concurrently with VRC07-523LS in healthy adults was paused and the administration of 10E8VLS terminated due to local reactogenicity. Seven of 8 recipients of 10E8VLS experienced erythema and induration within 24 hours and a biopsy from 1 participant with induration demonstrated panniculitis (39).

The utility of bnAbs for HIV prevention have been reviewed extensively (40–42) and thus will not be a focus of this article. The recently completed Antibody Mediated Protection (AMP) trials, 2 parallel phase 2b multicenter, randomized, double-blind, placebo-controlled trials involving over 4600 participants and over 3000 recipients of VRC01, every 8 weeks for 20 months have further demonstrated the safety, feasibility and scalability of intravenous bnAb infusion (43). Though VRC01 did not prevent overall HIV-1 acquisition, it did reduce the acquisition of viruses highly sensitive (an 80% inhibitory concentration, IC80 of <1 μg/mL) to VRC01, emphasizing the importance of breath and potency for bnAb efficacy.

In PWH and plasma viremia, bnAb monotherapy leads to transient reductions in HIV-1 RNA of ~1.5 $\log_{10}$ copies/mL (in the absence of pre-existing resistance), with mean HIV-1 RNA reductions of 1.48, 1.14, 1.52 and 1.7 $\log_{10}$ copies/mL for 3BNC117, VRC-01, 10-1074 and PGT121, respectively (30–32, 36). These safety and antiviral activity data supported the investigation of bnAbs as potential therapeutics for HIV-1. The two main therapeutic applications that are in clinical evaluations are the use of bnAbs in place of current antiretroviral regimens to maintain viral suppression and the use of bnAb as part of a therapeutic combination to target and eliminate the HIV-1 reservoir.

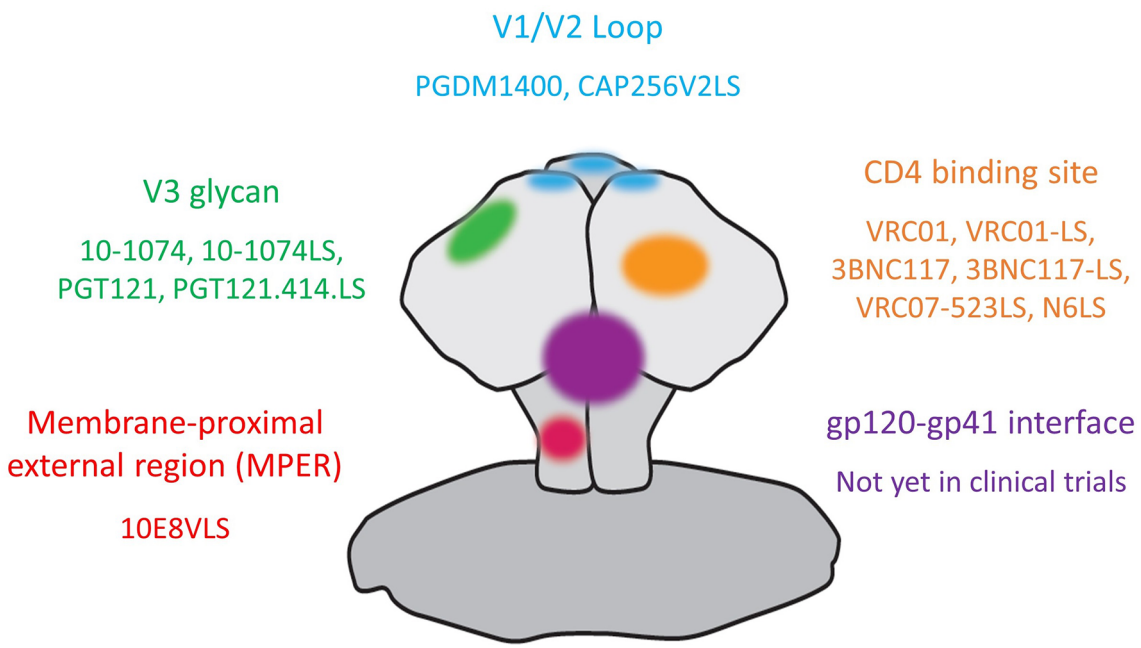


**FIGURE 1** | Anti-HIV-1 broadly neutralizing antibodies in clinical trials and their targets on the HIV-1 envelope.

## THE USE OF BNAB IN PLACE OF ART TO MAINTAIN VIRAL SUPPRESSION

The potential of bnAbs in maintaining viral suppression during analytical treatment interruption (ATI) has been assessed in a number of clinical trials. When 3BNC117 was administered during ATI to PWH with undetectable plasma HIV-1 RNA while on ART and with 3BNC117-sensitive outgrowth viruses, viral rebound was delayed to 8.4 weeks when compared to 2.6 weeks in matched historical controls. In the majority of participants, emerging viruses showed 3BNC117 resistance, indicating bnAb selection of escape variants. However, 30% of participants remained suppressed until 3BNC117 levels waned below 20 μg/mL, and the viruses emerging in all but one of these participants showed no apparent resistance to 3BCN117, suggesting failure of bnAb escape over a period of 9-19 weeks (44). In contrast, when 3BNC117 was administered to PWH at 24 weeks, 12 weeks and 2 days before ATI and 3 weeks after ATI, without pre-selection for 3NBC117 sensitivity, the time to rebound was strongly influenced by the neutralization sensitivity of the pre-treatment viruses, 3.6 vs 9.2 weeks in those with resistant vs sensitive viruses, respectively (45).

In 2 single arm clinical trials, AIDS Clinical Trials Group (ACTG) A5340, and National Institutes of Health (NIH) 15-I-0140, VRC01 during ATI was associated with a higher proportion of participants with undetectable HIV-1 RNA at 4 weeks post ATI when compared with historical controls. However, the difference was no longer significant at 8 weeks. VRC01 exerted pressure on the rebounding viruses, resulting in selection for preexisting and emerging bnAb-resistant viruses (46).

The aforementioned studies involved participants with treated chronic HIV-1 infection. PWH who initiated ART during acute HIV-1 infection (AHI) have smaller (47–49) and less diverse viral reservoirs (50, 51) as well as more preserved immune responses and thus may potentially display more favorable responses to bnAbs. VRC01 infusions during ATI in PWH who initiated ART during AHI did not significantly delay time to viral rebound of >20 copies/mL but did delay time to viral rebound of >1000 copies/mL, at a median of 33 days in VRC01 recipients when compared to 14 days in placebo recipients (52). Importantly, neutralization sensitivity was similar after viral rebound when compared to at the time of AHI diagnosis, indicating the lack of selection for VRC01 resistance during ATI. This was most likely secondary to the near-absence of diversity among these participants' sequences and short duration of viral replication due to prompt ART initiation. Consistent with studies in chronic HIV-1 infection, participants with strains most sensitive to VRC01 rebounded later. Interestingly, viral rebound occurred while the average serum VRC01 level was 50 times higher than *in vitro* IC80 values, suggesting that the VRC01 concentrations achieved were therapeutically insufficient. This may be a result of inadequate levels or speed of VRC01 penetration into tissue reservoirs, off target protein binding, or other factors, emphasizing that *in vitro* IC50 orIC80 values do not necessarily translate to therapeutic concentrations in humans (53).

Collectively, these clinical trials indicate that bnAb monotherapy does not have sufficient breadth to prevent rebound in most individuals. However, in the setting of adequate neutralization breadth to cover rebound competent viruses, bnAbs have the potential to maintain viral suppression during ATI as long as therapeutic levels are maintained in plasma and tissues, although further studies are needed to define adequate therapeutic levels.

## MECHANISMS TO IMPROVE POTENTIAL FOR BNABS TO SUPPRESS VIRAL REPLICATION

### Increasing Half-Life and Potency

The current requirement for frequent dosing (monthly) reduces the appeal of bnAbs to maintain ART-free viral suppression. Thus, two amino acid mutations (methionine-to-leucine substitution and an asparagine-to-serine substitution at amino acid positions 428 and 434, respectively, collectively referred to as "LS") have been introduced into the fragment crystallizable (Fc)-region of a number of bnAbs to improve affinity to the neonatal Fc-receptor (FcRn), leading to recirculation following cellular endocytosis and thereby extending the *in vivo* half-life (15, 17, 54).

In non-human primates (NHP), the LS substitution extended serum half-life by 2-3 fold (17) and also resulted in longer periods of protection against repeated mucosal challenges with Simian/Human Immunodeficiency Virus (SHIV), expressing HIV-1 envelope on a SIV backbone, with medians of 14.5 vs 8, 27 vs 12.5 and 17 vs 13 weeks for VRC01-LS, 10-1074-LS and 3BC117-LS, respectively when compared to the unmodified parental bnAb (17, 55). In people without HIV, the LS substitution extended serum half-life of VRC01 from 15 to 71 days (34). Serum half-life after intravenous infusion was 38 days for VRC07-523LS (35) and 44 days for N6LS (38). Pharmacokinetics data for 3BNC117-LS (NCT03254277), 10-1074LS (NCT03554408), PGT121.414.LS (NCT04212091) and CAP256V2LS (NCT04408963) are forthcoming, and the impact of LS mutations on bnAb half-life in tissues is yet to be quantified.

Other mutations to extend half-life have also been reported, including the Met252Tyr, Ser254Thr, and Thr256Glu (YTE) substitution that is associated with a 4-fold increase in serum half-life (56, 57). However, YTE substitution also reduces ADCC activity of the antibody (56), which potentially reduces its utility in HIV remission induction strategies that will likely require ADCC.

Subcutaneous administration of bnAb by direct needle and syringe injection obviates the need for venous access and volumetric pump infusion and is thus more scalable for widespread use. However, when compared with intravenous infusion, subcutaneous injections of VRC01, VRC01-LS, VRC07-523LS and N6LS showed markedly reduced maximal serum concentration ($C_{max}$) and delayed time to maximal concentration $T_{MAX}$ (29, 34, 35, 38).

Next-generation sequencing, computational bioinformatics, and structure-guided design can be employed to modify bnAbs to enhance neutralization potency and breadth. This approach was applied to VRC01 and resulted in the development of VRC07-523-LS, that is over 5-fold more potent than VRC01 and neutralized 96% of a panel of 171 HIV-1 pseudotyped viruses *in vitro* (18).

## Addressing the Issue of bnAb Activity, Breadth and Resistance

Certain HIV-1 strains are intrinsically resistant to bnAbs targeting specific epitopes. BnAbs targeting V3 glycans, including 10-1074 and PGT121, have little to no neutralizing activity against CRF01_AE and can only neutralize a minority of Clade D strains (22). In contrast, bnAbs targeting the V1/V2 loop have suboptimal activity against Clade B strains, with PGDM1400 neutralizing 70% (20) and CAP256-VRC26.25 neutralizing only 15% (58). Thus, data regarding the major prevalent subtypes for a particular geographic location must be considered in the selection of bnAbs.

In PWH with plasma viremia, bnAb mediated HIV-1 RNA reductions were mostly observed in those with sensitive HIV-1 strains. Furthermore, reduction in sensitivity developed within weeks of monotherapy, due to expansion of pre-existing resistant viruses or selection of new resistant variants (30–32, 36). Screening for pre-existing resistant variants is especially relevant for clinical trials assessing the utility of bnAbs during ATI. BnAb sensitivity of virus in plasma can be readily determined in participants with viremia; whereas in participants on suppressive ART, bnAb sensitivity can be determined using HIV-1 enveloped pseudovirus derived from proviral DNA in PBMC or directly using viruses from outgrowth cultures (31, 44, 59). However, these assays are labor intensive, impractical for widespread implementation, and may not capture the spectrum of minor viral variants that could emerge (60, 61).

An approach to expand neutralization coverage is to use bnAbs targeting different HIV-1 envelope epitopes in combination. Combinations of three and four bnAbs can neutralize 98-100% of viruses from a diverse panel of 125 Env-pseudotyped viruses *in vitro* (62, 63). In clinical trials, the combination of 3BNC117 and 10–1074 was safe and generally well tolerated and pharmacokinetics were similar to when these bnAbs were administered as monotherapy (61, 64).

Co-administration of 3BNC117 and 10–1074 to PWH and plasma viremia resulted in an average 1.65 $\log_{10}$copies/mL reduction in HIV-1 RNA. The four participants with dual antibody-sensitive viruses had greater and more prolonged HIV-1 RNA reduction (average of 2.05 $\log_{10}$ copies/mL for over 3 months). Suppression to undetectable levels was seen in one participant with low (730 copies/mL) pre-bnAb HIV-1 RNA. In 3 of the 4 initially sensitive participants, rebound viruses were resistant to 10–1074, but remained sensitive to 3BNC117 (as the shorter half-life of 3BNC117 resulted in a tail of 10–1074 monotherapy) (60). Thus, in PWH with plasma viremia, dual bnAbs are not sufficient to suppress viremia to undetectable levels.

In contrast, co-administration of 3BNC117 and 10–1074 during ATI to PWH who had undetectable plasma HIV-1 RNA while on ART and outgrowth viruses that were sensitivity to both 3BNC117 and 10-1074, maintained viral suppression for extended durations. The median time to rebound was 21 weeks compared to 8.4 weeks with 3BNC117 monotherapy and 2.3 weeks for historical controls. In participants with no detectable resistant viruses pre-infusion, viral rebound occurred when the levels of bnAb waned. Rebound viruses were resistant to 10–1074, but remained sensitive to 3BNC117 (due to the shorter half-life of 3BNC117) but none developed viruses resistant to both antibodies (61). This study supports that bnAbs used in combination can maintain long-term viral suppression in PWH with antibody-sensitive viruses as long as therapeutic levels are maintained. A number of clinical trials assessing the efficacy of combinations of bnAbs in maintaining viral suppression during ATI are currently ongoing (**Table 1**). Differential clearance of bnAbs used in combination that could result in a tail of bnAb monotherapy remains an issue to be addressed by thorough understanding of bnAb pharmacokinetics and interactions in clinical trials.

## Expanding bnAb Breadth

Newer technologies allow for the construction of antibodies with two, three, or four different binding sites on a single molecule. Targeting multiple HIV-1 envelope epitopes in a single bnAb molecule reduces the risk of developing viral resistance during periods of essential monotherapy due to differential half-lives of combination bnAbs, simplifies manufacturing and downstream product development and thus scalability. The 10E8V2.0/ibalizumab bispecific ab, generated using CrossMAbs technology, neutralized 100% of a panel of 118 HIV-1 pseudotyped viruses *in vitro* with mean IC50 values of 0.002 μg/mL. Furthermore, it also protected humanized mice against repeated intraperitoneal HIV-$1_{JR\text{-}CSF}$ challenges (65). Currently, a phase I dose-escalation study on the safety, tolerability, pharmacokinetics, and anti-HIV-1 activity of the 10E8.4/ibalizumab bispecific Ab is in progress (NCT03875209).

Tri-specific abs have also been generated using knob-in-hole heterodimerization to pair a single arm derived from a normal immunoglobulin (IgG) with a double-arm generated in the cross-over dual variable Ig-like proteins (CODV-Ig). Two lead tri-specific Ab, N6/PGDM1400-10E8v4 and VRC01/PGDM1400-10E8v4 were able to neutralize 207 and 204 of 208 pseudotyped viruses *in vitro*, respectively. When NHP were challenged intrarectally with a mix of $SHIV_{325c}$ (resistant to VRC01) and $SHIV_{BaLP4}$ (resistant to PGDM1400), 6 of 8 animals infused with VRC01 alone and 5 of 8 animals infused with PGDM1400 became infected. In contrast, none of the 8 animals infused with VRC01/PGDM1400-10E8v4 trispecific Ab were infected (66). This demonstrated that tri-specific ab conferred protection against viruses that otherwise showed resistance to single parental bnAbs. The VRC01-LS/PGDM1400-10E8v4 trispecific ab (SAR441236) is currently being evaluated in a dose escalation study to determine safety, pharmacokinetics and anti-HIV-1 activity (NCT03705169).

It is anticipated that the modified versions of 10E8 used in the aforementioned bi- and tri-specific bnAbs will not recapitulate

**TABLE 1 |** Ongoing clinical trials of bnAb as part of HIV-1 therapeutic or remission strategy.

| BnAb | Target site | Additional Intervention(s) | Study population | Study Endpoints | Clinicaltrials.gov identifier |
|---|---|---|---|---|---|
| **Studies on antiviral effects of bnAbs** | | | | | |
| VRC01-LS or VRC07-523LS | CD4bs | | Adults with HIV-1 and plasma viremia | Safety, PK and effects on plasma viremia | NCT02840474 |
| 3BNC117 + 10-1074 | CD4bs, V3 glycans | | Adults with HIV-1 and plasma viremia | Safety and effects on plasma viremia | NCT03571204 |
| 3BNC117-LS + 10-1074-LS | CD4bs, V3 glycans | | Adults with HIV-1 and plasma viremia | Safety, PK and effects on plasma viremia | NCT04250636 |
| VRC07-523LS + PGT121 + PGDM1400 | CD4bs, V3 glycans, V1/V2 loop | | Adults with HIV-1 and plasma viremia | Safety, PK and effects on plasma viremia | NCT03205917 |
| 10E8.4/iMab | MPER, CD4 | | Adults with HIV-1 and plasma viremia | Safety, PK and effects on plasma viremia | NCT03875209 |
| SAR441236 | Trispecific Ab targeting CD4bs, V2 loop, MPER | | Adults with HIV-1 and plasma viremia | Safety, PK and effects on plasma viremia | NCT03705169 |
| VRC01 | CD4bs | | Adults at the diagnosis of acute HIV-1 infection, in addition to ART | Safety and effects on plasma viremia | NCT02591420 |
| VRC01 | CD4bs | | Infants with HIV-1, in addition to ART | Safety, PK and effects on plasma viremia | NCT03208231 |
| 3BNC117 | CD4bs | Albuvirtide (Fusion inhibitor) | Adults with multi-drug resistant HIV-1 | Effects on plasma viremia | NCT04560569 |
| **Studies on efficacy in maintaining viral suppression during ATI** | | | | | |
| 3BNC117 + 10-1074 | CD4bs, V3 glycans | | Adults with HIV-1, on ART | Effects on the latent reservoir, impact on viral rebound and safety | NCT03526848 |
| 3BNC117 + 10-1074 | CD4bs, V3 glycans | | Adults with HIV-1, on ART, initiated during primary HIV-1 infection | Safety and impact on viral rebound | NCT03571204 |
| VRC01-LS + 10-1074 | CD4bs, V3 glycans | | Children with antepartum or peripartum HIV-1 infection, on ART, initiated early after diagnosis | Safety, impact on viral rebound and PK | NCT03707977 |
| VRC01 + 10-1074 | CD4bs, V3 glycans | | Adults with HIV-1, on ART | Safety and impact on viral rebound | NCT03831945 |
| 3BNC117-LS + 10-1074-LS | CD4bs, V3 glycans | | Adults with HIV-1, on ART, initiated during primary HIV-1 infection | Safety and impact on viral rebound | NCT04319367 |
| VRC07-523LS + PGT121 + PGDM1400 | CD4bs, V3 glycans, V1/V2 loop | | Adults with HIV-1, on ART | Safety, PK and impact on viral rebound | NCT03721510 |
| 3BNC117 | CD4bs | Albuvirtide (Fusion inhibitor) | Adults with HIV-1, on ART | Impact on viral rebound | NCT03719664 |
| 3BNC117-LS + 10-1074-LS | CD4bs, V3 glycans | Lenacapavir (capsid inhibitor) | Adults with HIV-1, on ART | Safety, impact on viral rebound and PK | NCT04811040 |
| VRC07-523LS | CD4bs | Long-acting cabotegravir | Adults with HIV-1, on ART | Safety and impact on viral rebound and PK | NCT03739996 |
| **Studies on bnAbs in combination with additional interventions to target and eliminate the viral reservoir** | | | | | |
| 3BNC117 | CD4bs | Romidepsin (LRA) | Adults at the diagnosis of HIV-1 infection, in addition to ART | Safety, effects on plasma viremia and the latent reservoir | NCT03041012 |
| 3BNC117 | CD4bs | Romidepsin | Adults with HIV-1, on ART | Safety, impacts on viral rebound and the latent reservoir | NCT02850016 |
| VRC07-523LS | CD4bs | Vorinostat (LRA) | Adults with HIV-1, on ART | Safety, effects on viral reservoir | NCT03803605 |
| 3BNC117 + 10-1074 | CD4bs, V3 glycans | Lefitolimod (TLR9 agonist) | Adults with HIV-1, on ART | Safety and impact on viral rebound | NCT03837756 |
| VRC07-523LS + 10-1074 | CD4bs, V3 glycans | N-803 (IL-15 superagonist) | Adults with HIV-1, on ART | Safety, impacts on viral rebound and the latent reservoir, PK | NCT04340596 |
| 3BNC117 + 10-1074 | CD4bs, V3 glycans | Pegylated Interferon alpha 2b | Adults with HIV-1, on ART | Safety, NK cell activity and impact on viral rebound | NCT03588715 |
| VRC07-523LS + 10-1074 | CD4bs, V3 glycans | HIV DNA vaccine, HIV MVA vaccine, lefitolimod | Adults with HIV-1, on ART | Safety, proportion with post treatment control, immunogenicity | NCT04357821 |
| 10-1074 | V3 glycans | HIV RNA vaccine, romidepsin | Adults with HIV-1, on ART | Safety, impacts on viral rebound and the latent viral reservoir, immunogenicity | NCT03619278 |

the local reactogenicity associated with 10E8VLS due to differences in amino acid sequences as well as antibody-antigen interactions between the bivalent 10E8VLS and the monovalent 10E8.4 arm of the bi- or tri-specific bnAbs. Due to their novel structures, recombinant multi-specific Abs have a higher theoretical possibility of inducing anti-drug Abs. However, this has not been reported in the preliminary trials to date and will need to be confirmed in larger scale studies in humans.

## THE USE OF BNABS TO TARGET, CONTROL AND POTENTIALLY ELIMINATE THE VIRAL RESERVOIR

### BnAbs Alone

Data from rhesus macaques inoculated with SHIV suggest that bnAb when administered alone may induce sustained ART free remission (**Table 2**). When 3BNC117 and 10-1074 were administered to animals 3 days post intra-rectal $SHIV_{AD8\text{-}EO}$ inoculation, plasma viremia was only detectable in 2 of 6 animals in the first month. Viral suppression was maintained for 8-25 weeks until bnAb levels waned. Importantly, 3 animals developed viral control. In a follow-on experiment, the same bnAb regimen was administered 3 days post intravenous $SHIV_{AD8\text{-}EO}$ inoculation. Plasma viremia was initially detected in all animals post inoculation (PI), but then declined to undetectable levels by 4 weeks post bnAb administration. Rebound occurred at 7-16 weeks PI when bnAb levels waned. Three of 7 animals developed post-rebound viral control. Subsequent CD8 T cell depletion in all 6 controllers resulted in increase in plasma viremia, suggesting a CD8 T cell dependent mechanism for control (67).

To evaluate the above strategy at a more clinically relevant post infection timepoint, $SHIV_{AD8\text{-}EO}$ -infected monkeys were treated with bnAbs (10-1074 and 3BNC117) alone or with ART plus bnAbs starting at 2 weeks PI. In the bnAb alone group, bnAbs reduced plasma viremia overall, but only 1 animal achieved full plasma viral suppression. This animal later rebounded and subsequently regained control. Three other animals also controlled virus, but much later, at 90-150 weeks post infection. Viral rebound occurred in all animals in the ART plus bnAbs group when bnAb levels waned. Three animals developed post-rebound viral control at weeks 70-160. CD8 T cell depletion in controllers from both groups also led to transient increases in plasma viremia (68).

Therefore, bnAbs initiated on day 3 or day 14 PI resulted in CD8 T cells dependent viral control in about half the animals. However, the time required to develop viral control was much more protracted when the initiation of bnAbs were delayed. The authors speculated that though bnAbs administered early post infection suppressed viremia, very-low levels of antigen production likely persisted and in the presence of bnAbs stimulated immune complex formation and dendritic cell activation leading to the induction of CD8 T cell responses. Immune responses were further augmented during viral rebound, culminating in viral control.

There is little data in humans on the efficacy of bnAbs to induce T cell responses leading to viral control. In the study by Mendoza et al, in which a combination of 3NBC117 and 10-1074 was administered during ATI, increased Gag-specific CD8+ and CD4+ T cell responses were seen in 9/9 and 8/9 participants with sensitive viruses and prolonged viral suppression. The increases were attributed to both newly detectable reactivity to HIV-1 Gag epitopes and the expansion of pre-existing measurable responses

**TABLE 2** | Non-human primate studies on the use of bnAbs to target, control and potentially eliminate the viral reservoir.

| | SHIV | ART initiation | BnAb | Additional Interventions | Outcome |
|---|---|---|---|---|---|
| Nishimura et al. (67) | $SHIV_{AD8\text{-}EO}$ | No ART | 3BNC117 + 10-1074 at days 3, 10 and 17 PI | | Viral control in 3 of 6 animals from intra-rectal and 3 of 7 animals from intravenous inoculation |
| Nishimura et al. (68) | $SHIV_{AD8\text{-}EO}$ | 2 weeks post infection | 3BNC117 + 10-1074 alone at weeks 2, 4 and 6 PI or ART initiation at week 2; 3BNC117 + 10-1074 at weeks 9, 11 and 13; ART discontinuation at week 10 | | Viral control in 4 of 6 animals in bnAb alone arm in 3 of 6 animals in bnAb and ART arm |
| Borducchi et al. (69) | $SHIV_{SF162P3}$ | 7 days post infection | PGT121 | TLR7 agonist | No rebound in 5/11 animals and delay in rebound when compared to controls (112 vs 21 days) |
| Hsu et al. (70) | $SHIV_{1157ipd3N4}$ | 2 weeks post infection | PGT121 + N6-LS | TLR7 agonist | Delay in rebound when compared to controls (6 versus 3 weeks) |
| Barouch et al. (71) | $SHIV_{SF162P3}$ | 12 months post infection | PGT121 or its FC modified version (GS9721) | TLR7 agonist | No rebound in 7/17 animals |
| Whitney et al. (72) | $SHIV_{AD8}$ | ~50 days post infection | 3BNC117 + 10-1074 | IL-15 superagonist | No difference in time to rebound. Post-rebound control in 6 of 8 animals |
| Barouch et al. (73) | $SHIV_{SF162P3}$ | 9 days post infection | PGT121 | TLR7 agonist, Ad26/MVA vaccine | 4 of 12 PGT121+TLR7 agonisttreated animals and 4 of 10 Ad26/MVA vaccine+PGT121 +TLR7 agonist-treated animals did not rebound post treatment interruption. Only 4 of 10 Ad26/MVA vaccine+PGT121+TLR7 agonist-treated animals remained viremic 140 days post treatment interruption. |

(74). However, whether the increase in responses contribute to viral control remains to be elucidated.

Data from human trials involving bnAbs infusions concurrent with ART [including VRC01 (31, 75) and 3BNC117 (45)] showed no measurable impact on the latent reservoir. The impact of bnAbs on the reservoir would likely be improved when used in combination with other strategies, including latency reversal agents to induce proviral activation and cell-surface expression of viral envelopes so that they can be targeted by bnAbs, immune activating agents to enhance anti-viral responses and Fc-mediated killing of infected cells, or therapeutic vaccination to stimulate T cell responses for viral control.

## BnAbs and Immune Activating Agents

In the study by Borducchi et al., toll-like receptor 7 (TLR7) agonist was incorporated to induce innate immune activation and enhance anti-viral responses (76, 77). In this study, TLR7 agonist and PGT121 were administered in addition to ART (initiated at 7 days post $SHIV_{SF162P3}$ inoculation). ART was discontinued after antibody washout at week 130. Only 6 of 11 (55%) animals that received PGT121+TLR7 agonist rebounded, at a median of 112 days vs 21 days in controls (p=0.0001) (69). Interestingly, no induction of CD8 T cell responses was seen. Importantly, in the animals that did not rebound, adoptive transfer experiments did not reveal infection of naïve hosts. Furthermore, SHIV RNA also remained undetectable after CD8 T cell depletion. These data suggest that the combination of immune stimulation with bnAb administration may potentially eliminate the viral reservoir.

In a follow-on study by Hsu et al., rhesus macaques inoculated with $SHIV_{1157ipd3N4}$ were initiated on ART on day 14 to more closely mirror what is logistically feasible in humans. ART initiation was followed by the administration of TLR7 agonist and dual bnAbs (N6-LS and PGT121). ART was discontinued after antibody washout. Though TLR7 agonist and dual bnAbs delayed viral rebound by 2-fold (3 vs 6 wks, p=0.024), viral rebound occurred in all animals (70). The delay in ART initiation, the shorter duration of ART and the lower number of doses of bnAbs administered (ranging from 2-5 doses, limited by the development of anti-drug antibody) may have contributed to the reduction in efficacy when compared with the Borducchi et al. study.

In a recent study, Barouch et al., demonstrated in $SHIV_{SF162P3}$-infected animals that initiated ART 12 months after infection, TLR7 agonist and PGT121 or its Fc-modified version, GS-9721 prevented viral rebound in 7 of 17 animals following ART discontinuation. These data suggest that TLR7 agonist and bnAb administration is efficacious for ART-free remission of chronic SHIV infection (71).

Whitney et al. explored the use of N-803 [IL-15 superagonist that has been shown to increase NK and CD8 T cells in the peripheral blood as well as SHIV-specific CD8 T cells in lymphoid follicles (78–80)] in combination with 3BNC117 and 10-1074 in macaques on ART for chronic $SHIV_{AD8}$ infection. ATI occurred after bnAb washout. Viral rebound occurred in all animals and no differences in time to rebound were seen between the active and control groups. However, post-rebound viral control occurred in 6 of 8 animals in the active group 4 months from the start of ATI (72).

Data regarding the effects of bnAbs in combination with additional strategies on the latent reservoir in humans is forthcoming. In a trial of 3BNC117 and romidepsin [a histone deacetylase inhibitor (81)], in 20 PWH on ART, the addition of 3BNC117 did not significantly reduce HIV-1 DNA or delay viral rebound when compared to romidepsin alone (82). A number of clinical trials, including 3BNC117+romidepsin (NCT03041012, NCT02850016), VRC07-523LS+vorinostat (NCT03803605), pegylated-interferon Alpha 2b+3BNC117+10-1074 (NCT03588715), lefitolimod (TLR9 agonist)+3BNC117+10-1074 (NCT03837756) and N-803+VRC07-523LS+10-1074 (NCT04340596) are currently on-going (**Table 1**).

## Use of bNabs With Vaccination

The effects of immune stimulation (TLR agonism) and bnAbs may be further enhanced by the addition of therapeutic vaccine to induce anti-HIV-1 CD8 T cell responses. This strategy was explored in $SHIV_{SF162P3}$-infected rhesus macaques that were initiated on ART day 9 post infection. Following ART discontinuation, all control animals rebounded. All 12 of the Ad26/MVA vaccine+TLR7 animals also rebounded, but 3 developed post-rebound viral control. In contrast, only 8 of 12 of PGT121+TLR7 treated animals and 6 of 10 of Ad26/MVA vaccine +PGT121+TLR7 treated animals rebounded. Moreover, some animals exhibited post-rebound viral control so that by day 140 following ART discontinuation, only 4 of 10 of Ad26/MVA vaccine +PGT121+TLR7 treated animals have detectable viremia (73). Thus, combined TLR7 agonist, active and passive immunization resulted in both delayed viral rebound and post-rebound control following ART. This strategy is also being explored in an upcoming clinical trial involving therapeutic conserved element DNA vaccine+MVA vaccine+VRC07-523LS+10-1074+lefitolimod (NCT04357821) and ChAdOx/MVA HIV mosaic vaccine +3BNC117LS+10-1074LS+vesatolimod (ACTG5374) in PWH who initiated ART during acute HIV infection. Such human data is essential to determine whether results in NHP can be reproduced.

Data regarding the use of bnAbs to target, control and potentially eliminate the viral reservoir are largely from small NHP studies. However, there are differences between SHIV-infected NHP and PWH including lower viral diversity and higher rate of natural control in SHIV infection. Furthermore, efficacy of bnAbs is reduced with delay in bnAb administration or ART initiation, suggesting a narrow window of opportunity to intervene. Finally, a prolonged duration of viremia is also required for the observation of post treatment control. Thus, feasibility and translatability in PWH who started ART during chronic HIV infection is yet to be demonstrated.

# INCORPORATING LESSONS LEARNED INTO CLINICAL TRIAL DESIGN

## The Use of bnAbs to Maintain Viral Suppression

Available data demonstrated that bnAbs are generally safe and suggest that bnAbs can maintain viral suppression during ATI as long as the pre-existing viruses are sensitive and therapeutic

levels are maintained. Judicious selection of bnAbs based on neutralization-sensitivity of the predominant variants in a given geographic location, screening for pre-existing resistance and the use of bnAbs in combination to increase breadth and coverage will minimize the selection of escape variants. These optimization strategies will need to be further assessed in phase II or III clinical trials involving participants with chronic HIV infection to determine longer term efficacy. The ultimate goal is to identify antibody combinations with adequate breath to cover for circulating variants to obviate the need for screening for pre-existing resistance, which is a major barrier to widespread use. When bnAbs are used in combination in the absence of ART, considerations must be given to differences in half-life of each respective bnAb. In addition to peripheral blood, collection of tissue samples including lymph node and gut biopsies should be incorporated into clinical trials to allow measurement of the levels of bnAbs so as to inform what constitutes therapeutic levels in reservoir sites.

The use of bnAbs with LS modifications will extend duration above therapeutic threshold and reduce infusion frequency. This, together with alternative routes of administration such as subcutaneous injection will facilitate scale-up and access. Data from clinical trials evaluating long-acting injectable anti-HIV drugs, including monthly intramuscular cabotegravir (integrase strand transfer inhibitor) and rilpivirine (nonnucleoside reverse-transcriptase inhibitor) (83) or 6-monthly subcutaneous lenacapavir (capsid inhibitor) (84) are becoming available. Monthly intramuscular cabotegravir and rilpivirine demonstrated non-inferior viral suppression when compared to standard ART. The development of resistance is infrequent. However, injection-related adverse events were common (>80% of participants) but only infrequently led to medication withdrawal (83). Long acting ART will contend with bnAbs as preferred agents to maintain long-term viral suppression with infrequent dosing. Given that both strategies have pros and cons, usage and uptake will likely be driven by considerations including availability, local HIV-variant sensitivity profile, tolerability, relative cost and availability, and individual and local cultural preferences. While some may prefer a daily oral pill, others may prefer a less frequent schedule of administration. Dosage route, frequency, and potential for bnAbs self-administration will be important factors in this consideration.

## The Use of bnAbs to Induce HIV Remission

BnAbs alone are unlikely to be adequate to eliminate the latent reservoir. A handful of NHP studies where bnAbs were used in combination with innate immune activating agents have shown promise. However, mechanisms for delay in viral rebound or post-rebound viral control have not been delineated. The strategy of innate stimulation, active and passive immunization are in the early stages of development and data is needed to inform decisions regarding optimal timing and order of administration of individual interventions to maximize therapeutic effects.

It is important to bear in mind that immune activating agents may potentially expand the reservoir through clonal proliferation. It remains possible that certain reservoir sites including the central nervous system may be exposed to latency activation and viral replication but little bnAb mediated anti-HIV-1 effects due to the blood brain barrier limiting bnAb penetrance. These questions can be addressed in NHP models where direct tissue sampling of the brain is more feasible. In parallel, clinical trials administering bnAb therapies can also monitor differential impact on bnAb therapies administered by varying routes on viral burden or cellular reservoirs in the cerebrospinal fluid relative to blood.

Data from NHP studies suggest that the opportunity to intervene may be narrow, with reduction in efficacy or substantial increase in time required to observe results when bnAb administration or ART initiation is delayed just by a few weeks. The MHRP RV217 prospective cohort involving seronegative high-incidence populations who underwent twice-weekly HIV-1 RNA testing estimated the eclipse phase (the time between HIV-1 infection and a diagnosable infection by nucleic acid testing) to be one week (85). Therefore, taking into account the time required to diagnose, screen and then enroll participants into a clinical trial, the earliest that interventions can realistically be administered is likely around 2 weeks post infection. The clinical trial NCT02591420 that explores the effects of VRC01 when administered at the time of diagnosis of AHI on the viral reservoir has just completed clinical follow-up, demonstrating that intervening early during HIV-1 infection is logistically feasible. However, the majority of PWH initiated ART during chronic infection and the impacts of these strategies in this setting are yet to be defined.

Though NHP studies demonstrated that post-rebound viral control is possible, a protracted period of viremia may be required prior to the development of control. The delicate balance between the utility of an extended ATI to observe post-rebound viral control versus the associated risks of transmission to sexual partners, symptomatic HIV disease, immune depletion, and emergence of new drug resistance mutation has generated much debate among researchers, ethicists and PWH (86–89). Research in delineating mechanisms and/or correlates for delay in viral rebound and sustained post-rebound viral control is urgently needed to reduce the reliance on extended ATI as an outcome measure.

BnAbs are generally safe and well tolerated and have been shown to maintain viral suppression in the setting of sensitive pre-treatment viruses. Mechanisms to improve antiviral effects and ease of use are becoming available. Thus, bnAbs used in combination have the potential to replace ART and obviate the need for high level adherence that is necessary for daily ART. The use of bnAbs as a component of combination strategies to target the reservoir has shown promise in NHP models. However, the window of opportunity to intervene for maximal effect may be narrow. A remission strategy should be effective across the spectrum of HIV infection. Thus, much work needs to be done to answer questions regarding the penetration into tissue sites, what constitutes therapeutic levels, and the mechanisms of action in the delay of viral rebound and post-rebound control before bnAb can become an important therapeutic advance for PWH.

## AUTHOR CONTRIBUTIONS

All authors reviewed the literature, drafted and revised the paper. All authors contributed to the article and approved the submitted version.

## FUNDING

SV reports funding from the U.S. Department of Defense with Henry M. Jackson Foundation for the Advancement of Military Medicine (Cooperative agreement numbers W81XWH-11-2-0174, W81XWH-07-2-0067, W81XWH-18-2-0040), funding from the NIH/NIAID (1UM1AI126603, 2UM1AI108568-08), and funding from the US Department of Defense (W81XWH1810579). DH reports funding from the U.S. Department of Defense with Henry M. Jackson Foundation for the Advancement of Military Medicine (Cooperative agreement number W81XWH-18-2-0040) and funding from the NIH/NIAID (1UM1AI126603, 2UM1AI108568-08). JM reports funding from NIH/NIAID to the I4C Martin Delaney Collaboratory (UM1AI126603), to the Pitt-Ohio State Clinical Trials Unit (UM1 AI069494), to the Pitt Virology Specialty Laboratory (UM1 AI106701), to the University of Pittsburgh (U01AI131285 and U01AI152969), from NCI through Leidos (75N91019D00024), and from the Bill & Melinda Gates Foundation (OPP1115715).

## REFERENCES

1. Palella FJJr., Baker RK, Moorman AC, Chmiel JS, Wood KC, Brooks JT, et al. Mortality in the Highly Active Antiretroviral Therapy Era: Changing Causes of Death and Disease in the HIV Outpatient Study. *J Acquir Immune Defic Syndr* (2006) 43(1):27–34. doi: 10.1097/01.qai.0000233310.90484.16
2. HIV-CAUSAL Collaboration, Ray M, Logan R, Sterne JA, Hernandez-Diaz S, Robins JM, et al. The Effect of Combined Antiretroviral Therapy on the Overall Mortality of HIV-Infected Individuals. *AIDS* (2010) 24(1):123–37. doi: 10.1097/QAD.0b013e3283324283
3. Chun TW, Stuyver L, Mizell SB, Ehler LA, Mican JA, Baseler M, et al. Presence of an Inducible HIV-1 Latent Reservoir During Highly Active Antiretroviral Therapy. *Proc Natl Acad Sci USA* (1997) 94(24):13193–7. doi: 10.1073/pnas.94.24.13193
4. Finzi D, Hermankova M, Pierson T, Carruth LM, Buck C, Chaisson RE, et al. Identification of a Reservoir for HIV-1 in Patients on Highly Active Antiretroviral Therapy. *Science* (1997) 278(5341):1295–300. doi: 10.1126/science.278.5341.1295
5. Chomont N, El-Far M, Ancuta P, Trautmann L, Procopio FA, Yassine-Diab B, et al. HIV Reservoir Size and Persistence Are Driven by T Cell Survival and Homeostatic Proliferation. *Nat Med* (2009) 15(8):893–900. doi: 10.1038/nm.1972
6. Li JZ, Etemad B, Ahmed H, Aga E, Bosch RJ, Mellors JW, et al. The Size of the Expressed HIV Reservoir Predicts Timing of Viral Rebound After Treatment Interruption. *AIDS* (2016) 30(3):343–53. doi: 10.1097/QAD.0000000000000953
7. Namazi G, Fajnzylber JM, Aga E, Bosch RJ, Acosta EP, Sharaf R, et al. The Control of HIV After Antiretroviral Medication Pause (Champ) Study: Posttreatment Controllers Identified From 14 Clinical Studies. *J Infect Dis* (2018) 218(12):1954–63. doi: 10.1093/infdis/jiy479
8. Govindasamy D, Ford N, Kranzer K. Risk Factors, Barriers and Facilitators for Linkage to Antiretroviral Therapy Care: A Systematic Review. *AIDS* (2012) 26 (16):2059–67. doi: 10.1097/QAD.0b013e3283578b9b
9. Ortego C, Huedo-Medina TB, Llorca J, Sevilla L, Santos P, Rodriguez E, et al. Adherence to Highly Active Antiretroviral Therapy (HAART): A Meta-Analysis. *AIDS Behav* (2011) 15(7):1381–96. doi: 10.1007/s10461-011-9942-x
10. Shubber Z, Mills EJ, Nachega JB, Vreeman R, Freitas M, Bock P, et al. Patient-Reported Barriers to Adherence to Antiretroviral Therapy: A Systematic Review and Meta-Analysis. *PloS Med* (2016) 13(11):e1002183. doi: 10.1371/journal.pmed.1002183
11. Dybul M, Attoye T, Baptiste S, Cherutich P, Dabis F, Deeks SG, et al. The Case for an HIV Cure and How to Get There. *Lancet HIV* (2021) 8(1):e51–8. doi: 10.1016/S2352-3018(20)30232-0
12. Beacroft L, Hallett TB. The Potential Impact of a "Curative Intervention" for HIV: A Modelling Study. *Glob Health Res Policy* (2019) 4:2. doi: 10.1186/s41256-019-0107-1
13. Lewin SR, Attoye T, Bansbach C, Doehle B, Dube K, Dybul M, et al. Multi-Stakeholder Consensus on a Target Product Profile for an HIV Cure. *Lancet HIV* (2021) 8(1):e42–50. doi: 10.1016/S2352-3018(20)30234-4
14. Wu X, Yang ZY, Li Y, Hogerkorp CM, Schief WR, Seaman MS, et al. Rational Design of Envelope Identifies Broadly Neutralizing Human Monoclonal Antibodies to HIV-1. *Science* (2010) 329(5993):856–61. doi: 10.1126/science.1187659
15. Ko SY, Pegu A, Rudicell RS, Yang ZY, Joyce MG, Chen X, et al. Enhanced Neonatal Fc Receptor Function Improves Protection Against Primate SHIV Infection. *Nature* (2014) 514(7524):642–5. doi: 10.1038/nature13612
16. Scheid JF, Mouquet H, Ueberheide B, Diskin R, Klein F, Oliveira TY, et al. Sequence and Structural Convergence of Broad and Potent HIV Antibodies That Mimic CD4 Binding. *Science* (2011) 333(6049):1633–7. doi: 10.1126/science.1207227
17. Gautam R, Nishimura Y, Gaughan N, Gazumyan A, Schoofs T, Buckler-White A, et al. A Single Injection of Crystallizable Fragment Domain-Modified Antibodies Elicits Durable Protection From SHIV Infection. *Nat Med* (2018) 24(5):610–6. doi: 10.1038/s41591-018-0001-2
18. Rudicell RS, Kwon YD, Ko SY, Pegu A, Louder MK, Georgiev IS, et al. Enhanced Potency of a Broadly Neutralizing HIV-1 Antibody *In Vitro* Improves Protection Against Lentiviral Infection *In Vivo*. *J Virol* (2014) 88 (21):12669–82. doi: 10.1128/JVI.02213-14
19. Huang J, Kang BH, Ishida E, Zhou T, Griesman T, Sheng Z, et al. Identification of a CD4-Binding-Site Antibody to HIV That Evolved Near-Pan Neutralization Breadth. *Immunity* (2016) 45(5):1108–21. doi: 10.1016/j.immuni.2016.10.027
20. Sok D, van Gils MJ, Pauthner M, Julien JP, Saye-Francisco KL, Hsueh J, et al. Recombinant HIV Envelope Trimer Selects for Quaternary-Dependent Antibodies Targeting the Trimer Apex. *Proc Natl Acad Sci USA* (2014) 111 (49):17624–9. doi: 10.1073/pnas.1415789111
21. Doria-Rose NA, Schramm CA, Gorman J, Moore PL, Bhiman JN, DeKosky BJ, et al. Developmental Pathway for Potent V1V2-Directed HIV-Neutralizing Antibodies. *Nature* (2014) 509(7498):55–62. doi: 10.1038/nature13036
22. Mouquet H, Scharf L, Euler Z, Liu Y, Eden C, Scheid JF, et al. Complex-Type N-Glycan Recognition by Potent Broadly Neutralizing HIV Antibodies. *Proc Natl Acad Sci USA* (2012) 109(47):E3268–77. doi: 10.1073/pnas.1217207109
23. Walker LM, Huber M, Doores KJ, Falkowska E, Pejchal R, Julien JP, et al. Broad Neutralization Coverage of HIV by Multiple Highly Potent Antibodies. *Nature* (2011) 477(7365):466–70. doi: 10.1038/nature10373
24. Huang J, Ofek G, Laub L, Louder MK, Doria-Rose NA, Longo NS, et al. Broad and Potent Neutralization of HIV-1 by a gp41-Specific Human Antibody. *Nature* (2012) 491(7424):406–12. doi: 10.1038/nature11544
25. Kwon YD, Georgiev IS, Ofek G, Zhang B, Asokan M, Bailer RT, et al. Optimization of the Solubility of HIV-1-Neutralizing Antibody 10E8 Through Somatic Variation and Structure-Based Design. *J Virol* (2016) 90 (13):5899–914. doi: 10.1128/JVI.03246-15
26. McCoy LE, Burton DR. Identification and Specificity of Broadly Neutralizing Antibodies Against HIV. *Immunol Rev* (2017) 275(1):11–20. doi: 10.1111/imr.12484
27. Sajadi MM, Dashti A, Rikhtegaran Tehrani Z, Tolbert WD, Seaman MS, Ouyang X, et al. Identification of Near-Pan-Neutralizing Antibodies Against HIV-1 by Deconvolution of Plasma Humoral Responses. *Cell* (2018) 173 (7):1783–1795 e14. doi: 10.1016/j.cell.2018.03.061
28. Liu Q, Zhang P, Miao H, Lin Y, Kwon YD, Kwong PD, et al. Rational Engraftment of Quaternary-Interactive Acidic Loops for Anti-HIV-1 Antibody Improvement. *J Virol* (2021) 95(12):e00159–21. doi: 10.1128/JVI.00159-21
29. Ledgerwood JE, Coates EE, Yamshchikov G, Saunders JG, Holman L, Enama ME, et al. Safety, Pharmacokinetics and Neutralization of the Broadly

Neutralizing HIV-1 Human Monoclonal Antibody VRC01 in Healthy Adults. *Clin Exp Immunol* (2015) 182(3):289–301. doi: 10.1111/cei.12692
30. Caskey M, Klein F, Lorenzi JC, Seaman MS, West APJr., Buckley N, et al. Viraemia Suppressed in HIV-1-Infected Humans by Broadly Neutralizing Antibody 3BNC117. *Nature* (2015) 522(7557):487–91. doi: 10.1038/nature14411
31. Lynch RM, Boritz E, Coates EE, DeZure A, Madden P, Costner P, et al. Virologic Effects of Broadly Neutralizing Antibody VRC01 Administration During Chronic HIV-1 Infection. *Sci Trans Med* (2015) 7(319):319ra206–319ra206. doi: 10.1126/scitranslmed.aad5752
32. Caskey M, Schoofs T, Gruell H, Settler A, Karagounis T, Kreider EF, et al. Antibody 10-1074 Suppresses Viremia in HIV-1-Infected Individuals. *Nat Med* (2017) 23(2):185. doi: 10.1038/nm.4268
33. Mayer KH, Seaton KE, Huang Y, Grunenberg N, Isaacs A, Allen M, et al. Safety, Pharmacokinetics, and Immunological Activities of Multiple Intravenous or Subcutaneous Doses of an anti-HIV Monoclonal Antibody, VRC01, Administered to HIV-Uninfected Adults: Results of a Phase 1 Randomized Trial. *PloS Med* (2017) 14(11):e1002435. doi: 10.1371/journal.pmed.1002435
34. Gaudinski MR, Coates EE, Houser KV, Chen GL, Yamshchikov G, Saunders JG, et al. Safety and Pharmacokinetics of the Fc-Modified HIV-1 Human Monoclonal Antibody VRC01LS: A Phase 1 Open-Label Clinical Trial in Healthy Adults. *PloS Med* (2018) 15(1):e1002493. doi: 10.1371/journal.pmed.1002493
35. Gaudinski MR, Houser KV, Doria-Rose NA, Chen GL, Rothwell RSS, Berkowitz N, et al. Safety and Pharmacokinetics of Broadly Neutralising Human Monoclonal Antibody VRC07-523LS in Healthy Adults: A Phase 1 Dose-Escalation Clinical Trial. *Lancet HIV* (2019) 6(10):e667–79. doi: 10.1016/S2352-3018(19)30181-X
36. Stephenson K, Julg B, Ansel J, Walsh SR, Tan CS, Maxfield L, et al. Therapeutic Activity of PGT121 Monoclonal Antibody in HIV-Infected Adults. In: *Conference on Retroviruses and Opportunistic Infections (Croi)* (2019).
37. Chen G, Coates E, Fichtenbaum C, Koletar S, Landovitz R, Presti R, et al. Safety and Virologic Effect of the HIV-1 Broadly Neutralizing Antibodies, VRC01LS or VRC07-523LS, Administered to HIV-Infected Adults in a Phase 1 Clinical Trial. In: *Journal of the International Aids Society*. SOUTHERN GATE, CHICHESTER PO19 8SQ, W: JOHN WILEY & SONS LTD THE ATRIUM (2019).
38. Widge AT, Houser KV, Gaudinski MR, Chen G, Carter C, Hickman SP, et al. A Phase I Dose-Escalation Trial of Human Monoclonal Antibody N6LS in Healthy Adults. In: *Conference on Retroviruses and Opportunistic Infections (Croi)* (2020).
39. Koup RA. Review of bNAbs in Clinical Development. In: *Hiv Research for Prevention Hivr4p, Satellite Session SA04 State of the Art of HIV bNAbs for Prevention of HIV Infection* (2018).
40. Pegu A, Hessell AJ, Mascola JR, Haigwood NL. Use of Broadly Neutralizing Antibodies for HIV-1 Prevention. *Immunol Rev* (2017) 275(1):296–312. doi: 10.1111/imr.12511
41. Julg B, Barouch DH. Neutralizing Antibodies for HIV-1 Prevention. *Curr Opin HIV AIDS* (2019) 14(4):318. doi: 10.1097/COH.0000000000000556
42. Karuna ST, Corey L. Broadly Neutralizing Antibodies for HIV Prevention. *Annu Rev Med* (2020) 71:329–46. doi: 10.1146/annurev-med-110118-045506
43. Corey L, Gilbert PB, Juraska M, Montefiori DC, Morris L, Karuna ST, et al. Two Randomized Trials of Neutralizing Antibodies to Prevent HIV-1 Acquisition. *N Engl J Med* (2021) 384(11):1003–14. doi: 10.1056/NEJMoa2031738
44. Scheid JF, Horwitz JA, Bar-On Y, Kreider EF, Lu CL, Lorenzi JC, et al. HIV-1 Antibody 3BNC117 Suppresses Viral Rebound in Humans During Treatment Interruption. *Nature* (2016) 535(7613):556–60. doi: 10.1038/nature18929
45. Cohen YZ, Lorenzi JCC, Krassnig L, Barton JP, Burke L, Pai J, et al. Relationship Between Latent and Rebound Viruses in a Clinical Trial of anti-HIV-1 Antibody 3BNC117. *J Exp Med* (2018) 215(9):2311–24. doi: 10.1084/jem.20180936
46. Bar KJ, Sneller MC, Harrison LJ, Justement JS, Overton ET, Petrone ME, et al. Effect of HIV Antibody VRC01 on Viral Rebound After Treatment Interruption. *N Engl J Med* (2016) 375(21):2037–50. doi: 10.1056/NEJMoa1608243
47. Ananworanich J, Chomont N, Eller LA, Kroon E, Tovanabutra S, Bose M, et al. HIV DNA Set Point Is Rapidly Established in Acute HIV Infection and Dramatically Reduced by Early Art. *EBioMedicine* (2016) 11:68–72. doi: 10.1016/j.ebiom.2016.07.024
48. Archin NM, Vaidya NK, Kuruc JD, Liberty AL, Wiegand A, Kearney MF, et al. Immediate Antiviral Therapy Appears to Restrict Resting CD4+ Cell HIV-1 Infection Without Accelerating the Decay of Latent Infection. *Proc Natl Acad Sci USA* (2012) 109(24):9523–8. doi: 10.1073/pnas.1120248109
49. Cheret A, Bacchus-Souffan C, Avettand-Fenoel V, Melard A, Nembot G, Blanc C, et al. Combined ART Started During Acute HIV Infection Protects Central Memory CD4+ T Cells and Can Induce Remission. *J Antimicrob Chemother* (2015) 70(7):2108–20. doi: 10.1093/jac/dkv084
50. Delwart E, Magierowska M, Royz M, Foley B, Peddada L, Smith R, et al. Homogeneous Quasispecies in 16 Out of 17 Individuals During Very Early HIV-1 Primary Infection. *AIDS* (2002) 16(2):189–95. doi: 10.1097/00002030-200201250-00007
51. Altfeld M, Rosenberg ES, Shankarappa R, Mukherjee JS, Hecht FM, Eldridge RL, et al. Cellular Immune Responses and Viral Diversity in Individuals Treated During Acute and Early HIV-1 Infection. *J Exp Med* (2001) 193 (2):169–80. doi: 10.1084/jem.193.2.169
52. Crowell TA, Colby DJ, Pinyakorn S, Sacdalan C, Pagliuzza A, Intasan J, et al. Safety and Efficacy of VRC01 Broadly Neutralising Antibodies in Adults With Acutely Treated HIV (RV397): A Phase 2, Randomised, Double-Blind, Placebo-Controlled Trial. *Lancet HIV* (2019) 6(5):e297–306. doi: 10.1016/S2352-3018(19)30053-0
53. Cale EM, Bai H, Bose M, Messina MA, Colby DJ, Sanders-Buell E, et al. Neutralizing Antibody VRC01 Failed to Select for HIV-1 Mutations Upon Viral Rebound. *J Clin Invest* (2020) 130(6):3299–304. doi: 10.1172/JCI134395
54. Zalevsky J, Chamberlain AK, Horton HM, Karki S, Leung IW, Sproule TJ, et al. Enhanced Antibody Half-Life Improves *In Vivo* Activity. *Nat Biotechnol* (2010) 28(2):157–9. doi: 10.1038/nbt.1601
55. Gautam R, Nishimura Y, Pegu A, Nason MC, Klein F, Gazumyan A, et al. A Single Injection of Anti-HIV-1 Antibodies Protects Against Repeated SHIV Challenges. *Nature* (2016) 533(7601):105–9. doi: 10.1038/nature17677
56. Dall'Acqua WF, Kiener PA, Wu H. Properties of Human IgG1s Engineered for Enhanced Binding to the Neonatal Fc Receptor (Fcrn). *J Biol Chem* (2006) 281(33):23514–24. doi: 10.1074/jbc.M604292200
57. Yu X-Q, Robbie GJ, Wu Y, Esser MT, Jensen K, Schwartz HI, et al. Safety, Tolerability, and Pharmacokinetics of MEDI4893, an Investigational, Extended-Half-Life, Anti-Staphylococcus Aureus Alpha-Toxin Human Monoclonal Antibody, in Healthy Adults. *Antimicrob Agents Chemother* (2017) 61(1):e01020–16. doi: 10.1128/AAC.01020-16
58. Doria-Rose NA, Bhiman JN, Roark RS, Schramm CA, Gorman J, Chuang GY, et al. New Member of the V1V2-Directed Cap256-Vrc26 Lineage That Shows Increased Breadth and Exceptional Potency. *J Virol* (2016) 90(1):76–91. doi: 10.1128/JVI.01791-15
59. Reeves J, Zheng Y, Olefsky M, Lie Y, Burke L, Taiwo B, et al. Susceptibility to BnAbs Is Concordant in Pre-ART Plasma and On-ART Pbmcs: ACTG Nwc413. In: *Conference on Retroviruses and Opportunistic Infections (Croi)* (2019).
60. Bar-On Y, Gruell H, Schoofs T, Pai JA, Nogueira L, Butler AL, et al. Safety and Antiviral Activity of Combination HIV-1 Broadly Neutralizing Antibodies in Viremic Individuals. *Nat Med* (2018) 24(11):1701. doi: 10.1038/s41591-018-0186-4
61. Mendoza P, Gruell H, Nogueira L, Pai JA, Butler AL, Millard K, et al. Combination Therapy With Anti-HIV-1 Antibodies Maintains Viral Suppression. *Nature* (2018) 561(7724):479. doi: 10.1038/s41586-018-0531-2
62. Kong R, Louder MK, Wagh K, Bailer RT, deCamp A, Greene K, et al. Improving Neutralization Potency and Breadth by Combining Broadly Reactive HIV-1 Antibodies Targeting Major Neutralization Epitopes. *J Virol* (2015) 89(5):2659–71. doi: 10.1128/JVI.03136-14
63. Wagh K, Seaman MS, Zingg M, Fitzsimons T, Barouch DH, Burton DR, et al. Potential of Conventional & Bispecific Broadly Neutralizing Antibodies for Prevention of HIV-1 Subtype A, C & D Infections. *PloS Pathog* (2018) 14(3): e1006860. doi: 10.1371/journal.ppat.1006860
64. Cohen YZ, Butler AL, Millard K, Witmer-Pack M, Levin R, Unson-O'Brien C, et al. Safety, Pharmacokinetics, and Immunogenicity of the Combination of the Broadly Neutralizing Anti-HIV-1 Antibodies 3BNC117 and 10-1074 in Healthy Adults: A Randomized, Phase 1 Study. *PloS One* (2019) 14(8): e0219142. doi: 10.1371/journal.pone.0219142
65. Huang Y, Yu J, Lanzi A, Yao X, Andrews CD, Tsai L, et al. Engineered Bispecific Antibodies With Exquisite HIV-1-Neutralizing Activity. *Cell* (2016) 165(7):1621–31. doi: 10.1016/j.cell.2016.05.024
66. Xu L, Pegu A, Rao E, Doria-Rose N, Beninga J, McKee K, et al. Trispecific Broadly Neutralizing HIV Antibodies Mediate Potent SHIV Protection in Macaques. *Science* (2017) 358(6359):85–90. doi: 10.1126/science.aan8630

67. Nishimura Y, Gautam R, Chun TW, Sadjadpour R, Foulds KE, Shingai M, et al. Early Antibody Therapy Can Induce Long-Lasting Immunity to SHIV. *Nature* (2017) 543(7646):559–63. doi: 10.1038/nature21435
68. Nishimura Y, Donau OK, Dias J, Ferrando-Martinez S, Jesteadt E, Sadjadpour R, et al. Immunotherapy During the Acute SHIV Infection of Macaques Confers Long-Term Suppression of Viremia. *J Exp Med* (2021) 218(1): e20201214. doi: 10.1084/jem.20201214
69. Borducchi EN, Liu J, Nkolola JP, Cadena AM, Yu WH, Fischinger S, et al. Antibody and TLR7 Agonist Delay Viral Rebound in SHIV-Infected Monkeys. *Nature* (2018) 563(7731):360–4. doi: 10.1038/s41586-018-0600-6
70. Hsu DC, Schuetz A, Imerbsin R, Silsorn D, Pegu A, Inthawong D, et al. TLR7 Agonist, N6-LS and PGT121 Delayed Viral Rebound in SHIV-Infected Macaques After Antiretroviral Therapy Interruption. *PloS Pathog* (2021) 17 (2):e1009339. doi: 10.1371/journal.ppat.1009339
71. Barouch D, Mercado N, Chandrashekar A, Borducchi E, Nkolola J, Carr BA, et al. PGT121 and Vesatolimod in Chronically Treated SHIV-Infected Rhesus Monkeys. In: *Conference on Retroviruses and Opportunistic Infections* (2020).
72. Lim SY, Osuna CE, Lee J, Silva-Ayala D, Vikhe P, Chen E, et al. Combination IL-15 Therapy in a SHIV Nhp Model. In: . *Conference on Retroviruses and Opportunistic Infections* (2020).
73. Barouch D, Mercado N, Chandrashekar A, Borducchi E, Nkolola J, Pau M, et al. Combined ACTIVE and PASSIVE Immunization IN SHIV-Infected RHESUS Monkeys. In: *Conference on Retroviruses and Opportunistic Infections* (2020).
74. Niessl J, Baxter AE, Mendoza P, Jankovic M, Cohen YZ, Butler AL, et al. Combination Anti-HIV-1 Antibody Therapy Is Associated With Increased Virus-Specific T Cell Immunity. *Nat Med* (2020) 26(2):222–7. doi: 10.1038/s41591-019-0747-1
75. Riddler SA, Zheng L, Durand CM, Ritz J, Koup RA, Ledgerwood J, et al. Randomized Clinical Trial to Assess the Impact of the Broadly Neutralizing HIV-1 Monoclonal Antibody VRC01 on HIV-1 Persistence in Individuals on Effective Art. *Open Forum Infect Dis* (2018) 5(10):ofy242. doi: 10.1093/ofid/ofy242
76. Hemmi H, Kaisho T, Takeuchi O, Sato S, Sanjo H, Hoshino K, et al. Small Anti-Viral Compounds Activate Immune Cells *Via* the TLR7 MyD88-Dependent Signaling Pathway. *Nat Immunol* (2002) 3(2):196–200. doi: 10.1038/ni758
77. Bam RA, Hansen D, Irrinki A, Mulato A, Jones GS, Hesselgesser J, et al. Tlr7 Agonist Gs-9620 Is a Potent Inhibitor of Acute HIV-1 Infection in Human Peripheral Blood Mononuclear Cells. *Antimicrob Agents Chemother* (2017) 61 (1):e01369–16. doi: 10.1128/AAC.01369-16
78. Ellis-Connell AL, Balgeman AJ, Zarbock KR, Barry G, Weiler A, Egan JO, et al. Alt-803 Transiently Reduces Simian Immunodeficiency Virus Replication in the Absence of Antiretroviral Treatment. *J Virol* (2018) 92 (3):e01748-17. doi: 10.1128/JVI.01748-17
79. Webb GM, Molden J, Busman-Sahay K, Abdulhaqq S, Wu HL, Weber WC, et al. The Human IL-15 Superagonist N-803 Promotes Migration of Virus-Specific CD8+ T and NK Cells to B Cell Follicles But Does Not Reverse Latency in ART-Suppressed, SHIV-Infected Macaques. *PloS Pathog* (2020) 16 (3):e1008339. doi: 10.1371/journal.ppat.1008339
80. McBrien JB, Mavigner M, Franchitti L, Smith SA, White E, Tharp GK, et al. Robust and Persistent Reactivation of SIV and HIV by N-803 and Depletion of CD8(+) Cells. *Nature* (2020) 578(7793):154–9. doi: 10.1038/s41586-020-1946-0
81. Shirakawa K, Chavez L, Hakre S, Calvanese V, Verdin E. Reactivation of Latent HIV by Histone Deacetylase Inhibitors. *Trends Microbiol* (2013) 21 (6):277–85. doi: 10.1016/j.tim.2013.02.005
82. Gruell H, Cohen Y, Gunst J. A Randomized Trial of the Impact of 3BNC117 and Romidepsin on the HIV-1 Reservoir. In: *Conference on Retroviruses and Opportunistic Infections (Croi)* (2020).
83. Swindells S, Andrade-Villanueva J-F, Richmond GJ, Rizzardini G, Baumgarten A, Masiá M, et al. Long-Acting Cabotegravir and Rilpivirine for Maintenance of HIV-1 Suppression. *New Engl J Med* (2020) 382 (12):1112–23. doi: 10.1056/NEJMoa1904398
84. Segal-Maurer S, Castagna A, Berhe M, Richmond G, Ruane PJ, Sinclair GI, et al. Potent Antiviral Acitivity of Lenacapavir in Phase 2/3 in Heavily Art-Experienced Pwh. In: *Conference on Retroviruses and Opportunistic Infections* (2021).
85. Rolland M, Tovanabutra S, Dearlove B, Li Y, Owen CL, Lewitus E, et al. Molecular Dating and Viral Load Growth Rates Suggested That the Eclipse Phase Lasted About a Week in HIV-1 Infected Adults in East Africa and Thailand. *PloS Pathog* (2020) 16(2):e1008179. doi: 10.1371/journal.ppat.1008179
86. Julg B, Dee L, Ananworanich J, Barouch DH, Bar K, Caskey M, et al. Recommendations for Analytical Antiretroviral Treatment Interruptions in HIV Research Trials-Report of a Consensus Meeting. *Lancet HIV* (2019) 6(4): e259–68. doi: 10.1016/S2352-3018(19)30052-9
87. Dawson L. Human Immunodeficiency Virus Transmission Risk in Analytical Treatment Interruption Studies: Relational Factors and Moral Responsibility. *J Infect Dis* (2019) 220(220 Suppl 1):S12–5. doi: 10.1093/infdis/jiz090
88. Henderson GE, Peay HL, Kroon E, Cadigan RJ, Meagher K, Jupimai T, et al. Ethics of Treatment Interruption Trials in HIV Cure Research: Addressing the Conundrum of Risk/Benefit Assessment. *J Med Ethics* (2018) 44(4):270–6. doi: 10.1136/medethics-2017-104433
89. Eyal N, Holtzman LG, Deeks SG. Ethical Issues in HIV Remission Trials. *Curr Opin HIV AIDS* (2018) 13(5):422–7. doi: 10.1097/COH.0000000000000489


**Disclaimer:** The U.S. Military HIV Research Program (MHRP) and the Emerging Infectious Diseases Branch (EIDB) at the Walter Reed Army Institute of Research are supported through a cooperative agreement with the Henry M. Jackson Foundation for the Advancement of Military Medicine (HJF). The views expressed are those of the authors and should not be construed to represent the positions of the U.S. Army, the Department of Defense or the Henry M. Jackson Foundation for the Advancement of Military Medicine, Inc.

**Conflict of Interest:** SV and DH report grants from the U.S. Department of Defense with Henry M. Jackson Foundation for the Advancement of Military Medicine and grants from the NIH/NIAID for the submitted work. SV also report grants from the U.S. Department of Defense. JM reports grants from the NIH for the submitted work, and grants from Gilead Sciences, Janssen Pharmaceuticals, USAID, and personal fees from Accelevir Diagnostics, Gilead Sciences, Merck, Xi'an Yufan Biotechnologies, and other from Infectious Diseases Connect, Co-Crystal Pharmaceuticals, Inc., and Abound Bio, Inc., outside the submitted work.

frontiers in Immunology

REVIEW
published: 20 July 2021
doi: 10.3389/fimmu.2021.712122

# Broadly Neutralizing Antibodies for HIV-1 Prevention

*Stephen R. Walsh*[1] *and Michael S. Seaman*[2]*

[1] Division of Infectious Diseases, Brigham and Women's Hospital, Harvard Medical School, Boston, MA, United States, [2] Center for Virology and Vaccine Research, Beth Israel Deaconess Medical Center, Harvard Medical School, Boston, MA, United States

Given the absence of an effective vaccine for protection against HIV-1 infection, passive immunization strategies that utilize potent broadly neutralizing antibodies (bnAbs) to block acquisition of HIV-1 are being rigorously pursued in the clinical setting. bnAbs have demonstrated robust protection in preclinical animal models, and several leading bnAb candidates have shown favorable safety and pharmacokinetic profiles when tested individually or in combinations in early phase human clinical trials. Furthermore, passive administration of bnAbs in HIV-1 infected individuals has resulted in prolonged suppression of viral rebound following interruption of combination antiretroviral therapy, and robust antiviral activity when administered to viremic individuals. Recent results from the first efficacy trials testing repeated intravenous administrations of the anti-CD4 binding site bnAb VRC01 have demonstrated positive proof of concept that bnAb passive immunization can confer protection against HIV-1 infection in humans, but have also highlighted the considerable barriers that remain for such strategies to effectively contribute to control of the epidemic. In this review, we discuss the current status of clinical studies evaluating bnAbs for HIV-1 prevention, highlight lessons learned from the recent Antibody Mediated Prevention (AMP) efficacy trials, and provide an overview of strategies being employed to improve the breadth, potency, and durability of antiviral protection.

**Keywords: HIV-1, antibody, neutralizing, Fc effector function, clinical trial**

OPEN ACCESS

***Edited by:***
*Philipp Schommers, University of Cologne, Germany*

***Reviewed by:***
*Nirianne Querijero Palacpac, Osaka University, Japan*
*Domenico Tortorella, Icahn School of Medicine at Mount Sinai, United States*

***Correspondence:**
*Michael S. Seaman*
*mseaman@bidmc.harvard.edu*

***Specialty section:***
*This article was submitted to Vaccines and Molecular Therapeutics, a section of the journal Frontiers in Immunology*

***Received:*** *19 May 2021*
***Accepted:*** *05 July 2021*
***Published:*** *20 July 2021*

***Citation:***
*Walsh SR and Seaman MS (2021) Broadly Neutralizing Antibodies for HIV-1 Prevention. Front. Immunol. 12:712122. doi: 10.3389/fimmu.2021.712122*

## INTRODUCTION

Human immunodeficiency virus (HIV) remains a major global health concern, with the World Health Organization (WHO) estimating that in 2019 there were 38 million HIV-1 infected individuals worldwide, 1.7 million new HIV infections, and 690,000 deaths from AIDS-related illness (1). Despite significant efforts over the past several decades, the development of an effective prophylactic vaccine against HIV-1 has yet to be realized. Thus, alternative biomedical strategies to prevent the transmission of HIV-1 are being actively pursued. Historically, passive immunization of pathogen-specific antibodies has proven to be an effective tool in the field of infectious disease for providing immediate yet transient protective immunity (2, 3). Recent advances in monoclonal antibody (mAb) engineering and production have accelerated the use of antibodies in the clinic for the treatment of cancers, autoimmune disease, and for targeting infectious pathogens or pathogen-

derived toxins (4, 5). Early attempts to utilize passive infusion of HIV-1-specific neutralizing mAbs for treatment of infected individuals demonstrated little if any clinical benefit (6, 7). Given the limited breadth and potency of these first generation neutralizing antibodies, enthusiasm for a passive immunization strategy for HIV-1 prevention or treatment largely waned.

As new standardized and high-throughput assay platforms were developed for measuring neutralizing antibody activity against HIV-1 (8, 9), it became possible to screen and identify rare HIV-1 infected individuals whose serum neutralizing activity exhibited exceptional potency and breadth when tested *in vitro* against genetically diverse strains of virus (10–13). Using newly developed technologies to single-cell sort antigen specific B cells and clone antibodies from such individuals (14), the floodgates opened for the discovery of a second generation of highly potent broadly neutralizing antibodies (bnAbs) against HIV-1 (15–21). All bnAbs target HIV-1 Envelope (Env) which is expressed as a trimer of glycoprotein 120 (gp120) – gp41 heterodimers, and is the only target exposed on the surface of the virion. Through epitope mapping and refined structural studies of bnAb-Env complexes, it has been possible to identify major sites of vulnerability on HIV-1 Env that are primarily targeted by these new generation bnAbs. These include the CD4 binding site (CD4bs), the V3-glycan super site, the V2-glycan epitope on the apex of the trimer, the membrane-proximal external region (MPER) on gp41, and an epitope at the interface of the gp120 and gp41 subunits. Details regarding these antibodies and their epitope targets have been extensively reviewed elsewhere (22, 23). Here, we provide an overview of the preclinical development of bnAbs, the current status of bnAb clinical prevention trials, and areas for future development.

## bnAb-MEDIATED PROTECTION IN ANIMAL MODELS

Both the humanized-mouse and non-human primate (NHP) animal models have been extensively used to characterize and model the protective-efficacy of bnAbs. The humanized mouse model relies on the reconstitution of immunodeficient mice with human hematopoietic and lymphoid cells, thus allowing for active HIV-1 replication and the ability to test investigational bnAbs for preventative or therapeutic potential with human immune cells (24). This model has been useful for initial proof-of-concept studies to demonstrate potent anti-viral protection *in vivo* by the newer generation bnAbs when delivered either as single antibodies, bnAb combination cocktails, or by vector-mediated expression using recombinant adeno-associated viruses (AAVs) (25–29). The potential utility of bnAbs for therapeutic treatment strategies has also been demonstrated using humanized mice. Treatment of animals with established HIV-1 YU2 infection using single bnAbs (PG16, 45-46$^{G54W}$, PGT128, 3BC176 or 10-1074) resulted in a transient decline in viremia that ultimately rebounded, in part through the development of escape mutations that arose from bnAb-induced selective immune pressure (27). In contrast, treatment of infected animals with a combination mixture of the five bnAbs resulted in sustained suppression of viral replication for up to 60 days without evidence of escape, thus providing the first evidence that combinations of bnAbs may be required for effective control of virus for therapeutic treatment strategies. While the humanized mouse model has thus far been useful for pre-clinical proof-of-concept studies, there are several potential disadvantages that limit its utility for assessing bnAb efficacy. These include, in part, incomplete immune reconstitution, the lack of a robust innate and adaptive immune repertoire (the former being critical for assessing Fc-mediated effector functions of bnAbs), and the frequent development of xenogeneic graft *vs* host responses that limit the lifespan of the host (24, 30). Continued efforts to optimize the humanized mouse model, especially in regards to the evaluation of Fc-mediated effector functions, will help improve its utility.

NHP provide a more relevant model of human infection as they have an intact innate and adaptive immune repertoire and can be infected with chimeric simian-human immunodeficiency viruses (SHIVs) that express HIV-1 Envelope on an SIV backbone. Repeated low-dose mucosal challenge models have also been developed in NHP to better mimic natural HIV-1 transmission events. Passive immunization of bnAbs in NHP prior to challenge has been an effective model to elucidate the protective efficacy of bnAbs in the setting of intravenous, intrarectal, intravaginal, penile, and oral SHIV infection (31, 32). bnAbs currently in advanced clinical development targeting the CD4 binding site (VRC01, 3BNC117, VRC07-523.LS), the V3-glycan site (PGT121, 10-1074), the V2-glycan site (PGDM1400, CAP256-VRC26.25) and MPER epitope (10E8) have all demonstrated various levels of protection against infection in SHIV challenge models (33–38). The level of protection observed has strongly correlated with the potency of the bnAb against the specific strain of SHIV used for challenge and the durability of serum bnAb levels. A study comparing three bnAbs targeting either the CD4bs (VRC01 and 3BNC117) or V3-glycan epitope (10-1074) demonstrated that a single infusion dose of 20 mg/kg could afford protection from weekly low-dose intrarectal challenges with $SHIV_{AD8}$ for up to 23 weeks (33). Animals receiving 3BNC117 infusion were protected for a median of 13 weeks, whereas those receiving VRC01, which is less potent against the $SHIV_{AD8}$ challenge virus, were only protected for a median of 8 weeks. A comparison of high-dose mucosal SHIV challenge studies using six bnAbs targeting the CD4bs or V3-glycan epitopes used regression analysis of the combined dataset to estimate that a serum 50% inhibitory dilution ($ID_{50}$) titer of 1:100 was sufficient to prevent acquisition in 50% of NHP (35). These findings were further supported by a more recent meta-analysis of data from 13 bnAb protection studies utilizing 274 NHP passively infused with 16 different bnAbs and eight strains of SHIV which demonstrated that serum neutralization titer on the day of SHIV challenge was strongly associated with protective efficacy against the challenge virus (32). Logistic modeling that adjusted for bnAb epitopes and challenge viruses estimated that serum $ID_{50}$ titers of 55, 219, and 685 would be required to achieve 50%, 75%, or 95% protection,

respectively. These analyses support the hypothesis that serum neutralization titer against the infecting strain of HIV-1 will be a key determinant of protection for bnAb prevention strategies in humans, and further highlight the possible requirement for substantial serum neutralization titers at the time of exposure for effective sterilizing immunity.

While NHP have been instrumental for investigating the potential protective efficacy of bnAbs for both HIV-1 prevention and therapeutic treatment strategies, there are several limitations to this model that should be taken into consideration. These include in part: (i) the limited genetic diversity of SHIVs compared to circulating strains of HIV-1 that are encountered in nature, (ii) the higher per exposure infection rate in SHIV challenge models compared to natural HIV-1 infection in humans, (iii) potential inefficiencies of human bnAbs to engage and activate innate immune effector functions in NHP, and (iv) the interference of anti-drug antibody (ADA) responses that often arise when NHPs elicit an autologous antibody response against the passively infused human bnAb (33, 39–43). Despite these potential drawbacks, NHP remain the best available animal model for bnAb protection studies. Recent advances in the development of genetically diverse panels of SHIVs that recapitulate many features of HIV-1 infection will certainly allow for more rigorous assessment of protection afforded by bnAbs and bnAb combinations (44–47). Together, both the humanized mouse and NHP models have been critical for accelerating the translation of bnAb passive immunity into human clinical trials.

## EFFECTOR MECHANISMS

Animal model studies have demonstrated that both Fab-mediated neutralization of virus and Fc-dependent effector functions can contribute to antiviral protection of bnAbs. The Fc-mediated component may be especially important for elimination of virus-infected cells and preventing the establishment of chronic infection (48–50). This may occur *via* binding to Fcγ-receptors (FcγRs) expressed on NK cells, macrophages and neutrophils to activate innate effector mechanisms such as antibody-dependent cellular cytotoxicity (ADCC) and antibody-dependent cellular phagocytosis (ADCP), or by activation of antibody-dependent complement-mediated lysis. Indeed, it has been demonstrated that passive protection afforded by PGT121 against a mucosal SHIV challenge in NHP involved clearance of disseminated virus in distal tissues rather than a complete blockade of virus at the mucosal surface (51). Elimination of these productively infected distal foci was hypothesized to involve Fc-effector mechanisms given evidence of innate immune activation in these tissues. Passive administration of bnAbs 3BNC117 and 10-1074 have also been shown to accelerate the clearance of HIV-1 infected CD4+ T cells in humanized mice through an FcγR-dependent mechanism (52).

Direct evaluation of the relative protective contribution of Fab-mediated neutralization versus Fc-mediated effector functions *in vivo* has also been investigated using antibodies with site-directed mutations to knock-out binding to FcγRs and/or complement. Results from such studies, however, have often come to conflicting conclusions. Hessell et al. first demonstrated the potential importance of Fc-mediated effector functions in NHP when protection afforded by passive immunization of b12, a first generation neutralizing mAb, was partially abrogated by elimination of Fc-receptor binding through the L234A/L235A (LALA) mutation (53). No reduction in protective effect was observed with a b12 variant that lacked complement binding (K332A). In contrast, two recent studies in NHP investigating the contribution of Fc effector functions with bnAb PGT121 in the setting of passive protection against $SHIV_{SF162P3}$ challenge (both cell-free and cell-associated viral infection models) found no evidence that effector functions contributed to bnAb-mediated protection, even when PGT121 wildtype and Fc-knock out variants were administered at sub-protective doses (54, 55). Furthermore, partial depletion of NK cells which are key mediators of Fc-dependent effector functions did not abrogate the protective efficacy of PGT121 (55).

Two recent studies utilized knowledge of HIV-1 dynamics and mathematical modeling to quantify the contribution of Fc-mediated effector functions to the antiviral activity of bnAbs in the context of therapeutic treatment of an established infection. By measuring the kinetics of viral load decline in response to a single dose treatment with either a wildtype bi-specific bnAb (composed of Fabs from 3BNC117 and PGDM1400) or a matched Fc-null variant, Wang and colleagues observed an earlier and sharper decline in viral load in both HIV-1-infected humanized mice and SHIV-infected NHP when treated with wildtype bnAb compared to the variant with deficient Fc effector function (56). Quantification of these observed differences suggested that Fc-mediated effector functions accounted for 25-45% of antiviral activity. Using similar methods, Asokan et al. observed that Fc-mediated effector functions contributed 21% of the anti-viral activity of bnAb VRC07-523-LS when infused into viremic SHIV-infected macaques (57). Interestingly, several studies that have examined passive administration of bnAb variants designed for enhanced binding to FcγRs, and therefore hypothesized to elicit greater ADCC activity, in fact observed no augmentation of protection in SHIV-infected NHP (57, 58).

Together, these data suggest that the predominant mechanism of bnAb-mediated protection is through direct neutralization of virions, but that Fc-mediated effector functions can contribute to overall protective efficacy. The latter may be more critical with the use of bnAbs in therapeutic settings in which virally infected cells must be targeted for elimination. Understanding whether individual bnAbs or bnAb-epitope classes differentially exhibit abilities to recruit Fc-mediated effector functions *in vivo* and whether these activities can be enhanced through Fc variant engineering will be important for exploring improved antibody-based strategies for HIV-1 prevention or therapeutic treatment (59).

## COMBINATIONS OF bnAbs

HIV-1 Env sequence diversity remains a major challenge for bnAb passive prevention strategies, as individuals may be

exposed to highly diverse swarms of virus that exhibit a range of neutralization sensitivities or complete resistance to any particular antibody. Furthermore, clade-specific resistance patterns have been identified for certain bnAbs which may complicate the use of these antibodies in geographical regions where these particular HIV-1 subtypes dominate. For example, CRF01_AE is the major circulating lineage in Southeast Asia, and viruses in this clade exhibit high level resistance to bnAbs targeting the V3-glycan epitope, such as PGT121 and 10-1074, due to the loss of the critical N332 glycosylation site (60). Similarly, clade B viruses demonstrate higher levels of resistance to bnAbs targeting the V2-glycan epitope, such as PGDM1400 and CAP256, compared to clade C viruses (60, 61). It is therefore likely that the clinical success of bnAb passive immunization strategies will require combinations of antibodies to increase the overall breadth and potency against diverse isolates and to prevent the emergence of resistance. A central question then arises as to which bnAbs and how many will be required to provide optimal protection. Mathematical modeling approaches have been developed that utilize *in vitro* neutralization data of clinically advanced bnAbs tested against large panels of genetically diverse HIV-1 Env pseudoviruses to help determine optimal combinations (62, 63). These analyses have demonstrated that combinations containing three or four bnAbs targeting different epitopes typically act additively to provide better breadth, potency, and extent of complete neutralization compared to two antibody combinations, and further increase the probability of having multiple bnAbs simultaneously active against a given virus. Combinations of bnAbs targeting independent epitopes are also more favorable than those containing antibodies targeting overlapping epitopes (e.g., two or more bnAbs targeting the CD4bs). Given that subtype-specific resistance patterns of bnAbs should be considered in decisions to test bnAbs in particular geographical regions, defining optimal combinations for clade-specific or regional use is an area of active investigation (64).

The optimal combination and number of bnAbs needed may also vary depending on the intended clinical use. For prevention of HIV-1 acquisition, it is possible that optimal combinations of two or three bnAbs may achieve sufficient breadth and potency to ensure reliable coverage against the transmitting virus. For therapeutic treatment strategies however, it is likely that larger numbers of bnAbs will be required to adequately cover the within-host diversity that exists as replicating virus or is present in the latent reservoir. The ability to accurately screen HIV-infected individuals to determine bnAb sensitivity profiles and compose optimal combinations to target the patient-specific viral quasispecies would be beneficial, similar to genotyping strategies used for optimizing combination antiretroviral drug regimens. While phenotyping the bnAb sensitivity of patient viruses can be performed using either bulk or limiting dilution T cell outgrowth cultures, these assays can be labor intensive, costly, and may fail to detect minor pre-existing resistant variants (65, 66). An alternative strategy for future development may be to use predictive modeling based on *env* sequencing of the patient's quasispecies to determine bnAb sensitivity patterns and optimize combination cocktails (67–69).

Combination bnAb regimens will also have additional complexities in manufacturing, product development, and clinical implementation that will need to be addressed. For example, each bnAb will have its own unique pharmacokinetic profile which may present challenges in formulation and delivery in order to maintain all antibodies in the combination above target therapeutic concentrations *in vivo* for optimal protective efficacy. Further development of multiple antibodies in a single co-formulated drug product will also need to take into account the specific formulation and stability characteristics of each bnAb. Recent reports have demonstrated that protein sequence optimization of several clinically advanced bnAbs can improve expression levels, conformational stability, and downstream processing and formulation conditions, all while maintaining the neutralization profile of the parental antibody (70, 71). A high concentration co-formulated drug product containing bnAbs 3BNC117-LS and 10-1074-LS that will allow for subcutaneous administration has also recently been described (72). As will be reviewed further below, the first 2- and 3-bnAb combinations have initiated clinical testing in HIV-infected and uninfected individuals. With the continued development of methods for predicting optimal bnAb combinations and improvement of manufacturing capabilities it is expected that the portfolio of bnAb combinations entering human clinical trials will continue to expand.

## CLINICAL EVALUATION OF bnAbs

The availability of clinical grade bnAbs capable of blocking HIV-1 *in vitro* and in animal challenge models has opened the possibility of antibody-mediated prevention (AMP) of HIV infection in humans (41). Several bnAbs have been tested in phase 1 studies to determine their safety, tolerability, and pharmacokinetic (PK) profiles in both HIV-infected and HIV-uninfected individuals (**Table 1**). Thus far, only the CD4bs targeting bnAb VRC01 has advanced to efficacy studies for protection against HIV infection, but ongoing combination bnAb trials will likely inform future efforts.

### CD4 Binding Site bnAbs

#### VRC01

VRC01 was originally discovered in an individual infected with HIV-1 for more than 15 years and whose immune system controlled the virus without antiretroviral therapy (ART) (20, 86). When tested *in vitro* against a genetically diverse panel of 190 HIV-1 Env pseudoviruses, VRC01 neutralized 91% with a 50% inhibitory concentration ($IC_{50}$) of < 50 μg/ml and 72% with an $IC_{50}$ < 1 μg/ml.

Clinical studies of VRC01 started in 2013, first in HIV-infected adults [VRC 601 (NCT01950325) (87)], and then in healthy adults [VRC 602 (NCT01993706) (88] and HVTN 104 (NCT02165267) (89)]. VRC01 was found to be safe and well tolerated at doses ranging from 5-40 mg/kg administered intravenously (IV) and at 5 mg/kg subcutaneously (SC). PK analyses across studies have shown that VRC01 has a half-life of approximately 15 days with little difference between dose groups.

**TABLE 1** | bnAbs in Clinical Trials.

| Epitope region targeted | bnAb | Half-life | Reference |
|---|---|---|---|
| CD4-binding site (CD4-BS) | VRC01 | 15 days; 71 days (-LS) | NCT02165267 (73, 74); |
| | VRC07-523 | 40 days (-LS) | NCT03015181 (75, 76); |
| | 3BNC117 | 18 days; 61 days (-LS) | NCT02018510 (77, 78); |
| | N6 | >30 days (-LS) | NCT03538626 (79); |
| Membrane-proximal external region (MPER) | 10E8 | N/A | NCT03565315 (80); |
| V1V2 loop glycan | PGDM1400 | N/A | NCT03205917 |
| | PG9[1] | N/A | NCT01937455 (81) |
| | CAP256-VRC26.25 | N/A | PACTR202003767867253 (82); |
| V3 loop glycan | PGT121 | 22 days | NCT02960581 (83); |
| | 10-1074 | 24 days; 73.5 days (-LS) | NCT02511990 (78, 84); |
| gp120 outer domain | 2G12 | 16.5 days[2] | (85) |

[1]*AAV delivery system.*
[2]*tested in HIV-infected participants.*
*NA, Not available.*

Importantly, VRC01 retained its expected neutralizing activity in participants' serum and no ADA responses were detected over the course of multiple infusions. In addition, a study of VRC01 in infants born to HIV-1 infected mothers is ongoing [IMPAACT P1112 (NCT02256631)].

VRC01 was further tested in two similar clinical trials, ACTG A5340 [NCT02463227] and NIH 15-I-0140 [NCT02471326], which were reported together and in which fully suppressed patients on stable ART underwent an analytic treatment interruption (ATI) after receiving VRC01 at a dose of 40 mg/kg (90). Disappointingly, viral rebound occurred despite VRC01 serum concentrations above 50 μg/ml with a mean time to rebound of 4 to 6 weeks. VRC01 was also found to exert selection pressure on emergent viruses which raises concerns about the development of resistance during treatment or prophylactic use.

## 3BNC117

3BNC117 is a more potent and broad CD4bs bnAb than VRC01 and was isolated from a chronically HIV-infected donor with high serum neutralization activity (21). In a first in human open-label study [NCT02018510], 3BNC117 was found to be safe and well-tolerated in HIV-infected participants and it was observed that a single IV dose of 30 mg/kg reduced viral loads of viremic participants for up to 28 days post-infusion (77). In HIV-uninfected participants, 3BNC117 is also safe and well tolerated across a range of doses *via* both the IV and SC routes and has a serum half-life of approximately 17 days (77, 91).

## VRC07-523LS

VRC07 is a CD4bs targeting bnAb that was cloned from the same HIV-infected donor from whom VRC01 was isolated. The VRC07 heavy chain was identified by deep sequencing based on its similarity to VRC01 and paired with the VRC01 light chain (92). VRC07 was then engineered with a series of mutations (called 523) which increased the breadth and potency compared to the parental antibody. As had also been done to VRC01 (73), modifications to the antibody Fc domain were introduced to improve antibody half-life. A common two amino acid substitution (M428L/N434S, referred to as "LS") increases the antibody's binding affinity for the neonatal Fc-receptor (FcRn), resulting in increased recirculation of functional IgG (93, 94) thereby prolonging the *in vivo* half-life. *In vitro*, VRC07-523LS is 5-to 8-fold more potent than VRC01, as well as broader, with an $IC_{50} < 1$ μg/ml against 92% of HIV-1 pseudoviruses from diverse clades (92).

A phase 1, first in human dose-escalation study of VRC07-523LS, [VRC 605 (NCT03015181)] has been completed in healthy, HIV-uninfected adults and evaluated the safety, tolerability, and PK of one to three administrations of the antibody (75). The doses evaluated ranged from a single administration of 1 mg/kg to 40 mg/kg IV, as well as three administrations (every 90 days) of 5 mg/kg SC and 20 mg/kg IV. VRC07-523LS was found to be safe and well-tolerated with a promising PK profile.

The HVTN 127/HPTN 087 trial (NCT03387150), which opened in February 2018, enrolled a total of 144 healthy, HIV-uninfected adult participants who received multiple injections of VRC07-523LS administered *via* IV, SC, and IM routes at a range of doses. The primary objectives are to assess safety and tolerability of repeated IV, SC, or IM administrations of VRC07-523LS as well as to characterize serum levels over time for the different doses and routes of administration. Additional objectives include building a population PK model of VRC07-523LS, and determining if ADA emerge in response to repeated administrations. A companion study, HVTN 128 (NCT03735849), is assessing the PK of VRC07-523LS in mucosal secretions (semen, cervical secretions, and rectal mucous) and mucosal biopsies (rectal, cervical, and vaginal tissue biopsies). Both studies have completed all follow-up visits and are in the analysis phase. Preliminary data from HVTN 127/HPTN 087 were presented at the virtual R4P conference in January 2021 and it was reported that VRC07-523LS was safe and well-tolerated with a serum half-life of about 40 days (76).

## N6

Another, even broader CD4bs targeting bnAb has been isolated from an HIV-infected donor found to have potent neutralizing serum activity and is called N6 (95). *In vitro*, N6 was found to

neutralize 98% of 181 pseudoviruses at an $IC_{50}$ < 50 μg/ml, including several isolates which are resistant to other VRC01-class bnAbs. Overall, N6 had a median $IC_{50}$ of 0.038 μg/ml. N6 was synthesized as an IgG1 with the –LS mutation to increase its *in vivo* half-life and administered in a first in human study [VRC 609 (NCT03538626)] at doses ranging from 5 mg/kg to 40 mg/kg. Preliminary data were presented at CROI 2020 and it was reported that N6LS was safe and well-tolerated with a half-life exceeding 30 days (79).

## V3 Glycan bnAbs

### PGT121

PGT121 was originally isolated from an HIV-infected donor in the IAVI Protocol G African cohort and was found to target the V3 glycan region on the gp120 Env protein. This epitope includes both peptide and glycan elements and is centered on the conserved residue N332 (96, 97). Although its coverage is somewhat less broad when assessed in *in vitro* pseudovirus neutralization assays (63% for PGT121 *vs.* 93% for VRC01 at an $IC_{50}$ < 50 μg/ml), PGT121 has about 10-fold higher median neutralizing potency than VRC01 and about 100-fold higher potency than first generation mAbs such as 2G12, b12, or 4E10 (18).

PGT121 has been tested in a phase 1 study called T001 which was a randomized, placebo-controlled trial of the safety, PK, and antiviral activity of this bnAb in both HIV-uninfected and HIV-infected adults [NCT 02960581]. IV infusions and SC injections were found to be safe and well-tolerated in all participants (83). The median half-life of PGT121 during the elimination phase was approximately 23 days (range 19 to 26 days).

### 10-1074

10-1074 was isolated from the same clade A infected African donor as PGT121 (13). Like PGT121, 10-1074 recognizes an epitope on the gp120 V3 outer domain that includes both peptides and glycans and is centered on the conserved amino acid residue N332 (98, 99). When tested against large panels of HIV-1 pseudoviruses *in vitro*, 10-1074 neutralized 65% of 306 strains comprising 13 subtypes with an average 80% inhibitory concentration ($IC_{80}$) titer of 0.18 μg/ml (84).

10-1074 has been tested in both HIV-infected and HIV-uninfected participants and found to be safe and well-tolerated at doses ranging from 3 mg/kg to 30 mg/kg [NCT02511990] (84). Amongst HIV-infected individuals with detectable viremia, 10-1074 infusion was found to induce a rapid decrease in plasma viral load, with one participant having a virologic response that was sustained for 58 days following a 30 mg/kg IV infusion.

## V2 Glycan bnAbs

### PGDM1400

PGDM1400 was isolated from another HIV-infected donor from the IAVI Protocol G African cohort and was found to interact with glycans in the region of residue N160 on the V2 loop of gp120 Env (100). PGDM1400 binding is highly quaternary-structure dependent and this bnAb is exceptionally potent, with 83% coverage of a globally representative panel of pseudoviruses at a median $IC_{50}$ of 0.003 μg/ml. Compared to three of the CD4bs antibodies (VRC01, VRC07, and 3BNC117), PGDM1400 is 10 to 100-fold more potent (18, 21, 100).

PGDM1400 has been tested in a phase 1 study called T002 which is a phase 1 randomized placebo-controlled clinical trial of the safety, pharmacokinetics, and antiviral activity of this bnAb in both HIV-uninfected and HIV-infected adults. [NCT03205917]. This study also tested the dual combination of PGDM1400 + PGT121 and a triple combination with the addition of VRC07-523LS. Results from this study are expected soon.

### CAP256

Another V2 loop targeting bnAb was isolated from an individual in the Centre for the AIDS Programme of Research in South Africa (CAPRISA) 002 Acute Infection study (101). This patient was infected with a clade C isolate and then superinfected with another clade C isolate and found to have broad serum neutralization activity (102, 103). One bnAb isolated was called CAP256-VRC26.25 and found to be exceptionally potent, especially against clade C isolates which predominate in southern Africa (62). A variant of this bnAb (CAP256V2LS) has been modified slightly to improve manufacturability and to include the –LS mutation, and is being tested in humans in a single-center phase 1 clinical trial called CAPRISA 012 [PACTR202003767867253] (82). Subsequent groups in CAPRISA 012 will evaluate CAP256V2LS in combination with VRC07-523LS and/or PGT121 (82).

## MPER bnAbs

### 10E8

Amongst the broadest in terms of overall global viral coverage are MPER targeting bnAbs. 10E8, like other bnAbs, was isolated from an HIV-infected donor with high serum neutralization activity and was found to bind to the same MPER gp41 epitopes as 4E10 (104). *In vitro* studies found that 10E8 did not bind phospholipids and did not bind to HEp-2 cells or a panel of autoantigens (104), unlike other MPER-targeting antibodies. A series of variants of 10E8 were developed for increased solubility as well as manufacturing ease (105). In NIH 18-I-0113 [NCT03565315], a leading candidate that had been engineered for a longer half-life (with the –LS mutation), 10E8VLS, was found to have a disappointing PK profile in terms of *in vivo* half-life. More concerning, however, was that one of the eight participants who received a single SC injection of 5 mg/kg 10E8VLS experienced severe injection site erythema and was found to have panniculitis. This led to the suspension of the study (80) and may have been due to a lipid-binding cross-reaction, although the mechanism remains under investigation.

## AMP Efficacy Trials

As VRC01 was found to be safe and well-tolerated in healthy HIV-uninfected volunteers and had modest anti-viral effects in viremic HIV-infected participants, an important question was whether VRC01 could prevent HIV infection (106). The NIAID-funded HIV Vaccine Trials Network (HVTN) and HIV Prevention Trials Network (HPTN) therefore collaborated on the design and conduct of the two Antibody Mediated Prevention

(AMP) trials, HVTN 704/HPTN 085 (NCT02716675) and HVTN 703/HPTN 081 (NCT02568215) (107). HVTN 704/HPTN 085 enrolled 2,699 cisgender men and transgender (TG) people who have sex with men in Brazil, Peru, Switzerland, and the US (108) while HVTN 703/HPTN 081 enrolled 1,924 cisgender women in Botswana, Kenya, Malawi, Mozambique, South Africa, Tanzania, and Zimbabwe (109).

The underlying hypothesis of the coordinated AMP trials was that passive transfer of an HIV-1 bnAb would be efficacious at preventing sexual transmission of HIV-1 in exposed individuals. A key secondary endpoint was to determine if an association existed between serum neutralization activity and the $ID_{50}$ or $ID_{80}$ titers required for protection as had been shown in NHP/SHIV models (41, 110). Based on the NHP models, it was estimated that protection would be achieved at serum antibody concentrations 50-100-fold higher than the measured $IC_{50}$ of the challenge (infecting) virus (32). Based on *in vitro* neutralization profiles of panels of HIV-1 isolates, it was anticipated that between 65% (clade C) and 81% (clade B) of infecting viruses would be susceptible to VRC01.

The two trials were each designed with 90% power to detect prevention efficacy (PE) of 60% comparing the two VRC01 groups *vs* the placebo group, based on an assumption of an annual background HIV-1 incidence of 5.5% in HVTN 703/HPTN 081 and 3% in HVTN 704/HPTN 085 and a dropout rate of 10% of participants per year (107). Participants were randomly assigned to one of three groups at a 1:1:1 ratio of VRC01 10 mg/kg, VRC01 30 mg/kg, or placebo. IV administration of VRC01 or placebo occurred every eight weeks for a total of 10 infusions. Pre-exposure prophylaxis (PrEP) was encouraged by the trial investigators and access to emtricitabine (FTC)/tenofovir disoproxil fumarate (TDF) was facilitated by the study.

Study conduct was very high quality. Loss to follow-up was low (9.4% per year in HVTN 704/HPTN 085 versus 6.3% per year in HVTN 703/HPTN 081) and 79% of participants in HVTN 704/HPTN 085 and 76% in HVTN 703/HPTN 081 received all 10 infusions (74). Rates of PrEP usage differed considerably between the two studies demonstrating some of the challenges in increasing PrEP uptake. Effective concentrations of FTC/TDF were detected in 28.9% of person-years in HVTN 704/HPTN 085 but only 0.4% of person-years in HVTN 703/HPTN 081 (74).

As had been noted in the Phase 1 studies, VRC01 infusions were safe and generally very well-tolerated. Moderate to severe adverse events which were deemed related to VRC01 were noted in 1.2% of participants in HVTN 704/HPTN 085 versus 3.0% of the participants in HVTN 703/HPTN 081. Infusion reactions were seen in a small number of participants and were generally mild to moderate, and typically resolved quickly (111).

The overall results from the AMP trials, however, were a disappointment. At week 80, the PE for the combined VRC01 groups *versus* placebo was 26.6% in HVTN 704/HPTN 085 and 8.8% in HVTN 703/HPTN 081 (p=0.15 *vs* placebo for HVTN 704/HPTN 085 and p=0.70 for HVTN 703/HPTN 081, respectively) (74). PE did not differ significantly by dose in either study. In HVTN 704/HPTN 085, PE was 22.4% in the low dose VRC01 group versus 30.9% in the high dose group, compared with –9.3% in the 10 mg/kg group, and 27.0% in the 30 mg/kg group in HVTN 703/HPTN 081 (74). While the point estimates of PE for the higher dose VRC01 groups are similar to the vaccine efficacy reported in the RV144 trial [31.2% (112)], the 95% confidence intervals (CIs) of the PEs in the AMP studies were quite large and all crossed the null.

Secondary analyses, however, demonstrated that for infecting HIV-1 isolates that were highly sensitive to VRC01 neutralization (prospectively defined as an $IC_{80}$ <1 μg/mL) protective efficacy was high, with an estimated PE of 75.4% and 95% CI from 45.5% to 88.9% (74). The majority of infecting HIV-1 isolates had $IC_{80}$ > 1 μg/mL (55% had $IC_{80}$ > 3 μg/mL) and there was no statistically significant protective efficacy seen against these more resistant viruses (74). Taken together, the infecting viruses in the combined VRC01 groups had a geometric mean $IC_{80}$ of 8.4 μg/mL versus 3.5 μg/mL in the placebo group (74), suggesting there was selection pressure on infecting viruses by VRC01 during acquisition. This immunologic selection pressure was also found to have an effect on viremia at the time of diagnosis amongst VRC01 recipients who were infected with highly sensitive strains HIV-1 with geometric mean viral loads of 9,800 copies/mL compared to 176,000 copies/mL for placebo recipients (74). This effect of mAb administration was not seen amongst participants infected with more resistant HIV-1 isolates.

These data provide several important lessons to help guide future trials. The AMP studies successfully enrolled at-risk participants and despite the complexities of intravenous infusions every two months, retention and engagement was high throughout the study. They also demonstrated the key proof-of-principle that a bnAb can prevent HIV infection in people. However, while VRC01 can prevent sexual HIV-1 acquisition, most circulating viruses have neutralization levels high enough to make them essentially resistant. Furthermore, *in vitro* neutralization sensitivity is a useful biomarker for preventive efficacy *in vivo*, although the threshold for protection (< 1 μg/mL) is considerably higher than had been predicted (10 μg/mL). These predictions were primarily based on *in vitro* testing of VRC01 against panels of HIV-1 Env pseudoviruses. Several studies have demonstrated that pseudoviruses produced *via* transfection of 293T cells are considerably more sensitive to neutralization by patient serum and bnAbs when compared to matched isolates expanded in peripheral blood mononuclear cells (PBMC) (113, 114). This point should be taken into consideration when incorporating *in vitro* neutralization data into clinical efficacy estimations for HIV-1 bnAbs. While bnAbs that are more potent and have broader coverage than VRC01 have been identified, it remains to be determined whether the threshold of protection identified by the AMP study will translate to other bnAbs targeting the CD4bs or other epitopes, or whether this threshold can be reliably achieved and maintained through repeated passive infusions. The AMP study suggests that a single monovalent bnAb is highly unlikely to have the breadth and potency required, but

nonetheless, the results do provide a benchmark for future bnAb studies to build upon.

## Clinical Testing of bnAb Combinations

To address the significant challenges of breadth and potency, combinations of bnAbs are being tested in early phase studies (**Table 2**). As bnAbs which target different regions of the Env protein have been found to have additive effects on inhibition *in vitro* (64), the combinations moving forward are complementary with respect to coverage. This concept is supported by NHP challenge studies showing that a combination of 2 bnAbs fully protected macaques against a mixed SHIV challenge when neither mAb administered alone was able to do so (39).

### HVTN130/HPTN089

In HVTN130/HPTN089 [NCT03928821], combinations of two or three complementary bnAbs are being tested for safety and PK parameters. The engineered CD4-binding site mAb VRC07-523LS is the broadest of the mAbs in this study and has the longest half-life due to the –LS mutation. Individually, PGT121 and PGDM1400 display more limited breadth than VRC07-523LS, but together they exhibit complementary coverage against diverse HIV-1 strains. Furthermore, they are remarkably potent, having amongst the lowest median $IC_{80}$ titers among the bnAbs identified to date (18). In silico modeling suggests that the triple combination of VRC07-523LS + PGT121 + PGDM1400 has >90% coverage of global isolates using a cutoff of $ID_{80}$ of 1 μg/ml and >80% coverage with a cutoff of 0.1 μg/ml (62–64). 10-1074 is being tested in this protocol as an alternative V3 glycan bnAb to compare versus PGT121 in combination with VRC07-523LS. This study is fully enrolled and data are expected to be presented soon.

### HVTN136/HPTN092

In HVTN136/HPTN092 [NCT04212091], an –LS variant of the V3 glycan targeting mAb PGT121 (PGT121.414.LS) is being tested alone and in a combination regimen, again with VRC07-523LS as the CD4bs targeting bnAb. The study is currently enrolling and the first groups will provide safety and PK data for PGT121.414.LS alone, which is being administered to people for the first time in this study, at doses ranging from 3 mg/kg to 30 mg/kg IV and 5mg/kg SC. The subsequent groups will combine the two mAbs at 20 mg/kg IV versus 5 mg/kg SC.

### IAVI C-100

A small single-center phase 1 study which combined the 3BNC117 and 10-1074 bnAbs was conducted and demonstrated that doses ranging from 3 mg/kg to 10 mg/kg were safe and well-tolerated (91). Importantly, there appeared to be no difference in the half-lives of the two bnAbs compared to when they were administered alone. This bnAb combination was also shown to maintain suppression of viremia and to prevent the emergence of resistant variants in HIV-1 infected individuals undergoing ART interruption (116), and to significantly reduce viral loads in viremic patients harboring dual sensitive viruses for up to 3 months following the last infusion (115). To improve the PK profile of this combination, -LS variants of the two bnAbs have been engineered and are being tested in a study called IAVI C100 [NCT04173819]. This study will evaluate the safety, tolerability, and PK of 3BNC117-LS-J and 10-1074-LS-J administered alone and in combination *via* IV and SC routes (78). The study is currently enrolling.

# FUTURE DIRECTIONS

The results from the AMP trials highlight that bnAbs with exceptional levels of breadth, potency and *in vivo* durability will be needed to have an appreciable impact on the prevention of HIV-1 acquisition. Efforts continue to identify new bnAbs with enhanced neutralization profiles that may be viable for clinical development either as single drug products, or to complement existing bnAbs for use in combination cocktails

**TABLE 2** | Selected Clinical Trials of bnAb Combinations.

| Name | bnAbs | Env region targeted | Reference |
|---|---|---|---|
| IAVI T002[1] | PGT121 | V3 glycan | NCT03205917 (83); |
| | PGDM1400 | V1V2 glycan | |
| YCO-0899[2] | 3BNC117 | CD4-binding site | NCT02824536 (91); |
| MCA-0906[3] | 10-1074 | V3 glycan | NCT02825797 (115); |
| HVTN130/HPTN089 | VRC07-523LS | CD4-binding site | NCT03928821 |
| | PGT121 or 10-1074 | V3 glycan | |
| | PGDM1400 | V1V2 glycan | |
| HVTN136/HPTN092 | VRC07-523LS | CD4-binding site | NCT04212091 |
| | PGT121.141.LS | V3 glycan | |
| IAVI C100 | 3BNC117-LS-J | CD4-binding site | NCT04173819 (78); |
| | 10-1074-LS-J | V3 glycan | |
| CAPRISA 012B | CAP256V2LS | V1V2 glycan | PACTR202003767867253 (82); |
| | VRC07-523LS | CD4-binding site | |
| | PGT121 | V3 glycan | |

[1]*Included both HIV-infected and HIV-uninfected participants.*
[2]*HIV-uninfected participants.*
[3]*HIV-infected participants.*

(117–119). Antibody engineering strategies are also being employed to improve the breadth and potency of existing bnAbs. Structure-guided rational design modifications of the antigen binding Fab domains have been successfully used to enhance interactions with the Env trimer resulting in improved neutralizing activity (92, 120, 121). Increasing the *in vivo* half-life of antibodies can also be achieved through engineering modifications to the antibody Fc domain, most notably the –LS mutations discussed above (93, 94). Multiple bnAbs currently in clinical development are being tested with the LS mutations, and it is hoped that such improvements in the pharmacokinetic profiles of bnAbs may make it possible to achieve and maintain therapeutic levels with lower-dose and less frequent administrations. Strategies for persistent expression of bnAbs *in vivo* by vectored antibody gene delivery using rAAV have shown promise in humanized mouse and NHP models of infection (122), and one clinical trial has evaluated rAAV1 delivery of the V2-glycan targeting bnAb PG9 in humans (NCT01937455) (81). While this study demonstrated that rAAV delivery was safe and well tolerated, there was no detection of PG9 in serum by ELISA, and the development of ADA and anti-vector antibody responses was observed in several volunteers, thus highlighting the challenges that remain for developing such approaches. A second phase I trial assessing rAAV8 delivery of the CD4bs targeting bnAb VRC07 in HIV-1-infected adults on antiretroviral therapy is currently ongoing (NCT03374202). Several initial proof-of-concept studies in mice have also evaluated the approach of gene-editing primary B cells to express bnAb antibody receptors on the cell surface (123, 124). Gene-edited B cells passively infused into wildtype recipients have the capacity to respond to vaccination with cognate antigen resulting in clonal expansion, affinity maturation, expression of high levels of serum bnAb, and establishment of durable memory. Future studies using the NHP/SHIV model will be important for further evaluating the potential of such approaches to provide durable sterilizing protection.

HIV-1 Env sequence diversity remains a major obstacle for the clinical development of antibody-based prevention strategies. As previously discussed, clinical trials are ongoing to assess antibody cocktails containing two or three bnAbs targeting independent epitopes on the Env trimer to provide greater coverage against circulating isolates and to circumvent viral escape. A parallel strategy being actively explored is to engineer bi- or tri-specific antibodies that combine Fabs from different bnAbs onto the same antibody molecule (125). Multiple bi-specific antibodies targeting various epitope combinations have demonstrated enhanced breadth and potency compared to single bnAb molecules in *in vitro* testing (95, 126). For example, the bi-specific antibody 10E8.4/iMab which targets the MPER epitope of Env and the host CD4 molecule has demonstrated exquisite breadth and potency when tested against large multiclade panels of viruses (100% breadth with mean $IC_{50}$ values of 0.002 μg/ml) and protection of humanized mice against HIV-1 infection (95). This molecule is currently being evaluated in a human clinical trial in HIV-1-infected and uninfected volunteers (NCT03875209). Another example is a tri-specific antibody that contains Fabs derived from the CD4bs antibody VRC01, the V2-glycan antibody PGDM1400 and the MPER antibody 10E8 (127). This antibody has also exhibited excellent neutralization breadth and potency *in vitro*, demonstrated complete protection in NHP against a mixed SHIV challenge, and is also currently being evaluated in a phase 1 human clinical trial (NCT03705169). Another strategy has been to engineer entry inhibitor molecules that target both the primary CD4 receptor and co-receptor binding sites on Env which are highly conserved across strains of HIV-1. One example in this class of molecules is eCD4-Ig which combines domains 1 and 2 of human CD4 fused to an IgG Fc with an attached sulfated CCR5-mimetic peptide. This molecule has also demonstrated 100% neutralization against all HIV-1, HIV-2, and SIV strains tested to date, and confers robust protection against SHIV and SIV challenges when delivered using rAAV vectors (128). While these strategies have theoretical benefits over cocktail combinations of individual bnAbs in regards to manufacturing and the complexity of clinical development, it remains to be determined how such engineered molecules will compare to naturally occurring antibodies in terms of pharmacokinetics, safety profiles, and the potential for inducing ADA responses in humans.

Currently the majority of bnAbs in clinical development are being evaluated as IgG1. Whether bnAbs expressed as IgA, IgM, or other IgG subclasses exhibit enhanced neutralization and/or effector activity is an area of active investigation. Indeed, several studies have demonstrated that certain bnAbs expressed as IgG3 have an increased ability to recruit ADCC and/or phagocytosis compared to their IgG1 counterparts (129, 130). These enhanced activities may be correlated with longer hinge length between the Fab and Fc domains and potentially higher affinity for FcγR-IIIA. Additional strategies in Fc engineering are being explored to increase antibody affinity to FcγRs expressed on innate immune cells and augment antibody-dependent effector activities. Modifications such as the AAA (S298A/E333A/K334A) or GASDALIE (G236A/S239D/A330L/I332E) mutations have been shown to increase antibody affinity for Fcγ-RIIIA and augment ADCC activity (131). Modifications of Fc-glycosylation patterns have also been demonstrated to enhance ADCC and ADCP activities (132). Additional evaluation in the NHP/SHIV model will be important to determine whether bnAbs expressed as alternative isotypes, IgG subclasses, or with modified Fc domains exhibit enhanced anti-viral protection *in vivo*, especially for therapeutic strategies in which activation of innate effector functions may be critical for eliminating infected cells. Additional understanding of the ability of bnAbs to inhibit cell-to-cell transmission versus cell-free transmission is also needed (133). While *in vitro* analyses have suggested that bnAbs may be less effective at inhibiting cell-to-cell transmission (134, 135), this may be dependent on the specific bnAb and/or epitope target, the virus strain and the degree of steric hindrance encountered at the virological synapse. Further insight into the mechanisms of cell-to-cell spread *in vivo* and the inhibitory potential of specific bnAbs will further inform optimal combinations for prevention and treatment strategies.

## CONCLUSIONS

HIV-1 bnAbs have shown significant promise for their potential use in the prevention and treatment of HIV-1 infection. Multiple bnAbs and bnAb combinations have been tested in human clinical trials and demonstrated favorable safety and pharmacokinetic profiles. The results from the first AMP efficacy trials have provided proof-of-concept that bnAbs can prevent acquisition of HIV-1, yet they also highlight the obstacles that must be addressed before bnAb passive immunization strategies can become integrated as a tool for standard clinical care. Combinations of highly potent bnAbs or engineered variants targeting multiple epitopes will likely be required to reliably inhibit the global diversity of circulating viruses encountered in nature and impede the development of resistance. Improving pharmacokinetic profiles and delivery methods such that bnAbs may be self-administered every 4-6 months by subcutaneous injection to attain persistent protective levels of serum neutralizing activity is a highly desired goal that the field continues to work towards. Additional efforts to optimize the Fc domain of bnAbs to enhance the activation of innate effector functions may further improve efficacy profiles, especially in the setting of therapeutic treatment of HIV-1 infection.

## AUTHOR CONTRIBUTIONS

All authors listed have made a substantial, direct, and intellectual contribution to the work, and approved it for publication.

## FUNDING

This work was supported by the Bill and Melinda Gates Foundation Collaboration for AIDS Vaccine Discovery (CAVD) grant #OPP1146996 (MS) and the National Institute of Allergy and Infectious Diseases (NIAID) grant # UM1 AI069412 (SW).

## REFERENCES

1. World Health Organization. *Data and Statistics*. Geneva, Switzerland: World Health Organization (2020).
2. Casadevall A, Dadachova E, Pirofski LA. Passive Antibody Therapy for Infectious Diseases. *Nat Rev Microbiol* (2004) 2:695–703. doi: 10.1038/nrmicro974
3. Graham BS, Ambrosino DM. History of Passive Antibody Administration for Prevention and Treatment of Infectious Diseases. *Curr Opin HIV AIDS* (2015) 10:129–34. doi: 10.1097/COH.0000000000000154
4. Walker LM, Burton DR. Passive Immunotherapy of Viral Infections: 'Super-Antibodies' Enter the Fray. *Nat Rev Immunol* (2018) 18:297–308. doi: 10.1038/nri.2017.148
5. Kumar D, Gauthami S, Bayry J, Kaveri SV, Hegde NR. Antibody Therapy: From Diphtheria to Cancer, COVID-19, and Beyond. *Monoclon Antib Immunodiagn Immunother* (2021) 40:36–49. doi: 10.1089/mab.2021.0004
6. Mehandru S, Vcelar B, Wrin T, Stiegler G, Joos B, Mohri H, et al. Adjunctive Passive Immunotherapy in Human Immunodeficiency Virus Type 1-Infected Individuals Treated With Antiviral Therapy During Acute and Early Infection. *J Virol* (2007) 81:11016–31. doi: 10.1128/JVI.01340-07
7. Trkola A, Kuster H, Rusert P, Joos B, Fischer M, Leemann C, et al. Delay of HIV-1 Rebound After Cessation of Antiretroviral Therapy Through Passive Transfer of Human Neutralizing Antibodies. *Nat Med* (2005) 11:615–22. doi: 10.1038/nm1244
8. Mascola JR, D'Souza P, Gilbert P, Hahn BH, Haigwood NL, Morris L, et al. Recommendations for the Design and Use of Standard Virus Panels to Assess Neutralizing Antibody Responses Elicited by Candidate Human Immunodeficiency Virus Type 1 Vaccines. *J Virol* (2005) 79:10103–7. doi: 10.1128/JVI.79.16.10103-10107.2005
9. Sarzotti-Kelsoe M, Bailer RT, Turk E, Lin CL, Bilska M, Greene KM, et al. Optimization and Validation of the TZM-Bl Assay for Standardized Assessments of Neutralizing Antibodies Against HIV-1. *J Immunol Methods* (2014) 409:131–46. doi: 10.1016/j.jim.2013.11.022
10. Doria-Rose NA, Klein RM, Daniels MG, O'Dell S, Nason M, Lapedes A, et al. Breadth of Human Immunodeficiency Virus-Specific Neutralizing Activity in Sera: Clustering Analysis and Association With Clinical Variables. *J Virol* (2010) 84:1631–6. doi: 10.1128/JVI.01482-09
11. Li Y, Migueles SA, Welcher B, Svehla K, Phogat A, Louder MK, et al. Broad HIV-1 Neutralization Mediated by CD4-Binding Site Antibodies. *Nat Med* (2007) 13:1032–4. doi: 10.1038/nm1624
12. Sather DN, Armann J, Ching LK, Mavrantoni A, Sellhorn G, Caldwell Z, et al. Factors Associated With the Development of Cross-Reactive Neutralizing Antibodies During Human Immunodeficiency Virus Type 1 Infection. *J Virol* (2009) 83:757–69. doi: 10.1128/JVI.02036-08
13. Simek MD, Rida W, Priddy FH, Pung P, Carrow E, Laufer DS, et al. Human Immunodeficiency Virus Type 1 Elite Neutralizers: Individuals With Broad and Potent Neutralizing Activity Identified by Using a High-Throughput Neutralization Assay Together With an Analytical Selection Algorithm. *J Virol* (2009) 83:7337–48. doi: 10.1128/JVI.00110-09
14. Scheid JF, Mouquet H, Feldhahn N, Walker BD, Pereyra F, Cutrell E, et al. A Method for Identification of HIV Gp140 Binding Memory B Cells in Human Blood. *J Immunol Methods* (2009) 343:65–7. doi: 10.1016/j.jim.2008.11.012
15. Corti D, Langedijk JP, Hinz A, Seaman MS, Vanzetta F, Fernandez-Rodriguez BM, et al. Analysis of Memory B Cell Responses and Isolation of Novel Monoclonal Antibodies With Neutralizing Breadth From HIV-1-Infected Individuals. *PloS One* (2010) 5:e8805. doi: 10.1371/journal.pone.0008805
16. Mouquet H, Klein F, Scheid JF, Warncke M, Pietzsch J, Oliveira TY, et al. Memory B Cell Antibodies to HIV-1 Gp140 Cloned From Individuals Infected With Clade A and B Viruses. *PloS One* (2011) 6:e24078. doi: 10.1371/journal.pone.0024078
17. Scheid JF, Mouquet H, Feldhahn N, Seaman MS, Velinzon K, Pietzsch J, et al. Broad Diversity of Neutralizing Antibodies Isolated From Memory B Cells in HIV-Infected Individuals. *Nature* (2009) 458:636–40. doi: 10.1038/nature07930
18. Walker LM, Huber M, Doores KJ, Falkowska E, Pejchal R, Julien JP, et al. Broad Neutralization Coverage of HIV by Multiple Highly Potent Antibodies. *Nature* (2011) 477:466–70. doi: 10.1038/nature10373
19. Walker LM, Phogat SK, Chan-Hui PY, Wagner D, Phung P, Goss JL, et al. Broad and Potent Neutralizing Antibodies From an African Donor Reveal a New HIV-1 Vaccine Target. *Science* (2009) 326:285–9. doi: 10.1126/science.1178746
20. Wu X, Yang ZY, Li Y, Hogerkorp CM, Schief WR, Seaman MS, et al. Rational Design of Envelope Identifies Broadly Neutralizing Human Monoclonal Antibodies to HIV-1. *Science* (2010) 329:856–61. doi: 10.1126/science.1187659
21. Scheid JF, Mouquet H, Ueberheide B, Diskin R, Klein F, Oliveira TY, et al. Sequence and Structural Convergence of Broad and Potent HIV Antibodies That Mimic CD4 Binding. *Science* (2011) 333:1633–7. doi: 10.1126/science.1207227
22. Sok D, Burton DR. Recent Progress in Broadly Neutralizing Antibodies to HIV. *Nat Immunol* (2018) 19:1179–88. doi: 10.1038/s41590-018-0235-7
23. Kwong PD, Mascola JR. Human Antibodies That Neutralize HIV-1: Identification, Structures, and B Cell Ontogenies. *Immunity* (2012) 37:412–25. doi: 10.1016/j.immuni.2012.08.012

24. Marsden MD. Benefits and Limitations of Humanized Mice in HIV Persistence Studies. *Retrovirology* (2020) 17:7. doi: 10.1186/s12977-020-00516-2
25. Deruaz M, Moldt B, Le KM, Power KA, Vrbanac VD, Tanno S, et al. Protection of Humanized Mice From Repeated Intravaginal HIV Challenge by Passive Immunization: A Model for Studying the Efficacy of Neutralizing Antibodies *In Vivo*. *J Infect Dis* (2016) 214:612–6. doi: 10.1093/infdis/jiw203
26. Sun M, Li Y, Yuan Z, Lu W, Kang G, Fan W, et al. VRC01 Antibody Protects Against Vaginal and Rectal Transmission of Human Immunodeficiency Virus 1 in Hu-BLT Mice. *Arch Virol* (2016) 161:2449–55. doi: 10.1007/s00705-016-2942-4
27. Klein F, Halper-Stromberg A, Horwitz JA, Gruell H, Scheid JF, Bournazos S, et al. HIV Therapy by a Combination of Broadly Neutralizing Antibodies in Humanized Mice. *Nature* (2012) 492:118–22. doi: 10.1038/nature11604
28. Stoddart CA, Galkina SA, Joshi P, Kosikova G, Long BR, Maidji E, et al. Efficacy of Broadly Neutralizing Monoclonal Antibody PG16 in HIV-Infected Humanized Mice. *Virology* (2014) 462-463:115–25. doi: 10.1016/j.virol.2014.05.036
29. Lin A, Balazs AB. Adeno-Associated Virus Gene Delivery of Broadly Neutralizing Antibodies as Prevention and Therapy Against HIV-1. *Retrovirology* (2018) 15:66. doi: 10.1186/s12977-018-0449-7
30. Akkina R, Allam A, Balazs AB, Blankson JN, Burnett JC, Casares S, et al. Improvements and Limitations of Humanized Mouse Models for HIV Research: NIH/NIAID "Meet the Experts" 2015 Workshop Summary. *AIDS Res Hum Retroviruses* (2016) 32:109–19. doi: 10.1089/aid.2015.0258
31. Garber DA, Adams DR, Guenthner P, Mitchell J, Kelley K, Schoofs T, et al. Durable Protection Against Repeated Penile Exposures to Simian-Human Immunodeficiency Virus by Broadly Neutralizing Antibodies. *Nat Commun* (2020) 11:3195. doi: 10.1038/s41467-020-16928-9
32. Pegu A, Borate B, Huang Y, Pauthner MG, Hessell AJ, Julg B, et al. A Meta-Analysis of Passive Immunization Studies Shows That Serum-Neutralizing Antibody Titer Associates With Protection Against SHIV Challenge. *Cell Host Microbe* (2019) 26:336–346 e333. doi: 10.1016/j.chom.2019.08.014
33. Gautam R, Nishimura Y, Pegu A, Nason MC, Klein F, Gazumyan A, et al. A Single Injection of Anti-HIV-1 Antibodies Protects Against Repeated SHIV Challenges. *Nature* (2016) 533:105–9. doi: 10.1038/nature17677
34. Pegu A, Yang ZY, Boyington JC, Wu L, Ko SY, Schmidt SD, et al. Neutralizing Antibodies to HIV-1 Envelope Protect More Effectively *In Vivo* Than Those to the CD4 Receptor. *Sci Transl Med* (2014) 6:243ra288. doi: 10.1126/scitranslmed.3008992
35. Shingai M, Donau OK, Plishka RJ, Buckler-White A, Mascola JR, Nabel GJ, et al. Passive Transfer of Modest Titers of Potent and Broadly Neutralizing Anti-HIV Monoclonal Antibodies Block SHIV Infection in Macaques. *J Exp Med* (2014) 211:2061–74. doi: 10.1084/jem.20132494
36. Julg B, Sok D, Schmidt SD, Abbink P, Newman RM, Broge T, et al. Protective Efficacy of Broadly Neutralizing Antibodies With Incomplete Neutralization Activity Against Simian-Human Immunodeficiency Virus in Rhesus Monkeys. *J Virol* (2017) 91:e01187–17. doi: 10.1128/JVI.01187-17
37. Julg B, Tartaglia LJ, Keele BF, Wagh K, Pegu A, Sok D, et al. Broadly Neutralizing Antibodies Targeting the HIV-1 Envelope V2 Apex Confer Protection Against a Clade C SHIV Challenge. *Sci Transl Med* (2017) 9:eaal1321. doi: 10.1126/scitranslmed.aal1321
38. Moldt B, Rakasz EG, Schultz N, Chan-Hui PY, Swiderek K, Weisgrau KL, et al. Highly Potent HIV-Specific Antibody Neutralization *In Vitro* Translates Into Effective Protection Against Mucosal SHIV Challenge *In Vivo*. *Proc Natl Acad Sci USA* (2012) 109:18921–5. doi: 10.1073/pnas.1214785109
39. Julg B, Liu PT, Wagh K, Fischer WM, Abbink P, Mercado NB, et al. Protection Against a Mixed SHIV Challenge by a Broadly Neutralizing Antibody Cocktail. *Sci Transl Med* (2017) 9:eaao4235. doi: 10.1126/scitranslmed.aao4235
40. Patel P, Borkowf CB, Brooks JT, Lasry A, Lansky A, Mermin J. Estimating Per-Act HIV Transmission Risk: A Systematic Review. *AIDS* (2014) 28:1509–19. doi: 10.1097/QAD.0000000000000298
41. Pegu A, Hessell AJ, Mascola JR, Haigwood NL. Use of Broadly Neutralizing Antibodies for HIV-1 Prevention. *Immunol Rev* (2017) 275:296–312. doi: 10.1111/imr.12511
42. Crowley AR, Ackerman ME. Mind the Gap: How Interspecies Variability in IgG and Its Receptors May Complicate Comparisons of Human and Non-Human Primate Effector Function. *Front Immunol* (2019) 10:697. doi: 10.3389/fimmu.2019.00697
43. Del Prete GQ, Lifson JD, Keele BF. Nonhuman Primate Models for the Evaluation of HIV-1 Preventive Vaccine Strategies: Model Parameter Considerations and Consequences. *Curr Opin HIV AIDS* (2016) 11:546–54. doi: 10.1097/COH.0000000000000311
44. Chang HW, Tartaglia LJ, Whitney JB, Lim SY, Sanisetty S, Lavine CL, et al. Generation and Evaluation of Clade C Simian-Human Immunodeficiency Virus Challenge Stocks. *J Virol* (2015) 89:1965–74. doi: 10.1128/JVI.03279-14
45. Li H, Wang S, Lee FH, Roark RS, Murphy AI, Smith J, et al. New SHIVs and Improved Design Strategy for Modeling HIV-1 Transmission, Immunopathogenesis, Prevention and Cure. *J Virol* (2021) 95:e00071–21. doi: 10.1101/2021.01.13.426578
46. O'Brien SP, Swanstrom AE, Pegu A, Ko SY, Immonen TT, Del Prete GQ, et al. Rational Design and *In Vivo* Selection of SHIVs Encoding Transmitted/Founder Subtype C HIV-1 Envelopes. *PloS Pathog* (2019) 15:e1007632. doi: 10.1371/journal.ppat.1007632
47. Tartaglia LJ, Chang HW, Lee BC, Abbink P, Ng'ang'a D, Boyd M, et al. Production of Mucosally Transmissible SHIV Challenge Stocks From HIV-1 Circulating Recombinant Form 01_AE Env Sequences. *PloS Pathog* (2016) 12:e1005431. doi: 10.1371/journal.ppat.1005431
48. Carpenter MC, Ackerman ME. Recent Insights Into Fc-Mediated Effector Responses to HIV-1. *Curr Opin HIV AIDS* (2020) 15:282–9. doi: 10.1097/COH.0000000000000638
49. Danesh A, Ren Y, Brad Jones R. Roles of Fragment Crystallizable-Mediated Effector Functions in Broadly Neutralizing Antibody Activity Against HIV. *Curr Opin HIV AIDS* (2020) 15:316–23. doi: 10.1097/COH.0000000000000644
50. Su B, Dispinseri S, Iannone V, Zhang T, Wu H, Carapito R, et al. Update on Fc-Mediated Antibody Functions Against HIV-1 Beyond Neutralization. *Front Immunol* (2019) 10:2968. doi: 10.3389/fimmu.2019.02968
51. Liu J, Ghneim K, Sok D, Bosche WJ, Li Y, Chipriano E, et al. Antibody-Mediated Protection Against SHIV Challenge Includes Systemic Clearance of Distal Virus. *Science* (2016) 353:1045–9. doi: 10.1126/science.aag0491
52. Lu CL, Murakowski DK, Bournazos S, Schoofs T, Sarkar D, Halper-Stromberg A, et al. Enhanced Clearance of HIV-1-Infected Cells by Broadly Neutralizing Antibodies Against HIV-1 *In Vivo*. *Science* (2016) 352:1001–4. doi: 10.1126/science.aaf1279
53. Hessell AJ, Hangartner L, Hunter M, Havenith CE, Beurskens FJ, Bakker JM, et al. Fc Receptor But Not Complement Binding is Important in Antibody Protection Against HIV. *Nature* (2007) 449:101–4. doi: 10.1038/nature06106
54. Hangartner L, Beauparlant D, Rakasz E, Nedellec R, Hoze N, McKenney K, et al. Effector Function Does Not Contribute to Protection From Virus Challenge by a Highly Potent HIV Broadly Neutralizing Antibody in Nonhuman Primates. *Sci Transl Med* (2021) 13:eabe3349. doi: 10.1126/scitranslmed.abe3349
55. Parsons MS, Lee WS, Kristensen AB, Amarasena T, Khoury G, Wheatley AK, et al. Fc-Dependent Functions are Redundant to Efficacy of Anti-HIV Antibody PGT121 in Macaques. *J Clin Invest* (2019) 129:182–91. doi: 10.1172/JCI122466
56. Wang P, Gajjar MR, Yu J, Padte NN, Gettie A, Blanchard JL, et al. Quantifying the Contribution of Fc-Mediated Effector Functions to the Antiviral Activity of Anti-HIV-1 IgG1 Antibodies *In Vivo*. *Proc Natl Acad Sci USA* (2020) 117:18002–9. doi: 10.1073/pnas.2008190117
57. Asokan M, Dias J, Liu C, Maximova A, Ernste K, Pegu A, et al. Fc-Mediated Effector Function Contributes to the *In Vivo* Antiviral Effect of an HIV Neutralizing Antibody. *Proc Natl Acad Sci USA* (2020) 117:18754–63. doi: 10.1073/pnas.2008236117
58. Moldt B, Schultz N, Dunlop DC, Alpert MD, Harvey JD, Evans DT, et al. A Panel of IgG1 B12 Variants With Selectively Diminished or Enhanced Affinity for Fcgamma Receptors to Define the Role of Effector Functions in Protection Against HIV. *J Virol* (2011) 85:10572–81. doi: 10.1128/JVI.05541-11
59. Richardson SI, Moore PL. Targeting Fc Effector Function in Vaccine Design. *Expert Opin Ther Targets* (2021). doi: 10.1080/14728222.2021.1907343
60. Bricault CA, Yusim K, Seaman MS, Yoon H, Theiler J, Giorgi EE, et al. HIV-1 Neutralizing Antibody Signatures and Application to Epitope-Targeted Vaccine Design. *Cell Host Microbe* (2019) 25:59–72.e58. doi: 10.1016/j.chom.2018.12.001

61. Doria-Rose NA, Bhiman JN, Roark RS, Schramm CA, Gorman J, Chuang GY, et al. New Member of the V1V2-Directed CAP256-VRC26 Lineage That Shows Increased Breadth and Exceptional Potency. *J Virol* (2016) 90:76–91. doi: 10.1128/JVI.01791-15
62. Wagh K, Bhattacharya T, Williamson C, Robles A, Bayne M, Garrity J, et al. Optimal Combinations of Broadly Neutralizing Antibodies for Prevention and Treatment of HIV-1 Clade C Infection. *PloS Pathog* (2016) 12:e1005520. doi: 10.1371/journal.ppat.1005520
63. Kong R, Louder MK, Wagh K, Bailer RT, deCamp A, Greene K, et al. Improving Neutralization Potency and Breadth by Combining Broadly Reactive HIV-1 Antibodies Targeting Major Neutralization Epitopes. *J Virol* (2015) 89:2659–71. doi: 10.1128/JVI.03136-14
64. Wagh K, Seaman MS, Zingg M, Fitzsimons T, Barouch DH, Burton DR, et al. Potential of Conventional & Bispecific Broadly Neutralizing Antibodies for Prevention of HIV-1 Subtype A, C & D Infections. *PloS Pathog* (2018) 14: e1006860. doi: 10.1371/journal.ppat.1006860
65. Lorenzi JC, Cohen YZ, Cohn LB, Kreider EF, Barton JP, Learn GH, et al. Paired Quantitative and Qualitative Assessment of the Replication-Competent HIV-1 Reservoir and Comparison With Integrated Proviral DNA. *Proc Natl Acad Sci USA* (2016) 113:E7908–16. doi: 10.1073/pnas.1617789113
66. Scheid JF, Horwitz JA, Bar-On Y, Kreider EF, Lu CL, Lorenzi JC, et al. HIV-1 Antibody 3BNC117 Suppresses Viral Rebound in Humans During Treatment Interruption. *Nature* (2016) 535:556–60. doi: 10.1038/nature18929
67. Hake A, Pfeifer N. Prediction of HIV-1 Sensitivity to Broadly Neutralizing Antibodies Shows a Trend Towards Resistance Over Time. *PloS Comput Biol* (2017) 13:e1005789. doi: 10.1371/journal.pcbi.1005789
68. Rawi R, Mall R, Shen CH, Farney SK, Shiakolas A, Zhou J, et al. Accurate Prediction for Antibody Resistance of Clinical HIV-1 Isolates. *Sci Rep* (2019) 9:14696. doi: 10.1038/s41598-019-50635-w
69. Magaret CA, Benkeser DC, Williamson BD, Borate BR, Carpp LN, Georgiev IS, et al. Prediction of VRC01 Neutralization Sensitivity by HIV-1 Gp160 Sequence Features. *PloS Comput Biol* (2019) 15:e1006952. doi: 10.1371/journal.pcbi.1006952
70. Kerwin BA, Bennett C, Brodsky Y, Clark R, Floyd JA, Gillespie A, et al. Framework Mutations of the 10-1074 bnAb Increase Conformational Stability, Manufacturability, and Stability While Preserving Full Neutralization Activity. *J Pharm Sci* (2020) 109:233–46. doi: 10.1016/j.xphs.2019.07.009
71. Patel A, Gupta V, Hickey J, Nightlinger NS, Rogers RS, Siska C, et al. Coformulation of Broadly Neutralizing Antibodies 3BNC117 and PGT121: Analytical Challenges During Preformulation Characterization and Storage Stability Studies. *J Pharm Sci* (2018) 107:3032–46. doi: 10.1016/j.xphs.2018.08.012
72. Sharma VK, Misra B, McManus KT, Avula S, Nellaiappan K, Caskey M, et al. Characterization of Co-Formulated High-Concentration Broadly Neutralizing Anti-HIV-1 Monoclonal Antibodies for Subcutaneous Administration. *Antibodies (Basel)* (2020) 9:36. doi: 10.3390/antib9030036
73. Gaudinski MR, Coates EE, Houser KV, Chen GL, Yamshchikov G, Saunders JG, et al. Safety and Pharmacokinetics of the Fc-Modified HIV-1 Human Monoclonal Antibody VRC01LS: A Phase 1 Open-Label Clinical Trial in Healthy Adults. *PloS Med* (2018) 15:e1002493. doi: 10.1371/journal.pmed.1002493
74. Corey L, Gilbert PB, Juraska M, Montefiori DC, Morris L, Karuna ST, et al. Two Randomized Trials of Neutralizing Antibodies to Prevent HIV-1 Acquisition. *N Engl J Med* (2021) 384:1003–14. doi: 10.1056/NEJMoa2031738
75. Gaudinski MR, Houser KV, Doria-Rose NA, Chen GL, Rothwell RSS, Berkowitz N, et al. Safety and Pharmacokinetics of Broadly Neutralising Human Monoclonal Antibody VRC07-523LS in Healthy Adults: A Phase 1 Dose-Escalation Clinical Trial. *Lancet HIV* (2019) 6:e667–79. doi: 10.1016/S2352-3018(19)30181-X
76. Walsh SR, Gay CL, Karuna ST, Hyrien O, Skalland T, Mayer KH, et al. *Safety and Single-Dose Pharmacokinetics of VRC07-523ls Administered via Different Routes and Doses*. Cape Town, South Africa: R4P Virtual (2021).
77. Caskey M, Klein F, Lorenzi JC, Seaman MS, West APJr., Buckley N, et al. Viraemia Suppressed in HIV-1-Infected Humans by Broadly Neutralizing Antibody 3BNC117. *Nature* (2015) 522:487–91. doi: 10.1038/nature14411
78. Caskey M. *Preclinical to Clinical: 3BNC117 and 10-1074 bNAb Combination for HIV Prophylaxis*. Cape Town, South Africa: R4P Virtual (2021).
79. Widge AT, Houser KV, Gaudinski MR, Chen G, Carter C, Hickman SP, et al. *A Phase I Dose-Escalation Trial of Human Monoclonal Antibody N6LS in Healthy Adults*. Boston, MA, USA: CROI (2020).
80. Koup RA. *Review of Bnabs in Clinical Development*. Madrid, Spain: R4P (2018).
81. Priddy FH, Lewis DJM, Gelderblom HC, Hassanin H, Streatfield C, LaBranche C, et al. Adeno-Associated Virus Vectored Immunoprophylaxis to Prevent HIV in Healthy Adults: A Phase 1 Randomised Controlled Trial. *Lancet HIV* (2019) 6: e230–9. doi: 10.1016/S2352-3018(19)30003-7
82. Mahomed S, Garrett N, Karim QA, Zuma NY, Capparelli E, Baxter C, et al. Assessing the Safety and Pharmacokinetics of the Anti-HIV Monoclonal Antibody CAP256V2LS Alone and in Combination With VRC07-523LS and PGT121 in South African Women: Study Protocol for the First-in-Human CAPRISA 012B Phase I Clinical Trial. *BMJ Open* (2020) 10:e042247. doi: 10.1136/bmjopen-2020-042247
83. Stephenson KE, Julg B, Ansel J, Walsh SR, Tan CS, Maxfield L, et al. *Therapeutic Activity of PGT121 Monoclonal Antibody in HIV-Infected Adults*. Seattle, WA, USA: CROI (2019).
84. Caskey M, Schoofs T, Gruell H, Settler A, Karagounis T, Kreider EF, et al. Antibody 10-1074 Suppresses Viremia in HIV-1-Infected Individuals. *Nat Med* (2017) 23:185–91. doi: 10.1038/nm.4268
85. Armbruster C, Stiegler GM, Vcelar BA, Jäger W, Michael NL, Vetter N, et al. A Phase I Trial With Two Human Monoclonal Antibodies (hMAb 2F5, 2G12) Against HIV-1. *AIDS* (2002) 16:227–33. doi: 10.1097/00002030-200201250-00012
86. Zhou T, Georgiev I, Wu X, Yang ZY, Dai K, Finzi A, et al. Structural Basis for Broad and Potent Neutralization of HIV-1 by Antibody VRC01. *Science* (2010) 329:811–7. doi: 10.1126/science.1192819
87. Lynch RM, Boritz E, Coates EE, DeZure A, Madden P, Costner P, et al. Virologic Effects of Broadly Neutralizing Antibody VRC01 Administration During Chronic HIV-1 Infection. *Sci Transl Med* (2015) 7:319ra206. doi: 10.1126/scitranslmed.aad5752
88. Ledgerwood JE, Coates EE, Yamshchikov G, Saunders JG, Holman L, Enama ME, et al. Safety, Pharmacokinetics and Neutralization of the Broadly Neutralizing HIV-1 Human Monoclonal Antibody VRC01 in Healthy Adults. *Clin Exp Immunol* (2015) 182:289–301. doi: 10.1111/cei.12692
89. Mayer KH, Seaton KE, Huang Y, Grunenberg N, Isaacs A, Allen M, et al. Safety, Pharmacokinetics, and Immunological Activities of Multiple Intravenous or Subcutaneous Doses of an Anti-HIV Monoclonal Antibody, VRC01, Administered to HIV-Uninfected Adults: Results of a Phase 1 Randomized Trial. *PloS Med* (2017) 14:e1002435. doi: 10.1371/journal.pmed.1002435
90. Bar KJ, Sneller MC, Harrison LJ, Justement JS, Overton ET, Petrone ME, et al. Effect of HIV Antibody VRC01 on Viral Rebound After Treatment Interruption. *N Engl J Med* (2016) 375:2037–50. doi: 10.1056/NEJMoa1608243
91. Cohen YZ, Butler AL, Millard K, Witmer-Pack M, Levin R, Unson-O'Brien C, et al. Safety, Pharmacokinetics, and Immunogenicity of the Combination of the Broadly Neutralizing Anti-HIV-1 Antibodies 3BNC117 and 10-1074 in Healthy Adults: A Randomized, Phase 1 Study. *PloS One* (2019) 14: e0219142. doi: 10.1371/journal.pone.0219142
92. Rudicell RS, Kwon YD, Ko SY, Pegu A, Louder MK, Georgiev IS, et al. Enhanced Potency of a Broadly Neutralizing HIV-1 Antibody *In Vitro* Improves Protection Against Lentiviral Infection *In Vivo*. *J Virol* (2014) 88:12669–82. doi: 10.1128/JVI.02213-14
93. Ko SY, Pegu A, Rudicell RS, Yang ZY, Joyce MG, Chen X, et al. Enhanced Neonatal Fc Receptor Function Improves Protection Against Primate SHIV Infection. *Nature* (2014) 514:642–5. doi: 10.1038/nature13612
94. Zalevsky J, Chamberlain AK, Horton HM, Karki S, Leung IW, Sproule TJ, et al. Enhanced Antibody Half-Life Improves *In Vivo* Activity. *Nat Biotechnol* (2010) 28:157–9. doi: 10.1038/nbt.1601
95. Huang Y, Yu J, Lanzi A, Yao X, Andrews CD, Tsai L, et al. Engineered Bispecific Antibodies With Exquisite HIV-1-Neutralizing Activity. *Cell* (2016) 165:1621–31. doi: 10.1016/j.cell.2016.05.024
96. Julien JP, Sok D, Khayat R, Lee JH, Doores KJ, Walker LM, et al. Broadly Neutralizing Antibody PGT121 Allosterically Modulates CD4 Binding *via*

Recognition of the HIV-1 Gp120 V3 Base and Multiple Surrounding Glycans. *PloS Pathog* (2013) 9:e1003342. doi: 10.1371/journal.ppat.1003342
97. Sok D, Doores KJ, Briney B, Le KM, Saye-Francisco KL, Ramos A, et al. Promiscuous Glycan Site Recognition by Antibodies to the High-Mannose Patch of Gp120 Broadens Neutralization of HIV. *Sci Transl Med* (2014) 6:236ra263. doi: 10.1126/scitranslmed.3008104
98. Garces F, Sok D, Kong L, McBride R, Kim HJ, Saye-Francisco KF, et al. Structural Evolution of Glycan Recognition by a Family of Potent HIV Antibodies. *Cell* (2014) 159:69–79. doi: 10.1016/j.cell.2014.09.009
99. Mouquet H, Scharf L, Euler Z, Liu Y, Eden C, Scheid JF, et al. Complex-Type N-Glycan Recognition by Potent Broadly Neutralizing HIV Antibodies. *Proc Natl Acad Sci USA* (2012) 109:E3268–3277. doi: 10.1073/pnas.1217207109
100. Sok D, van Gils MJ, Pauthner M, Julien JP, Saye-Francisco KL, Hsueh J, et al. Recombinant HIV Envelope Trimer Selects for Quaternary-Dependent Antibodies Targeting the Trimer Apex. *Proc Natl Acad Sci USA* (2014) 111:17624–9. doi: 10.1073/pnas.1415789111
101. van Loggerenberg F, Mlisana K, Williamson C, Auld SC, Morris L, Gray CM, et al. Establishing a Cohort at High Risk of HIV Infection in South Africa: Challenges and Experiences of the CAPRISA 002 Acute Infection Study. *PloS One* (2008) 3:e1954. doi: 10.1371/journal.pone.0001954
102. Bhiman JN, Anthony C, Doria-Rose NA, Karimanzira O, Schramm CA, Khoza T, et al. Viral Variants That Initiate and Drive Maturation of V1V2-Directed HIV-1 Broadly Neutralizing Antibodies. *Nat Med* (2015) 21:1332–6. doi: 10.1038/nm.3963
103. Sheward DJ, Marais J, Bekker V, Murrell B, Eren K, Bhiman JN, et al. HIV Superinfection Drives De Novo Antibody Responses and Not Neutralization Breadth. *Cell Host Microbe* (2018) 24:593–9.e593. doi: 10.1016/j.chom.2018.09.001
104. Huang J, Ofek G, Laub L, Louder MK, Doria-Rose NA, Longo NS, et al. Broad and Potent Neutralization of HIV-1 by a Gp41-Specific Human Antibody. *Nature* (2012) 491:406–12. doi: 10.1038/nature11544
105. Kwon YD, Georgiev IS, Ofek G, Zhang B, Asokan M, Bailer RT, et al. Optimization of the Solubility of HIV-1-Neutralizing Antibody 10E8 Through Somatic Variation and Structure-Based Design. *J Virol* (2016) 90:5899–914. doi: 10.1128/JVI.03246-15
106. Cohen MS, Corey L. Broadly Neutralizing Antibodies to Prevent HIV-1. *Science* (2017) 358:46–7. doi: 10.1126/science.aap8131
107. Gilbert PB, Juraska M, deCamp AC, Karuna S, Edupuganti S, Mgodi N, et al. Basis and Statistical Design of the Passive HIV-1 Antibody Mediated Prevention (AMP) Test-Of-Concept Efficacy Trials. *Stat Commun Infect Dis* (2017) 9:20160001. doi: 10.1515/scid-2016-0001
108. Edupuganti S, Mgodi N, Karuna ST, Andrew P, Rudnicki E, Kochar N, et al. Feasibility and Successful Enrollment in a Proof-Of-Concept HIV Prevention Trial of VRC01, a Broadly Neutralizing HIV-1 Monoclonal Antibody. *J Acquir Immune Defic Syndr* (2021) 87:671–9. doi: 10.1097/QAI.0000000000002639
109. Mgodi NM, Takuva S, Edupuganti S, Karuna S, Andrew P, Lazarus E, et al. A Phase 2b Study to Evaluate the Safety and Efficacy of VRC01 Broadly Neutralizing Monoclonal Antibody in Reducing Acquisition of HIV-1 Infection in Women in Sub-Saharan Africa: Baseline Findings. *J Acquir Immune Defic Syndr* (2021) 87:680–7. doi: 10.1097/QAI.0000000000002649
110. Huang Y, Naidoo L, Zhang L, Carpp LN, Rudnicki E, Randhawa A, et al. Pharmacokinetics and Predicted Neutralisation Coverage of VRC01 in HIV-Uninfected Participants of the Antibody Mediated Prevention (AMP) Trials. *EBioMedicine* (2021) 64:103203. doi: 10.1016/j.ebiom.2020.103203
111. Takuva S, Karuna S, Juraska M, Rudnicki E, Edupuganti S, Anderson M, et al. *Infusion Reactions in the Phase 2b Antibody Mediated Prevention (AMP) Studies*. San Francisco, CA, USA: Virtual CROI (2021).
112. Rerks-Ngarm S, Pitisuttithum P, Nitayaphan S, Kaewkungwal J, Chiu J, Paris R, et al. Vaccination With ALVAC and AIDSVAX to Prevent HIV-1 Infection in Thailand. *N Engl J Med* (2009) 361:2209–20. doi: 10.1056/NEJMoa0908492
113. Cohen YZ, Lorenzi JCC, Seaman MS, Nogueira L, Schoofs T, Krassnig L, et al. Neutralizing Activity of Broadly Neutralizing Anti-HIV-1 Antibodies Against Clade B Clinical Isolates Produced in Peripheral Blood Mononuclear Cells. *J Virol* (2018) 92:e01883–17. doi: 10.1128/JVI.01883-17
114. Lorenzi JCC, Mendoza P, Cohen YZ, Nogueira L, Lavine C, Sapiente J, et al. Neutralizing Activity of Broadly Neutralizing Anti-HIV-1 Antibodies Against Primary African Isolates. *J Virol* (2020) 95:e01909–20. doi: 10.1101/2020.09.24.310938
115. Bar-On Y, Gruell H, Schoofs T, Pai JA, Nogueira L, Butler AL, et al. Safety and Antiviral Activity of Combination HIV-1 Broadly Neutralizing Antibodies in Viremic Individuals. *Nat Med* (2018) 24:1701–7. doi: 10.1038/s41591-018-0186-4
116. Mendoza P, Gruell H, Nogueira L, Pai JA, Butler AL, Millard K, et al. Combination Therapy With Anti-HIV-1 Antibodies Maintains Viral Suppression. *Nature* (2018) 561:479–84. doi: 10.1038/s41586-018-0531-2
117. Pinto D, Fenwick C, Caillat C, Silacci C, Guseva S, Dehez F, et al. Structural Basis for Broad HIV-1 Neutralization by the MPER-Specific Human Broadly Neutralizing Antibody Ln01. *Cell Host Microbe* (2019) 26:623–37.e628. doi: 10.1016/j.chom.2019.09.016
118. Sajadi MM, Dashti A, Rikhtegaran Tehrani Z, Tolbert WD, Seaman MS, Ouyang X, et al. Identification of Near-Pan-Neutralizing Antibodies Against HIV-1 by Deconvolution of Plasma Humoral Responses. *Cell* (2018) 173:1783–1795 e1714. doi: 10.1016/j.cell.2018.03.061
119. Schommers P, Gruell H, Abernathy ME, Tran MK, Dingens AS, Gristick HB, et al. Restriction of HIV-1 Escape by a Highly Broad and Potent Neutralizing Antibody. *Cell* (2020) 180:471–489 e422. doi: 10.1016/j.cell.2020.01.010
120. Diskin R, Scheid JF, Marcovecchio PM, West APJr., Klein F, Gao H, et al. Increasing the Potency and Breadth of an HIV Antibody by Using Structure-Based Rational Design. *Science* (2011) 334:1289–93. doi: 10.1126/science.1213782
121. Liu Q, Zhang P, Miao H, Lin Y, Kwon YD, Kwong PD, et al. Rational Engraftment of Quaternary-Interactive Acidic Loops for Anti-HIV-1 Antibody Improvement. *J Virol* (2021) 95:e00159–21. doi: 10.1128/JVI.00159-21
122. Gardner MR. Promise and Progress of an HIV-1 Cure by Adeno-Associated Virus Vector Delivery of Anti-HIV-1 Biologics. *Front Cell Infect Microbiol* (2020) 10:176. doi: 10.3389/fcimb.2020.00176
123. Hartweger H, McGuire AT, Horning M, Taylor JJ, Dosenovic P, Yost D, et al. HIV-Specific Humoral Immune Responses by CRISPR/Cas9-Edited B Cells. *J Exp Med* (2019) 216:1301–10. doi: 10.1084/jem.20190287
124. Huang D, Tran JT, Olson A, Vollbrecht T, Tenuta M, Guryleva MV, et al. Vaccine Elicitation of HIV Broadly Neutralizing Antibodies From Engineered B Cells. *Nat Commun* (2020) 11:5850. doi: 10.1038/s41467-020-20304-y
125. Padte NN, Yu J, Huang Y, Ho DD. Engineering Multi-Specific Antibodies Against HIV-1. *Retrovirology* (2018) 15:60. doi: 10.1186/s12977-018-0439-9
126. Bournazos S, Gazumyan A, Seaman MS, Nussenzweig MC, Ravetch JV. Bispecific Anti-HIV-1 Antibodies With Enhanced Breadth and Potency. *Cell* (2016) 165:1609–20. doi: 10.1016/j.cell.2016.04.050
127. Xu L, Pegu A, Rao E, Doria-Rose N, Beninga J, McKee K, et al. Trispecific Broadly Neutralizing HIV Antibodies Mediate Potent SHIV Protection in Macaques. *Science* (2017) 358:85–90. doi: 10.1126/science.aan8630
128. Gardner MR, Kattenhorn LM, Kondur HR, von Schaewen M, Dorfman T, Chiang JJ, et al. AAV-Expressed Ecd4-Ig Provides Durable Protection From Multiple SHIV Challenges. *Nature* (2015) 519:87–91. doi: 10.1038/nature14264
129. Chu TH, Crowley AR, Backes I, Chang C, Tay M, Broge T, et al. Hinge Length Contributes to the Phagocytic Activity of HIV-Specific IgG1 and IgG3 Antibodies. *PloS Pathog* (2020) 16:e1008083. doi: 10.1371/journal.ppat.1008083
130. Richardson SI, Lambson BE, Crowley AR, Bashirova A, Scheepers C, Garrett N, et al. IgG3 Enhances Neutralization Potency and Fc Effector Function of an HIV V2-Specific Broadly Neutralizing Antibody. *PloS Pathog* (2019) 15:e1008064. doi: 10.1371/journal.ppat.1008064
131. Shields RL, Namenuk AK, Hong K, Meng YG, Rae J, Briggs J, et al. High Resolution Mapping of the Binding Site on Human IgG1 for Fc Gamma RI, Fc Gamma RII, Fc Gamma RIII, and FcRn and Design of IgG1 Variants With Improved Binding to the Fc Gamma R. *J Biol Chem* (2001) 276:6591–604. doi: 10.1074/jbc.M009483200
132. Li T, DiLillo DJ, Bournazos S, Giddens JP, Ravetch JV, Wang LX. Modulating IgG Effector Function by Fc Glycan Engineering. *Proc Natl Acad Sci USA* (2017) 114:3485–90. doi: 10.1073/pnas.1702173114
133. Liu Y, Cao W, Sun M, Li T. Broadly Neutralizing Antibodies for HIV-1: Efficacies, Challenges and Opportunities. *Emerg Microbes Infect* (2020) 9:194–206. doi: 10.1080/22221751.2020.1713707
134. Reh L, Magnus C, Schanz M, Weber J, Uhr T, Rusert P, et al. Capacity of Broadly Neutralizing Antibodies to Inhibit HIV-1 Cell-Cell Transmission Is Strain- and Epitope-Dependent. *PloS Pathog* (2015) 11:e1004966. doi: 10.1371/journal.ppat.1004966
135. Li H, Zony C, Chen P, Chen BK. Reduced Potency and Incomplete Neutralization of Broadly Neutralizing Antibodies Against Cell-To-Cell

Transmission of HIV-1 With Transmitted Founder Envs. *J Virol* (2017) 91: e02425–16. doi: 10.1128/JVI.02425-16

**Conflict of Interest:** The authors declare that the research was conducted in the absence of any commercial or financial relationships that could be construed as a potential conflict of interest.

frontiers in Immunology

ORIGINAL RESEARCH
published: 13 August 2021
doi: 10.3389/fimmu.2021.710273

# Elimination of SHIV Infected Cells by Combinations of Bispecific HIVxCD3 DART® Molecules

*Marina Tuyishime[1]*, Amir Dashti[2], Katelyn Faircloth[1†], Shalini Jha[1], Jeffrey L. Nordstrom[3], Barton F. Haynes[4,5,6], Guido Silvestri[2], Ann Chahroudi[2,7,8], David M. Margolis[9,10,11,12] and Guido Ferrari[1,13]*

[1] Department of Surgery, Duke University Medical Center, Durham, NC, United States, [2] Department of Pediatrics, Emory University, Atlanta, GA, United States, [3] Research Department, MacroGenics, Rockville, MD, United States, [4] Duke Human Vaccine Institute, Durham, NC, United States, [5] Department of Medicine, Duke University Medical Center, Durham, NC, United States, [6] Department of Immunology, Duke University Medical Center, Durham, NC, United States, [7] Yerkes National Primate Research Center, Emory University, Atlanta, GA, United States, [8] Center for Childhood Infections and Vaccines of Children's Healthcare of Atlanta and Emory University, Atlanta, GA, United States, [9] University of North Carolina (UNC) HIV Cure Center, University of North Carolina at Chapel Hill, Chapel Hill, NC, United States, [10] Department of Medicine, University of North Carolina at Chapel Hill, Chapel Hill, NC, United States, [11] Department of Microbiology and Immunology, University of North Carolina at Chapel Hill, Chapel Hill, NC, United States, [12] Department of Epidemiology, University of North Carolina at Chapel Hill, Chapel Hill, NC, United States, [13] Department of Molecular Genetics and Microbiology, Duke University Medical Center, Durham, NC, United States

OPEN ACCESS

**Edited by:**
*Philipp Schommers, University of Cologne, Germany*

**Reviewed by:**
*Maxim Rosario, Johns Hopkins Medicine, United States*
*Elizabeth Connick, University of Arizona, United States*

***Correspondence:**
*Marina Tuyishime*
*marina.tuyishime@duke.edu*

*[†]Currently research analyst at City of Hope, kfaircloth@coh.org*

**Specialty section:**
*This article was submitted to Vaccines and Molecular Therapeutics, a section of the journal Frontiers in Immunology*

**Received:** *15 May 2021*
**Accepted:** *26 July 2021*
**Published:** *13 August 2021*

**Citation:**
*Tuyishime M, Dashti A, Faircloth K, Jha S, Nordstrom JL, Haynes BF, Silvestri G, Chahroudi A, Margolis DM and Ferrari G (2021) Elimination of SHIV Infected Cells by Combinations of Bispecific HIVxCD3 DART® Molecules. Front. Immunol. 12:710273. doi: 10.3389/fimmu.2021.710273*

Bispecific HIVxCD3 DART molecules that co-engage the viral envelope glycoprotein (Env) on HIV-1-infected cells and the CD3 receptor on CD3+ T cells are designed to mediate the cytolysis of HIV-1-infected, Env-expressing cells. Using a novel *ex vivo* system with cells from rhesus macaques (RMs) infected with a chimeric Simian-Human Immunodeficiency Virus (SHIV) CH505 and maintained on ART, we tested the ability of HIVxCD3 DART molecules to mediate elimination of *in vitro*-reactivated CD4+ T cells in the absence or presence of autologous CD8+ T cells. HIVxCD3 DART molecules with the anti-HIV-1 Env specificities of A32 or 7B2 (non-neutralizing antibodies) or PGT145 (broadly neutralizing antibody) were evaluated individually or combined. DART molecule-mediated antiviral activity increased significantly in the presence of autologous CD8+ T cells. In this *ex vivo* system, the PGT145 DART molecule was more active than the 7B2 DART molecule, which was more active than the A32 DART molecule. A triple combination of the DART molecules exceeded the activity of the individual PGT145 DART molecule. Modified quantitative virus outgrowth assays confirmed the ability of the DART molecules to redirect RM CD3+ T cells to eliminate SHIV-infected RM CD4+ T cells as demonstrated by the decreased propagation of *in vitro* infection by the infected cells pre-incubated with DART molecules in presence of effector CD8+ T cells. While mediating cytotoxic activity, DART molecules did not increase proinflammatory cytokine production. In summary, combination of HIVxCD3 DART molecules that have broadly-neutralizing and non-neutralizing anti-HIV-1 Env specificities can leverage the host immune system for treatment of HIV-1 infection but will require appropriate reactivation of the latent reservoir.

**Keywords: HIV, bispecific DART molecules, redirected cytotoxicity, cytotoxic T cells, broadly neutralizing antibodies, non-neutralizing antibodies**

## INTRODUCTION

Since the first reported cases of Acquired Immunodeficiency Syndrome (AIDS) in 1981, infection with Human Immunodeficiency Virus type 1 (HIV-1) has been deemed a global and persistent epidemic. The treatment of HIV-1 infection with antiretroviral therapy (ART) has been effective in controlling virus replication, delaying disease progression, and reducing HIV-1 transmission (1). The inability of ART to eradicate HIV-1 infection is primarily due to the establishment of a latent reservoir that cannot be successfully targeted by current therapeutic strategies. Due to the presence of integrated but transcriptionally silent proviral HIV DNA, ART has had limited effects in preventing the elimination of the latent reservoir (2, 3) and achieving HIV-1 remission (4, 5). Due to the slow decay rate of the HIV reservoir, computational data suggest that it might take up to 70 years on ART to completely eradicate the infection (5, 6). Latency Reversing Agents (LRAs) have been identified and used to induce proviral transcription in latently infected cells (7–10) with subsequent expression of viral antigens on the cell surface that can be targeted by HIV-1-specific antibodies (Abs).

Broadly neutralizing anti-HIV-1 envelope (Env) antibodies (bNAbs) have been shown to reduce viremia, eliminate sensitive viruses in chronically infected individuals, delay virus rebound (11–17) and provide protection in non-human primate studies (18–25). In addition to virus neutralization, Abs can also eliminate infected cells *via* Fc-mediated functions that include antibody dependent cellular cytotoxicity (ADCC). ADCC activities have been correlated with slow disease progression in HIV-1-infected individuals (26–29). ADCC, driven by bNAbs and non-neutralizing antibodies (non-NAbs), can also mediate killing of cells infected with neutralization resistant viruses (30, 31). Based on these properties of anti-HIV-1 Env Abs, bispecific DART molecules were generated. DART molecules bind to CD3 with one arm and to HIV-1 Env with another, with the ability to engage Env expressed on HIV-1-infected CD4+ T cells, representing the target cells, and CD3 expressed on cytotoxic effector T cells (32). *In vitro* studies show that DART molecules with anti-HIV-1 Env specificities of bNAbs retain the neutralization breadth and potency of the bNAb component (8, 33), and can neutralize newly produced virions post latency reversal. DART and other mAb-based molecules mediated elimination of HIV Env-expressing infected CD4 cell lines and primary human CD4+ T by recruiting *via* anti-CD3 arm cytotoxic CD8+ T from HIV-seronegative and ART-suppressed HIV-seropositive participants (8, 33–36). The original DART molecules had limited *in vivo* pharmacokinetics (bioavailability, solubility, stability, and half-life) compared to traditional Abs (37, 38); therefore, a new molecule was designed to add an Fc region to DART which demonstrated improvement in its half-life (39). One HIVxCD3 DART molecule (MGD014, also known as A32xCD3) is currently in clinical testing in people living with HIV-1 on ART (40).

We previously reported that DART molecules with anti-HIV-1 Env arms based on non-neutralizing A32 (gp120 C1C2, epitope cluster A), non-neutralizing 7B2 (gp41 cluster I) and neutralizing PGT145 (V2 apex) antibodies, redirected human CD8+ T cells to eliminate HIV-1-infected primary autologous CD4+ T cells (41) and latently infected cells from ART-suppressed, HIV-1-seropositive donors that had been reactivated *ex vivo* (33, 34). A triple combination of A32xCD3, 7B2xCD3 and PGT145xCD3 DART molecules, which have anti-CD3 arms that cross-react with rhesus CD3 and were engineered with rhesus Fc domains, was tested *in vivo* in rhesus macaques (RMs) infected with Simian-Human Immunodeficiency Virus expressing the CH505 T/F envelope (SHIV.CH505.375H) (41, 42). However, we reported that the limited sizes of the viral reservoir and the absence of detectable latency reactivation in animals following LRA administration most likely affected our ability to fully assess the anti-viral activity of HIVxCD3 DART molecules (41). In the current study, we further confirm the ability of three DART molecules individually and in combination to eliminate reactivated SHIV.CH505.375H-infected cells using a novel *ex vivo* primary RM system utilizing purified populations of infected target (CD4+) and effector (CD8+) cells. In this autologous system we evaluated whether a combination of DART molecules is more effective than individual DART molecules in mediating clearance of CD4+ T cells isolated from SHIV.CH505.375H-infected RMs by autologous CD8+ T cells. These data support an active role of the DART molecule that will require a more efficient activation of the latent reservoir regardless its size.

## MATERIALS AND METHODS

### DART Molecules

HIVxCD3 DART molecules are bispecific, Fc-bearing molecules with an anti-HIV-1 Env specificity paired with an anti-human CD3 specificity. The anti-HIV-1 Env specificities were derived from A32 (non-neutralizing antibody (Ab) specific for the cluster A epitope in gp120 C1, C2), 7B2 (non-neutralizing Ab specific for gp41 cluster I) and PGT145 (neutralizing Ab specific for gp120 V2) (33, 34). The anti-human CD3 specificity cross-reacts with rhesus monkey CD3ϵ. The rhesus IgG1 Fc domain utilized for these DART molecules is inactivated for Fc-gamma receptor and complement binding but retains neonatal Fc receptor binding (41). HIVxRSV DART molecules contain anti-respiratory syncytial virus (RSV) specificities instead of anti-CD3 specificities.

### SHIV-Infection of A66 Cells

SHIV.CH505.375H challenge virus stocks, a chimeric simian/human immunodeficiency virus with a SIVmac766 backbone and the clinically relevant HIV-1 transmitted/founder clade C envelope CH505 (41) grown in rhesus PBMCs were titrated to determine the input required for optimal viral gene expression within 72 hours post-infection of A66 cells as measured by intracellular p27 expression, using anti-SIV Gag anti-p27 antibody (WNPRC Immunology Services). A66 cells (provided by James Hoxie, University of Pennsylvania, Philadelphia, PA) are SupT1 cells [non-BC7 variant (43)] that have been stably

transfected to express both rhesus CD4 and rhesus CCR5 receptors after knockout of endogenous human CXCR4 and CD4 (44). A66 cells ($1 \times 10^6$ cells/infection) were incubated with 100 ng/mL p27 of SHIV.CH505.375H for 4 hours at 37°C and 5% $CO_2$ in the presence of DEAE-Dextran (10 μg/mL, Sigma Aldrich). The cells were subsequently resuspended at $0.33 \times 10^6$/mL and cultured for 3 days in complete medium containing 10 μg/mL DEAE-Dextran. On assay day, infection was monitored by measuring the frequency of cells expressing intracellular p27. The assays performed using the SHIV.CH505.375H-infected target cells were considered reliable if the percentage of viable p27+ target cells on assay day was ≥10%. Assay data generated using infected cells was normalized to the frequency of live target cells positive for intracellular p27.

## Binding of HIVxRSV DART Molecules to SHIV-Infected A66 Cells

SHIV.CH505.375H-infected A66 cells were obtained as described above. Cells incubated in the absence of virus (mock infected) were used as a negative control. Infected and mock-infected cells were washed in PBS, dispensed into 96-well V-bottom plates at 2 x $10^5$ cells/well and incubated with 1 μg/mL of indicated DART molecule for 2 hours at 37 °C. To eliminate CD3 binding, these studies were conducted with HIVxRSV DART molecules in which anti-HIV-1 Env arms were paired with anti-RSV arms instead of anti-CD3 arms. After two washes with 250 μL/well wash buffer (1% FBS in PBS, WB), the cells were stained with vital dye (Live/Dead Fixable Aqua Dead Cell Stain, Invitrogen) to exclude nonviable cells from subsequent analysis. Cells were washed with WB and stained with anti-CD4-PerCP-Cy5.5 (clone Leu-3; BD Biosciences) to a final dilution of 1:20 in the dark for 20 min at room temperature (RT). Cells were then washed again, and permeabilized using Cytofix/Cytoperm (BD Biosciences) for 20 min at 4°C. After wash with 1x Cytoperm wash solution (BD Biosciences), anti-p27 antibody (WNPRC Immunology Services, 1:500 dilution in 1x Cytoperm Solution, BD Biosciences) and a secondary PE-conjugated antibody (goat anti-human Ig Fc-PE, eBioscience, San Diego, CA., final dilution of 1:400) were added to each well and incubated in the dark for 25 min at 4 °C. The secondary anti-human Ig Fc antibody detects the Fc portion of DART molecules bound to the surface of infected cells. Cells were washed 3 times with Cytoperm wash solution and resuspended in PBS-1% paraformaldehyde. The samples were acquired within 24 hours using a BD Fortessa cytometer. A minimum of 50,000 total events was acquired for each analysis. Gates were set to include singlet and live events. The appropriate compensation beads were used to compensate the spill-over signal for the four fluorophores. Data analysis was performed using FlowJo 9.6.6 software (BD Biosciences). Final data represents the PE MFI and frequency of infected cells bound by DART molecules (%p27 +/DART+), after normalization by subtracting PE MFI for cells stained with the secondary antibody alone. Assays were repeated twice and the average results are shown.

## *In Vitro* Killing Assays With SHIV-Infected A66 Cells and Human CD8+ T Cells

SHIV.CH505.375H-infected A66 cells, as described above, were used as target cells using a previously described assay (34). Briefly, infected and uninfected target cells were washed in R10 and labelled with a fluorescent target-cell marker (TFL4; OncoImmunin) and a viability marker (NFL1; OncoImmunin) for 15 min at 37°C, as specified by manufacturer. Cells were washed twice in R10 and adjusted to a concentration of 0.2 x $10^6$ cells/mL. On assay day, resting human $CD8^+$ effector T cells were isolated by negative selection from PBMCs from healthy donors using a $CD8^+$ T cell isolation kit (Miltenyi Biosciences) and were used as effectors with E:T ratio at 33:1. Cells were incubated in the absence or presence of HIVxCD3 DART molecules for 6 hours at the starting concentration of 50 μg/mL with subsequent 6 dilutions at 1:5. Uninfected and infected target cells alone were included as additional controls. Each condition was tested in duplicate. After the incubation period, cells were washed with WB and stained with anti-CD4-PerCP-Cy5.5 (BD Biosciences, clone Leu-3) at a final dilution of 1:20 in the dark for 20 min at RT. After washing with WB, cells were resuspended in 100 μL/well Cytofix/Cytoperm (BD Biosciences), incubated in the dark for 20 min at 4°C, washed in 1x Cytoperm wash solution (BD Biosciences) and co-incubated with anti-SIV Gag p27 antibody (WNPRC Immunology Services) to a final dilution of 1:500 in the dark for 25 min at 4°C. Three washes were performed with Cytoperm wash solution before resuspending the cells in 125 μL PBS-1% paraformaldehyde for acquisition. The samples were acquired within 24 hours using a BD Fortessa cytometer. The appropriate compensation beads were used to compensate the spill-over signal for the four fluorophores. Data analysis was performed using FlowJo 9.6.6 software (BD Biosciences). Mock-infected cells were used to appropriately position live cell p27+/- gates. Redirecting killing activity mediated by the DART molecules was determined by measuring the reduction in the percentage of p27+ cells according to the following formula: % specific killing = [(Frequency of p27 positive cells in wells containing target and effector cells alone – Frequency of p27 positive cells in wells containing target and effector cells plus DART molecules)/ Frequency of p27 positive cells in wells containing target and effector cells alone] ×100.

## *Ex Vivo* DART Molecule Treatment of Reactivated, SHIV-Infected RM CD4+ T Cells in the Presence or Absence Of Autologous RM CD8+ T Cells

A novel *ex vivo* assay system was developed to evaluate the ability of HIVxCD3 DART molecules to mediate killing of *in vitro* reactivated CD4+ T cells isolated from SHIV.CH505.375H-infected RMs in the presence or absence of autologous RM CD8+ T cells (**Figure 2A**). PBMCs collected from SHIV-infected RMs at the peak of viremia (week 2 post-infection) were used as the source of SHIV-infected RM CD4+ T cells

(targets). PBMCs collected from SHIV-infected RMs on ART (at week 36, when plasma VL levels < 60 copies/mL) were used as the source of CD8+ T cells (effectors). The primary SHIV-infected RM CD4+ T cells were activated for 24 hours with a mixture of antibodies specific for nonhuman primate CD2/CD3/CD28. Reactivated SHIV-infected RM CD4 T cells ($1x10^5$ cells/well) were incubated for 48 hours in the absence or presence of autologous CD8 T cells ($3x10^3$ cells/well at E:T ratio of 0.03:1) in absence (No DART) or presence of DART molecules individually at 1 μg/mL or combined at 1 μg/mL each. DART molecule-mediated activity was analyzed as % reduction (in absence of autologous CD8+ T cells) and % killing (in presence of autologous CD8+ T cells) by measuring p27 levels in supernatants as following: % p27 reduction/killing = [(p27 ng/mL in wells containing target cells alone − p27 ng/mL in wells containing target and DART molecules (or effector cells, or DART molecules plus effector cells)/p27 ng/mL in wells containing target cells alone] ×100.

## Modified Quantitative Viral Outgrowth Assay

Following the 48-hour incubations of the *ex vivo* killing assays, DART molecules were washed off and A66 feeder cells were added ($1x10^6$ cells per well) to allow the propagation of replication competent virus. Cells were passaged with fresh media in the absence of DART molecules every two to three days for a total duration of 9 days. Supernatants from each condition were collected at days 4 and 9 and stored frozen. Supernatants were then thawed and analyzed for SIV Gag p27 levels by ELISA to determine the amounts of SHIV virus that was produced.

## Cytokine and Chemokine Release

Cultures of primary reactivated SHIV-infected CD4+ T cells alone ($1x10^5$ cells) or mixed with autologous CD8 T cells ($3x10^3$ cells) at E:T ratio of 0.03:1 were incubated without (No DART) or with individual DART molecules at 1 μg/mL or the triple DART molecule combination at 1 μg/mL each for 48 hours. Supernatants were collected and levels of GM-CSF, IFN-γ, IL-1β, IL-6, IL-8, IL-12p40, IL-18, and TNFα determined using a Milliplex® MAP kit (Millipore # HCYTMAG-60K-PX41) on a Luminex MAGPIX™ instrument according to the manufacturer's protocol. Plates were read on a Sector s600 MSD plate reader and data analyzed using MSD Discovery Workbench analysis software.

# RESULTS

## HIVxCD3 DART Molecule Binding and Specific CD8+ T-Cell Killing of SHIV-Infected A66 Cells

The ability of the individual DART molecules with A32, 7B2 or PGT145 anti-HIV-1 envelope (Env) specificities to bind to primary human CD4+ T cells activated and infected *in vitro* with HIV-1 transmitted/founder clade C envelope CH505 Infectious Molecular Clone (IMC), and to mediate specific killing by autologous human CD8+ T cells was previously reported (41). Here we first analyzed the ability of the DART molecules to bind to and to redirect human CD8+ T cells to kill SHIV.CH505.375H-infected A66 cells, a human SupT1 cell line modified to stably express RM CD4 and CCR5 receptors. To specifically interrogate binding to CH505 Env on the surface of the SHIV-infected A66 cells, variant DART molecules were generated with anti-HIV-1 Env arms paired with anti-respiratory syncytial virus (anti-RSV) arms instead of anti-CD3 arms. All three HIVxRSV DART molecules demonstrated binding to the SHIV.CH505.375H-infected A66 cells as shown by the frequency (%p27+/DART+) and median fluorescent intensity (MFI) of infected cells bound by the DART molecules (**Figures 1A, B**). The frequency of SHIV.CH505.375H-infected A66 cells bound by A32xRSV, 7B2xRSV or PGT145xRSV was 56%, 2% or 2.5% with MFI of 310, 35 or 30, respectively. Despite the variations in binding, all 3 HIVxCD3 DART molecules mediated specific killing of the SHIV.CH505.375H-infected A66 cells by primary human CD8+ T cells. The killing activity of HIVxCD3 DART molecule, which requires binding to both target and effector cells, occurs at $EC_{50}$ values that range from 1-10 ng/mL (33). Only a small fraction of the binding sites on targets and effectors need to be occupied to enable the formation of immunological synapses that lead to target cell killing. This is consistent with the small number of interactions required for cytotoxic synapses between CTLs and peptide-MHC complexes (45). Thus, dose-dependent effect was observed for specific killing by the individual DART molecules (**Figure 1C**). We chose 1 μg/mL of each DART molecule that shows 20% (A32xCD3), 20% (7B2xCD3) and 40% (PGT145xCD3) specific killing against SHIV.CH505.375H-infected A66 cells and hypothesized that combination of DART molecules each at 1μg/mL will lead to an increase in specific killing compared to individual DART molecules. No binding or specific killing was observed with negative control DART, 4420xRSV, where the anti-HIV arm is substituted for anti-fluorescein.

## *Ex Vivo* Study Design

To evaluate DART molecule-mediated killing of RM CD4+ T cells collected from SHIV.CH505.375H-infected animals, we developed a novel primary *ex vivo* assay system. PBMCs collected from SHIV.CH505.375H-infected RMs (41) at the peak of viremia (week 2 post-infection) were used as the source of target SHIV-infected RM CD4+ T cells (**Figure 2A**). This time point was chosen because we expected it to provide the highest frequency of circulating infected CD4+ T cells capable of expressing Env on their surface upon reactivation (46) and, thus, represent the most optimal targets for recognition by DART molecules. PBMCs collected from RMs on ART at week 36, when plasma viral load (VL) levels were < 60 copies/mL, were used as the source of effectors CD8+ T cells (41). This time point was chosen to recapitulate pre-clinical studies and clinical trials with administration of DART molecules that rely on post-ART functionality of cytotoxic CD8+ T cells to eliminate reactivated Env-expressing targets (47–49). Primary RM CD4+ T cells were isolated and *in vitro* activated for 24 hours with anti-CD2/CD3/

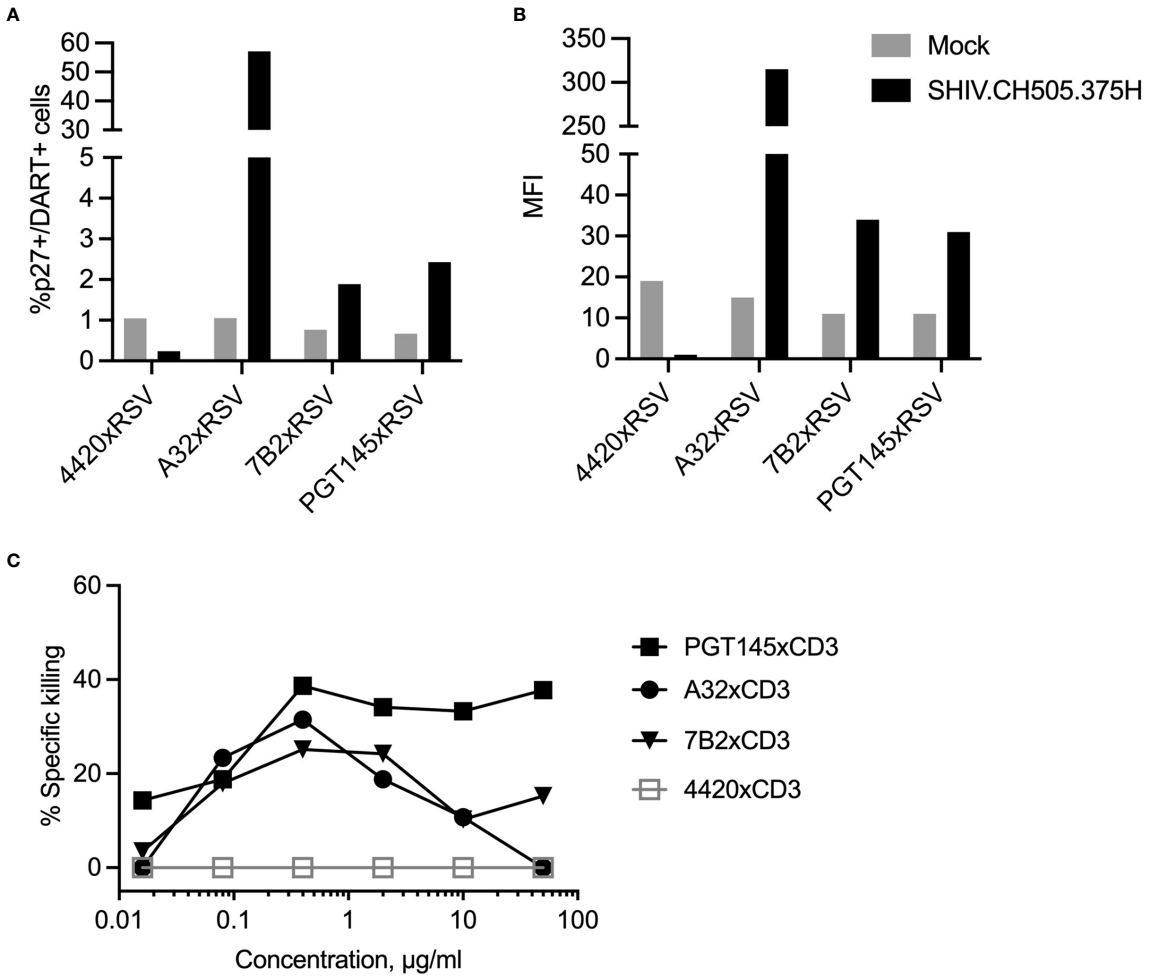


**FIGURE 1** | DART molecule binding to SHIV-infected A66 cells and their redirected killing in the presence of human CD8 T cells. The binding of HIVxRSV DART molecules with A32, 7B2 or PGT145 anti-HIV-1 Env specificities to SHIV.CH505.375H-infected A66 cells was evaluated to determine **(A)** frequency of SHIV-infected cells bound by DART molecules (%p27+/DART+) and **(B)** median fluorescent intensity (MFI). The 4420 DART molecule, which contains an anti-fluorescein specificity instead of an anti-HIV-1 Env specificity, was used as the negative control. **(C)** Titration curves represent DART-mediated killing of SHIV.CH505.375H-infected A66 cells as targets (T) by human CD8+ T cells as effectors (E) with E:T ratio of 33:1. The % Specific killing was determined 6 hours post by incubation of T+E+DART molecules measuring the reduction in the percentage of p27+ cells in presence of DART molecules compared to T+E alone.

CD28 non-human primate (NHP) Abs and then cultured for 48 hours by themselves or with autologous RM CD8+ T cells at an effector to target (E:T) ratio of 0.03:1 in the absence or presence of DART molecules. The experimental design is shown schematically in **Figure 2B**. This novel system is designed to reflect the diversity of target cells infected by virus isolates circulating *in vivo* and allow evaluation of autologous target and effector cell interactions mediated by DART molecules.

## Virologic Assessment of Primary RM CD4+ T Cells

The 9 animals in this *ex vivo* study, which were selected based on availability of cryopreserved cellular samples, had peak plasma viral loads (PVL) ranging from $1.5x10^6$ to $9x10^6$ SHIV RNA copies/ml of plasma [**Figure 3A,** (41)]. All animals had established viral reservoirs which were measured by cell-associated SHIV.CH505.375H DNA and RNA (**Figures 3B, C**). The RNA reservoir was smaller than the DNA reservoir, as expected (50). *In vitro* activation of viral gene expression in primary CD4+ T cells from SHIV.CH505.375H-infected RMs with anti-CD2/CD3/CD28 NHP Abs was monitored by measuring SIV Gag p27 levels in supernatants using p27 ELISA; p27 levels ranged from 0.074 to 3.9 ng/mL (**Figure 3D**). We did not observe significant correlations between p27 level in supernatants from cultures of reactivated cells, PVL, level of cell-associated viral RNA, or level of cell-associated viral DNA, as shown by the heat map in **Figure 3E** ($R^2$ values ranged from -0.18 to 0.39, with non-significant p values).

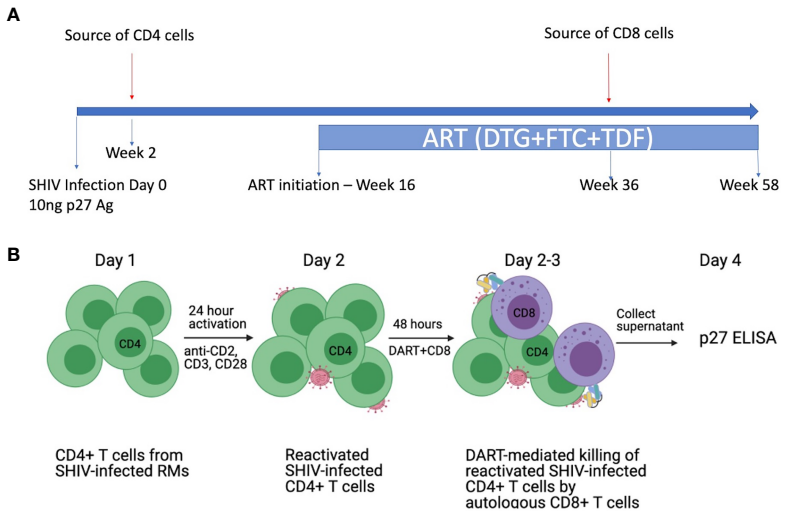


**FIGURE 2** | *Ex vivo* killing assays with SHIV-infected RM CD4+ T cells and autologous RM CD8+ T cells. **(A)** Schematic of the *in vivo* study. Rhesus macaques (RMs) were infected intravenously (i.v.) with SHIV.CH505.375H at a dose of 10 ng of SIV Gag p27 antigen (41). SHIV.CH505.375H is a chimeric simian/human immunodeficiency virus with SIVmac backbone and HIV-1 transmitted/founder clade C envelope CH505. The RMs were treated with an ART regimen consisting of tenofovir (TDF: 5.1 mg/kg), emtricitabine (FTC: 40 mg/kg), and dolutegravir (DTG: 2.5 mg/kg) administered subcutaneously daily from week 16 post-infection (p.i.) to the end of the study. PBMCs were collected from the SHIV-infected RMs at week 2 post-infection (prior to ART) to isolate SHIV-infected CD4+ T cells (targets) and at week 36 post-infection (while on ART) to isolate CD8+ T cells (effectors). **(B)** Design of the *ex vivo* killing assays. Primary CD4+ T cells from SHIV.CH505.375H-infected RMs were isolated and activated *in vitro* for 24 hours with antibodies specific for nonhuman primate CD2/CD3/CD28. Activated SHIV-infected RM CD4+ T cells were cultured for 48 hours alone or with autologous RM CD8+ T cells at an E:T ratio of 0.03:1 in the absence or presence of DART molecules. The % killing of the SHIV-infected RM CD4+ T cells was determined by measuring the reduction in supernatant SIV Gag p27 levels compared to CD4+ T cells alone.

## DART Molecule Treatment of Reactivated, SHIV-Infected RM CD4+ T Cells

Supernatant p27 levels in cultures of *in vitro*-reactivated primary CD4+ T cells from SHIV.CH505.375H-infected RMs, incubated without addition of canonical cytotoxic CD8+ T cells, declined noticeably compared to the '*No DART*' control following incubation with A32 DART molecule in 7 of 9 cultures (median reduction 2.5%, range 0.7-30% **Figure 4A**), 7B2 DART molecule in 7 of 9 cultures (median reduction of 10%, range 2.4-39%), PGT145 DART molecule in 7 of 9 cultures (median reduction of 53.6%, range 23-90%), and triple DART combination in 7 of 9 cultures (median reduction of 42%: range 27-68%). Two of the 9 cultures showed no reduction in supernatant p27 level following incubation with the DART molecules. The ranked activities of the DART molecules were PGT145 > 7B2 > A32, and the activity of the triple DART combination was comparable to that of the PGT145 DART molecule alone. Both CD4+ and CD8+ T cell subsets are capable of being redirected to kill HIV-infected Env-expressing target cells, although CD8 cells are generally more potent effectors than CD4 cells (34). Thus, since A32 and 7B2 have non-neutralizing anti-HIV-1 Env specificities, the declines in supernatant p27 observed in presence of A32 and 7B2 DART molecules are interpreted to be due to the killing of Env-expressing SHIV.CH505.375H-infected CD4+ cells by redirected cytotoxic CD4+ T cells. In addition, PGT145 has virus neutralizing activity; therefore, the declines in supernatant p27 mediated by the PGT145 DART molecule may result from both virus neutralization and killing of Env-expressing SHIV-infected CD4+ T cells by redirected cytotoxic CD4+ T cells.

## DART Molecule Treatment of Reactivated, SHIV-Infected RM CD4+ T Cells in the Presence of Autologous RM CD8+ T Cells

We first assessed the elimination of SHIV-infected RM CD4+ T cells by autologous CD8+ T cells at an E:T ratio of 0.03:1 in the absence of DART molecules (**Figure 4B**, *No DART*). We observed a diversity in killing activity in cultures from 7 of 9 animals (median killing 17%, range 10-46%). These results demonstrate that, in this cohort, CD8+ T cells alone are unable to eliminate >50% of the reactivated SHIV-infected RM CD4+ T cells. Next, we analyzed the killing of reactivated SHIV-infected RM CD4+ T cells by autologous CD8 + T cells in the presence of DART molecules. The A32 DART molecule mediated killing in 7 of 9 cultures and increased killing in 6 of 9 cultures compared to CD8+ T cells alone (median killing 15%, range 14-61%). The 7B2 DART molecule mediated killing in 8 of 9 cultures (median killing 41%, range 17-71%), and the PGT145 DART molecule mediated killing in all 9 cultures (median killing 72%, range 27-88%). The ranked activities of the DART molecules were PGT145 > 7B2 > A32. The greater activity of the PGT145 DART molecule observed here is consistent with its greater activity in mediating human CD8+ T-cell killing of HIV-1 CH505 IMC-infected human CD4+ cells *in vitro*, compared to A32 and 7B2 DART molecules, as was previously shown by Dashti et al. (41). It is also consistent with the greater activity of

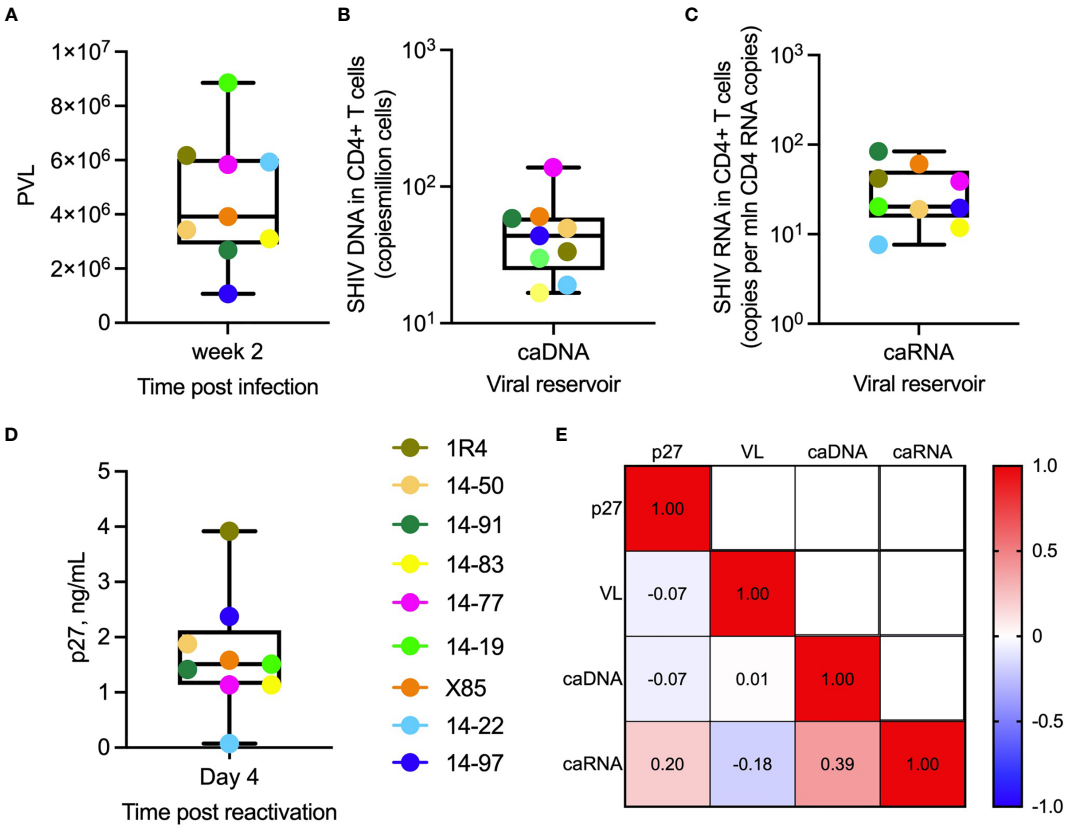


**FIGURE 3** | Virologic parameters. **(A)** Plasma viral load (SHIV RNA copies/mL) in individual animals (indicated by their ID designations) following 2 weeks post infection with SHIV.CH505.375H. **(B)** Cell-associated viral DNA (caDNA) and **(C)** cell-associated viral RNA (caRNA) prior to ART initiation at week 16 post-infection. **(D)** SIV Gag p27 levels in supernatants of primary RM CD4+ T cells collected at week 2 post-infection, activated for 24 hours *in vitro* with anti-CD2, CD3, and CD28 antibodies and cultures for 3 days in fresh media. **(A–D)** In the box plots, horizontal lines within boxes denote median values, ends of boxes denote 25$^{th}$ and 75$^{th}$ percentiles, and lines outside of boxes denote minimum and maximum values. **(E)** Spearman correlation analysis of p27 levels in supernatants following *in vitro* activation of RM CD4+ T cells, peak plasma viral load, cell-associated viral RNA, and cell-associated viral DNA. Values are $R^2$ values.

the PGT145 DART molecule in mediating human CD8+ T-cell killing of SHIV.CH505.375H-infected A66 cells (**Figure 1C**). Interestingly, the PGT145 DART molecule was able to mediate low-level killing of reactivated, SHIV-infected RM CD4+ cells from animal 14-19 which exhibited resistance to the activity of the A32 and 7B2 DART molecules. The triple DART molecule combination mediated killing in 9 animals (median killing 76%, range 23.5-99%, **Figure 4B**) and demonstrated an increase in killing activity in 4 of 9 cultures compared to the PGT145 DART molecule alone increasing median killing in those animals from 65% (range 51.8-74.8% by PGT145 DART) to 77.4% (range 68-99% by DART combination). Although DART combination demonstrated an increase in killing activity compared to PGT145 DART alone, the difference did not reach statistical significance (**Figure 4D**).

Despite the limited number of animals, an in-depth analysis of DART molecule-mediated killing activity among the cultures from the 9 animals identifies possible differences in functional profiles. DART combination mediated 99.9% killing of the SHIV-infected RM CD4+ T cells by autologous CD8+ T cells from animal 14-22 however, *in vitro* activation of SHIV-infected RM CD4+ T cells showed the lowest supernatant p27 levels (0.074 ng/mL, **Figure 3C**). These data suggest that low level reactivation of latent infected target cells is sufficient to allow recognition and clearance by DART molecules. However, nearly complete elimination of infected cells could also be due to the lowest numbers of the reactivated SHIV-infected cells present in the *ex vivo* assay. In animal X85, we detected similar levels of % p27 reduction (~90%) when reactivated SHIV-infected CD4+ T cells were cultured with PGT145 DART in the absence (**Figure 4A**) or presence (**Figure 4B**) of CD8 effector cells, suggesting that addition of autologous CD8 cells to these cultures did not increase % killing. These results indicate that CD8 cells from animal X85 could mediate limited cytotoxic activity compared to other animals. In cultures from 5 animals (14-91, 1R4, 14-83, 14-77 and 14-19) the addition of PGT145 DART molecule alone and DART combination drastically increase the % killing of SHIV-infected RM CD4+ T cells by CD8 cells compared to '*No DART*' control, demonstrating the PGT145-driven killing of infected cells in cultures from these animals. The addition of autologous

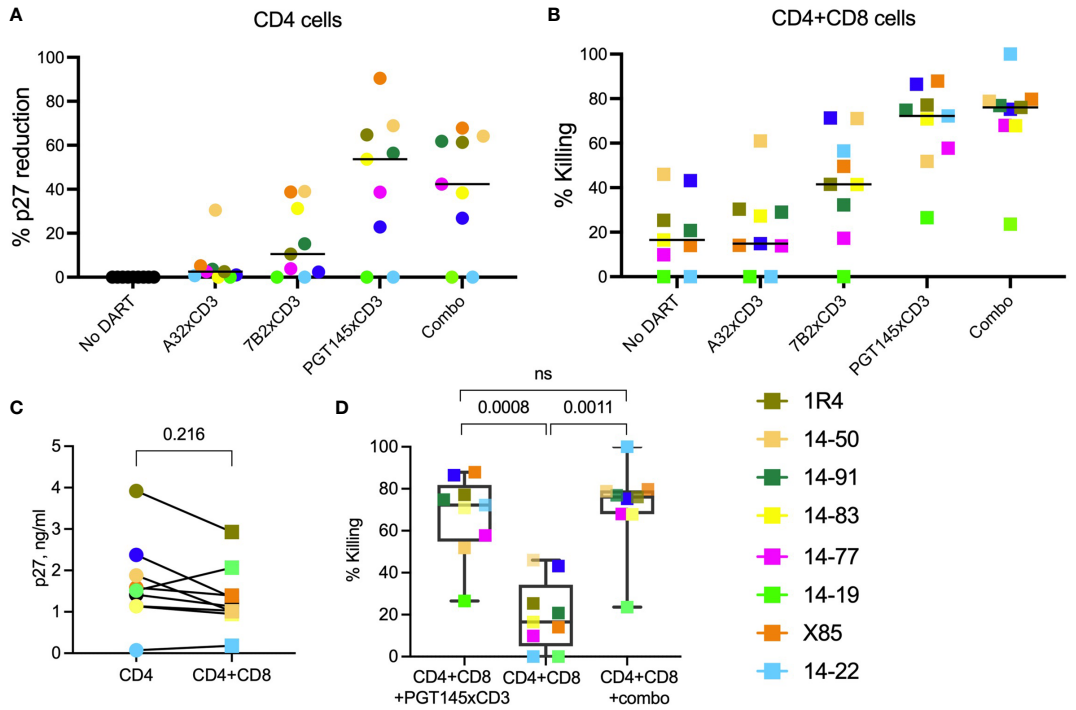


**FIGURE 4** | HIVxCD3 DART molecule-mediated killing of SHIV-infected RM CD4+ T cells. *In vitro* activated primary CD4+ T cells from SHIV.CH505.375H-infected RMs were cultured without or with DART molecules in the absence **(A)** or presence **(B)** of autologous CD8+ effector cells at an E:T ratio of 0.03:1. The A32, 7B2 and PGT145 DART molecules at 1 μg/mL were added individually or as a triple combination (Combo) at 1 μg/mL each. The reduction in p27 levels **(A)** and DART-mediated killing **(B)** was analyzed by p27 ELISA in culture supernatants 48 hours post treatment. The circles represent cultures with CD4 cells, squares represent cultures with CD4 and CD8 cells. Each colored symbol represents an individual animal. The horizontal black bars represent median values. Statistical analysis of p27 levels **(C)** or % killing **(D)** between indicated groups was performed using Wilcoxon Test at the significance level of 0.05. NS, not significant.

CD8+ T cells did not significantly reduce supernatant p27 levels compared to cultures with CD4 cells alone (**Figure 4C**), while we noticed significantly increased killing of infected cells in presence of PGT145 DART and DART combination compared to CD8 cells alone (**Figure 4D**).

To investigate the differences in cytotoxic activity mediated by CD8+ T cells among animals, we analyzed the CD8+ T cells isolated from PBMCs from each animal using an intracellular cytokine staining (ICS) assay. The cytotoxicity of CD8 cells isolated from each animal did not correlate with production of cytokines (GzB, INFg, TNFa, IL-2) post *in vitro* stimulation of CD8 cells with nonspecific T cell stimulator PMA and ionomycin (PMI). The expression of exhaustion marker PD-1 and the negative checkpoint receptor TIGID also did not show statistical significance or correlation with the cytotoxic activity of CD8 cells from each individual animal (data not shown).

## DART Molecule-Mediated Activity Measured by Modified Quantitative Viral Outgrowth Assay (QVOA)

We sought to determine whether the 48-hour treatment with DART molecules would inhibit the number of infected cells responsible for cell-to-cell transmission of replication competent virus. To do so, we modified the Quantitative Viral Outgrowth Assay (QVOA) assay (9). Given the limited numbers of primary RM CD4+ T cells available from SHIV.CH505.375H-infected animals, we utilized the A66 cells as feeder cells. Forty-eight hours following incubation of reactivated SHIV-infected RM CD4+ T cells and autologous RM CD8+ T cells in the absence or presence of DART molecules, the cell cultures were washed to remove DART molecules. The high dissociation rate constants of the HIVxCD3 DART molecules and rhesus CD3-epsilon (5.2-5.8 x $10^{-3}$ $s^{-1}$) and monovalent binding of anti-CD3 arm to CD3, which is does not have an avidity component, allows efficient elimination of DART molecules from cultures by three washing steps. Following the washed A66 feeders ($1x10^6$ per well) were added. Cells were passaged every two to three days with fresh media without DART molecules (**Supplementary Figure 1A**). Culture supernatants from each condition were collected at day 9 and the amount of virus recovered was determined by measuring supernatant levels of SIV Gag p27 by ELISA. Increases in supernatant p27 levels occurred with 8 of 9 cultures that contained reactivated SHIV-infected RM CD4+ T cells alone (in the absence of autologous RM CD8 cells or DART molecules), which indicates presence of residual SHIV-infected RM CD4+ T cells capable to transmit replication-competent virus (**Supplementary Figure 1B**).

As shown in **Figure 5A**, on Day 9 the median p27 level in the supernatants of cultures with reactivated SHIV-infected RM CD4

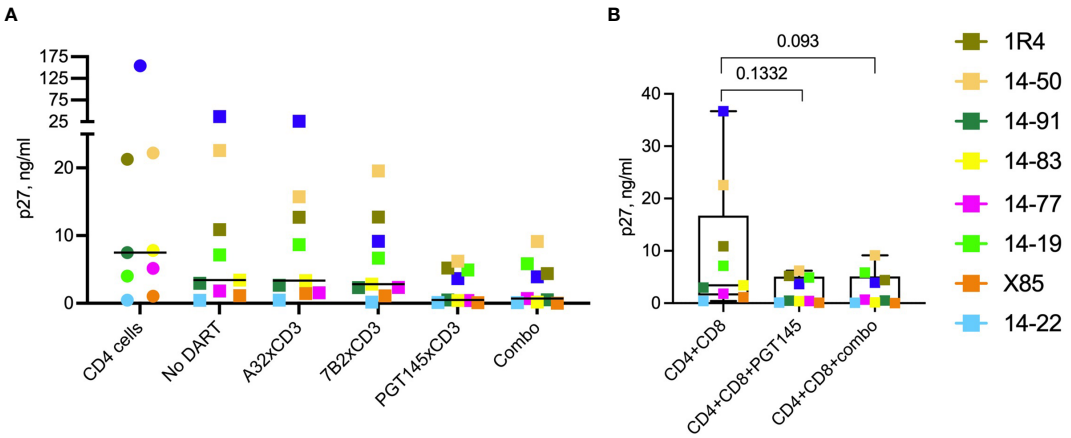


**FIGURE 5** | Effect of DART molecules on virus propagation. Cultures of reactivated SHIV-infected RM CD4+ T cells alone (CD4 cells) or mixed with autologous RM CD8+ T cells and incubated in the absence (No DART) or presence of DART molecules for 48 hours. DART molecules were then washed away and the cultures were mixed with A66 feeder cells to allow virus propagation. On day 9 cultures supernatants were analyzed for SIV Gag p27 levels by ELISA **(A)**. The horizontal lines represent the median values. **(B)** Statistical comparison between the indicated groups was performed using the Wilcoxon test at a significance level of 0.05. Combo is a combination of A32, 7B2 and PGT145 DART molecules.

cells and autologous RM CD8 cells in the absence of DART molecules (*No DART*) declined to 3.4 ng/mL (range 0.4-35 ng/mL) compared to 7.5 ng/mL (range 0.4-154 ng/mL) detected in the cultures of reactivated SHIV-infected RM CD4+ T cells alone (*CD4 cells*). Compared to observed reduction in p27 in cultures with CD8 cells (*No DART*), single 48-hour treatment with A32 DART molecule reduced the levels of p27 in 2 of 9 cultures (median p27 3.4 ng/mL, range 0.4-28 ng/mL), with 7B2 DART molecule in 3 of 9 cultures (median p27 2.8 ng/mL, range 0.4-20 ng/mL). The minor reductions in p27 levels in cultures treated with A32 and 7B2 DART molecules was not significant compared to p27 levels observed in cultures with CD8 cells alone. Treatment with PGT145 DART molecule reduced supernatant p27 in 9 of 9 cultures with a median of 0.5 ng/mL (range 0.04-8 ng/mL). The triple DART combination reduced supernatant p27 levels in 9 of 9 cultures similar to PGT145 DART alone demonstrating a median p27 level of 0.7 ng/mL (range 0.04-12 ng/mL) (**Figure 5A**). The ranked ability to inhibit the virus propagation was PGT145 > 7B2 > A32. Cultures from animal 14-97 demonstrated the greatest reduction in virus recovery; supernatant p27 levels were 154 ng/mL for the reactivated SHIV-infected RM CD4 cells alone, which declined to 35 ng/mL following addition of autologous RM CD8 cells (*No DART*), which further declined to 3.6 ng/mL following addition of PGT145 DART molecule or triple DART molecule combination (**Figure 5A**). The average reduction in virus recovery mediated by the addition of PGT145 or combination of DART molecules to the cultures with CD4 and CD8 cells was 8-fold, but the difference was not statistically significant (**Figure 5B**).

## Assessment of Cytokine Release Concomitant With Cytolytic Activity

We measured *in vitro* cytokine production when cultures of primary reactivated SHIV-infected RM CD4+ T cells alone or mixed with autologous RM CD8+ T cells were incubated without (*No DART*) or with DART molecules for 48 hours. Cytokines measured included IL-1b, IL-6, IL-8, IL-12p40, IL-18, GM-CSF, IFN-γ and TNF-α (**Supplementary Figure 1**). None of the cytokines were detected when reactivated SHIV-infected RM CD4+ T cells were incubated alone. The addition of individual DART molecules or DART combination without or with autologous CD8+ T cells did not change production of IL-1b, IL-6, IL-8, IL-12p40, IL-18 cytokines (**Supplementary Figure 1A**). Low levels of GM-CSF, IFN-g and TNF-a (median <16pg/mL, <2pg/mL, and <4pg/mL, respectively) were detected following incubation of SHIV-infected RM CD4+ T cells with individual DART molecules or their combination. Incubation of SHIV-infected RM CD4+ T cells with autologous RM CD8+ T cells in absence of DART molecules resulted in production of GM-CSF, IFN-γ and TNF-α with median 4pg/mL, 15pg/mL, and 5pg/mL, respectively. The addition of DART molecules to CD4+CD8 autologous mixture had no or minimal effect on production of GM-CSF, IFN-γ and TNF-α (**Supplementary Figure 1A**). These small increases in cytokines did not correlate with the cytotoxic activity exhibited by these cultures (**Supplementary Figure 1B**).

# DISCUSSION

Eradication of persistently infected cells is key to a functional cure of HIV infection. While ART treatment can successfully prevent viremia and disease progression, it does not lead to elimination of the virus, which persists as a quiescent provirus in rare latent infected cells. Life-long ART, which is required to prevent rebound of viremia and return of disease, is a financial and social burden. Novel immunotherapy-based strategies to treat HIV-1 need to address viral diversity and leverage the

immune system's ability to more efficiently target the latent viral reservoir. One potential approach is the "shock and kill" strategy where infected cells harboring latent virus are reactivated with latency reversing agents (LRAs) and eliminated by immunotherapies.

In the prior study, administration of a mixture of three HIVxCD3 DART molecules (having A32, 7B2 and PGT145 anti-HIV-1 Env specificities) and AZD5582 (latency reversing agent) to SHIV.CH505.375H-infected RMs that had been on ART for ~3 months did not result in reduction of the viral reservoir (41). The lack of DART molecule-mediated clearance activity in this animal model is attributed to the small size of the viral reservoir in the SHIV-infected animals maintained on ART and the absence of detectable latency reversal in response to AZD5582 treatment. The question persisted on whether DART molecules could engage the CD3-expressing effector cells of the animals to mediate target killing of reactivated Env-expressing SHIV-infected CD4+ T cells.

We, therefore, sought to confirm that DART molecules were capable of engaging primate effector cells and exerting an antiviral effect. We utilized primary cells isolated from the SHIV.CH505.375H-infected animal studied in Dashti et al. (41) and developed an *ex vivo* autologous system to assess DART molecule-mediated activities. We focused our work on the clearance of infected cells and utilized CD4+ T cells isolated from RMs at the peak of viremia (week 2 post infection), when the highest frequency of circulating infected cells expressed is expected and could be targeted for clearance. In order to assess whether DART molecules can recruit CD8 cells post ART treatment, we used autologous CD8+ T cells isolated from animals 20 weeks post ART initiation, when viremia was below the level of detection (47–49). According to our data, CD8+ T cells isolated from the RMs at this time may have only partially regained their cytotoxic function *in vivo*; under these conditions, the RM CD8+ T cells may not fully recapitulate the functionality of CD8+ T cells in PLWH who are maintained on ART before they can enroll in the clinical trials that evaluate the potency of these molecules.

Our data demonstrate that HIVxCD3 DART molecules were able to redirect RM CD8+ T cells to kill reactivated SHIV.CH505.375H-infected RM CD4+ cells and to reduce the level of replication competent virus released from the reactivated SHIV-infected RM CD4+ cells. The PGT145 DART molecule was more active than the 7B2 or A32 DART molecules, which is consistent with the ranked activities of these DART molecules in redirecting human CD8+ T cells to kill CH505 HIV-1 infectious molecular clone-infected human CD4+ cells. The PGT145 DART molecule, which is based on a broadly neutralizing antibody, is highly active toward CD4 cells infected by a more limited set of HIV-1 isolates than the 7B2 and A32 DART molecules, which are based on non-neutralizing, broadly reactive antibodies that recognize highly conserved epitopes in HIV-1 Env (34). We hypothesized that a combination of DART molecules based on a broadly neutralizing Ab (PGT145) and 2 non-neutralizing Abs (A32 and 7B2) can cover a broader spectrum of HIV-1 envelope conformations that are expressed on the membrane of the infected cells and upon reactivation of the latent virus (51–54). The principal finding of this study is that the triple DART molecule combination mediated optimal *ex vivo* redirected killing activity and inhibited propagation of replication competent virus. The combination of DART molecules demonstrated increase in killing in 4 of 9 animals, although the difference did not reach statistical significance compared to the PGT145 DART alone. Thus, the triple combination of DART molecules administered to the SHIV.CH505.375H-infected rhesus monkeys had potential to reduce the size of the virus reservoir if the co-administered LRA had generated targets for the DART molecules by reactivating latent infected cells to express HIV-1 Env on their surface.

Our data suggests that HIVxCD3 DART molecules have the potential to mediate elimination of the viral reservoir by cytotoxic CD8+ T cells after latency reversal. The effectiveness of viral eradication strategies requires both potent LRAs and cell-mediated cytotoxicity. Future studies designed to eradicate the viral reservoir in chronic infection should be powered to take in consideration the individual variability in the level of exhaustion and susceptibility to activation of the infection-induced immune responses.

## DATA AVAILABILITY STATEMENT

The original contributions presented in the study are included in the article/**Supplementary Material**. Further inquiries can be directed to the corresponding author.

## ETHICS STATEMENT

The animal study was reviewed and approved by the Institutional Animal Care and Use Committee (IACUC) of Emory University and Yerkes National Primate Research Center.

## AUTHOR CONTRIBUTIONS

MT, GF, and DM designed the experimental procedures. MT, AD, and KF conducted the experiments. SJ analyzed the data. JN generated the DART molecules. MT, GF, JN, and DM wrote the manuscript. AC and GS provided critical review of the results. All authors contributed to the article and approved the submitted version.

## FUNDING

This work was supported by Collaboratory of AIDS Researchers for Eradication (CARE), a Martin Delaney Collaboratory

program; NIAID, National Institute of Neurological Disorders and Stroke, National Institute on Drug Abuse, and National Institute of Mental Health grant 1UM1AI126619-01, and NIH NIAID P01 grant AI120756. MT was supported by the NIH Ruth L. Kirschstein National Research Service Award (5T32AI007392). Work was also supported by federal funds from NIAID, NIH, Dept. of Health and Human Services under Contract No. HHSN272201500032C. Research was also supported by the Emory Consortium for Innovative AIDS Research in Nonhuman Primates (UM1 AI124436), the Yerkes National Primate Research Center (P51 OD011132), and the Translational Virology and Reservoir Cores of the Center for AIDS Research at Emory University (P30 AI050409). The content is solely the responsibility of the authors. The funders had no role in study design, data collection and analysis, decision to publish, or preparation of the manuscript.

## ACKNOWLEDGMENTS

We thank Dr. James Hoxie for contributing the A66 cell line used in this study. (SIV)mac239 Gag was obtained through the HIV Reagent Program, Division of AIDS (DAIDS), National Institute of Allergy and Infectious Diseases (NIAID), National Institutes of Health (NIH). Peptide Pool, Simian Immunodeficiency Virus (SIV)mac239 Gag Protein, ARP-12364, was contributed by DAIDS/NIAID.

## SUPPLEMENTARY MATERIAL

The Supplementary Material for this article can be found online at: https://www.frontiersin.org/articles/10.3389/fimmu.2021.710273/full#supplementary-material

**Supplementary Figure 1 |** Modified quantitative viral outgrowth assay (QVOA). **(A)** Transmission of infection from reactivated SHIV-infected RM CD4+ T cells to A66 feeder cells. Primary CD4+ T cells from SHIV.CH505.375H-infected RMs were isolated and activated *in vitro* for 24 hours with anti-CD2/CD3/CD28 antibodies. The activated SHIV-infected RM CD4+ T cells were cultured alone or with autologous RM CD8+ cells for 48 hours in the absence or presence of DART molecules. On Day 4 the DART molecules were washed off and feeder A66 cells were added. Cells were split and media changed every 2-3 days. Supernatants collected at Day 4 and Day 9 were analyzed for SIV Gag p27 levels by ELISA to determine the amounts of SHIV virus that was produced. **(B)** p27 levels (ng/mL) in supernatants collected from cultures of activated SHIV-infected RM CD4+ T cells incubated in the absence of autologous CD8 cells or DART molecules. Each symbol indicates an individual animal. Animal 14-97 is graphed separately due to the difference in scare supernatant p27 level.

**Supplementary Figure 2 |** Cytokine release concomitant with cytolytic activity. Cultures of primary reactivated SHIV-infected RM CD4+ T cells alone or mixed with autologous RM CD8+ T cells were incubated without (No DART) or with DART molecules for 48 hours. Cytokines measured in supernatants included IL-1b, IL-6, IL-8, IL-12p40, IL-18, GM-CSF, IFN-γ and TNF-α. Each symbol represents an individual animal; circles represent supernatants from CD4 cells and squares represent supernatants from mixtures of CD4 + CD8 cells. Limit of detection was set by the manufacturer at 1.6 pg/ml. (**C**) Statistical correlation between killing of infected cells by autologous CD8 cells in absence of DART molecules (refer to **Figure 4B**) and levels of GM-CSF, IFN-γ or TNF-α using two-tailed Pearson correlation coefficient with 95% confidence interval.

## REFERENCES

1. Cohen MS. "Successful Treatment of HIV Eliminates Sexual Transmission". In: *Lancet*. England: London (2019).
2. Finzi D, Hermankova M, Pierson T, Carruth LM, Buck C, Chaisson RE, et al. Identification of a Reservoir for HIV-1 in Patients on Highly Active Antiretroviral Therapy. *Science (New York NY)* (1997) 278(5341):1295–300. doi: 10.1126/science.278.5341.1295
3. Chun TW, Stuyver L, Mizell SB, Ehler LA, Mican JA, Baseler M, et al. Presence of an Inducible HIV-1 Latent Reservoir During Highly Active Antiretroviral Therapy. *Proc Natl Acad Sci USA* (1997) 94(24):13193–7. doi: 10.1073/pnas.94.24.13193
4. Siliciano JD, Siliciano RF. The Latent Reservoir for HIV-1 in Resting CD4+ T Cells: A Barrier to Cure. *Curr Opin HIV AIDS* (2006) 1(2):121–8. doi: 10.1097/01.COH.0000209582.82328.b8
5. Siliciano JD, Kajdas J, Finzi D, Quinn TC, Chadwick K, Margolick JB, et al. Long-Term Follow-Up Studies Confirm the Stability of the Latent Reservoir for HIV-1 in Resting CD4+ T Cells. *Nat Med* (2003) 9(6):727–8. doi: 10.1038/nm880
6. Klatt NR, Chomont N, Douek DC, Deeks SG. Immune Activation and HIV Persistence: Implications for Curative Approaches to HIV Infection. *Immunol Rev* (2013) 254(1):326–42. doi: 10.1111/imr.12065
7. Deeks SG. HIV: Shock and Kill. *Nature* (2012) 487(7408):439–40. doi: 10.1038/487439a
8. Pegu A, Asokan M, Wu L, Wang K, Hataye J, Casazza JP, et al. Activation and Lysis of Human CD4 Cells Latently Infected With HIV-1. *Nat Commun* (2015) 6:8447. doi: 10.1038/ncomms9447
9. Nixon CC, Mavigner M, Sampey GC, Brooks AD, Spagnuolo RA, Irlbeck DM, et al. Systemic HIV and SIV Latency Reversal *via* Non-Canonical NF-κb Signalling In Vivo. *Nature* (2020) 578(7793):160–5. doi: 10.1038/s41586-020-1951-3
10. Archin NM, Liberty AL, Kashuba AD, Choudhary SK, Kuruc JD, Crooks AM, et al. Administration of Vorinostat Disrupts HIV-1 Latency in Patients on Antiretroviral Therapy. *Nature* (2012) 487(7408):482–5. doi: 10.1038/nature11286
11. Moody MA, Gao F, Gurley TC, Amos JD, Kumar A, Hora B, et al. Strain-Specific V3 and CD4 Binding Site Autologous HIV-1 Neutralizing Antibodies Select Neutralization-Resistant Viruses. *Cell Host Microbe* (2015) 18(3):354–62. doi: 10.1016/j.chom.2015.08.006
12. Caskey M, Klein F, Lorenzi JCC, Seaman MS, West APJr., Buckley N, et al. Viraemia Suppressed in HIV-1-Infected Humans by Broadly Neutralizing Antibody 3BNC117. *Nature* (2015) 522(7557):487–91. doi: 10.1038/nature14411
13. Scheid JF, Horwitz JA, Bar-On Y, Kreider EF, Lu CL, Lorenzi JC, et al. HIV-1 Antibody 3BNC117 Suppresses Viral Rebound in Humans During Treatment Interruption. *Nature* (2016) 535(7613):556–60. doi: 10.1038/nature18929
14. Bar KJ, Sneller MC, Harrison LJ, Justement JS, Overton ET, Petrone ME, et al. Effect of HIV Antibody VRC01 on Viral Rebound After Treatment Interruption. *N Engl J Med* (2016) 375(21):2037–50. doi: 10.1056/NEJMoa1608243
15. Bar-On Y, Gruell H, Schoofs T, Pai JA, Nogueira L, Butler AL, et al. Safety and Antiviral Activity of Combination HIV-1 Broadly Neutralizing Antibodies in Viremic Individuals. *Nat Med* (2018) 24(11):1701–7. doi: 10.1038/s41591-018-0186-4
16. Mendoza P, Gruell H, Nogueira L, Pai JA, Butler AL, Millard K, et al. Combination Therapy With Anti-HIV-1 Antibodies Maintains Viral Suppression. *Nature* (2018) 561(7724):479–84. doi: 10.1038/s41586-018-0531-2
17. Caskey M, Schoofs T, Gruell H, Settler A, Karagounis T, Kreider EF, et al. Antibody 10-1074 Suppresses Viremia in HIV-1-Infected Individuals. *Nat Med* (2017) 23(2):185–91. doi: 10.1038/nm.4268
18. Mascola JR, Lewis MG, Stiegler G, Harris D, VanCott TC, Hayes D, et al. Protection of Macaques Against Pathogenic Simian/Human Immunodeficiency Virus 89.6PD by Passive Transfer of Neutralizing Antibodies. *J Virol* (1999) 73(5):4009–18. doi: 10.1128/JVI.73.5.4009-4018.1999
19. Hofmann-Lehmann R, Vlasak J, Rasmussen RA, Smith BA, Baba TW, Liska V, et al. Postnatal Passive Immunization of Neonatal Macaques With a Triple Combination of Human Monoclonal Antibodies Against Oral Simian-Human Immunodeficiency Virus Challenge. *J Virol* (2001) 75(16):7470–80. doi: 10.1128/JVI.75.16.7470-7480.2001

20. Burton DR, Hessell AJ, Keele BF, Klasse PJ, Ketas TA, Moldt B, et al. Limited or No Protection by Weakly or Nonneutralizing Antibodies Against Vaginal SHIV Challenge of Macaques Compared With a Strongly Neutralizing Antibody. *Proc Natl Acad Sci USA* (2011) 108(27):11181–6. doi: 10.1073/pnas.1103012108
21. Saunders KO, Pegu A, Georgiev IS, Zeng M, Joyce MG, Yang Z-Y, et al. Sustained Delivery of a Broadly Neutralizing Antibody in Nonhuman Primates Confers Long-Term Protection Against Simian/Human Immunodeficiency Virus Infection. *J Virol* (2015) 89(11):5895–903. doi: 10.1128/JVI.00210-15
22. Shingai M, Donau OK, Plishka RJ, Buckler-White A, Mascola JR, Nabel GJ, et al. Passive Transfer of Modest Titers of Potent and Broadly Neutralizing Anti-HIV Monoclonal Antibodies Block SHIV Infection in Macaques. *J Exp Med* (2014) 211(10):2061–74. doi: 10.1084/jem.20132494
23. Mascola JR, Stiegler G, VanCott TC, Katinger H, Carpenter CB, Hanson CE, et al. Protection of Macaques Against Vaginal Transmission of a Pathogenic HIV-1/SIV Chimeric Virus by Passive Infusion of Neutralizing Antibodies. *Nat Med* (2000) 6(2):207–10. doi: 10.1038/72318
24. Hessell AJ, Rakasz EG, Poignard P, Hangartner L, Landucci G, Forthal DN, et al. Broadly Neutralizing Human Anti-HIV Antibody 2G12 is Effective in Protection Against Mucosal SHIV Challenge Even at Low Serum Neutralizing Titers. *PLoS Pathog* (2009) 5(5):e1000433. doi: 10.1371/journal.ppat.1000433
25. Moldt B, Rakasz EG, Schultz N, Chan-Hui PY, Swiderek K, Weisgrau KL, et al. Highly Potent Hiv-Specific Antibody Neutralization *In Vitro* Translates Into Effective Protection Against Mucosal Shiv Challenge In Vivo. *Proc Natl Acad Sci USA* (2012) 109(46):18921–5. doi: 10.1073/pnas.1214785109
26. Baum LL, Cassutt KJ, Knigge K, Khattri R, Margolick J, Rinaldo C, et al. HIV-1 Gp120-Specific Antibody-Dependent Cell-Mediated Cytotoxicity Correlates With Rate of Disease Progression. *J Immunol (Baltimore Md: 1950)* (1996) 157 (5):2168–73.
27. Lambotte O, Ferrari G, Moog C, Yates NL, Liao HX, Parks RJ, et al. Heterogeneous Neutralizing Antibody and Antibody-Dependent Cell Cytotoxicity Responses in HIV-1 Elite Controllers. *AIDS (Lond Engl)* (2009) 23(8):897–906. doi: 10.1097/QAD.0b013e328329f97d
28. Smalls-Mantey A, Doria-Rose N, Klein R, Patamawenu A, Migueles SA, Ko SY, et al. Antibody-Dependent Cellular Cytotoxicity Against Primary HIV-Infected CD4+ T Cells Is Directly Associated With the Magnitude of Surface Igg Binding. *J Virol* (2012) 86(16):8672–80. doi: 10.1128/JVI.00287-12
29. Wren LH, Chung AW, Isitman G, Kelleher AD, Parsons MS, Amin J, et al. Specific Antibody-Dependent Cellular Cytotoxicity Responses Associated With Slow Progression of HIV Infection. *Immunology* (2013) 138(2):116–23. doi: 10.1111/imm.12016
30. Lewis GK. Role of Fc-Mediated Antibody Function in Protective Immunity Against HIV-1. *Immunology* (2014) 142(1):46–57. doi: 10.1111/imm.12232
31. von Bredow B, Arias JF, Heyer LN, Moldt B, Le K, Robinson JE, et al. Comparison of Antibody-Dependent Cell-Mediated Cytotoxicity and Virus Neutralization by HIV-1 Env-Specific Monoclonal Antibodies. *J Virol* (2016) 90(13):6127–39. doi: 10.1128/JVI.00347-16
32. Moore PA, Zhang W, Rainey GJ, Burke S, Li H, Huang L, et al. Application of Dual Affinity Retargeting Molecules to Achieve Optimal Redirected T-Cell Killing of B-Cell Lymphoma. *Blood* (2011) 117(17):4542–51. doi: 10.1182/blood-2010-09-306449
33. Sloan DD, Lam CY, Irrinki A, Liu L, Tsai A, Pace CS, et al. Targeting HIV Reservoir in Infected CD4 T Cells by Dual-Affinity Re-Targeting Molecules (Darts) That Bind HIV Envelope and Recruit Cytotoxic T Cells. *PLoS Pathog* (2015) 11(11):e1005233. doi: 10.1371/journal.ppat.1005233
34. Sung JA, Pickeral J, Liu L, Stanfield-Oakley SA, Lam CY, Garrido C, et al. Dual-Affinity Re-Targeting Proteins Direct T Cell-Mediated Cytolysis of Latently HIV-Infected Cells. *J Clin Invest* (2015) 125(11):4077–90. doi: 10.1172/JCI82314
35. Pollara J, Edwards RW, Jha S, Lam CK, Liu L, Diedrich G, et al. Redirection of Cord Blood T Cells and Natural Killer Cells for Elimination of Autologous HIV-1-Infected Target Cells Using Bispecific DART® Molecules. *Front Immunol* (2020) 11:713. doi: 10.3389/fimmu.2020.00713
36. Petrovas C, Ferrando-Martinez S, Gerner MY, Casazza JP, Pegu A, Deleage C, et al. Follicular CD8 T Cells Accumulate in HIV Infection and can Kill Infected Cells In Vitro via Bispecific Antibodies. *Sci Trans Med* (2017) 9(373). doi: 10.1126/scitranslmed.aag2285
37. Lameris R, de Bruin RC, Schneiders FL, van Bergen en Henegouwen PM, Verheul HM, de Gruijl TD, et al. Bispecific Antibody Platforms for Cancer Immunotherapy. *Crit Rev Oncol Hematol* (2014) 92(3):153–65. doi: 10.1016/j.critrevonc.2014.08.003
38. Kontermann RE. Strategies to Extend Plasma Half-Lives of Recombinant Antibodies. *BioDrugs* (2009) 23(2):93–109. doi: 10.2165/00063030-200923020-00003
39. Liu L, Lam CK, Long V, Widjaja L, Yang Y, Li H, et al. MGD011, a CD19 X CD3 Dual-Affinity Retargeting Bi-Specific Molecule Incorporating Extended Circulating Half-Life for the Treatment of B-Cell Malignancies. *Clin Cancer Res* (2017) 23(6):1506–18. doi: 10.1158/1078-0432.CCR-16-0666
40. Bohac C. *A Phase 1 Study to Evaluate the Safety, Immunologic and Virologic Responses of MGD014 Therapy in HIV-Infected Individuals on Suppressive Antiretroviral Therapy*. ClinicalTrials.gov (2018).
41. Dashti A, Waller C, Mavigner M, Schoof N, Bar KJ, Shaw GM, et al. SMAC Mimetic Plus Triple-Combination Bispecific Hivxcd3 Retargeting Molecules in SHIV.C.CH505-Infected, Antiretroviral Therapy-Suppressed Rhesus Macaques. *J Virol* (2020) 94(21). doi: 10.1128/JVI.00793-20
42. Li H, Wang S, Kong R, Ding W, Lee FH, Parker Z, et al. Envelope Residue 375 Substitutions in Simian-Human Immunodeficiency Viruses Enhance CD4 Binding and Replication in Rhesus Macaques. *Proc Natl Acad Sci USA* (2016) 113(24):E3413–22. doi: 10.1073/pnas.1606636113
43. Hoxie JA, LaBranche CC, Endres MJ, Turner JD, Berson JF, Doms RW, et al. CD4-Independent Utilization of the CXCR4 Chemokine Receptor by HIV-1 and HIV-2. *J Reprod Immunol* (1998) 41(1-2):197–211. doi: 10.1016/S0165-0378(98)00059-X
44. Schouest B, Leslie GJ, Hoxie JA, Maness NJ. Tetherin Downmodulation by Sivmac Nef Lost With the H196Q Escape Variant is Restored by an Upstream Variant. *PloS One* (2020) 15(8):e0225420. doi: 10.1371/journal.pone.0225420
45. Huppa JB, Davis MM. The Interdisciplinary Science of T-Cell Recognition. *Adv Immunol* (2013) 119:1–50. doi: 10.1016/B978-0-12-407707-2.00001-1
46. Goonetilleke N, Moore S, Dally L, Winstone N, Cebere I, Mahmoud A, et al. Induction of Multifunctional Human Immunodeficiency Virus Type 1 (HIV-1)-Specific T Cells Capable of Proliferation in Healthy Subjects by Using a Prime-Boost Regimen of DNA- and Modified Vaccinia Virus Ankara-Vectored Vaccines Expressing HIV-1 Gag Coupled to CD8+ T-Cell Epitopes. *J Virol* (2006) 80(10):4717–28. doi: 10.1128/JVI.80.10.4717-4728.2006
47. Kalams SA, Goulder PJ, Shea AK, Jones NG, Trocha AK, Ogg GS, et al. Levels of Human Immunodeficiency Virus Type 1-Specific Cytotoxic T-Lymphocyte Effector and Memory Responses Decline After Suppression of Viremia With Highly Active Antiretroviral Therapy. *J Virol* (1999) 73(8):6721–8. doi: 10.1128/JVI.73.8.6721-6728.1999
48. Migueles SA, Weeks KA, Nou E, Berkley AM, Rood JE, Osborne CM, et al. Defective Human Immunodeficiency Virus-Specific CD8+ T-Cell Polyfunctionality, Proliferation, and Cytotoxicity are Not Restored by Antiretroviral Therapy. *J Virol* (2009) 83(22):11876–89. doi: 10.1128/JVI.01153-09
49. Warren JA, Clutton G, Goonetilleke N. Harnessing CD8(+) T Cells Under Hiv Antiretroviral Therapy. *Front Immunol* (2019) 10:291. doi: 10.3389/fimmu.2019.00291
50. Yukl SA, Shergill AK, Ho T, Killian M, Girling V, Epling L, et al. The Distribution of HIV DNA and RNA in Cell Subsets Differs in Gut and Blood of HIV-Positive Patients on ART: Implications for Viral Persistence. *J Infect Dis* (2013) 208(8):1212–20. doi: 10.1093/infdis/jit308
51. Ferrari G, Pollara J, Kozink D, Harms T, Drinker M, Freel S, et al. An HIV-1 Gp120 Envelope Human Monoclonal Antibody That Recognizes a C1 Conformational Epitope Mediates Potent Antibody-Dependent Cellular Cytotoxicity (ADCC) Activity and Defines a Common ADCC Epitope in Human HIV-1 Serum. *J Virol* (2011) 85(14):7029–36. doi: 10.1128/JVI.00171-11
52. Pollara J, Bonsignori M, Moody MA, Liu P, Alam SM, Hwang KK, et al. HIV-1 Vaccine-Induced C1 and V2 Env-Specific Antibodies Synergize for Increased Antiviral Activities. *J Virol* (2014) 88(14):7715–26. doi: 10.1128/JVI.00156-14
53. Tuyishime M, Garrido C, Jha S, Moeser M, Mielke D, LaBranche C, et al. Improved Killing of HIV-Infected Cells Using Three Neutralizing and Non-Neutralizing Antibodies. *J Clin Invest* (2020) 130(10):5157–70. doi: 10.1172/JCI135557
54. Richard J, Pacheco B, Gohain N, Veillette M, Ding S, Alsahafi N, et al. Co-Receptor Binding Site Antibodies Enable CD4-Mimetics to Expose Conserved

Anti-cluster A ADCC Epitopes on HIV-1 Envelope Glycoproteins. *EBioMedicine* (2016) 12:208–18. doi: 10.1016/j.ebiom.2016.09.004

**Conflict of Interest:** JN is employed by MacroGenics and owns MacroGenics stock. JN, BH, and GF have pending patents on some of the molecules.

The remaining authors declare that the research was conducted in the absence of any commercial or financial relationships that could be construed as a potential conflict of interest.

**Publisher's Note:** All claims expressed in this article are solely those of the authors and do not necessarily represent those of their affiliated organizations, or those of the publisher, the editors and the reviewers. Any product that may be evaluated in this article, or claim that may be made by its manufacturer, is not guaranteed or endorsed by the publisher.

frontiers in Immunology

METHODS
published: 24 August 2021
doi: 10.3389/fimmu.2021.709994

# Validation of a Triplex Pharmacokinetic Assay for Simultaneous Quantitation of HIV-1 Broadly Neutralizing Antibodies PGT121, PGDM1400, and VRC07-523-LS

*Martina S. Wesley[1,2], Kelvin T. Chiong[1,2], Kelly E. Seaton[1,2], Christine A. Arocena[1], Sheetal Sawant[1,2], Jonathan Hare[3,4], Kasey Hernandez[1], Michelle Rojas[1], Jack Heptinstall[1,2], David Beaumont[1,2], Katherine Crisafi[4], Joseph Nkolola[5,6], Dan H. Barouch[5,6], Marcella Sarzotti-Kelsoe[2,7], Georgia D. Tomaras[1,2,7,8] and Nicole L. Yates[1,2]**

[1] Center for Human Systems Immunology, Duke University, Durham, NC, United States, [2] Department of Surgery, Duke University, Durham, NC, United States, [3] International AIDS Vaccine Initiative (IAVI), Human Immunology Laboratory, Imperial College, London, United Kingdom, [4] International AIDS Vaccine Initiative (IAVI), New York, NY, United States, [5] Center for Virology and Vaccine Research, Beth Israel Deaconess Medical Center, Boston, MA, United States, [6] Ragon Institute of Massachusetts General Hospital (MGH), Massachusetts Institute of Technology (MIT) and Harvard, Cambridge, MA, United States, [7] Department of Immunology, Duke University, Durham, NC, United States, [8] Department of Molecular Genetics and Microbiology, Duke University, Durham, NC, United States

The outcome of the recent Antibody Mediated Prevention (AMP) trials that tested infusion of the broadly neutralizing antibody (bnAb) VRC01 provides proof of concept for blocking infection from sensitive HIV-1 strains. These results also open up the possibility that triple combinations of bnAbs such as PGT121, PGDM1400, as well as long-lasting LS variants such as VRC07-523 LS, have immunoprophylactic potential. PGT121 and PGDM1400 target the HIV-1 V3 and V2 glycan regions of the gp120 envelope protein, respectively, while VRC07-523LS targets the HIV-1 CD4 binding site. These bnAbs demonstrate neutralization potency and complementary breadth of HIV-1 strain coverage. An important clinical trial outcome is the accurate measurement of *in vivo* concentrations of passively infused bnAbs to determine effective doses for therapy and/or prevention. Standardization and validation of this testing method is a key element for clinical studies as is the ability to simultaneously detect multiple bnAbs in a specific manner. Here we report the development of a sensitive, specific, accurate, and precise multiplexed microsphere-based assay that simultaneously quantifies the respective physiological concentrations of passively infused bnAbs in human serum to ultimately define the threshold needed for protection from HIV-1 infection.

**Keywords: antibody, immunoprophilaxis, HIV - human immunodeficiency virus, pharmacokinetics, validation, broadly neutralizing antibodies**

OPEN ACCESS

***Edited by:***
*Marit Van Gils, Academic Medical Center, Netherlands*

***Reviewed by:***
*Owen Kavanagh, York St. John University, United Kingdom*
*James Even Voss, The Scripps Research Institute, United States*

***Correspondence:**
*Nicole L. Yates*
*Nicole.yates@duke.edu*

***Specialty section:***
*This article was submitted to Vaccines and Molecular Therapeutics, a section of the journal Frontiers in Immunology*

***Received:*** *14 May 2021*
***Accepted:*** *02 August 2021*
***Published:*** *24 August 2021*

***Citation:***
*Wesley MS, Chiong KT, Seaton KE, Arocena CA, Sawant S, Hare J, Hernandez K, Rojas M, Heptinstall J, Beaumont D, Crisafi K, Nkolola J, Barouch DH, Sarzotti-Kelsoe M, Tomaras GD and Yates NL (2021) Validation of a Triplex Pharmacokinetic Assay for Simultaneous Quantitation of HIV-1 Broadly Neutralizing Antibodies PGT121, PGDM1400, and VRC07-523-LS. Front. Immunol. 12:709994. doi: 10.3389/fimmu.2021.709994*

## INTRODUCTION

The rate of Acquired Immunodeficiency Syndrome (AIDS)-related deaths is not decreasing, despite the existence of highly efficient drugs that suppress Human Immunodeficiency Virus (HIV) replication and provide patients a life expectancy close to that of healthy individuals (1). This is partially due to the lack of sufficient access to antiretroviral therapy (ART) and due to the fact that ART does not eliminate viral reservoirs from HIV-1 infected individuals. Therefore, continuous therapy is needed for a lifetime. Additionally, most currently available ART regimens require daily adherence and have negative side effects, including risk of adverse short- and long-term effects on kidneys, bone density and the cardiovascular system (2–4). Thus, alternate prevention and treatment strategies are needed to increase accessibility and uptake. In particular, effective, long-acting prevention strategies with fewer off-target or other side effects may increase trust and acceptance in communities affected by or at high-risk for HIV-1 acquisition.

Recent studies have shown that passively infused broadly neutralizing monoclonal antibodies (bnAbs) exhibit favorable safety profiles and are promising strategies for therapy and prevention of HIV-1 (5–7). The Antibody Mediated Prevention (AMP) studies substantiated the concept that a bnAb can prevent HIV acquisition (5, 8–10). In addition to prevention of HIV-1 infection, bnAbs are being investigated as an approach to achieve viral control without the use of antiretroviral therapy (11–13). For treatment, as well as for prevention, suitable combinations of antibodies are essential to increase overall breadth and potency of coverage and to prevent the emergence of resistant variants. More than a decade ago, the first bnAbs were successfully isolated from chronically HIV-1 infected individuals (14–16), including VRC01, PGT121 and PGDM1400. PGT121 targets HIV-1 gp120 envelope protein at the base of the V3 glycan loop, PGDM1400 binds to the V1/V2 glycan region (16–18) and VRC01 targets the CD4 binding site. While these are naturally occurring HIV-1 broadly neutralizing antibodies, next generation antibodies have been engineered for increased potency, half-life and ability to target 2 or 3 independent viral sites to achieve better neutralization (19). A good example of this is VRC07-523-LS. VRC07-523-LS is a modified variant of VRC01 and targets the CD4 binding site of the HIV-1 gp120 (20). PGT121, PGDM1400 and VRC07-523-LS in any combination are currently being tested in various clinical trials (ClinicalTrials.gov Identifier NCT02960581, NCT03205917), highlighting the importance of measuring the pharmacokinetics (PK) of more than one antibody simultaneously. These results describe the Triplex PK Assay, a validated method to simultaneously measure the PK of PGT121, PGDM1400 and VRC07-523-LS monoclonal antibody (mAb) concentrations in human serum. This assay utilizes a mixture of three microsphere sets that are each bound to specific anti-idiotype (anti-ID) antibodies to capture either PGT121, PGDM1400 or VRC07-523-LS mAbs. The microsphere mixture is incubated with sample serum and bound mAbs are then detected using a phycoerythrin (PE)-labelled anti-human IgG antibody. Each microsphere set, and therefore, the binding to each mAb, can be distinguished from each other by a Bio-Plex 200 system. It has proven to be sensitive, specific, accurate, and precise in both HIV-1 seronegative and seropositive human serum (Supplementary Material). This method can therefore be applied for analyzing results of both prevention and/or therapeutic human trials and is, hence, an important tool for the effort to end HIV-1 infections and AIDS.

## MATERIAL AND METHODS

### Antibody Capture

Anti-ID antibodies bind specifically to the antigen binding site, or idiotype, of another antibody. All anti-ID antibodies utilized here are recombinant and generated to bind specifically to their corresponding mAb drug product. Therefore, anti-ID antibodies are important reagents for specific drug development since they can be used to measure free and total drug levels in samples. In the Triplex PK Assay, anti-idiotype antibodies are loaded onto MagPlex microspheres (Luminex Corp, Austin, TX) such that their antigen binding sites are free to bind the antigen binding site of the target antibody drug product. This is done by first binding biotinylated anti-mouse IgG to neutravidin-coupled microspheres, followed by binding to one of the three anti-IDs (**Figure 1**). Each MagPlex microsphere region is labeled with varying concentrations of two different fluorescent dyes, to be individually identified using the Bio-Plex Manager and Bio-Plex 200 Systems (Bio-Rad, Hercules, CA). Covalent coupling of free amines on the side chains of NeutrAvidin (16.65 µg/5x$10^6$ microspheres) (ThermoFisher, Waltham, MA) to the intermediate Sulfo-NHS (N-hydroxysulfosuccinimide) ester of activated carboxylated fluorescent MagPlex microspheres was performed according to the xMAP® Antibody Coupling Kit User Manual (Luminex Corp, Austin, TX) (21–24). NeutrAvidin-coupled microspheres were then bound to 5 µg/5x$10^6$ microspheres of biotinylated goat anti-mouse IgG antibody, adsorbed against human immunoglobins and pooled sera (SouthernBiotech, Birmingham, AL) for one hour, followed by washing. Goat anti-mouse IgG bound microspheres were then bound to 250 µg/ml of the anti-PGT121-idiotype (Covance, Princeton, NJ, customized and expressed by cell line: IV1737.939.26(A-I0715)) or 25 µg/ml of the anti-PGDM1400-idiotype (Covance, Princeton, NJ, customized and expressed by cell line: IV1919.265.37(A-F0914)) diluted in 500 µl Phosphate Buffered Saline (PBS) for 30 minutes. For detection of VRC07-523-LS mAb, 5 µg/ml of a biotinylated goat anti-mouse IgG Fc antibody, cross- adsorbed against bovine, horse and human serum (ThermoFisher, Waltham, MA) was bound to neutravidin beads for 1 hour, followed by 20 µg/ml anti-VRC07-523-LS-idiotype (5C9)(NIH, Bethesda, MD, Vaccine Research Center, customized and expressed by cell line: CHO DG44) antibody diluted in 500 µl PBS for 30 minutes. Thus, the F (ab) arms are oriented outward to freely bind the paratopes of PGDM1400, PGT121 or VRC07-523-LS (**Figure 1**). Both the capture antibody and anti-ID antibody incubations were done at room temperature (RT) and shaking at 1100rpm. Microspheres

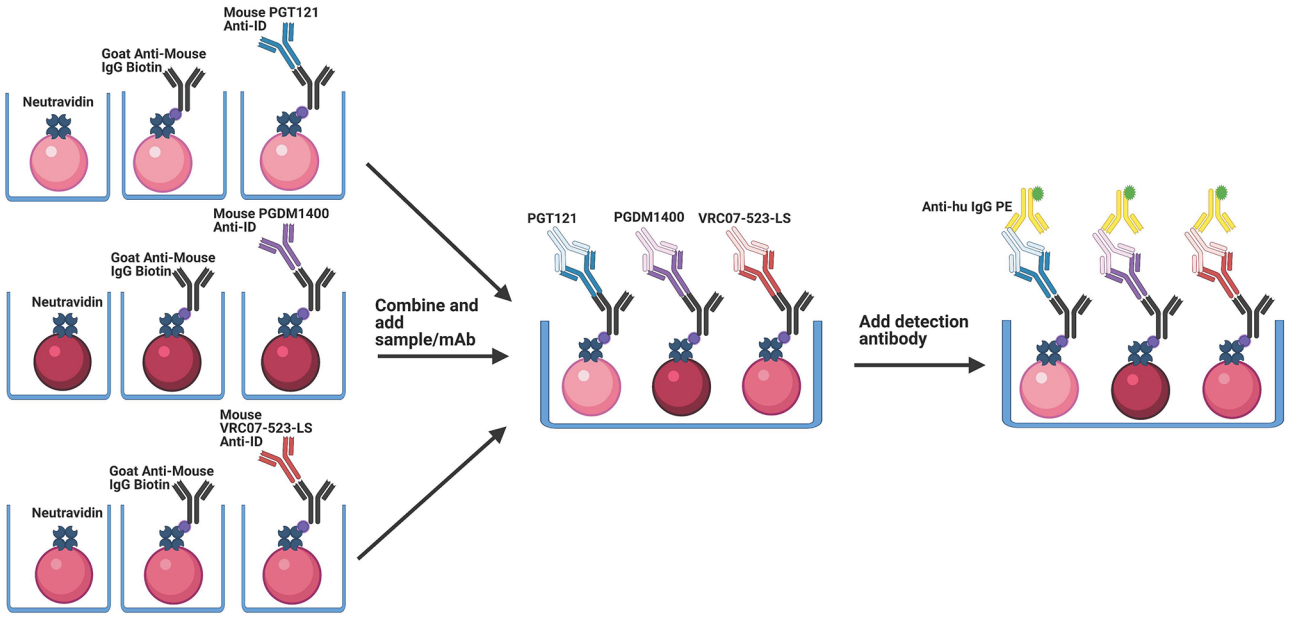


**FIGURE 1** | Schematic of the Triplex PK setup. Magnetic microspheres are coupled to NeutrAvidin, which binds to the biotin conjugated goat anti-mouse IgG. This antibody is in an orientation that allows for binding of the anti-ID antibody in the correct orientation to allow for optimal binding of the corresponding mAb. In a multiplex setup, the anti-ID antibodies are bound to the goat anti-mouse IgG Biotin in separate reactions, are washed, and then combined. PGT121, PGDM1400 and VRC07-523-LS mAbs are then added simultaneously into the solution. The microspheres are then washed, and detection antibody is added.

were washed and blocked in between incubations with wash buffer (1% Bovine Serum Albumin (w/v)/0.05% Tween-20 (v/v)/ 0.05% Sodium Azide (w/v) in PBS).

## Triplex PK Assay for HIV-1 bnAbs

The assay was conducted in a 96-well flat bottom plate (Bio-Rad, Hercules, CA). Human sera and controls were diluted in assay diluent (1% Milk Blotto (w/v)/5% Normal Goat Sera (v/v)/0.05% Tween-20 (v/v) in PBS) to the desired dilution factor. Prepared capture microspheres (5000 microspheres/well) were incubated with human sera as unknown samples alongside mAb dilution series of known concentration for generation of standard curves and mAb spiked serum controls (25 µl total volume per well) for 2 hours shaking at 750 rpm and at 22˚C in a temperature controlled incubator. Sample incubation is then followed by 3 washing and blocking steps with 100 µl per well wash buffer using a magnetic separator (Luminex Corp, Austin, TX). Subsequently, 25 µl per well of a goat anti-human IgG detection antibody conjugated to phycoerythrin (PE) at 2 µg/ml for 30 minutes (SouthernBiotech, Birmingham, AL) was used to detect bound PGDM1400, PGT121 and VRC07-523-LS. Known amounts of purified PGT121 IgG mAb (0.5 µg/ml, 2-fold, 14 serial dilutions) (Catalent, Somerset, NJ), PGDM1400 IgG mAb (0.1 µg/ml, 2-fold, 14 serial dilutions) (Catalent, Somerset, NJ) and VRC07-523-LS IgG mAb (1 µg/ml, 3-fold, 14 serial dilutions) (NIH, Bethesda, MD) were co-titrated as a standard curves on every assay plate to quantify PGT121 IgG, PGDM1400 IgG and VRC07-523-LS IgG present in human serum using fluorescence intensity (FI) readouts with the unit of median fluorescence intensity (MFI). All controls, samples, standards, and blanks were assayed as a duplicate, and the mean value was reported. The blank well (background, referred to as Bkgd) is subtracted from the FI and the resultant value was reported as FI-Bkgd. Additionally, PGDM1400 IgG mAb, PGT121 IgG mAb and VRC07-523-LS IgG mAbs were spiked into 1:100 normal human reference serum (NHS) at 5 specific known concentrations (1. PGDM1400 starting at 0.04 µg/ml, 4-fold, for 5 serial dilutions; 2. PGT121 starting at 0.08 µg/ml, 2-fold, for 4 serial dilutions plus a fifth concentration of 0.002 µg/ml; and 3. VRC07-523-LS starting at 0.002 µg/ml, 2-fold, for 5 serial dilutions) and were used as antibody-specific controls for standard curve accuracy. Negative controls and blank (uncoupled) microspheres were included in each assay to ensure specificity. Assay plates were read using Bio-Plex Manager and Bio-Plex 200 Systems (Bio-Rad, Hercules, CA). The Bio-Plex 200 System detects the fluorescent dyes (microsphere region) within the each MagPlex microsphere region and then quantifies the associated PE signal intensities from the detection antibody. The level of bound mAbs is identified by the intensity of the PE (reporter signal) in FI-Bkgd. This enables the quantification of all three mAbs simultaneously using Bio-Plex Manager software.

## Specimens

Human sera were obtained from HIV seronegative and seropositive individuals, with Institutional Review Board (IRB) approval. Both seronegative and seropositive samples were assessed to test assay parameters in the sample-specific matrix, with applications for both HIV-1 prevention and therapeutic studies. 132 HIV seronegative human sera were obtained from

BioIVT, Westbury, NY (formerly Bioreclamation), and 66 HIV seropositive samples were obtained from the University of Washington Center For AIDS Research (Seattle, WA). An additional 17 samples were obtained from group 3B in the CAVD study Barouch 693 (IAVI T002, ClinicalTrials.gov Identifier NCT03205917), from seropositive study participants off ART and infused with PGDM1400 and/or PGT121.

## Quality Control/Quality Assurance and Data Management

Quality control (QC) acceptance criteria for Triplex PK assay include but are not limited to: 1) FI-Bkgd readout must have a percentage of coefficient of variation (%CV) between replicates < 20% for each dilution in the titration series and < 15% for a sample that is assayed at a single dilution when fluorescence- background (FI-Bkgd)>100, 2) Three out of five spiked controls must have a recovery between 70 -130% of their input concentration, and 3) the positive control antibody titer, defined as the half maximal effective concentration (EC50) from a five parameter logistic curve fit (5PL) and the highest FI-Bkgd in the positive control standard curve must be within three standard deviations of the historical mean as tracked with Levey-Jennings charts [Portal, Labkey, Seattle, WA (25)]. Guide sets for Levey-Jennings charts that enable tracking of positive controls to historical data were established from >10 standardized assays. Experiments were performed in a Good Clinical Laboratory Practice (GCLP) compliant laboratory with oversight by the Quality assurance for Duke Vaccine Immunogenicity Programs (QADVIP). Assay documentation was recorded and stored in an Electronic Laboratory Notebook (ELN) (Agilent Technologies, Santa Clara, CA). Raw experimental data and analyses are securely stored with an audit trail through Electronic Content Manager (ECM) (Agilent Technologies, Santa Clara, CA).

## Analysis

Validation described herein was performed in accordance with the FDA document "Guidance for Industry: Bioanalytical Method Validation, May 2018" and the ICH Tripartite Guideline "Validation of Analytical Procedures: Text and Methodology. Q2 (R1)" (26, 27). Qualification of the method for HIV-1 seropositive serum followed the same aspects and parameters, with a smaller sample size than for validation. Should a need for validation of this method using seropositive serum be deemed necessary, established cut points from qualification will be used for validation. The parameters tested and reported here are Accuracy, Specificity, Positivity, Limit of Detection and Quantitation, and Precision. Range and linearity testing were not specifically tested since samples can be diluted to fall within the quantifiable range of the assay, and samples are screened at the beginning of the trial to determine optimal dilution factor. This is a newly developed assay and is not performed in another laboratory, so reproducibility could not be tested. The recommended sample size for establishing limit of detection (LOD) and lower limit of quantitation (LLOQ) is 60 (28). Therefore, at least 66 (110% of required minimum) samples were tested because it is anticipated that some samples might not pass the QC criteria and are, therefore, not included in the calculations. 5PL curve fit for the standard curves as well as the equation for EC50 calculation were generated with Bio-Plex Manager (Bio-Rad). For validation in seronegative samples and to enhance the significance in establishing the background cutoffs (LOD and LLOQ), the FI-Bkgd of two samples sets (66 each, 132 seronegative samples in total) were combined to calculate the 95$^{th}$ percentile FI-Bkgd. The LOD in FI-Bkgd (mean + 3.3 standard deviations of the FI-Bkgd from these samples) was plugged into the 5PL equation generated by Bio-Plex Manager from the PGDM1400 IgG, PGT121 IgG or VRC07-523-LS IgG standard curve to obtain the concentration for the LOD. LLOQ was calculated in a similar way, except that the mean + 10 standard deviations of the FI-Bkgd from these samples was be used. The LLOQ in FI-Bkgd was then also plugged into the 5PL equation from respective standard curve to calculate the concentrations of the LLOQ. Alternatively, LLOQ can be determined as the lowest accurately-recovered concentration on the standard curve that it was above the LOD. Microsoft Excel was used to calculate %CV (standard deviation/mean *100) between curves for repeatability and intermediate precision, Levey-Jennings plots, and calculating concentration for LOD and LLOQ with the 5PL curve. Data processing for automated QC report was performed on a secure and validated data repository [Portal, Labkey (25)]. SAS software, Version 9.4 of the SAS System for Windows, Copyright © [2002-2012] by SAS Institute Inc., Cary, NC, USA, was used for generating histograms. R Core Team (2018). R: A language and environment for statistical computing, R Foundation for Statistical Computing, Vienna, Austria. URL https://www.R-project.org/ and package ggplot2 was used for generating plots for positivity.

# RESULTS

## Specificity

The specificity of an analytical method is the capability of assessing the analyte in the presence of other components, which may have a positive or negative effect on the resulting values. This can also be defined as non-specific background. Components that may be expected are impurities, degradation products and/or sample matrix. Whether the presence of one mAb affects the background and specificity of the detection of the other mAb concentrations are of particular interest for co-infusion studies. The goal of this experiment was to assess how the three mAbs influence each other or the output values of this method.

### Non-Specific Background Activity of HIV-1 Seronegative Human Serum

To assess non-specific background activity in human serum, 132 HIV-1 seronegative sera (2 subsets of each 66 samples) were diluted at 1:100 and tested for non-specific background binding. Seropositive sera were also tested, and data is shown in Supplementary Material. The FI-Bkgd values (excluding samples that did not meet QC acceptance criteria) were used to calculate a mAb specific positivity threshold. The 95$^{th}$ percentile is an established method for antigen specific cutoff determination from baseline or seronegative status samples and is commonly used for immunoassays (29, 30). The positivity cutoff was calculated as the

95th percentile of the mAb and sample set specific response from the tested samples (**Table 1** and **Supplementary Table 1**). Positivity cutoffs for PGDM1400, PGT121 and VRC07-523-LS in HIV-1 seronegative serum are as low as 1049 FI-Bkgd, 1419 FI-Bkgd and 1126 FI-Bkgd, respectively (**Table 1**). **Figure 2** shows the FI-Bkgd distribution of binding to anti-IDs for PGDM1400 (**Figure 2A**), PGT121 (**Figure 2B**) and VRC07-523-LS (**Figure 2C**) in seronegative (**Figures 2A–C)** and seropositive (**Supplementary Figures 1A–C)** human serum. Thus, these results demonstrate a sensitive assay with low positivity cutoffs.

### Positivity

To determine if the reported method could detect and quantify accurate amounts of PGDM1400, PGT121, and VRC07-523-LS mAb in 33 HIV-1 seronegative serum samples, commercially available samples were spiked with known amounts of each mAb (0.006 μg/ml of PGDM1400, 0.020 μg/ml of PGT121, and 0.003 μg/ml of VRC07-523-LS). These concentrations were selected since they are within the limits of accurate recovery (70-130%) for the respective mAb and above the calculated limit of detection. Percent recovery was calculated using following formula: (observed concentration/expected concentration)*100. Of all included samples, 100% of seronegative samples (**Figure 3**) and at least 80% of seropositive (**Supplementary Figures 2A–C)** samples had an observed concentration that was within 2-fold of the expected concentration.

## Accuracy

Accuracy of an analytical method is expressed by the degree to which the value found conforms with a particular value, which is either the accepted conventional true values or an accepted reference value. It also demonstrates how reliably a method can produce true values, which is an essential parameter for the pharmacokinetic measurement of passively-infused bnAbs. To determine the accuracy of antibody concentration detection, or antibody recovery, in the sample matrix, PGDM1400 IgG, PGT121 IgG and VRC07-523-LS IgG mAbs were co-titrated into assay diluent as well as into pooled HIV-1 seronegative sera diluted at 1:100 in assay diluent. Additionally, as an additional test of antibody recovery to ensure the accuracy of the standard curve, PGDM1400, PGT121 and VRC07-523-LS mAbs at several known concentrations (low, medium, high) were spiked into assay diluent and into 30 pooled HIV-1 seronegative human serum samples, diluted 1:100 diluted in assay diluent. The known concentrations for each mAb spiked controls were as follows: 1. PGDM1400 starting at 0.04 μg/ml, 4-fold, for 5 serial dilutions; 2. PGT121 starting at 0.08 μg/ml, 2-fold, for 4 serial dilutions plus a fifth concentration of 0.002 μg/ml; and 3. VRC07-523-LS starting at 0.002 μg/ml, 2-fold, for 5 serial dilutions. A PGDM1400/PGT121/VRC07-523-LS IgG co-titrated standard curve was assayed on the same plate to determine observed concentration of the spiked serum samples. It was also critical to determine if the bnAbs tested had any cross-reactivity to anti-idiotypes of mis-matched specificity. Therefore, a co-titrated PGDM1400/PGT121 and a VRC07-523-LS standard curve, both from validated assays, were compared to the co-titrated PGMD1400/PGT121/VRC07-523-LS standard curve. All three curves were titrated in 1:100 NHS diluted in assay

**TABLE 1** | Limit of detection and quantification in HIV-1 seronegative human serum.

| mAb | Serostatus | 95th percentile (FI-Bkgd) | LOD ng/ml | Physiological LOD μg/ml | LLOQ ng/ml (mean +10 stdev) | Physiological LLOQ μg/ml | ULOQ ng/ml (highest concentration with accurate recovery) | Physiological ULOQ μg/ml | LLOQ ng/ml (lowest accurate point above LOD) | Physiological LLOQ μg/ml |
|---|---|---|---|---|---|---|---|---|---|---|
| ***PGDM1400*** | Seronegative | 1049 | 0.26 | 0.026 | 0.76 | 0.076 | 50 | 5 | 0.391 | 0.039 |
| ***PGT121*** | Seronegative | 1419 | 0.91 | 0.091 | 2.6 | 0.26 | 250 | 25 | 0.977 | 0.098 |
| ***VRC07-523-LS*** | Seronegative | 1126 | 0.14 | 0.014 | 0.41 | 0.041 | 37 | 3.7 | 0.152 | 0.098 |

*LOD, LLOQ and ULOQ as well as the corresponding physiological concentrations observed in the PGDM1400/PGT121/VRC07-523-LS Triplex PK for HIV-1 seronegative human serum.*

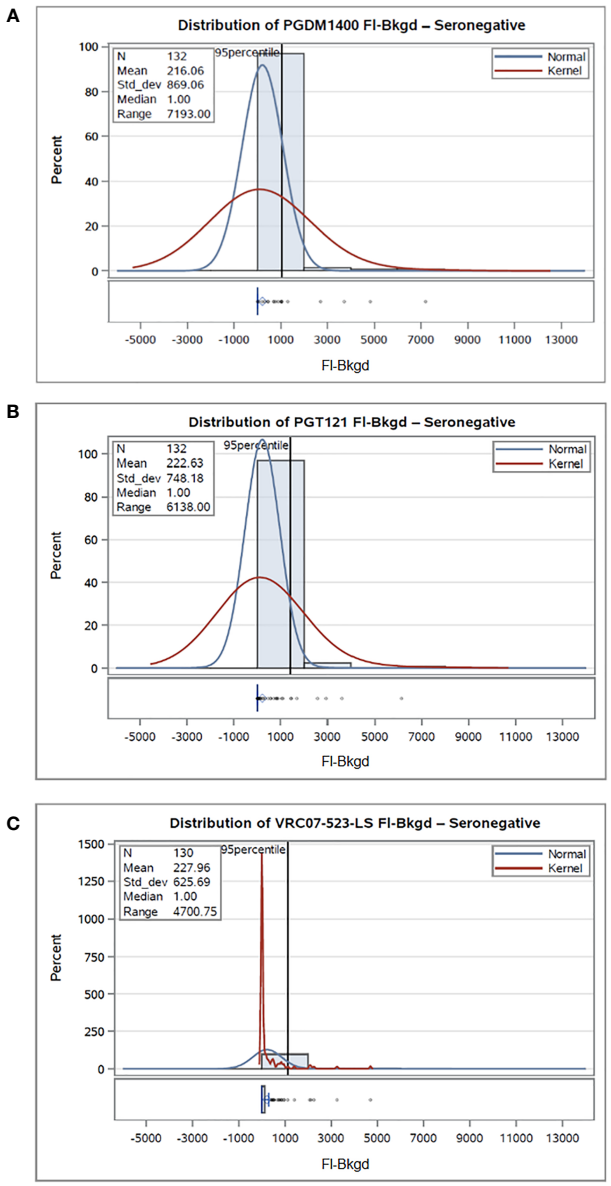


**FIGURE 2** | Non-specific background activity of HIV-1 seronegative human serum. 132 HIV-1 seronegative samples were tested at 1:100 in the PGDM1400/PGT121/VRC07-523-LS PK BAMA, and the distribution of binding to the PGDM1400 anti-ID **(A)**, PGT121 anti-ID **(B)**, and VRC07-523-LS anti-ID **(C)** was plotted. Normal and kernel density estimates are used to visualize the data distribution. Normal shows the fit of a normal distribution to the FI-Bkgd measurements, and a superimposed fitted density curve on the histogram. Kernel density estimates on histograms help smoothen the data distribution and help visualize the non-normal data distribution and patterns.

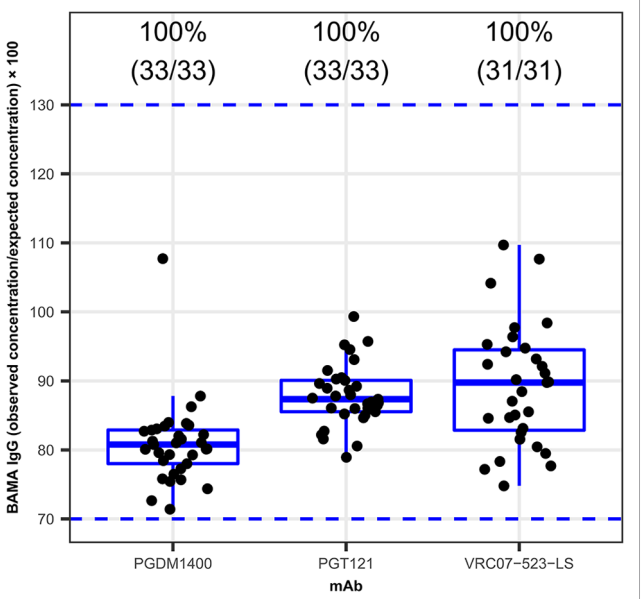


**FIGURE 3** | Positivity of the PGDM1400, PGT121 and VRC07-523-LS Triplex PK. 33 HIV-1 seronegative serum samples were spiked with specific concentrations of the PGDM1400, PGT121, and VRC07-523-LS. Percent recovery, calculated as (observed concentration ÷ expected concentration) × 100, for PGMD1400, PGT121 and VRC07-523-LS, respectively is shown on y-axis. The blue dashed lines at levels 70 and 130, show preset acceptance criteria for percent recovery [70-130%]. Numbers on top of each box plot show the percentage and counts (number of samples that met the present acceptance criteria/total number of samples) of samples with a percent recovery between 70-130%. 100% of the samples, for all three bnAbs tested here, had acceptable percent recovery.

diluent and FI-Bkgd as well as percent recovery were compared. Observed concentrations and percent recovery (observed concentration/expected concentration x 100) were calculated using the Bio-Plex Manager software. Additionally, to determine if each bnAb demonstrated cross-reactivity to the un-matched anti-ID antibodies, each bnAb was solely spiked into assay diluent at defined concentrations as mentioned above and incubated with a microsphere mixture containing all three anti-ID antibodies.

The FI-Bkgd observed for the co-titrated PGDM1400/PGT121/VRC07-523-LS standard curves in assay diluent were comparable at most points to those observed in pooled HIV-1 seronegative (**Figure 4**) and seropositive serum (**Supplementary Figure 3**). At least 6 and 7 (for VRC07-523-LS) or 13 and 11 (for PGDM1400 and PGT121) consecutive points had accurate recovery within the range of 70-130% for the co-titrated standard curve in assay diluent and in HIV-1 seronegative serum, respectively (**Figures 4A, C, E**). These results meet the defined validation criteria, which required at least 5 consecutive points in each titration curve to have an observed concentration that is between 70 and 130% of the expected concentration. Recovery for each spiked concentration in pooled HIV-1 seronegative serum was within the accurate recovery range of 70-130% (**Figures 4B, D, F).** The 5PL (5 parameter logistic) EC50 (Effective Concentration-50) values of PGDM1400/PGT121/VRC07-523-LS standard curve in assay diluent, HIV-1 seronegative and seropositive serum are within the mean +/- 3 standard deviations criteria established for tracking in Levey-Jennings (**Figure 5** and **Supplementary Figure 4**). Results for FI-Bkgd and percent recovery for the PGDM1400/PGT121 and VRC07-523-LS standard curves and comparable to the co-titrated PGDM1400/PGT121/VRC07-523-LS standard curve, demonstrating that VR07-

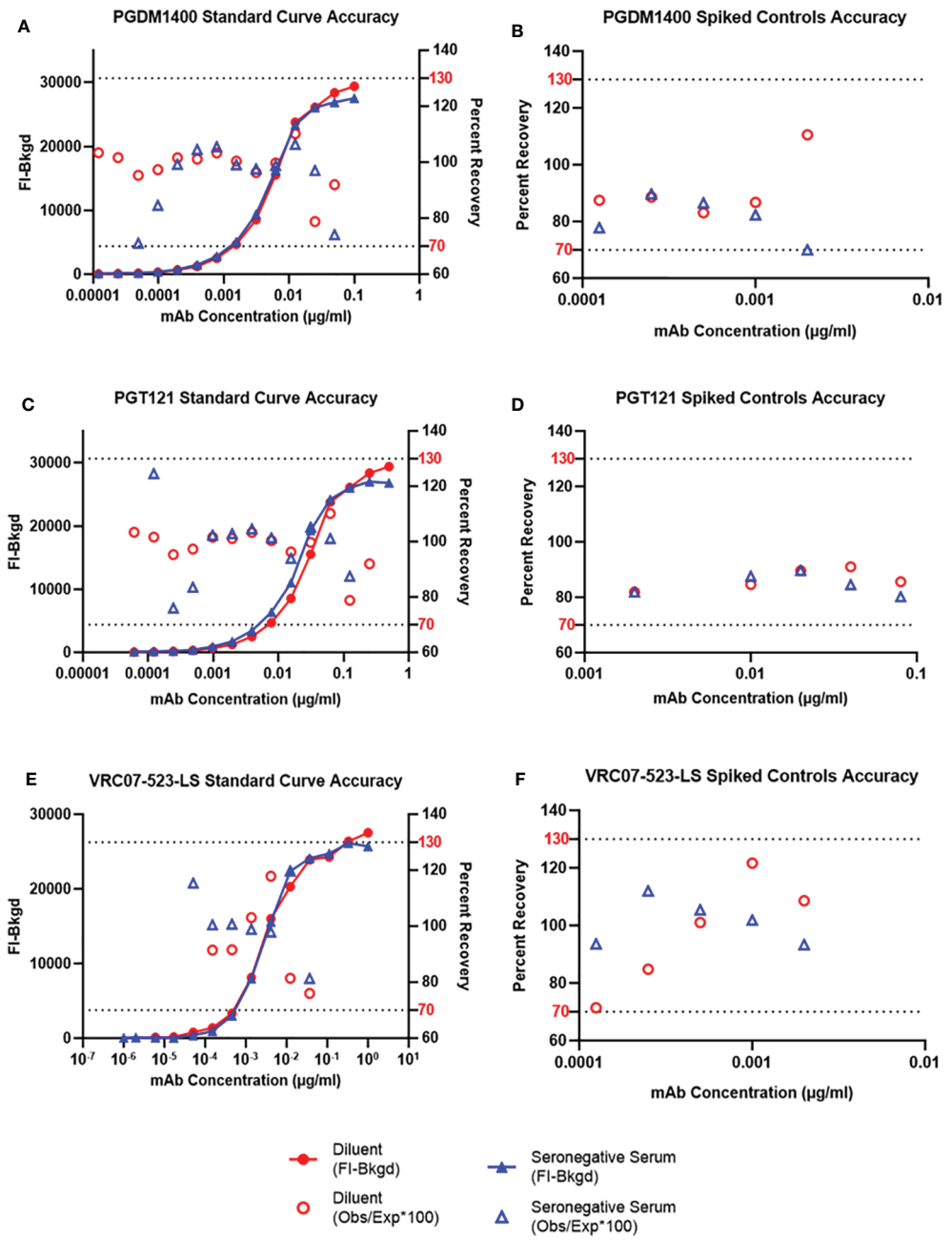


**FIGURE 4** | Accuracy of Standard Curves and Spiked Sample Recovery. PGDM1400 IgG **(A)**, PGT121 IgG **(C)** and VRC07-523-LS IgG **(E)** mAbs were titrated in diluent (red), in pooled 1:100 diluted HIV-1 seronegative human serum. PGDM1400 IgG **(B)**, PGT121 IgG **(D)** and VRC07-523-LS IgG **(F)** mAbs were spiked in pooled 1:100 diluted seronegative serum at 5 different concentrations. Observed concentration for each point in the curve was calculated and used to determine accuracy of recovery of each mAb. The dotted lines denote the upper (130% of the expected concentration) and lower (70% of the expected concentration) limits of acceptable percent recovery.

523-LS did not bind to the PGT121 or PGDM1400 anti-ID antibodies and no cross-reactivity was observed (**Figure 6**). Binding was only observed between specific mAb and anti-ID antibodies, indicating that they are highly specific (**Figure 7**). These results demonstrate that the co-titrated PGDM1400/PGT121/VRC07-523-LS standard curves in assay diluent, HIV-1 seronegative as well as seropositive serum can accurately and simultaneously quantify each mAb concentration respectively, in the serum matrix diluted to be within the linear range of the assay.

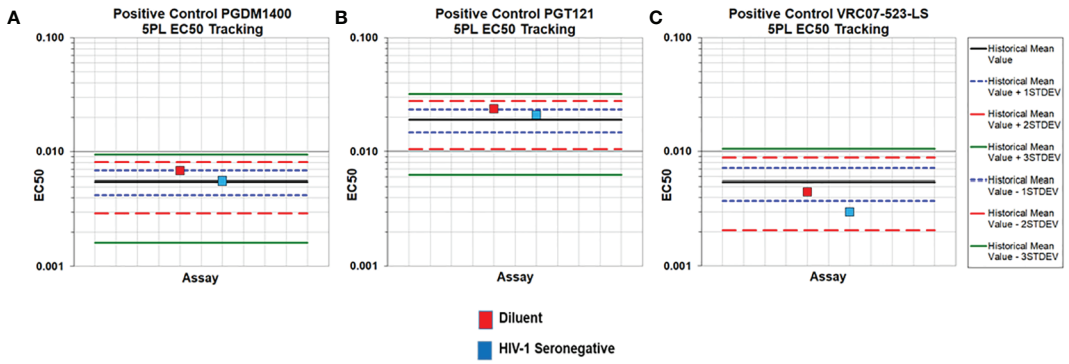


**FIGURE 5** | Accuracy of the PGDM1400/PGT121/VRC07-523-LS Triplex PK standard curves in diluent and HIV-1 seronegative human serum. PGDM1400 **(A)**, PGT121 **(B)** and VRC07-523-LS **(C)** were co-titrated in assay diluent and 1:100 HIV-1 seronegative serum diluted in assay diluent. 5PL EC50 values of each mAb fell within 3 standard deviations of the historical mean (solid black line).

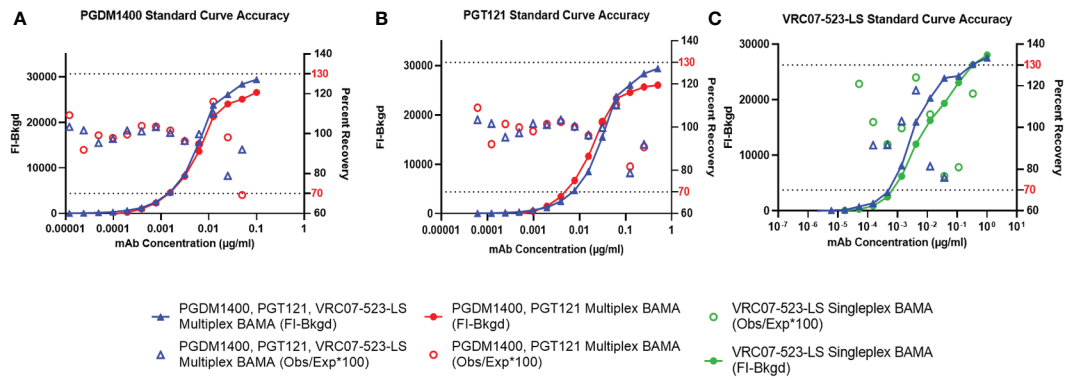


**FIGURE 6** | Accuracy of multiplexed PGDM1400, PGT121 and VRC07-523-LS. Co-titrated PGDM1400 **(A)** PGT121 **(B)** as well as a VRC07-523-LS **(C)** standard curve (all from validated assays) are compared to the co-titrated PGMD1400/PGT121/VRC07-523-LS standard curve. All three curves were titrated in 1:100 NHS diluted in assay diluent and Fl-Bkgd as well as percent recovery were compared. Curves and percent recovery are comparable indicating that VRC07-523-LS does not bind to any other anti-ID other than the one specific to VRC07-523-LS.

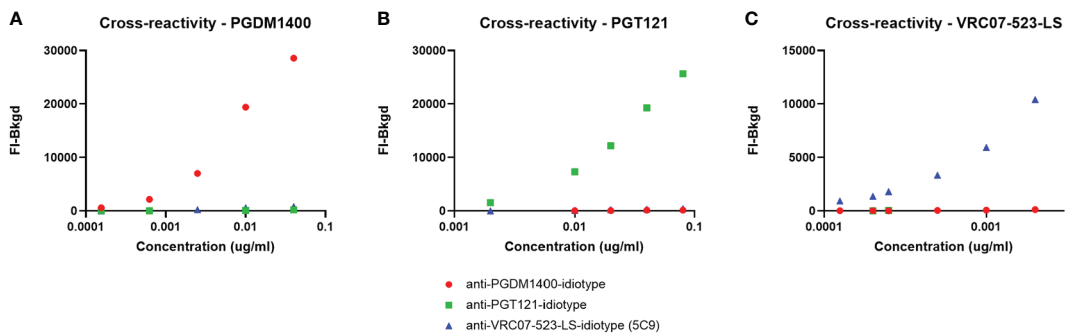


**FIGURE 7** | Lack of Cross-reactivity and competition between PGDM1400, PGT121 and VRC07-523-LS and their respective anti-ID antibodies. PGDM1400 **(A)**, PGT121 **(B)** and VRC07-523-LS **(C)** were each titrated in assay diluent and incubated with a microsphere mixture containing all three anti-ID antibodies. Binding can only be observed between specific mAb and anti-ID antibodies, indicating that the anti-ID's are highly specific and no cross-reactivity can be expected.

## Limits of Detection and Quantitation

The limit of detection (LOD) is the lowest concentration of an analyte that can be detected but not necessarily quantified, while the lower limit of quantitation (LLOQ) is the lowest concentration that can be quantified with acceptable precision. The upper limit of quantitation (ULOQ) is the highest concentration at which each mAb can be consistently and accurately recovered. The level of background binding and therefore, the LOD (mean + 3.3 standard deviations of FI-Bkgd) and LLOQ (mean + 10 standard deviations of FI-Bkgd), may be highly dependent on the sample set tested, therefore study-specific LOD/LLOQ should be determined using baseline samples, population-specific or drug naïve samples. For validation in seronegative samples and to enhance the significance in establishing the background cutoffs (LOD and LLOQ), the FI-Bkgd of two samples sets (66 each, 132 seronegative samples in total) were combined to calculate the 95$^{th}$ percentile. The physiological LOD and LLOQ are the values multiplied by the dilution factor and therefore, corresponding to the concentration in the sample before diluting for the assay.

PGDM1400, PGT121 and VRC07-523-LS were co-titrated in 30 pooled HIV-1 seronegative serum samples diluted at 1:100 in assay diluent for the standard curve. 132 HIV-1 seronegative samples were diluted at 1:100. All samples that fell below the 95$^{th}$ percentile cutoff (**Table 1**) were used for the analysis. The LOD, LLOQ (using both calculations mentioned above), ULOQ and their corresponding physiological concentrations for each mAb in HIV-1 seronegative human serum are summarized in **Table 1**, and **Supplementary Table 1** for HIV-1 seropositive human serum.

## Precision

Precision is a measurement of the random error or degree of scatter between repeated measurements, which are repeated under the same conditions. Precision may be considered at two levels: repeatability and intermediate precision.

### Repeatability

Repeatability testing was performed to assess the variation in the PGDM1400/PGT121/VRC07-523-LS co-titrated standard curve when tested repeatedly. 12 repeats for each 12 dilutions of the standard curve were analyzed and performed by the same operator (**Figure 8**). The %CV between each replicate was less than 18% for all dilutions within the linear range of the curve for

**TABLE 2** | Repeatability of PGDM1400/PGT121/VRC07-523-LS standard curve.

| mAb | Conc (μg/ml) | Mean FI-Bkgd | %CV (12 curves) |
|---|---|---|---|
| ***PGDM1400*** | **0.1** | **28526.25** | **3.92** |
| | **0.05** | **28256.63** | **4.24** |
| | **0.025** | **26743.50** | **5.74** |
| | **0.0125** | **24070.25** | **8.12** |
| | **0.00625** | **16543.88** | **13.69** |
| | **0.003125** | **9521.50** | **15.43** |
| | **0.001563** | **5346.25** | **17.43** |
| | **0.000781** | **2826.75** | **17.70** |
| | **0.000391** | **1519.00** | **17.22** |
| | 0.000195 | 746.38 | 19.99 |
| | 0.000098 | 360.25 | 22.11 |
| | 0.000049 | 180.13 | 27.32 |
| | 0.000024 | 157.38 | 28.16 |
| | 0.000012 | 85.50 | 25.79 |
| ***PGT121*** | **0.5** | **27582.50** | **3.90** |
| | **0.25** | **27293.38** | **3.94** |
| | **0.125** | **26578.63** | **3.16** |
| | **0.0625** | **24460.25** | **2.84** |
| | **0.03125** | **18272.13** | **4.46** |
| | **0.015625** | **11092.50** | **4.59** |
| | **0.007813** | **6342.63** | **6.82** |
| | **0.003906** | **3342.13** | **5.66** |
| | **0.001953** | **1720.25** | **10.49** |
| | 0.000977 | 843.13 | 7.20 |
| | 0.000488 | 393.75 | 13.52 |
| | 0.000244 | 188.13 | 23.56 |
| | 0.000122 | 144.50 | 25.80 |
| | 0.000061 | 78.38 | 29.48 |
| ***VRC07-523-LS*** | **1** | **26137.25** | **5.03** |
| | **0.333333** | **25989.13** | **3.75** |
| | **0.111111** | **24656.63** | **5.46** |
| | **0.037037** | **22778.63** | **8.45** |
| | **0.012346** | **20545.50** | **11.35** |
| | **0.004115** | **13522.25** | **11.35** |
| | **0.001372** | **6874.38** | **11.24** |
| | **0.000457** | **2803.50** | **13.58** |
| | 0.000152 | 919.63 | 16.44 |
| | 0.000051 | 372.00 | 28.22 |
| | 0.000017 | 131.38 | 65.48 |
| | 0.000006 | 50.75 | 173.37 |
| | 0.000002 | 84.25 | 66.03 |
| | 0.000001 | 48.38 | 157.62 |

*The table shows the average binding (Mean FI-Bkgd) of each of the 12 titrated curves at each dilution as well as the %CV, which was less than 18% at each dilution within the linear range of the curves. Values in bold are above the FI-Bkgd LOD for the respective mAb and curve.*

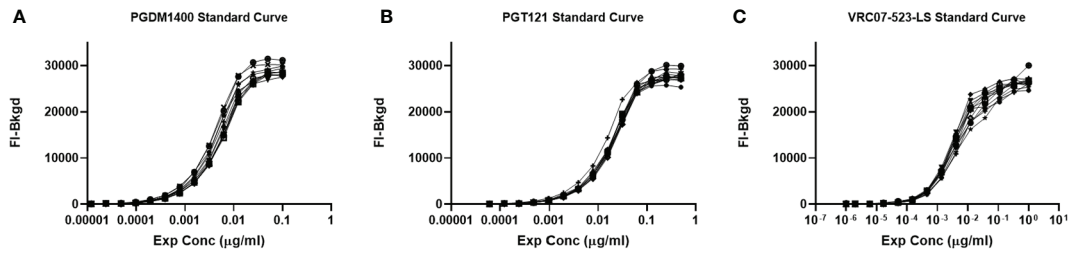


**FIGURE 8** | Repeatability of the PGDM1400/PGT121/VRC07-523-LS standard curve. PGDM1400, PGT121 and VRC07-523-LS were co-titrated in 1:100 NHS in assay diluent for a total of 12 repeats by the same operator. Curves for PGDM1400 **(A)**, PGT121 **(B)** and VRC07-523-LS **(C)** are graphed to demonstrate the repeatability of this assay.

each mAb (**Table 2**). Thus, this assay passes the preset validation criteria, which is defined that the %CV between each replicate has to be below 30% within the accurate range of the standard curve.

### Intermediate Precision

Intermediate precision assesses the variation across days, assay operators and/or equipment (27). To determine the intra-operator variability over 40 days, 3 assays including a PGDM1400/PGT121/VRC07-523-LS standard curve were performed. Resulting FI-Bkgd and observed concentrations were compared (**Figure 9** and **Table 3**). Similar to the parameters for repeatability, the %CV of each point of the standard curve within the linear range was less than 30%. Thus, this method demonstrates intermediate intra-operator precision over the time course of 40 days due to the %CV being a maximum of 14% for each point within the linear range (**Table 3**).

**TABLE 3** | Intermediate precision of PGDM1400/PGT121/VRC07-523-LS standard curve.

| mAb | Conc (μg/ml) | Mean FI-Bkgd | %CV (3 curves) |
|---|---|---|---|
| ***PGDM1400*** | **0.1** | **28018.88** | **1.79** |
| | **0.05** | **27914.25** | **2.13** |
| | **0.025** | **26289.13** | **1.38** |
| | **0.0125** | **23187.63** | **3.55** |
| | **0.00625** | **15701.00** | **11.94** |
| | **0.003125** | **9146.88** | **12.46** |
| | **0.001563** | **5118.38** | **20.86** |
| | **0.000781** | **2746.13** | **12.31** |
| | **0.000391** | **1424.63** | **12.34** |
| | 0.000195 | 726.00 | 10.88 |
| | 0.000098 | 373.75 | 15.55 |
| | 0.000049 | 180.13 | 26.74 |
| | 0.000024 | 166.88 | 4.53 |
| | 0.000012 | 103.63 | 18.23 |
| ***PGT121*** | **0.5** | **27042.75** | **3.67** |
| | **0.25** | **27073.38** | **2.77** |
| | **0.125** | **26298.25** | **3.13** |
| | **0.0625** | **24228.63** | **1.99** |
| | **0.03125** | **18661.75** | **4.51** |
| | **0.015625** | **11092.50** | **3.39** |
| | **0.007813** | **6351.63** | **8.40** |
| | **0.003906** | **3392.25** | **7.07** |
| | **0.001953** | **1719.13** | **8.48** |
| | 0.000977 | 877.63 | 9.35 |
| | 0.000488 | 398.75 | 15.16 |
| | 0.000244 | 201.50 | 26.83 |
| | 0.000122 | 160.00 | 13.07 |
| | 0.000061 | 84.75 | 33.69 |
| ***VRC07-523-LS*** | **1** | **25855.00** | **5.03** |
| | **0.333333** | **26093.88** | **3.75** |
| | **0.111111** | **24698.63** | **5.46** |
| | **0.037037** | **23454.38** | **8.45** |
| | **0.012346** | **21074.75** | **11.35** |
| | **0.004115** | **14348.63** | **11.35** |
| | **0.001372** | **7102.88** | **11.24** |
| | **0.000457** | **2736.75** | **13.58** |
| | 0.000152 | 940.63 | 16.44 |
| | 0.000051 | 341.63 | 28.22 |
| | 0.000017 | 173.75 | 65.48 |
| | 0.000006 | 50.75 | 173.37 |
| | 0.000002 | 120.50 | 66.03 |
| | 0.000001 | 48.38 | 157.62 |

*The table shows the average binding (Mean FI-Bkgd) of each standard curve performed by the same operator over the time course of 40 days at each dilution as well as the %CV, which was less than 14% at each dilution within the linear range of the curves. Values in bold are above the LOD in FI-Bkgd for the respective mAb and curve.*

## DISCUSSION

The PK method for the simultaneous detection of three bnAbs was validated for HIV-1 seronegative human serum as well as qualified for HIV-1 seropositive human serum for the measurement of antibody concentrations in human clinical trials. Results demonstrated that the PGDM1400/PGT121/VRC07-523-LS PK BAMA is specific, accurate, sensitive, precise, and capable for repeatable simultaneous quantitation of three bnAbs, namely PGT121, PGDM1400, and VRC07-523-LS. This innovative Triplex immunoassay reported here measures the pharmacokinetics of PGDM1400, PGT121 and VRC07-523-LS mAbs simultaneously using PGDM1400-, PGT121- and VRC-07-523-LS-specific anti-idiotype antibodies. This assay accurately quantified each mAb in HIV-1 seronegative specimens at physiological concentrations in serum starting at 0.026 μg/mL, 0.091 μg/mL, and 0.014 μg/mL for PGDM1400, PGT121 and VRC07-523-LS, respectively. This was similar to the LOD of PGDM1400, PGT121 and VRC07-523-LS in HIV-1 seropositive human serum starting at physiological concentrations of 0.032 μg/mL, 0.098 μg/mL, and 0.021 μg/mL, respectively. The upper limits of quantitation in diluted serum for PGDM1400, PGT121 and VRC07-523-LS were 5 μg/mL,

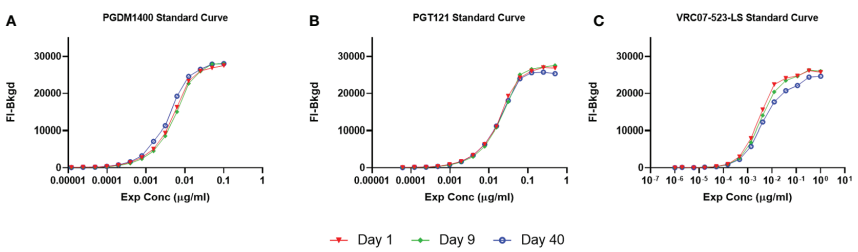


**FIGURE 9** | Intermediate Precision of the PGDM1400/PGT121/VRC07-523-LS standard curve. PGDM1400, PGT121 and VRC07-523-LS were co-titrated in 1:100 NHS in assay diluent by the same operator over a timeframe of 40 days. Curves for PGDM1400 **(A)**, PGT121 **(B)** and VRC07-523-LS **(C)** are graphed to demonstrate the intermediate precision of this assay.

25 μg/mL, and 3.7 μg/mL, respectively, and highly concentrated serum samples can be diluted to fall within the upper and lower quantification limits. Other common parameters like range and linearity were not tested for this report since samples can be diluted to fall within the quantifiable range of the assay. Therefore, samples for a new study will be tested in the beginning of the trial to determine the optimal dilution factor. This assay can not only be used to quantify bnAb concentration after infusion for HIV prevention studies, but also for therapeutic studies in HIV-infected subjects. There is a critical need for reliable methods to analyze the pharmacokinetics of mAbs in the human body, especially with increased abilities to engineer next generation antibodies as well as to verify pharmacokinetic modelling approaches *in vivo* (31, 32). A reliable method is the enzyme-linked immunosorbent assay (ELISA), which has been utilized in most PK studies in the past (12, 13, 17, 33–35). However, traditional ELISA protocols can only assay one analyte at a time. The PK BAMA is a microsphere-based assay that can be customized to assay up to 50 analytes simultaneously and is readily adapted to new bnAbs as well as new bnAb combinations. The simultaneous measurement of multiple bnAbs is an efficient tool to inform the selection of the most promising bnAb combinations for HIV-1 prevention and therapeutics strategies.

## DATA AVAILABILITY STATEMENT

The original contributions presented in the study are included in the article/**Supplementary Material**. Further inquiries can be directed to the corresponding author.

## ETHICS STATEMENT

The studies involving human participants were reviewed and approved by Duke IRB. The patients/participants provided their written informed consent to participate in this study.

## AUTHOR CONTRIBUTIONS

MW contributed to the design of the work, performed experiments, analyzed and interpreted data, and helped with writing the manuscript. KTC, CA, KH, and MR contributed to the conception/design of the work, performed experiments, and analyzed and interpreted data. KS and JHe contributed to the conception/design of the work, analysis and interpretation of data, and revising the manuscript. SS and DB contributed to data analysis and interpretation. JHa, KC, MS-K, and GT contributed to design of work and data interpretation and manuscript revision. JN and DHB contributed to conception and design of the work. NY contributed to conception/design of the work, analysis and interpretation of data, and writing and revising the manuscript. All authors critically reviewed the manuscript for intellectual content and agree to be accountable for all aspects of the work. All authors contributed to the article and approved the submitted version.

## FUNDING

This work was supported by the Bill & Melinda Gates Foundation, Collaboration for AIDS Vaccine Discovery, Vaccine Immune Monitoring Center (CAVIMC) (OPP1146996); and the National Institutes of Health (NIH), National Institute of Allergy and Infectious Diseases (NIAID, Duke Center for AIDS Research (CFAR) (P30 AI064518) and HIV Vaccine Trials Network Laboratory Program (NIH U01 AI068618).

## ACKNOWLEDGMENTS

We thank Wes Rountree for statistical analysis advice, Judith T. Lucas and Dan Ozaki for quality assurance oversight, Michael Archibald for technical assistance, Hongmei Gao and Kelli Greene, for project management, Peter Abbink and Vaneet Sharma for provision of reagents, the University of Washington/Fred Hutch Center for AIDS Research, an NIH-funded program under award number AI027757 which is supported by the following NIH Institutes and Centers: NIAID, NCI, NIMH, NIDA, NICHD, NHLBI, NIA, NIGMS, NIDDK and Boris Juelg at the Ragon Institute of MGH and MIT at Harvard for coordinating serum samples, and the patients and volunteers for clinical trial samples. **Figure 1** was created with BioRender.com.

## SUPPLEMENTARY MATERIAL

The Supplementary Material for this article can be found online at: https://www.frontiersin.org/articles/10.3389/fimmu.2021.709994/full#supplementary-material

## REFERENCES

1. Marcus JL, Leyden WA, Alexeeff SE, Anderson AN, Hechter RC, Hu H, et al. Comparison of Overall and Comorbidity-Free Life Expectancy Between Insured Adults With and Without HIV Infection, 2000-2016. *JAMA Network Open* (2020) 3(6):e207954–e. doi: 10.1001/jamanetworkopen.2020.7954
2. Schouten J, Wit FW, Stolte IG, Kootstra NA, van der Valk M, Geerlings SE, et al. Cross-Sectional Comparison of the Prevalence of Age-Associated Comorbidities and Their Risk Factors Between HIV-Infected and Uninfected Individuals: The AGEhIV Cohort Study. *Clin Infect Dis* (2014) 59(12):1787–97. doi: 10.1093/cid/ciu701
3. Rasmussen LD, May MT, Kronborg G, Larsen CS, Pedersen C, Gerstoft J, et al. Time Trends for Risk of Severe Age-Related Diseases in Individuals With and Without HIV Infection in Denmark: A Nationwide Population-Based Cohort Study. *Lancet HIV* (2015) 2(7):e288–98. doi: 10.1016/S2352-3018(15)00077-6

4. Hoy JF, Grund B, Roediger M, Schwartz AV, Shepherd J, Avihingsanon A, et al. Immediate Initiation of Antiretroviral Therapy for HIV Infection Accelerates Bone Loss Relative to Deferring Therapy: Findings From the START Bone Mineral Density Substudy, A Randomized Trial. *J Bone Mineral Res* (2017) 32(9):1945–55. doi: 10.1002/jbmr.3183
5. Gilbert PB, Juraska M, deCamp AC, Karuna S, Edupuganti S, Mgodi N, et al. Basis and Statistical Design of the Passive HIV-1 Antibody Mediated Prevention (AMP) Test-Of-Concept Efficacy Trials. *Stat Commun Infect Dis* (2017) 9(1):20160001. doi: 10.1515/scid-2016-0001
6. Ledgerwood JE, Coates EE, Yamshchikov G, Saunders JG, Holman L, Enama ME, et al. Safety, Pharmacokinetics and Neutralization of the Broadly Neutralizing HIV-1 Human Monoclonal Antibody VRC01 in Healthy Adults. *Clin Exp Immunol* (2015) 182(3):289–301. doi: 10.1111/cei.12692
7. Mayer KH, Seaton KE, Huang Y, Grunenberg N, Isaacs A, Allen M, et al. Safety, Pharmacokinetics, and Immunological Activities of Multiple Intravenous or Subcutaneous Doses of an Anti-HIV Monoclonal Antibody, VRC01, Administered to HIV-Uninfected Adults: Results of a Phase 1 Randomized Trial. *PloS Med* (2017) 14(11):e1002435. doi: 10.1371/journal.pmed.1002435
8. Huang Y, Naidoo L, Zhang L, Carpp LN, Rudnicki E, Randhawa A, et al. Pharmacokinetics and Predicted Neutralisation Coverage of VRC01 in HIV-Uninfected Participants of the Antibody Mediated Prevention (AMP) Trials. *EBioMedicine* (2021) 64:103203. doi: 10.1016/j.ebiom.2020.103203
9. Corey L, Gilbert PB, Juraska M, Montefiori DC, Morris L, Karuna ST, et al. Two Randomized Trials of Neutralizing Antibodies to Prevent HIV-1 Acquisition. *New Engl J Med* (2021) 384(11):1003–14. doi: 10.1056/NEJMoa2031738
10. Edupuganti S, Mgodi N, Karuna ST, Andrew P, Rudnicki E, Kochar N, et al. Feasibility and Successful Enrollment in a Proof-Of-Concept HIV Prevention Trial of VRC01, A Broadly Neutralizing HIV-1 Monoclonal Antibody. *JAIDS J Acquired Immune Deficiency Syndromes* (2021) 87(1):671–79. Publish Ahead of Print. doi: 10.1097/QAI.0000000000002639
11. Caskey M, Klein F, Lorenzi JCC, Seaman MS, West AP, Buckley N, et al. Viraemia Suppressed in HIV-1-Infected Humans by Broadly Neutralizing Antibody 3BNC117. *Nature* (2015) 522(7557):487–91. doi: 10.1038/nature14411
12. Bar-On Y, Gruell H, Schoofs T, Pai JA, Nogueira L, Butler AL, et al. Safety and Antiviral Activity of Combination HIV-1 Broadly Neutralizing Antibodies in Viremic Individuals. *Nat Med* (2018) 24(11):1701–7. doi: 10.1038/s41591-018-0186-4
13. Mendoza P, Gruell H, Nogueira L, Pai JA, Butler AL, Millard K, et al. Combination Therapy With Anti-HIV-1 Antibodies Maintains Viral Suppression. *Nature* (2018) 561(7724):479–84. doi: 10.1038/s41586-018-0531-2
14. Li Y, Migueles SA, Welcher B, Svehla K, Phogat A, Louder MK, et al. Broad HIV-1 Neutralization Mediated by CD4-Binding Site Antibodies. *Nat Med* (2007) 13(9):1032–4. doi: 10.1038/nm1624
15. Wu X, Yang Z-Y, Li Y, Hogerkorp C-M, Schief WR, Seaman MS, et al. Rational Design of Envelope Identifies Broadly Neutralizing Human Monoclonal Antibodies to HIV-1. *Science* (2010) 329(5993):856. doi: 10.1126/science.1187659
16. Walker LM, Huber M, Doores KJ, Falkowska E, Pejchal R, Julien J-P, et al. Broad Neutralization Coverage of HIV by Multiple Highly Potent Antibodies. *Nature* (2011) 477(7365):466–70. doi: 10.1038/nature10373
17. Rosenberg YJ, Montefiori DC, LaBranche CC, Lewis MG, Sack M, Lees JP, et al. Protection Against SHIV Challenge by Subcutaneous Administration of the Plant-Derived PGT121 Broadly Neutralizing Antibody in Macaques. *PloS One* (2016) 11(3):e0152760. doi: 10.1371/journal.pone.0152760
18. Sok D, van Gils MJ, Pauthner M, Julien J-P, Saye-Francisco KL, Hsueh J, et al. Recombinant HIV Envelope Trimer Selects for Quaternary-Dependent Antibodies Targeting the Trimer Apex. *Proc Natl Acad Sci* (2014) 111 (49):17624. doi: 10.1073/pnas.1415789111
19. Grobben M, Stuart RAL, van Gils MJ. The Potential of Engineered Antibodies for HIV-1 Therapy and Cure. *Curr Opin Virol* (2019) 38:70–80. doi: 10.1016/j.coviro.2019.07.007
20. Rudicell RS, Kwon YD, Ko S-Y, Pegu A, Louder MK, Georgiev IS, et al. Enhanced Potency of a Broadly Neutralizing HIV-1 Antibody In Vitro Improves Protection Against Lentiviral Infection In Vivo. *J Virol* (2014) 88 (21):12669. doi: 10.1128/JVI.02213-14
21. Tomaras GD, Yates NL, Liu P, Qin L, Fouda GG, Chavez LL, et al. Initial B-Cell Responses to Transmitted Human Immunodeficiency Virus Type 1: Virion-Binding Immunoglobulin M (IgM) and IgG Antibodies Followed by Plasma Anti-Gp41 Antibodies With Ineffective Control of Initial Viremia. *J Virol* (2008) 82(24):12449. doi: 10.1128/JVI.01708-08
22. Fouda GG, Yates NL, Pollara J, Shen X, Overman GR, Mahlokozera T, et al. HIV-Specific Functional Antibody Responses in Breast Milk Mirror Those in Plasma and Are Primarily Mediated by IgG Antibodies. *J Virol* (2011) 85 (18):9555. doi: 10.1128/JVI.05174-11
23. Yates NL, Lucas JT, Nolen TL, Vandergrift NA, Soderberg KA, Seaton KE, et al. Multiple HIV-1-Specific IgG3 Responses Decline During Acute HIV-1: Implications for Detection of Incident HIV Infection. *AIDS* (2011) 25(17) 2089–97. doi: 10.1097/QAD.0b013e32834b348e
24. Liu P, Overman RG, Yates NL, Alam SM, Vandergrift N, Chen Y, et al. Dynamic Antibody Specificities and Virion Concentrations in Circulating Immune Complexes in Acute to Chronic HIV-1 Infection. *J Virol* (2011) 85 (21):11196. doi: 10.1128/JVI.05601-11
25. Eckels J, Nathe C, Nelson EK, Shoemaker SG, Nostrand EV, Yates NL, et al. Quality Control, Analysis and Secure Sharing of Luminex® Immunoassay Data Using the Open Source LabKey Server Platform. *BMC Bioinf* (2013) 14 (1):145. doi: 10.1186/1471-2105-14-145
26. Bioanalytical Method Validation FDA. *Guidance for Industry. Www.Fda.Com: Food and Drug Administration, Centre for Drug Evaluation and Research (CDER)*. Available at: https://www.fda.gov/files/drugs/published/Bioanalytical-Method-Validation-Guidance-for-Industry.pdf.
27. ICH. *Validation of Analytical Procedures: Text and Methodology. Q2(R1): ICH Harmonised Tripartite Guidline* (2005). Available at: https://database.ich.org/sites/default/files/Q2_R1:Guideline.pdf.
28. Armbruster D, Pry T. Limit of Blank, Limit of Detection and Limit of Quantitation. *Clin biochemist Reviews/Australian Assoc Clin Biochemists* (2008) 29(Suppl 1):S49–52.
29. Zhang J, Li W, Roskos LK, Yang H. Immunogenicity Assay Cut Point Determination Using Nonparametric Tolerance Limit. *J Immunol Methods* (2017) 442:29–34. doi: 10.1016/j.jim.2017.01.001
30. Shankar G, Devanarayan V, Amaravadi L, Barrett YC, Bowsher R, Finco-Kent D, et al. Recommendations for the Validation of Immunoassays Used for Detection of Host Antibodies Against Biotechnology Products. *J Pharm Biomed Anal* (2008) 48(5):1267–81. doi: 10.1016/j.jpba.2008.09.020
31. Haraya K, Tachibana T, Igawa T. Improvement of Pharmacokinetic Properties of Therapeutic Antibodies by Antibody Engineering. *Drug Metab Pharmacokinetics* (2019) 34(1):25–41. doi: 10.1016/j.dmpk.2018.10.003
32. Glassman PM, Balthasar JP. Physiologically-Based Modeling of Monoclonal Antibody Pharmacokinetics in Drug Discovery and Development. *Drug Metab Pharmacokinetics* (2019) 34(1):3–13. doi: 10.1016/j.dmpk.2018.11.002
33. Liu Q, Lai Y-T, Zhang P, Louder MK, Pegu A, Rawi R, et al. Improvement of Antibody Functionality by Structure-Guided Paratope Engraftment. *Nat Commun* (2019) 10(1):721. doi: 10.1038/s41467-019-08658-4
34. Gaudinski MR, Houser KV, Doria-Rose NA, Chen GL, Rothwell RSS, Berkowitz N, et al. Safety and Pharmacokinetics of Broadly Neutralising Human Monoclonal Antibody VRC07-523LS in Healthy Adults: A Phase 1 Dose-Escalation Clinical Trial. *Lancet HIV* (2019) 6(10):e667–79. doi: 10.1016/S2352-3018(19)30181-X
35. Julg B, Tartaglia LJ, Keele BF, Wagh K, Pegu A, Sok D, et al. Broadly Neutralizing Antibodies Targeting the HIV-1 Envelope V2 Apex Confer Protection Against a Clade C SHIV Challenge. *Sci Transl Med* (2017) 9 (406):eaal1321. doi: 10.1126/scitranslmed.aal1321


**Conflict of Interest:** The authors declare that the research was conducted in the absence of any commercial or financial relationships that could be construed as a potential conflict of interest.

frontiers in Immunology

ORIGINAL RESEARCH
published: 31 August 2021
doi: 10.3389/fimmu.2021.710012

# Modeling HIV-1 Within-Host Dynamics After Passive Infusion of the Broadly Neutralizing Antibody VRC01

*E. Fabian Cardozo-Ojeda*[1] *and Alan S. Perelson*[2]*

[1] Vaccine and Infectious Disease Division, Fred Hutchinson Cancer Research Center, Seattle, WA, United States,
[2] Theoretical Biology and Biophysics, Los Alamos National Laboratory, Los Alamos, NM, United States

VRC01 is a broadly neutralizing antibody that targets the CD4 binding site of HIV-1 gp120. Passive administration of VRC01 in humans has assessed the safety and the effect on plasma viremia of this monoclonal antibody (mAb) in a phase 1 clinical trial. After VRC01 infusion, the plasma viral load in most of the participants was reduced but had particular dynamics not observed during antiretroviral therapy. In this paper, we introduce different mathematical models to explain the observed dynamics and fit them to the plasma viral load data. Based on the fitting results we argue that a model containing reversible Ab binding to virions and clearance of virus-VRC01 complexes by a two-step process that includes (1) saturable capture followed by (2) internalization/degradation by phagocytes, best explains the data. This model predicts that VRC01 may enhance the clearance of Ab-virus complexes, explaining the initial viral decay observed immediately after antibody infusion in some participants. Because Ab-virus complexes are assumed to be unable to infect cells, i.e., contain neutralized virus, the model predicts a longer-term viral decay consistent with that observed in the VRC01 treated participants. By assuming a homogeneous viral population sensitive to VRC01, the model provides good fits to all of the participant data. However, the fits are improved by assuming that there were two populations of virus, one more susceptible to antibody-mediated neutralization than the other.

**Keywords: virus dynamics, HIV-1, VRC01, mathematical modeling, ODE**

OPEN ACCESS

***Edited by:***
*Marit Van Gils, Academic Medical Center, Netherlands*

***Reviewed by:***
*Alvin X. Han, Academic Medical Center, Netherlands*
*Taina Immonen, Frederick National Laboratory for Cancer Research (NIH), United States*

***Correspondence:**
*Alan S. Perelson*
*asp@lanl.gov*

***Specialty section:***
*This article was submitted to Vaccines and Molecular Therapeutics, a section of the journal Frontiers in Immunology*

***Received:*** *14 May 2021*
***Accepted:*** *02 August 2021*
***Published:*** *31 August 2021*

***Citation:***
*Cardozo-Ojeda EF and Perelson AS (2021) Modeling HIV-1 Within-Host Dynamics After Passive Infusion of the Broadly Neutralizing Antibody VRC01. Front. Immunol. 12:710012. doi: 10.3389/fimmu.2021.710012*

## INTRODUCTION

Passive administration of broadly neutralizing antibodies (bnAbs) in infected humanized-mice, macaques and humans has suggested that bnAb infusion may be a therapeutic modality against HIV-1 infection (1–3). One of the more potent bnAbs that has been isolated and characterized is VRC01 (4–6). VRC01 is a monoclonal antibody that recognizes the CD4 binding site of HIV gp120, emulating the binding of the CD4 receptor (5, 7).

To determine the pharmacokinetics, safety and effect of VRC01 on plasma viral load, this antibody was infused into HIV-1 chronically infected individuals in a phase 1 clinical trial (1, 8). After a single infusion of 40 mg/kg of VRC01, the plasma viral load was reduced by more than 1-log in 6/8 infected individuals, but there was no significant response in the other two participants (1). In the responding individuals, the major viral reduction occurred after a plateau phase that lasted about 2 days, which is longer than what is normally seen in infected participants under antiretroviral treatment (9, 10). In three participants, there was a rapid decay of virus immediately after VRC01 infusion, followed by a rebound to baseline over the next 24-48 hours. The other three responding participants presented a steady or an initial increase in the viral load to values higher than baseline. Both patterns were then followed by a decline in viral load that persisted but slowly returned to baseline as the VRC01 concentration declined (see **Figure 1**).

The aim of this paper is to obtain insight into the mechanisms that lead to these viral load dynamics. A pioneering study modeling the impact of antibodies during acute HIV infection adapted the basic model of virus dynamics to account for the possible effect of antibodies on viral infectivity, virion clearance, and infected cell death (11). More elaborated models including the explicit binding and dissociation of antibody to virus, in one or multiple steps have also been developed (12–14). More recently a mathematical model was used to determine if the bnAb 3BNC117 leads to antibody-dependent cellular cytotoxicity (ADCC) *in-vivo* (15). Here we develop mathematical models to fit the plasma HIV RNA data obtained after VRC01 infusion, with the goal of quantifying the mechanisms by which this mAb reduces viral load.

# MODELS AND RESULTS

## VRC01 Pharmacokinetics

After infusion of 40 mg/kg of VRC01, the serum antibody concentration decayed in a biphasic manner, similar to decays previously observed with other monoclonal antibodies (8, 16). The biphasic decay results from antibody distribution from the blood into the tissue followed by elimination from the body. As done previously (16, 17), we modeled these dynamics by using a two-compartment pharmacokinetic model presented in equation (1), where $A_1$ and $A_2$ represent the concentration of VRC01 in compartments one and two, respectively. In this model, VRC01 is infused at rate $R$ for the period $0 < t < T_{end}$ into the first compartment with volume $Vol_1$. VRC01 is transported to the second compartment of volume $Vol_2$ at rate $k_{12}$, where it is cleared at rate $k_0$. VRC01 is transported back to the first compartment at a rate $k_{21}$. Following these assumptions, the model has the form,

$$\begin{aligned} \frac{dA_1}{dt} &= R - k_{12}A_1 + k_{21}A_2\frac{Vol_2}{Vol_1} \\ \frac{dA_2}{dt} &= k_{12}A_1\frac{Vol_1}{Vol_2} - k_{21}A_2 - k_0A_2 \\ R &= \begin{cases} \frac{A_{\max}}{T_{end}}, & t \le T_{end} \\ 0, & t > T_{end} \end{cases} \end{aligned} \quad . \tag{1}$$

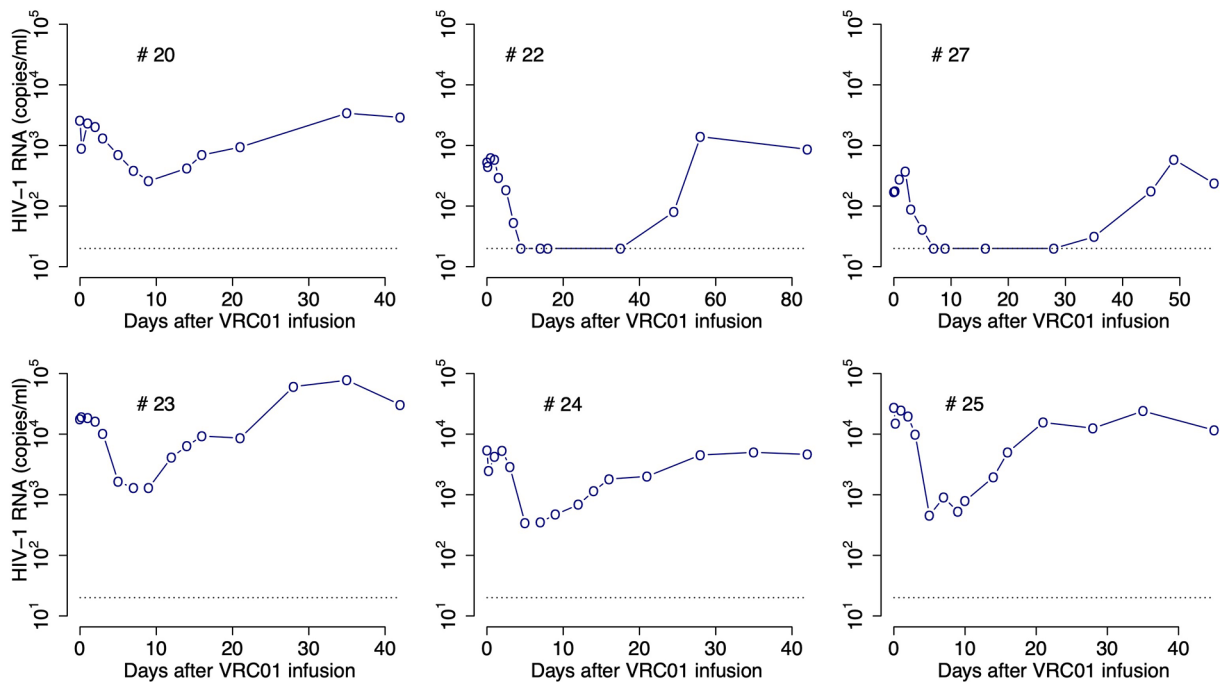


**FIGURE 1** | HIV-RNA levels in plasma after infusion of VRC01. Patient identifiers are given at the top of each graph.

We assume $T_{end}$ = 1 hour and $A_{max}$ equals the maximum measured VRC01 serum concentration. During the time of infusion ($0 < t < T_{end}$) the equation for VRC01 concentration in the first compartment can be approximated by $\frac{dA_1}{dt} = R$, i.e., the antibody concentration $A_1$ increases during the infusion at rate $R$, with solution

$$A_1(t) = \frac{A_{\max} t}{T_{inf}}, 0 < t < T_{end} \quad (2)$$

Substituting equation (2) into equation (1), we obtain for $0 < t < T_{end}$, $\frac{dA_2}{dt} = \frac{k_{12} A_{\max} t Vol_1}{T_{end} Vol_2} - (k_{21} + k_0)A_2$ . Since $A_2(0) = 0$, the solution for $A_2(t)$ yields

$$A_2(t) = \frac{k_{12} A_{\max} Vol_1}{T_{end} Vol_2} e^{-(k_{21}+k_0)t} \int_0^t \tau e^{(k_{21}+k_0)\tau} d\tau$$

$$= \frac{k_{12} A_{\max} Vol_1}{T_{end} Vol_2 (k_{21} + k_0)} \left[(k_{21} + k_0)t - 1 + e^{-(k_{21}+k_0)t}\right]. \quad (3)$$

Note that by substituting $A_2(t)$ back into Eq. (1) for $A_1$ one can obtain a higher order approximation of $A_1(t)$. However, for our purposes with a short infusion the solution given by Eq. (2) suffices.

At the end of the infusion (i.e., $t = T_{end}$) the predicted Ab concentration in the first and second compartments are $A_1(T_{end}) = A_{max}$, and

$$A_2(T_{end}) = \frac{k_{12} A_{\max} Vol_1}{Vol_2 (k_{21} + k_0)} \left[\frac{1}{(k_{21} + k_0) T_{end}} \left\{e^{-(k_{21}+k_0)t} - 1\right\} + 1.\right]$$

After the end of infusion, $t > T_{end}$, $R$=0, and the antibody concentration decays as,

$$A_1(t) = A_{\max}[k e^{-\lambda_1 (t - T_{end})} + (1 - k) e^{-\lambda_2 (t - T_{end})}], t > T_{end}. \quad (4)$$

The parameters $\lambda_1$ and $\lambda_2$ are the eigenvalues of the system in equation (1) when $R = 0$, with form $\lambda_{1,2} = \frac{1}{2}(k_{21} + k_0 + k_{12}) \pm \sqrt{(k_{21} + k_0 - k_{12})^2 + 4 k_{21} k_{12}}$ . The parameter $k$ is obtained by equating the derivatives of $A_1(t)$ from equations (1) and (4) when $t = T_{end}$, yielding $A_{\max}(-\lambda_1 k - \lambda_2(1 - k)) = -k_{12} A_{\max} + \frac{k_{21} A_2(T_{end}) Vol_2}{Vol_1}$ or $k = \frac{k_{12} A_2(T_{end}) Vol_2}{Vol_1 A_{\max}(\lambda_2 - \lambda_1)} + \frac{\lambda_2 - k_{12}}{\lambda_2 - \lambda_1}$, which upon substituting $A_2(T_{end})$ gives,

$$k = \frac{k_{21} k_{12}}{(\lambda_2 - \lambda_1)(k_{21} + k_0)} \left[\frac{1}{(k_{21} + k_{10}) T_{end}} \left\{e^{-(k_{21}+k_0)t} - 1\right\} + 1\right] + \frac{\lambda_2 - k_{12}}{\lambda_2 - \lambda_1}. \quad (5)$$

Notice that the values of $\lambda_1$, $\lambda_2$ and $k$ do not depend on the values of $Vol_1$ and $Vol_2$. Therefore, the behavior of $A_1(t)$ in equations (2)

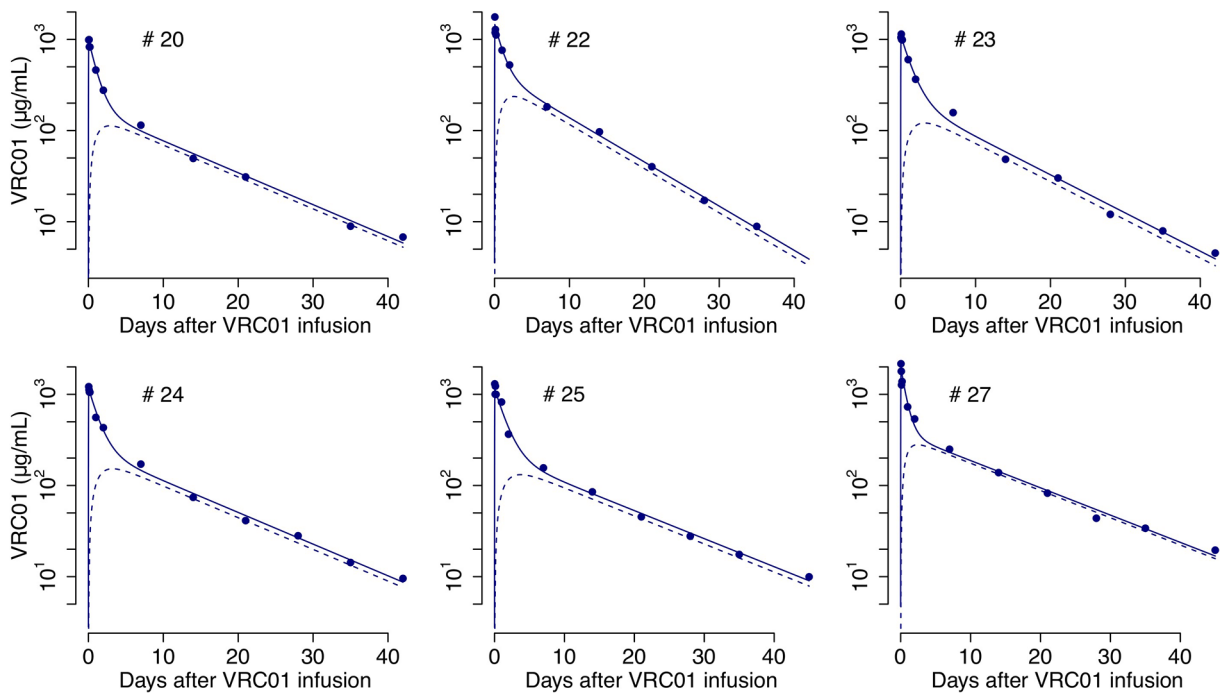


**FIGURE 2** | Best-fits of the two-compartment model in equations (2)-(6) to the PK data from infected individuals. Blue circles represent the measured VRC01 serum concentration, and solid lines the best fit from the model in equations (2) and (4) of the VRC01 concentration in the blood. Dashed lines represent the predicted concentration of VRC01 in the second compartment from the model in equations (3) and (6), assuming plasma volume, $Vol_1 = 3L$ and $Vol_2 = \frac{k_{12} Vol_1}{k_{21}}$ (see **Table S1** for each participant's parameter estimates).

and (4) does not depend on $Vol_1$ and $Vol_2$. However, as we show below, $A_2(t)$ does depend on the volume ratio, $\frac{Vol_1}{Vol_2}$.

We fit $A_1(t)$ given by equations (2) and (4) to the VRC01 serum concentration from the six infected individuals that responded to the mAb, estimating the rates of VRC01 distribution from blood to tissues, clearance, and transport from tissue to plasma: $k_{12}$, $k_0$ and $k_{21}$, respectively. From the best fits (**Figure 2**) we obtain estimates for the clearance rate, $k_0$, the rate of distribution from blood to tissues, $k_{12}$, and rate of distribution from tissues to blood, $k_{21}$, to be 0.09 $day^{-1}$, 0.13 $day^{-1}$ and 0.7 $day^{-1}$, respectively (see the estimate for each participant in **Table S1**).

The VRC01 concentration was also measured in a group of uninfected, *i.e.* aviremic, volunteers in whom the same amount of VRC01 was infused. Doing the same analysis, we found that the biphasic decline was not significantly different between infected and aviremic participants, suggesting that the presence of HIV in infected participants did not significantly perturb their plasma VRC01 concentrations. For that reason, for the viral kinetic models in the following sections we simply assumed that the VRC01 concentration that affects the measured serum viremia, $A(t)$, can be determined by the PK model, *i.e.*, $A(t) = A_1(t)$.

In more complex models where one also models the HIV-1 levels in tissue one could use $A_2(t)$ for the interactions of HIV-1 with VRC01 in tissue. We obtained a closed form solution for $A_2(t)$ when $t > T_{end}$, by plugging in the solution of $A_1(t)$ in equation (4) into the differential equation for $A_2(t)$, in equation (1), yielding,

$$A_2(t) = A_2(T_{end})e^{-(k_{21}+k_0)(t-T_{end})} + \frac{k_{12}A_{\max}Vol_1}{Vol_2}e^{-(k_{21}+k_0)t}$$

$$\left[k\int_{T_{end}}^{t} e^{(k_{21}+k_0-\lambda_1)\tau}d\tau + (1-k)\int_{T_{end}}^{t} e^{(k_{21}+k_0-\lambda_2)\tau}d\tau\right]$$

$$= A_2(T_{end})e^{-(k_{21}+k_0)(t-T_{end})} + \frac{k_{12}A_{\max}Vol_1}{Vol_2}e^{-(k_{21}+k_0)t} \quad (6)$$

$$\left\{\left[\frac{k}{k_{21}+k_0-\lambda_1} + \frac{(1-k)}{k_{21}+k_0-\lambda_2}\right]e^{-(k_{21}+k_0)(t-T_{end})} + \left[\frac{\lambda_1 k e^{-\lambda_1(t-T_{end})}}{k_{21}+k_0-\lambda_1} - \frac{\lambda_2(1-k)e^{-\lambda_2(t-T_{end})}}{k_{21}+k_0-\lambda_2}\right]\right\}.$$

Unlike $A_1(t)$, the dynamics of $A_2(t)$, as presented in equations (3) and (6), depends on the ratio $\frac{Vol_1}{Vol_2}$. Without knowledge of how VRC01 is distributed in tissues, one cannot determine $A_2(t)$. However, if we assume that the transport of the Ab keeps a balanced total flow imposing the constraint, $k_{21}Vol_2 = k_{12}Vol_1$ (17), then, assuming that $Vol_1 = 3L$ corresponds to the plasma volume one can estimate $Vol_2$ and predict $A_2(t)$. Predictions of the VRC01 concentration in compartment two under this assumption, using the parameter estimates from fitting $A_1(t)$ to the serum VRC01 concentration samples given in **Table S1**, are presented in **Figure 2**.

## Virus Dynamics Modeling Approach

### Description of the Virus Load Data in the Presence of VRC01

After a single passive administration of 40 mg/kg of VRC01, the change in plasma viral load in the responding infected individuals (with ID #20, #22, #23, #24, #25, and #27) can be separated into three phases (1): (i) an initial period during which there is a rapid viral decline followed by a rebound to baseline (in participants #20, #24, and #25), a plateau phase (in participant #23), or an initial viral increase in viral load (in participants #22 and #27). This initial period is followed by (ii) a long-term viral decline of about 1-log, and finally (iii) a viral rebound as the antibody concentration declines (see **Figure 1**).

The initial period lasted about 2-3 days. Using the viral load measurements at baseline and 4 hours after VRC01 infusion, we estimated the viral load reduction in the three participants that presented a rapid decline and rebound, and found viral decay slopes of 5, 4 and 3 $day^{-1}$ in participants #20, #24 and #25, respectively. We further estimated the slope of the long-term decay beginning after the initial viral load rebound for the four participants whose viral load remained over the limit of detection (#20, #23, #24 and #25). We found that the long-term decline had slopes ranging from 0.28 to 0.78 $day^{-1}$. These decline slopes are smaller than those estimated during potent ART of about 1 $day^{-1}$ (9, 10, 18). Finally, between 5 or 10 days after VRC01 infusion, the viral load began to rebound to baseline values.

### Modeling Approach

To model the virus dynamics in participants receiving VRC01, we modified the basic model of virus dynamics (19, 20). The basic model includes only the key players during HIV infection, but it has been able to describe the decline of the viral load in chronically infected participants during the first couple of weeks after receiving antiretroviral therapy (ART), and also the viral rebound after ART cessation (10, 21, 22). This basic model includes target cells for HIV, $T$, productively infected cells, $I$, and free virus, $V$. In the model target cells are created (e.g. in the thymus) at a constant rate $\lambda$ and have a net per capita loss rate $d$. Target cells are infected by the virus and become productively infected with rate constant $\beta$. Productively infected cells, $I$, die at per capita rate $\delta$ and produce virus at a rate $p$ per cell. Finally, free virus is cleared at rate $c$ per virion. Under these assumptions the basic model has the form,

$$\begin{aligned}\frac{dT}{dt} &= \lambda - dT - \beta VT\\ \frac{dI}{dt} &= \beta VT - \delta I\\ \frac{dV}{dt} &= pI - cV\end{aligned} \quad . \quad (7)$$

Due to abortive HIV infection (23, 24), only a small fraction, $f$, of cells that are infected become productively infected (1 - $f$ would be the fraction abortively infected). We included this feature by modifying the infection term to $f\beta VT$ in the infected cell equation. Furthermore, it has been suggested that the death rate of infected cells is not constant, as in equation (7), but it might vary proportionally to the density of effector cells (i.e. $\delta \propto E(t)$, being $E(t)$ the effector cell density) (25–27). Holte et al. (28) presented one of the simplest versions of this approach where the effector cell density in turn depends on the infected cell density with form $E(t) \propto I(t)^{\omega-1}$. In this case, the death rate of infected cells is expressed as $\delta = \hat{\delta}I(t)^{\omega-1}$ (notice that assuming $\omega = 1$ yields a constant death rate of infected cells as in equation (7)).

Adding these features, we have a virus dynamic model of the form,

$$\begin{aligned}\frac{dT}{dt} &= \lambda - dT - \beta VT \\ \frac{dI}{dt} &= f\beta VT - \hat{\delta} I^{\omega} \\ \frac{dV}{dt} &= pI - cV\end{aligned} \quad . \tag{8}$$

## Modeling the Effect of VRC01 on HIV-1 Viral Load

As presented in (11), the simplest way to model the effect of antibodies on viral infection is by increasing or decreasing parameters in the basic model corresponding to processes that HIV-specific antibodies might affect. For example, neutralization of the virus due to opsonization can be included in this basic model, by reducing the infection rate constant $\beta$ in equation (8) by a factor $1 + \alpha A(t)$, where $\alpha$ is a constant (11). Therefore, in the presence of HIV-specific antibodies target cells would become infected at rate $\frac{\beta VT}{1+\alpha A(t)}$.

One can deduce this simplification by including into the basic model reversible binding of the antibody to the virus to produce neutralized immune complexes, $C$. We assume antibodies bind to the virus with rate constant $k_{on}$ and dissociates from it with rate constant $k_{off}$. Assuming that immune complexes are cleared from the plasma at rate $\gamma$, one ends up with a model of the form,

$$\begin{aligned}\frac{dT}{dt} &= \lambda - dT - \beta VT \\ \frac{dI}{dt} &= f\beta VT - \hat{\delta} I^{\omega} \\ \frac{dV}{dt} &= pI - cV - k_{on} VA(t) + k_{off} C \\ \frac{dC}{dt} &= k_{on} VA(t) + k_{off} C - \gamma C\end{aligned} \quad . \tag{9}$$

Assuming that immune complexes come into a quasi-steady state with the viral load, one obtains: $k_{on}VA(t) = (k_{off} + \gamma)C$. Thus, the fraction of free/non-neutralized virus in the presence of HIV-specific antibodies, $\frac{V}{V+C}$, will be equal to $\frac{1}{1+\frac{k_{on}A(t)}{k_{off}+\gamma}}$. Defining $\alpha = \frac{k_{on}}{k_{off}+\gamma}$, the model in equation (9) can be simplified to the form,

$$\begin{aligned}\frac{dT}{dt} &= \lambda - dT - \frac{\beta V_T T}{1+\alpha A(t)} \\ \frac{dI}{dt} &= \frac{f\beta V_T T}{1+\alpha A(t)} - \hat{\delta} I^{\omega}\end{aligned} \quad ,$$

where $V_T = V + C$ is the total amount of virus per unit volume and the $\frac{dV}{dt}$ and $\frac{dC}{dt}$ equations are the same as in Eq. (9). Assuming that immune complexes are cleared at the same rate as free virus (*i.e.*, $\gamma = c$), as would be the case *in vitro* where $\gamma = c = 0$, and then adding the equations for $\frac{dV}{dt}$ and $\frac{dC}{dt}$ one finds

$$\begin{aligned}\frac{dT}{dt} &= \lambda - dT - \frac{\beta V_T T}{1+\alpha A(t)} \\ \frac{dI}{dt} &= \frac{f\beta V_T T}{1+\alpha A(t)} - \hat{\delta} I^{\omega} \\ \frac{dV_T}{dt} &= pI - cV_T\end{aligned} \quad . \tag{10}$$

Note that the model in equation (10) has the same structure of the basic model in equation (8), with the infectivity reduction proposed in Tomaras et al. (11). Also notice that from this approach, one may glean information about the dissociation constant $K_d = \frac{k_{off}}{k_{on}}$ from the parameter $\alpha$. For simplicity from now on variable $V$ will represent total viral load (i.e., $V_T$) unless a $\frac{dC}{dt}$ equation is distinctly specified for virus-VRC01 complexes. In the latter case $V$ will represent free virus only.

To analyze the effect of virus neutralization by VRC01 on the viral load, we propose in the following sections adaptations of the models in equations (9) and (10), and show the best-fits of those adaptations to the HIV-RNA data. Model symbols and parameter values are described in **Table 1**.

**TABLE 1** | Description of model parameters.

| Parameters | Description | Value | Unit | Reference |
|---|---|---|---|---|
| $f$ | Fraction of target cells that after infection become productively infected cells. | 0.05 | | (23, 24) |
| $\hat{\delta}\hat{I}(0)^{\omega-1}$ | Initial productively infected cell decay rate. | 1.5 (See *Materials and Methods* section) | $day^{-1}$ | (29) |
| $\omega$ | Parameter that quantifies the density dependent rate of infected cells. | Fitted | | (28) |
| $c$ | Clearance rate of virus in plasma. | 23 | $day^{-1}$ | (30) |
| $\beta_s$, $\beta_r$ | Density dependent infection rate for sensitive and less-sensitive virus. | See *Materials and Methods* section | $ml\ day^{-1}$ | |
| $\lambda$ | Target cell production rate. | See *Materials and Methods* section | $ml^{-1}\ day^{-1}$ | |
| $d$ | Death rate of target cells and cells that are not productively infected. | 0.01 | $day^{-1}$ | (31) |
| $p$ | Virus production rate per infected cell | Fitted | $day^{-1}$ | |
| $\alpha_s$, $\alpha_r$ | Sensitive and less-sensitive virus neutralization sensitivity to VRC01 (delayed neutralization models) | Fitted | ml | |
| $\tau$ | Delay in the neutralization of VRC01 (delayed neutralization models) | Fitted | days | |
| $k_{off_s}$, $k_{off_r}$ | VRC01-virus neutralized complex dissociation rate (phagocytosis-based clearance models). | 2.75 | $day^{-1}$ | (32, 33) |
| $k_{on_s}$, $k_{on_r}$ | VRC01-senstive and less-sensitive virus neutralized complex formation rate (phagocytosis-based clearance models). | Fitted | $ml\ day^{-1}$ | |
| $\gamma$ | Maximum clearance rate of immune complexes (phagocytosis-based clearance models). | Fitted | $day^{-1}$ | |
| $m$ | Degradation rate of immune complexes captured by phagocytes (phagocytosis-based clearance models). | Fitted | $day^{-1}$ | |
| $K$ | Carrying capacity of captured immune complexes (phagocytosis-based clearance models). | Fitted | copies $ml^{-1}$ | |

## Delayed-Neutralization Model

During passive infusion of a potent broadly neutralizing antibody, such as VRC01, one would assume that infection of target cells would be significantly reduced when the serum concentration of the antibody is high. Thus, we would expect that the VRC01-mediated neutralization of the virus will block *de novo* infection events, and the rate of viral load decline will reflect the death rate of infected cells, similar to what is observed after initiation of therapy with protease, reverse transcriptase, and integrase strand transfer inhibitors (PIs, RTIS and InSTI, respectively) (10, 21, 22). However, the data shows that there is a delay, which is longer than the one observed after initiation of therapy with PIs, RTIs and InSTIs, before there is a major reduction of plasma viral load (10, 21, 22).

An empirical way to account for this delay, without explicitly explaining the mechanism behind it, is to assume that the presence of VRC01 decreases virus infectivity, as presented in the previous section, with a delay $\tau$ after the mAb infusion. Thus, in the presence of VRC01 target cells become infected at a rate $\hat{\beta}VT$, where

$$\hat{\beta} = \begin{cases} \beta & t < \tau \\ \frac{\beta}{(1+\alpha A(t))}, & t \geq \tau \end{cases}. \tag{11}$$

Adding this feature to the model in equation (8), we have a model with form (see **Figure 3**),

$$\begin{aligned} \frac{dT}{dt} &= \lambda - dT - \hat{\beta}VT \\ \frac{dI}{dt} &= f\hat{\beta}VT - \hat{\delta}I^{\omega} \\ \frac{dV}{dt} &= pI - cV \end{aligned} \quad . \tag{12}$$

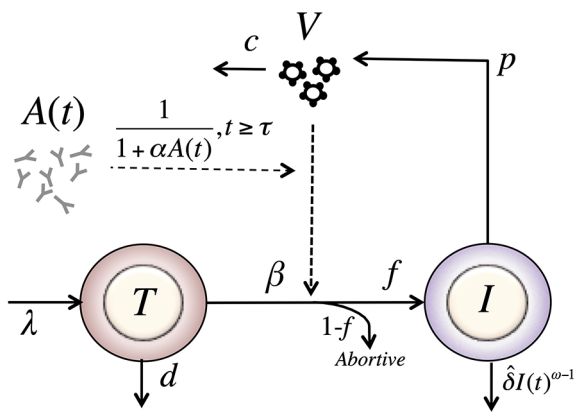


**FIGURE 3** | Schematic of the delayed-neutralization model. The model includes three variables: target cells ($T$), productively infected cells ($I$), and free virus ($V$), Parameters $\lambda$, $d$ and $\beta$ are the production, death and infection rates of target cells; $\delta$ is the death rate of infected cells; $p$ and $c$ are the production and clearance rates of free virus. Antibodies decrease the infectivity after a delay $\tau$, with sensitivity $\alpha$. The antibody concentration, $A(t)$, is determined from the best fits of the two-compartmental model to VRC01 concnetration measurements for each individual (see text).

We fit the model in equation (12) to the viral load data after VRC01 infusion as described in the *Materials and Methods* section, estimating the parameters $\tau$, $\alpha$, $pT(0)$, $V(0)$ and $\omega$ (see individual parameter estimates in **Table S2**). From the best fits, as shown in **Figure 4**, we found that, in general, the model is able to predict a delay, followed by viral decay and rebound as observed in the viral load data after VRC01 infusion in all participants. However, the data for participants #24 and #25 appear to have a faster decline than that predicted by the model. In addition, the model predicts a median delay of $\tau$ = 2.3 days before the neutralization effect of VRC01 is observed in the viral load data. Using the relation $\alpha = \frac{k_{on}}{k_{off}+\gamma}$ from the previous section, assuming that $\gamma = c$ = 23 day$^{-1}$, and that $k_{off}$ is equivalent to the VRC01 off-rate constant measured *in vitro* on a YU2 gp120 subunit, i.e. $k_{off}$ = 2.75 day$^{-1}$ (32, 33), with our estimate of $\alpha$ we calculate a dissociation coefficient $K_d = \frac{k_{off}}{k_{on}}$ of about 1.7 μg ml$^{-1}$. This dissociation coefficient is higher than the value estimated *in vitro* [~0.3 μg ml$^{-1}$ (32, 33)]. Nevertheless, the estimated dissociation coefficient seems reasonable, as viral rebound is observed when the VRC01 serum concentration has levels around 10 μg ml$^{-1}$. Besides, the conditions in which the *in vitro* $K_d$ values are obtained may be significantly different than the *in vivo* conditions in chronically infected individuals, which may explain the difference in the estimates.

### Delayed-Neutralization Model With Two Viral Populations

Lynch et al. (1) detected virus populations less sensitive to VRC01 a month after antibody infusion. It is possible that selection pressure leads to the growth of less sensitive (i.e. partially VRC01 resistant) populations when the antibody concentration is high (1). Here, we combine all the less sensitive virus into a second viral population with a different infectivity and sensitivity to VRC01, $\beta_r$ and $\alpha_r$, respectively. In the model, the less-sensitive virus population infects target cells at rate $\beta_r V_r T$. As in the one viral population model, the infectivity is only affected by VRC01 after a delay $\tau$,

$$\hat{\beta}_r = \begin{cases} \beta_r, & t < \tau \\ \frac{\beta_r}{(1+\alpha_r A(t))}, & t \geq \tau \end{cases} \tag{13}$$

We include two more equations for the population of productively infected cells, $I_r$, infected by the less-sensitive virus population, and the virus population $V_r$, using the same structure as for the sensitive-population. Therefore, assuming $V_s$ represents the virus sensitive to VRC01, with infectivity and sensitivity to VRC01, $\beta_s$ and $\alpha_s$, respectively, the model in equation (12) is adjusted to

$$\begin{aligned} \frac{dT}{dt} &= \lambda - dT - \hat{\beta}_s V_s T - \hat{\beta}_r V_r T \\ \frac{dI_s}{dt} &= f\hat{\beta}_s V_s T - \hat{\delta} I_s^{\omega} \\ \frac{dI_r}{dt} &= f\hat{\beta}_r V_r T - \hat{\delta} I_r^{\omega} \\ \frac{dV_s}{dt} &= pI_s - cV_s \\ \frac{dV_r}{dt} &= pI_r - cV_r \end{aligned} \tag{14}$$

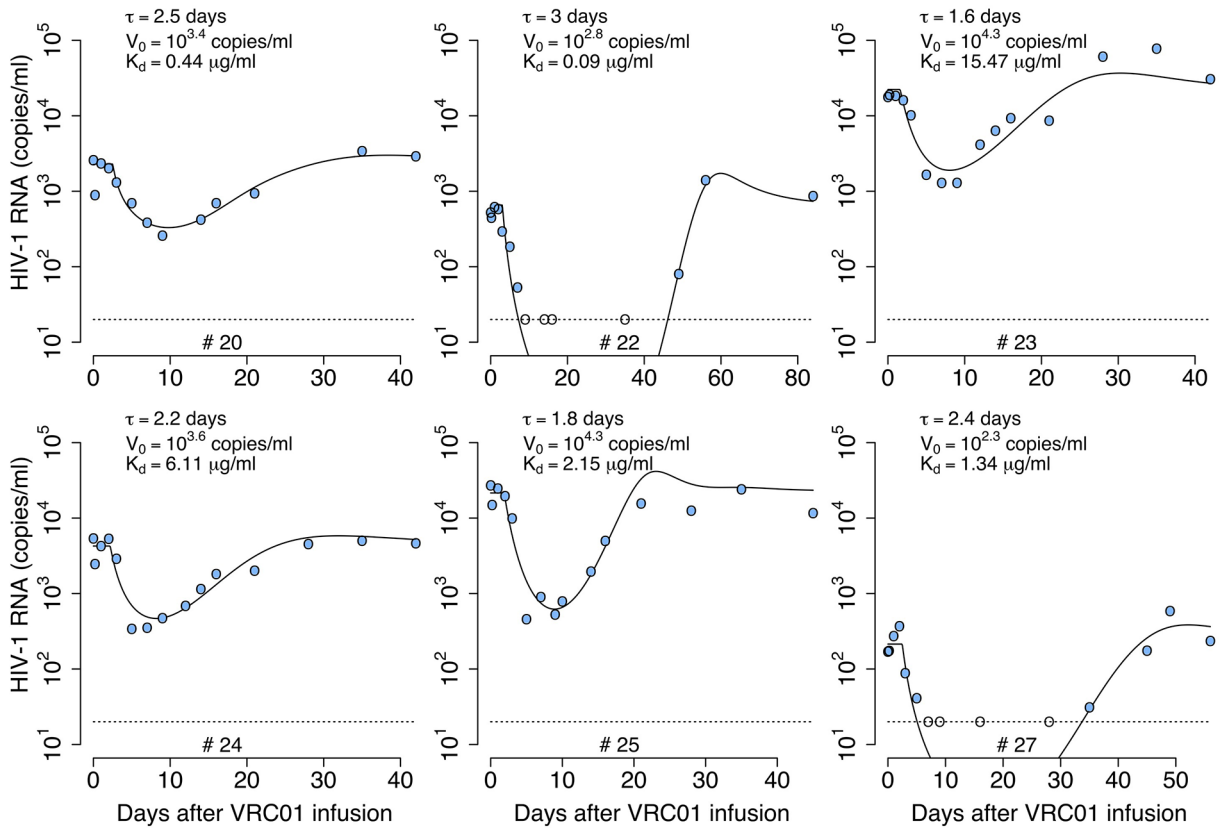


**FIGURE 4** | Best-fits of the delayed neutralization model, equation (12), to viral load data from participants receiving a single infusion of VRC01. Blue-filled and unfilled circles are the HIV-RNA over and below the limit of detection, respectively. Solid black lines are the best-fit of the model in equation (12) to the data. Fixed parameter values are described in **Table 1**. See all parameters estimates in **Table S2**. Other parameters and initial values were derived by assuming the system was in steady state before VRC01 infusion.

As before, we fit the model in equation (14) to the viral load data, now estimating the parameters $\tau$, $\alpha_s$, $\alpha_r$, % $V_s(0)$, $pT(0)$, $V(0)$ and $\omega$ (see best-fit parameter estimates in **Table S3**). As shown in **Figure 5**, this model also recapitulates the viral load data, but the fits to all participants data had similar or worst statistical support compared to the delayed neutralization model with one viral population (See **Table S3**). Nevertheless, this model predicts a similar delay of $\tau$ = 2.4 days for the virus neutralization effect. The model also predicts 96% of the virus is sensitive to VRC01 at baseline. However, because the less-sensitive virus population is less efficiently neutralized it can ultimately dominate the viral population (e.g., participants #23, 24 and 25, **Figure 5**). Since, the less sensitive viral population is important in viral rebound, the model predicts a lower dissociation constant of VRC01 for the sensitive virus, $K_{ds}$~0.6 μg ml$^{-1}$, than the one predicted with a model with only one viral population of 1.7 μg ml$^{-1}$. Interestingly, this $K_{ds}$ value is close to the average $K_d$ value of 0.3 μg ml$^{-1}$ estimated *in-vitro*.

A disadvantage of this model is that it does not provide a mechanistic explanation of the initial delay in the neutralization effect. The delay in the viral load decline in chronically infected individuals initiating ART is thought to be due to a combination of the pharmacological delay after oral uptake of the drug and the step in the viral cycle at which the drug acts (9, 10, 34). However, in the case of VRC01, the mAb is infused directly into bloodstream, and it is not clear why there is such a long delay. One possibility is that the delay reflects the time for the infused mAb to be transported into tissues where the majority of virus replication occurs and accumulate to a high enough concentration to effectively neutralize the virus. Another possibility is that the delay may reflect other mAb-mediated mechanisms of action against the virus. We will explore the latter case in the following sections.

## Phagocytosis-Based Saturated Clearance Model

If one assumes that the viral load is measured accurately, then the rapid decay of virus immediately after VRC01 infusion followed by a rebound to baseline over the next 24-48 hours in participants #20, #24 and #25 needs to be explained. Further, in participant #27, there was an initial increase in the viral load to values higher than baseline. These observations may indicate that

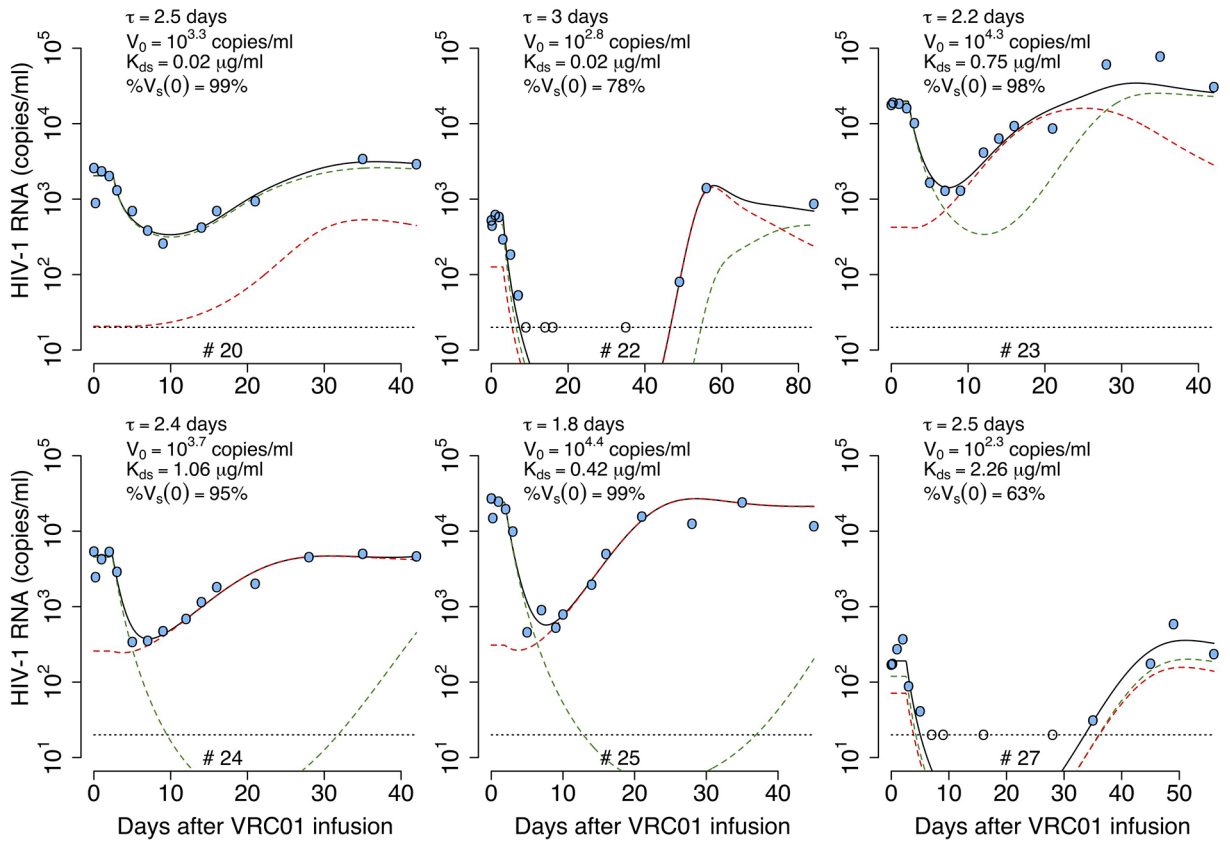


**FIGURE 5** | Best-fits of the two viral population delayed neutralization model, equation (14), to viral load data from participants receiving a single infusion of VRC01. Blue-filled and unfilled circles are the HIV-RNA over and below the limit of detection, respectively. Solid black lines are the best-fit of the model to the data ($V_s + V_r$). Green and red dashed lines show the sensitive ($V_s$) and less sensitive ($V_r$) virus concentration prediction of the model, respectively. Fixed parameter values are described in **Table 1**. See all parameter estimates in **Table S3**. Other parameters and initial values were derived by assuming the system was in steady state before VRC01 infusion.

after VRC01 infusion, there is not a physiological delay, but rather that VRC01 has an immediate effect on the virus. The early fast decay seen in some of the individuals have slopes ≥3 day$^{-1}$, faster than the viral decline rate seen after the initiation ART, of about 1 day$^{-1}$, suggesting that this fast decline does not reflect the death of infected cells. Rather, VRC01 maybe disrupting the viral set point by enhancing the clearance of the virus. The simplest way to codify this effect in the basic model is by adding an antibody-dependent enhanced factor to the virus clearance rate (11):

$$\frac{dV}{dt} = pI - c[1 + \gamma A(t)]V \tag{15}$$

This approach would account for the rapid early decay of the virus but not for the fast rebound. To have an early viral decline and a rebound, the model has to include a viral clearance rate that varies over time. A simple model to account for this effect can be obtained by adjusting the model in equation (9) assuming a time varying clearance of immune complexes. Thus, the equation for immune complexes in equation (9) can be adjusted to (see **Figure 6**),

$$\frac{dC}{dt} = k_{on}VA(t) - k_{off}C - \hat{\gamma}(t)C\,. \tag{16}$$

Assuming that the viral load reflects the total viral load, i.e. the free- and complexed-virus $V + C$, the value of $\hat{\gamma}(t)$ has to be initially greater than the clearance of free virus, $c$, to disrupt the set point leading to an initial fast decay. Then, at some point the value of $\hat{\gamma}(t)$ has to decrease below $c$ to account for the viral rebound.

One plausible biological explanation for this behavior of $\hat{\gamma}(t)$ is that immune complexes, $C$, are cleared as they interact with Fc receptors on phagocytes with a phenomenological carrying capacity $K$. Then, when the concentration of immune complexes is low, $C << K$, $\hat{\gamma}(t)$ will be high. As VRC01 interacts with free virus, the concentration of immune complexes, $C$, increases, and the likelihood of interaction of immune complexes with phagocytes decreases as fewer free Fc receptors might be available, or other Fc-Fc receptor interaction obstacles may

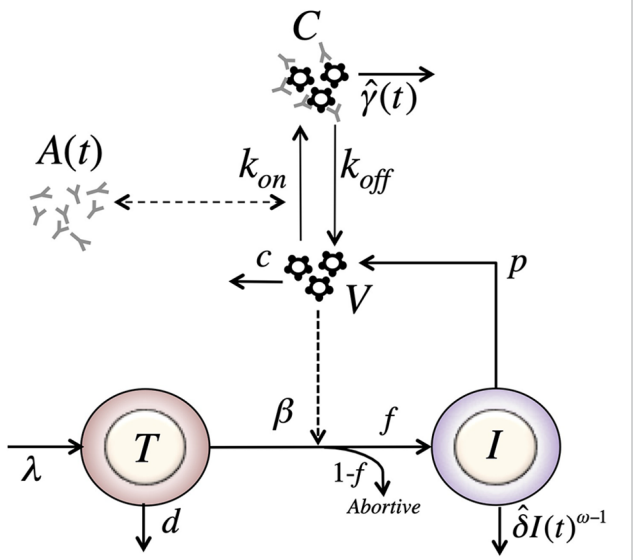


**FIGURE 6** | Schematic of the model with reversible binding of Ab to HIV and a time-varying clearance rate of immune complexes. The model include four variables: target cells ($T$), productively infected cells ($I$), free virus ($V$), and VRC01-HIV immune complexes ($C$). Parameters $\lambda$, $d$ and $\beta_s$ are the production, death and infection rates of target cells; $\delta$ is the death rate of infected cells; $p$ and $c$ are the production and clearance rates of free virus; $k_{on}$ and $k_{off}$ are the binding and dissociation rate constants of VRC01 to free virus; $\hat{\gamma}(t)$ is the time varying clearance rate of VRC01-HIV immune complexes. The antibody concentration, $A(t)$, is determined from the best-fit of the two-compartmental model to VRC01 concentration measurements for each individual (see text).

appear, reducing the clearance rate. We can describe this phenomenologically using a clearance rate with the form $\hat{\gamma}(t) = \gamma\frac{K}{K+C}$. At low concentrations, $c$, immune complexes are cleared at a rate close to $\gamma$. If VRC01 enhances the clearance of virus by forming immune complexes, this would be reflected in the model by $\gamma > c$, and one would expect a rapid viral decay disrupting the steady state. As more complexes form, they might not be cleared as efficiently, if the phagocytic capacity of the host becomes exhausted (35–38), and when $\gamma\frac{K}{K+C} < c$, we would expect a rebound in the viral load. Under these assumptions, the model has the form,

$$\begin{aligned}\frac{dT}{dt} &= \lambda - dT - \beta VT\\ \frac{dI}{dt} &= f\beta VT - \hat{\delta}I^{\omega}\\ \frac{dV}{dt} &= pI - cV - k_{on}VA(t) + k_{off}C\\ \frac{dC}{dt} &= k_{on}VA(t) + k_{off}C - \gamma\frac{K}{K+C}C\end{aligned}. \quad (17)$$

We fit the model in equation (17) to the data, estimating the parameters $\gamma$, $K$, $pT(0)$, $k_{on}$ and $\omega$. As before, we assume that $k_{off}$ is equivalent to the off-rate constant of VRC01 measured *in vitro* equal to 2.75 day$^{-1}$ (32, 33). As presented in **Figure S1**, this model is not able to capture the early fast decay and rebound of the viral load after VRC01 infusion nor the long-term decline. Thus, this model does not improve the fits of the two previous models in any of the participants (See **Table 2**).

## Phagocytosis-Based Saturated Clearance Model With Two Viral Populations

As before, we considered a variant of the previous model including a preexisting viral population less sensitive to VRC01. VRC01 also binds to this second viral population to form VRC01-HIV complexes, $C_r$, but with reduced affinity We assume in this model that phagocytic cells capture both types of immune complexes, $C_s$ and $C_r$. If the same maximum clearance rate $\gamma$ is used for both viral populations, the model makes a similar prediction than with the one with only one viral population (simulations not shown). Therefore, we assume that the immune complexes, $C_s$ and $C_r$, have clearance rates $\gamma_s$ and $\gamma_r$. In this case, the clearance rate of immune complexes has the form $\hat{\gamma}_s(t) = \gamma_s\frac{K}{K+\gamma_sC_s+\gamma_rC_r}$ and $\hat{\gamma}_r(t) = \gamma_r\frac{K}{K+\gamma_sC_s+\gamma_rC_r}$ for immune complexes with sensitive and resistant virus, respectively. Notice that the clearance of immune complexes depends on the competition of $C_s$ and $C_r$ to be captured by Fc receptors, and the advantage of one over the other depends on the rates $\gamma_s$ and $\gamma_r$. Because VRC01 has higher affinity for sensitive virus, $V_s$, than the partially resistant virus, $V_r$, the $V_s$-Ab complexes should have more antibody in them, and hence be taken up preferentially by phagocytes, i.e., we expect $\gamma_s > \gamma_r$. Therefore, the sensitive virus will decay faster in the initial hours after VRC01 infusion, but the clearance of the less-sensitive virus might be reduced leading to an early increase of this population, reflected in the early viral rebound. With these assumptions, the model has the form,

$$\begin{aligned}\frac{dT}{dt} &= \lambda - dT - \beta_sV_sT - \beta_rV_rT\\ \frac{dI_s}{dt} &= f\beta_sV_sT - \hat{\delta}I_s^{\omega}\\ \frac{dI_r}{dt} &= f\beta_rV_rT - \hat{\delta}I_r^{\omega}\\ \frac{dV_s}{dt} &= pI_s - cV_s - k_{on_s}V_sA(t) + k_{off}C_s\\ \frac{dV_r}{dt} &= pI_r - cV_r - k_{on_r}V_rA(t) + k_{off}C_r\\ \frac{dC_s}{dt} &= k_{on_s}V_sA(t) - k_{off}C_s - \hat{\gamma}_s(t) - \gamma_s\frac{K}{K+\gamma_sC_s+\gamma_rC_r}C_s\\ \frac{dC_r}{dt} &= k_{on_r}V_rA(t) - k_{off}C_r - \gamma_r(t) - \gamma_s\frac{K}{K+\gamma_sC_s+\gamma_rC_r}C_r\end{aligned}. \quad (18)$$

We fit the model in equation (18) to the data, estimating the parameters $\gamma_s$, $\gamma_r$, $K$, $pT(0)$,$k_{on_s}$, $k_{on_r}$, $\%V_s(0)$ and $\omega$ (see best-fit parameter estimates in **Table S5**). In general, this model is able to reproduce the data well (**Figure 7**) and predicts a fast viral decline and rebound in most of the cases (except participant #25). The fast decline is due to the loss of sensitive virus to VRC01, and the rebound is due to the formation of VRC01/less-sensitive virus complexes. However, this model only improved the fits to the data from participants #20 and #22 compared to all previous models. Nonetheless, from the fits the model predicts a dissociation coefficient for the sensitive virus, ($K_{d_s} = \frac{k_{off}}{k_{on_s}}$) around 0.04 μg ml$^{-1}$, smaller than the $K_d$ estimates of VRC01 *in-vitro*.

**TABLE 2** | BIC values from the best fits of each model to each participant's viral load data.

| ID | BIC | | | | | |
|---|---|---|---|---|---|---|
| | DNM | | PSCM | | PLCM | |
| | 1 Viral pop. | 2 Viral pops. | 1 Viral pop. | 2 Viral pops. | 1 Viral pop. | 2 Viral pops. |
| **#20** | -39.1 | -35.7 | -28.7 | -39.4 | **-54.0** | -49.7 |
| **#22** | -4.0 | 1.1 | -13.3 | -38.0 | **-50.9** | -45.3 |
| **#23** | -34.8 | -34.2 | -30.4 | -29.0 | -34.8 | **-42.1** |
| **#24** | -44.0 | -45.8 | -27.8 | -27.6 | -53.4 | **-68.7** |
| **#25** | -32.2 | -31.7 | -18.7 | -13.3 | -26.0 | **-34.6** |
| **#27** | -37.9 | -32.0 | -15.6 | -25.7 | **-40.4** | -36.1 |

*DNM, Delayed neutralization model; PSCM, Phagocytosis-based saturated clearance model; PLCM, Phagocytosis-based logistic clearance model. In bold, the lowest BIC of each row.*

However, because this model predicts that most of the virus during the early rebound comes from the less-sensitive population, the value of $K_{d_s}$ might be overestimated. The model also predicts that the sensitive virus corresponds to the majority (~84%) of the initial viral population. The model also predicts that the ratio between the capture rates of the immune complexes, $\frac{\gamma_s}{\gamma_r}$, is between 10 and $10^2$ (except participant #25), implying that complexes $C_s$ are much more likely to be cleared than complexes $C_r$.

In summary, the model predicts that during the first hours after VRC01 infusion, sensitive immune complexes are formed and are cleared faster than free virus by phagocytic activity

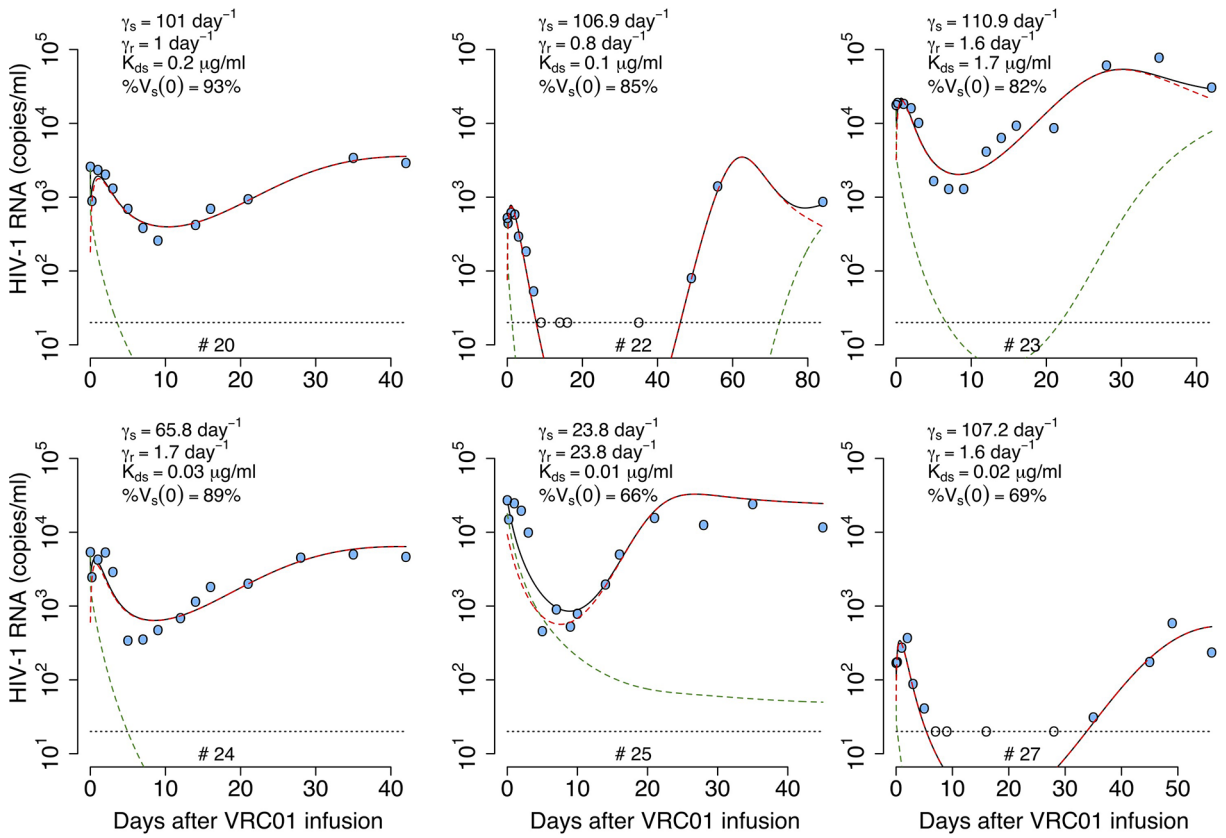


**FIGURE 7** | Best-fits of the phagocytosis-based saturated clearance model with two viral populations, equation (18), to viral load data from participants receiving a single infusion of VRC01. Blue-filled and unfilled circles are the HIV-RNA over and below the limit of detection, respectively. Solid black lines are the prediction of best fit of the model in equation (18) to the data ($V_s + V_r + C_s + C_r$). Green and red dashed lines show the sensitive ($V_s + C_s$) and less sensitive ($V_r + C_r$) virus concentration prediction of the model, respectively. Fixed parameter values are described in **Table 1**. See all parameter estimates in **Table S5**. Other parameters and initial values were derived by assuming the system was in steady state before VRC01 infusion.

(green dashed lines in **Figure 7**), explaining the initial fast decay. As the phagocytic capture is smaller for less sensitive immune complexes, fewer such complexes (red dashed lines in **Figure 7**) are cleared producing a fast rebound over the next hours. Neutralization of virus by VRC01 leads to a reduction of *de novo* infection events and coupled with death of already infected cells leads to a decrease of productively infected cells reflected in the viral decay observed over the next couple of days. While the concentration of VRC01 is still high enough to affect the sensitive virus, the less VRC01-sensitive virus population might be selected (red dashed lines in **Figure 7**) producing the final rebound in viral load.

While the model accurately captures the early viral decline, and rebound in participant #20, it does not do so for participants #24 and #25. Thus, we consider another variant of the model.

## Phagocytosis-Based Logistic Clearance Model

In our final model, we assume that immune complexes first become "captured" immune complexes, $C_p$, i.e. bind to Fc receptors. However, in a second step the captured complexes need to be internalized and degraded. Modeling this two-step process assuming a logistic form for capture of complexes with carrying capacity $K$, and an internalization and degradation rate $m$ of captured complexes, we obtain a model of the form (**Figure 8**)

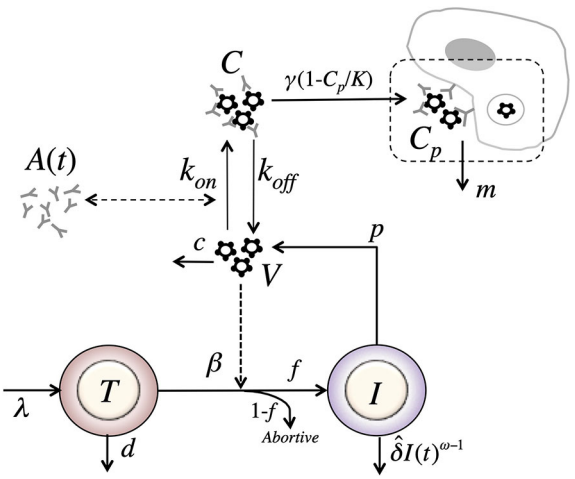


**FIGURE 8** | Schematic of the phagocytosis-based logistic clearance model (for one virus population) used to analyze the virus dynamics after VRC01 infusion. The model includes five variables: target cells ($T$), productively infected cells ($I$), free virus ($V$), VRC01-HIV immune complexes ($C$), and complexes cleared by phagocytes ($C_p$). Parameters $\lambda$, $d$ and $\beta_s$ are the production, death and infection rates of target cells; $\delta$ is the death rate of infected cells; $p$ and $c$ are the production and clearance rates of free virus; $k_{on}$ and $k_{off}$ are the binding and dissociation rate constants of VRC01 to free virus; $\gamma$, $K$ and $m$ are the phagocytosis mediated maximum clearance rate, carrying capacity and degradation rate of VRC01-HIV immune complexes. The antibody concentration, $A(t)$, is determined from the best-fits of the two-compartmental model to VRC01 concentration measurements for each individual (see text).

$$\begin{aligned}
\frac{dT}{dt} &= \lambda - dT - \beta VT \\
\frac{dI}{dt} &= f\beta VT - \hat{\delta} I^{\omega} \\
\frac{dV}{dt} &= pI - cV - k_{on} VA(t) + k_{off} C \\
\frac{dC}{dt} &= k_{on} VA(t) - k_{off} C - \gamma\left(1 - \frac{C_p}{K}\right) C \\
\frac{dC_p}{dt} &= \gamma\left(1 - \frac{C_p}{K}\right) C - mC_p
\end{aligned} \qquad (19)$$

Notice that if we assume that the captured complexes, $C_p$, are in quasi-stationary state, then $\frac{dC_p}{dt} = 0$, and $>\bar{C}_p = \frac{\frac{\gamma}{m} KC}{K + \frac{\gamma}{m} C}$. Substituting $\bar{C}_p$ in equation (19), we get, $\frac{dC}{dt} = k_{on} VA(t) - k_{off} C - \gamma \frac{K}{K + \frac{\gamma}{m} C} C$, identical to the form of the equation for immune complexes in equation (17). Therefore, the model in equation (17) is a special case of the model in equation (19) where $\frac{\gamma}{m} = 1$ (the same applies for the case with two viral populations).

Notice that as described in the previous model, if VRC01 enhances the clearance of virus by forming immune complexes, then $\gamma > c$ and one would expect a rapid viral decay disrupting the steady state when the levels of $C_p$ are low. Then, as immune complexes are captured and degraded by phagocytes with a carrying capacity $K$, the early decline gets disrupted when the number of captured complexes $C_p$ approaches the carrying capacity. Thus, when $\gamma(1 - \frac{C_p}{K}) < c$ or equivalently when $(\frac{C_p}{K}) > 1 - \frac{c}{\gamma}$ the model predicts a switch to a viral increase rather than a decease. This is easy to see since the rate of change of the total virus, $\frac{d(V+C)}{dt} = pI - cV - \gamma(1 - \frac{C_p}{K})C$. When $\gamma(1 - \frac{C_p}{K}) = c, \frac{d(V+C)}{dt} = pI - c(V + C)$ and because $c$ is large the system will rapidly reach a quasi-steady state where total virus production and clearance balance. When $\gamma(1 - \frac{C_p}{K}) < c$, total viral clearance will be less than total production and the total amount of virus will increase.

We fit the model in equation (19) to the viral load data, estimating the parameters $\gamma$, $K$, $m$, $pT(0)$, $k_{on}$ and $\omega$. In general, this model can capture the early fast viral decline and rebound in participant #20 and #24, the early viral rebound or plateau phase in participants #22 and #27, and the long-term viral decline and rebound in all four participants (see **Figure 9**). However, it misses several features in participants #23 and #25 (See individual parameter estimates in **Table S6**). This is demonstrated by the statistical improvement of the fits to the viral load only from participants #20, #22, #24 and #27 ($\Delta$BIC>2.5 only by comparing the fits of this model to data from participants #20, #22, #24 and #27 with respect to the fits with all the previous models in **Table 2**).

The model predicts that the VRC01 dissociation constant for the sensitive virus ($K_{d_s} = \frac{k_{off}}{k_{on}}$) is ~11.4 μg ml$^{-1}$. This dissociation coefficient is higher than that estimated by the delayed neutralization model with one viral population and is also higher than the value estimated *in vitro*. Finally, the model predicts that the initial decay is due to the maximum clearance of the immune complexes $\gamma$, being between 1 and 4 times greater than the clearance rate of the free virus ($c$ = 23 day$^{-1}$), suggesting that VRC01 enhances the virus clearance.

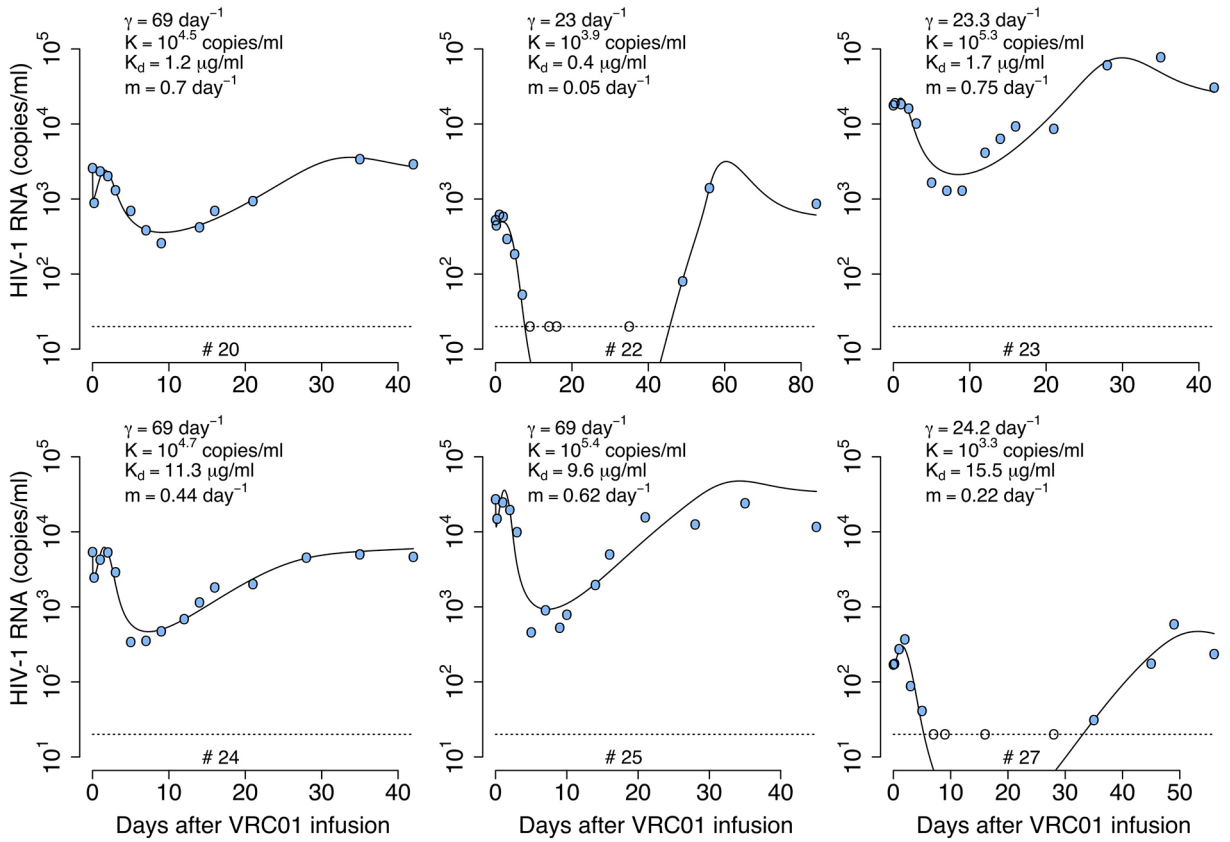


**FIGURE 9** | Best-fits of the phagocytosis-based logistic clearance model (PLCM), equation (19), to viral load data from participants receiving a single infusion of VRC01. Blue-filled and unfilled circles are the HIV-RNA over and below the limit of detection, respectively. Solid black lines are of best fit of the model, $(V + C)$ in equation (19), to the data. Relevant parameter estimates for each participant are shown in each plot. Fixed parameter values are described in **Table 1**. See all parameter estimates in **Table S6**. Other parameters and initial values were derived by assuming the system was in steady state before VRC01 infusion.

## Phagocytosis-Based Logistic Clearance Model With Two Viral Populations

Generalizing to two viral populations, the model becomes

$$\begin{aligned}
\frac{dT}{dt} &= \lambda - dT - \beta_s V_s T - \beta_r V_r T \\
\frac{dI_s}{dt} &= f\beta_s V_s T - \hat{\delta} I_s^{\omega} \\
\frac{dI_r}{dt} &= f\beta_r V_r T - \hat{\delta} I_r^{\omega} \\
\frac{dV_s}{dt} &= pI_s - cV_s - k_{on_s} V_s A(t) + k_{off} C_s \\
\frac{dV_r}{dt} &= pI_r - cV_r - k_{on_r} V_r A(t) + k_{off} C_r \\
\frac{dC_s}{dt} &= k_{on_s} V_s A(t) - k_{off} C_s - \gamma\left(1 - \frac{C_p}{K}\right) C_s \\
\frac{dC_r}{dt} &= k_{on_r} V_r A(t) - k_{off} C_r - \gamma\left(1 - \frac{C_p}{K}\right) C_r \\
\frac{dC_p}{dt} &= \gamma\left(1 - \frac{C_p}{K}\right)(C_s + C_r) - mC_p
\end{aligned} \quad . \qquad (20)$$

We fit this model to the data, estimating the parameters $\%V_s(0)$, $\gamma$, $K$, $m$, $pT(0)$, $k_{on_s}$, $k_{on_r}$ and $\omega$. In general, this model is able to reproduce all the features of the viral load data from all participants well (**Figure 10**). However, the model only has better statistical support for the fits to participants #23, #24 and #25 compared to the best previous models (see **Table 2**). The model did not improve the fitting with respect to the one viral population version for participants #20, #22 and #27, but the estimated parameters reflect the same results for participants #20 and #22 (See **Table S7** for all best-fit estimates). For the best fits of participant #22 the model predicts that the sensitive virus population corresponds to almost 100% of the viral population, which is the same as having just a model with one viral population. Also, the model predicts that for participant #20, the dissociation constants for the sensitive and less-sensitive virus populations ( $K_{d_s} = \frac{k_{off}}{k_{on_s}}$ and $K_{d_r} = \frac{k_{off}}{k_{on_r}}$, respectively) are very similar, which also is equivalent to have a model with one viral population.

This model predicts a dissociation constant for the sensitive virus around 0.8 μg ml$^{-1}$, also similar to the estimates from the delayed-neutralization model. The model also predicts that the sensitive virus corresponds to the majority (~90%) of the initial viral population. This value is relevant as it is similar to the 90% breadth of VRC01 estimated *in vitro* (32). As for the one viral

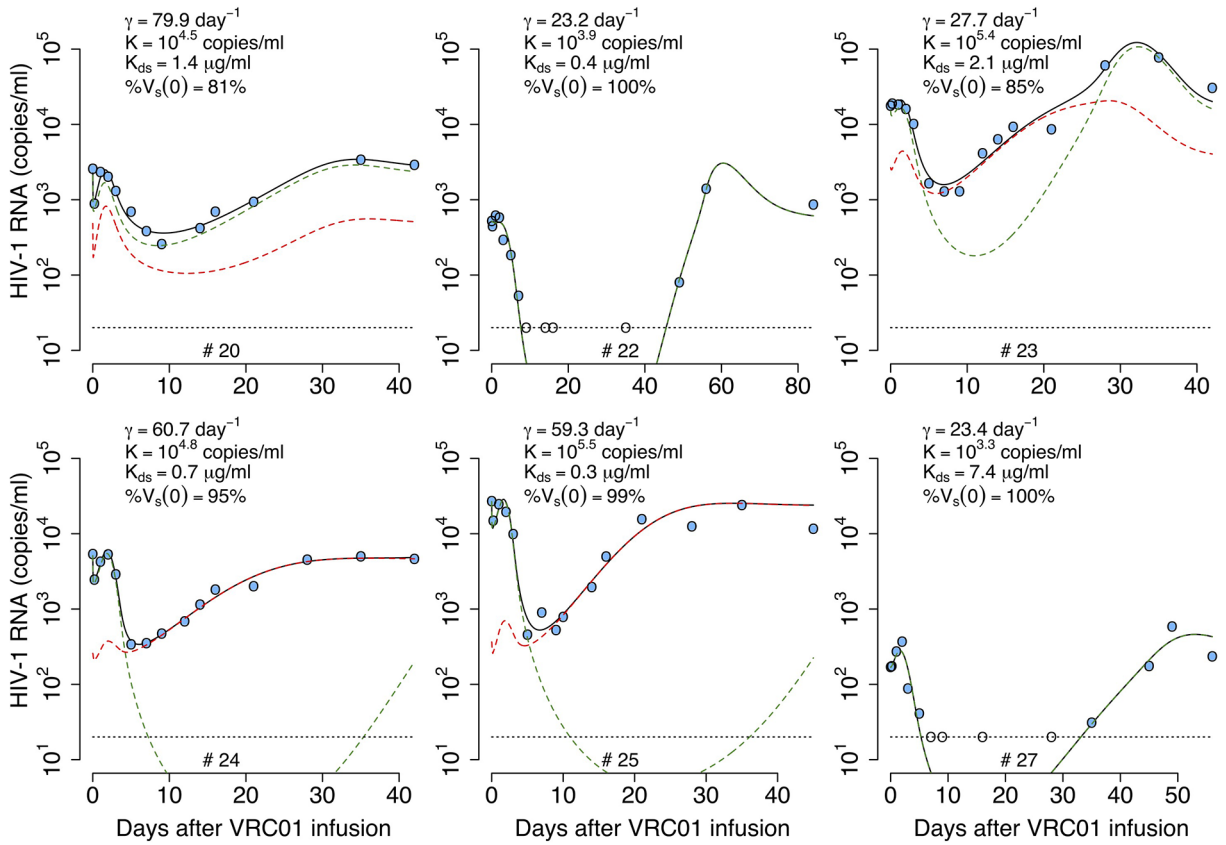


**FIGURE 10** | Best-fits of the two viral population phagocytosis-based logistic clearance model, equation (20), to viral load data from participants receiving a single infusion of VRC01. Blue-filled and unfilled circles are the HIV-RNA over and below the limit of detection, respectively. Solid black lines are the best-fit of the model, ($V_s + V_r + C_s + C_r$) in equation (20) to the data. Green and red dashed lines show the sensitive ($V_s + C_s$) and less sensitive ($V_r + C_r$) virus concentration prediction of the model, respectively. Relevant parameter estimates for each participant are shown in each plot and all parameter estimates are given in **Table S7**. Fixed parameter values are described in **Table 1**. Other parameters and initial values were derived by assuming the system was in steady state before VRC01 infusion.

population model, this model predicts VRC01 enhances the clearance of the virus by increasing the clearance rate of immune complexes up to ~4-fold, i.e., from 23 day$^{-1}$ to 80 day$^{-1}$. Finally, the model reproduces the rapid initial viral load decline and rebound, and estimates that captured immune complexes have a half-life of ~72 hrs.

To understand how the parameters drive the virus dynamics, we used the estimated parameter values for participant #24 to simulate the model and then did a sensitivity analysis by varying one parameter at a time. As presented in **Figure S2**, once the value of $\gamma$ increases over the value of $c$ = 23 day$^{-1}$ a rapid, early virus decline is predicted by the model (**Figure S2A**). Since the following rebound depends on how quickly the captured immune complexes $C_p$ grow, the rebound is modulated by the parameters $K$ and $m$. Thus, a higher and longer early viral rebound is predicted when $K$ and $m$ decrease (**Figures S2B, C**). Specifically, $K$ must be smaller than the early viral load concentration, for an early viral rebound to appear. Since HIV complexed with VRC01 is assumed be neutralized and thus does not infect cells, if $K_{d_s} = \frac{k_{off}}{k_{on_s}}$ is sufficiently small compared to the VRC01 concentration the model predicts a long-term viral load decline (**Figure S2D**). However, if $K_{d_s}$ is close to or greater than the VRC01 concentration (i.e. $K_{d_s} > 50$ μg ml$^{-1}$) the viral decline slows down or is not seen because less virus is neutralized allowing viral replication and there is no early viral rebound because immune complexes are rarely formed (**Figure S2D**). A similar, non-responding behavior is seen if the fraction of the viral population sensitive to VRC01, $\%V_s(0)$ is smaller than 50% (**Figure S2E**).

As an illustration, **Figure 11** presents the predicted fate of the virus in volunteer #24 according to this model. At baseline, sensitive virus comprises 95% of the viral population (green dashed lines). During the first hours after VRC01 infusion, immune complexes are formed and are cleared faster than free virus, explaining the initial fast decay. As the phagocytic carrying capacity is reached, fewer immune complexes (green dot lines) are cleared producing a fast rebound over the next hours. Neutralization of virus by VRC01 leads to reduced *de novo* infection, and coupled with the death of already infected cells leads to the viral decay observed over the next couple of days. While the concentration of VRC01 is still high enough to affect the sensitive virus, a less VRC01-sensitive virus population can

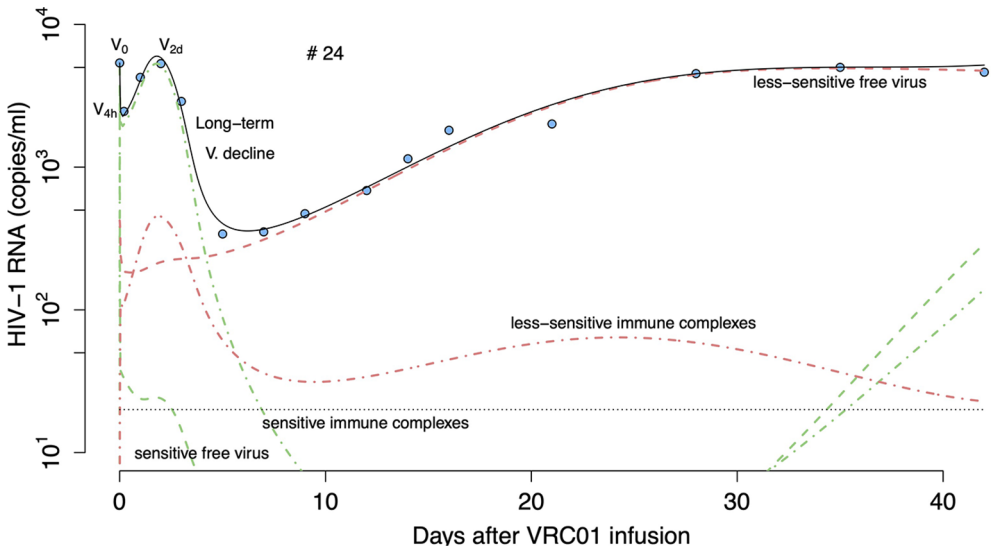


**FIGURE 11** | Prediction of the two viral population phagocytosis-based logistic clearance model, equation (20), for free virus and immune complexes in participant #24. Blue-filled circles are the HIV-RNA and the solid black line is the model predictions ($V_s + V_r + C_s + C_r$). Green and red dashed lines show the sensitive ($V_s$) and less sensitive ($V_r$) free virus concentration prediction. Red and green dotted-dashed lines present the complexes formed by VRC01 and the sensitive ($C_s$) or less sensitive virus ($C_r$).

have selective advantage (red dashed lines) producing the final rebound in viral load.

## Comparison of All Models

We compared the ability of each model to explain the data by using model selection theory (39). In this approach, we computed the Bayesian information criterion (BIC) for the fit of each model to each participant and also by comparing a global Bayesian information criterion for all participants ($BIC_{all}$), as described in the *Materials and Methods* section.

When comparing the BIC of the model for each participant (see **Table 2**) we found that the data from participants #20, #22 and #27 are better explained by the phagocytosis-based logistic clearance model with one viral population, while the data for participants #23, #24 and #25 are better explained by the same model but with two viral populations. From the estimates of the best model for each individual (**Table 3**) we found a dissociation constant for the sensitive virus around 0.9 μg $ml^{-1}$, and that the sensitive virus corresponds to the ~95% of the initial viral population.

To evaluate the robustness of the model selection process we fit each model again to ten viral load profiles constructed artificially by adding noise to participants' viral load observations over the limit of detection. We assumed the noise was lognormally distributed with zero mean and a standard deviation of 0.2 $\log_{10}$ (**Figure S3**). Then, for each participant we computed the BIC of the models using the median of the sum of squares errors from the fits of each model to the ten profiles. As before, we found that the phagocytosis-based logistic clearance model better explains the data, with the model with one viral population better for #20, #22 and #27, and with two viral populations better for participants #23, #24 and #25 (**Tables S12, S13**).

When comparing the models using a global approach, we found that the model that best fit the data was the phagocytosis-based logistic clearance model with two viral populations ($\Delta BIC_{all}$>2.9, **Table 4**). As described in the previous section,

**TABLE 3** | Parameter estimate of the models with the lowest BIC values in **Table 2** for each individual.

| | $\%V_s(0)$ (-) | $\log_{10}(pT_0)$ $\log_{10}$(1/ml/day) | $K_{d_s}$ (μg/ml) | $K_{d_r}$ (μg/ml) | $\gamma$ (1/day) | $\log_{10}(K)$ $\log_{10}$(1/ml) | $m$ (1/day) | $\omega$ (-) |
|---|---|---|---|---|---|---|---|---|
| **#20** | – | 8.3 | 1.1 | – | 75.9 | 4.5 | 0.8 | 2.5 |
| **#22** | – | 7.6 | 0.4 | – | 23.0 | 3.9 | 0.1 | 1.2 |
| **#23** | 0.85 | 8.3 | 2.1 | 28.9 | 27.7 | 5.4 | 0.3 | 1.3 |
| **#24** | 0.95 | 7.8 | 0.7 | 217.3 | 60.7 | 4.8 | 0.2 | 1.2 |
| **#25** | 0.99 | 8.3 | 0.3 | 91.5 | 59.3 | 5.5 | 0.3 | 1.2 |
| **#27** | – | 7.2 | 15.9 | – | 24.3 | 3.3 | 0.2 | 1.1 |
| **Median** | 0.95 | 8.1 | 0.9 | 91.5 | 43.5 | 4.7 | 0.2 | 1.2 |
| **min** | 0.85 | 7.2 | 0.29 | 28.9 | 23.0 | 3.3 | 0.1 | 1.1 |
| **max** | 0.99 | 8.3 | 15.9 | 217.3 | 75.9 | 5.5 | 0.8 | 2.5 |

**TABLE 4** | Sum of squared error (SSE) and global Bayesian information criterion ($BIC_{all}$) values.

| ID | SSE | | | | | |
|---|---|---|---|---|---|---|
| | DNM | | PSCM | | PLCM | |
| | 1 Viral pop. | 2 Viral pops. | 1 Viral pop. | 2 Viral pops. | 1 Viral pop. | 2 Viral pops. |
| **#20** | 0.24 | 0.21 | 0.53 | 0.13 | 0.06 | 0.06 |
| **#22** | 4.09 | 4.03 | 2.11 | 0.21 | 0.12 | 0.12 |
| **#23** | 0.60 | 0.43 | 0.80 | 0.51 | 0.50 | 0.21 |
| **#24** | 0.32 | 0.20 | 0.95 | 0.56 | 0.14 | 0.04 |
| **#25** | 0.71 | 0.51 | 1.75 | 1.45 | 0.89 | 0.35 |
| **#27** | 0.36 | 0.38 | 1.79 | 0.49 | 0.25 | 0.24 |
| **Σ(SSE)** | 6.32 | 5.77 | 7.93 | 3.36 | 1.97 | 1.02 |
| $M_{all}$ | 30 | 42 | 30 | 48 | 36 | 48 |
| $BIC_{all}$ | -87.6 | -42.0 | -68.3 | -61.5 | -160.0 | **-162.9** |
| $\Delta BIC_{all}$ | 75.3 | 120.9 | 94.6 | 101.4 | 2.9 | 0.0 |

*DNM, Delayed-neutralization model; PSCM, Phagocytosis-based saturated clearance model; PLCM, Phagocytosis-based logistic clearance model. The lowest $BIC_{all}$ is given in bold type.*

although this model globally fits the data better, the estimated parameters for participants #20, #22 and #27 suggested that the sensitive viral population correspond to almost 100% of the final population or with very similar dissociation constant with respect to the less sensitive viral population, equivalent to have a model with a single viral population.

We finally compared the best model obtained by the global selection, with the equivalent model but assuming that the death rate of infected cells was constant (i.e. $\omega = 1$). However, we found that the model with $\omega = 1$ resulted in worse fits to the data (see **Table S11**).

## DISCUSSION

A single infusion of 40mg/kg of VRC01 was able to reduce the viral load in chronically infected individuals more than 1-log (1). Since VRC01 is a bnAb with breadth of 90% *in-vitro*, one would expect that *in-vivo* it neutralizes the majority of virus strains preventing *de-novo* infection events. Thus, one would expect the virus dynamics during treatment with VRC01 would reflect the death rate of infected cells similarly to what is observed during treatment with reverse transcriptase inhibitors (RTIs). However, the observed kinetics after VRC01 passive administration are quite distinct from those observed after initiation of treatment with RTIs (1, 18, 21). The data shows that the major reduction in viral load occurs after a delay of about 2-3 days, which is longer than the one observed after initiation of antiretroviral therapy (9, 10, 18, 21, 40). If one assumes the data is accurate, in three of the individuals the virus declined rapidly during the initial 4 hours and then rebounded to baseline by day 1, and in two other treated individuals, the early decline was not captured but an initial viral increase to above baseline was observed.

The measured serum concentration of VRC01 decayed in a biphasic manner, similar to the dynamics observed with other monoclonal antibodies (16). Therefore, we fit the antibody concentration data to a two-compartment pharmacokinetics model (representing the VRC01 concentration in plasma and tissues) where the first phase decay occurs as the antibody is distributed from blood to tissue, and the second phase represents antibody elimination from the body (17). We developed closed form solutions for the serum VRC01 concentration in both compartments and showed that the volume of the compartments do not affect the VRC01 dynamics in the first compartment (plasma), but it affect its concentration in second compartment (tissues). Pharmacokinetic analysis showed that infusion of VRC01 in viremic and aviremic individuals did not have significant differences. This result suggests that the concentration of VRC01 was sufficiently high that the binding of VRC01 to the virus in infected individuals did not noticeable affect the serum VRC01 concentration during the first 6 weeks following infusion. Our pharmacokinetic model predicts that VRC01 in infected individuals is eliminated with a half-life of 7.1 days. This value is smaller than the 12 days estimated previously in infected individuals using a non-compartmental PK analysis (1, 8). However, our PK model includes transport of the Ab between blood and tissue, codifying explicitly the mechanisms for both the first (distribution) and second (elimination) decay phases observed in the VRC01 concentration time course data (17).

To explain the viral dynamics in chronically infected individuals after a single infusion of VRC01 we developed models by modifying the standard model of virus dynamics in (19, 20). Since Lynch et al. (1) detected virus resistant VRC01 in 2 individuals at baseline, who were not modeled here as their viral load did not decline, and in the six individuals studied here a virus population less sensitive to VRC01 a month after infusion, we generalized each model to include two viral populations with one more sensitive to VRC01 than the other, assuming that the observed viral load reflects the sum of the two viral populations. Here we presented three different mathematical models, with one or two viral populations, that could explain the observed viral load data. The first model assumed that VRC01 neutralizes the virus after a delay. However, this model did not explain the mechanism behind the initial delay. The other two models assumed that the mechanism behind the "delay" has to do with the capacity of VRC01 to opsonize HIV-1 and increase

the rate of phagocytosis to clear the virus, reflected in the initial rapid decline in the viral load after VRC01 infusion. To capture that mechanism these models included an explicit term for the formation of immune complexes and explored different approaches regarding their clearance. The best-fit model assumed that clearance of immune complexes comprises a two-step process that includes capture of immune complexes on the surface of phagocytes that have a maximum carrying (binding) capacity followed by the internalization/degradation of the complexes, which then allows the phagocytes to bind additional immune complexes. Based on BIC, we found that this model, with capture and internalization/degradation of immune complexes, consistently explained the data better for each participant than the other models we examined; with one viral population for participants #20, #22, and #27, and two viral populations for participants #23, #24, and #25.

One of the main implications of this result is that it suggests that VRC01, through the formation of HIV-VRC01 immune complexes, has the capacity to enhance the clearance of the virus up to 3–fold compared to estimates of free virus clearance. This process is necessary to explain the rapid viral decline during the initial hours after VRC01 infusion. This result concurs with early studies that demonstrated rhesus macaques receiving a continuous infusion of HIV and high titers of virus-targeted antibodies experienced an enhancement in virus clearance of up to 4-fold in the presence of the antibodies (41). It also agrees with a recent study in humanized mice showing the ability of 3BNC117, a bnAb also targeting the CD4 binding site, to enhance the clearance of mAb-opsonized virus from the circulation (42). The second main implication is that the best model suggests that the clearance of VRC01-HIV immune complexes behaves as a phagocytosis-like process, but predicts that this process is constrained during immune complex capture and possibly internalization/degradation of HIV-VRC01 immune complexes. This limitation is necessary to explain the viral rebound before the major viral load reduction.

It has been shown that besides neutralization antibodies can activate phagocytic cells *in-vivo* following the opsonization of antigens by antibodies, particularly $IgG_1$, the isotype of VRC01, and the binding of their Fc region to Fcγ receptors on the surface of phagocytes (43). Previous *in-vitro* studies have suggested that monocyte-derived macrophages use Fcγ receptors (FcγR) to phagocytose and clear HIV-IgG complexes (44). Additionally, *in-vivo* studies in humanized mice have revealed that viral opsonization by mAbs targeting the CD4bs enhanced their clearance by circulating or tissue-resident cells expressing FcγR (42). More recently, a study has shown that the majority of effectors cells expressing FcγR in human mucosal tissues are phagocytes, with significant phagocytic activity (45). Thus, our results, along with the findings mentioned above, suggest that effector mechanisms like phagocytosis of VRC01-HIV immune complexes are likely to clear virus-mAb immune complexes, and if it enhances the clearance of the virus it can explain the early virus dynamics observed after VRC01 infusion.

Our results also suggest that in order to have the initial viral load rebound (or plateau phase) at day 1, phagocytic capacity has to be constrained. A similar rebound over baseline was present in 10 of 18 infected participants one day after receiving a single infusion of 3BNC117 (3), and in 7 of 13 participants receiving 30 mg/kg of the bnAb 10-1074 (46). Interestingly, our model can recapitulate the viral loads of individuals receiving 3BNC117, suggesting the same mechanism may drive those early viral rebounds (manuscript in preparation). The nature behind this phagocytic impairment is unclear, but it might be due either to the loss of Fc receptors by internalization, high amounts of circulating immune complexes prior to VRC01 infusion that may block access to FcγRs (37, 38) or due to a finite capacity to internalize and degrade immune complexes, among other reasons. In any event, our model predicts that phagocytic capacity returns with a $t_{1/2}$ of ~3 days. In lymphoid tissues, where the majority of HIV-1 infection events occur, FcγR expressing macrophages and neutrophils are present (45). However, in HIV-1 infected individuals the capacity of FcγR-expressing phagocytes can be impaired (47–50) as the expression of FcγRs is significantly reduced in chronic infection (36). This reduction in FcγR expression may make it easier to saturate the cellular phagocytic capacity. Furthermore, phagocytosis can be impaired in the presence of HIV proteins, as they might prevent the recruitment of key proteins into the phagocytic cup (51), or perturb phagosome formation (52) and fusion to lysosomes (53). Thus, although in the absence of HIV-1 phagocytosis of viruses or bacteria by neutrophils or macrophages may take from several minutes (54) to a couple of hours (55), our results along with the studies referenced above may indicate that the capacity of this process might be impaired and the degradation activity delayed in chronic HIV-1 infection.

Our model predicts that VRC01 has a maximum *in-vivo* dissociation constant for the sensitive virus ($\frac{k_{off_S}}{k_{on_S}}$) of 0.9 μg/ml. Since VRC01 has *in-vitro* neutralization potency with $IC_{50}$ estimates similar to the dissociation constant estimated here (32), our findings indicate that *in-vitro* estimates of neutralization potency might be surrogates for *in-vivo* virologic effects (1). Furthermore, in agreement with neutralization and sequence analyses (1), the model predicts that in several participants a second less VRC01-sensitive viral population might be selected, and that the majority of virus in the observed viral rebound might come from this second population. In those cases, the sensitive virus was around 95% of the initial virus population. This fraction is relevant as it might be related to the previous estimate of the 90% breadth of VRC01 (32).

The phagocytosis-based logistic clearance model included the reversible formation and dissociation of sensitive-virus/VRC01 neutralized complexes. As in the model of Lu et al. (15), this is the simplest model of viral neutralization in which only a single antibody binds to each virion, leading to its neutralization. In reality, a number of antibodies can bind to a virion, but as VRC01 is in great excess this extra binding does not appear to affect the free antibody concentration. However, these extra antibodies could bind free Fc receptors and more detailed models of phagocytosis and viral neutralization would be needed to take this into account.

Finally, our model predicts that the death rate of infected cells is not constant, as traditionally modeled to fit virus dynamics (10, 19–21), but it depends on the density of infected cells, codified by the parameter $\omega$, as first introduced by Holte et al. (28). We found that assuming a constant rate of infected cell death ($\omega = 1$) the fits of the model to the data are significantly degraded, and that viral rebound cannot be reproduced accurately. Interpretations of this non-linear, infected cell-density dependent rate may suggest that cytolytic processes that are activated by an increased number of infected cells may be present, such as CD8+ T cell mediated cell killing (28, 56).

In conclusion, we have compared several models to understand the mechanism behind the virus dynamics observed in chronically infected participants treated with a single infusion of VRC01. From our comparison, the best model suggests that a single infusion of VRC01 induces an enhancement of virus clearance by a phagocytic mechanism that rapidly clears VRC01-HIV complexes. Our analysis also suggests that this phagocytic mechanism is limited, and that VRC01-HIV complex clearance might slow as the process becomes saturated, possibly due to internalization or blocking of Fc receptors. This explains the initial fast decay and rebound in the plasma viral load observed after VRC01 infusion. The long-term viral decline is due to neutralization of the virus by VRC01 with similar efficacy estimated by *in-vitro* methods. However, selection pressure may lead to the outgrowth of a less-susceptible virus population to VRC01 with lowered neutralization potency reflected in the viral load final rebound.

# MATERIALS AND METHODS

## Clinical Data

We fit our proposed models to data from the VRC 601 single-site, phase 1, open-label, dose escalation study conducted at the NIH Clinical Center by the VRC Clinical Trials Program, NIAID, NIH (ClinicalTrials.gov NCT 01950325) (1, 8).

For the VRC01 pharmacokinetic analysis we used two sets of data. The first came from the six HIV-1 infected individuals who had a significant decrease in their viral load after a single VRC01 infusion of 40 mg/kg. We did not use the VRC01 concentration data from the two infected individuals who did not respond to the mAb as we wanted to know if the binding of VRC01 to HIV-1 significantly changed the VRC01 serum concentration. The data comprises serum VRC01 concentration measurements collected before infusion and at 0, 1, 2, 4, and 24 hours, and days 2, 7, 14, 21, 28, 35, 42, 49, 56, and 84 after infusion (1). The second set of data comes from the three-aviremic participants who received one or two VRC01 infusions of 40 mg/kg. Two of them were infused at days 0 and 28, and samples were collected at 0, 1, 2, 4, 8, 12, and 24 hours, as well as 2, 7, 14, 21 and 28 days after each infusion (8). One of the three-aviremic individuals completed only one infusion following the same collection of data until day 28 after VRC01 administration. VRC01 serum concentration quantification was performed in 96-well plates on a Beckman Biomek–based automation platform using the anti-idiotype mAb 5C9. VRC01 concentration was undetectable at levels smaller than 0.098 μg/ml.

For the viral kinetic model analysis, we used HIV RNA plasma samples from six HIV-1 infected participants after VRC01 infusion. Measurements were performed by the NIH Clinical Center using the standard diagnostic assay COBAS AmpliPrep/COBAS TaqManHIV-1 Test, version 2.0. We used samples collected at baseline, 4 hours, as well as days 1, 2, 3, 5, 7, 14, 16, 21, 28, 35 and 42 after VRC01 administration for all participants, but also days 49, 56, and 84 for participants #22 and #27 (1), for a total of 85 data points from all infected participants who responded to VRC01 combined (participants #20, #22, #23, #24, #25 and #27). Virus load was undetectable at concentrations below 20 copies/ml.

## Pharmacokinetic Model Fitting

We separately fit the two-compartment PK model solution in Eqs. (2) and (4) to the VRC01 serum concentration measurements from the six HIV-1 infected participants and from three aviremic, presumably non-infected, volunteers infused with 40 mg/kg of VRC01 using a non-linear least-squares approach. We estimated the parameters $k_0$, $k_{12}$ and $k_{21}$.

To convert from units of [μg/ml], we assumed that VRC01 has the IgG molecular weight of 160 kDa. Thus, we computed a conversion factor as follows,

$$160\,\text{kDa} = 1.6 \times 10^5 \text{g/mol} \times 6.022 \times 10^{-23} \text{mol/molecule} \times 10^6 \mu\text{g/g} = 2.7 \times 10^{-13} \mu\text{g/molecule}\,.$$

## Viral Kinetic Model Fitting and Selection

Using the best-fit of the VRC01 concentration in blood for each infected individual as $A(t)$, we then fit the viral kinetic models with one or two viral populations to the plasma HIV RNA data of the six participant that responded to VRC01.

Because the viral production rate $p$ cannot be estimated from the standard viral dynamics model using only viral load data (57, 58) we redefined the variables in all the virus dynamics models so that $\hat{I} = pI$, and $\hat{T} = pT$, so we can re-write, without loss of generality, the equations for $T$, $I$ and $V$ as,

$$\begin{aligned} \frac{d\hat{T}}{dt} &= \hat{\lambda} - d\hat{T} - \beta V \hat{T} \\ \frac{d\hat{I}}{dt} &= \beta V \hat{T} - \tilde{\delta} \hat{I}^{\omega} \\ \frac{dV}{dt} &= \hat{I} - cV \end{aligned} \tag{21}$$

Where $\tilde{\delta} = p^{1-\omega}\delta$ and $\hat{\lambda} = p\lambda$. We did the same for the models with two viral populations.

For each participant, we determined a parameter set minimizing the sum of squared error function $\sum_i [log(y_i) - \log f(t_i)]^2$, where $f(t_i)$ represents the numerical solution for the viral load at time $t_i$ derived from the model, and $y_i$ represents the measured HIV RNA value at time $t_i$. For the models with an explicit term for immune complexes, the model viral loads were calculated as $V_s + C_s$, and $V_s + C_s + V_r + C_r$, for the case of one and two viral populations, respectively.

Otherwise, the model viral loads were calculated as $V_s$, and $V_s + V_r$. For participants #22 and #27, in which the viral loads fell below the limit of detection, we fit each model to the data by minimizing the following adjusted sum of squared error, that takes into consideration censored data:

$$SSE = \sum_{i\in I_{v>LD}}[\log(\gamma_i) - \log f(t_i)]^2 + \sum_{i\in I_{v<LD}} - \log[F_{LN}\{LD, \log f(t_i), \sigma_i\}] \quad (22)$$

where $F_{LN}$ represents the lognormal cumulative distribution at the limit of detection level with mean $f(t_i)$ and variance $\sigma_i^2$ (where the negative symbol in the censored-data-term in equation (22) is used to minimize the function, and $F_{LN}\left\{LD, \log f(t_i), \sigma_i\right\} = \frac{1}{\sqrt{2\pi\sigma_i^2}}\int_{-\infty}^{LD} e^{-\left(u-\log f(t_i)\right)^2} du$) (59). The sets $I_{v>LD}$ and $I_{v<LD}$ represent the sets of HIV RNA measurements above and below the limit of detection, respectively. Since there was no additional single copy assay data to obtain information about the values below the limit of detection, we used an approach for censored data with a model for $\sigma_i^2$ fit to single-copy assay (SCA) data proposed elsewhere (60, 61).

Fixed parameter values used are the target cell death rate $d$ = 0.01 day$^{-1}$ (31) and the virus clearance rate c = 23 day$^{-1}$ (30). Since the death rate of infected cells is density-dependent, we computed the value of $\tilde{\delta}$ by assuming that the initial infected cell death rate $\tilde{\delta}\hat{I}(0)^{\omega-1}$ = 1.5 day$^{-1}$ [close to the maximum constant death rate estimates during ART (18)], so that $\tilde{\delta} = \frac{1.5}{\hat{I}(0)^{\omega-1}}$, where the value of $\omega$ is fitted, and $\hat{I}(0)$ is obtained using the steady-state assumption at the beginning of VRC01 infusion as described below. We used the maximum estimate of $\delta$ from (18) as we expect the density of infected cells and hence $\delta = \tilde{\delta}\hat{I}^{\omega-1}$ to decrease with time. In the models that have binding and dissociation of VRC01 to the virus, we used a dissociation rate of 2.75 day$^{-1}$ (32, 33). For all models, we assumed that the initial values of the variables in the model correspond to the participant being at steady state (set-point of chronic infection) before the VRC01 infusion. In the case of models with two viral populations, we assumed that the initial value of the sensitive viral population to VRC01, $V_s(0)$, was equal to the measured baseline viral load data multiplied by the estimated fraction $\frac{V_s(0)}{V(0)}$, from the fitting procedure. During the fitting we estimated the fraction $\frac{V_s(0)}{V(0)}$. Similarly, $V(0)[1 - \frac{V_s(0)}{V(0)}]$ . We assumed $C_s(0) = C_r(0) = 0$. We calculated the initial values of infected cells from the steady-state equations before the infusion of VRC01 with forms $\hat{I}_s(0) = cV_s(0)$ and $\hat{I}_r(0) = cV_r(0)$. Also using the initial values presented above we estimated the production rate of target cells as $\hat{\lambda} = d\hat{T}(0) + \beta_s V_s(0)\hat{T}(0) + \beta_r V_r(0)\hat{T}(0)$ (we also performed fits assuming $\hat{\lambda} = d\hat{T}(0)$ but obtained equivalent results), with infectivity rates for the sensitive and less-sensitive virus $\beta_S = \frac{\delta\hat{I}_s(0)^{\omega}}{fV_s(0)\hat{T}(0)}$ and $\beta_r = \frac{\delta\hat{I}_r(0)^{\omega}}{fV_r(0)\hat{T}(0)}$.

We used the Differential Evolution package in R to find initial parameter estimates and improved them using the L-BFGS-B algorithm in the R-optim package. We performed model selection for each participant using the Bayesian information criterion ($BIC = n\log(\frac{SSE}{n}) + M\log(n)$), where $M$ is the number of estimated parameters for the model and $n$ is the number of data points. Then, we compared the $BIC$ values from different models and computed the values of $\Delta BIC$ by subtracting the minimum $BIC$ from each model's $BIC$. We assumed there is substantial evidence against models with higher $BIC$ if their corresponding $\Delta BIC > 2$ (39). We also performed model selection globally for all participants by computing $BIC_{all} = n_{all}\log(\frac{SSE_{all}}{n_{all}}) + M_{all}\log(n_{all})$, where $SSE_{all}$ is the sum of squared error of the fits from all participants viral load data using a specific model, $M_{all}$ is the total number of parameter estimated for all participants, i.e. $M_{all} = M \times 6$, and $n_{all}$ the total number of data points (in this case, $n_{all}$ = 85). We computed the values of $\Delta BIC_{all}$ by comparing the $BIC_{all}$ of each model with the minimum $BIC_{all}$ from all models. We also assumed a substantial evidence against the models with higher $BIC_{all}$ if their corresponding $\Delta BIC_{all} > 2$.

## DATA AVAILABILITY STATEMENT

Publicly available datasets were analyzed in this study. This data can be found here: Lynch, R. M. et al. Sci Trans Med 7, 319ra206 (2015).

## ETHICS STATEMENT

The studies involving human participants were reviewed and approved by Los Alamos National Laboratory Institutional Review Board. The patients/participants provided their written informed consent to participate in this study.

## AUTHOR CONTRIBUTIONS

EC and AP conceived the study and developed the models. EC assembled data, wrote all code, performed all calculations and derivations, ran the models, and analyzed output data. AP and EC wrote the manuscript. All authors contributed to the article and approved the submitted version.

## FUNDING

Portions of this work were one under the auspices of the U.S. Department of Energy under contract 89233218CNA000001. This study was supported by grants from the National Institutes of Health, R01 AI150500 (EC) and R01 AI028433, R01 OD011095 and P01 AI131365 (AP). The funders had no role in study design, data collection and analysis, decision to publish, or preparation of the manuscript.

## ACKNOWLEDGMENTS

We thank the Clinical Trials Program and Vaccine Immunology Program at the Vaccine Research Center, NIAID, NIH and the VRC 601 Study Team for providing the data.

## SUPPLEMENTARY MATERIAL

The Supplementary Material for this article can be found online at: https://www.frontiersin.org/articles/10.3389/fimmu.2021.710012/full#supplementary-material

## REFERENCES

1. Lynch RM, Boritz E, Coates EE, DeZure A, Madden P, Costner P, et al. Virologic Effects of Broadly Neutralizing Antibody VRC01 Administration During Chronic HIV-1 Infection. *Sci Trans Med* (2015) 7:319ra206–319ra206. doi: 10.1126/scitranslmed.aad5752
2. Barouch DH, Whitney JB, Moldt B, Klein F, Oliveira TY, Liu J, et al. Therapeutic Efficacy of Potent Neutralizing HIV-1-Specific Monoclonal Antibodies in SHIV-Infected Rhesus Monkeys. *Nature* (2013) 503:224–8. doi: 10.1038/nature12744
3. Caskey M, Klein F, Lorenzi JCC, Seaman MS, West APJr., Buckley N, et al. Viraemia Suppressed in HIV-1-Infected Humans by Broadly Neutralizing Antibody 3BNC117. *Nature* (2015) 522:487–91. doi: 10.1038/nature14411
4. Li Y, O'Dell S, Walker LM, Wu X, Guenaga J, Feng Y, et al. Mechanism of Neutralization by the Broadly Neutralizing HIV-1 Monoclonal Antibody VRC01. *J Virol* (2011) 85:8954–67. doi: 10.1128/JVI.00754-11
5. Zhou T, Georgiev I, Wu X, Yang Z-Y, Dai K, Finzi A, et al. Structural Basis for Broad and Potent Neutralization of HIV-1 by Antibody VRC01. *Science* (2010) 329:811–7. doi: 10.1126/science.1192819
6. Zhou T, Zhu J, Wu X, Moquin S, Zhang B, Acharya P, et al. Multidonor Analysis Reveals Structural Elements, Genetic Determinants, and Maturation Pathway for HIV-1 Neutralization by VRC01-Class Antibodies. *Immunity* (2013) 39:245–58. doi: 10.1016/j.immuni.2013.04.012
7. Zhou T, Xu L, Dey B, Hessell AJ, Van Ryk D, Xiang S-H, et al. Structural Definition of a Conserved Neutralization Epitope on HIV-1 Gp120. *Nature* (2007) 445:732–7. doi: 10.1038/nature05580
8. Ledgerwood JE, Coates EE, Yamshchikov G, Saunders JG, Holman L, Enama ME, et al. Safety, Pharmacokinetics and Neutralization of the Broadly Neutralizing HIV-1 Human Monoclonal Antibody VRC01 in Healthy Adults. *Clin Exp Immunol* (2015) 182:289–301. doi: 10.1111/cei.12692
9. Andrade A, Guedj J, Rosenkranz SL, Lu D, Mellors J, Kuritzkes DR, et al. Early HIV RNA Decay During Raltegravir-Containing Regimens Exhibits Two Distinct Subphases (1a and 1b). *AIDS* (2015) 29:2419–26. doi: 10.1097/QAD.0000000000000843
10. Perelson AS, Neumann AU, Markowitz M, Leonard JM, Ho DD. HIV-1 Dynamics *In Vivo*: Virion Clearance Rate, Infected Cell Life-Span, and Viral Generation Time. *Science* (1996) 271:1582–6. doi: 10.1126/science.271.5255.1582
11. Tomaras GD, Yates NL, Liu P, Qin L, Fouda GG, Chavez LL, et al. Initial B-Cell Responses to Transmitted Human Immunodeficiency Virus Type 1: Virion-Binding Immunoglobulin M (IgM) and IgG Antibodies Followed by Plasma Anti-Gp41 Antibodies With Ineffective Control of Initial Viremia. *J Virol* (2008) 82:12449–63. doi: 10.1128/JVI.01708-08
12. Ciupe SM, Ribeiro RM, Perelson AS. Antibody Responses During Hepatitis B Viral Infection. *PloS Comput Biol* (2014) 10:e1003730. doi: 10.1371/journal.pcbi.1003730
13. Ciupe SM, De Leenheer P, Kepler TB. Paradoxical Suppression of Poly-Specific Broadly Neutralizing Antibodies in the Presence of Strain-Specific Neutralizing Antibodies Following HIV Infection. *J Theoret Biol* (2011) 277:55–66. doi: 10.1016/j.jtbi.2011.01.050
14. McKinley SA, Chen A, Shi F, Wang S, Mucha PJ, Forest MG, et al. Modeling Neutralization Kinetics of HIV by Broadly Neutralizing Monoclonal Antibodies in Genital Secretions Coating the Cervicovaginal Mucosa. *PLoS One* (2014) 9:e100598. doi: 10.1371/journal.pone.0100598
15. Lu C-L, Murakowski DK, Bournazos S, Schoofs T, Sarkar D, Halper-Stromberg A, et al. Enhanced Clearance of HIV-1–Infected Cells by Broadly Neutralizing Antibodies Against HIV-1 *In Vivo*. *Science* (2016) 352 (6288):1001–4. doi: 10.1126/science.aaf1279
16. Joos B, Trkola A, Kuster H, Aceto L, Fischer M, Stiegler G, et al. Long-Term Multiple-Dose Pharmacokinetics of Human Monoclonal Antibodies (MAbs) Against Human Immunodeficiency Virus Type 1 Envelope Gp120 (MAb 2G12) and Gp41 (MAbs 4E10 and 2F5). *Antimicrob Agents Chemother* (2006) 50:1773–9. doi: 10.1128/AAC.50.5.1773-1779.2006
17. Gabrielsson J, Weiner D. *Pharmacokinetic and Pharmacodynamic Data Analysis: Concepts and Applications*. *3rd ed*. Swedish Pharmaceutical Press: Stockholm. (2001).
18. Markowitz M, Louie M, Hurley A, Sun E, Mascio MD, Perelson AS, et al. A Novel Antiviral Intervention Results in More Accurate Assessment of Human Immunodeficiency Virus Type 1 Replication Dynamics and T-Cell Decay *In Vivo*. *J Virol* (2003) 77:5037–8. doi: 10.1128/JVI.77.8.5037-5038.2003
19. Perelson AS, Ribeiro RM. Modeling the Within-Host Dynamics of HIV Infection. *BMC Biol* (2013) 11(1):96. doi: 10.1186/1741-7007-11-96
20. Perelson AS. Modelling Viral and Immune System Dynamics. *Nat Rev Immunol* (2002) 2(1):28–36. doi: 10.1038/nri700
21. Perelson AS, Essunger P, Cao Y, Vesanen M, Hurley A, Saksela K, et al. Decay Characteristics of HIV-1-Infected Compartments During Combination Therapy. *Nature* (1997) 387(6629):188–91. doi: 10.1038/387188a0
22. Luo R, Piovoso MJ, Martinez-Picado J, Zurakowski R. HIV Model Parameter Estimates From Interruption Trial Data Including Drug Efficacy and Reservoir Dynamics. *PLoS One* (2012) 7(7):e40198. doi: 10.1371/journal.pone.0040198
23. Doitsh G, Cavrois M, Lassen KG, Zepeda O, Yang Z, Santiago ML, et al. Abortive HIV Infection Mediates CD4 T Cell Depletion and Inflammation in Human Lymphoid Tissue. *Cell* (2010) 143:789–801. doi: 10.1016/j.cell.2010.11.001
24. Doitsh G, Galloway NLK, Geng X, Yang Z, Monroe KM, Zepeda O, et al. Cell Death by Pyroptosis Drives CD4 T-Cell Depletion in HIV-1 Infection. *Nature* (2014) 505:509–14. doi: 10.1038/nature12940
25. Conway JM, Perelson AS. Post-Treatment Control of HIV Infection. *Proc Natl Acad Sci USA* (2015) 112(17):5467–72. doi: 10.1073/pnas.1419162112
26. Bonhoeffer S, Rembiszewski M, Ortiz GM, Nixon DF. Risks and Benefits of Structured Antiretroviral Drug Therapy Interruptions in HIV-1 Infection. *AIDS* (2000) 14(15):2313–22. doi: 10.1097/00002030-200010200-00012
27. Gadhamsetty S, Coorens T, de Boer RJ. Notwithstanding Circumstantial Alibis, Cytotoxic T Cells can be Major Killers of HIV-1-Infected Cells. *J Virol* (2016) 90(16):7066–83. doi: 10.1128/JVI.00306-16
28. Holte SE, Melvin AJ, Mullins JI, Tobin NH, Frenkel LM. Density-Dependent Decay in HIV-1 Dynamics. *J Acquir Immune Defic Syndr* (2006) 41:266–76. doi: 10.1097/01.qai.0000199233.69457.e4
29. Brandin E, Thorstensson R, Bonhoeffer S, Albert J. Rapid Viral Decay in Simian Immunodeficiency Virus-Infected Macaques Receiving Quadruple Antiretroviral Therapy. *J Virol* (2006) 80:9861–4. doi: 10.1128/JVI.00394-06
30. Ramratnam B, Bonhoeffer S, Binley J, Hurley A, Zhang L, Mittler JE, et al. Rapid Production and Clearance of HIV-1 and Hepatitis C Virus Assessed by Large Volume Plasma Apheresis. *Lancet* (1999) 354:1782–5. doi: 10.1016/S0140-6736(99)02035-8
31. Mohri H, Perelson AS, Tung K, Ribeiro RM, Ramratnam B, Markowitz M, et al. Increased Turnover of T Lymphocytes in HIV-1 Infection and Its Reduction by Antiretroviral Therapy. *J Exp Med* (2001) 194:1277–88. doi: 10.1084/jem.194.9.1277
32. Wu X, Yang Z-Y, Li Y, Hogerkorp C-M, Schief WR, Seaman MS, et al. Rational Design of Envelope Identifies Broadly Neutralizing Human Monoclonal Antibodies to HIV-1. *Science* (2010) 329:856–61. doi: 10.1126/science.1187659
33. Scheid JF, Mouquet H, Ueberheide B, Diskin R, Klein F, Oliveira TYK, et al. Sequence and Structural Convergence of Broad and Potent HIV Antibodies That Mimic CD4 Binding. *Science* (2011) 333:1633–7. doi: 10.1126/science.1207227
34. Murray JM, Kelleher AD, Cooper DA. Timing of the Components of the HIV Life Cycle in Productively Infected CD4+ T Cells in a Population of HIV-Infected Individuals. *J Virol* (2011) 85(20):10798–805. doi: 10.1128/JVI.05095-11

35. Mellman I, Plutner H. Internalization and Degradation of Macrophage Fc Receptors Bound to Polyvalent Immune Complexes. *J Cell Biol* (1984) 98:1170–7. doi: 10.1083/jcb.98.4.1170
36. Dugast A-S, Tonelli A, Berger CT, Ackerman ME, Sciaranghella G, Liu Q, et al. Decreased Fc Receptor Expression on Innate Immune Cells is Associated With Impaired Antibody-Mediated Cellular Phagocytic Activity in Chronically HIV-1 Infected Individuals. *Virology* (2011) 415:160–7. doi: 10.1016/j.virol.2011.03.012
37. Wieland A, Shashidharamurthy R, Kamphorst Alice O, Han J-H, Aubert Rachael D, Choudhury Biswa P, et al. Antibody Effector Functions Mediated by Fcgamma-Receptors Are Compromised During Persistent Viral Infection. *Immunity* (2015) 42(2):367–78. doi: 10.1016/j.immuni.2015.01.009
38. Yamada Douglas H, Elsaesser H, Lux A, Timmerman John M, Morrison Sherie L, de la Torre Juan C, et al. Suppression of Fcgamma-Receptor-Mediated Antibody Effector Function During Persistent Viral Infection. *Immunity* (2015) 42(2):379–90. doi: 10.1016/j.immuni.2015.01.005
39. Burnham KP, Anderson DR. *Model Selection and Multimodel Inference: A Practical Information-Theoretic Approach. 2nd ed*. New York: Springer (2003). p. 488.
40. Cardozo EF, Andrade A, Mellors JW, Kuritzkes DR, Perelson AS, Ribeiro RM. Treatment With Integrase Inhibitor Suggests a New Interpretation of HIV RNA Decay Curves That Reveals a Subset of Cells With Slow Integration. *PLoS Pathog* (2017) 13(7):e1006478. doi: 10.1371/journal.ppat.1006478
41. Igarashi T, Brown C, Azadegan A, Haigwood N, Dimitrov D, Martin MA, et al. Human Immunodeficiency Virus Type 1 Neutralizing Antibodies Accelerate Clearance of Cell–Free Virions From Blood Plasma. *Nat Med* (1999) 5:211–6. doi: 10.1038/5576
42. Bournazos S, Klein F, Pietzsch J, Seaman MS, Nussenzweig MC, Ravetch JV. Broadly Neutralizing Anti-HIV-1 Antibodies Require Fc Effector Functions for *In Vivo* Activity. *Cell* (2014) 158:1243–53. doi: 10.1016/j.cell.2014.08.023
43. Janeway CA Jr., Travers P, Walport M, Shlomchik MJ. *Immunobiology. 5th ed*. New York: Garland Publishing (2001).
44. Holl V, Hemmerter S, Burrer R, Schmidt S, Bohbot A, Aubertin A-M, et al. Involvement of FcγRI (CD64) in the Mechanism of HIV-1 Inhibition by Polyclonal IgG Purified From Infected Patients in Cultured Monocyte-Derived Macrophages. *J Immunol* (2004) 173:6274–83. doi: 10.4049/jimmunol.173.10.6274
45. Sips M, Krykbaeva M, Diefenbach TJ, Ghebremichael M, Bowman BA, Dugast A-S, et al. Fc Receptor-Mediated Phagocytosis in Tissues as a Potent Mechanism for Preventive and Therapeutic HIV Vaccine Strategies. *Mucosal Immunol* (2016) 9:1584–95. doi: 10.1038/mi.2016.12
46. Caskey M, Schoofs T, Gruell H, Settler A, Karagounis T, Kreider EF, et al. Antibody 10-1074 Suppresses Viremia in HIV-1-Infected Individuals. *Nat Med* (2017) 23(2):185–91. doi: 10.1038/nm.4268
47. Collini P, Noursadeghi M, Sabroe I, Miller RF, Dockrell DH. Monocyte and Macrophage Dysfunction as a Cause of HIV-1 Induced Dysfunction of Innate Immunity. *Curr Mol Med* (2010) 10:727–40. doi: 10.2174/156652410793384141
48. Ganji R, Dhali S, Rizvi A, Sankati S, Vemula MH, Mahajan G, et al. Proteomics Approach to Understand Reduced Clearance of Mycobacteria and High Viral Titers During HIV–mycobacteria Co-Infection. *Cell Microbiol* (2016) 18:355–68. doi: 10.1111/cmi.12516
49. Jambo KC, Banda DH, Kankwatira AM, Sukumar N, Allain TJ, Heyderman RS, et al. Small Alveolar Macrophages are Infected Preferentially by HIV and Exhibit Impaired Phagocytic Function. *Mucosal Immunol* (2014) 7:1116–26. doi: 10.1038/mi.2013.127
50. Torre D, Gennero L, Baccino FM, Speranza F, Biondi G, Pugliese A. Impaired Macrophage Phagocytosis of Apoptotic Neutrophils in Patients With Human Immunodeficiency Virus Type 1 Infection. *Clin Diagn Lab Immunol* (2002) 9:983–6. doi: 10.1128/CDLI.9.5.983-986.2002
51. Debaisieux S, Lachambre S, Gross A, Mettling C, Besteiro S, Yezid H, et al. HIV-1 Tat Inhibits Phagocytosis by Preventing the Recruitment of Cdc42 to the Phagocytic Cup. *Nat Commun* (2015) 6:6211. doi: 10.1038/ncomms7211
52. Mazzolini J, Herit F, Bouchet J, Benmerah A, Benichou S, Niedergang F. Inhibition of Phagocytosis in HIV-1–Infected Macrophages Relies on Nef-Dependent Alteration of Focal Delivery of Recycling Compartments. *Blood* (2010) 115:4226–36. doi: 10.1182/blood-2009-12-259473
53. Dumas A, Lê-Bury G, Marie-Anaïs F, Herit F, Mazzolini J, Guilbert T, et al. The HIV-1 Protein Vpr Impairs Phagosome Maturation by Controlling Microtubule-Dependent Trafficking. *J Cell Biol* (2015) 211:359–72. doi: 10.1083/jcb.201503124
54. Hampton MB, Vissers MC, Winterbourn CC. A Single Assay for Measuring the Rates of Phagocytosis and Bacterial Killing by Neutrophils. *J Leukoc Biol* (1994) 55:147–52. doi: 10.1002/jlb.55.2.147
55. Rigden RC, Carrasco CP, Summerfield A, MCCullough KC. Macrophage Phagocytosis of Foot-and-Mouth Disease Virus May Create Infectious Carriers. *Immunology* (2002) 106:537–48. doi: 10.1046/j.1365-2567.2002.01460.x
56. Callaway DS, Perelson AS. HIV-1 Infection and Low Steady State Viral Loads. *Bull Math Biol* (2002) 64:29–64. doi: 10.1006/bulm.2001.0266
57. Miao H, Xia X, Perelson AS, Wu H. On Identifiability of Nonlinear ODE Models and Applications in Viral Dynamics. *SIAM Rev* (2011) 53(1):3–39. doi: 10.1137/090757009
58. Stafford MA, Corey L, Cao Y, Daar ES, Ho DD, Perelson AS. Modeling Plasma Virus Concentration During Primary HIV Infection. *J Theoret Biol* (2000) 203(3):285–301. doi: 10.1006/jtbi.2000.1076
59. Di Mascio M, Dornadula G, Zhang H, Sullivan J, Xu Y, Kulkosky J, et al. In a Subset of Subjects on Highly Active Antiretroviral Therapy, Human Immunodeficiency Virus Type 1 RNA in Plasma Decays From 50 to <5 Copies Per Milliliter, With a Half-Life of 6 Months. *J Virol* (2003) 77(3):2271–5. doi: 10.1128/JVI.77.3.2271-2275.2003
60. Luo R, Cardozo EF, Piovoso MJ, Wu H, Buzon MJ, Martinez-Picado J, et al. Modelling HIV-1 2-LTR Dynamics Following Raltegravir Intensification. *J Roy Soc Interface* (2013) 10(84):20130186. doi: 10.1098/rsif.2013.0186
61. Luo R, Piovoso MJ, Zurakowski R. Modeling Uncertainty in Single-Copy Assays for HIV. *J Clin Microbiol* (2012) 50(10):3381–2. doi: 10.1128/JCM.01254-12


**Conflict of Interest:** The authors declare that the research was conducted in the absence of any commercial or financial relationships that could be construed as a potential conflict of interest.

**Publisher's Note:** All claims expressed in this article are solely those of the authors and do not necessarily represent those of their affiliated organizations, or those of the publisher, the editors and the reviewers. Any product that may be evaluated in this article, or claim that may be made by its manufacturer, is not guaranteed or endorsed by the publisher.

frontiers in Immunology

ORIGINAL RESEARCH
published: 10 September 2021
doi: 10.3389/fimmu.2021.733958

# HIV Broadly Neutralizing Antibodies Expressed as IgG3 Preserve Neutralization Potency and Show Improved Fc Effector Function

*Simone I. Richardson*[1,2], *Frances Ayres*[1], *Nelia P. Manamela*[1], *Brent Oosthuysen*[1], *Zanele Makhado*[1], *Bronwen E. Lambson*[1,2], *Lynn Morris*[1,2,3] *and Penny L. Moore*[1,2,3]*

[1] Centre for HIV and STI's, National Institute for Communicable Diseases, a Division of the National Health Laboratory Service, Johannesburg, South Africa, [2] Medical Research Council (MRC) Antibody Immunity Research Unit, Faculty of Health Sciences, University of the Witwatersrand, Johannesburg, South Africa, [3] Centre for the AIDS Programme of Research in South Africa (CAPRISA), University of KwaZulu-Natal, Durban, South Africa

OPEN ACCESS

**Edited by:**
*Philipp Schommers, University of Cologne, Germany*

**Reviewed by:**
*Thorsten Demberg, Marker Therapeutics, United States*
*Michael Seaman, Beth Israel Deaconess Medical Center and Harvard Medical School, United States*

***Correspondence:**
*Penny L. Moore*
*pennym@nicd.ac.za*

**Specialty section:**
*This article was submitted to Vaccines and Molecular Therapeutics, a section of the journal Frontiers in Immunology*

**Received:** *30 June 2021*
**Accepted:** *19 August 2021*
**Published:** *10 September 2021*

**Citation:**
*Richardson SI, Ayres F, Manamela NP, Oosthuysen B, Makhado Z, Lambson BE, Morris L and Moore PL (2021) HIV Broadly Neutralizing Antibodies Expressed as IgG3 Preserve Neutralization Potency and Show Improved Fc Effector Function. Front. Immunol. 12:733958. doi: 10.3389/fimmu.2021.733958*

The ability of several broadly neutralizing antibodies (bNAbs) to protect against HIV infection is enhanced through Fc receptor binding. Antibody isotype modulates this effect, with IgG3 associated with improved HIV control and vaccine efficacy. We recently showed that an IgG3 variant of bNAb CAP256-VRC26.25 exhibited more potent neutralization and phagocytosis than its IgG1 counterpart. Here, we expanded this analysis to include additional bNAbs targeting all major epitopes. A total of 15 bNAbs were expressed as IgG1 or IgG3, and pairs were assessed for neutralization potency against the multi-subtype global panel of 11 HIV strains. Binding to the neonatal Fc receptor (FcRn) and Fcγ receptors were measured using ELISA and antibody-dependent cellular cytotoxicity (ADCC) and phagocytosis were measured using infectious viruses and global panel Env SOSIP trimers, respectively. IgG3 bNAbs generally showed similar or increased (up to 60 fold) neutralization potency than IgG1 versions, though the effect was virus-specific. This improvement was statistically significant for CAP256-VRC26.25, 35022, PGT135 and CAP255.G3. IgG3 bNAbs also showed significantly improved binding to FcγRIIa which correlated with enhanced phagocytosis of all trimeric Env antigens. Differences in ADCC were epitope-specific, with IgG3 bNAbs to the MPER, CD4 binding site and gp120-gp41 interface showing increased ADCC. We also explored the pH dependence of IgG1 and IgG3 variants for FcRn binding, as this determines the half-life of antibodies. We observed reduced pH dependence, associated with shorter half-lives for IgG3 bNAbs, with κ-light chains. However, IgG3 bNAbs that use λ-light chains showed similar pH dependence to their IgG1 counterparts. This study supports the manipulation of the constant region to improve both the neutralizing and Fc effector activity of bNAbs, and suggests that IgG3 versions of bNAbs may be preferable for passive immunity given their polyfunctionality.

**Keywords: broadly neutralizing antibodies (bnAbs), Fc effector function, IgG3, phagocytosis, ADCC (antibody dependent cellular cytotoxicity)**

## INTRODUCTION

Antibodies mediate pathogen neutralization through the binding of the Fab portion to antigen, and also elicit several effector functions through interaction of the Fc with a variety of receptors. Both neutralization and Fc effector function have been shown to be critical *in vivo*. The importance of neutralization has been confirmed by passive transfer studies, where bNAbs provide sterilizing immunity in animal models (1–3) and robust antiviral activity in chronically infected humans (4, 5). Despite this, combinations of bNAbs with high levels of potency and breadth will be needed to improve on the results of the antibody-mediated protection (AMP) passive immunization trial with VRC01 (6). Fc receptor engagement results in the recruitment of cytotoxic functions which have been shown in HIV infection to restrict the number of transmitted/founder viruses that establish infection, reduce viral load, and drive viral escape (7–10) and are associated with spontaneous HIV control (11) and slowed disease progression (12). Polyfunctional Fc effector function has also been associated with vaccine protection in humans and non-human primates (13–19) and with the development of broadly neutralizing antibodies (bNAbs) during infection (20, 21). Further, Fc receptor binding is required for several bNAbs to optimally protect from infection or clear infected cells in different animal models (22–28). Thus, while the elicitation of HIV bNAbs is likely necessary for an efficacious vaccine, Fc effector function can complement this function to improve efficacy.

Among the factors that contribute to modulating Fc effector function is antibody isotype (IgM, IgA, IgG and IgE) and subclass (IgG1-4 and IgA1-2), determined by sequence variation in the constant regions of the heavy chain (CH1-3) genes. The unique structures of each isotype result in differential binding to multiple Fc receptors, and this translates to diversity of Fc effector functions, varying half-lives and immune complex formation (29). Furthermore, there is substantial evidence that isotype can significantly alter antigen affinity and/or neutralization capacity of monoclonal antibodies (30–35), indicating the importance of the isotype well beyond Fc receptor binding. Isotype therefore potentially represents an important factor to improve the function of bNAbs for passive immunization.

Of the IgG subclasses, IgG3 antibodies are the most polyfunctional, owing to their increased affinity for Fc receptors (36). IgG3 is highly polymorphic with 29 reported alleles (37), and this variability is known to alter antibody activity and half-life (34, 38, 39). Structurally, IgG3 is distinct from other subclasses, with a long flexible hinge, enabling high rotational freedom about the Fc-Fab and Fab-Fab axes (40, 41). In HIV infection, skewing towards IgG3 has been associated with reduced risk of infection in the RV144 and HVTN 505 vaccine trials (14, 15, 42) and in viral control (11). IgG3 specific bNAbs have also been shown to mediate greater antibody-dependent cellular phagocytosis (ADCP) compared to IgG1 (43, 44), largely through their elongated hinge (34, 45). In addition to better ADCP, we previously demonstrated that IgG3 variants of the V2-specific bNAb CAP256-VRC26.25 showed enhanced antibody-dependent cellular trogocytosis (ADCT) and significantly improved neutralization potency when compared to IgG1 (34).

IgG3 is however not currently used for any therapeutic antibodies in a clinical setting. One of the major reasons for this is its reduced half-life of approximately 7 days compared to 21 days for IgG1 (41). Half-life is largely mediated by antibody binding to the neonatal Fc receptor (FcRn). IgG is able to bind FcRn at acidic conditions (pH6) within endosomes. FcRn–IgG complexes are then routed away from the lysosomal degradation pathway, and through the merging of vesicles with the plasma membrane, returned to physiological pH (pH 7.4), where IgG is released (46). Unlike IgG1*01 which contains a histidine at position 435, IgG3 alleles such as IgG3*01 contain an arginine at position 435. This does not deprotonate at neutral pH, resulting in IgG3 binding to FcRn being less pH-dependent (39, 47), an undesirable feature for a therapeutic antibody. However several IgG3 alleles (IgG3*17, *18 and *19), like IgG1, have a histidine at position 435. Furthermore, other variable region structures of the antibody are known to affect half-life (48, 49), demonstrating alternative ways to engineer IgG3 bNAbs with enhanced pH dependence for FcRn binding.

Here, we examine the impact of IgG3 isotype on Fc effector function and neutralization activity of 15 bNAbs that target the five major bNAb epitopes on the HIV trimer. We engineered paired IgG1 and IgG3 variants of the bNAbs and assayed them for ADCP and antibody-dependent cellular cytotoxicity (ADCC) activity. We show that ADCP was globally improved by IgG3, however ADCC was improved in an epitope-dependent manner. We examine the features of IgG3 bNAb light chains that result in similar binding to FcRn compared to their IgG1 counterparts and show that IgG3 has increased binding to Fcγ receptors. Finally we demonstrate that neutralization potency of these IgG3 bNAbs is maintained or enhanced. This suggests that IgG3 variants of bNAbs may be preferable for use in passive immunity as they not only display improved Fc effector function but also show enhanced neutralization potency in a virus-specific manner.

## MATERIALS AND METHODS

### Ethics

Approval for use of PBMCs from healthy HIV uninfected individuals was approved by the Human Research Ethics Committee of the University of the Witwatersrand (M150313).

### Cell Lines

THP-1 cells obtained from the AIDS Reagent Program (Division of AIDS, NIAID, NIH contributed by Dr. Li Wu and Vineet N. KewalRamani) were used for the ADCP assay. Cells were cultured at 37°C, 5% $CO_2$ in RPMI containing 10% heat-inactivated fetal bovine serum (Gibco, Gaithersburg, MD), 1% Penicillin Streptomycin (Gibco, Gaithersburg, MD) and 2-mercaptoethanol to a final concentration of 0.05 mM. CEM-$NK_R$.CCR5, a CEM-natural killer resistant T lymphoblast cell line transduced with CCR5 served as targets in the ADCC assay.

These were obtained from the AIDS Reagent Program (Division of AIDS, NIAID, NIH developed by Dr Alexander Trkola) and were cultured at 37°C, 5% $CO_2$ in RPMI containing 10% heat-inactivated fetal bovine serum (Gibco, Gaithersburg, MD) and 1% Penicillin Streptomycin (Gibco, Gaithersburg, MD). TZM-bl cells, previously designated JC53-bl (clone 13) cells, are a HeLa cell line expressing high levels of CD4 and CCR5 and transduced with a luciferase gene under the control of the HIV promoter. These were obtained from the AIDS Reagent Program (Division of AIDS, NIAID, NIH developed by Dr. John C. Kappes, and Dr. Xiaoyun Wu) and used in neutralization assays. HEK293T cells were obtained from Dr. George Shaw (University of Alabama, Birmingham, AL) and were used for pseudovirus expression. These adherent cell lines were cultured at 37°C, 5% $CO_2$, in DMEM containing 10% heat-inactivated fetal bovine serum (Gibco BRL Life Technologies) and supplemented with 50 μg/ml gentamicin (Sigma). Cells were disrupted at confluence with 0.25% trypsin in 1 mM EDTA (Sigma) every 48–72 hours. HEK293F suspension cells were cultured in 293Freestyle media (Gibco BRL Life Technologies) and grown in a shaking incubator at 37°C, 5% $CO_2$, 70% humidity at 125rpm.

## Proteins and Peptides

Constructs of avitagged SOSIP trimers of 246.F3.C10.2, BJOX002000.03.2 and CE1176.A3 from the global virus panel (50) were a gift from Dr Christopher Cottrell (The Scripps Research Institute). These were transfected into HEK293F suspension cells with PEIMax, incubated for 6 days in a shaking incubator at 37°C, 5% $CO_2$, 70% humidity at 125 rpm and purified by sequential Ni-NTA and size exclusion chromatography (SEC) as described elsewhere (51). Prior to use, trimers were subjected to quality control by ELISA binding of monoclonal antibodies CAP256-VRC26.25 and PGT151 (which trimeric Env forms only) and F105 and 447-D (which do not bind native-like Env trimers). Biotinylated MPR.03 peptide was purchased from Peptide 2.0 (Chantilly, Virginia).

## Antibody Engineering and Production

The heavy and light chain variable regions of bNAbs of interest were cloned into both IgG1 and IgG3 (received from Dr Bart Haynes, Duke University, Durham, NC) expression vectors. The allelic variants of each subclass were IgG1*01 and IgG3*01 respectively. IgG3*01 differs from IgG1*01 with a hinge length of 62 compared to 15 amino acids as well as at many key Fc receptor binding sites. This includes position 435, a key site for FcRn interaction and enhanced half-life for which IgG1*01 contains a histidine and IgG3*01 contains an arginine. For antibody expression, plasmids encoding heavy or light chain genes were co-transfected into HEK293F cells with PEI-MAX 40,000 (Polysciences) head-to-head. Cells were cultured for six days in 293Freestyle media at 37°C, 10% $CO_2$, then harvested supernatants were filtered and purified using Protein G (Thermoscientific). Antibody concentrations of all variants were quantified by nanodrop using sequence-specific extinction coefficients as determined by ProtParam (ExPASy) and confirmed by ELISA. SDS-PAGE was used to confirm IgG1 and IgG3 stability and size.

## Antibody-Dependent Cellular Phagocytosis (ADCP) Assay

The THP-1 phagocytosis assay was performed as in (52) using 1 μM neutravidin beads (Molecular Probes Inc, Eugene, OR) coated with 246.F3.C10.2, BJOX002000.03.2 or CE1176.A3 SOSIP trimer or MPR.03 peptide. SOSIP was biotinylated on an avitag to ensure correct orientation when binding to the beads. Antibodies were tested starting at 10 μg/ml with 5-fold dilutions. Phagocytic scores were calculated as the geometric mean fluorescent intensity (MFI) of the beads that have been taken up by THP-1 cells, multiplied by the percentage bead uptake on a FACSAria II (BD Biosciences, Franklin Lakes, New Jersey). Pooled IgG from HIV-positive donors from the NIH AIDS Reagent programme (HIVIG) was used in all assays to normalize for plate to plate variation and Palivizumab (MedImmune, LLC; Gaithersburg, MD) was used as negative control.

## Infectious Antibody-Dependent Cellular Cytotoxicity (ADCC) Assay

The HIV-1 reporter viruses used in the ADCC assays were replication-competent infectious molecular clones (IMC) encoding the 246.F3.C10.2, BJOX002000.03.2 and CE1176 env within an isogenic backbone Env-IMC-6ATRi, that also expresses the Renilla luciferase reporter gene, and preserves all viral open reading frames produced as described previously (53). These constructs were kindly provided by Dr Christina Ochsenbauer (University of Alabama at Birmingham). Reporter virus stocks were generated by transfection of HEK293T cells (NIH AIDS Reagent Program) with proviral IMC plasmid DNA, and titered for infectivity in CEM.$NK_R$CCR5 cells (NIH AIDS Reagent Program) by p24 staining (Beckman-Coulter). CD4 downregulation was also measured with co-staining with anti-CD4. ADCC activity as previously described (54). Briefly, a CEM.$NK_R$CCR5 cell line (NIH AIDS Reagent Program) was used as the target for ADCC luciferase assays after infection with the HIV-1 IMCs listed above. The target cell line was infected with IMC using titered stocks that generated more than 50% infected cells after 72 hours of infection. These were incubated with 5-fold serially diluted mAbs starting at 50 μg/ml. Cryopreserved peripheral blood mononuclear cells (PBMC) obtained from a HIV-negative donor with a high-affinity 158V/V FcγRIIIa phenotype were used as source of effector cells. After thawing, the cryopreserved PBMCs were rested overnight and used at an effector-to-target ratio of 30:1. The effector cells, target cells, and Ab dilutions were plated in white 96-well half area plates and incubated for 6 hours at 37°C in 5% $CO_2$. The final readout was the luminescence intensity (in relative light units) generated by the presence of residual intact target cells that had not been lysed by the effector population in the presence of any ADCC-mediating mAb. The percentage of killing was calculated using the formula:

$$\%\ killing = \frac{(RLU\ of\ target\ and\ effector\ well) - (RLU\ of\ sample\ well)}{RLU\ of\ target\ and\ effector\ well} \times 100$$

In this analysis, the RLU of the target plus effector wells represents non-antibody background. The RSV-specific mAb

Palivizumab (Medimmune; Synagis) and A32 that does not bind to prefusion trimer (NIH AIDS Reagent Program) were used as negative controls and a polyclonal mixture of IgG from HIV infected individuals (HIVIG) from the NIH AIDS Reagent Program was used to normalize between plates. Data are represented as the area under the curve (AUC) of percentage specific killing over the serially diluted antibodies.

## FcγR Binding ELISA

Antibody binding to FcγR was measured by ELISA as described previously (55). Briefly, FcγRI, FcγRIIa, FcγRIIb and FcγRIIIa His6-tagged receptors (R&D Systems Minneapolis, MN) were coated on nickel plates (Qiagen) at 2 μg/ml or 4 μg/ml. Five-fold serial dilutions starting at 5 μg/ml of bNAbs were added. Binding was detected by a goat Anti-Human IgG (Fab specific) antibody goat at 1 in 10,000 (Sigma). Results were visualized with tetramethylbenzidine (TMB).

## Neonatal Fc Receptor (FcRn) ELISA

Binding to the neonatal Fc receptor was measured as described in (24). Nickel plates (Qiagen) were coated with 2 μg/ml his-tagged FcRn/β2 (Sinobiological, Bejing) for a minimum of 1 hour, washed with PBS 0.05% Tween-20, and blocked with 5% milk/PBS. Five-fold serial dilutions starting at 5 μg/ml of bNAbs were incubated with the receptor in 100mM NaPO4, 0.05% (v/v) Tween20, pH 6.0 for 1 hour at room temperature. Following this, plates were either washed with 100 mM $NaPO_4$, 0.05% (v/v) Tween20, pH 6.0 or 100 mM $NaPO_4$, 0.05% (v/v) Tween20, pH 7.4 three times with 30 minute incubations in between washes. Residual binding of antibodies was detected by a goat Anti-Human IgG (Fab specific) antibody at 1 in 5,000 (Sigma) and were visualized with tetramethylbenzidine (TMB) at OD450nm.

## Pseudovirus Production

Pseudovirus plasmids expressing the HIV Env of interest were co-transfected with pSG3DEnv backbone-expressing plasmids (obtained from the NIH AIDS Research and Reference Reagent Program, Division of AIDS, NIAID, NIH) into HEK293T cells using PEI-MAX 40,000 (Polysciences). Cultures were incubated for 48 hours at 37°C, then supernatants filtered through 0.45 μm and frozen in DMEM/20% FBS to yield Env-pseudotyped viruses capable of a single round of infection only as previously described (56).

## Neutralization Assay

Neutralization assays were performed in TZM-bl cells as previously described (57). Neutralization was measured as a reduction in RLUs after a single round of pseudovirus infection in the presence of the monoclonal antibody. bNAbs were serially diluted 1:3 and the $IC_{50}$ calculated as the dilution at which the infection was reduced by 50%. All subclass switch variants were run head-to-head on the same plate to limit intra-experimental variation. Eleven viruses from the global panel (50) including 246.F3.C10.2, 25710.2.43, 398.F1.F6.20, 703010217.B6, BJOX002000.03.2, CE1176.A3, CH119.10, CNE55, TRO.11, X1632.S2.B10 and X2278.C2.B6 were tested against all bNAbs. For combinations of IgG1 and IgG3 bNAbs, the Bliss-Hill model was calculated by the tool COMBINABER (http://www.hiv.lanl.gov/content/sequence/COMBINABER/combinaber.html) as described in (58).

## SOSIP Trimer ELISA

Avitagged SOSIP trimers were biotinylated using BirA ligase as described elsewhere (59). Biotinylated trimer was coated on to streptavidin ELISA plates (Thermofisher) at 4 μg/ml in PBS and incubated for 1 hour at room temperature. Following PBS washes, the plates were blocked for 30 minutes in 5% milk/PBS and washed in PBS. Fifty μl of bNAb variants as well as negative controls 447-52D and F105 (starting at 10μg/ml) were incubated for 1 hour at room temperature, followed by PBS washes. Secondary antibody, goat anti-human Fab-HRP (Sigma) was incubated in the plate for 1 hour at room temperature, the plate washed three times with PBS and 100μl TMB added to each well. The reaction was stopped with 1M $H_2SO_4$ and read at 450nm.

## Statistical Analysis

Analysis of all flow cytometry based experiments was done using FlowJo (FlowJo LLC, Ashland, OR). Sequencing to confirm cloning was analyzed with Sequencher 5.4.1. All statistical analysis was performed in GraphPad Prism 6 (GraphPad Software, Inc, La Jolla, CA). All comparisons between groups were done with non-parametric tests including Mann-Whitney U tests (for two unmatched groups) and Wilcoxon matched pairs signed rank test (for two matched groups). All confidence intervals were set to 95%. All correlations reported are non-parametric Spearman's correlations and all statistical analysis was done with two-sided testing with using an alpha level of 0.05.

# RESULTS

## IgG3 Improves Antibody-Dependent Cellular Phagocytosis (ADCP)

We and others have previously shown both CAP256-VRC26.25 (referred to as CAP256.25) (34) and VRC01 (45) had improved ADCP when engineered as IgG3. Here we investigated whether this was applicable to bNAbs that targeted other epitopes on the trimer. To do this, we selected 13 additional bNAbs that target different epitopes on the HIV trimer as shown in **Figure 1A**, and included both CAP256.25 and VRC01 as positive controls. These bNAbs, several of which are under clinical development (60), have a wide range of neutralization potencies and breadth as measured against a multiclade 200-virus panel (**Figure 1B**). We cloned the variable regions of each bNAb into IgG1*01 and IgG3*01 antibody heavy chain expression plasmids and expressed both variants head-to-head in HEK293F cells. Following purification, we determined the protein concentration of each antibody, accounting for the different sizes of IgG1 and IgG3.

All 15 bNAb pairs were tested for ADCP activity against three SOSIP trimers from the global panel; 246.F3.C10.2 (clade AC), BJOX002000.03.2 (clade CRF07) and CE1176.A3 (clade C) (**Figure 2A** and **Supplementary Figures 1A–F**). We compared two scores of ADCP activity, area under the curve (AUC) which encompasses the full titration, or activity measured at 10 μg/ml,

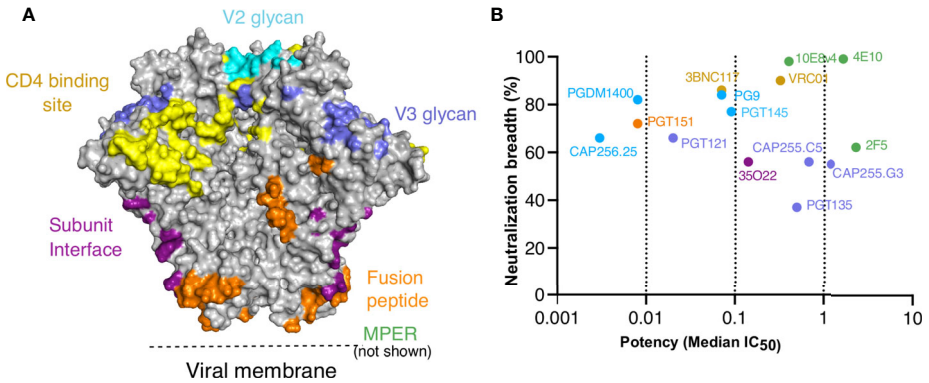


**FIGURE 1** | Targets, neutralization breadth and potency of selected HIV broadly neutralizing antibodies. IgG1*01 and IgG3*01 variants of 15 bNAbs that target the six major epitopes of vulnerability were expressed. **(A)** Major contacts of each of the bNAbs on the BG505 SOSIP.664 trimer (PDB: 6V0R). **(B)** Neutralization breadth and potency of IgG1 bNAb variants represented by median $IC_{50}$ (μg/ml) against a 200 multiclade virus panel as obtained from CATNAP.

the highest concentration tested. Both measures of ADCP activity were highly correlated for all three trimers (**Supplementary Figures 1B, D, F**), and therefore we used AUC in all subsequent analyses. IgG3 bNAb variants showed significantly improved ADCP compared to IgG1, for all three trimers (**Figure 2A**). In line with previous studies (34, 45), though against different antigens, we confirmed higher ADCP for both VRC01 and CAP256.25 IgG3 variants compared to IgG1 (**Supplementary Figures 1A, C, E**). As SOSIP trimers lack the membrane-proximal external region (MPER), the MPER bNAbs showed no ADCP activity against the trimers (**Supplementary Figures 1A, C, E**). In order to test their ADCP activity, MPER bNAbs were tested using an MPER consensus peptide MPR.03. Unlike the other bNAbs, MPER bNAbs overall showed no significant difference in IgG3 compared to IgG1, perhaps because MPR.03 is linear, rather than being in a native structural conformation (**Supplementary Figures 1G, H**).

In order to investigate whether the higher IgG3 ADCP activity could be attributed to differences in binding to the trimer, we measured their ability to bind 246.F3.C10.2, BJOX002000.03.2 and CE1176.A3 trimers by ELISA (**Supplementary Figure 2**). bNAb pairs that failed to bind the trimer, or did so weakly, were unable to mediate high levels of ADCP. Examples include PGT135 against 246.F3.C10.2 (**Supplementary Figures 1A** and **2A**), 3BNC117 against BJOX002000.03.2 (**Supplementary Figure 1C** and **2B**) or PGT145 against CE1176.A3 (**Supplementary Figures 1E** and **2C**). The IgG1 and IgG3 MPER bNAbs showed no difference in binding to the MPR.03 peptide (**Supplementary Figure 2D**), reflecting their lack of difference in ADCP against this antigen. While binding was significantly correlated with ADCP mediated by IgG1 bNAbs these were not observed for IgG3 (**Supplementary Figure 2E**). We also observed no significant change in trimer binding between IgG1 and IgG3 variants (**Supplementary Figure 2F**). Together this data shows that enhanced ADCP activity of IgG3 bNAbs is not simply a result of improved binding to trimer but likely an enhancement in avidity, perhaps through the longer hinge as shown elsewhere (34, 45).

## IgG3 Mediated Antibody-Dependent Cellular Cytotoxicity (ADCC) Is Enhanced in an Epitope-Specific Manner

We next assessed the effect of IgG3 on the ability of bNAbs to mediate ADCC. We used infectious Renilla reporter viruses made from 246.F3.C10.2, BJOX002000.03.2 and CE1176.A3 in the Env-IMC-6ATRi backbone. These were used to infect a lymphocytic cell line CEM.NKR.CCR5 which showed substantial downregulation of CD4 and >30% infection of the cells as determined through p24 expression (**Supplementary Figure 3A**) compared to a mock infection. ADCC was measured as the decrease in luminescence of cells in the presence of antibody and effector PBMCs, relative to a "no mAb" control, representative of the killing of infected target cells.

In contrast to ADCP, ADCC of IgG3 variants did not show overall improvement compared to IgG1 (**Figure 2B**, **Supplementary Figures 3B–G**). As for ADCP, area under the curve was used to represent ADCC which also correlated with peak ADCC activity (**Supplementary Figures 3C, E, G**). However, while ADCC activity against CE1176.A3 was significantly improved by IgG3, particularly for PGT151, 10E8v4, 3BNC117 and VRC01 (**Supplementary Figure 3F**), this was not true of 246.F3.C10.2 or BJOX002000.03.2, where mixed isotype-driven effects were observed.

To understand epitope effects, we assessed the effect of IgG3 variant for each bNAb pair, represented as fold change between IgG3 and IgG1 (**Figure 2C**). Interface and CD4 binding site directed bNAbs, particularly, showed an overall improvement of ADCC when expressed as IgG3. This was especially true for 3BNC117 and VRC01, where all three viruses tested showed improved ADCC as IgG3. MPER bNAbs 10E8v4 and 2F5 also showed improved ADCC as IgG3 with the former showing significant improvement. In contrast, PGDM1400 and both CAP255 mAbs showed increased ADCC as IgG1 variants. This finding suggests that engineering bNAbs as IgG3 to improve ADCC is both virus- and bNAb-specific.

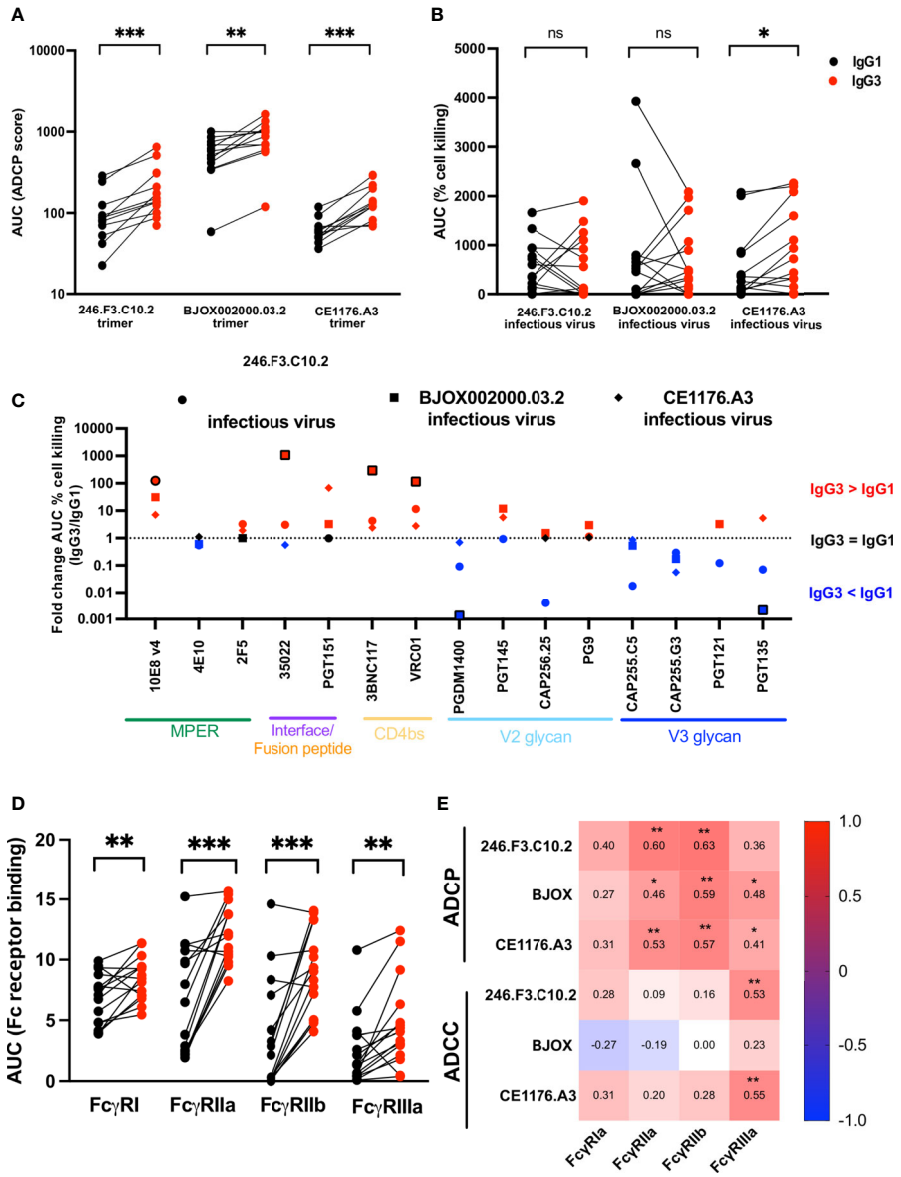


**FIGURE 2** | IgG3 bNAb variants show improved ADCP, epitope specific ADCC and Fc receptor binding enhancement compared to IgG1. IgG1 and IgG3 variants of bNAbs were tested for **(A)** antibody-dependent cellular phagocytosis (ADCP) measured against SOSIP trimer coated beads (246.F3.C10.2, BJOX002000.03.2 and CE1176.A3). ADCP scores are represented as the area under the curve (AUC) and MPER-specific bNAbs are not included. **(B)** Antibody-dependent cellular cytotoxicity (ADCC) measured as the cell killing of CEM.NKR.CCR5 cells infected with Renilla-expressing infectious molecular clones 246.F3.C10.2, BJOX002000.03.2 and CE1176.A3. ADCC activity represented here as the area under the curve of the percentage reduction of luminescence. Red indicates IgG3 and black IgG1. **(C)** Fold change of the AUC of ADCC cell killing between IgG3 and IgG1 bNAbs targeting multiple epitopes, with the shapes indicating the virus used to infect target cells. Red indicates instances where IgG3 was more effective at mediating ADCC, with blue indicating IgG1 showed greater ADCC than IgG3, and black those cases where the difference equals 1 fold. Outlined shapes indicate instances where there is a knock-out of activity of one IgG variant. **(D)** Fc receptor binding of IgG1 (black) and IgG3 (red) bNAb variants measured by ELISA and represented as AUC and **(E)** Spearman's correlations of antigen-specific ADCP and ADCC and Fc receptor binding of IgG1 and IgG3 variants. Wilcoxon matched pairs signed rank t test were used to compare IgG1 and IgG3 activity with significance indicated as *p < 0,05; **p < 0,01; ***p < 0,001; ns, non-significant. Plots are representative of at least two independent experiments.

## Fcγ Receptor Binding Is Enhanced by IgG3

We next examined the affinity of the IgG1 and IgG3 pairs for Fc receptors, as this modulates Fc effector function, and IgG3 mAb variants have increased binding to Fcγ receptors compared to IgG1 (61). One of the major contributors to differences in Fc receptor binding is Fc glycosylation which differs by cell line in which the antibody is produced (62). We therefore tested IgG1 and IgG3 variants produced in the same cell line, head to head. We tested bNAb binding to FcγRI, FcγRIIa, FcγRIIb and FcγRIIIa by ELISA, and showed that IgG3 showed significantly improved

binding to all receptors tested (**Figure 2D** and **Supplementary Figures 4A–D**). However, Fc receptor binding levels varied for different bNAbs despite the fact that all utilize the same IgG1 or IgG3 backbones, suggesting a role for Fab-Fc interactions in determining Fc receptor affinity (**Supplementary Figure 4**).

We next assessed the relationship between binding to Fc receptors and functional assays as it is known that FcγRIIa and FcγRIIb modulate ADCP function (63), whereas FcγRIIIa mediates ADCC (64). In line with this, bNAb binding to FcγRIIa and FcγRIIb correlated with ADCP activity across all SOSIP trimers tested and FcγRIIIa binding correlated with ADCC activity (**Figure 2E**). However, Spearman's correlations were relatively low (less than or equal to 0.6) perhaps suggesting that factors other than Fc receptor binding contribute to the enhanced activity of IgG3 version of these antibodies.

## pH Dependence for Binding to the Neonatal Fc Receptor Is Similar for IgG1 and IgG3 bNAbs That Use a Lambda Light Chain

One of the major reasons that IgG3 is not widely considered for therapeutic use is that it has a reduced half-life of approximately 7 days compared to that of 21 days for IgG1 (41). It is known that the reduced pH dependence of IgG3 compared to IgG1 is the major contributor to poor half-life, with antibody binding to FcRn being a good proxy of half-life (39).

We measured the relative abilities of IgG3 and IgG1 bNAbs to bind FcRn by ELISA at pH 6 and pH 7.4, to establish pH dependence. IgG3 bNAbs generally showed increased binding to FcRn under acidic conditions (measured as area under the curve at pH 6) but reduced pH dependence, defined as the ratio of binding at pH 6 and pH 7.4 (**Figure 3A** and **Supplementary Figure 5A**).

The observation that bNAbs with shared constant regions showed differential pH dependence suggests that the variable region impacts antibody binding to the FcRn receptor. Several studies have shown that the light chain affects FcRn binding (48, 49). Comparison of the bNAbs showed that although IgG1 bNAbs were similar in their pH dependence for FcRn binding regardless of whether they used kappa or lambda light chains, there was a striking difference in pH dependence of IgG3 bNAbs based on light chain use (**Figure 3B**). Specifically IgG3 bNAbs using kappa light chains were significantly less pH dependent for FcRn binding than those with a lambda light chains. We further show that IgG3 bNAbs exhibiting enhanced pH dependence were enriched for CDRL3s greater than 9 amino acids in length (**Figure 3C**) and that lambda light chains were significantly longer overall (**Supplementary Figure 5B**). Finally we examined whether the charge of the light chain, or different regions thereof, impacted the pH dependence of IgG3 bNAbs. While there was no correlation between the net charge at pH7.4 of the entire light chain or of the variable region of the light chain for either IgG1 or IgG3, the charge of the CDRL3 for IgG3 bNAbs was significantly correlated with improved pH dependence (**Figure 3D**).

Overall, this indicates that CDRL3 charge and length is associated with increased pH dependence in IgG3 bNAbs, which results in binding profiles similar to that of IgG1.

## IgG3 Enhances or Maintains Neutralization Potency of bNAbs

Although Fc receptor binding contributes to protection afforded by bNAbs (65), the major mechanism for protection is neutralization. We therefore measured neutralization of IgG1 and IgG3 bNAb pairs against 11 viruses from the multiclade global virus panel, widely used to define broadly neutralizing sera in HIV infected individuals (50).

Overall, these bNAbs either maintained neutralization activity (1-3 fold differences in either direction) or showed improved neutralization (>3 fold enhancement compared to IgG1) across several viruses at both $IC_{50}$ and $IC_{80}$ (**Figures 4A, B** and **Supplementary Figure 6A**). BNAbs 35O22, CAP255.G3, PGT135 and, as we previously showed CAP256.25 (34) showed significant improvement across the 11 viruses tested as IgG3 at $IC_{50}$ (**Figure 4A** and **Supplementary Figure 6B**) with 35O22 losing significance at $IC_{80}$ owing to its plateau (**Figure 4B**). An exception was 10E8v4, which despite the fact that the parent antibody, 10E8, was originally isolated as an IgG3 (66), showed reduced neutralization as IgG3 at both $IC_{50}$ and $IC_{80}$.

Binding of IgG1 bNAbs to the global panel trimers 246.F3.C10.2, BJOX002000.03.2 and CE1176.A3 generally reflected the neutralization of these viruses as expected (**Supplementary Figures 2C–E**). BNAbs unable to neutralize were similarly unable to bind the trimer at all or bound at low levels, with the exception of 35O22 which bound strongly to the BJOX002000.03.2 SOSIP trimer but was unable to neutralize it. This may be as a result of differences in the conformation of the soluble SOSIP trimer compared to the trimer on viral particles. However, despite differences in neutralization between IgG1 and IgG3, their capacity to bind was generally similar for the three viruses we tested (**Supplementary Figure 2F**). This may be because neutralization is impacted by factors in addition to trimer binding, such as the potential ability of IgG3 bNAbs which have increased rotational freedom, to cross-link trimers on a virus, compared to IgG1.

## IgG3 bNAbs Show More Potent Neutralization in Combination Than IgG1

Interventions based on passive immunization of bNAbs will likely require combinations of antibodies that target different epitopes in order to overcome viral resistance (58). We thus investigated whether the increase in neutralization potency of some IgG3 bNAbs conferred a benefit in combinations of bNAbs. We used the Bliss-Hill model (58) to predict the best double and triple combinations of either IgG1 or IgG3 bNAbs against the global virus panel. While the best triple combination of either IgG1 or IgG3 included the same bNAbs (35O22 +PGT121+CAP256.25), the best double combination for IgG1 bNAbs was PGDM1400+PGT121 whereas for IgG3, it was PGT121+CAP256.25 (**Figure 4C**). The best IgG3 double and triple combinations were more potent than the best IgG1 combinations. Furthermore, when all combinations that showed 100% breadth were compared, IgG3 bNAbs showed a trend to increased potency in double combinations, and significantly improved potency in triple combinations

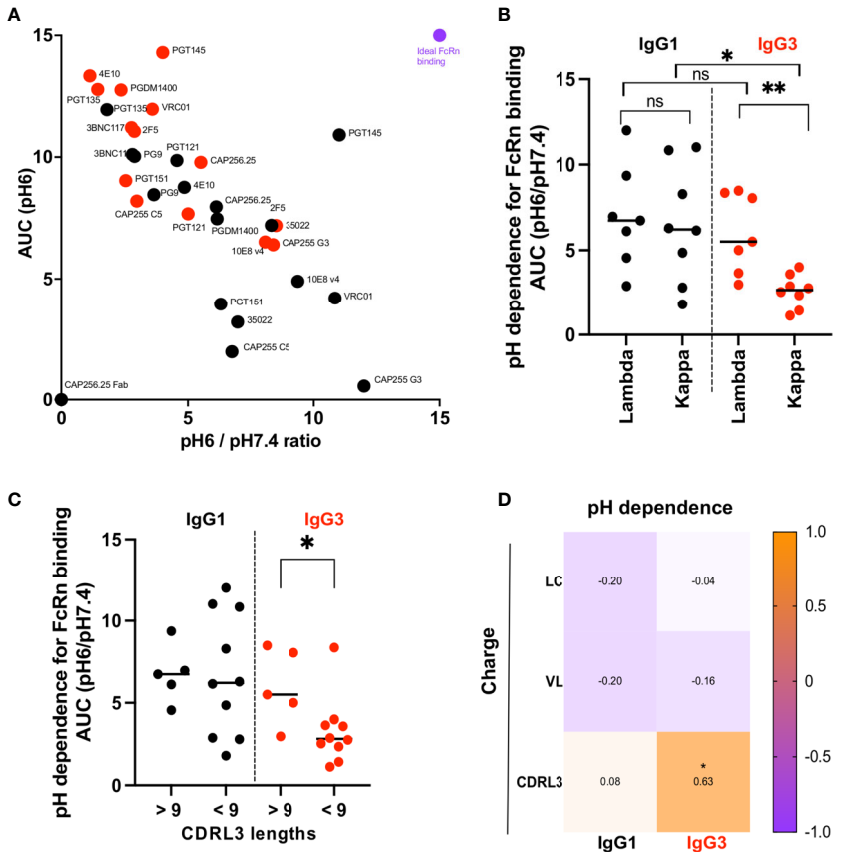


**FIGURE 3** | IgG3 bNAb variants with a Lambda light chain show significantly improved dependence on pH for FcRn binding. **(A)** Binding to the FcRn receptor measured by ELISA at pH6 and pH7.4. Y axis shows binding to the receptor at pH6 area under the curve (AUC) and the X axis the ratio of the area under the curve of binding to the FcRn receptor at pH6 and pH7.4. Red dots indicate the IgG3 and black the IgG1 bNAb variants. Purple denotes an example of an antibody with optimal FcRn binding. **(B)** pH dependence (AUC pH6/pH7.4) for antibodies with lambda or kappa light chains. Significance is indicated by a Mann Whitney t test for unpaired samples (** denotes $p < 0,01$) and a Wilcoxon paired test for paired samples (* denotes $p < 0,05$). **(C)** pH dependence (AUC pH6/pH7.4) for antibodies with CDRL3 lengths below and above 9 are shown with significance indicated by a Mann Whitney t test where * denotes $p < 0,05$. **(D)** Net charge at pH7.4 of the light chain (LC), the variable region of the light chain (VL) and the complementarity determining region 3 of the light chain (CDRL3) correlated with the pH dependence of IgG1 and IgG3 bNAbs (represented as AUC pH6/pH7.4) are shown as Spearman's correlations where * denotes $p < 0.05$ and ns denotes non-significant.

(**Figure 4D**). Therefore, the potency of combinations may be further enhanced through as the use of IgG3 bNAbs, to improve both neutralization and Fc effector function.

## DISCUSSION

The contribution of the constant region of bNAbs has emerged as being important for optimal protection from infection as well as for the elimination of already infected cells (67, 68). Given our previous observation that both the Fc effector function and the neutralization potency of CAP256.25, a V2-directed bNAb, was significantly enhanced as an IgG3 variant (34), we expanded this to additional bNAbs. We show that the IgG3 isotype enhances ADCP and, in an epitope specific manner, ADCC, for several bNAbs. Furthermore, IgG3 maintains or improves neutralization against a small but globally relevant panel. This suggests the potential broader applicability of this subclass in passive immunization.

Fc receptor mediated cytotoxic functions are likely to be beneficial at transmission, especially at the mucosa where phagocytes predominate (69). In line with several previous studies (34, 43, 45), we show that IgG3 bNAb variants show enhanced ADCP compared to matched IgG1 variants. We further show that this enhancement could not be attributed to increased binding of IgG3 variants to trimer, similar to what has been observed for other bNAbs (34, 43, 45). We also found that IgG3 binding to FcγRIIa, the Fc receptor that largely facilitates ADCP, was significantly increased compared to IgG1. This is in contrast to a previous study that saw no differences in IgG1 or IgG3 bNAb binding to Fc receptors or antigen by surface plasmon resonance (45). These discrepancies may be a consequence of the use of ELISA, and it is also possible that variation in Fc glycosylations as a result of cell line used may result in differences in binding. We note that in our study, although there is a correlation between FcγRIIa binding and function, this was not very strong, suggesting other features of

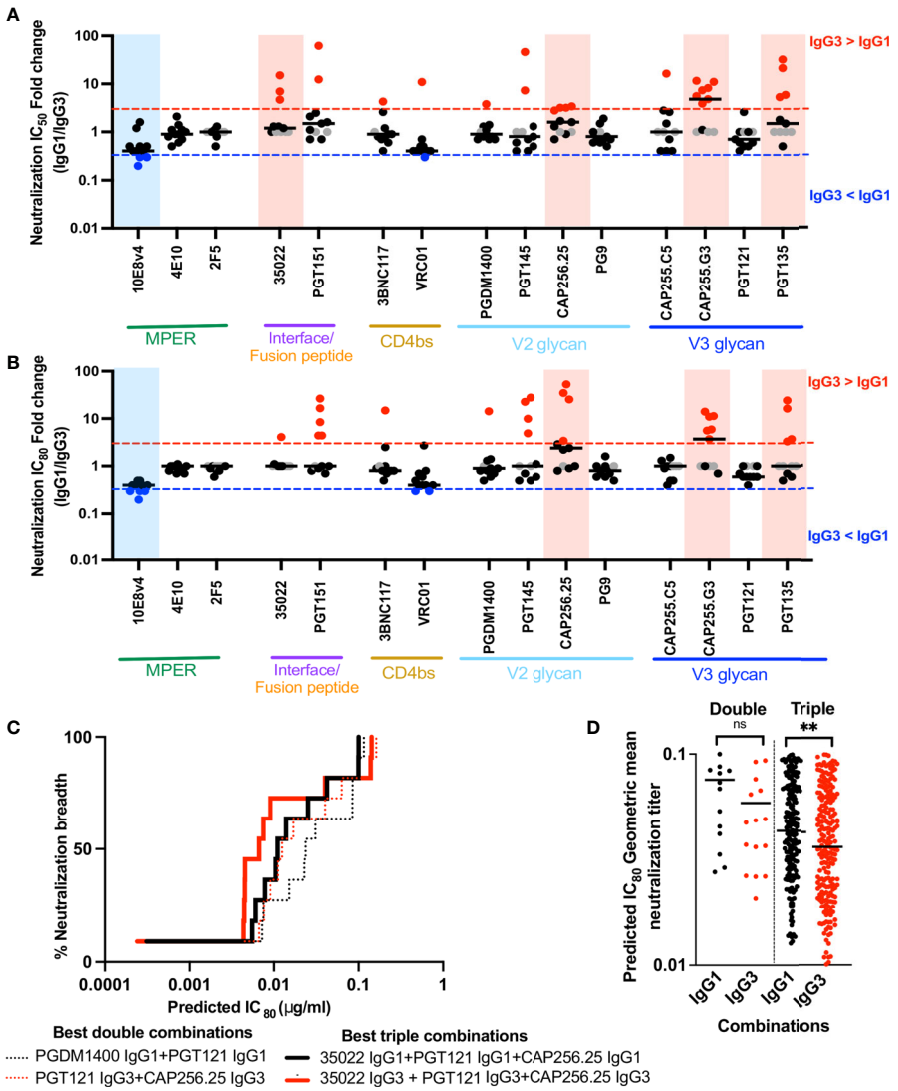


**FIGURE 4** | IgG3 bNAb variants enhance or maintain neutralization of a multiclade panel of viruses and IgG3 combinations are are more potent that IgG1 combinations. **(A)** Fold changes of $IC_{50}$ and **(B)** $IC_{80}$ between IgG3 and IgG1 bNAb variants, by epitope targets against 11 viruses from the multiclade global panel where the neutralization is represented by individual dots. The red and blue lines indicate 3 fold difference where IgG3 > IgG1 and IgG3 < IgG1 respectively. Grey dots indicate instances where a virus is resistance to neutralization and shaded blue and red areas indicating those instances where there is a statistically significant difference between IgG1 and IgG3 activity against all viruses, for that bNAb pair. **(C)** Neutralization breadth potency curves of the best double (dotted) and triple (bold) combinations of antibodies as defined by the Bliss-Hill model. IgG1 in black, IgG3 in red. **(D)** All double or triple combinations of antibodies that show 100% breadth against the 11 virus panel are shown as the predicted $IC_{80}$ geomean titers. ** denotes $p < 0.01$ and ns denotes non-significant, Mann-Whitney t test.

the antibody may contribute to increased ADCP. One possibility is that the longer IgG3 hinge may result in cross-linking of antigen. Ultimately, while improved ADCP as IgG3 has previously been studied in a small number of HIV bNAbs (34, 43, 45), we show here that it is broadly applicable across bNAbs targeting different epitopes.

While IgG3 showed marked improvement of ADCP regardless of the antigen that was tested, or the epitope targeted, ADCC capacities of IgG3 bNAb variants were epitope and antigen specific. Overall, while ADCC activity was not uniformly enhanced by IgG3, the isotype was advantageous for several MPER, gp41-gp120 interface and CD4 binding site bNAbs. This is in line with previous studies that show highly virus specific IgG1 bNAb ADCC activity which was dependent on the ability of these antibodies to bind infected cells (67, 70–72). In a study that examined the ADCC of bNAbs, those that induced the strongest FcγRIIIa stimulation were most active (67), which is similar to our study where ADCC correlated with binding to this Fc receptor. Given that antibody angle-of-approach influences how the Fc is presented to the receptor and the level of avidity induced (73, 74), the increased reach of IgG3 may be advantageous against certain epitopes. Similarly the

nature of the distribution of trimer on the surface of the cell, which likely differs between viruses, may influence Fc presentation as it does for other pathogens (75). This may explain the virus dependent ADCC enhancement seen between IgG1 and IgG3. While the hinge length of IgG3 does not influence the ADCC of VRC01 (45), it is interesting that short hinge variants of non-HIV antibodies show enhanced ADCC, confirming that this region should be further investigated in HIV bNAbs (38). Further, beyond ADCP and ADCC other Fc effector functions should be investigated. Given IgG3 can enhance complement-mediated lysis relative to IgG1, specifically in cases of sparse antigen density (76), and this function is important for HIV bNAb mediated killing (70), it is likely of relevance.

The reduced half-life of IgG3, compared to IgG1, has limited their potential as therapeutics. This shorter half-life is determined by its low pH dependence during FcRn-mediated recycling (39). In this study we show that as expected, IgG3 bNAbs overall display lower pH dependence compared to IgG1. However, individual bNAbs showed significantly different binding profiles, indicating the involvement of the Fab in FcRn binding. Several previous studies have shown this, either by comparing antibodies with identical Fc portions and different variable regions (77, 78) or using the hydrogen deuterium exchange method (79). Minor contributions from complementarity determining regions light chain 3 (CDRL3) of antibodies have been shown to strengthen the interaction with the FcRn (48, 49). Particularly for IgG3 it is possible that residues in CDRs could directly contact FcRn following the first interaction at the putative binding site, owing to the inherent flexibility of the Fab arms (41). Here we show that IgG3 dependence on pH was significantly lower for those bNAbs that use a kappa light chain, in contrast to those that use a lambda light chain. Given that IgG1 bNAbs showed no such difference, this preference appears to be unique to the IgG3 molecule. There was no difference in pH dependence between lambda IgG3 bNAbs and matched IgG1. This suggests these may have similar half-lives to IgG1 *in vivo*, although this yet to be assessed. Lambda light chains overall showed longer CDRL3 chains, which along with charge was associated with improved pH dependence of IgG3 bNAbs. These data suggest that the Fab portion may strengthen FcRn binding and compensate for the otherwise poor pH dependence of IgG3 constant regions.

We further showed that 14 of the 15 bNAb pairs tested in this study, to multiple epitopes, showed either enhancement or maintenance of neutralization activity as IgG3, with only 10E8v4 showing loss of neutralization. This extends previous studies showing that the constant region can alter neutralization potency of bNAbs (30, 32–34, 80, 81). As in previous studies VRC01 as well as MPER bNAbs 2F5 and 4E10 which were isolated as IgG3 (45, 82, 83), showed no difference in potency between IgG1 and IgG3. While for several bNAbs, we find large fold differences in neutralization potency between IgG1 and IgG3, binding to a subset of three trimers showed minimal difference. This suggests other mechanisms for enhanced neutralization, which may include cross linking of trimers or intra-trimeric binding, with the longer hinge length of IgG3 likely able to increase Fab–Fc distance, Fab–Fab distance and flexibility (40). A key immune evasion mechanism of HIV-1 against host antibody responses is the remarkably low density of Env molecules on the viral surface (84), a feature that IgG3 is able to circumvent in other pathogens due to its enhanced reach (75). This is supported in HIV by data showing that bispecific bNAbs, particularly 3BNC117/PGT135, with engineered hinge lengths equivalent to that of IgG3, showed increased neutralization potency by favoring intra-trimeric, bivalent interactions and increasing avidity of the construct (85). Interestingly, the IgG3 variant of PGT135 also showed significant enhancement in our study. Overall our findings suggest that the unique structure of IgG3 may be an advantage for neutralization.

For passive immunization strategies, there is an increased focus on combinations of antibodies to increase viral coverage and counteract resistance. We show that combinations of IgG3 bNAbs show enhanced potency, compared to IgG1 combinations against the small panel of viruses tested. In addition to enhanced neutralization, combinations of potent IgG3 bNAbs would also have the advantage of increased Fc effector function, which may be advantageous for future passive immunization strategies. This represents an alternative strategy to the engineering of specific residues within IgG1 bNAbs to increase effector function, an approach which has shown variable improvement in protection *in vivo* (25).

The paucity of therapeutic IgG3 bnAbs is largely borne out of concerns about half-life, which we show here also depends on the Fab portion of the antibody. These findings may enable strategies to mitigate the poor pH dependence of IgG3. An additional concern frequently raised is allotypic mismatch resulting in adverse reactions owing to the polymorphic nature of IgG3. However as many of the changes are isoallotypic (occurring in other IgG subclasses) (29) this is unlikely to be a major issue in passive immunization. The stability of IgG3 can also be improved through mutations in the CH3 (86). Most importantly, IgG3 has shown tolerability and benefit in humans for the treatment of lung cancer and *Staphylococcus aureus* bacteraemia (41). Our study shows that the polyfunctional enhancement of bNAbs by IgG3 is substantial and these should be considered for passive immunization. Ultimately, this study leverages the IgG3 subclass to improve antibody function and shows that antibodies should be optimised based not only on their antigen binding characteristics but also on the intrinsic properties of their constant regions.

## DATA AVAILABILITY STATEMENT

The original contributions presented in the study are included in the article/**Supplementary Material**. Further inquiries can be directed to the corresponding author.

## ETHICS STATEMENT

The studies involving human participants were reviewed and approved by Human Research Ethics Committee of the

University of the Witwatersrand. The patients/participants provided their written informed consent to participate in this study.

## AUTHOR CONTRIBUTIONS

SR conceptualized, performed experiments, analyzed data, generated the figures and wrote the manuscript. FA, BO, ZM, and BL produced antibodies and proteins. NM performed Fc experiments. LM and PM assisted in data interpretation. PM wrote the manuscript. All authors contributed to the article and approved the submitted version.

## FUNDING

SR and PM are supported by the South African Research Chairs Initiative of the Department of Science and Innovation and National Research Foundation of South Africa, the SA Medical Research Council SHIP program, the Centre for the AIDS Program of Research (CAPRISA) and an H3 Africa grant (U01A136677). SR is also supported by the Poliomyelitis Research Foundation and is a L'Oreal/UNESCO Women in Science South Africa Young Talents awardee. The funder was not involved in the study design, collection, analysis, interpretation of data, the writing of this article or the decision to submit it for publication. Related research by the authors is conducted as part of the DST-NRF Centre of Excellence in HIV Prevention, which is supported by the Department of Science and Technology and the National Research Foundation.

## ACKNOWLEDGMENTS

We thank Dr. Christina Ochsenbauer (University of Alabama at Birmingham) for the Env.IMC constructs and Dr. Christopher Cottrell (The Scripps Research Institute) for the SOSIP trimer constructs.

## SUPPLEMENTARY MATERIAL

The Supplementary Material for this article can be found online at: https://www.frontiersin.org/articles/10.3389/fimmu.2021.733958/full#supplementary-material

## REFERENCES

1. Moldt B, Rakasz EG, Schultz N, Chan-Hui P-Y, Swiderek K, Weisgrau KL, et al. Highly Potent HIV-Specific Antibody Neutralization *In Vitro* Translates Into Effective Protection Against Mucosal SHIV Challenge *In Vivo*. *Proc Natl Acad Sci U S A* (2012) 109(46):18921–5. doi: 10.1073/pnas.1214785109
2. Gautam R, Nishimura Y, Pegu A, Nason MC, Klein F, Gazumyan A, et al. A Single Injection of Anti-HIV-1 Antibodies Protects Against Repeated SHIV Challenges. *Nature* (2016) 533(7601):105–9. doi: 10.1038/nature17677
3. Julg B, Tartaglia LJ, Keele BF, Wagh K, Pegu A, Sok D, et al. Broadly Neutralizing Antibodies Targeting the HIV-1 Envelope V2 Apex Confer Protection Against a Clade C SHIV Challenge. *Sci Transl Med* (2017) 9(406): eaal1321. doi: 10.1126/scitranslmed.aal1321
4. Caskey M, Klein F, Lorenzi JCC, Seaman MS, West APJr., Buckley N, et al. Viraemia Suppressed in HIV-1-Infected Humans by Broadly Neutralizing Antibody 3BNC117. *Nature* (2015) 522(7557):487–91. doi: 10.1038/nature14411
5. Lynch RM, Boritz E, Coates EE, DeZure A, Madden P, Costner P, et al. Virologic Effects of Broadly Neutralizing Antibody VRC01 Administration During Chronic HIV-1 Infection. *Sci Transl Med* (2015) 7(319):319ra206 LP–319ra206. doi: 10.1126/scitranslmed.aad5752
6. Corey L, Gilbert PB, Juraska M, Montefiori DC, Morris L, Karuna ST, et al. Two Randomized Trials of Neutralizing Antibodies to Prevent HIV-1 Acquisition. *N Engl J Med* (2021) 384(11):1003–14. doi: 10.1056/NEJMoa2031738
7. Hessell AJ, Shapiro MB, Powell R, Malherbe DC, McBurney SP, Pandey S, et al. Reduced Cell-Associated DNA and Improved Viral Control in Macaques Following Passive Transfer of a Single Anti-V2 Monoclonal Antibody and Repeated Simian/Human Immunodeficiency Virus Challenges. *J Virol* (2018) 92(11):e02198–17. doi: 10.1128/JVI.02198-17
8. Horwitz JA, Bar-On Y, Lu CL, Fera D, Lockhart AAK, Lorenzi JCC, et al. Non-Neutralizing Antibodies Alter the Course of HIV-1 Infection *In Vivo*. *Cell* (2017) 170(4):637–48.e10. doi: 10.1016/j.cell.2017.06.048
9. Moog C, Dereuddre-Bosquet N, Teillaud J-L, Biedma ME, Holl V, Van Ham G, et al. Protective Effect of Vaginal Application of Neutralizing and Nonneutralizing Inhibitory Antibodies Against Vaginal SHIV Challenge in Macaques. *Mucosal Immunol* (2014) 7(1):46–56. doi: 10.1038/mi.2013.23
10. Santra S, Tomaras GD, Warrier R, Nicely NI, Liao HX, Pollara J, et al. Human Non-Neutralizing HIV-1 Envelope Monoclonal Antibodies Limit the Number of Founder Viruses During SHIV Mucosal Infection in Rhesus Macaques. *PLoS Pathog* (2015) 11(8):e1005042:1–38. doi: 10.1371/journal.ppat.1005042
11. Ackerman ME, Mikhailova A, Brown EP, Dowell KG, Walker BD, Bailey-Kellogg C, et al. Polyfunctional HIV-Specific Antibody Responses Are Associated With Spontaneous HIV Control. *PLoS Pathog* (2016) 12(1): e1005315. doi: 10.1371/journal.ppat.1005315
12. Forthal DN, Landucci G, Daar ES. Antibody From Patients With Acute Human Immunodeficiency Virus (HIV) Infection Inhibits Primary Strains of HIV Type 1 in the Presence of Natural-Killer Effector Cells. *J Virol* (2001) 75 (15):6953–61. doi: 10.1128/JVI.75.15.6953-6961.2001
13. Haynes BF, Gilbert PB, McElrath MJ, Zolla-Pazner S, Tomaras GD, Alam SM, et al. Immune-Correlates Analysis of an HIV-1 Vaccine Efficacy Trial. *N Engl J Med* (2012) 366(14):1275–86. doi: 10.1056/NEJMoa1113425
14. Chung AW, Ghebremichael M, Robinson H, Brown E, Choi I, Lane S, et al. Polyfunctional Fc-Effector Profiles Mediated by IgG Subclass Selection Distinguish RV144 and VAX003 Vaccines. *Sci Transl Med* (2014) 6 (228):228ra38–228ra38. doi: 10.1126/scitranslmed.3007736
15. Yates NL, Liao H-X, Fong Y, DeCamp A, Vandergrift NA, Williams WT, et al. Vaccine-Induced Env V1-V2 IgG3 Correlates With Lower HIV-1 Infection Risk and Declines Soon After Vaccination. *Sci Transl Med* (2014) 6 (228):228ra39–228ra39. doi: 10.1126/scitranslmed.3007730
16. Om K, Paquin-Proulx D, Montero M, Peachman K, Shen X, Wieczorek L, et al. Adjuvanted HIV-1 Vaccine Promotes Antibody-Dependent Phagocytic Responses and Protects Against Heterologous SHIV Challenge. *PLoS Pathog* (2020) 16(9):e1008764. doi: 10.1371/journal.ppat.1008764
17. Ackerman ME, Das J, Pittala S, Broge T, Linde C, Suscovich TJ, et al. Route of Immunization Defines Multiple Mechanisms of Vaccine-Mediated Protection Against SIV. *Nat Med* (2018) 24(10):1590–8. doi: 10.1038/s41591-018-0161-0
18. Bradley T, Pollara J, Santra S, Vandergrift N, Pittala S, Bailey-Kellogg C, et al. Pentavalent HIV-1 Vaccine Protects Against Simian-Human Immunodeficiency Virus Challenge. *Nat Commun* (2017) 8(1):15711. doi: 10.1038/ncomms15711
19. Richardson SI, Moore PL. Targeting Fc Effector Function in Vaccine Design. *Expert Opin Ther Targets* (2021) 25:1–11. doi: 10.1080/14728222.2021.1907343

20. Richardson SI, Chung AW, Natarajan H, Mabvakure B, Mkhize NN, Garrett N, et al. HIV-Specific Fc Effector Function Early in Infection Predicts the Development of Broadly Neutralizing Antibodies. *PLoS Pathog* (2018) 14(4): e1006987. doi: 10.1371/journal.ppat.1006987
21. Lofano G, Gorman MJ, Yousif AS, Yu W-H, Fox JM, Dugast A-S, et al. Antigen-Specific Antibody Fc Glycosylation Enhances Humoral Immunity *via* the Recruitment of Complement. *Sci Immunol* (2018) 3: (26):eaat7796. doi: 10.1126/sciimmunol.aat7796
22. Hessell AJ, Hangartner L, Hunter M, Havenith CEG, Beurskens FJ, Bakker JM, et al. Fc Receptor But Not Complement Binding is Important in Antibody Protection Against HIV. *Nature* (2007) 449(7158):101–4. doi: 10.1038/nature06106
23. Hessell AJ, Poignard P, Hunter M, Hangartner L, Tehrani DM, Bleeker WK, et al. Effective, Low-Titer Antibody Protection Against Low-Dose Repeated Mucosal SHIV Challenge in Macaques. *Nat Med* (2009) 15(8):951–4. doi: 10.1038/nm.1974
24. Bournazos S, Klein F, Pietzsch J, Seaman MS, Nussenzweig MC, Ravetch JV. Broadly Neutralizing Anti-HIV-1 Antibodies Require Fc Effector Functions for *In Vivo* Activity. *Cell* (2014) 158(6):1243–53. doi: 10.1016/j.cell.2014.08.023
25. Asokan M, Dias J, Liu C, Maximova A, Ernste K, Pegu A, et al. Fc-Mediated Effector Function Contributes to the *In Vivo* Antiviral Effect of an HIV Neutralizing Antibody. *Proc Natl Acad Sci* (2020) 117(31):18754–63. doi: 10.1073/pnas.2008236117
26. Wang P, Gajjar MR, Yu J, Padte NN, Gettie A, Blanchard JL, et al. Quantifying the Contribution of Fc-Mediated Effector Functions to the Antiviral Activity of Anti–HIV-1 IgG1 Antibodies *In Vivo*. *Proc Natl Acad Sci* (2020) 117 (30):18002–9. doi: 10.1073/pnas.2008190117
27. Halper-Stromberg A, Lu C-L, Klein F, Horwitz JA, Bournazos S, Nogueira L, et al. Broadly Neutralizing Antibodies and Viral Inducers Decrease Rebound From HIV-1 Latent Reservoirs in Humanized Mice. *Cell* (2014) 158(5):989–99. doi: 10.1016/j.cell.2014.07.043
28. Lu C-L, Murakowski DK, Bournazos S, Schoofs T, Sarkar D, Halper-Stromberg A, et al. Enhanced Clearance of HIV-1-Infected Cells by Broadly Neutralizing Antibodies Against HIV-1 *In Vivo*. *Science* (2016) 352 (6288):1001–4. doi: 10.1126/science.aaf1279
29. Vidarsson G, Dekkers G, Rispens T. IgG Subclasses and Allotypes: From Structure to Effector Functions. *Front Immunol* (2014) 5:520/abstract(OCT). doi: 10.3389/fimmu.2014.00520/abstract
30. Tudor D, Yu H, Maupetit J, Drillet A-S, Bouceba T, Schwartz-Cornil I, et al. Isotype Modulates Epitope Specificity, Affinity, and Antiviral Activities of Anti-HIV-1 Human Broadly Neutralizing 2F5 Antibody. *Proc Natl Acad Sci U.S.A.* (2012) 109(31):12680–5. doi: 10.1073/pnas.1200024109
31. Klein K, Veazey RS, Warrier R, Hraber P, Doyle-Meyers LA, Buffa V, et al. Neutralizing IgG at the Portal of Infection Mediates Protection Against Vaginal Simian/Human Immunodeficiency Virus Challenge. *J Virol* (2013) 87(21):11604–16. doi: 10.1128/JVI.01361-13
32. Astronomo RD, Santra S, Ballweber-Fleming L, Westerberg KG, Mach L, Hensley-McBain T, et al. Neutralization Takes Precedence Over IgG or IgA Isotype-Related Functions in Mucosal HIV-1 Antibody-Mediated Protection. *EBioMedicine* (2016) 14:97–111. doi: 10.1016/j.ebiom.2016.11.024
33. Cheeseman HM, Olejniczak NJ, Rogers PM, Evans AB, King DFL, Ziprin P, et al. Broadly Neutralizing Antibodies Display Potential for Prevention of HIV-1 Infection of Mucosal Tissue Superior to That of Nonneutralizing Antibodies. *J Virol* (2016) 91(1):e01762–16. doi: 10.1128/JVI.01762-16
34. Richardson SI, Lambson BE, Crowley AR, Bashirova A, Scheepers C, Garrett N, et al. IgG3 Enhances Neutralization Potency and Fc Effector Function of an HIV V2-Specific Broadly Neutralizing Antibody. *PLoS Pathog* (2019) 15 (12):1–25. doi: 10.1371/journal.ppat.1008064
35. Scheepers C, Bekker V, Anthony C, Richardson SI, Oosthuysen B, Moyo T, et al. Antibody Isotype Switching as a Mechanism to Counter HIV Neutralization Escape. *Cell Rep* (2020) 33(8):108430. doi: 10.1016/j.celrep.2020.108430
36. Bruhns P, Iannascoli B, England P, Mancardi DA, Fernandez N, Jorieux S, et al. Specificity and Affinity of Human Fcγ Receptors and Their Polymorphic Variants for Human IgG Subclasses. *Blood* (2009) 113(16):3716–25. doi: 10.1182/blood-2008-09-179754
37. Lefranc M-P, Lefranc G. *Human Gm, Km, and Am Allotypes and Their Molecular Characterization: A Remarkable Demonstration of Polymorphism BT - Immunogenetics: Methods and Applications in Clinical Practice*. FT Christiansen, BD Tait, editors. Totowa, NJ: Humana Press (2012) p. 635–80. doi: 10.1007/978-1-61779-842-9_34
38. de Taeye SW, Bentlage AEH, Mebius MM, Meesters JI, Lissenberg-Thunnissen S, Falck D, et al. FcγR Binding and ADCC Activity of Human IgG Allotypes. *Front Immunol* (2020) 11:740. doi: 10.3389/fimmu.2020.00740
39. Stapleton NM, Andersen JT, Stemerding AM, Bjarnarson SP, Verheul RC, Gerritsen J, et al. Competition for FcRn-Mediated Transport Gives Rise to Short Half-Life of Human IgG3 and Offers Therapeutic Potential. *Nat Commun* (2011) 2:599. doi: 10.1038/ncomms1608
40. Roux KH, Strelets L, Michaelsen TE. Flexibility of Human IgG Subclasses. *J Immunol* (1997) 159(7):3372–82.
41. Chu TH, Patz EFJr., Ackerman ME. Coming Together at the Hinges: Therapeutic Prospects of IgG3. *MAbs* (2021) 13(1):1882028. doi: 10.1080/19420862.2021.1882028
42. Neidich SD, Fong Y, Li SS, Geraghty DE, Williamson BD, Young WC, et al. Antibody Fc Effector Functions and IgG3 Associate With Decreased HIV-1 Risk. *J Clin Invest* (2019) 129(11):4838–49. doi: 10.1172/JCI126391
43. Tay MZ, Liu P, Williams LD, McRaven MD, Sawant S, Gurley TC, et al. Antibody-Mediated Internalization of Infectious HIV-1 Virions Differs Among Antibody Isotypes and Subclasses. *PLoS Pathog* (2016) 12(8): e1005817. doi: 10.1371/journal.ppat.1005817
44. Pollara J, Tay MZ, Edwards RW, Goodman D, Crowley AR, Edwards RJ, et al. Functional Homology for Antibody-Dependent Phagocytosis Across Humans and Rhesus Macaques. *Front Immunol* (2021) 12:678511. doi: 10.3389/fimmu.2021.678511
45. Chu TH, Crowley AR, Backes I, Chang C, Tay M, Broge T, et al. Hinge Length Contributes to the Phagocytic Activity of HIV-Specific IgG1 and IgG3 Antibodies. *PLoS Pathog* (2020) 16(2):1–25. doi: 10.1371/journal.ppat.1008083
46. Pyzik M, Sand KMK, Hubbard JJ, Andersen JT, Sandlie I, Blumberg RS. The Neonatal Fc Receptor (FcRn): A Misnomer? *Front Immunol* (2019) 10:1540. doi: 10.3389/fimmu.2019.01540
47. Raghavan M, Bonagura VR, Morrison SL, Bjorkman PJ. Analysis of the pH Dependence of the Neonatal Fc Receptor/Immunoglobulin G Interaction Using Antibody and Receptor Variants. *Biochemistry* (1995) 34(45):14649–57. doi: 10.1021/bi00045a005
48. Piche-Nicholas NM, Avery LB, King AC, Kavosi M, Wang M, O'Hara DM, et al. Changes in Complementarity-Determining Regions Significantly Alter IgG Binding to the Neonatal Fc Receptor (FcRn) and Pharmacokinetics. *MAbs* (2018) 10(1):81–94. doi: 10.1080/19420862.2017.1389355
49. Schoch A, Kettenberger H, Mundigl O, Winter G, Engert J, Heinrich J, et al. Charge-Mediated Influence of the Antibody Variable Domain on FcRn-Dependent Pharmacokinetics. *Proc Natl Acad Sci* (2015) 112(19):5997–6002. doi: 10.1073/pnas.1408766112
50. deCamp A, Hraber P, Bailer RT, Seaman MS, Ochsenbauer C, Kappes J, et al. Global Panel of HIV-1 Env Reference Strains for Standardized Assessments of Vaccine-Elicited Neutralizing Antibodies. *J Virol* (2014) 88(5):2489–507. doi: 10.1128/JVI.02853-13
51. Sanders RW, Derking R, Cupo A, Julien J-P, Yasmeen A, de Val N, et al. A Next-Generation Cleaved, Soluble HIV-1 Env Trimer, BG505 SOSIP.664 Gp140, Expresses Multiple Epitopes for Broadly Neutralizing But Not Non-Neutralizing Antibodies. *PLoS Pathog* (2013) 9(9):e1003618. doi: 10.1371/journal.ppat.1003618
52. Ackerman ME, Moldt B, Wyatt RT, Dugast AS, McAndrew E, Tsoukas S, et al. A Robust, High-Throughput Assay to Determine the Phagocytic Activity of Clinical Antibody Samples. *J Immunol Methods* (2011) 366:8–19. doi: 10.1016/j.jim.2010.12.016
53. Alberti MO, Jones JJ, Miglietta R, Ding H, Bakshi RK, Edmonds TG, et al. Optimized Replicating Renilla Luciferase Reporter HIV-1 Utilizing Novel Internal Ribosome Entry Site Elements for Native Nef Expression and Function. *AIDS Res Hum Retroviruses* (2015) 31(12):1278–96. doi: 10.1089/aid.2015.0074
54. Pollara J, Bonsignori M, Moody MA, Liu P, Alam SM, Hwang K-K, et al. HIV-1 Vaccine-Induced C1 and V2 Env-Specific Antibodies Synergize for

Increased Antiviral Activities. *J Virol* (2014) 88(14):7715–26. doi: 10.1128/JVI.00156-14
55. Moldt B, Schultz N, Dunlop DC, Alpert MD, Harvey JD, Evans DT, et al. A Panel of IgG1 B12 Variants With Selectively Diminished or Enhanced Affinity for Fcγ Receptors To Define the Role of Effector Functions in Protection Against HIV. *J Virol* (2011) 85(20):10572–81. doi: 10.1128/JVI.05541-11
56. Gray ES, Moore PL, Choge IA, Decker JM, Bibollet-Ruche F, Li H, et al. Neutralizing Antibody Responses in Acute Human Immunodeficiency Virus Type 1 Subtype C Infection. *J Virol* (2007) 81(12):6187–96. doi: 10.1128/JVI.00239-07
57. Montefiori DC. Evaluating Neutralizing Antibodies Against HIV, SIV, and SHIV in Luciferase Reporter Gene Assays. *Curr Protoc Immunol* (2004) 64 (1):12.11.1–12.11.17. doi: 10.1002/0471142735.im1211s64
58. Wagh K, Bhattacharya T, Williamson C, Robles A, Bayne M, Garrity J, et al. Optimal Combinations of Broadly Neutralizing Antibodies for Prevention and Treatment of HIV-1 Clade C Infection. *PLoS Pathog* (2016) 12(3): e1005520–e1005520. doi: 10.1371/journal.ppat.1005520
59. Doria-Rose NA, Bhiman JN, Roark RS, Schramm CA, Gorman J, Chuang G-Y, et al. New Member of the V1V2-Directed CAP256-VRC26 Lineage That Shows Increased Breadth and Exceptional Potency. *J Virol* (2016) 90(1):76–91. doi: 10.1128/JVI.01791-15
60. Mahomed S, Garrett N, Baxter C, Abdool Karim Q, Abdool Karim SS. Clinical Trials of Broadly Neutralizing Monoclonal Antibodies for Human Immunodeficiency Virus Prevention: A Review. *J Infect Dis* (2021) 223 (3):370–80. doi: 10.1093/infdis/jiaa377
61. Bruhns P. Properties of Mouse and Human IgG Receptors and Their Contribution to Disease Models. *Blood* (2012) 119(24):5640–9. doi: 10.1182/blood-2012-01-380121
62. Jennewein MF, Alter G. The Immunoregulatory Roles of Antibody Glycosylation. *Trends Immunol* (2017) 38(5):358–72. doi: 10.1016/j.it.2017.02.004
63. Ackerman ME, Dugast A-S, McAndrew EG, Tsoukas S, Licht AF, Irvine DJ, et al. Enhanced Phagocytic Activity of HIV-Specific Antibodies Correlates With Natural Production of Immunoglobulins With Skewed Affinity for FcγR2a and FcγR2b. *J Virol* (2013) 87(10):5468–76. doi: 10.1128/JVI.03403-12
64. Bournazos S, Ravetch JV. Diversification of IgG Effector Functions. *Int Immunol* (2017) 29(7):303–10. doi: 10.1093/intimm/dxx025
65. Danesh A, Ren Y, Brad Jones R. Roles of Fragment Crystallizable-Mediated Effector Functions in Broadly Neutralizing Antibody Activity Against HIV. *Curr Opin HIV AIDS* (2020) 15(5):316–23. doi: 10.1097/COH.0000000000000644
66. Huang J, Ofek G, Laub L, Louder MK, Doria-Rose NA, Longo NS, et al. Broad and Potent Neutralization of HIV-1 by a Gp41-Specific Human Antibody. *Nature* (2012) 491(7424):406–12. doi: 10.1038/nature11544
67. Bruel T, Guivel-Benhassine F, Amraoui S, Malbec M, Richard L, Bourdic K, et al. Elimination of HIV-1-Infected Cells by Broadly Neutralizing Antibodies. *Nat Commun* (2016) 7(1):10844. doi: 10.1038/ncomms10844
68. Parsons MS, Chung AW, Kent SJ. Importance of Fc-Mediated Functions of Anti-HIV-1 Broadly Neutralizing Antibodies. *Retrovirology* (2018) 15(1):58–70. doi: 10.1186/s12977-018-0438-x
69. Sips M, Krykbaeva M, Diefenbach TJ, Ghebremichael M, Bowman BA, Dugast A-S, et al. Fc Receptor-Mediated Phagocytosis in Tissues as a Potent Mechanism for Preventive and Therapeutic HIV Vaccine Strategies. *Mucosal Immunol* (2016) 9(6):1584–95. doi: 10.1038/mi.2016.12
70. Mujib S, Liu J, Rahman AKMN-U, Schwartz JA, Bonner P, Yue FY, et al. Comprehensive Cross-Clade Characterization of Antibody-Mediated Recognition, Complement-Mediated Lysis, and Cell-Mediated Cytotoxicity of HIV-1 Envelope-Specific Antibodies Toward Eradication of the HIV-1 Reservoir. *J Virol* (2017) 91(16):e00634–17. doi: 10.1128/JVI.00634-17
71. von Bredow B, Arias JF, Heyer LN, Moldt B, Le K, Robinson JE, et al. Comparison of Antibody-Dependent Cell-Mediated Cytotoxicity and Virus Neutralization by HIV-1 Env-Specific Monoclonal Antibodies. *J Virol* (2016) 90(13):6127–39. doi: 10.1128/JVI.00347-16
72. Pinto D, Fenwick C, Caillat C, Silacci C, Guseva S, Dehez F, et al. Structural Basis for Broad HIV-1 Neutralization by the MPER-Specific Human Broadly Neutralizing Antibody Ln01. *Cell Host Microbe* (2019) 26(5):623–637.e8. doi: 10.1016/j.chom.2019.09.016
73. Murin CD. Considerations of Antibody Geometric Constraints on NK Cell Antibody Dependent Cellular Cytotoxicity. *Front Immunol* (2020) 11:1635. doi: 10.3389/fimmu.2020.01635
74. Patel KR, Roberts JT, Barb AW. Multiple Variables at the Leukocyte Cell Surface Impact Fc γ Receptor-Dependent Mechanisms. *Front Immunol* (2019) 10:223. doi: 10.3389/fimmu.2019.00223
75. Giuntini S, Granoff DM, Beernink PT, Ihle O, Bratlie D, Michaelsen TE. Human IgG1, IgG3, and IgG3 Hinge-Truncated Mutants Show Different Protection Capabilities Against Meningococci Depending on the Target Antigen and Epitope Specificity. *Clin Vaccine Immunol* (2016) 23(8):698–706. doi: 10.1128/CVI.00193-16
76. Michaelsen TE, Garred P, Aase A. Human IgG Subclass Pattern of Inducing Complement-Mediated Cytolysis Depends on Antigen Concentration and to a Lesser Extent on Epitope Patchiness, Antibody Affinity and Complement Concentration. *Eur J Immunol* (1991) 21(1):11–6. doi: 10.1002/eji.1830210103
77. Wang W, Lu P, Fang Y, Hamuro L, Pittman T, Carr B, et al. Monoclonal Antibodies With Identical Fc Sequences Can Bind to FcRn Differentially With Pharmacokinetic Consequences. *Drug Metab Dispos* (2011) 39(9):1469–77. doi: 10.1124/dmd.111.039453
78. Schlothauer T, Rueger P, Stracke JO, Hertenberger H, Fingas F, Kling L, et al. Analytical FcRn Affinity Chromatography for Functional Characterization of Monoclonal Antibodies. *MAbs* (2013) 5(4):576–86. doi: 10.4161/mabs.24981
79. Jensen PF, Larraillet V, Schlothauer T, Kettenberger H, Hilger M, Rand KD. Investigating the Interaction Between the Neonatal Fc Receptor and Monoclonal Antibody Variants by Hydrogen/Deuterium Exchange Mass Spectrometry *. *Mol Cell Proteomics* (2015) 14(1):148–61. doi: 10.1074/mcp.M114.042044
80. Jia M, Liberatore RA, Guo Y, Chan KW, Pan R, Lu H, et al. VSV-Displayed HIV-1 Envelope Identifies Broadly Neutralizing Antibodies Class-Switched to IgG and IgA. *Cell Host Microbe* (2020) 27(6):63–975.e5. doi: 10.1016/j.chom.2020.03.024
81. Magri G, Cerutti A. IgA Summons IgG to Take a Hit at HIV-1. *Cell Host Microbe*. (2020) 27(6):854–56. doi: 10.1016/j.chom.2020.05.017
82. Kunert R, Steinfellner W, Purtscher M, Assadian A, Katinger H. Stable Recombinant Expression of the Anti HIV-1 Monoclonal Antibody 2F5 After IgG3/IgG1 Subclass Switch in CHO Cells. *Biotechnol Bioeng* (2000) 67 (1):97–103. doi: 10.1002/(SICI)1097-0290(20000105)67:1<97::AID-BIT11>3.0.CO;2-2
83. Cavacini LA, Kuhrt D, Duval M, Mayer K, Posner MR. Binding and Neutralization Activity of Human IgG1 and IgG3 From Serum of HIV-Infected Individuals. *AIDS Res Hum Retroviruses* (2003) 19(9):785–92. doi: 10.1089/088922203769232584
84. Zhu P, Liu J, Bess J, Chertova E, Lifson JD, Grisé H, et al. Distribution and Three-Dimensional Structure of AIDS Virus Envelope Spikes. *Nature* (2006) 441(7095):847–52. doi: 10.1038/nature04817
85. Bournazos S, Gazumyan A, Seaman MS, Nussenzweig MC, Ravetch JV. Bispecific Anti-HIV-1 Antibodies With Enhanced Breadth and Potency. *Cell* (2016) 165(7):1609–20. doi: 10.1016/j.cell.2016.04.050
86. Saito S, Namisaki H, Hiraishi K, Takahashi N, Iida S. A Stable Engineered Human IgG3 Antibody With Decreased Aggregation During Antibody Expression and Low pH Stress. *Protein Sci* (2019) 28(5):900–9. doi: 10.1002/pro.3598

**Conflict of Interest:** The authors declare that the research was conducted in the absence of any commercial or financial relationships that could be construed as a potential conflict of interest.

**Publisher's Note:** All claims expressed in this article are solely those of the authors and do not necessarily represent those of their affiliated organizations, or those of the publisher, the editors and the reviewers. Any product that may be evaluated in this article, or claim that may be made by its manufacturer, is not guaranteed or endorsed by the publisher.

frontiers in Immunology

REVIEW
published: 15 September 2021
doi: 10.3389/fimmu.2021.734304

# Contribution to HIV Prevention and Treatment by Antibody-Mediated Effector Function and Advances in Broadly Neutralizing Antibody Delivery by Vectored Immunoprophylaxis

*Meredith Phelps and Alejandro Benjamin Balazs* *

*Ragon Institute of MGH, MIT and Harvard, Cambridge, MA, United States*

HIV-1 broadly neutralizing antibodies (bNAbs) targeting the viral envelope have shown significant promise in both HIV prevention and viral clearance, including pivotal results against sensitive strains in the recent Antibody Mediated Prevention (AMP) trial. Studies of bNAb passive transfer in infected patients have demonstrated transient reduction of viral load at high concentrations that rebounds as bNAb is cleared from circulation. While neutralization is a crucial component of therapeutic efficacy, numerous studies have demonstrated that bNAbs can also mediate effector functions, such as antibody-dependent cellular cytotoxicity (ADCC), antibody-dependent cellular phagocytosis (ADCP), and antibody-dependent complement deposition (ADCD). These functions have been shown to contribute towards protection in several models of HIV acquisition and in viral clearance during chronic infection, however the role of target epitope in facilitating these functions, as well as the contribution of individual innate functions in protection and viral clearance remain areas of active investigation. Despite their potential, the transient nature of antibody passive transfer limits the widespread use of bNAbs. To overcome this, we and others have demonstrated vectored antibody delivery capable of yielding long-lasting expression of bNAbs *in vivo*. Two clinical trials have shown that adeno-associated virus (AAV) delivery of bNAbs is safe and capable of sustained bNAb expression for over 18 months following a single intramuscular administration. Here, we review key concepts of effector functions mediated by bNAbs against HIV infection and the potential for vectored immunoprophylaxis as a means of producing bNAbs in patients.

**Keywords: vectored immunoprophylaxis, HIV, broadly neutralizing antibody, VRC07, humanized mice, AAV, Fc receptor, innate immunity**

OPEN ACCESS

***Edited by:***
*Marit Van Gils, Academic Medical Center, Netherlands*

***Reviewed by:***
*Simone Richardson, National Institute of Communicable Diseases (NICD), South Africa*
*Lars Hangartner, The Scripps Research Institute, United States*

***Correspondence:**
*Alejandro Benjamin Balazs*
*abalazs@mgh.harvard.edu*

***Specialty section:***
*This article was submitted to Vaccines and Molecular Therapeutics, a section of the journal Frontiers in Immunology*

***Received:*** *30 June 2021*
***Accepted:*** *24 August 2021*
***Published:*** *15 September 2021*

***Citation:***
*Phelps M and Balazs AB (2021) Contribution to HIV Prevention and Treatment by Antibody-Mediated Effector Function and Advances in Broadly Neutralizing Antibody Delivery by Vectored Immunoprophylaxis. Front. Immunol. 12:734304. doi: 10.3389/fimmu.2021.734304*

## INTRODUCTION

Despite the success of pre-exposure prophylaxis (PrEP) and antiretroviral therapy (ART) in reducing HIV incidence in developed countries, the HIV pandemic remains a major burden in developing nations (1). Among the novel interventions that continue to be developed, those employing broadly neutralizing antibodies are among the most promising as potential prevention (2), therapeutic (3) or cure modality *via* elimination of the latent viral reservoir (4). Broadly neutralizing antibodies (bNAbs) are defined by their capacity for potent neutralization of large panels of diverse strains (5–8). Numerous studies in non-human primates (NHP) and humanized mice have explored the potential for passive transfer of various bNAbs to prevent HIV acquisition. Testing of various antibodies has shown that bNAb-mediated prevention can be highly effective, however, at low concentrations a loss of protection against challenge is observed (9–11).

In addition to direct neutralization of virus entry, antibodies are capable of mediating non-neutralizing functions that are important in the context of HIV prevention and viral clearance, such as antibody-dependent cellular cytotoxicity (ADCC), antibody-dependent cellular phagocytosis (ADCP) and antibody-dependent complement deposition (ADCD), through engagement of the Fragment crystallizable (Fc) region with various Fc receptors expressed on the surface of innate cells or complement proteins in the circulation (**Figure 1**) (12–16). Therefore, understanding the parameters that influence bNAb

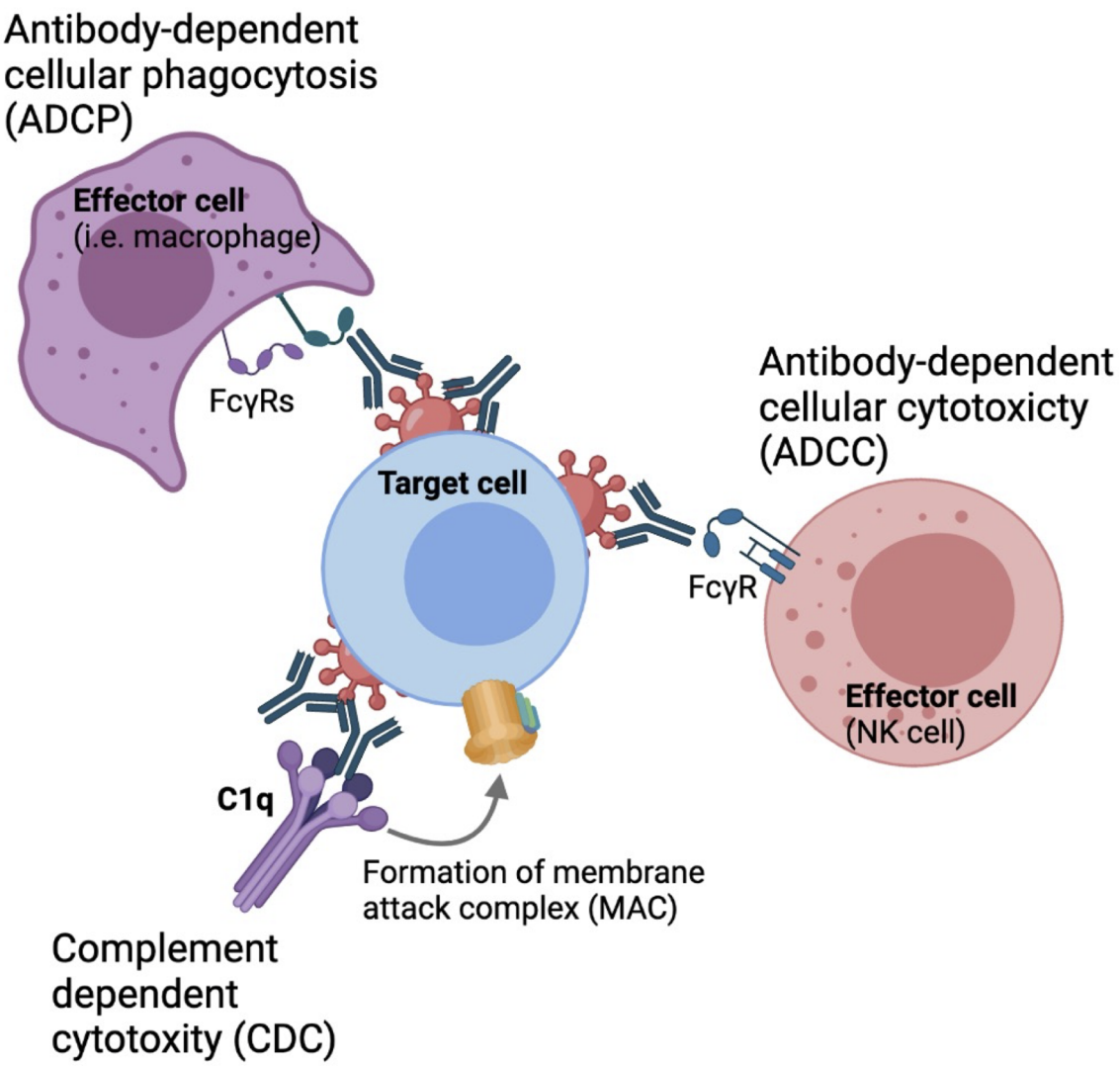


**FIGURE 1** | Fc-mediated effector functions. Antibodies can engaged with phagocytes, such as monocytes macrophages and neutrophyls through FcγRIa and FcγRIIa to drive antibody-dependent cellular phagocytosis.Nk cells can engaged with antibodies through engagement with FcγRIIIa to drive antibody-dependent cellular cytotoxicity. Antibodies can also activate the classical complement pathway to derive complement dependent cytotoxicity.

engagement with these innate cell subsets is critical for the development of maximally effective protective and therapeutic strategies.

Recent results from the AMP study, in which patients were passively transferred with VRC01 to prevent HIV acquisition, has shown that transmission risk is increased as antibody concentrations fall (17) (ClinicalTrials.gov: HVTN 703/HPTN 081). To overcome the short-lived nature of passive transfer, we and others have described recombinant adeno-associated viruses (rAAVs) as a delivery modality, termed Vectored ImmunoProphylaxis (VIP), that utilizes a single intramuscular administration to yield sustained expression of a given antibody (18). To maximize packaging capacity and minimize any potential toxicity, all viral sequences are removed with the exception of two 145 base pair inverted terminal repeats. These innovations allow for a full-length antibody sequence to be successfully packaged and efficiently expressed in animal models (19, 20).

Humanized mice are a valuable model in which to test both prophylactic and therapeutic interventions for HIV. These mice are the product of genetic engineering to express human genes or xenografting of immunocompromised mice with stem human cells and tissues. Humanized mouse models have shown long-lasting expression of various HIV-1 bNAbs delivered through VIP resulting in protection from viral challenge (21, 22). Given the pre-clinical success of vectored antibody strategies, a clinical trial testing the safety and efficacy of bNAb delivery using VIP is currently underway with recent results showing up to microgram per mL concentrations in circulation which were sustained for at least 18 months post-administration. In this review, we discuss the role of Fc-mediated effector functions during antibody-mediated protection from HIV particularly at low concentrations and the potential for vectored immunoprophylaxis to harness effector functions to yield durable protection through sustained bNAb delivery.

## PROTECTION FROM HIV ACQUISITION BY BROADLY NEUTRALIZING ANTIBODIES

The first-generation of HIV-1 broadly neutralizing antibodies including b6, 4E10, 2F5, and b12 were described over twenty years ago and showed limited breadth or potency (23–26). Since then, several second generation bNAbs such as PGDM1400, VRC01, and PGT121 have been characterized with far greater potency and breadth (27). BNAbs target distinct sites of vulnerability on the viral envelope; these include the CD4-binding site (CD4bs), the V1V2 loops (V1V2), the V3 loop (V3), the membrane-proximal external region (MPER), and more recently the gp120-41 interface or fusion peptide (28–31). Studies in non-human primates (NHPs) have investigated bNAb-mediated protection from SHIV acquisition using various bNAbs targeting each of these sites, including b12 (13), VRC01 (11, 32), 3BNC117 (CD4bs) (9, 33), PGDM1400, CAP256-VRC26.25 (V1V2) (10), 10-1074 (34) and PGT121 (V3) (9, 35). A recent meta-analysis of passive immunization studies performed by Pegu et al. (32) measured the rates of SHIV infection after a single administration of a given antibody (32). Collectively, these studies showed that antibody serum concentration against the challenge virus was strongly correlated with protection and that antibody inhibitory concentration required to reduce viral infectivity by fifty or eighty percent ($IC_{50}$ and $IC_{80}$, respectively) were also strong predictors of protection. Other work has shown that the protective concentration of an antibody *in vivo* is often 50-200 times greater than the *in vitro* $IC_{50}$ value calculated in an *in vitro* neutralization assay suggesting that the more potent an antibody is, the lower the concentration required to protect (36). Collectively, this work shows that antibody concentration and potency are crucial factors that contribute to protection. However, antibodies are also capable of mediating non-neutralizing effector functions that have been shown to contribute to protection and driving viral clearance (12, 13, 16, 37, 38).

## CONTRIBUTION OF FC-MEDIATED EFFECTOR FUNCTIONS IN HIV PREVENTION AND VIRAL CLEARANCE

Innate immune cells such as natural killer cells, monocytes, macrophage and neutrophils express a variety of activating and inhibitory Fc-gamma receptors (FcγRs) which can engage with the Fc-region of antibodies to drive Fc-mediated effector functions (39–41). Four different subclasses of Fc receptors have been defined, including three activating receptors FcγRI, FcγRII and FcγRIIIa, as well as the inhibitory receptor FcγRIIb. These molecules drive antibody-dependent innate functions including ADCC, ADCP, ADCD. ADCC occurs when NK and other innate cells form immunological synapses with a target cell through FcγRIIIa engagement to release perforin and granzyme B. These cytotoxic granules create pores in the membrane of the target cell, causing it to lyse and die (42–44). Phagocytosis is mediated by monocytes, macrophages, and neutrophils, where immune complex-opsonized cells are engulfed by mononuclear phagocytes through engagement of FcγRIa and FcγRIIa. Cross-linking of these FcγRs leads to downstream degradation of these engulfed target cells (45). Additionally, antibodies can also engage the complement system to drive ADCD. Antibodies bound to envelopes expressed by infected cells can form stable hexameric immune complexes that can recruit complement (45). Antibody-mediated complement activation occurs through the classical pathway in which C1q is recruited to antibody-immune complexes (46). This results in the formation of a membrane attack complex (MAC) that leads to lysis of the target cell (47).

The role of Fc-mediated effector functions in HIV prevention in patients has been suggested by the analysis of the partially successful RV144 vaccine trial in Thailand, in which patients were administered a heterologous prime-boost vaccine regimen (48). Analysis of uninfected participants showed that antibodies capable of driving Fc-mediated effector functions were positively associated with protection (14). Two antibody-dependent innate

functions that were strong correlates of decreased risk were ADCC and ADCP (49–51). Interestingly non-neutralizing IgG1 and IgG3 subclass antibodies targeting the V1V2 site mediated these effector functions, raising the possibility that there may be an optimal envelope epitopes to target to best drive these Fc functions. Bradley et al. performed a similar study to that of the RV144 trial in non-human primates, however they designed a vaccine cocktail of various gp120s to increase the diversity of antigen seen by the immune system in the hopes of eliciting broadly neutralizing antibodies (52). Analysis of the elicited antibodies also found that ADCC by NK cells was a major correlate of protection in the monkeys. More recent studies investigating the correlates of protection in a phase 1B trial attempting to replicate the RV144 regimen in South Africa (HVTN 097) found that innate immune pathways were highly upregulated, including signatures of ADCC and ADCP however it failed to demonstrate significant protection (53). Collectively, these findings suggest antibodies capable of driving Fc-mediated effector functions may hold promise in future interventions designed to prevent HIV transmission.

In addition to HIV prevention, polyfunctional antibodies have also been found to be associated with HIV control (54). Similar to findings described in RV144 subjects, elite controllers, who maintain low viral loads in the absence of therapy, harbor higher levels of IgG1 and IgG3 antibodies capable of mediating ADCC and ADCP. Antibodies isolated from elite controllers, viremic controllers, infected patients on ART, and infected patients off ART were compared for polyfunctionality and breakdown of IgG isotype. Interestingly, antibodies from elite controllers did not have enhanced polyfunctionality compared to other groups, but there was a higher prevalence of IgG1 and IgG3 subclasses seen in these patients. These antibodies were also able to mediate ADCC, ADCP, ADCD, and antibody-dependent neutrophil phagocytosis (ADNP) at lower serum titers compared to the other groups (54). Additionally, patients harboring antibodies that could mediate ADCC were also more likely to develop antibodies that could drive phagocytosis by both monocytes and neutrophils. Collectively, this data suggests that polyfunctional antibodies may have a significant impact on viral clearance in chronically infected individuals.

Understanding the role effector functions play in both prevention and control in chronic infection has largely focused on non-neutralizing antibodies elicited by patients. Although the vaccine regimen administered in the RV144 trial showed promising results, when an analogous regimen was given in South Africa in the HVTN02 trial it failed to achieve statistically significant protection, demonstrating the need for continued development of alternative strategies. Additionally, a study by Dugast et al. (55) demonstrated that passive transfer of ADCC-inducing non-neutralizing antibodies isolated from elite controllers failed to protect rhesus monkeys from SHIV challenge, suggesting that Fc-mediated effector functions alone are insufficient to protect against viral acquisition (55). In another study, Burton et al. (56) showed that rhesus macaques had limited protection against mucosal SHIV challenge when administered weakly or non-neutralizing antibodies compared to monkeys given a potent bNAb (56). Given these findings, highly potent neutralizing antibodies appear to afford better protection than polyfunctional non-neutralizing antibodies in HIV prevention. However, understanding the capacity for bNAbs to elicit these Fc-mediated effector functions has been of considerable interest as a potential way to harness the polyfunctionality of these antibodies. Additionally, given the promise shown by bNAbs in prevention, there has also been a push to investigate how these antibodies may be employed therapeutically.

A number of groups have independently performed assays designed to measure the protective and therapeutic efficacy of bNAbs across a wide-range of animal models (**Table 1**). Seminal work in this area by Hessell et al. demonstrated the importance of Fc-mediated effector functions of bNAbs in SHIV prevention. Variants of b12, a first-generation CD4bs bNAb, designed to abrogate Fc-interaction and engagement with FcγRs, were passively transferred into rhesus macaques to evaluate the contribution of Fc effector functions against SHIV challenge (13). Interestingly, NHPs that were given b12-LALA, an Fc variant in which mutations were engineered into the Fc region to diminish engagement with FcγRs and abrogate ADCD, ADCC, ADCP, and ADNP, were more susceptible to infection compared to macaques that were administered wildtype antibody. However, recent work by Hangartner et al. (60) performing a similar study with PGT121 found differing results (60). Demonstrating no difference in protection among NHPs given PGT121-WT and PGT121-LALA or PGT121-LALAPG, a variant that further reduces engagement with rhesus FcγRI and rhesus FcγRIIa, thereby reducing Fc-mediated function. Another recent study found similar results also comparing PGT121 and PGT121-LALA to measure protection afforded by Fc effector function in pigtail marques, finding that the neutralization potency of this bNAb renders Fc effector functions partially redundant (61). It may be more difficult to ascertain the role Fc-mediated effector functions play in protection with a highly potent bNAb, such as PGT121, compared to bNAbs that may be less potent, such as b12 where there may be a more clear distinction in the contribution of effector function (61). Given the results of these studies, it is possible that the protective efficacy of some bNAbs do not benefit from Fc-effector functions. As such, additional work will be needed to fully define the protective properties of Fc-mediated functions.

In addition to prevention, Fc-mediated effector functions of bNAbs have also been investigated in the context of driving viral clearance of established HIV infection. Recently, Asokan et al. measured the contribution of bNAb-mediated effector function in chronically infected rhesus macaques. SHIV-infected monkeys were treated with a CD4bs-directed bNAb, VRC07-LS, or variants harboring Fc mutations that either enhanced or diminished engagement with FcγRs. Using this panel of mutant antibodies, they determined that innate effector functions, such as ADCC, ADCP and complement fixation contributed approximately 21% of the observed rate of viral clearance (16). Interestingly, this study did find that VRC07-LS

**TABLE 1 |** Protective and therapeutic efficacy of bNAbs *in vivo*.

| Reference | Model System | bNAb | Human or Monkey Ab | Dose given (mg/kg) | Passive Transfer or AAV | Route | Challenge Virus | Virus Route | Dose | In vitro IC50 | Projected Conc at time of challenge | Isotype | Effector function | Outcome |
|---|---|---|---|---|---|---|---|---|---|---|---|---|---|---|
| Moldt et al. (35) | rhesus macaques | PGT121 | Human | 5<br>1<br>0.2 | P.T. | I.V. | SHIV-SF162P3 | intravaginal challenge | 300 TCID50 | 0.005μg/ml | High: 95μg/ml Medium: 15μg/ml Low:1/8μg/ml | IgG1 | N.A. | Protection at 5 and 1mg/kg and 3/5 protected at 0.2mg/kg, suggesting that protective serum concentrations for PGT121 is <10μg/ml |
| Shingai et al. (57) | rhesus macaques | VRC01<br>NIH45-46<br>45-46G54W<br>45-46m2<br>3BNC117<br>12A12<br>1NC9<br>8ANC195<br>10-1074<br>PGT121<br>PGT126 | Human | **Against AD8EO:** VRC01: 50, 20<br>PGT121 and 10-10-74: 20, 5, 1, 0.2<br>3BNC117: 5, 1<br>45-46m2: 20, 5<br>**Against DH12-V3AD8:** VRC01: 30<br>PGT121, 10-1074 and 3BNC117: 20, 1, 0.2, 0.05<br>45-46m2: 5 | P.T. | I.V. | SHIV-DH12-V3AD8<br>SHIV-AD8EO | rectal challenge | | AD8EO:<br>V3:0.09-0.15μg/ml,<br>CD4bs: 0.14μg/ml-6.36μg/ml<br>DH12-V3AD8 V3:<br>V3: 0.01-0.16μg/ml<br>CD4bs: 0.39-86.27μg/ml | AD8EO:<br>VRC01: 188-711μg/ml<br>PGT121: 1.8-267μg/ml<br>10-1074: 19-289μg/ml'<br>3BNC117: 215-105μg/ml<br>45-46m2: 2-15μg/ml<br>DH12-V3AD8:<br>VRC01: 306-395μg/ml<br>PGT121: 1-282μg/ml<br>10-1074: 19-290μg/ml<br>3BNC117: 3-294μg/ml<br>45-46m2: 2-4μg/ml | IgG1 | N.A. | Neutralizing titers were predictive of protection against both viruses; the higher the antibody conentration the more likely a monkey was to be protected |
| Pegu et al. (32) | rhesus macaques | 2D5<br>VRC01 | Human | 2D5:40 | P.T. | I.V. | SHIV-SF162P3 | rectal challenge | 300 TCID50 | | 2D5: 352μg/ml VRC01 high 60μg/ml, medium | IgG1 | N.A. | Protection with 2D5 (2/4) despite high concentration, VRC01 against SHIV-SF162P3 afforded complete protection, BalP4 challenges: all monkeys at high and medium doses of VRC01 |

*(Continued)*

**TABLE 1** | Continued

| Reference | Model System | bNAb | Human or Monkey Ab | Dose given (mg/kg) | Passive Transfer or AAV | Route | Challenge Virus | Virus Route | Dose | In vitro IC50 | Projected Conc at time of challenge | Isotype | Effector function | Outcome |
|---|---|---|---|---|---|---|---|---|---|---|---|---|---|---|
| | | | | | | | | | | | 22μg/ml, low 1.31μg/ml | | | were protected, at low dose (4/10), 10E8 protected all monkeys at high and medium doses, at low dose (3/6), PG9 protected (4/6) at high dose, (3/6) at medium and no moneys at low dose |
| | | 1E9 | | VRC01, 10E8, PG9: 20, 5, 0.3 | | | BALP4 | | | | 10E8 high 133μg/ml, medium 31μg/ml, low 1.8μg/ml | | | |
| | | PG9 | | | | | | | | | PG9 high 32μg/ml, medium 3.7μg/ml, low 0.28μg/ml | | | |
| Julg et al. (10) | rhesus macaques | PGDM1400 CAP256-VRC26.25-LS | Human | 2 0.4 0.08 | P.T. | I.V. | SHIV-325c | rectal challenge | 500 TCID50 | PGDM1400=0.037 CAP256-VRC26.25=0.003 | ~0.1-10μg/ml | IgG1 | N.A. | CAP256.VRC26 protection at high dose (3/3), medium (3/3), low (3/3), PGMD1400 protection at high dose (4/5), medium (5/5/), low (1/3) |
| Balazs et al. (18) | Hu-PBMC mice | 2G12 | Human | N.A. | AAV | I.V. | NL4-3 | I.P. and I.V. | 1ng p24 | | b12: 100μg/ml | IgG1 | N.A. | Mice given b12 were completely protected, mice given 2G12, 2F5 and 4E10 were partially protected. Mice expressing varying doses of VRC01 showed partial protection: Mice expressing less than 10μg/ml succumbed to infection but mice expressing >10μg/ml were protected |
| | | b12 | | | | | | | | | 2G12: 150μg/ml | | | |
| | | 2F5 | | | | | | | | | 2F5: 20μg/ml | | | |
| | | 4E10 | | | | | | | 10ng p24 | | 4E10: 20μg/ml | | | |
| | | VRC01 | | | | | | | | | VRC01: 0.1-200μg/ml | | | |
| Balazs et al. (21) | BLT humanized mice | b12 | Human | N.A. | AAV | I.V. | REJO.c | intravaginal challenge | 16ng p24 REJO.c | | b12: ~100-300μg/ml | IgG1 | N.A. | bNAbs can maintain long lasting expression using VIP, can also reach high concentrations that are protective against repeated mucosal challenge |
| | | VRC01 | | | | | JR-CSF | | 50ng p24 JR-CSF | | VRC01: ~100-300μg/ml | | | |
| | | VRC07W | | | | | | | | | VRC07W: ~100μg/ml | | | |
| Moldt et al. (58) | rhesus macaques | PGT126 | Human | 10 | P.T. | I.V. | SHIV-SF162P3 | intravaginal and rectal | unknown | 0.3μg/ml | 10mg/kg: 100-125μg/ml | IgG1 | N.A. | No difference in protection between either route of challenge, suggesting that there is similar efficacy of bNAb proteection against both primary transmission routes |
| | | | | 0.4 | | | | | | | 2mg/kg:25μg/ml | | | |

*(Continued)*

**TABLE 1** | Continued

| Reference | Model System | bNAb | Human or Monkey Ab | Dose given (mg/kg) | Passive Transfer or AAV | Route | Challenge Virus | Virus Route | Dose | In vitro IC50 | Projected Conc at time of challenge | Isotype | Effector function | Outcome |
|---|---|---|---|---|---|---|---|---|---|---|---|---|---|---|
| Rudicell et al. (59) | rhesus macaques | VRC01-LS<br>VRC07-523-LS | Human | 0.3<br>0.2<br>0.05 | P.T. | I.V. | SHIV-BalP4 | rectal challenge | 12,800 TCID50 | VRC01-LS: 0.028µg/ml<br>VRC07-523-LS: 0.005µg/ml | 0.4mg/kg: 4µg/ml<br>VRC01-LS: 2.5µg/ml<br>VRC07-523-LS: 0.47µg/ml | IgG1 | N.A. | VRC07-523-LS afforded better protection compared to VRC01-LS, suggesting that a more potent antibody can protect at these lower concentrations |
| Saunders et al. (11) | rhesus macaques | VRC01<br>VRC01-LS | Simian | 5 | P.T. | I.V. | SHIV-BalP4 | rectal challenge | unknown | 0.019µg/ml | VRC01: 0.1-1µg/ml<br>VRC01-LS: 2-6µg/ml | IgG1 | N.A. | Introducing an LS mutation into the antibody led to elevated antibody levels for a longer period of time and protected against mucosal challenge for up to two months after last antibody administration |
| Ko et al. (59) | rhesus macaques | VRC01, VRC01-LS VRC01-LS | Human | 0.3 | P.T. | I.V. | SHIV-BalP4 | rectal challenge | unknown | unknown | ~20-100µg/ml | IgG1 | FcRn and FcγRIIIa binding, ADCC | VRC01-LS affords better protection against viral challenge than VRC01, due to its enhanced binding with FcRn. No detectable difference in the ability to bind FcRIIIa, suggesting that ADCC is intact |
| Hessell et al. (13) | rhesus macaques | b12-WT<br>b12-LALA | Human | 1 | P.T. | I.V. | SHIV-SF162P3 | intravaginal challenge | TCID50 10 | 0.18µg/ml | b12: ~45-70µg/ml<br>b12-LALA: ~5-55µg/ml, | IgG1 | b12-WT can mediate effector functions, LALA variant cannot mediate any function | Two-fold difference in hazard ratio between WT and LALA variant number of challenges to infection, effector function appears to play a role in this difference in protection |
| Hessell et al. (38) | rhesus macaques | b12-WT<br>b12-LALA<br>b12-KA | Human | 25 | P.T. | I.V. | SHIV-SF162P3 | intravaginal challenge | 300 TCID50 | unknown | b12-WT: 562µg/ml<br>b12-KA: 616µg/ml<br>b12-LALA: 534µg/ml | IgG1 | C1q and FcγR binding | No difference in protection between b12-WT and b12-KA (8/9 protected), but monkeys given b12-LALA were less protected (5/9) |
| Bournazos et al. (37) | Luciferase reporter mice transduced with AdV hCCR5-A2-hCD4 | 3BNC117<br>Jan-74<br>3BCN60<br>Jan-79<br>3BC176<br>PGT121<br>PG16 | mouse-human chimeric (human bNAbs with mouse | 200µg | P.T. | S.C. | HIV-YU-2 Cre pseudovirus | I.V. | unknown | 3BNC117: 0.021<br>1-74: >50<br>3BNC60: 0.018<br>1-79: 24.8<br>3BNC176: 1.278<br>PGT121: 0.44<br>PG16: 0.8 | unknown | mIgG2a and mIgG1 D265A | FcγR binding as a surrogate for Fc effector function | mIgG1 and mIgG1 D265A (Fc-null) variants of bNAbs had higher rates of infection compared to mIgG2a (intact Fc function) variants of all bNAbs, suggesting that Fc-mediated effector functions play a role in protection |

*(Continued)*

**TABLE 1** | Continued

| Reference | Model System | bNAb | Human or Monkey Ab | Dose given (mg/kg) | Passive Transfer or AAV | Route | Challenge Virus | Virus Route | Dose | In vitro IC50 | Projected Conc at time of challenge | Isotype | Effector function | Outcome |
|---|---|---|---|---|---|---|---|---|---|---|---|---|---|---|
| | | | constant region heavy chains) | | | | | | | | | | | |
| Bournazos et al. (37) | NRG humanized mice | 3BNC117-WT 3BNC117-GRLR 3BNC117-GASDALIE | Human | 100μg/ml (high dose) 20μg/ml (low dose) | P.T. | S.C. | HIV-YU-2 | I.V. | 57.5ng p24 | 0.021μg/ml | >10μg/ml | IgG1 | FcγR binding as a surrogate for Fc effector function | Mice given 3BNC117-GASDALIE (Fc enahncing) exhibited lower rates of infection compared to WT and 3BNC117-GRLR (Fc-null) |
| Julg et al. (10) | rhesus macaques | 3BNC117, PGT121 | Human | 10<br>2 | P.T. | I.V. | SHIV-327c | rectal challenge | 300 TCID50 | PGT121=0.11μg/ml 3BNC117=0.84μg/ml | ~50-150μg/ml | IgG1 | ADCP and CDC | PGT121 protected monkeys at both doses (high dose 4/4, low dose 2/2), 3BNC117 did not protect at low dose (0/3) and only protect 1/4 monkeys at high dose, no dfference in mediating effector function |
| Hangartner et al. (60) | rhesus macaques | PGT121<br>PGT121-LALA,<br>PGT121-LALAPG | Human | 1 | P.T. | I.V. | SHIV-SF162P3 | intravaginal challenge | 300 TCID50 | | PGT121: 5-10μg/ml PGT121-LALA: 5-18μg/ml PGT121-LALAPG: 5-20μg/ml | IgG1 | ADCP and ADCC | No difference in protection between PGT121 and PGT121-LALA, suggesting that effector function for this antibody maynot contribute to protection against this given virus |

*N.A., not applicable; S.C., subcutaneous.*

with Fc mutations to enhance FcγR binding led to NK cell death one hour after bnAb infusion, likely due to FcγRIIIa cross-linking on the cell surface and driving necroptosis, in turn leading to reduced ADCC. It is possible that over-optimization of an antibody may have detrimental effects early on in delivery, and this should be taken into consideration if these antibodies are to be used therapeutically.

Humanized mice have also been an effective model in which to study the role of antibody effector functions (12, 37, 62). Similar to NHP studies, several groups have investigated the protective effects of various bNAbs and their ability to drive effector functions in the context of both HIV prevention and viral clearance during infection. In one study, humanized NOD *Rag1*$^{-/-}$*Il2g*$^{null}$ (NRG) mice given the CD4-binding site targeting bNAb 3BNC117 and challenged with HIV were found to have enhanced viral clearance 24 hours-post challenge compared to the control mice given a non-specific antibody (37). 3BNC117 has also been used to measure the role of innate immunity in ART treated humanized NRG mice (62). Mutations were introduced into the Fc-region of the antibody to abrogate binding to both murine and human FcγRs. HIV-infected mice taken off ART and given Fc-null (3BNC117-GRLR) antibody exhibited slower viral clearance as compared to mice given the wild-type antibody and similar clearance to control mice given a non-specific antibody. These studies implicate innate cells through Fc engagment in viral clearance in humanized mice. Other work has also aimed to measure the contribution of Fc-mediated viral clearance during early infection (12). In this study, a bi-specific bNAb composed of 3BNC117 and PGDM1400 was administered to infected mice. Another group of infected mice were given the same bNAb harboring mutations in the Fc-region to prevent FcγR engagement and downstream effector functions. Results showed that innate effector functions contributed 25-31% of the antiviral activity seen in humanized mice while 75% was due to antibody neutralization.

Considerable effort has been made to determine whether there are optimal epitopes on the viral envelope that may facilitate these activities. BNAbs targeting each of the major epitopes have been assessed for their ability to mediate innate functions, including ADCC, ADCP, and antibody-dependent complement mediated cell lysis (ADCML) against diverse viruses that span various clades (63, 64). Interestingly, while neutralization potency does not appear to predict effector function, there is a weak correlation between antibody binding and effector function (63, 64). Other groups have confirmed these findings, showing that neither neutralization potency nor breadth are strong predictors of effector activity (64–68). Instead they have shown that binding avidity is better correlated with function (64–68). As of yet, there is no clear consensus of which target epitope for bNAbs best mediates Fc-driven functions. Instead, it has been suggested that modes of binding by non-neutralizing antibodies can have a dramatic effect on the resulting potency of the downstream effector function such as ADCC (67). Two monoclonal antibodies targeting the C1 and C4 gp120 regions with similar antigen affinities exhibit markedly different responses in driving ADCC (67). Interestingly, when crystal structures were determined for each of the antibodies with the corresponding antigen, they showed that antibody orientation on the bound antigen may have enhanced formation of an immune complex, resulting in increased potency of downstream innate immunity (67). The angle of approach for a given bNAb likely affects how these immune complexes can form and engage with FcγRs (67). Additionally, numerous structural studies have elucidated FcγR-Fc interactions to determine the precise mechanism of antibody binding to FcγRs (40, 69–72). Antibody-antigen structures have also provided insight on Fc presentation and angle of antibody binding to an antigen may influence optimal FcγR engagement to lead to downstream effector function, such as ADCC (73). There is still much work to be done to understand how modes of antibody engagement can drive effector functions across diverse viral strains and how antibodies function post antigen-binding.

Other avenues of investigation have looked to optimize bNAbs to elicit more potent Fc effector function. One potential approach has been the use of bNAbs expressed as different isotypes that have enhanced effector function, such as IgG3. Recent work by Richardson et al. (74) compared IgG1 and IgG3 variants of V2-specific bNAbs CAP256-VRC26.25 and CAP256-VRC29 to measure how isotype contributed to potent Fc effector functions (74). The group was able to isolate these two bNAbs from an HIV-infected individual that had mounted a potent V2-specific response and elicited high levels of IgG3 antibodies that significantly contributed to the total effector function activity measured in the serum (74). These two bNAbs, CAP256-VRC26.25 and CAP256-VRC29, were constructed as IgG3 variants using different IGHG3 alleles to measure Fc function and neutralization. They also expressed these bNAbs as IgG1 isotypes and found reduced neutralization and Fc function compared to the IgG3 variants but no difference in antigen binding. They found IgG3 potency was likely due to its longer hinge length than that of IgG1. Therapeutically, however, employing IgG3 in patients may pose a challenge as the affinity for the neonatal receptor FcRn is drastically reduced compared to IgG1, leading to a far shorter half-life (75). However, recent work demonstrated that alteration of the hinge length of IgG1 and IgG3 bNAbs VRC01 and 447-52D contributed to Fc mediated effector functions (76). To make the IgG1 variants, exons derived from IgG3, including exon a which encodes the upper and core hinge regions, and exons b-d that encode the core hinge repeat sequence were sequentially added, resulting in hinge variants up to 5 times longer than wild-type IgG1. They repeated the same hinge alteration for IgG3, and included the IgG1 hinge length as an additional variant. When measuring phagocytosis by all these variants, they found that a longer hinge length significantly enhanced the Fc effector function, suggesting that the length can lead to a more potent response. In addition, *in vivo* stability of hinge variants of IgG1 were measured and the rate of plasma decay in mice was similar to that of the wild-type, suggesting that such alterations may be viable approaches to harness Fc mediated effector function by bNAbs.

In addition to understanding how hinge length, isotype and subclass contribute to optimal Fc effector function, considerable

effort has identified point mutations in the Fc region capable of enhancing FcγR engagement and downstream function (77). In 2001, Shields et al. mapped the binding site of IgG1 for FcγRs, including FcγRII, FcγRIIIa and FcRn by mutagenesis of an IgG1 antibody. From these variants, specific point mutations in the Fc region of the antibody emerged that could enhance or diminish binding to the FcγRs described above (78). One modification, S298A/E333A/K334A, showed enhanced binding to FcγRIIIa but decreased binding to FcγRIIa, resulting in improved ADCC response. Further work has elucidated alternative Fc modifications that have led to enhanced FcγRIIIa binding and ADCC, including S239D/I332E, S329D/A330L/I332E, G236A/S239D/I332E and F243L/R292P/Y300L/V305I/P396L (79–81). Other Fc modifications have led to increased FcγRIIa binding and ADCP, including G236A, G236A/A330I/I332E, and G236A/S239D/A330L/I332E (80, 82). Some mutations have led to both enhanced ADCC and ADCP, including S239D/I332E, S239D/A330L/I332E and G236A/S239D/I332E. In addition to introduction of Fc point mutations, afucosylation of IgG1 antibodies led to dramatically increased ADCC (83). Minimal alterations to antibodies can maximize downstream Fc functionality, and these modifications can be used therapeutically to improve bNAb-mediated protection.

Given the potential for bNAb-mediated protection in HIV prevention and viral clearance, the question of implementation has come to the forefront. The AMP clinical trials utilized passive transfer of VRC01, a CD4bs bNAb, to measure HIV prevention in different populations, including HIV-uninfected men who have sex with men (MSM), transgender men who have sex with men, and sexually active women in sub-Saharan Africa (17, 84–86) ClinicalTrials.gov: NCT02716675 (17, 84–86). The results from these trials have been promising, with excellent safety and tolerability to bNAb administration and reduced transmission of sensitive strains. However, one drawback to passive immunization is the need for constant re-administration in order to maintain steady-state bNAb concentrations. This requirement poses significant challenges to feasibly scale and implement as a widespread prophylaxis. In order to overcome this challenge, other methods of delivery can be employed, such as vector-mediated delivery. Adeno Associated Virus (AAV) based gene replacement therapies have been used to treat a variety of diseases, and recent advances in AAV technology have demonstrated sustained bNAb expression in humans in an ongoing clinical trial.

## UTILIZING AAV-DELIVERY OF BROADLY NEUTRALIZING ANTIBODIES

AAVs are non-enveloped viruses that belong to the Parvoviridae family (85, 86). AAVs are unable to replicate on their own, and as such require a helper virus, such as an adenovirus or herpesvirus to productively replicate within cells (87–90). They are composed of an icosahedral protein capsid surrounding a single stranded DNA genome of approximately 4700 base pairs. The natural AAV genome consists of a *rep* and *cap* gene flanked by two inverted terminal repeats (ITRs) (91). The *rep* gene encodes proteins necessary for virion assembly, including Rep78, Rep68, Rep52 and Rep40. The *cap* gene encodes for three capsid proteins, VP1, VP2 and VP3 and the assembly activating protein (AAP) and membrane-associated accessory protein (MAAP) in alternative reading frames (87, 92–97). AAV virions are comprised of 60 VP subunits, and each subunit has nine variable regions that dictate tropism and intracellular trafficking (91). Currently, there are more than 100 AAV serotypes identified that all differ in primary receptor usage and tissue tropism (98). During infection, AAVs bind to receptors on target cells which trigger endocytosis into endosomes from which they escape and traffic to the nucleus. Here, the inverted terminal repeats (ITRs) present on either end of the genome self-prime second strand synthesis, which is the rate-limiting step prior to gene expression (99–102). The ITRs are the only requirement for packaging DNA into the capsid (103) As a consequence, recombinant AAV vectors have approximately 96% of their genome removed, including all viral coding sequences. This allows for greater packaging capacity and lowers the potential for viral toxicity (91). In place of these coding sequences, a transgene of interest, up to approximately 4,500 base pairs, can be introduced between the ITRs (104). Following transduction, these recombinant viral genomes form head-to-tail concatemers within the nucleus, where they persist as non-integrated episomal genomes (105, 106).

To date, AAV gene therapies have been successful in treating diseases in the therapeutic areas of ophthalmology, neurology, hematology, metabolic and musculoskeletal disorders (99, 107). This platform can also be used for delivering biological therapeutics for chronic infectious diseases, such as HIV, through delivery of small molecule inhibitors, immunoadhesins, or HIV broadly neutralizing antibodies. This platform has the benefit of enabling specific gene-encoded antibodies to be delivered, representing a viable approach to incorporating Fc-enhancing mutations to improve innate immune functionality of the delivered protein. In 2002, Lewis et al. demonstrated the use of a dual promoter rAAV vector to express full-length b12 in $Rag1^{-/-}$ mice (20). Subsequent enhancements were made to the viral vector by Fang et al. improved packaging and cleavage of these antibodies *in vivo* using a picornavirus 2A self-processing peptide in order to express both the heavy and light chains of an antibody from a single open reading frame (19). A furin cleavage site was also introduced between the C-terminus of the heavy chain and N-terminus of the 2A sequence to enable removal of remaining 2A residues (108). These alterations led to significant improvement in antibody expression, resulting in concentrations well over 1mg/ml in serum.

Johnson et al. first demonstrated the efficacy of a self-complementary AAV (scAAV) vector that expressed SIV-specific immunoadhesins composed of recombinant antibody fragments (109). They administered one intramuscular injection of this scAAV1 into rhesus macaques, resulting in serum expression of the immunoadhesins four weeks after

administration. Our lab utilized AAV serotype 8 capsid to express a full-length HIV bNAb *in vivo*. Enhancements were made to the vector, including designing a novel promoter that combined the CMV enhancer and chicken β-actin promoter followed by an artificial intron containing the ubiquitin enhancer region (18). These changes led to significantly improved antibody expression which enabled this improved vector system to deliver various HIV bNAbs targeting different viral epitopes and measured protection against repeated HIV mucosal challenge in humanized mice (21). This system has also been used to deliver CAP256-antibodies and CAP228-antibodies in immunocompetent mice, both of which target the V2 loops and have been shown to mediate ADCC (110). NHP studies have also demonstrated expression of a simianized form of VRC07, a CD4bs-directed bNAb, and anti-SIV neutralizing antibodies, ITS01 and ITS06.02 (111, 112). As a result of these promising proof-of-concept animal studies, two separate Phase I clinical trials were initiated to test VIP in humans.

In one study, AAV was used to deliver PG9, a V1V2-directed bNAb, chosen for its potent neutralization capacity (ClinicalTrials.gov: NCT01937455) (113). This clinical trial looked at the safety and efficacy of PG9 delivery using an rAAV-1 vector. The PG9 heavy and light chains were codon optimized to increase expression in the rAAV vector. Additionally, a 21-amino acid synthetic signal peptide was included in order to improve secretion into the serum. The transgene consisted of a dual promoter system to independently express the variable heavy and variable light chains of the IgG1 antibody. The heavy chain was expressed under a CMV promoter and the light chain was expressed by the EF1a promoter (**Figure 2**). Healthy, non-HIV infected, men aged 18-45 were administered rAAV1-PG9DP through intramuscular injection. Results showed that the AAV caused no harmful side effects to the volunteers, and muscle biopsies showed detectable PG9 by RT-PCR as well as IgG within muscle cells and extracellular tissues by immunohistochemistry. However, PG9 was not detectable in the serum by ELISA, although it is important to note that the limit of detection in the assay was 2.5μg/ml. In support of these findings, no HIV neutralizing activity was detectable in the sera. Importantly, they observed anti-drug antibody responses in many of the participants of the study, suggesting that these may have limited the potential for PG9 expression (113).

Independently, a second on-going clinical trial by the NIH is testing the safety and efficacy of VRC07 delivery through an rAAV8 viral vector to HIV-infected adults aged 18-60 (AAV8-VRC07; ClinicalTrials.gov: NCT03374202). The vector design used in this study was analogous to those described in previous papers from our laboratory and include the CASI promoter and optimized F2A-containing VRC07 transgene (**Figure 2**). Recent results from this clinical trial presented at the 2021 Conference on Retroviruses and Opportunistic Infections meeting showed detectable expression of VRC07 antibody as high as 1μg/mL in circulation, with several patients maintaining VRC07 concentrations well over a year after administration. In contrast to results from the earlier study, VRC07 neutralizing activity was detected in trial participants, suggesting that antibodies produced as a result of VIP retained their activity *in vivo*. This trial represents the first demonstration of long-lived systemic production of a broadly neutralizing antibody in humans, providing strong evidence for the potential of vectored antibody delivery. Despite this success, some participants developed anti-drug antibodies against the VRC07 antibody variable regions, leading to loss of antibody expression.

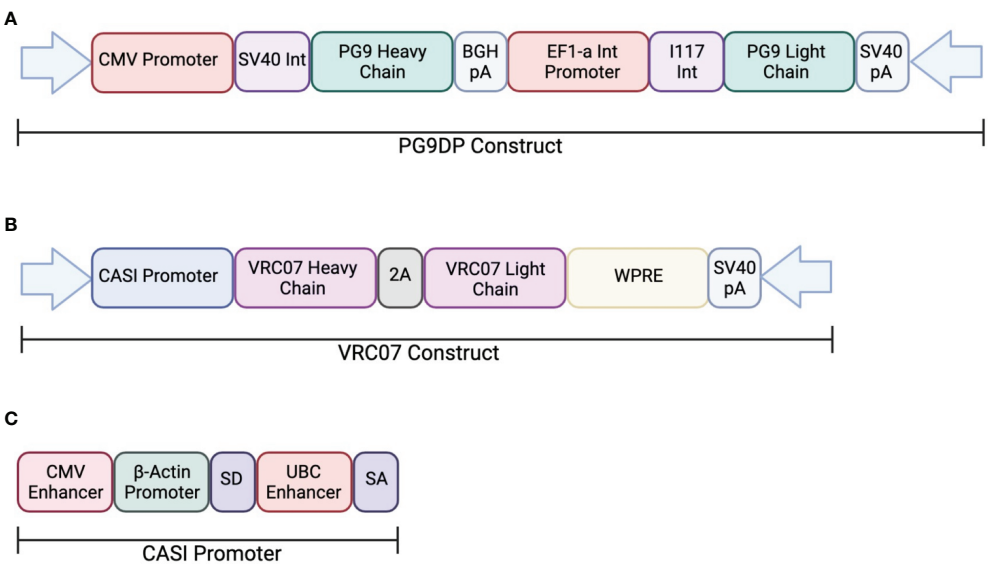


**FIGURE 2** | Transgene construct used in clinical trials testing AAV delivery of bNAbs. **(A)** The dual promotor transgene cassette was used to expressed PG9 in an rAAV-1 vector. The heavy chain is expressed the CMV promoter while the light chain is expressed by the EF1a promoter. **(B)** The transgene cassette used to express VRC07 in an rAAV-8 vector. Both heavy and light chains are expressed through the CASI promotor shown in **(C)**.

As such, additional improvements to the AAV transgene may be necessary to enable widespread use of VIP for HIV prevention. Looking forward, this system could be utilized for delivery of optimized bNAbs that contain altered Fc-regions with hinge length changes or even different isotypes to improve FcγR binding. The use of such optimized transgenes has the potential to reduce the concentrations of bNAbs necessary to prevent HIV acquisition.

## DISCUSSION

Broadly neutralizing antibodies have been shown to be promising candidates for HIV prevention, therapy and possibly cure. Passive administration of bNAbs have demonstrated that antibody concentration and potency are important parameters correlated with protection against HIV acquisition. Other non-neutralizing functions, including ADCC, ADCP and ADCD have also been shown to be critical in this context. As a result, there is growing interest in understanding whether there are optimal viral epitopes that antibodies can target to effectively elicit protective responses. Early findings from the RV144 vaccine study suggested that non-neutralizing antibodies targeting the V2 site were implicated in preventing disease acquisition. However, when bNAbs targeting different sites of vulnerability were tested for their ability to mediate these same non-neutralizing functions, results were variable and largely dependent upon the challenge virus. Further work is needed to understand if there is an optimal site that can facilitate these functions across a wide range of diverse strains. Additionally, several *in vivo* studies measured the contribution of these effector functions in protection, but questions remain as to contributions of individual functions, such as ADCC, to mediating protection. Future work could help to identify which effector functions contribute most to bNAb-mediated protection, and armed with this improved understanding, specific Fc mutations or hinge length modifications could be made to the antibody to improve therapeutic outcomes. These are especially relevant in the context of vectored antibody delivery, which represents a promising approach capable of integrating advances made in our understanding of antibody-mediated innate immune function into future clinical products. However, transduction efficiency is relatively low as compared to pre-clinical models and there appears to be a significant proportion of recipients who mount an immune response against the antibody transgene. Future studies will be needed to improve the consistency of antibody delivery using this system, including optimizing the vector to improve antibody concentrations and minimizing anti-drug antibodies elicited in response to existing rAAV vectors.

## AUTHOR CONTRIBUTIONS

MP and AB conceived of and wrote the manuscript. All authors contributed to the article and approved the submitted version.

## REFERENCES


1. Pandey A, Galvani AP. The Global Burden of HIV and Prospects for Control. *Lancet HIV*. (2019) 6(12):e809–11. doi: 10.1016/S2352-3018(19)30230-9
2. Morris L, Mkhize NN. Prospects for Passive Immunity to Prevent HIV Infection. *PloS Med* (2017) 14(11):e1002436. doi: 10.1371/journal.pmed.1002436
3. Martinez-Navio JM, Fuchs SP, Pantry SN, Lauer WA, Duggan NN, Keele BF, et al. Adeno-Associated Virus Delivery of Anti-HIV Monoclonal Antibodies can Drive Long-Term Virologic Suppression. *Immunity* (2019) 50(3):567–75. doi: 10.1016/j.immuni.2019.02.005
4. Gardner MR. Promise and Progress of an HIV-1 Cure by Adeno-Associated Virus Vector Delivery of Anti-HIV-1 Biologics. *Front Cell Infect Microbiol* (2020) 10:176. doi: 10.3389/fcimb.2020.00176
5. Gray ES, Madiga MC, Hermanus T, Moore PL, Wibmer CK, Tumba NL, et al. The Neutralization Breadth of HIV-1 Develops Incrementally Over Four Years and Is Associated With CD4+ T Cell Decline and High Viral Load During Acute Infection. *J Virol* (2011) 85(10):4828–40. doi: 10.1128/JVI.00198-11
6. Hraber P, Seaman MS, Bailer RT, Mascola JR, Montefiori DC, Korber BT. Prevalence of Broadly Neutralizing Antibody Responses During Chronic HIV-1 Infection. *AIDS* (2014) 28(2):163–9. doi: 10.1097/QAD.0000000000000106
7. Klein F, Mouquet H, Dosenovic P, Scheid JF, Scharf L, Nussenzweig MC. Antibodies in HIV-1 Vaccine Development and Therapy. *Science* (2013) 341(6151):1199–204. doi: 10.1126/science.1241144
8. Walker LM, Huber M, Doores KJ, Falkowska E, Pejchal R, Julien J-P, et al. Broad Neutralization Coverage of HIV by Multiple Highly Potent Antibodies. *Nature* (2011) 477(7365):466–70. doi: 10.1038/nature10373
9. Julg B, Sok D, Schmidt SD, Abbink P, Newman RM, Broge T, et al. Protective Efficacy of Broadly Neutralizing Antibodies With Incomplete Neutralization Activity Against Simian-Human Immunodeficiency Virus in Rhesus Monkeys. *J Virol* (2017) 91(20):e.1187–17. doi: 10.1128/JVI.01187-17
10. Julg B, Tartaglia LJ, Keele BF, Wagh K, Pegu A, Sok D, et al. Broadly Neutralizing Antibodies Targeting the HIV-1 Envelope V2 Apex Confer Protection Against a Clade C SHIV Challenge. *Sci Trans Med* (2017) 9:eaal1321. doi: 10.1126/scitranslmed.aal1321
11. Saunders KO, Pegu A, Georgiev IS, Zeng M, Joyce MG, Yang Z-Y, et al. Sustained Delivery of a Broadly Neutralizing Antibody in Nonhuman Primates Confers Long-Term Protection Against Simian/Human Immunodeficiency Virus Infection. *J Virol* (2015) 89(11):5895–903. doi: 10.1128/JVI.00210-15
12. Wang P, Gajjar MR, Yu J, Padte NN, Gettie A, Blanchard JL, et al. Quantifying the Contribution of Fc-Mediated Effector Functions to the Antiviral Activity of Anti–HIV-1 Igg1 Antibodies *In Vivo*. *Proc Natl Acad Sci* (2020) 117:18002–9. doi: 10.1073/pnas.2008190117
13. Hessell AJ, Poignard P, Hunter M, Hangartner L, Tehrani DM, Bleeker WK, et al. Effective, Low-Titer Antibody Protection Against Low-Dose Repeated Mucosal SHIV Challenge in Macaques. *Nat Med* (2009) 15:951–4. doi: 10.1038/nm.1974
14. Liao H-X, Bonsignori M, Munir Alam S, McLellan JS, Tomaras GD, Anthony Moody M, et al. Vaccine Induction of Antibodies Against a Structurally Heterogeneous Site of Immune Pressure Within HIV-1 Envelope Protein Variable Regions 1 and 2. *Immunity* (2013) 38:176–86. doi: 10.1016/j.immuni.2012.11.011
15. Ackerman ME, Barouch DH, Alter G. Systems Serology for Evaluation of HIV Vaccine Trials. *Immunol Rev* (2017) 275(1):262–70. doi: 10.1111/imr.12503
16. Asokan M, Dias J, Liu C, Maximova A, Ernste K, Pegu A, et al. Fc-Mediated Effector Function Contributes to the *In Vivo* Antiviral Effect of an HIV Neutralizing Antibody. *Proc Natl Acad Sci U S A* (2020) 117(31):18754–63. doi: 10.1073/pnas.2008236117

17. Corey L, Gilbert PB, Juraska M, Montefiori DC, Morris L, Karuna ST, et al. Two Randomized Trials of Neutralizing Antibodies to Prevent HIV-1 Acquisition. *N Engl J Med* (2021) 384(11):1003–14. doi: 10.1056/NEJMoa2031738
18. Balazs AB, Chen J, Hong CM, Rao DS, Yang L, Baltimore D. Antibody-Based Protection Against HIV Infection by Vectored Immunoprophylaxis. *Nature* (2012) 481:81–4. doi: 10.1038/nature10660
19. Fang J, Qian J-J, Yi S, Harding TC, Tu GH, VanRoey M, et al. Stable Antibody Expression at Therapeutic Levels Using the 2A Peptide. *Nat Biotechnol* (2005) 23(5):584–90. doi: 10.1038/nbt1087
20. Lewis AD, Chen R, Montefiori DC, Johnson PR, Reed Clark K. Generation of Neutralizing Activity Against Human Immunodeficiency Virus Type 1 in Serum by Antibody Gene Transfer. *J Virol* (2002) 76:8769–75. doi: 10.1128/jvi.76.17.8769-8775.2002
21. Balazs AB, Ouyang Y, Hong CM, Chen J, Nguyen SM, Rao DS, et al. Vectored Immunoprophylaxis Protects Humanized Mice From Mucosal Hiv Transmission. *Nat Med* (2014) 20(3):296–300. doi: 10.1038/nm.3471
22. Fuchs SP, Martinez-Navio JM, Piatak MJr, Lifson JD, Gao G, Desrosiers RC. AAV-Delivered Antibody Mediates Significant Protective Effects Against Sivmac239 Challenge in the Absence of Neutralizing Activity. *PloS Pathog* (2015) 11(8):e1005090. doi: 10.1371/journal.ppat.1005090
23. Burton DR, Barbas CF, Persson MA, Koenig S, Chanock RM, Lerner RA. A Large Array of Human Monoclonal Antibodies to Type 1 Human Immunodeficiency Virus From Combinatorial Libraries of Asymptomatic Seropositive Individuals. *Proc Natl Acad Sci* (1991) 88:10134–7. doi: 10.1073/pnas.88.22.10134
24. Burton DR, Pyati J, Koduri R, Sharp SJ, Thornton GB, Parren PW, et al. Efficient Neutralization of Primary Isolates of HIV-1 by a Recombinant Human Monoclonal Antibody. *Science* (1994) 266(5187):1024–7. doi: 10.1126/science.7973652
25. Purtscher M, Trkola A, Gruber G, Buchacher A, Predl R, Steindl F, et al. A Broadly Neutralizing Human Monoclonal Antibody Against Gp41 of Human Immunodeficiency Virus Type 1. *AIDS Res Hum Retroviruses* (1994) 10p:1651–8. doi: 10.1089/aid.1994.10.1651
26. Muster T, Guinea R, Trkola A, Purtscher M, Klima A, Steindl F, et al. Cross-Neutralizing Activity Against Divergent Human Immunodeficiency Virus Type 1 Isolates Induced by the Gp41 Sequence ELDKWAS. *J Virol* (1994) 68 (6):4031–4. doi: 10.1128/jvi.68.6.4031-4034.1994
27. Burton DR, Hangartner L. Broadly Neutralizing Antibodies to HIV and Their Role in Vaccine Design. *Annu Rev Immunol* (2016) 34:635–59. doi: 10.1146/annurev-immunol-041015-055515
28. Munro JB, Mothes W. Structure and Dynamics of the Native HIV-1 Env Trimer. *J Virol* (2015) 89(11):5752–5. doi: 10.1128/JVI.03187-14
29. McCoy LE. The Expanding Array of HIV Broadly Neutralizing Antibodies. *Retrovirology* (2018) 15(1):70. doi: 10.1186/s12977-018-0453-y
30. Bonsignori M, Liao H-X, Gao F, Williams WB, Munir Alam S, Montefiori DC, et al. Antibody-Virus Co-Evolution in HIV Infection: Paths for HIV Vaccine Development. *Immunological Rev* (2017) 275:145–60. doi: 10.1111/imr.12509
31. Yuan M, Cottrell CA, Ozorowski G, van Gils MJ, Kumar S, Wu NC, et al. Conformational Plasticity in the HIV-1 Fusion Peptide Facilitates Recognition by Broadly Neutralizing Antibodies. *Cell Host Microbe* (2019) 25(6):873–83.e5. doi: 10.1016/j.chom.2019.04.011
32. Pegu A, Yang Z-Y, Boyington JC, Wu L, Ko S-Y, Schmidt SD, et al. Neutralizing Antibodies to HIV-1 Envelope Protect More Effectively In Vivo Than Those to the CD4 Receptor. *Sci Transl Med* (2014) 6 (243):243ra88. doi: 10.1126/scitranslmed.3008992
33. Barouch DH, Whitney JB, Moldt B, Klein F, Oliveira TY, Liu J, et al. Therapeutic Efficacy of Potent Neutralizing HIV-1-Specific Monoclonal Antibodies in SHIV-Infected Rhesus Monkeys. *Nature* (2013) 503 (7475):224–8. doi: 10.1038/nature12744
34. Gautam R, Nishimura Y, Pegu A, Nason MC, Klein F, Gazumyan A, et al. A Single Injection of Anti-HIV-1 Antibodies Protects Against Repeated SHIV Challenges. *Nature* (2016) 533(7601):105–9. doi: 10.1038/nature17677
35. Moldt B, Rakasz EG, Schultz N, Chan-Hui P-Y, Swiderek K, Weisgrau KL, et al. Highly Potent Hiv-Specific Antibody Neutralization *In Vitro* Translates Into Effective Protection Against Mucosal Shiv Challenge *In Vivo*. *Proc Natl Acad Sci* (2012) 109:18921–5. doi: 10.1073/pnas.1214785109
36. Sok D, Burton DR. Publisher Correction: Recent Progress in Broadly Neutralizing Antibodies to HIV. *Nat Immunol* (2019) 20(3):374. doi: 10.1038/s41590-019-0329-x
37. Bournazos S, Klein F, Pietzsch J, Seaman MS, Nussenzweig MC, Ravetch JV. Broadly Neutralizing Anti-HIV-1 Antibodies Require Fc Effector Functions for *In Vivo* Activity. *Cell* (2014) 158(6):1243–53. doi: 10.1016/j.cell.2014.08.023
38. Hessell AJ, Hangartner L, Hunter M, Havenith CEG, Beurskens FJ, Bakker JM, et al. Fc Receptor But Not Complement Binding Is Important in Antibody Protection Against HIV. *Nature* (2007) 449(7158):101–4. doi: 10.1038/nature06106
39. Nimmerjahn F, Ravetch JV. Fcgamma Receptors as Regulators of Immune Responses. *Nat Rev Immunol* (2008) 8(1):34–47. doi: 10.1038/nri2206
40. Nimmerjahn F, Gordan S, Lux A. Fcγr Dependent Mechanisms of Cytotoxic, Agonistic, and Neutralizing Antibody Activities. *Trends Immunol* (2015) 36 (6):325–36. doi: 10.1016/j.it.2015.04.005
41. Bruhns P. Properties of Mouse and Human Igg Receptors and Their Contribution to Disease Models. *Blood* (2012) 119(24):5640–9. doi: 10.1182/blood-2012-01-380121
42. Bryceson YT, March ME, Ljunggren H-G, Long EO. Activation, Coactivation, and Costimulation of Resting Human Natural Killer Cells. *Immunol Rev* (2006) 214:73–91. doi: 10.1111/j.1600-065X.2006.00457.x
43. Belizário JE, Neyra JM, Rodrigues MFS. When and How NK Cell-Induced Programmed Cell Death Benefits Immunological Protection Against Intracellular Pathogen Infection. *Innate Immun* (2018) 24:452–65. doi: 10.1177/1753425918800200
44. Prager I, Watzl C. Mechanisms of Natural Killer Cell-Mediated Cellular Cytotoxicity. *J Leukoc Biol* (2019) 105(6):1319–29. doi: 10.1002/JLB.MR0718-269R
45. Lu LL, Suscovich TJ, Fortune SM, Alter G. Beyond Binding: Antibody Effector Functions in Infectious Diseases. *Nat Rev Immunol* (2018) 18(1):46–61. doi: 10.1038/nri.2017.106
46. Dunkelberger JR, Song W-C. Complement and its Role in Innate and Adaptive Immune Responses. *Cell Res* (2010) 20(1):34–50. doi: 10.1038/cr.2009.139
47. Merle NS, Church SE, Fremeaux-Bacchi V, Roumenina LT. Complement System Part I - Molecular Mechanisms of Activation and Regulation. *Front Immunol* (2015) 6:262. doi: 10.3389/fimmu.2015.00262
48. Karasavvas N, Billings E, Rao M, Williams C, Zolla-Pazner S, Bailer RT, et al. The Thai Phase III HIV Type 1 Vaccine Trial (RV144) Regimen Induces Antibodies That Target Conserved Regions Within the V2 Loop of Gp120. *AIDS Res Hum Retroviruses* (2012) 28(11):1444–57. doi: 10.1089/aid.2012.0103
49. Chung AW, Crispin M, Pritchard L, Robinson H, Gorny MK, Yu X, et al. Identification of Antibody Glycosylation Structures That Predict Monoclonal Antibody Fc-Effector Function. *AIDS* (2014) 28(17):2523–30. doi: 10.1097/QAD.0000000000000444
50. Yates NL, Liao H-X, Fong Y, deCamp A, Vandergrift NA, Williams WT, et al. Vaccine-Induced Env V1-V2 Igg3 Correlates With Lower HIV-1 Infection Risk and Declines Soon After Vaccination. *Sci Transl Med* (2014) 6(228):228ra39. doi: 10.1126/scitranslmed.3007730
51. Haynes BF, Gilbert PB, McElrath MJ, Zolla-Pazner S, Tomaras GD, Alam SM, et al. Immune-Correlates Analysis of an HIV-1 Vaccine Efficacy Trial. *N Engl J Med* (2012) 366(14):1275–86. doi: 10.1056/NEJMoa1113425
52. Bradley T, Pollara J, Santra S, Vandergrift N, Pittala S, Bailey-Kellogg C, et al. Pentavalent Hiv-1 Vaccine Protects Against Simian-Human Immunodeficiency Virus Challenge. *Nat Commun* (2017) 8:15711. doi: 10.1038/ncomms15711
53. Andersen-Nissen E, Fiore-Gartland A, Ballweber Fleming L, Carpp LN, Naidoo AF, Harper MS, et al. Innate Immune Signatures to a Partially-Efficacious HIV Vaccine Predict Correlates of HIV-1 Infection Risk. *PloS Pathog* (2021) 17(3):e1009363. doi: 10.1371/journal.ppat.1009363
54. Ackerman ME, Mikhailova A, Brown EP, Dowell KG, Walker BD, Bailey-Kellogg C, et al. Polyfunctional Hiv-Specific Antibody Responses are Associated With Spontaneous Hiv Control. *PloS Pathog* (2016) 12(1): e1005315. doi: 10.1371/journal.ppat.1005315
55. Dugast A-S, Chan Y, Hoffner M, Licht A, Nkolola J, Li H, et al. Lack of Protection Following Passive Transfer of Polyclonal Highly Functional Low-Dose Non-Neutralizing Antibodies. *PloS One* (2014) 9(5):e97229. doi: 10.1371/journal.pone.0097229

56. Burton DR, Hessell AJ, Keele BF, Klasse PJ, Ketas TA, Moldt B, et al. Limited or No Protection by Weakly or Nonneutralizing Antibodies Against Vaginal SHIV Challenge of Macaques Compared With a Strongly Neutralizing Antibody. *Proc Natl Acad Sci* (2011) 108:11181–6. doi: 10.1073/pnas.1103012108
57. Shingai M, Donau OK, Plishka RJ, Buckler-White A, Mascola JR, Nabel GJ, et al. Passive Transfer of Modest Titers of Potent and Broadly Neutralizing Anti-HIV Monoclonal Antibodies Block SHIV Infection in Macaques. *J Exp Med* (2014) 211(10):2061–74. doi: 10.1084/jem.20132494
58. Moldt B, Le KM, Carnathan DG, Whitney JB, Schultz N, Lewis MG, et al. Neutralizing Antibody Affords Comparable Protection Against Vaginal and Rectal Simian/Human Immunodeficiency Virus Challenge in Macaques. *AIDS* (2016) 30(10):1543–51. doi: 10.1097/QAD.0000000000001102
59. Rudicell RS, Kwon YD, Ko S-Y, Pegu A, Louder MK, Georgiev IS, et al. Enhanced Potency of a Broadly Neutralizing HIV-1 Antibody In Vitro Improves Protection Against Lentiviral Infection *In Vivo*. *J Virol* (2014) 88 (21):12669–82.
60. Ko S-Y, Pegu A, Rudecill RS, Yang Z-Y, Joyce MG, Chen X, et al. Enhanced Neonatal Fc Receptor Function Improves Protection Against Primate SHIV Infection. *Nature* (2014) 514(7524):642–5. doi: 10.1038/nature13612
61. Hangartner L, Beauparlant D, Rakasz E, Nedellec R, Hozé N, McKenney K, et al. Effector Function Does Not Contribute to Protection From Virus Challenge by a Highly Potent HIV Broadly Neutralizing Antibody in Nonhuman Primates. *Sci Transl Med* (2021) 13(585). doi: 10.1126/scitranslmed.abe3349
62. Parsons MS, Lee WS, Kristensen AB, Amarasena T, Khoury G, Wheatley AK, et al. Fc-Dependent Functions are Redundant to Efficacy of Anti-HIV Antibody PGT121 in Macaques. *J Clin Invest.* (2019) 129(1):182–91. doi: 10.1172/JCI122466
63. Lu C-L, Murakowski DK, Bournazos S, Schoofs T, Sarkar D, Halper-Stromberg A, et al. Enhanced Clearance of HIV-1-Infected Cells by Broadly Neutralizing Antibodies Against HIV-1 In Vivo. *Science* (2016) 352(6288):1001–4. doi: 10.1126/science.aaf1279
64. Mujib S, Liu J, Rahman AKMN-U, Schwartz JA, Bonner P, Yue FY, et al. Comprehensive Cross-Clade Characterization of Antibody-Mediated Recognition, Complement-Mediated Lysis, and Cell-Mediated Cytotoxicity of HIV-1 Envelope-Specific Antibodies Toward Eradication of the HIV-1 Reservoir. *J Virol* (2017) 91(16):e00634-17. doi: 10.1128/JVI.00634-17
65. von Bredow B, Arias JF, Heyer LN, Moldt B, Le K, Robinson JE, et al. Comparison of Antibody-Dependent Cell-Mediated Cytotoxicity and Virus Neutralization by HIV-1 Env-Specific Monoclonal Antibodies. *J Virol* (2016) 90(13):6127–39. doi: 10.1128/JVI.00347-16
66. von Bredow B, Andrabi R, Grunst M, Grandea AG 3rd, Le K, Song G, et al. Differences in the Binding Affinity of an HIV-1 V2 Apex-Specific Antibody for the SIV Envelope Glycoprotein Uncouple Antibody-Dependent Cellular Cytotoxicity From Neutralization. *MBio* (2019) 10(4):e01255–19. doi: 10.1128/mBio.01255-19
67. Bonsignori M, Pollara J, Moody MA, Alpert MD, Chen X, Hwang K-K, et al. Antibody-Dependent Cellular Cytotoxicity-Mediating Antibodies From an HIV-1 Vaccine Efficacy Trial Target Multiple Epitopes and Preferentially Use the VH1 Gene Family. *J Virol* (2012) 86(21):11521–32. doi: 10.1128/JVI.01023-12
68. Acharya P, Tolbert WD, Gohain N, Wu X, Yu L, Liu T, et al. Structural Definition of an Antibody-Dependent Cellular Cytotoxicity Response Implicated in Reduced Risk for HIV-1 Infection. *J Virol* (2014) 88 (21):12895–906. doi: 10.1128/JVI.02194-14
69. Bruel T, Guivel-Benhassine F, Amraoui S, Malbec M, Richard L, Bourdic K, et al. Elimination of HIV-1-Infected Cells by Broadly Neutralizing Antibodies. *Nat Commun* (2016) 7:10844. doi: 10.1038/ncomms10844
70. Lu J, Chu J, Zou Z, Hamacher NB, Rixon MW, Sun PD. Structure of Fcγri in Complex With Fc Reveals the Importance of Glycan Recognition for High-Affinity Igg Binding. *Proc Natl Acad Sci U S A*. (2015) 112(3):833–8. doi: 10.1073/pnas.1418812112
71. Subedi GP, Barb AW. The Immunoglobulin G1 N-Glycan Composition Affects Binding to Each Low Affinity Fc γ Receptor. *mAbs* (2016) 8:1512–24. doi: 10.1080/19420862.2016.1218586
72. Subedi GP, Barb AW. The Structural Role of Antibody N-Glycosylation in Receptor Interactions. *Structure* (2015) 23(9):1573–83. doi: 10.1016/j.str.2015.06.015
73. Murin CD. Considerations of Antibody Geometric Constraints on NK Cell Antibody Dependent Cellular Cytotoxicity. *Front Immunol* (2020) 11:1635. doi: 10.3389/fimmu.2020.01635
74. Murin CD, Wilson IA, Ward AB. Antibody Responses to Viral Infections: A Structural Perspective Across Three Different Enveloped Viruses. *Nat Microbiol* (2019) 4(5):734–47. doi: 10.1038/s41564-019-0392-y
75. Richardson SI, Lambson BE, Crowley AR, Bashirova A, Scheepers C, Garrett N, et al. Igg3 Enhances Neutralization Potency and Fc Effector Function of an HIV V2-Specific Broadly Neutralizing Antibody [Internet. *PloS Pathog* (2019) 15:e1008064. doi: 10.1371/journal.ppat.1008064
76. Stapleton NM, Andersen JT, Stemerding AM, Bjarnarson SP, Verheul RC, Gerritsen J, et al. Competition for Fcrn-Mediated Transport Gives Rise to Short Half-Life of Human Igg3 and Offers Therapeutic Potential. *Nat Commun* (2011) 2:599. doi: 10.1038/ncomms1608
77. Chu TH, Crowley AR, Backes I, Chang C, Tay M, Broge T, et al. Hinge Length Contributes to the Phagocytic Activity of HIV-Specific Igg1 and Igg3 Antibodies. *PloS Pathog* (2020) 16(2):e1008083. doi: 10.1371/journal.ppat.1008083
78. Liu R, Oldham R, Teal E, Beers S, Cragg M. Fc-Engineering for Modulated Effector Functions—Improving Antibodies for Cancer Treatment. *Antibodies* (2020) 9:64. doi: 10.3390/antib9040064
79. Shields RL, Namenuk AK, Hong K, Meng YG, Rae J, Briggs J, et al. High Resolution Mapping of the Binding Site on Human Igg1 for Fc Gamma RI, Fc Gamma RII, Fc Gamma RIII, and Fcrn and Design of Igg1 Variants With Improved Binding to the Fc Gamma R. *J Biol Chem* (2001) 276(9):6591–604. doi: 10.1074/jbc.M009483200
80. Lazar GA, Dang W, Karki S, Vafa O, Peng JS, Hyun L, et al. Engineered Antibody Fc Variants With Enhanced Effector Function. *Proc Natl Acad Sci* (2006) 103:4005–10. doi: 10.1073/pnas.0508123103
81. Richards JO, Karki S, Lazar GA, Chen H, Dang W, Desjarlais JR. Optimization of Antibody Binding to Fcgammariia Enhances Macrophage Phagocytosis of Tumor Cells. *Mol Cancer Ther* (2008) 7(8):2517–27. doi: 10.1158/1535-7163.MCT-08-0201
82. Stavenhagen JB, Gorlatov S, Tuaillon N, Rankin CT, Li H, Burke S, et al. Fc Optimization of Therapeutic Antibodies Enhances Their Ability to Kill Tumor Cells In Vitro and Controls Tumor Expansion In Vivo *via* Low-Affinity Activating Fcγ Receptors. *Cancer Res* (2007) 67:8882–90. doi: 10.1158/0008-5472.can-07-0696
83. Ahmed AA, Keremane SR, Vielmetter J, Bjorkman PJ. Structural Characterization of GASDALIE Fc Bound to the Activating Fc Receptor Fcγriiia. *J Struct Biol* (2016) 194(1):78–89. doi: 10.1016/j.jsb.2016.02.001
84. Yamane-Ohnuki N, Kinoshita S, Inoue-Urakubo M, Kusunoki M, Iida S, Nakano R, et al. Establishment of FUT8 Knockout Chinese Hamster Ovary Cells: An Ideal Host Cell Line for Producing Completely Defucosylated Antibodies With Enhanced Antibody-Dependent Cellular Cytotoxicity. *Biotechnol Bioeng.* (2004) 87(5):614–22. doi: 10.1002/bit.20151
85. Gilbert PB, Juraska M, deCamp AC, Karuna S, Edupuganti S, Mgodi N, et al. Basis and Statistical Design of the Passive HIV-1 Antibody Mediated Prevention (AMP) Test-of-Concept Efficacy Trials. *Stat Commun Infect Dis* (2017) 9(1). doi: 10.1515/scid-2016-0001
86. Gilbert PB. Ongoing Vaccine and Monoclonal Antibody HIV Prevention Efficacy Trials and Considerations for Sequel Efficacy Trial Designs. *Stat Commun Infect Diseases.* (2019) 11. doi: 10.1515/scid-2019-0003
87. McFarland EJ, Cunningham CK, Muresan P, Capparelli EV, Perlowski C, Morgan P, et al. Safety, Tolerability, and Pharmacokinetics of a Long-Acting Broadly Neutralizing HIV-1 Monoclonal Antibody VRC01LS in HIV-1-Exposed Newborn Infants. *J Infect Dis* (2021). doi: 10.1093/infdis/jiab229
88. Samulski RJ, Muzyczka N. AAV-Mediated Gene Therapy for Research and Therapeutic Purposes. *Annu Rev Virol* (2014) 1(1):427–51. doi: 10.1146/annurev-virology-031413-085355
89. Atchison RW, Casto BC, McD. Hammon W. Adenovirus-Associated Defective Virus Particles. *Science* (1965) 149p:754–5. doi: 10.1126/science.149.3685.754
90. Buller RML, Janik JE, Sebring ED, Rose JA. Herpes Simplex Virus Types 1 and 2 Completely Help Adenovirus-Associated Virus Replication. *J Virol* (1981) 40:241–7. doi: 10.1128/jvi.40.1.241-247.1981
91. Urabe M, Nakakura T, Xin K-Q, Obara Y, Mizukami H, Kume A, et al. Scalable Generation of High-Titer Recombinant Adeno-Associated Virus

Type 5 in Insect Cells. *J Virol* (2006) 80:1874–85. doi: 10.1128/jvi.80.4.1874-1885.2006
92. Li C, Jude Samulski R. Engineering Adeno-Associated Virus Vectors for Gene Therapy. *Nat Rev Genet* (2020) 21:255–72. doi: 10.1038/s41576-019-0205-4
93. Sonntag F, Schmidt K, Kleinschmidt JA. A Viral Assembly Factor Promotes AAV2 Capsid Formation in the Nucleolus. *Proc Natl Acad Sci* (2010) 107:10220–5. doi: 10.1073/pnas.1001673107
94. King JA. DNA Helicase-Mediated Packaging of Adeno-Associated Virus Type 2 Genomes Into Preformed Capsids. *EMBO J* (2001) 20:3282–91. doi: 10.1093/emboj/20.12.3282
95. Sonntag F, Bleker S, Leuchs B, Fischer R, Kleinschmidt JA. Adeno-Associated Virus Type 2 Capsids With Externalized VP1/VP2 Trafficking Domains are Generated Prior to Passage Through the Cytoplasm and are Maintained Until Uncoating Occurs in the Nucleus. *J Virol* (2006) 80:11040–54. doi: 10.1128/jvi.01056-06
96. Girod A, Wobus CE, Zádori Z, Ried M, Leike K, Tijssen P, et al. The VP1 Capsid Protein of Adeno-Associated Virus Type 2 is Carrying a Phospholipase A2 Domain Required for Virus Infectivity. *J Gen Virol* (2002) 83:973–8. doi: 10.1099/0022-1317-83-5-973
97. Becerra SP, Koczot F, Fabisch P, Rose JA. Synthesis of Adeno-Associated Virus Structural Proteins Requires Both Alternative Mrna Splicing and Alternative Initiations From a Single Transcript. *J Virol* (1988) 62:2745–54. doi: 10.1128/jvi.62.8.2745-2754.1988
98. Ogden PJ, Kelsic ED, Sinai S, Church GM. Comprehensive AAV Capsid Fitness Landscape Reveals a Viral Gene and Enables Machine-Guided Design. *Science* (2019) 366(6469):1139–43. doi: 10.1126/science.aaw2900
99. Hammond SL, Leek AN, Richman EH, Tjalkens RB. Cellular Selectivity of AAV Serotypes for Gene Delivery in Neurons and Astrocytes by Neonatal Intracerebroventricular Injection. *PloS One* (2017) 12(12):e0188830. doi: 10.1371/journal.pone.0188830
100. Wang D, Tai PWL, Gao G. Adeno-Associated Virus Vector as a Platform for Gene Therapy Delivery. *Nat Rev Drug Discov* (2019) 18(5):358–78. doi: 10.1038/s41573-019-0012-9
101. Kotin RM, Siniscalco M, Samulski RJ, Zhu XD, Hunter L, Laughlin CA, et al. Site-Specific Integration by Adeno-Associated Virus. *Proc Natl Acad Sci U S A* (1990) 87(6):2211–5. doi: 10.1073/pnas.87.6.2211
102. Samulski RJ, Zhu X, Xiao X, Brook JD, Housman DE, Epstein N, et al. Targeted Integration of Adeno-Associated Virus (AAV) Into Human Chromosome 19. *EMBO J* (1991) 10:3941–50. doi: 10.1002/j.1460-2075.1991.tb04964.x
103. Hüser D, Weger S, Heilbronn R. Kinetics and Frequency of Adeno-Associated Virus Site-Specific Integration Into Human Chromosome 19 Monitored by Quantitative Real-Time PCR. *J Virol* (2002) 76:7554–9. doi: 10.1128/jvi.76.15.7554-7559.2002
104. Schultz BR, Chamberlain JS. Recombinant Adeno-Associated Virus Transduction and Integration. *Mol Ther* (2008) 16:1189–99. doi: 10.1038/mt.2008.103
105. Chamberlain K, Riyad JM, Weber T. Expressing Transgenes That Exceed the Packaging Capacity of Adeno-Associated Virus Capsids. *Hum Gene Ther Methods* (2016) 27(1):1–12. doi: 10.1089/hgtb.2015.140
106. Duan D, Sharma P, Yang J, Yue Y, Dudus L, Zhang Y, et al. Circular Intermediates of Recombinant Adeno-Associated Virus Have Defined Structural Characteristics Responsible for Long-Term Episomal Persistence in Muscle Tissue. *J Virol* (1998) 72(11):8568–77. doi: 10.1128/JVI.72.11.8568-8577.1998
107. Duan D, Yan Z, Yue Y, Engelhardt JF. Structural Analysis of Adeno-Associated Virus Transduction Circular Intermediates. *Virol* (1999) 261(1):8–14. doi: 10.1006/viro.1999.9821
108. Kuzmin DA, Shutova MV, Johnston NR, Smith OP, Fedorin VV, Kukushkin YS, et al. The Clinical Landscape for AAV Gene Therapies. *Nat Rev Drug Discovery* (2021) 20(3):173–4. doi: 10.1038/d41573-021-00017-7
109. Fang J, Yi S, Simmons A, Tu GH, Nguyen M, Harding TC, et al. An Antibody Delivery System for Regulated Expression of Therapeutic Levels of Monoclonal Antibodies *In Vivo*. *Mol Ther* (2007) 15(6):1153–9. doi: 10.1038/sj.mt.6300142
110. Johnson PR, Schnepp BC, Zhang J, Connell MJ, Greene SM, Yuste E, et al. Vector-Mediated Gene Transfer Engenders Long-Lived Neutralizing Activity and Protection Against SIV Infection in Monkeys. *Nat Med* (2009) 15(8):901–6. doi: 10.1038/nm.1967
111. van den Berg FT, Makoah NA, Ali SA, Scott TA, Mapengo RE, Mutsvunguma LZ, et al. AAV-Mediated Expression of Broadly Neutralizing and Vaccine-Like Antibodies Targeting the HIV-1 Envelope V2 Region. *Mol Ther Methods Clin Dev* (2019) 14:100–12. doi: 10.1016/j.omtm.2019.06.002
112. Saunders KO, Wang L, Joyce MG, Yang Z-Y, Balazs AB, Cheng C, et al. Broadly Neutralizing Human Immunodeficiency Virus Type 1 Antibody Gene Transfer Protects Nonhuman Primates From Mucosal Simian-Human Immunodeficiency Virus Infection. *J Virol* (2015) 89(16):8334–45. doi: 10.1128/JVI.00908-15
113. Welles HC, Jennewein MF, Mason RD, Narpala S, Wang L, Cheng C, et al. Vectored Delivery of Anti-SIV Envelope Targeting Mab *via* AAV8 Protects Rhesus Macaques From Repeated Limiting Dose Intrarectal Swarm Sivsme660 Challenge. *PloS Pathog* (2018) 14(12):e1007395. doi: 10.1371/journal.ppat.1007395
114. Priddy FH, Lewis DJM, Gelderblom HC, Hassanin H, Streatfield C, LaBranche C, et al. Adeno-Associated Virus Vectored Immunoprophylaxis to Prevent HIV in Healthy Adults: A Phase 1 Randomised Controlled Trial [Internet]. *Lancet HIV* (2019) 6:e230–9. doi: 10.1016/s2352-3018(19)30003-7

**Conflict of Interest:** The authors declare that the research was conducted in the absence of any commercial or financial relationships that could be construed as a potential conflict of interest.

**Publisher's Note:** All claims expressed in this article are solely those of the authors and do not necessarily represent those of their affiliated organizations, or those of the publisher, the editors and the reviewers. Any product that may be evaluated in this article, or claim that may be made by its manufacturer, is not guaranteed or endorsed by the publisher.

frontiers in Immunology

ORIGINAL RESEARCH
published: 15 September 2021
doi: 10.3389/fimmu.2021.710327

# Characterizing the Relationship Between Neutralization Sensitivity and *env* Gene Diversity During ART Suppression

*Andrew Wilson*[1], *Leyn Shakhtour*[1], *Adam Ward*[2,3], *Yanqin Ren*[2], *Melina Recarey*[1], *Eva Stevenson*[2], *Maria Korom*[1], *Colin Kovacs*[4], *Erika Benko*[4], *R. Brad Jones*[2] *and Rebecca M. Lynch*[1]*

[1] Lynch Lab, Department of Microbiology, Immunology, and Tropical Medicine, The George Washington University School of Medicine and Health Sciences, Washington, DC, United States, [2] Jones Lab, Department of Medicine, Division of Infectious Diseases, Weill Cornell Medicine, New York, NY, United States, [3] PhD Program in Epidemiology, The George Washington University Milken Institute School of Public Health, Washington, DC, United States, [4] Department of Internal Medicine, Maple Leaf Medical Clinic, Toronto, ON, Canada

OPEN ACCESS

**Edited by:**
*Kshitij Wagh,*
*Los Alamos National Laboratory (DOE), United States*

**Reviewed by:**
*Shubhanshi Trivedi,*
*The University of Utah, United States*
*Sandhya Vasan,*
*Henry M. Jackson Foundation for the Advancement of Military Medicine (HJF), United States*
*Denise Hsu,*
*United States Military HIV Research Program, United States*

***Correspondence:**
*Rebecca M. Lynch*
*rmlynch@gwu.edu*

**Specialty section:**
*This article was submitted to Vaccines and Molecular Therapeutics, a section of the journal Frontiers in Immunology*

**Received:** *15 May 2021*
**Accepted:** *18 August 2021*
**Published:** *15 September 2021*

**Citation:**
*Wilson A, Shakhtour L, Ward A, Ren Y, Recarey M, Stevenson E, Korom M, Kovacs C, Benko E, Jones RB and Lynch RM (2021) Characterizing the Relationship Between Neutralization Sensitivity and env Gene Diversity During ART Suppression. Front. Immunol. 12:710327. doi: 10.3389/fimmu.2021.710327*

Although antiretroviral therapy (ART) successfully suppresses HIV-1 replication, ART-treated individuals must maintain therapy to avoid rebound from an integrated viral reservoir. Strategies to limit or clear this reservoir are urgently needed. Individuals infected for longer periods prior to ART appear to harbor more genetically diverse virus, but the roles of duration of infection and viral diversity in the humoral immune response remain to be studied. We aim to clarify a role, if any, for autologous and heterologous antibodies in multi-pronged approaches to clearing infection. To that end, we have characterized the breadths and potencies of antibody responses in individuals with varying durations of infection and HIV-1 envelope (*env)* gene diversity as well as the sensitivity of their inducible virus reservoir to broadly neutralizing antibodies (bNAbs). Plasma was collected from 8 well-characterized HIV-1$^+$ males on ART with varied durations of active infection. HIV *envs* from reservoir-derived outgrowth viruses were amplified and single genome sequenced in order to measure genetic diversity in each participant. IgG from plasma was analyzed for binding titers against gp41 and gp120 proteins, and for neutralizing titers against a global HIV-1 reference panel as well as autologous outgrowth viruses. The sensitivity to bNAbs of these same autologous viruses was measured. Overall, we observed that greater *env* diversity was associated with higher neutralizing titers against the global panel and also increased resistance to certain bNAbs. Despite the presence of robust anti-HIV-1 antibody titers, we did not observe potent neutralization against autologous viruses. In fact, 3 of 8 participants harbored viruses that were completely resistant to the highest tested concentration of autologous IgG. That this lack of neutralization was observed regardless of ART duration or viral diversity suggests that the inducible reservoir harbors 'escaped' viruses (that co-evolved with autologous antibody responses), rather than proviruses archived from earlier in infection. Finally, we observed that viruses resistant to autologous neutralization remained sensitive to bNAbs,

especially CD4bs and MPER bNAbs. Overall, our data suggest that the inducible reservoir is relatively resistant to autologous antibodies and that individuals with limited virus variation in the *env* gene, such as those who start ART early in infection, are more likely to be sensitive to bNAb treatment.

**Keywords: broadly neutralizing antibodies, HIV-1, diversity, *env* gene, autologous antibodies, ART suppression**

## INTRODUCTION

Although effective antiretroviral therapy (ART) suppresses HIV-1 replication, ART-treated individuals must maintain life-long therapy to avoid rebound from a persistent viral reservoir, and may experience adverse effects. This long-lived virus reservoir of integrated provirus poses an obstacle to curing HIV-1, and a deeper qualitative understanding of its composition may hold clues for improving therapeutic as well as cure strategies. Antibodies mediate effector functions such as neutralization and opsonization that could aid in suppressing virus replication, clearing infected cells, and boosting immune responses (1). Anti-HIV-1 antibodies could therefore, be used to prevent mother to child transmission (2) or reformatted as bi-specific or tri-specific molecules (3). The characterization of broadly neutralizing antibodies (bNAbs) capable of recognizing genetically diverse HIV-1 Env proteins has led to robust exploration of how to effectively use antibodies against the HIV-1 reservoir. To date, the results of clinical trials passively infusing bNAbs as IgG1 into chronically infected participants have been modest (4–10). Infusion with a single bNAb can increase time to rebound during analytic treatment interruption (ATI) (4, 10) or reduce viral load in participants not on suppressive ART (5, 6, 9), and these effects are improved with combination therapy (7, 8). The modest nature of these effects may reflect the presence of virus strains that are either completely resistant to the infused bNAb or insufficient antibody concentration and/or penetration. Ultimately the data suggest that the virus becomes sufficiently resistant to replicate faster than the available concentration of bNAb can neutralize. One clear lesson from these trials is that bNAbs were more effective when participants were prescreened for neutralization sensitivity, clearly indicating that further methods for overcoming bNAb resistance are needed.

HIV-1 sexual transmission often begins with a single founder virus (11–13) that diversifies over the course of infection resulting in a diverse quasispecies (14, 15). This genetic diversity is reflected in the integrated proviral reservoir as reviewed in (16) and is a consequence of rapid virus mutation during replication as well as selection pressure exerted by the immune system. In particular, the autologous antibody response exerts pressure on the HIV-1 *env* gene (17–20). Therefore, there is a circular relationship after virus transmission that starts with an antibody response that drives viral diversification, and results in escape from the antibody response. This inherent tension between the host immune system and virus replication is frequently called an "arms race" (21), but the effects of the arms race on efficacy of bNAb treatment during chronic infection remain unknown. We therefore perceived a need to define the complicated relationship between genetic diversity of *env*, duration of active viral infection, autologous antibody titers and reservoir virus sensitivity to bNAbs. We hypothesized longer durations of HIV-1 replication before ART suppression would lead to higher autologous antibody titers and to greater Env diversity within the reservoir, which would be associated with increased resistance to bNAbs.

## MATERIALS AND METHODS

### Study Participants

All participants were HIV-1 infected males on ART recruited from the Maple Leaf Medical Clinic in Toronto, Canada, through a protocol approved by the University of Toronto Institutional Review Board. Secondary use of the samples from Toronto was approved through the George Washington University Institutional Review Boards. All subjects were adults and gave written informed consent. Clinical data for these participants are described in **Table 1**. We calculated an estimated date of infection to be midway between the last negative test and first positive test. The estimated duration of active infection was

**TABLE 1** | Clinical characteristics of study cohort.

| Participant ID | Age | Sex | Viral Load (copies/ml) | CD4 Count (cells/mm$^3$) | IUPM | HIV Subtype | Estimated duration of unsuppressed infection (months) | Duration of ART (years) | QVOA wells (number) |
|---|---|---|---|---|---|---|---|---|---|
| OM5334 | 33 | Male | Undetectable | 812 | 1.57 | B | 3 | 3 | 5 |
| OM5267 | 29 | Male | Undetectable | 429 | 2.34 | B | 10.5 | 3 | 4 |
| OM5346 | 48 | Male | Undetectable | 1182 | 0.27 | B, AG | 25.5 | 5 | 4 |
| OM5148 | 47 | Male | Undetectable | 733 | 1.02 | B | 69 | 10 | 5 |
| CIRC0196 | 56 | Male | Undetectable | 679 | 0.49 | B | 81.5 | 3 | 5 |
| OM5162 | 53 | Male | Undetectable | 478 | 0.65 | B | >3 | 14 | 5 |
| OM5001 | 43 | Male | 42 | 540 | 10.46 | B | >14 | 9 | 4 |
| OM5365 | 56 | Male | Undetectable | 624 | 0.42 | B | >18 | 25 | 3 |

calculated to be the months between the estimated date of infection and the date of documented ART initiation.

## QVOA

Leukapheresis was performed on ART-treated participants. Peripheral blood mononuclear cells (PBMCs) were isolated by centrifugation with Ficoll (GE Life Sciences). CD4 T cells were enriched from PBMCs (Stemcell Technologies). Cells were serially diluted (2 million, 1 million, 0.5 million, 0.2 million, and 0.1 million cells/well) and plated in 24-well plates, with 12 replicates at each concentration. Phytohemagglutinin (PHA) and irradiated allogenic HIV-negative PBMCs were added to activate the CD4 T cells. $CCR5^+$ MOLT-4 cells [NIH AIDS reagent program (22)] were added 24 hours later for viral replication. Media were changed every 3-4 days and ELISA for p24 protein was performed after 14 days of culture as described in (23). In general, supernatants were collected from $p24^+$ wells for which fewer than 50% of dilution replicates were positive. To increase the volume of outgrowth virus available for use, viruses were re-grown for 6 days by infecting and proliferating in new HIV-negative $CD4^+$ T cells.

## Single Genome Sequencing

SGS was performed as previously described (24)} with the following modifications. Viral RNA was extracted from culture supernatants by QIAmp kit (Qiagen, Germantown MD). cDNA was synthesized as previously described in (9), and *env* genes were amplified by nested PCR using the Platinum Taq High Fidelity polymerase (Invitrogen). Template cDNA was serially diluted so that fewer than 33% of PCR replicates were positive, ensuring that a majority of amplicons would be generated from a single cDNA template. Well-described primers Env_outF1 (TAGAGCCCTGGAAGCATCCAGGAAG) and Env_outR1 (TTGCTACTTGTGATTGCTCCATGT) were used for first round amplification, and Env_inF2 (CACCTTAGGCATCT CCTATGGCAGGAAGAAG) and Env_inR2 (GTCTC GAGATACTGCTCCCACCC) for the second round. In the case of Subtype AG viruses from participant OM5346, customized primer Env_innR3 (GATACTGCTCCCACC CCATCTGC) was used in lieu of Env_inR2. All PCR mixes were generated in PCR clean rooms free of post-PCR or plasmid DNA. Amplicons were run on 1% agarose gels and sequenced by ACGT Inc. A minimum of three single-template sequences were obtained from each well. Sequences that contained stop codons, large deletions, or mixed bases were removed from further analysis.

## Maximum Likelihood Trees

All QC'ed sequences were translation aligned by participant to generate individual nucleic acid alignments. Due to the additive chances of mutation during replication in the QVOA assay, cDNA synthesis, and PCR (25–27), wells were considered to contain a single virus if no sequence contained more than four amino acid mutations from the consensus sequence for that well, and that each mutation was unique to that sequence. These consensus sequences for all single-virus wells were translated and protein sequences from all participants were aligned with MUSCLE to Consensus B and AG sequences (www.hiv.lanl.gov). All alignments were hand-edited and gap-stripped for regions that could not unambiguously be aligned. All sequence analysis was performed in the Geneious suite version (9.0.5) [http://www.geneious.com (28)]. Maximum likelihood trees were generated from these alignments using RAxML-HPC BlackBox (8.2.12) run on the Cyberinfrastructure for Phylogenetic Research (CIPRES) Science Gateway. Trees are rooted on midpoint for visualization using MEGA version X (29, 30). Bootstraps greater than 90 are shown.

## Average Pairwise Distance

Average pairwise distance was calculated using DIVEIN (https://indra.mullins.microbiol.washington.edu/DIVEIN/diver.html). Briefly, consensus protein sequences for viruses from each individual were aligned with MUSCLE. Alignments were input into DIVEIN using the HIVb substitution model to generate average pairwise distance for each individual.

## ELISA

IgG purification from plasma was performed with the Melon Gel IgG purification kit (Thermo Fisher) according to the manufacturer's instructions. ELISAs against recombinant proteins YU2 gp120 (provided by Dr. John Mascola) and DIII gp41 (Abcam) were run as previously described (31), with the following modifications. IgG was diluted to 50μg/mL and serially diluted 5-fold to 0.0032μg/mL in B3T buffer (150 mM NaCl, 50 mM Tris-HCl, 1 mM EDTA, 3.3% fetal bovine serum, 2% bovine albumin, 0.07% Tween 20). Briefly, 96-well ELISA plates were coated with 2 μg/ml of the specified recombinant protein in phosphate-buffered saline (PBS) overnight at 4°C. The following day, the plates were blocked with B3T buffer. IgGs were detected using peroxidase-conjugated goat anti-human IgG antibody (Jackson ImmunoResearch). All incubations were for 1 h at 37°C, and all volumes were 100 μl, except for the blocking step, which was 200 μl. The plates were washed between incubations with 0.1% Tween 20 in PBS, detected using SureBlue TMB substrate (SeraCare, VWR), and subsequently read at 450 nm.

## Neutralization Assay

Single-round neutralization assays in Tzm-bl target cells [NIH AIDS Reagent Program (32)] were performed as described previously (23, 31, 33). Briefly, neutralization activity of isolated plasma IgG samples were tested against both heterologous HIV-Env pseudotyped viruses and replication-competent autologous outgrowth viruses. IgG was diluted to 50μg/mL and serially diluted 5-fold to 0.0032μg/mL in duplicate. Plasmids for pseudovirus production were from the global panel of 12 reference *env* clones [NIH AIDS Reagent Program (34)]. Outgrowth viruses were kept in the presence of 3.5uM Indinavir (Sigma-Aldrich) to prevent replication. Viruses were titered on Tzm-bl target cells before use and diluted to target 5500 relative luciferase units (RLU) for virus isolates (which were very low volume) and 45,000 RLU for pseudovirus. Virus and antibody pairings were incubated at 37°C for 30 min in 96-well clear flat-bottom black culture plates (Greiner Bio-One) before Tzm-bl cells were added at a concentration of $10^4$ per well in the presence of DEAE-Dextran (Sigma Aldrich) diluted to 20μg/ml. After

48 hours, plates were read by removing 100µl of media from each well, and adding 100 µl of SpectraMax Glo Steady-Luc reporter assay reagent (Molecular Devices). Luminescence intensity was measured using a SpectraMax i3x multimode detection platform (Molecular Devices). per the manufacturer's instructions. Neutralization curves were generated after background subtraction of mean RLU of cell only wells by calculating the change in RLUs in the presence of antibody to the mean RLU of virus-only control wells. Curves were fit by nonlinear regression using the asymmetric five-parameter logistic equation in Prism 9 (GraphPad). The 50% and 80% inhibitory concentrations ($IC_{50}$ and $IC_{80}$) were defined as the antibody dilutions that neutralize 50% and 80% of the virus, respectively.

## Statistics

All statistical analyses were performed in Prism 9 (GraphPad). Comparisons were performed using Mann Whitney and correlations using non-parametric Spearman.

# RESULTS

## Association Between Genetic Diversity and bNAb Sensitivity

To successfully contribute to curing HIV-1, bNAbs will need to both neutralize circulating virus to prevent new infections, while also tagging infected cells displaying viral antigen for killing by immune cells. Previously we studied the abilities of bNAbs to recognize both cell-free HIV virions as well as matched infected cells from the inducible reservoir of 8 individuals. From these studies, we observed both inter-and intra-individual variation in bNAb sensitivity (23). Earlier studies have indicated that diversity within the persistent HIV reservoir increases with duration of active infection (13, 15, 35, 36), but it remains unknown how this diversity could affect sensitivity to bNAb neutralization. To study this question, we performed single genome sequencing (SGS) on the 35 quantitative virus outgrowth assay (QVOA) cultures from these 8 individuals (**Table 1**). These 8 males represented a wide range of reservoir sizes as measured by QVOA in infectious units per million cells (IUPM) (**Table 1**). A minimum of 3 *env* sequences were generated from each of the 3-5 QVOA supernatants. Outgrowth wells were considered to contain a single virus if all amplified sequences were within 4 amino acids of the consensus and all mutations from consensus were unique (i.e., not fixed in multiple sequences). We chose this definition to allow for mutations that may have been caused during viral outgrowth, reverse transcription, or PCR amplification (25–27). The majority (77%) of QVOA wells contained only a single virus by this criterion, and wells containing multiple viruses were excluded from further analyses (**Supplementary Figure 1**). We performed these analyses to ensure we only studied wells containing a single virus, so that we could pair our functional data to our genetic data and be confident that the sequence studied was indeed the one being tested *in vitro*. In particular, QVOA outgrowths for OM5148 contained multiple viruses in 4 out of the 5 wells, leading to only one well that passed our criteria for further phenotypic and phylogenetic studies. For all wells containing a single virus, consensus sequences were generated and aligned to produce a maximum-likelihood tree of all Env proteins (**Figure 1A**). This sequencing revealed that OM5346 was co-infected with both subtype B and AG viruses, introducing a secondary source of diversity beyond viral evolution.

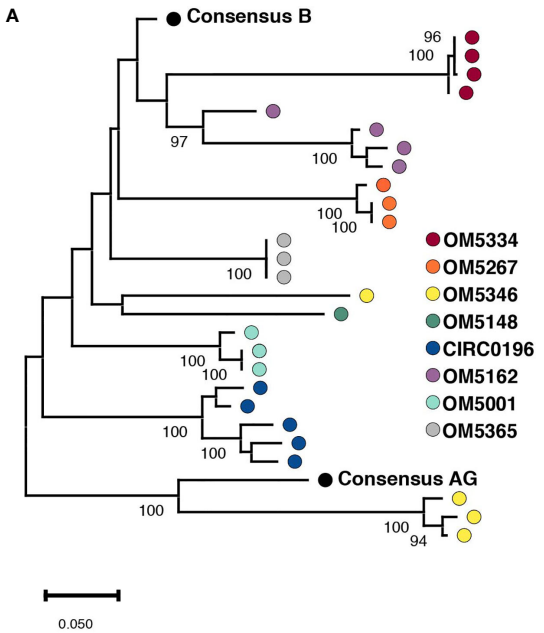


B

| Participant | Time to ART (months) | APD |
|---|---|---|
| OM5334 | 3 | 0.28% |
| OM5267 | 10.5 | 0.37% |
| OM5346 | 25.5 | N.D. |
| OM5148 | 69 | N.D. |
| CIRC0196 | 81.5 | 6.64% |
| OM5162 | >3 | 8.26% |
| OM5001 | >14 | 1.59% |
| OM5365 | >18 | 0.00% |

**FIGURE 1** | Genetic diversity of participant reservoir virus increases with active infection length. **(A)** A minimum of 3 SGS sequences were used to generate consensus sequences for each QVOA well. The protein sequence of each well was aligned to consensus subtype B and AG and a maximum likelihood tree was generated. Wells containing multiple viruses were excluded. Each dot represents one QVOA outgrowth virus well and is color-coded by participant. The tree is midpoint rooted for visualization and bootstraps over 90% are shown. **(B)** For all participants a minimum duration of infection was calculated using the date of diagnosis and date of ART initiation. For individuals for whom an $HIV^-$ date was confirmed, an estimated length of infection was calculated using an estimated date of infection as the midpoint between confirmed $HIV^-$ and $HIV^+$ time points. For each person, these estimated times of active infection are listed next to the average pairwise distance (APD) of Env for their inducible reservoir viruses.

We next quantified genetic diversity for each individual by calculating average pairwise distance (APD) between the consensus protein sequences of their QVOA wells. OM5148 and OM5346 were excluded from this analysis for either having only one sequence or multiple subtypes respectively; therefore, we could only calculate APD for 6 of 8 participants (**Figure 1B**). APDs varied among individuals, ranging from 0% to 8.26%, but appeared to group into "high" diversity with APDs greater than 6% (CIRC0196 and OM5162) or "low" diversity with APDs less than 2% (OM5334, OM5267, OM5001 and OM5365). We hypothesized that diversity was linked to duration of actively replicating virus before ART suppression. For 5 individuals there were clinical records documenting an HIV-1 negative test date. We calculated an estimated date of infection to be midway between the last negative test and first positive test. We then estimated the duration of active infection to be the months between the estimated date of infection and the date of documented ART initiation. Of these 5 individuals, only 3 had calculated APDs because of lack of sequences or multiple subtypes in the other individuals. The 2 individuals with an estimated length of infection of less than a year were in the low diversity group, and the person with an estimated length of greater than six years was in the high diversity group (**Figure 1B**). These observations are consistent with previous literature demonstrating that length of infection correlates with increased genetic diversity (13, 15, 35, 36).

To investigate the relationship between genetic diversity and bNAb sensitivity, we re-analyzed data on the neutralization sensitivity of these QVOA outgrowths to 10 bNAbs (23). We could now exclude wells that contained multiple viruses because of the sequencing analyses. To quantify the bNAb sensitivity of each individuals' reservoir, the geometric mean $IC_{50}$ for all outgrowth viruses against bNAbs was calculated (**Supplementary Table 1**). When graphed by APD, the geometric mean $IC_{50}$s of high diversity individuals' viruses were not significantly different from the low group when tested against CD4bs bNAbs (**Figure 2A**) or 10E8v4-V5F-100cF (**Figure 2B**). There are significant differences between these groups, however, for bNAbs targeting V2-apex (**Figure 2C**) and V3-glycan (**Figure 2D**) epitopes. High diversity people exhibited more resistance to these bNAbs, although it is important to note that OM5267 has very low diversity and is completely resistant to the anti-V2-apex bNAbs.

## Association Between Genetic Diversity and Autologous Antibody

Recent papers have highlighted the role of autologous antibodies in restricting virus from rebounding *in vivo* after ATI (37, 38). To study the titers of autologous antibodies in each individual,

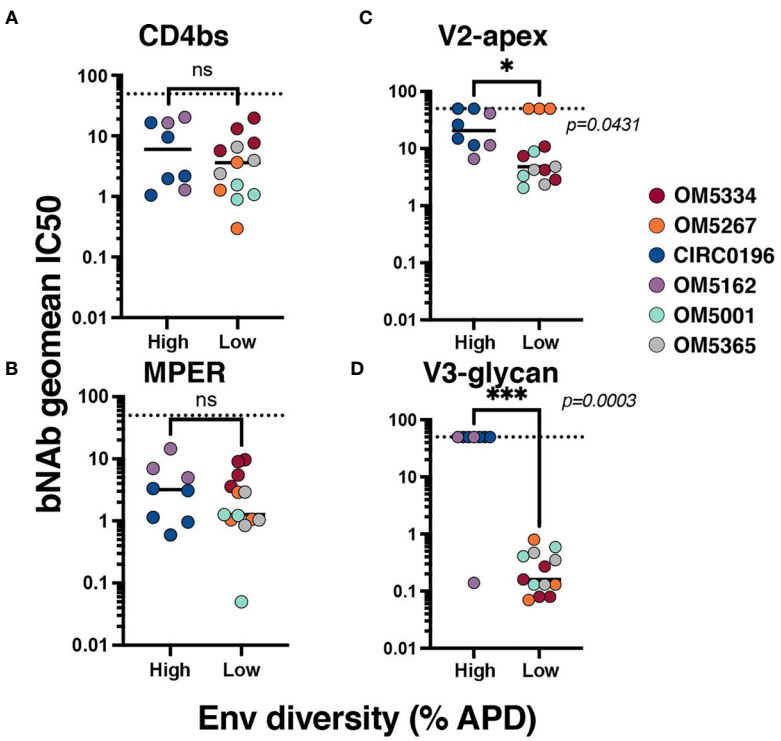


**FIGURE 2** | Association between reservoir diversity and bNAb resistance. Each virus was tested for neutralization sensitivity against a panel of 10 HIV-1 bNAbs. The geometric $IC_{50}$ of each individuals' virus-bNAb pairing was calculated by bNAb epitope: **(A)** CD4bs antibodies include VRC01, VRC07-523, 3BNC117, and N6, **(B)** MPER antibody 10E8v4-V5F-100cF (because there is only one bNAb, $IC_{50}$ is plotted), **(C)** V2-apex antibodies PGDM1400, CAP256.VRC26.25, and PG09, and **(D)** V3-glycan targeting antibodies PGT121 and 10-1074. Geometric mean $IC_{50}$s for each virus are color-coded by individual and grouped by high (>6%APD) or low (<2% APD) Env diversity. Comparisons were performed by Mann-Whitney. * signifies $p < 0.05$. *** signifies $p < 0.001$. ns signifies $p > 0.05$.

we first isolated IgG from plasma because circulating ART can confound anti-viral antibody assays. We next measured binding titers against subtype B HIV-1 gp120 (**Figure 3A**) and gp41 proteins (**Figure 3B**). All participants exhibited similar gp41 binding curves with slightly more variation in binding to gp120. Titers were quantified by calculating $EC_{50}$ values, and there was no apparent difference between people with high or low *env* diversity (**Figures 3C, D**). There was also no correlation between gp120 (**Figure 3E**) or gp41 (**Figure 3F**) titers and duration of ART in our study samples.

Once it was established that all individuals had robust antibody titers despite years of ART suppression (ranging between 3 to 25), we next tested their abilities to neutralize virus on a well-established global reference panel of HIV-1 pseudoviruses (34). On average, our study participants neutralized 65.6% of these viruses, but this neutralization was typically not potent, with a geometric mean $IC_{50}$ of 25.5μg/mL for neutralized viruses (**Table 2**). These neutralization patterns are consistent with antibody responses during chronic infection (34, 39, 40). We assigned an overall titer on the global panel for each person by calculating a geometric mean $IC_{50}$ for all viruses, designating resistant viruses "50". We observed an apparent trend toward increased breadth and potency (lower geometric mean $IC_{50}$) associated with increased *env* diversity (r = -0.77; **Figure 4A**), but no detectable trend between this overall $IC_{50}$ and duration of ART (r = -0.27; **Figure 4B**).

To assess if these IgGs were effective against autologous viruses, we performed neutralization assays against the same QVOA outgrowth cultures we had sequenced. Importantly, these polyclonal IgGs were derived from the plasma samples matched to the leukapheresis cells used in the QVOA. Therefore, these were the antibodies circulating at the time point from which the reservoir viruses were isolated. Interestingly, across 22 pairings of virus and autologous IgG, we observed no instances of potent neutralization, suggesting that these viruses were mostly escaped from circulating antibodies (**Figure 5A**).

## Combination of Autologous and Heterologous Antibody Sensitivity

Recent studies have demonstrated that autologous neutralization can restrict which viruses rebound after ATI (37, 38). Therefore, viruses that have not completely escaped the autologous antibody response can be neutralized by these antibodies, and bNAb therapy would need to particularly target autologous-resistant virus. One of these studies demonstrated that autologous neutralization with an $IC_{50}$ less than 35 μg/ml was sufficient to

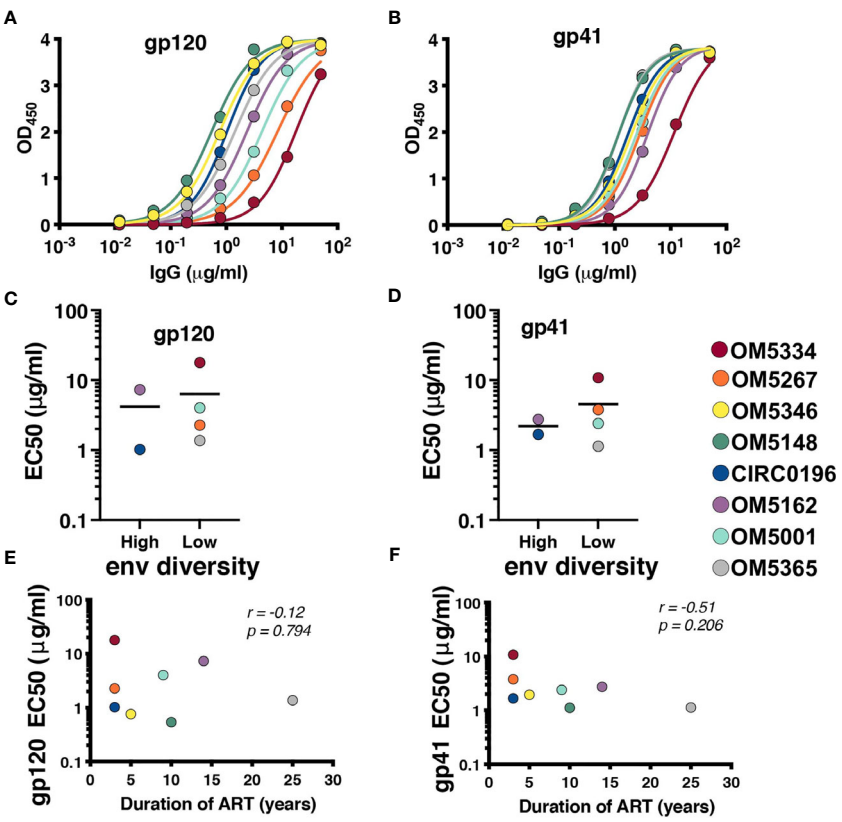


**FIGURE 3** | All participants exhibit detectable anti-HIV antibodies. IgG binding for each person was assessed by indirect ELISA against **(A)** YU2 gp120 and **(B)** DIII gp41. $EC_{50}$s for each participant against gp120 **(C)** and gp41 **(D)** were graphed by high (>6%APD) and low (<2% APD) Env diversity. $EC_{50}$s for gp120 **(E)** and gp41 **(F)** were graphed against duration of ART. Comparisons were performed by Mann-Whitney and correlations by nonparametric Spearman.

**TABLE 2** | $IC_{50}$s of IgG on a 12-virus panel.

| IC50 (µg/ml) | Subtype B | | Subtype C | Subtype A | | Subtype BC | | | Subtype AE | | | Subtype G | | | | |
|---|---|---|---|---|---|---|---|---|---|---|---|---|---|---|---|---|
| Tier | 2 | 2 | 1B or 2 | 2 | 2 | 2 | 2 | 2 | 2 or 3 | 2 | 2 | 2 | | GeoMean of Neutralized Virus | Percent of viruses neutralized | GeoMean of all viruses |
| Ab Sample | TRO11 | X2278 | 25710 | CEO217 | CE1176 | 398F1 | 246F3 | BJOX2000 | CH119 | CNE8 | CNE55 | X1632 | $SIV_{mac239}$ | | | |
| OM5334 | 42.1 | 40.7 | >50 | 47.4 | >50 | 18.4 | 49.7 | >50 | >50 | >50 | >50 | >50 | >50 | 37.5 | 41.7 | 44.4 |
| OM5267 | 35.9 | 44.5 | 45.3 | 46.6 | 19.5 | 15.3 | 45.1 | >50 | >50 | >50 | 22.5 | 15.6 | >50 | 29.3 | 75.0 | 33.5 |
| OM5346 | 23.0 | 45.6 | >50 | 14.8 | 38.8 | 15.0 | >50 | 43.7 | >50 | >50 | >50 | 18.4 | >50 | 25.6 | 58.3 | 33.8 |
| OM5148 | 8.11 | >50 | >50 | 49.7 | 38.7 | 15.3 | 49.5 | >50 | >50 | >50 | 16.6 | 11.5 | >50 | 21.7 | 58.3 | 30.7 |
| CIRC0196 | 21.7 | 8.78 | >50 | >50 | 30.9 | 8.33 | 10.8 | 18.9 | >50 | 18.8 | 18.1 | 32.7 | >50 | 16.9 | 75.0 | 22.1 |
| OM5162 | 23.5 | 9.65 | >50 | 46.7 | 19.1 | 17.7 | 36.9 | 20.5 | >50 | 45.5 | 35.8 | 17.6 | >50 | 24.5 | 83.3 | 27.6 |
| OM5001 | >50 | 10.5 | 14.8 | 46.9 | 36.8 | 17.1 | 10.8 | >50 | >50 | 46.3 | 45.7 | 33.3 | >50 | 24.8 | 75.0 | 29.5 |
| OM5365 | 10.2 | 46.9 | >50 | 12.0 | >50 | 15.5 | >50 | >50 | >50 | 48.8 | 21.0 | 46.1 | >50 | 23.7 | 58.3 | 32.4 |

*IC (µg/ml)*
*>50*
*10-50*
*1-10*
*0.1-1*
*<0.1*

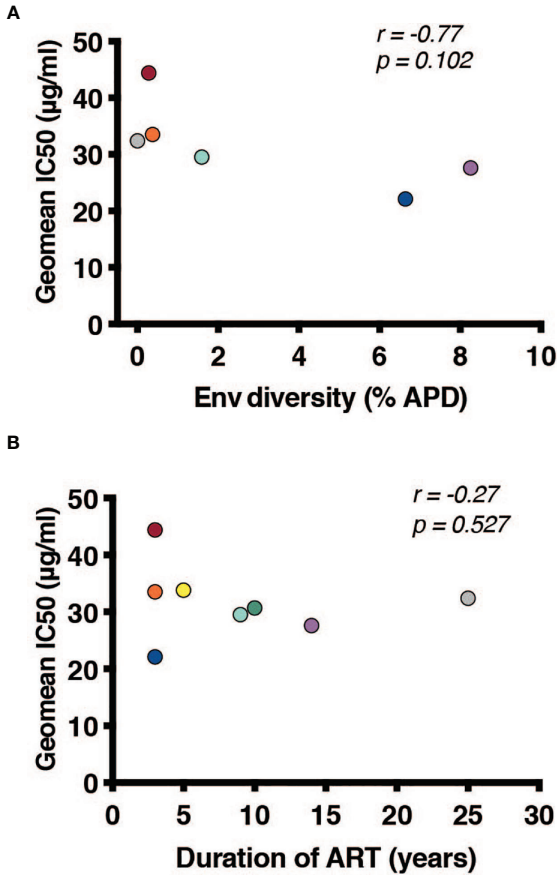


**FIGURE 4** | Duration of infection and reservoir diversity are associated with neutralization of global HIV-1 viruses. Geometric mean $IC_{50}$ of IgGs against a global HIV-1 reference panel were calculated for each individual and graphed against **(A)** Env diversity and **(B)** duration of ART. Correlations were calculated by nonparametric Spearman.

block outgrowth in the QVOA (38). We therefore, re-analyzed our data using this suggested cutoff for autologous resistance. We measured sensitivity to bNAbs targeting the CD4bs (**Figure 5B**), V2-apex (**Figure 5C**), MPER (**Figure 5D**) or V3-glycan (**Figure 5E**) by both autologous-resistant or sensitive viruses. Interestingly although there was no difference in sensitivity to bNAbs targeting the variable loop epitopes such as V3-glycan or V2-apex, viruses resistant to autologous neutralization were more sensitive to CD4bs antibodies (p = 0.011) and MPER-targeting antibody10E8-v4-V5R-100cF (p = 0.0002).

## DISCUSSION

Genetic diversity in the HIV-1 reservoir poses challenges for long-term supplemental therapies to current ART and cure strategies. To gain insight into how this diversity might be overcome to improve antibody efficacy, we first explored the role of ART suppression in decreasing the overall diversity of the viral quasispecies. We found that 2 individuals with an estimated

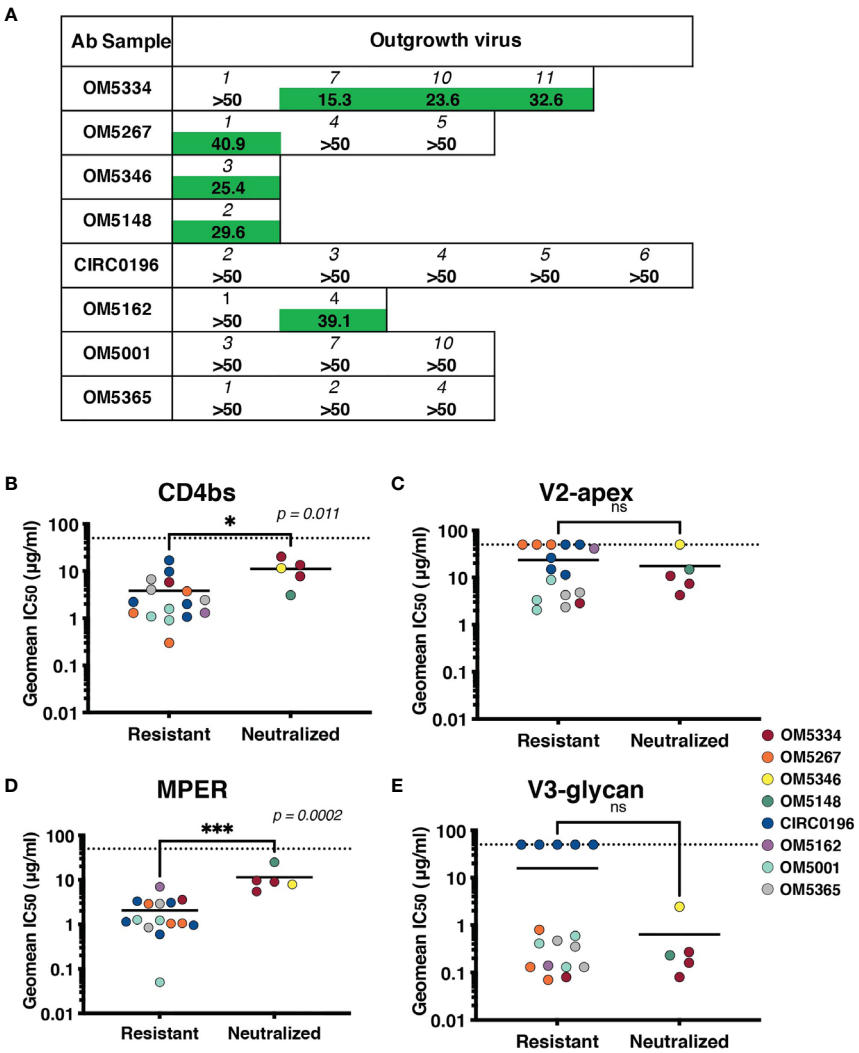


**FIGURE 5** | Sensitivity of the inducible reservoir to autologous IgG and to bNAbs targeting multiple epitopes. **(A)** $IC_{50}$ values for each individual's IgG against autologous QVOA-derived viruses. Viruses resistant at 50µg/mL of IgG were denoted with ">50". **(B–E)** Geometric mean $IC_{50}$s of bNAbs were calculated for viruses resistant to autologous neutralization ($IC_{50}$ >35µg/mL) and those that were sensitive. $IC_{50}$s were graphed by epitope targeted: **(B)** CD4bs antibodies include VRC01, VRC07-523, 3BNC117, and N6, **(C)** V2-apex antibodies include PGDM1400, CAP256.VRC26.25, and PG09, **(D)** MPER antibody 10E8v4-V5F-100cF, and **(E)** V3-glycan antibodies include PGT121 and 10-1074. Geometric mean $IC_{50}$s are color-coded by individual, and the limit of detection (50µg/ml) is indicated with a dotted line. * signifies $p < 0.05$. *** signifies $p < 0.001$. ns signifies $p > 0.05$.

duration of active viral replication before ART suppression of less than a year had 'low' diversity whereas an individual with an estimated duration of infection of greater than six years had 'high' diversity. Our limited sample size precluded correlation analysis but is consistent with earlier studies (13, 15, 35, 36). We extended these findings to assess how Env diversity related to bNAb neutralization. Overall, geometric mean $IC_{50}$s to CD4bs or MPER bNAbs were not significantly different between individuals with high or low Env diversity, but those with high diversity were more likely to be resistant to V2-apex and V3-glycan bNAbs. Interestingly, these are two epitopes highly affected by glycosylation, and in fact glycans comprise part of the epitope for some of these antibodies. Therefore, it seems plausible that longer duration of infection might affect glycans associated with bNAb neutralization (41, 42). These data suggest that individuals with shorter active infections, and by extension less reservoir diversity, may be more effectively treated with bNAbs. However, OM5267 did not follow this trend, and was completely resistant to V2 antibodies despite very low Env diversity. This observation highlights that even people who started ART early may harbor bNAb resistant viruses, but it may be easier to pre-screen for this resistance before enrolling in a clinical trial as there is less likelihood of a minor resistant variant existing.

The role of autologous antibody responses is another area of interest when considering cure strategies. During the course of infection, antibodies generated against HIV-1 are insufficient to

prevent the spread of the virus, but can typically neutralize viruses from earlier timepoints in the infection (17, 18, 42, 43). Similarly, these antibodies are inadequate to prevent rebound during an interruption of ART suppression; however, autologous antibodies likely play a selective role in restricting which viruses rebound from latently infected cells (37, 38). It also remains incompletely understood how stable antibody responses remain during ART. It is known that individuals who are suppressed early after HIV-1 infection have low antibody titers (44), and it has been observed that titers wane over time during durable ART suppression, but not dramatically (45). We therefore hypothesized that longer ART suppression would correlate with lower antibody titers. In testing isolated IgG for the ability to bind and neutralize heterologous virus, we observed detectable binding titers and 'average' neutralization, suggesting that autologous antibodies are both present and functional irrespective of length of ART treatment – even up to 25 years. It is important to note that our samples are cross-sectional, and without longitudinal time points, we cannot directly address this question of durability. We did observe a trend for individuals with greater reservoir diversity and longer durations of infection to have increased breadth and potency against a global HIV-1 reference panel. This trend was not statistically significant, likely because of our small sample size, but is consistent with studies of breadth development during chronic infection (46–49).

After establishing that HIV-1 specific antibodies were still detectable and circulating, we examined their efficacy against the participants' own inducible reservoir viruses. We observed no instances of potent neutralization, and indeed, many viruses were completely resistant to autologous IgG at the highest concentration tested (50 μg/mL). It is important to note that these viruses were not cloned, and are T-cell derived, which can result in increased resistance to antibody neutralization, likely due to the number of HIV trimers expressed on the virion as well as glycosylation patterns (50–53). Our data are consistent with other reported autologous neutralizing antibody titers from chronically suppressed individuals (38) and suggest that the viruses have mainly evolved away from the circulating antibodies and are already escaped or nearly-escaped. These data are consistent with descriptions of autologous neutralization during active chronic infection (17, 18, 42, 43), and therefore, also consistent with reports that the majority of the reservoir is established at the time of ART initiation (54). If the inducible reservoir did harbor archival variants from earlier infection timepoints, we would expect to see more potent autologous neutralization. Because we were not able to deeply sample the reservoir, we cannot exclude the possibility that rare, sensitive variants also exist. Finally, we investigated the potential cooperation between autologous antibodies and bNAbs by measuring bNAb sensitivity of autologous-resistant viruses. If autologous antibodies can restrict some proportion of viruses from rebounding from the integrated reservoir, then potentially bNAb therapy could focus on autologous-resistant viruses. Because of our small sample size, we observed only 5 outgrowth viruses that were neutralized by autologous antibodies, 3 of which were from a single individual. Nevertheless, these viruses were more resistant to CD4bs antibodies and MPER-targeting antibody 10E8v4-V5F-100cF. It would be of interest to examine if CD4bs and MPER bNAbs would in fact better restrict autologous-resistant viruses.

In conclusion, our study finds that antibody titers and functionality during ART suppression are quite similar to those described during chronic infection. We found that the inducible reservoir from these 8 individuals studied was fairly refractory to autologous neutralization. This observation is consistent with the reservoir being comprised of viruses that had co-evolved with these antibodies and therefore, were mostly escaped. We also observed a trend toward individuals with shorter active infections, and by extension less reservoir diversity, harboring reservoir viruses more sensitive to bNAbs. These data suggest that individuals able to suppress virus replication with ART early in infection may be more effectively treated with bNAbs, and that particular care should be taken when screening for bNAb resistant variants in individuals who were infected for longer periods of time before starting ART.

## DATA AVAILABILITY STATEMENT

All sequence data is submitted to GenBank with accession numbers OK011845-OK011988.

## AUTHOR CONTRIBUTIONS

MK, CK, EB, and YR contributed data. AWa performed data analysis. AWi, LS, MR, and ES collected data. RJ contributed data and helped write the paper. AWi and RL conceived and designed the experiments, performed analyses and wrote the paper. All authors contributed to the article and approved the submitted version.

## FUNDING

Research reported in this publication was supported by the National Institute of Allergy and Infectious Diseases of the National Institutes of Health under award number UM1AI126617 (to the Martin Delaney BELIEVE Collaboratory). It was also supported by a supplement from the District of Columbia Center for AIDS Research, an NIH funded program (P30AI117970), which is supported by the following NIH Co-Funding and Participating Institutes and Centers: NIAID, NCI, NICHD, NHLBI, NIDA, NIMH, NIA, NIDDK, NIMHD, NIDCR, NINR, FIC and OAR.

## ACKNOWLEDGMENTS

We acknowledge the participants from the Toronto Maple Leaf Medical clinic, who devoted time and effort toward HIV research. We thank Sam Nicholes, Jumana Akoad and Michelle Papa for

helpful feedback. The following reagents were obtained through the NIH AIDS Reagent Program, NIAID, NIH: MOLT-4/CCR5 from Dr. Masanori Baba, Dr. Hiroshi Miyake, Dr. Yuji Iizawa, TZM-bl from Dr. John C. Kappes, Dr. Xiaoyun Wu and Tranzyme Inc., and the Panel of Global Human Immunodeficiency Virus 1 (HIV-1) Env Clones, ARP-12670, from Dr. David Montefiori. Andrew Wilson is a predoctoral student in the Microbiology and Immunology Program of the Institute for Biomedical Sciences at the George Washington University. This work is from a dissertation to be presented to the above program in partial fulfillment of the requirements for the Ph.D. degree.

## SUPPLEMENTARY MATERIAL

The Supplementary Material for this article can be found online at: https://www.frontiersin.org/articles/10.3389/fimmu.2021.710327/full#supplementary-material

**Supplementary Figure 1 |** Single genome amplification sequences obtained from each individual. Maximum likelihood trees of all SGS sequences obtained for each individual. **(A)** Trees of individuals with low diversity (<2% predicted APD). Scale bars are 0.001 for these individuals, with the exception of OM5365 (grey), where the scale bar is 0.0002. **(B)** Trees for individuals with high diversity (>2% predicted APD). Scale bars are 0.01 for these individuals.

## REFERENCES

1. Wang X-Y, Wang B, Wen Y-M. From Therapeutic Antibodies to Immune Complex Vaccines. *NPJ Vaccines* (2019) 4:2–8. doi: 10.1038/s41541-018-0095-z
2. Voronin Y, Mofenson LM, Cunningham CK, Fowler MG, Kaleebu P, McFarland EJ, et al. HIV Monoclonal Antibodies: A New Opportunity to Further Reduce Mother-to-Child HIV Transmission. *PloS Med* (2014) 11: e1001616. doi: 10.1371/journal.pmed.1001616
3. Ferrari G, Haynes BF, Koenig S, Nordstrom JL, Margolis DM, Tomaras GD. Envelope-Specific Antibodies and Antibody-Derived Molecules for Treating and Curing HIV Infection. *Nat Rev Drug Discov* (2016) 15(12):823–34. doi: 10.1038/nrd.2016.173
4. Scheid JF, Horwitz JA, Bar-On Y, Kreider EF, Lu C-L, Lorenzi JCC, et al. HIV-1 Antibody 3BNC117 Suppresses Viral Rebound in Humans During Treatment Interruption. *Nature* (2016) 535(7613):1–21. doi: 10.1038/nature18929
5. Caskey M, Klein F, Lorenzi JCC, Seaman MS, West AP, Buckley N, et al. Viraemia Suppressed in HIV-1-Infected Humans by Broadly Neutralizing Antibody 3BNC117. *Nature* (2015) 522:487–91. doi: 10.1038/nature14411
6. Caskey M, Schoofs T, Gruell H, Settler A, Karagounis T, Kreider EF, et al. Antibody 10-1074 Suppresses Viremia in HIV-1-Infected Individuals. *Nat Med* (2017) 23:185–91. doi: 10.1038/nm.4268
7. Mendoza P, Gruell H, Nogueira L, Pai JA, Butler AL, Millard K, et al. Combination Therapy With Anti-HIV-1 Antibodies Maintains Viral Suppression. *Nature* (2018) 561:479–84. doi: 10.1038/s41586-018-0531-2
8. Bar-On Y, Gruell H, Schoofs T, Pai JA, Nogueira L, Butler AL, et al. Safety and Antiviral Activity of Combination HIV-1 Broadly Neutralizing Antibodies in Viremic Individuals. *Nat Med* (2018) 24:1701–7. doi: 10.1038/s41591-018-0186-4
9. Lynch RM, Boritz E, Coates EE, DeZure A, Madden P, Costner P, et al. Virologic Effects of Broadly Neutralizing Antibody VRC01 Administration During Chronic HIV-1 Infection. *Sci Transl Med* (2015) 7:319ra206–319ra206. doi: 10.1126/scitranslmed.aad5752
10. Bar KJ, Sneller MC, Harrison LJ, Justement JS, Overton ET, Petrone ME, et al. Effect of HIV Antibody VRC01 on Viral Rebound After Treatment Interruption. *N. Engl J Med* (2016) 375:2037–50. doi: 10.1056/NEJMoa1608243
11. Keele BF, Giorgi EE, Salazar-Gonzalez JF, Decker JM, Pham KT, Salazar MG, et al. Identification and Characterization of Transmitted and Early Founder Virus Envelopes in Primary HIV-1 Infection. *Proc Natl Acad Sci USA* (2008) 105:7552–7. doi: 10.1073/pnas.0802203105
12. Derdeyn CA, Decker JM, Bibollet-Ruche F, Mokili JL, Muldoon M, Denham SA, et al. Envelope-Constrained Neutralization-Sensitive HIV-1 After Heterosexual Transmission. *Science* (2004) 303:2019–22. doi: 10.1126/science.1093137
13. Kearney M, Maldarelli F, Shao W, Margolick JB, Daar ES, Mellors JW, et al. Human Immunodeficiency Virus Type 1 Population Genetics and Adaptation in Newly Infected Individuals. *J Virol* (2009) 83:2715–27. doi: 10.1128/JVI.01960-08
14. Zanini F, Brodin J, Thebo L, Lanz C, Bratt G, Albert J, et al. Population Genomics of Intrapatient HIV-1 Evolution. *Elife* (2015) 4:e11282. doi: 10.7554/eLife.11282
15. Shankarappa R, Gupta P, Learn GH, Rodrigo AG, Rinaldo CR, Gorry MC, et al. Evolution of Human Immunodeficiency Virus Type 1 Envelope Sequences in Infected Individuals With Differing Disease Progression Profiles. *Virology* (1998) 241:251–9. doi: 10.1006/viro.1997.8996
16. van Zyl G, Bale MJ, Kearney MF. HIV Evolution and Diversity in ART-Treated Patients. *Retrovirology* (2018) 15(14):1–12. doi: 10.1186/s12977-018-0395-4
17. Moore PL, Ranchobe N, Lambson BE, Gray ES, Cave E, Abrahams M-R, et al. Limited Neutralizing Antibody Specificities Drive Neutralization Escape in Early HIV-1 Subtype C Infection. *PloS Pathog* (2009) 5:e1000598. doi: 10.1371/journal.ppat.1000598
18. Rong R, Li B, Lynch RM, Haaland RE, Murphy MK, Mulenga J, et al. Escape From Autologous Neutralizing Antibodies in Acute/Early Subtype C HIV-1 Infection Requires Multiple Pathways. *PloS Pathog* (2009) 5:e1000594. doi: 10.1371/journal.ppat.1000594
19. Bar KJ, Tsao CY, Iyer SS, Decker JM, Yang Y, Bonsignori M, et al. Early Low-Titer Neutralizing Antibodies Impede HIV-1 Replication and Select for Virus Escape. *PloS Pathog* (2012) 8:e1002721. doi: 10.1371/journal.ppat.1002721
20. Mahalanabis M, Jayaraman P, Miura T, Pereyra F, Chester EM, Richardson B, et al. Continuous Viral Escape and Selection by Autologous Neutralizing Antibodies in Drug-Naive Human Immunodeficiency Virus Controllers. *J Virol* (2009) 83:662–72. doi: 10.1128/JVI.01328-08
21. Bonsignori M, Liao H-X, Gao F, Williams WB, Alam SM, Montefiori DC, et al. Antibody-Virus Co-Evolution in HIV Infection: Paths for HIV Vaccine Development. *Immunol. Rev* (2017) 275:145–60. doi: 10.1111/imr.12509
22. Baba M, Miyake H, Okamoto M, Iizawa Y, Okonogi K. Establishment of a CCR5-Expressing T-Lymphoblastoid Cell Line Highly Susceptible to R5 HIV Type 1. *AIDS Res Hum Retroviruses* (2000) 16:935–41. doi: 10.1089/08892220050058344
23. Ren Y, Korom M, Truong R, Chan D, Huang S-H, Kovacs CC, et al. Susceptibility to Neutralization by Broadly Neutralizing Antibodies Generally Correlates With Infected Cell Binding for a Panel of Clade B HIV Reactivated From Latent Reservoirs. *J Virol* (2018) 92:e00895–18. doi: 10.1128/JVI.00895-18
24. Salazar-Gonzalez JF, Salazar MG, Keele BF, Learn GH, Giorgi EE, Li H, et al. Genetic Identity, Biological Phenotype, and Evolutionary Pathways of Transmitted/Founder Viruses in Acute and Early HIV-1 Infection. *J Exp Med* (2009) 206:1273–89. doi: 10.1084/jem.20090378
25. Palmer S, Kearney M, Maldarelli F, Halvas EK, Bixby CJ, Bazmi H, et al. Multiple, Linked Human Immunodeficiency Virus Type 1 Drug Resistance Mutations in Treatment-Experienced Patients Are Missed by Standard Genotype Analysis. *J Clin Microbiol* (2005) 43:406–13. doi: 10.1128/JCM.43.1.406-413.2005
26. McInerney P, Adams P, Hadi MZ. Error Rate Comparison During Polymerase Chain Reaction by DNA Polymerase. *Mol Biol Int* (2014) 2014:287430. doi: 10.1155/2014/287430
27. Mansky LM, Temin HM. Lower *In Vivo* Mutation Rate of Human Immunodeficiency Virus Type 1 Than That Predicted From the Fidelity of Purified Reverse Transcriptase. *J Virol* (1995) 69:5087–94. doi: 10.1128/JVI.69.8.5087-5094.1995
28. Kearse M, Moir R, Wilson A, Stones-Havas S, Cheung M, Sturrock S, et al. Geneious Basic: An Integrated and Extendable Desktop Software Platform for the Organization and Analysis of Sequence Data. *Bioinformatics* (2012) 28:1647–9. doi: 10.1093/bioinformatics/bts199
29. Kumar S, Stecher G, Li M, Knyaz C, Tamura K. MEGA X: Molecular Evolutionary Genetics Analysis Across Computing Platforms. *Mol Biol Evol* (2018) 35:1547–9. doi: 10.1093/molbev/msy096

30. Stecher G, Tamura K, Kumar S. Molecular Evolutionary Genetics Analysis (MEGA) for macOS. *Mol Biol Evol* (2020) 37:1237–9. doi: 10.1093/molbev/msz312
31. Lynch RM, Tran L, Louder MK, Schmidt SD, Cohen MCHAVI 001 Clinical Team Members, et al. The Development of CD4 Binding Site Antibodies During HIV-1 Infection. *J Virol* (2012) 86:7588–95. doi: 10.1128/JVI.00734-12
32. Wei X, Decker JM, Liu H, Zhang Z, Arani RB, Kilby JM, et al. Emergence of Resistant Human Immunodeficiency Virus Type 1 in Patients Receiving Fusion Inhibitor (T-20) Monotherapy. *Antimicrobial Agents Chemother.* (2002) 46:1896–905. doi: 10.1128/AAC.46.6.1896-1905.2002
33. Montefiori DC. Measuring HIV Neutralization in a Luciferase Reporter Gene Assay. *Methods Mol Biol* (2009) 485:395–405. doi: 10.1007/978-1-59745-170-3_26
34. deCamp A, Hraber P, Bailer RT, Seaman MS, Ochsenbauer C, Kappes J, et al. Global Panel of HIV-1 Env Reference Strains for Standardized Assessments of Vaccine-Elicited Neutralizing Antibodies. *J Virol* (2014) 88:2489–507. doi: 10.1128/JVI.02853-13
35. Brumme ZL, Sudderuddin H, Ziemniak C, Luzuriaga K, Jones BR, Joy JB, et al. Genetic Complexity in the Replication-Competent Latent HIV Reservoir Increases With Untreated Infection Duration in Infected Youth. *Aids* (2019) 33:211–8. doi: 10.1097/QAD.0000000000002045
36. Maldarelli F, Kearney M, Palmer S, Stephens R, Mican J, Polis MA, et al. HIV Populations Are Large and Accumulate High Genetic Diversity in a Nonlinear Fashion. *J Virol* (2013) 87:10313–23. doi: 10.1128/JVI.01225-12
37. Salantes DB, Zheng Y, Mampe F, Srivastava T, Beg S, Lai J, et al. HIV-1 Latent Reservoir Size and Diversity Are Stable Following Brief Treatment Interruption. *J Clin Invest* (2018) 128:3102–15. doi: 10.1172/JCI120194
38. Bertagnolli LN, Varriale J, Sweet S, Brockhurst J, Simonetti FR, White J, et al. Autologous IgG Antibodies Block Outgrowth of a Substantial But Variable Fraction of Viruses in the Latent Reservoir for HIV-1. *Proc Natl Acad Sci USA* (2020) 117:32066–77. doi: 10.1073/pnas.2020617117
39. Doria-Rose NA, Klein RM, Daniels MG, O'Dell S, Nason M, Lapedes A, et al. Breadth of Human Immunodeficiency Virus-Specific Neutralizing Activity in Sera: Clustering Analysis and Association With Clinical Variables. *J Virol* (2010) 84:1631–6. doi: 10.1128/JVI.01482-09
40. Hraber P, Seaman MS, Bailer RT, Mascola JR, Montefiori DC, Korber BT. Prevalence of Broadly Neutralizing Antibody Responses During Chronic HIV-1 Infection. *Aids* (2014) 28:163–9. doi: 10.1097/QAD.0000000000000106
41. Sagar M, Wu X, Lee S, Overbaugh J. Human Immunodeficiency Virus Type 1 V1-V2 Envelope Loop Sequences Expand and Add Glycosylation Sites Over the Course of Infection, and These Modifications Affect Antibody Neutralization Sensitivity. *J Virol* (2006) 80:9586–98. doi: 10.1128/JVI.00141-06
42. Wei X, Decker JM, Wang S, Hui H, Kappes JC, Wu X, et al. Antibody Neutralization and Escape by HIV-1. *Nature* (2003) 422:307–12. doi: 10.1038/nature01470
43. Moody MA, Gao F, Gurley TC, Amos JD, Kumar A, Hora B, et al. Strain-Specific V3 and CD4 Binding Site Autologous HIV-1 Neutralizing Antibodies Select Neutralization-Resistant Viruses. *Cell Host Microbe* (2015) 18:354–62. doi: 10.1016/j.chom.2015.08.006
44. Stephenson KE, Neubauer GH, Bricault CA, Shields J, Bayne M, Reimer U, et al. Antibody Responses After Analytic Treatment Interruption in Human Immunodeficiency Virus-1-Infected Individuals on Early Initiated Antiretroviral Therapy. *Open Forum Infect Dis* (2016) 3:ofw100–9. doi: 10.1093/ofid/ofw100
45. Keating SM, Pilcher CD, Jain V, Lebedeva M, Hampton D, Abdel-Mohsen M, et al. HIV Antibody Level as a Marker of HIV Persistence and Low-Level Viral Replication. *J Infect Dis* (2017) 216:72–81. doi: 10.1093/infdis/jix225
46. Gray ES, Madiga MC, Hermanus T, Moore PL, Wibmer CK, Tumba NL, et al. The Neutralization Breadth of HIV-1 Develops Incrementally Over Four Years and Is Associated With CD4+ T Cell Decline and High Viral Load During Acute Infection. *J Virol* (2011) 85:4828–40. doi: 10.1128/JVI.00198-11
47. Piantadosi A, Panteleeff D, Blish CA, Baeten JM, Jaoko W, McClelland RS, et al. Breadth of Neutralizing Antibody Response to Human Immunodeficiency Virus Type 1 Is Affected by Factors Early in Infection But Does Not Influence Disease Progression. *J Virol* (2009) 83:10269–74. doi: 10.1128/JVI.01149-09
48. Rusert P, Kouyos RD, Kadelka C, Ebner H, Schanz M, Huber M, et al. Determinants of HIV-1 Broadly Neutralizing Antibody Induction. *Nat Med* (2016) 22(11):1260–7. doi: 10.1038/nm.4187
49. Sather DN, Armann J, Ching LK, Mavrantoni A, Sellhorn G, Caldwell Z, et al. Factors Associated With the Development of Cross-Reactive Neutralizing Antibodies During Human Immunodeficiency Virus Type 1 Infection. *J Virol* (2009) 83:757–69. doi: 10.1128/JVI.02036-08
50. Cohen YZ, Lorenzi JCC, Seaman MS, Nogueira L, Schoofs T, Krassnig L, et al. Neutralizing Activity of Broadly Neutralizing Anti-HIV-1 Antibodies Against Clade B Clinical Isolates Produced in Peripheral Blood Mononuclear Cells. *J Virol* (2017) 92(5):e01883-17. doi: 10.1128/JVI.01883-17
51. Louder MK, Sambor A, Chertova E, Hunte T, Barrett S, Ojong F, et al. HIV-1 Envelope Pseudotyped Viral Vectors and Infectious Molecular Clones Expressing the Same Envelope Glycoprotein Have a Similar Neutralization Phenotype, But Culture in Peripheral Blood Mononuclear Cells Is Associated With Decreased Neutralization Sensitivity. *Virology* (2005) 339:226–38. doi: 10.1016/j.virol.2005.06.003
52. Mann AM, Rusert P, Berlinger L, Kuster H, Günthard HF, Trkola A. HIV Sensitivity to Neutralization Is Determined by Target and Virus Producer Cell Properties. *Aids* (2009) 23:1659–67. doi: 10.1097/QAD.0b013e32832e9408
53. Raska M, Takahashi K, Czernekova L, Zachova K, Hall S, Moldoveanu Z, et al. Glycosylation Patterns of HIV-1 Gp120 Depend on the Type of Expressing Cells and Affect Antibody Recognition. *J Biol Chem* (2010) 285:20860–9. doi: 10.1074/jbc.M109.085472
54. Abrahams M-R, Joseph SB, Garrett N, Tyers L, Moeser M, Archin N, et al. The Replication-Competent HIV-1 Latent Reservoir Is Primarily Established Near the Time of Therapy Initiation. *Sci Transl Med* (2019) 43(1):406–13. doi: 10.1126/scitranslmed.aaw5589


**Author Disclaimer:** The content is solely the responsibility of the authors and does not necessarily represent the official views of the NIH.

**Conflict of Interest:** The authors declare that the research was conducted in the absence of any commercial or financial relationships that could be construed as a potential conflict of interest.

**Publisher's Note:** All claims expressed in this article are solely those of the authors and do not necessarily represent those of their affiliated organizations, or those of the publisher, the editors and the reviewers. Any product that may be evaluated in this article, or claim that may be made by its manufacturer, is not guaranteed or endorsed by the publisher.

frontiers in Immunology

ORIGINAL RESEARCH
published: 16 September 2021
doi: 10.3389/fimmu.2021.734110

# Combinations of Single Chain Variable Fragments From HIV Broadly Neutralizing Antibodies Demonstrate High Potency and Breadth

*Rebecca T. van Dorsten*[1,2], *Kshitij Wagh*[3], *Penny L. Moore*[1,2,4] *and Lynn Morris*[1,2,4]*

[1] Center for HIV and STIs, National Institute for Communicable Diseases of the National Health Laboratory Service, Johannesburg, South Africa, [2] Medical Research Council (MRC) Antibody Immunity Research Unit, Faculty of Health Sciences, University of the Witwatersrand, Johannesburg, South Africa, [3] Theoretical Division, Los Alamos National Laboratory, Los Alamos, NM, United States, [4] Center for the AIDS Programme of Research in South Africa (CAPRISA), University of KwaZulu-Natal, Durban, South Africa

OPEN ACCESS

**Edited by:**
*Susu M. Zughaier, Qatar University, Qatar*

**Reviewed by:**
*Christopher Andrew Cottrell, The Scripps Research Institute, United States*
*Michael Zwick, The Scripps Research Institute, United States*

***Correspondence:**
*Lynn Morris*
*lynnm@nicd.ac.za*

**Specialty section:**
*This article was submitted to Vaccines and Molecular Therapeutics, a section of the journal Frontiers in Immunology*

**Received:** *30 June 2021*
**Accepted:** *31 August 2021*
**Published:** *16 September 2021*

**Citation:**
*van Dorsten RT, Wagh K, Moore PL and Morris L (2021) Combinations of Single Chain Variable Fragments From HIV Broadly Neutralizing Antibodies Demonstrate High Potency and Breadth. Front. Immunol. 12:734110. doi: 10.3389/fimmu.2021.734110*

Broadly neutralizing antibodies (bNAbs) are currently being assessed in clinical trials for their ability to prevent HIV infection. Single chain variable fragments (scFv) of bNAbs have advantages over full antibodies as their smaller size permits improved diffusion into mucosal tissues and facilitates vector-driven gene expression. We have previously shown that scFv of bNAbs individually retain significant breadth and potency. Here we tested combinations of five scFv derived from bNAbs CAP256-VRC26.25 (V2-apex), PGT121 (N332-supersite), 3BNC117 (CD4bs), 8ANC195 (gp120-gp41 interface) and 10E8v4 (MPER). Either two or three scFv were combined in equimolar amounts and tested in the TZM-bl neutralization assay against a multiclade panel of 17 viruses. Experimental $IC_{50}$ and $IC_{80}$ data were compared to predicted neutralization titers based on single scFv titers using the Loewe additive and the Bliss-Hill model. Like full-sized antibodies, combinations of scFv showed significantly improved potency and breadth compared to single scFv. Combinations of two or three scFv generally followed an independent action model for breadth and potency with no significant synergy or antagonism observed overall although some exceptions were noted. The Loewe model underestimated potency for some dual and triple combinations while the Bliss-Hill model was better at predicting $IC_{80}$ titers of triple combinations. Given this, we used the Bliss-Hill model to predict the coverage of scFv against a 45-virus panel at concentrations that correlated with protection in the AMP trials. Using $IC_{80}$ titers and concentrations of 1μg/mL, there was 93% coverage for one dual scFv combination (3BNC117+10E8v4), and 96% coverage for two of the triple combinations (CAP256.25 +3BNC117+10E8v4 and PGT121+3BNC117+10E8v4). Combinations of scFv, therefore, show significantly improved breadth and potency over individual scFv and given their size advantage, have potential for use in passive immunization.

**Keywords: HIV, broadly neutralizing antibodies, single chain variable fragments, combinations of scFv, HIV prevention**

## INTRODUCTION

Broadly neutralizing antibodies (bNAbs), isolated from a subset of HIV-1 positive individuals, are capable of neutralizing a wide range of HIV viruses. Crucially, bNAbs have been shown to provide protection in non-human primate studies and it is thought that such antibodies are needed for an effective HIV vaccine (1–4). However, to date, no candidate HIV vaccines have been able to elicit bNAbs in humans (5–8). This has led the field to actively explore the possibility of using bNAbs as biological drugs for passive immunization against HIV (9–13).

The results of the first efficacy trials of an antibody for HIV prevention tested in Africa and the Americas have recently been published (14–17). These two Antibody-Mediated Prevention (AMP www.ampstudy.org.za) trials showed that VRC01 had 75% prevention efficacy in high-risk men and women if the infecting virus was sensitive to the antibody at <1μg/ml ($IC_{80}$). Therefore, to target the extensive envelope diversity, minimize escape, and provide sufficient potency a combination of multiple antibodies will be needed. Several studies have investigated the potential of antibody combinations and observed, as expected, an increase in breadth and potency (18, 19). These studies demonstrate that the complementary neutralization profiles of individual bNAbs can improve the overall breadth and provide higher coverage of multiclade panels of viruses at much lower antibody concentrations (18, 20). By using those antibodies that specifically target the HIV subtypes predominant in a specific area, a geographically relevant set of antibodies may be selected to provide optimal coverage and potency (20). For example, CAP256.25, which shows high potency against clade C viruses, is currently being assessed in combination with PGT121 and VRC07-523LS in dual and triple combination in the South African CAPRISA 012B trial (21, 22). Similarly, there are several ongoing phase 1 trials, testing multispecific antibodies or dual and triple combinations. These trials test the aforementioned antibodies in addition to V3 (10–1074) and V2 (PGDM1400) antibodies and the broadly neutralizing MPER-targeting antibody 10E8v4 (23, 24).

The ability to accurately predict the breadth and potency of antibody combinations without experimental validation enables the rapid identification of optimal combinations. Two models have been used to predict the $IC_{50}$ and $IC_{80}$ of antibody combinations based on single antibody titers, the Loewe Additive model, and the Bliss-Hill Independence model. Both models assume that there is no interaction between the different antibodies and that neutralization by combinations of antibodies will be additive, however, owing to different formulations of independence, their predicted results differ (18, 25). These models can also be used to determine whether synergy or antagonism occurs by comparing the predicted data with experimental results. When using the Loewe Additive model most combinations of two antibodies were demonstrated to show additive potency where the experimental potency was close to the predicted $IC_{50}$ (19). This model in comparison to experimental results has in cases also indicated synergy or antagonism between antibodies targeting specific epitopes such as the CD4 binding site, MPER, and V1/V2 antibodies. However, comprehensive analyses have shown that the Bliss-Hill model tended to be better at predicting IgG combination titers (18, 19) and this model did not predict synergy between these epitopes when predictions were compared to experimental results.

Experimental synergy between anti-HIV antibodies has only been rarely observed, and only in the context of bispecific antibodies. A bispecific antibody that simultaneously engaged the V2 and V3 epitopes showed moderate levels of synergy (26). Another bispecific employing a CAP256.25 scFv and the antibody binding fragment (Fab) of 10-1074, showed moderate levels of improved potency against a few viruses (26). In this case, neutralization was compared to single scFv-Fc or IgG rather than to the predicted combination titers or experimental combinations of the two arms, which may have overestimated the level of synergy (20, 26–30). More convincing evidence of synergy was observed when antibodies targeting a host cell protein and the viral Env protein were combined particularly as part of bispecific or trispecific antibody constructs. This effect is due to the localization of the anti-HIV antibody close to the host cell membrane through CCR5 or CD4 binding, for example, the 10E8-iMab, which targets the MPER region on the HIV virion and the CD4 receptor on the HIV target cell. This bispecific antibody has a geometric mean $IC_{50}$ potency of 0.002μg/mL compared to 0.4μg/mL for 10E8 and 0.05μg/mL for the iMab indicating a 25-fold improvement over the expected activity (27, 31).

Single chain variable fragments (scFv) are small molecules, which contain the variable heavy and light chain of antibodies connected through a glycine linker. These molecules have some enhanced pharmacokinetic properties such as improved distribution and absorption into mucosal tissues despite a loss of half-life due to lacking an Fc region (32–35). They may also display less steric hindrance when used in combination with other molecules and other bNAbs or scFv (36). This may be especially true for epitopes in close proximity such as the V2 and V3, or V3 and CD4bs. A recent study demonstrated that scFv targeting the V3 and CD4bs could display synergy when combined with fusion inhibitors (37).

We previously demonstrated that scFv of bNAbs retain significant breadth and potency against a multiclade panel of viruses despite potency differences linked to differential affinity for the epitope (38). In particular, 10E8v4 maintained the same breadth and most of its potency as an scFv. Single antibodies may be limited in their ability to prevent HIV infection, however, as evidenced by the recent AMP results. We, therefore, tested combinations of scFv that target major bNAb epitopes on the HIV trimer, namely CAP256.25 (V2 apex), PGT121 (N332-supersite), 3BNC117 (CD4bs), 8ANC195 (gp120-gp41), and 10E8v4 (MPER) and show that they generally follow a model of additive potency and complementary breadth. No significant antagonism or synergy was observed compared to the models, although antibody combinations tested against individual viruses could show variation. Overall, combinations of three scFv antibodies reached considerable breadth and potency indicating that scFv in combinations should be further investigated for passive immunity purposes.

# METHODS

## scFv Construction

scFv were designed and cloned previously as described (38). In short, single constructs containing the variable heavy and light chain interspaced with a 15 or 18 amino acid glycine-serine linker of five HIV-directed bNAbs (CAP256.25, PGT121, 3BNC117, 8ANC195, and 10E8v4) were generated through overlapping PCR or ordered from GenScript (New Jersey, USA) (38). These scFv genes were then cloned into a CMV/R expression plasmid (AIDS Reagent Program, Division of AIDS, NIAID, NIH. For the lambda chain of PGT121, the pBR322 based lambda expression vector was used (AIDS Reagent Program, Division of AIDS, NIAID, NIH).

## scFv Protein Expression

The constructs were grown in JM109 bacterial cells and extracted using a plasmid Maxiprep kit (Qiagen, Hilden Germany). Sequences were confirmed using the Applied Biosystems 3500xL Genetic Analyzer. Constructs were expressed as previously described (39). In short, HEK293F suspension cells at $1.5x10^6$ to $2x10^6$ cells/ml were cotransfected with linear Polyethylenimine hydrochloride (molecular weight, 40,000) at a 3:1 ratio with 1µg of plasmid per 1 ml of culture. Supernatants were harvested after 6 days.

scFv proteins were purified using Ni-Sepharose beads (GE Healthcare, Massachusetts USA), washed using a 30mM imidazole–phosphate-buffered saline (PBS) solution and eluted using 400mM imidazole in PBS. Glycerol was added to the elution at a final concentration of 5% to limit aggregation. Eluates were applied to Hiload Superdex 75 or Superdex 200 columns (GE Healthcare) equilibrated with PBS at pH 6.5 (5% glycerol with 0.02% sodium azide). The fractions corresponding to the size of the scFv were collected, pooled, and concentrated using Vivaspin concentrators or Vivapore static concentrators (GE Healthcare). The samples were dialyzed overnight at room temperature to remove sodium azide. Concentrations were measured on a NanoDrop device (Thermofisher, MA, USA), with extinction coefficients at 1% calculated using Expasy ProtParam (40) and characterized by SDS-PAGE. Molar weight was determined by using Expasy ProtParam (CAP256.25: 31.35kDa, PGT121: 28.89kDa, 3BNC117 28.47kDa, 10E8v4: 29.30kDa and 8ANC195 29.00kDa). scFv proteins were stored at -75°C.

## IgG Production

IgG constructs were expressed in HEK293F cells as described previously (39). Supernatants were harvested after 6 days and purified using a protein A affinity column. Proteins were eluted using a 0.15M glycine buffer at pH 2.5 buffer into 1M Tris, pH 8, and were concentrated and dialyzed into PBS pH 6.5 containing 5% glycerol. Concentrations were measured on a Nanodrop using an Extinction Coefficient of 13.7 at a 1% solution. The molecular weight of the IgG was calculated using the Expasy ProtParam (40) of CAP256.25 (150.71kDa), 10E8v4 (147.29kDa), 3BNC117: (146.24kDa), PGT121: (146.2kDa), 8ANC195: (147.43kDa). IgG and proteins were stored at -75°C.

## Pseudovirus production for TZM-bl Assay

Plasmids containing HIV-1 envelope (gp160) genes cloned in the pcDNA™3.1D/V5-His-TOPO® vector were co-transfected with $pSG3^{\Delta env}$ into HEK293T cells and cultured for 48-72hrs at 37°C. Supernatants were harvested and filtered through a 45µm filter and frozen at -80°C. Virus stocks were titrated on TZM-bl cells using a luciferase assay to determine a dilution yielding RLU at least 10-fold above the "cell only" background (40,000-100,000 RLU).

## Neutralization Assay

A panel of 43 viruses (41) plus BG505 N332 and CAP256_SU (CAP256.3mo.9C) (42, 43) representing HIV-1 clades A, B, and C was used to compare neutralization titers of IgG and scFv. Neutralization assays were performed in TZM-bl cells as described previously (44–46). Proteins were tested at 200µg/mL for the IgG (~146kDa) and 50µg/mL for the scFv (28-32 kDa). All assays were repeated at least twice. $IC_{50}$ and $IC_{80}$ of each antibody tested was calculated and geometric mean potency was calculated for both IgG and scFv using sensitive viruses only.

## Experimental Testing of scFv Combinations

Combinations were tested by adding equimolar amounts of two or three scFv proteins in a neutralization assay as described above. A panel of 17 subtype A, B and C viruses were selected based on their sensitivity to at least 2 of the scFv in order to test neutralization of scFv combinations and confirm the Loewe Additivity and Bliss-Hill Independence models. Pre-dilutions containing scFv at 2µM and 10µM each were used to facilitate the assay set up. As a control, the single scFv were diluted to 10µM and 2µM as well and run alongside the combinations as a comparison. The highest concentration tested for the combinations was 30µg/mL or 1000nM. $IC_{50}$ and $IC_{80}$ of each experimental antibody combination was calculated, where each antibody is present at the concentration determined at $IC_{50}$ or $IC_{80}$.

## Loewe Additivity and Bliss-Hill Independence Models

The $IC_{50}$ and $IC_{80}$ values from experimental combinations were compared to the predicted $IC_{50}$ and $IC_{80}$ based on the Loewe Additive model and the Bliss-Hill model as previously described (18, 19).

The following formula is used to calculate Loewe Additivity.

$$Predicted IC_{50} = 1/\left(\frac{1}{IC_{50}(A)} + \frac{1}{IC_{50}(B)} + \ldots \frac{1}{IC_{50}(N)}\right)$$

Post analysis values were recalculated from nM into µg/mL based on the following formula.

$$IC_{50} in \quad \mu g/mL = \frac{(Mw(A) \times IC_{50} \quad in \quad nM) + (Mw(B) \times IC_{50} \quad in \quad nM) + \ldots (Mw(N) \times IC_{50} \quad in \quad nM)}{n \times 1000}$$

Where (n) is the number of antibodies, Mw the molecular weight of the antibodies in the combination, and $IC_{50}$ the experimental $IC_{50}$ or theoretical $IC_{50}$ obtained. The same formula is used for

$IC_{80}$ values replacing the $IC_{50}$ with $IC_{80}$ in the formula above. For resistant viruses, the model assumes the titer of the active scFv.

For the Bliss-Hill Independence model, the following formula was used to calculate the Hill function

$$f(c) = \frac{c^m}{(k^m + c^m)}$$

Where c= bNAb concentration, k = $IC_{50}$, and

$$m = \frac{\log(4)}{\log(IC_{80}) - \log(IC_{50})}$$

The combination neutralization curve is then calculated using the Bliss Independence model,

$$f = 1 - (1 - f(A))(1 - f(B))(\ldots)$$

with f(A), f(B), etc. being the individual functions of the scFv antibodies. Combination molar $IC_{50}$ and $IC_{80}$ titers are calculated by setting f = 0.5 or 0.8 and assuming each scFv is present at the same molarity, and converted to μg/ml using the above formula.

Dual/triple coverage was calculated by considering a virus resistant if less than 2/3 antibodies in the combination were able to neutralize that virus at set concentrations.

We used the following formula for both models to determine which is more accurate in predicting the combination potencies for $IC_{50}$ and $IC_{80}$.

$$Absolute(Log10(experimental \quad IC_{50}) - Log10(predicted \quad IC_{50}))$$

## Synergy and/or Antagonism Predictions Based on Loewe Additivity and Bliss-Hill Independence Models

Synergy was predicted based on whether the experimental $IC_{50}$ and $IC_{80}$ were improved compared to the Loewe Additive model or the Bliss-Hill model. The formula below was used to characterize this effect, with the Bliss-Hill $IC_{50}$ replacing the Loewe $IC_{50}$ in the formula below.

$$LogFold = Log10(\frac{Loewe^{50}}{Experimental\, IC_{50}})$$

Positive values indicate experimental titers lower (i.e. more potent) than predicted and imply synergy, while negative values indicate less potent experimental titers than predicted and imply antagonism. For a given combination of antibodies, the mean and the 95% Confidence interval were calculated using LogFold values for this combination against each virus in the panel.

## Statistics

All statistics were done using the GraphPad Prism 8 software. Fold differences of the experimental combinations were calculated with the most potent scFv in the mixture for both $IC_{50}$ and $IC_{80}$. A Wilcoxon signed-rank test was performed to test which model was more accurate at predicting the experimental titers for both $IC_{50}$ and $IC_{80}$. Pearson's Correlation between experimental neutralization titers and titers based on the two models was calculated using the GraphPad software. A nonlinear fit model (log-log) was used to predict the slope between the experimental and predicted data, using a robust regression. A log-fold with a 95% confidence interval was used to determine if the fold difference is significantly different from 0, indicating either synergy or antagonism. Breadth-potency curves were drawn using a survival model in GraphPad. Significance was tested using the log-rank Mantel-Cox significance test.

# RESULTS

## Dual and Triple Combinations of scFv of HIV bNAbs

To assess whether scFv of HIV bNAbs showed increased breadth and potency when used in combination, we tested five different scFv as part of dual and triple combinations. The scFv included those targeting the V2 (CAP256.25), the N332 supersite (PGT121), the CD4bs (3BNC117), and the MPER region (10E8v4), all of which were previously shown to retain significant activity compared to IgG (38). For this study, we added the antibody 8ANC195 that targets the gp120-gp41 interface so that all five major epitopes on the HIV trimer were covered (see single $IC_{50}$ and $IC_{80}$ data in nM **Supplementary 1A** and **1B** and in μg/ml **1C** and **1D** respectively, (38)]. All scFv were expressed and purified by size exclusion columns and, with size and purity confirmed SDS-PAGE gels. scFv were stored in buffers containing 5% glycerol as determined previously to prevent aggregation (38).

Combinations of scFv were tested against a panel of 17 pseudoviruses from subtypes A, B, and C (n=3, 4 and 10, respectively). These were selected based on their sensitivity to at least three of the five scFv under investigation. Equimolar amounts (based on their molecular weights), of each scFv in combinations of two or three were tested, giving a total of 20 different combinations of antibodies (10 dual and 10 triple combinations), which were compared to single scFv neutralization titers. To standardize the output data, the concentration of the single scFv and the scFv combinations in μg/mL were calculated from the nM titers and the molecular weight of the scFvs (**Figure 1**, **Supplementary Figure 2**) (38). Combination titers $IC_{50}$ and $IC_{80}$ are reported as the concentration of each scFv in the mix in μg/mL or nM.

As expected, combinations of two scFv improved the coverage, with active scFv making up for the inactive scFv. For all dual and triple combinations, breadth reached 100% at $IC_{50}$ against this 17-virus panel (**Figure 1**). The neutralization of individual viruses by two or three scFv was usually similar to the $IC_{50}$ of the most potent scFv in the combination (**Figure 1**; fold differences are shown in the columns next to the $IC_{50}$s). Except for a few cases, the virus neutralization titers of the dual and triple combinations fell within 3-fold of the titer of the

**A**

| | Pseudovirus | $IC_{50}$ of single scFv in µg/mL (converted from nM) | | | | |
|---|---|---|---|---|---|---|
| | | CAP256.25 | PGT121 | 3BNC117 | 8ANC195 | 10E8v4 |
| Subtype A | Q23 | 0.30 | 0.0054 | 0.042 | 7.2 | 0.42 |
| | Q168 | 1.1 | >30 | 0.030 | 0.67 | 0.51 |
| | Q842 | 3.7 | 0.058 | 0.012 | >30 | 0.54 |
| Subtype B | AC10 | 7.3 | 0.042 | >30 | 1.8 | 0.10 |
| | RHPA | >30 | 0.013 | 0.016 | 0.25 | 0.35 |
| | PV04 | 0.83 | 0.15 | 0.044 | 1.9 | 0.65 |
| | 6535 | >30 | 0.0035 | 5.4 | 0.56 | 0.16 |
| Subtype C | Du156 | 0.015 | 0.015 | 1.5 | 2.5 | 0.11 |
| | ZM53 | 0.0020 | 0.066 | 1.7 | 0.15 | 0.33 |
| | ZM233 | 0.042 | >30 | 4.2 | 2.5 | 0.100 |
| | ZM249 | 0.50 | 0.34 | 0.065 | 8.3 | 0.40 |
| | CAP8.6F | 8.1 | 0.0098 | >30 | 2.9 | 0.18 |
| | CAP61 | 4.5 | 0.019 | 2.7 | 13 | 0.31 |
| | CAP84.32 | 9.2 | 0.0040 | >30 | >30 | 0.34 |
| | CAP88 | >30 | 4.4 | 28 | 5.1 | 0.0098 |
| | CAP256_SU | 0.0024 | 0.018 | 0.41 | 0.27 | 0.68 |
| | ConC | 0.0054 | 0.016 | 2.0 | 1.1 | 0.17 |
| | Geomean | 0.28 | 0.031 | 0.40 | 1.6 | 0.23 |

**B**

| | Pseudovirus | $IC_{50}$ of Combinations of scFv in µg/mL (converted from nM) | | | | | | | | | | | | | | | | | |
|---|---|---|---|---|---|---|---|---|---|---|---|---|---|---|---|---|---|---|---|
| | | CAP256.25 PGT121 | | CAP256.25 3BNC117 | | CAP256.25 8ANC195 | | CAP256.25 10E8v4 | | PGT121 3BNC117 | | PGT121 8ANC195 | | PGT121 10E8v4 | | 3BNC117 8ANC195 | | 3BNC117 10E8v4 | | 8ANC195 10E8v4 | |
| Subtype A | Q23 | 0.0074 | 0.7 | 0.028 | 1.5 | 0.18 | 1.7 | 0.058 | **5.2** | 0.0065 | 0.8 | 0.0076 | 0.7 | 0.0091 | 0.6 | 0.046 | 0.9 | 0.042 | 1.0 | 0.44 | 1.0 |
| | Q168 | 1.1 | 1.0 | 0.028 | 1.1 | 0.29 | 2.3 | 0.14 | **3.5** | 0.031 | 1.0 | 0.97 | 0.7 | 0.46 | 1.1 | 0.025 | 1.2 | 0.024 | 1.2 | 0.20 | 2.6 |
| | Q842 | 0.041 | 1.4 | 0.0078 | 1.5 | 2.1 | 1.7 | 0.39 | 1.4 | 0.0064 | 1.8 | 0.043 | 1.3 | 0.030 | 2.0 | 0.0084 | 1.4 | 0.0078 | 1.5 | 0.52 | 1.0 |
| Subtype B | AC10 | 0.042 | 1.0 | 18 | 0.4 | 1.1 | 1.7 | 0.093 | 1.1 | 0.033 | 1.3 | 0.044 | 1.0 | 0.016 | 2.6 | 2.7 | 0.7 | 0.11 | 1.0 | 0.10 | 1.0 |
| | RHPA | 0.029 | 0.4 | 0.013 | 1.2 | 0.22 | 1.1 | 0.20 | 1.8 | 0.012 | 1.1 | 0.025 | 0.5 | 0.027 | 0.5 | 0.023 | 0.7 | 0.024 | 0.7 | 0.16 | 1.6 |
| | PV04 | 0.16 | 1.0 | 0.034 | 1.3 | 0.30 | 2.8 | 0.16 | **4** | 0.036 | 1.2 | 0.083 | 1.9 | 0.11 | 1.5 | 0.034 | 1.3 | 0.032 | 1.4 | 0.24 | 2.7 |
| | 6535 | 0.0032 | 1.1 | 7.0 | 0.8 | 0.31 | 1.8 | 0.080 | 2.0 | 0.0035 | 1.0 | 0.0040 | 0.9 | 0.0033 | 1.0 | 0.26 | 2.1 | 0.11 | 1.5 | 0.086 | 1.9 |
| Subtype C | Du156 | 0.011 | 1.4 | 0.011 | 1.4 | 0.012 | 1.2 | 0.0096 | 1.5 | 0.012 | 1.2 | 0.012 | 1.2 | 0.0071 | 2.1 | 0.52 | 2.8 | 0.071 | 1.6 | 0.069 | 1.7 |
| | ZM53 | 0.0039 | 0.5 | 0.0040 | 0.5 | 0.0035 | 0.6 | 0.0039 | 0.5 | 0.083 | 0.8 | 0.049 | 1.3 | 0.028 | 2.3 | 0.16 | 1.0 | 0.28 | 1.2 | 0.28 | 0.6 |
| | ZM233 | 0.025 | 1.2 | 0.017 | 1.8 | 0.026 | 1.2 | 0.014 | 2.2 | 2.9 | 1.0 | 3.7 | 0.7 | 0.12 | 0.8 | 1.4 | 1.8 | 0.18 | 0.6 | 0.13 | 0.8 |
| | ZM249 | 0.26 | 1.3 | 0.043 | 1.5 | 0.99 | 0.5 | 0.045 | **9** | 0.21 | **0.3** | 0.67 | 0.5 | 0.091 | **3.7** | 0.076 | 0.9 | 0.068 | 1.0 | 0.31 | 1.3 |
| | CAP8.6F | 0.0083 | 1.2 | 4.3 | 1.9 | 1.5 | 2.0 | 0.069 | 2.5 | 0.0087 | 1.1 | 0.0076 | 1.3 | 0.0082 | 1.2 | 3.6 | 0.8 | 0.24 | 0.7 | 0.15 | 1.1 |
| | CAP61 | 0.013 | 1.4 | 0.82 | **3.2** | 1.5 | **3.1** | 0.10 | **3.1** | 0.016 | 1.2 | 0.012 | 1.6 | 0.012 | 1.6 | 2.5 | 1.1 | 0.22 | 1.5 | 0.17 | 1.9 |
| | CAP84.32 | 0.0051 | 0.8 | 9.6 | 1.0 | 11 | 0.8 | 0.16 | 2.1 | 0.0041 | 1.0 | 0.0050 | 0.8 | 0.0043 | 0.9 | 6.9 | **4.3** | 0.25 | 1.3 | 0.31 | 1.1 |
| | CAP88 | 2.0 | 2.3 | 30 | 1.0 | 4.6 | 1.1 | 0.0089 | 1.1 | 4.1 | 1.1 | 0.15 | **29** | 0.0052 | 1.9 | 9.6 | 0.5 | 0.0092 | 1.1 | 0.011 | 0.9 |
| | CAP256_SU | 0.0041 | 0.6 | 0.0050 | 0.5 | 0.0038 | 0.6 | 0.0048 | 0.5 | 0.018 | 1.0 | 0.018 | 1.0 | 0.014 | 1.3 | 0.12 | 2.3 | 0.21 | 2.0 | 0.28 | 1.0 |
| | ConC | 0.0047 | 1.2 | 0.0075 | 0.7 | 0.0093 | 0.6 | 0.0099 | 0.5 | 0.0073 | 2.2 | 0.0063 | 2.6 | 0.0059 | 2.8 | 0.38 | 2.8 | 0.087 | 2.0 | 0.076 | 2.3 |
| | Geomean | 0.026 | 1.2 | 0.12 | 2.2 | 0.23 | 1.2 | 0.044 | **4.9** | 0.030 | 1.1 | 0.040 | 0.80 | 0.019 | 1.6 | 0.30 | 1.3 | 0.072 | **3.0** | 0.16 | 1.4 |

**C**

| | Pseudovirus | $IC_{50}$ Combinations of scFv in µg/mL (converted from nM) | | | | | | | | | | | | | | | | | |
|---|---|---|---|---|---|---|---|---|---|---|---|---|---|---|---|---|---|---|---|
| | | CAP256.25 PGT121 3BNC117 | | CAP256.25 PGT121 8ANC195 | | CAP256.25 PGT121 10E8v4 | | CAP256.25 3BNC117 8ANC195 | | CAP256.25 3BNC117 10E8v4 | | CAP256.25 8ANC195 10E8v4 | | PGT121 3BNC117 8ANC195 | | PGT121 3BNC117 10E8v4 | | PGT121 8ANC195 10E8v4 | | 3BNC117 8ANC195 10E8v4 | |
| Subtype A | Q23 | 0.003 | 1.9 | 0.004 | 1.5 | 0.003 | 1.8 | 0.023 | 1.8 | 0.022 | 1.9 | 0.075 | 4.1 | 0.006 | 1.0 | 0.005 | 1.1 | 0.005 | 1.2 | 0.045 | 0.9 |
| | Q168 | 0.031 | 1.0 | 0.28 | 2.4 | 0.16 | **3.1** | 0.021 | 1.5 | 0.016 | 1.9 | 0.093 | **5.5** | 0.033 | 0.9 | 0.023 | 1.3 | 0.13 | **3.9** | 0.029 | 1.0 |
| | Q842 | 0.007 | 1.8 | 0.040 | 1.5 | 0.046 | 1.3 | 0.008 | 1.5 | 0.008 | 1.4 | 0.38 | 1.4 | 0.006 | 2.0 | 0.006 | 2.1 | 0.023 | 2.5 | 0.008 | 1.5 |
| Subtype B | AC10 | 0.028 | 1.5 | 0.024 | 1.7 | 0.030 | 1.4 | 1.9 | 0.9 | 0.051 | 2.0 | 0.046 | 2.2 | 0.041 | 1.0 | 0.022 | 1.9 | 0.021 | 2.0 | 0.061 | 1.7 |
| | RHPA | 0.005 | 2.6 | 0.008 | 1.6 | 0.025 | 0.5 | 0.014 | 1.1 | 0.011 | 1.5 | 0.095 | 2.6 | 0.007 | 1.7 | 0.007 | 1.7 | 0.006 | 2.1 | 0.015 | 1.1 |
| | PV04 | 0.025 | 1.7 | 0.074 | 2.1 | 0.12 | 1.3 | 0.038 | 1.2 | 0.023 | 1.9 | 0.100 | **6.5** | 0.034 | 1.3 | 0.029 | 1.5 | 0.075 | 2.1 | 0.035 | 1.2 |
| | 6535 | 0.002 | 1.7 | 0.002 | 1.7 | 0.003 | 1.0 | 0.39 | 1.4 | 0.079 | 2.1 | 0.082 | 2.0 | 0.005 | 0.7 | 0.004 | 0.9 | 0.003 | 1.0 | 0.081 | 2.0 |
| Subtype C | Du156 | 0.004 | **3.7** | 0.003 | **4.5** | 0.004 | **3.7** | 0.029 | 0.5 | 0.009 | 1.6 | 0.010 | 1.5 | 0.008 | 1.9 | 0.007 | 2.0 | 0.005 | **3.1** | 0.084 | 1.4 |
| | ZM53 | 0.001 | 1.7 | 0.002 | 1.3 | 0.002 | 1.2 | 0.002 | 0.8 | 0.001 | 1.4 | 0.002 | 1.3 | 0.045 | 1.5 | 0.047 | 1.4 | 0.032 | 2.0 | 0.090 | 1.7 |
| | ZM233 | 0.068 | 0.5 | 0.050 | 0.6 | 0.023 | 1.3 | 0.048 | 0.7 | 0.023 | 1.4 | 0.018 | 1.8 | 1.9 | 1.3 | 0.18 | 0.5 | 0.10 | 1.0 | 0.15 | 0.7 |
| | ZM249 | 0.032 | 2.0 | 0.15 | 2.2 | 0.074 | **4.5** | 0.063 | 1.0 | 0.013 | **4.9** | 0.063 | **6.3** | 0.15 | 0.4 | 0.054 | 1.2 | 0.11 | **3.2** | 0.068 | 1.0 |
| | CAP8.6F | 0.010 | 1.0 | 0.007 | 1.5 | 0.006 | 1.7 | 3.0 | 1.0 | 0.11 | 1.5 | 0.077 | 2.3 | 0.013 | 0.7 | 0.011 | 0.9 | 0.006 | 1.6 | 0.11 | 1.5 |
| | CAP61 | 0.016 | 1.2 | 0.010 | 1.8 | 0.008 | 2.4 | 1.3 | 2.0 | 0.15 | 2.2 | 0.11 | 2.9 | 0.015 | 1.3 | 0.013 | 1.5 | 0.007 | **2.7** | 0.24 | 1.3 |
| | CAP84.32 | 0.003 | 1.3 | 0.003 | 1.2 | 0.007 | 0.6 | 3.8 | 2.4 | 0.20 | 1.7 | 0.18 | 1.9 | 0.006 | 0.7 | 0.004 | 1.0 | 0.005 | 0.9 | 0.15 | 2.3 |
| | CAP88 | 1.9 | 2.0 | 0.58 | **6.7** | 0.004 | 2.2 | 1.4 | **3.5** | 0.003 | **3.6** | 0.002 | **5.4** | 1.3 | 2.9 | 0.005 | 1.9 | 0.004 | 2.5 | 0.004 | 2.6 |
| | CAP256_SU | 0.002 | 1.2 | 0.004 | 0.5 | 0.002 | 1.0 | 0.003 | 0.9 | 0.003 | 0.8 | 0.002 | 1.0 | 0.022 | 0.9 | 0.012 | 1.6 | 0.013 | 1.4 | 0.098 | 2.8 |
| | ConC | 0.003 | 2.1 | 0.002 | 2.7 | 0.003 | 1.9 | 0.008 | 0.7 | 0.006 | 0.9 | 0.006 | 0.9 | 0.009 | 1.8 | 0.008 | 2.1 | 0.008 | 1.9 | 0.048 | **3.6** |
| | Geomean | 0.010 | **3.0** | 0.014 | 2.2 | 0.011 | 2.8 | 0.078 | **3.5** | 0.018 | **12** | 0.033 | **6.6** | 0.027 | 1.2 | 0.013 | 2.4 | 0.015 | 2.1 | 0.052 | **4.2** |

**FIGURE 1** | Neutralization titers of single, dual, and triple combinations of scFv. Heat map showing $IC_{50}$ neutralization titers in µg/mL for single **(A)**, dual **(B)**, and triple **(C)** combinations of scFv against a panel of 17 subtype A, B, and C viruses. Viruses insensitive to individual bNAbs are shown as >30µg/mL. The fold improvement in $IC_{50}$ titers of the dual and triple combinations relative to the $IC_{50}$ of the best scFv in the combination is included in **(B, C)**. Values with >3-fold increase or decrease in neutralization are shown in bold. Geometric mean potency is included at the bottom of each table. Each scFv is present in the combination at the titer indicated.

most potent single scFv in that combination. There was little to no loss of potency noted compared to the most potent scFv for the entire panel for all 20 scFv combinations tested (a total of 340 single test titers). A few instances of potential gain of potency compared to the most potent scFv were noted, with most of these linked to specific scFv combinations (bolded values in **Figure 1**).(See **Supplementary Figure 2** for $IC_{50}$ titers in nM **(A)** and μg/mL **(B)** and for $IC_{80}$ values in nM **(C)** and μg/mL **(D)** respectively).

The combination of CAP256.25+10E8v4 scFv stood out, demonstrating an overall 4.9-fold improvement in geometric mean titer (**Figure 1B**). This was driven by five viruses of which two were subtype A, one was subtype B and two were subtype C indicating this was not subtype-specific. Five other dual scFv combinations showed improved potency over single scFv for single viruses but this was not linked to any specific combination of antibodies. The 3BNC117+10E8v4 combination showed an overall significant improvement in the geometric mean titer although this was not seen for individual viruses indicating complementarity of neutralization potency of the scFv rather than synergy.

For the triple combinations, five of the ten combinations showed >3-fold improved geometric means compared to the most potent single scFv with a 12-fold improvement for the CAP256.25+3BNC117+10E8v4 combination (**Figure 1C**). This was higher than for the dual combinations where only two out of ten showed an improvement in geometric mean potency and was driven by improvement in potency against single viruses (16 of the 170 virus-scFv combination pairings). This was due to the scFv (e.g. CAP256.25 and 3BNC117 scFv), in the combinations being potent against different viruses allowing for complementarity in neutralization potency and coverage. Triple combinations overall showed higher improvements in breadth compared to dual combinations or single scFv as a consequence of having more antibodies.

Some viruses appeared to be more sensitive to the effects of combined scFv. For example, a slight potency improvement was observed against the CAP61 and ZM249 viruses for the dual combinations, although for the latter loss of potency was also noted (fold difference <0.33 see **Figure 1B**). Some enhancement in potency was also seen with these viruses plus Du156 and CAP88 for the triple combinations (**Figure 1C**).

Overall, we found either improved or similar titers for combinations compared to the most potent single scFv, particularly for triple combinations, indicating that combinations of scFv improve the coverage of a panel of viruses and the potency at which viruses are neutralized. We overlaid neutralization curves of the combinations with the single scFv used in the combination, to determine if there were distinct patterns associated with improved $IC_{50}$s or where we observed similar $IC_{50}$ for the combinations compared to the single scFv. For most dual and triple combinations (314/340), an additive effect was seen where the combination curve overlapped with the best scFv in the combination (**Figure 2A**). Here $IC_{50}$ did not show a potency improvement compared to the single scFv. A few combinations shifted the curve to the left compared to the curve of the most potent single scFv corresponding with fold potency improvements as seen in **Figure 1** and indicating potential synergy (10/170 virus-dual combination pairings and 16/170 in the triple combinations showed improved $IC_{50}$s) (**Figure 2B**). In one case we observed decreased potency for the combination compared to the most potent scFv possibly indicating some antagonism (**Figure 2C**). With the addition of a third antibody this was partially negated (**Figure 2C** right panel). Overall, most combinations did not show significant potency improvements or loss of potency, suggesting that they largely followed an additive model of potency.

## scFv Follow an Additive Model of Interaction in HIV Neutralization

To further explore whether combinations of scFv follow an additive model of interaction we compared the experimental results with predictions based on the single scFv titers using the Loewe Additive model and the Bliss-Hill models. As mentioned before, both these models assume no synergistic or antagonistic interactions between antibodies (18, 19). We calculated the combination scFv $IC_{50}$ and $IC_{80}$ titers based on these 2 models (Methods) and based on the geometric mean $IC_{50}$ and $IC_{80}$ of the repeats of single scFv obtained in the experiment. All scFv predicted data titers were compared to the $IC_{50}$ and $IC_{80}$ titers of the experimentally tested combinations.

There was a strong significant ($p<0.0001$) correlation between the experimental $IC_{50}$ and $IC_{80}$ and the predicted $IC_{50}$ and $IC_{80}$ of the dual combinations for both the Loewe and Bliss Hill model (Loewe, Pearson's r=0.94 and r=0.79 respectively, Bliss-Hill, r=0.94 and 0.91 respectively) (**Figures 3A, B**). Similarly, for the triple combinations, there was a strong correlation between the predicted values and the experimental values (Loewe r=0.78 and r=0.79, Bliss-Hill: r=0.70 and r=0.95 respectively) (**Figures 3C, D**). For each combination, we also determined which model was better by comparing the mean absolute log difference between the experimental values and the predicted values for each individual combination. For the dual combinations, the Bliss Hill model was better at predicting two out of the 10 combinations (10E8v4 combined with CAP256.25 or PGT121), whereas no significant difference between the models was observed for any of the other combinations (**Figures 3E, F**). Similarly, for the triple combinations, most combinations did not show differences between the two models in the $IC_{50}$ with the Bliss-Hill model being better at predicting two combinations (8ANC195 + 10E8v4 with either CAP256.25 or PGT121) (**Figure 3G**). For the $IC_{80}$ of the triple combinations, 6/10 combinations were significantly better predicted by the Bliss-Hill model compared to the Loewe model (**Figure 3H**). This indicated that for most combinations both Loewe and Bliss-Hill could predict combination $IC_{50}$ titers well with a slight advantage for the Bliss-Hill model. However, the Bliss-Hill model is significantly better at predicting triple $IC_{80}$ titers compared to the Loewe model, with the latter underestimating the potency of the triple combinations at $IC_{80}$.

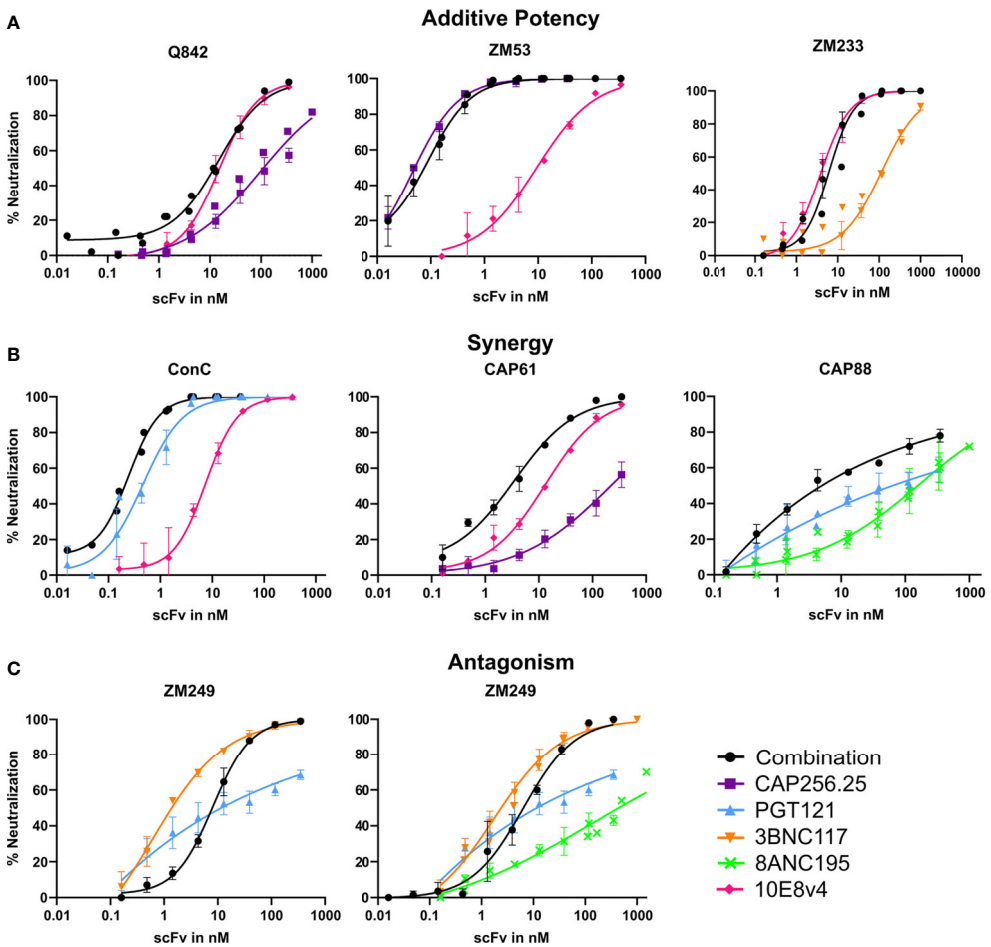


**FIGURE 2** | Combinations of scFv that show improved neutralization potency over single scFv. Neutralization curves showing potential additive, synergistic and antagonistic potency effects of combinations of antibodies. Combinations of scFv compared to single scFv neutralization curves with CAP256.25 in purple, PGT121 in light blue, 3BNC117 in orange, 8ANC195 in green and 10E8v4 in pink. The dual or triple combinations are represented in black. Geometric mean values are used for each data point with error bars representing repeat experiments. **(A)** Examples of combinations where neither synergy nor antagonism is observed for three viruses tested against dual combinations of scFv. Additive potency is represented by the combination curve (black) overlapping with the best scFv in the mixture. **(B)** Potential synergy as observed in dual combinations of scFv against three different virus strains. Synergy was represented by a left shift of the combination curve (black) relative to the most potent scFv in the mixture, or by steeper neutralization curves resulting in improved IC80. **(C)** Potential antagonism as represented by a right shift of the combination curve relative to the most potent scFv in the mixture, observed in combinations of two or three scFv tested against ZM249, which was sensitive to all scFv in the combinations.

## No Synergy or Antagonism Observed for scFv Combinations Against a Panel of HIV Pseudovirus

We next sought to determine if any of the combinations showed significant potency improvement or potency loss in either $IC_{50}$ or $IC_{80}$ by comparing the experimental data to the expected titers based on the Bliss Hill model. These analyses allowed us to determine if there is potential synergy (higher potency than predicted), as indicated by a log-fold difference >0.4 (~2.5 fold) and/or antagonism (lower potency than predicted) as indicated by a log-fold difference <-0.4 (**Figure 4**). The dual combinations had a mean log-fold difference close to 0 (log-fold -0.4<CI<0.4) for both $IC_{50}$ and $IC_{80}$ indicating that there was neither antagonism nor synergy, although a few antibody combinations showed some improved potency (red dots, $IC_{50}$ n=3, 1.7% and $IC_{80}$: n=0, 0%) or decreased potency (blue dots, $IC_{50}$ and $IC_{80}$: n=6, 3.5%) for individual viruses these were relatively few and most showed less than 0.4 log fold difference when compared to model predictions (**Figures 4A, B**).

For the triple combinations, similar results were observed with 157/170 of the $IC_{50}$ and 154/170 of the $IC_{80}$ values showing less than a Log (2.5) difference. The mean on triple combinations was also close to 0 (log-fold -0.4<CI<0.4) for both $IC_{50}$ and $IC_{80}$. Similarly, only a few individual viral titers showed a potential loss of potency for the $IC_{50}$ (n=8, 4.7%) and $IC_{80}$ (n=11, 6.5%) or a potential gain of potency ($IC_{50}$ and $IC_{80}$: n=5, 3%) for triple combinations compared to the model (**Figures 4C, D**). None of the outliers in dual or triple combinations could be linked to

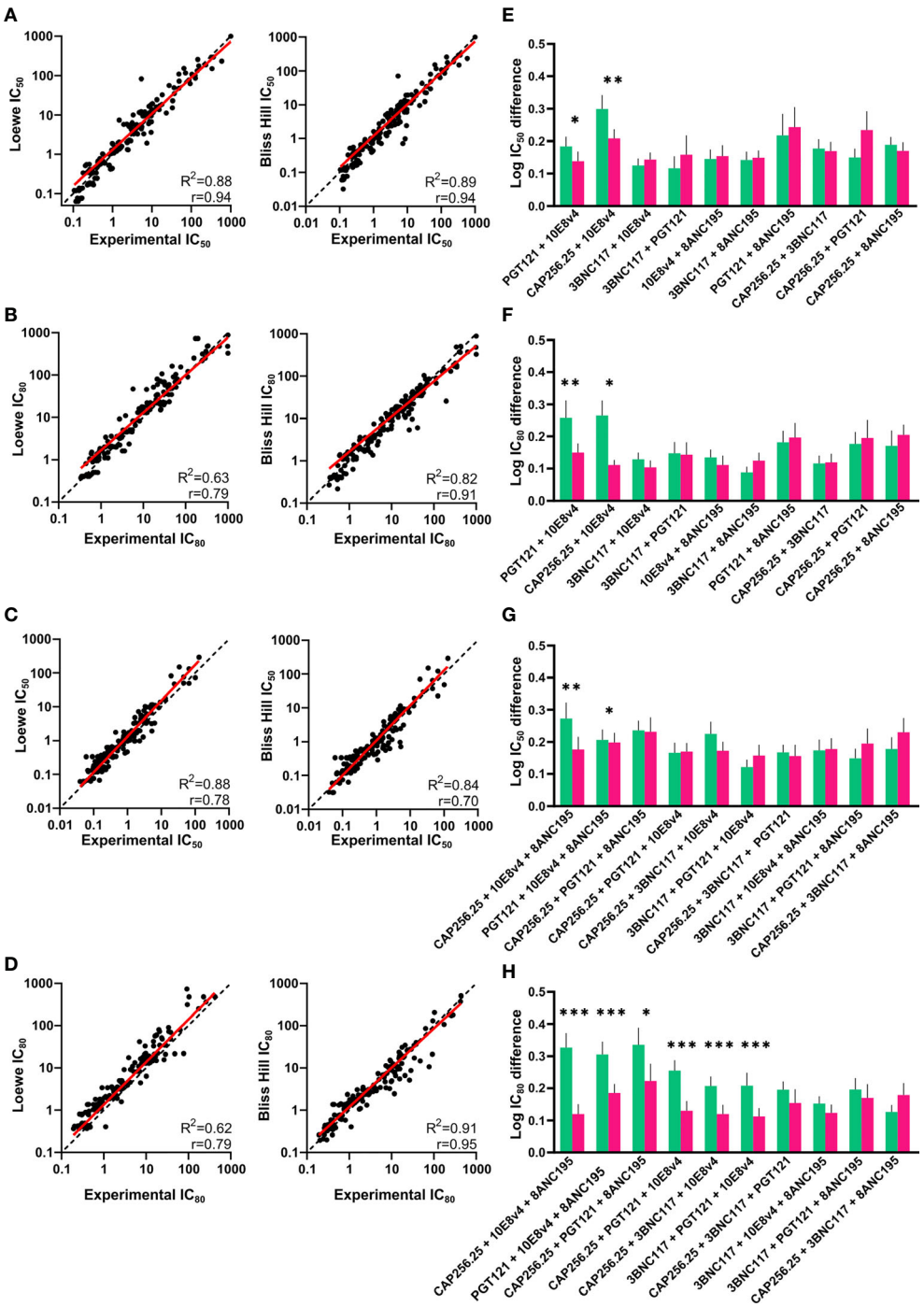


**FIGURE 3** | Comparison of experimental and predicted combinations of dual and triple scFv. **(A, B)** $IC_{50}$ and $IC_{80}$ titers of dual antibody combinations plotted against the predicted $IC_{50}$ and $IC_{80}$ titers according to the Loewe Additive (left) and Bliss-Hill Independence (right) models. **(C, D)** Predicted $IC_{50}$ and $IC_{80}$ titers of triple combinations *versus* the experimental $IC_{50}$ and $IC_{80}$ titers. Values where both or all titers of single scFv >30µg/mL are excluded. **(E, F)** Comparison of the absolute Log($IC_{50}$) and Log($IC_{80}$) difference between the experimental titers and predicted titers according to the Loewe Additive (green) and Bliss-Hill independence (purple) for the dual combinations. **(G, H)** Comparison of the absolute Log($IC_{50}$) and Log($IC_{80}$) difference between the experimental titers and predicted titers according to the Loewe Additive (green) and Bliss-Hill independence (purple) models for the triple combinations. For **(A, B, E, F)**, a nonlinear robust regression log-log line (red) and an equity line (black dotted) as well as r, R2, are shown and p<0.0001. For **(C, D, G, H)**, mean values are given with a standard error of the mean. A paired, Wilcoxon t-test was performed on each pair with significant p values above the graphs ($p < 0.05$ = * $p < 0.01$ = ** $p < 0.001$= ***).

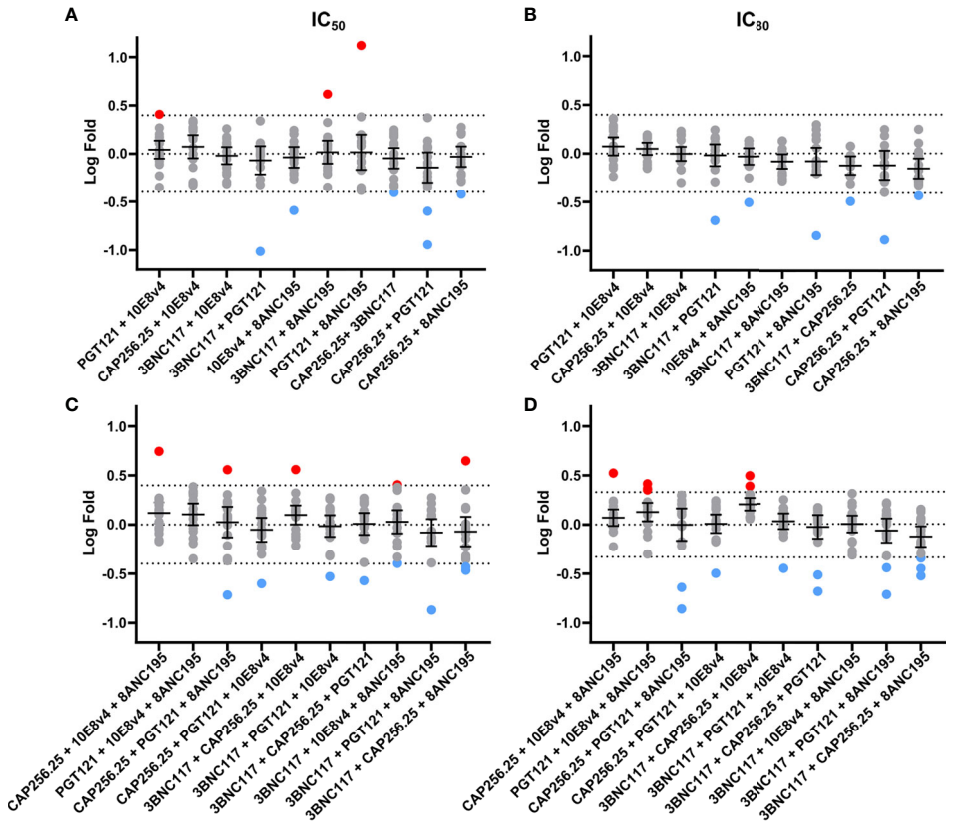


**FIGURE 4** | No synergy observed using fold difference between experimental and Bliss-Hill predictions of dual and triple scFv combinations. Log-fold differences of double and triple $IC_{50}$ **(A, C)** and $IC_{80}$ **(B, D)** experimental combinations to the Bliss-Hill Independence model prediction. Mean and the 95% confidence interval are shown with a dotted line indicating no fold change. Log (2.5) fold difference dotted lines (0.4 or -0.4) are also shown. Red and blue are used to indicate more than a log difference of 0.4 (~2.5x) with red dots indicating potential synergy and blue dots indicating potential antagonism.

specific viral signatures (data not shown). Notwithstanding these few outliers, we, did not observe any significant synergy nor antagonism for dual or triple combinations of scFv.

## Using the Bliss-Hill Model to Predict $IC_{50}$ and $IC_{80}$ Titers of scFv Combinations Against a Larger HIV Panel

In order to assess their breadth-potency on a larger virus panel, we used the $IC_{50}$ and $IC_{80}$ data of single scFv to predict neutralization titers for combinations of two and three scFv, now including 8ANC195, on a 45-virus panel described in our previous study (38) (see **Supplementary Figure 1** for single $IC_{50}$ in nM **(A)** and $IC_{80}$ in nM **(B)** or μg/mL **(C, D)** titers) (38). These theoretical scFv combinations were ranked based on their geometric mean potency using both $IC_{50}$ and $IC_{80}$ data for dual and triple combinations (**Figures 5A, B, E, F**). Combinations with the expected highest breadth and potency were plotted using breadth-potency curves (**Figures 5C, D, G, H**).

The best dual combinations, namely PGT121+10E8v4 (red), 3BNC117+10E8v4 (pink), and CAP256.25+10E8v4 (orange) were able to neutralize most viruses barring one at $IC_{50}$ and $IC_{80}$ (**Figures 5A, B**). The breadth-potency curves of the three 10E8v4-containing combinations reached 100% neutralization at the $IC_{50}$ and 98% neutralization at the $IC_{80}$ (colored breadth-potency plots *versus* grey, **Figures 5C, D**) with most viruses neutralized between 0.1 and 1μg/mL at $IC_{80}$. The fourth combination of 10E8v4 with 8ANC195 was less effective due to the low potency of both antibodies and the limited breadth of 8ANC195, [see **Supplementary Figure 3** (38)]. The other dual combinations showed reduced breadth (up to 30% at 50μg/mL) or reduced potency especially at $IC_{80}$ (grey dots and lines). Some combinations such as PGT121+3BNC117 had a potent geometric mean below 0.1μg/mL at $IC_{50}$, but there was a larger spread of neutralization titers and so breadth was lost at $IC_{80}$ (**Figures 5A, B**). (See **Supplementary Figure 4** for $IC_{50}$ in nM **(A)** and μg/mL **(B)** and $IC_{80}$ in nM **(C)** and μg/mL **(D)** titers of dual, and triple combinations predicted by the Bliss-Hill Independence model).

The triple combinations showed higher levels of potency and complete neutralization with 8/10 combinations showing complete neutralization of the viral panel at $IC_{50}$, and 6/10 showing near-complete neutralization at $IC_{80}$ (**Figures 5E–H**). Moreover, 7/10 triple combinations had a geometric mean potency below 0.1μg/mL at $IC_{50}$ (**Figure 5E**, green, dark green, and blue). Of these, three combinations all had a geometric mean $IC_{80}$ below 1μg/mL and neutralized up to

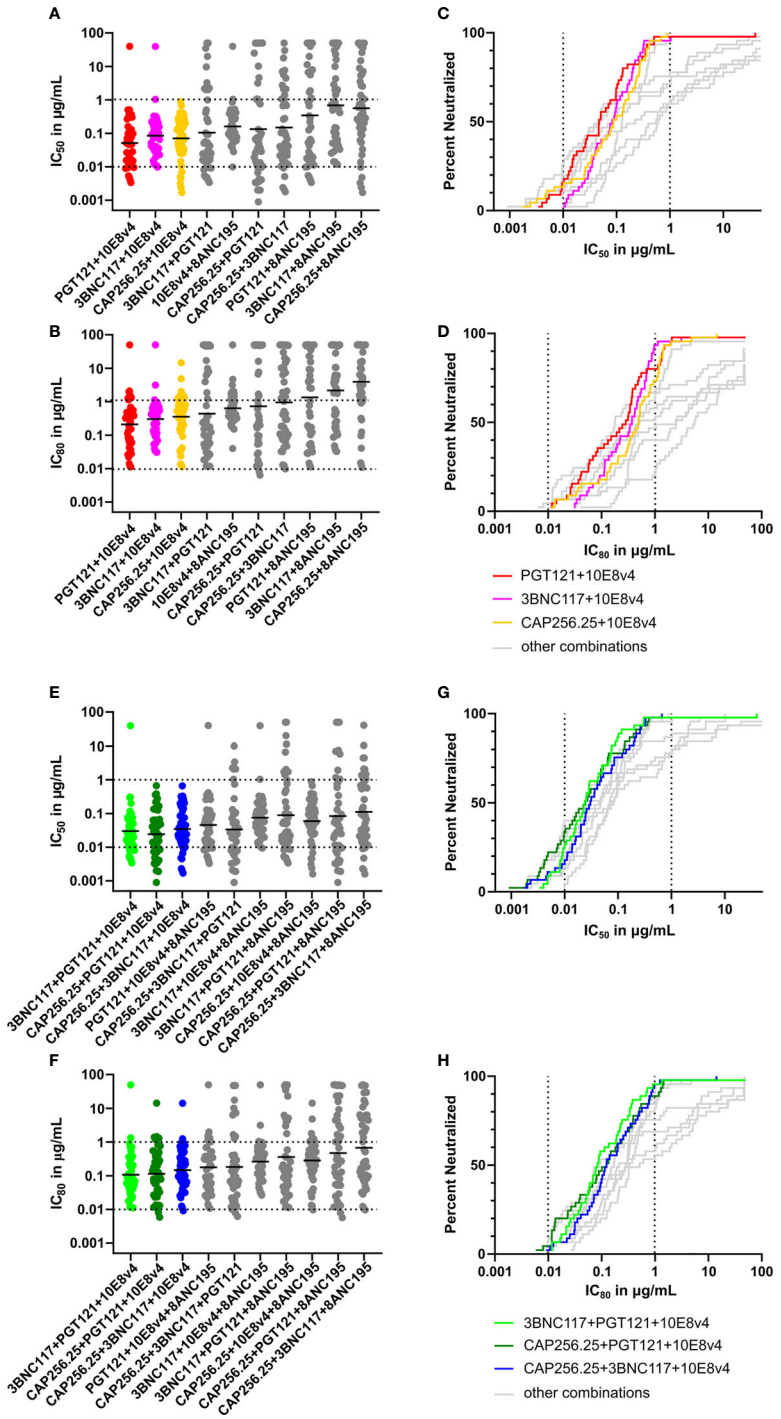


**FIGURE 5** | Predicted breadth and potency of scFv combinations against large virus panel. **(A)** Scatter plot showing predicted $IC_{50}$ titers of dual combinations based on single scFv data for a panel of 45 viruses using the Bliss-Hill Independence model. The $IC_{50}$ data is plotted in µg/mL recalculated from nM based on the formula given in the methods section. **(B)** Predicted $IC_{80}$ titers of dual combinations based on the Bliss-Hill Independence model ranked by geometric mean. **(C)** Breadth-potency curves of $IC_{50}$ titers of most potent and broad dual combinations were plotted for the $IC_{50}$.with the others in grey. **(D)** Breadth-potency curves from $IC_{80}$ data for the most potent and broad dual combinations. **(E)** $IC_{50}$ titers for triple combinations based on the Bliss-Hill Independence model. **(F)** Predicted $IC_{80}$ titers for the triple combinations ranked based on geometric mean. **(G)** Breadth potency curves for the $IC_{50}$ of the most potent and broad triple combinations are plotted. **(H)** The breadth-potency curves are based on $IC_{80}$ titers of the most potent and broad combinations. The maximum neutralization for the $IC_{50}$ and $IC_{80}$ data is set at 50µg/mL for all plots. Geometric mean is indicated by a black line in **A, C, E**, and **G** Dotted lines are shown at 0.01µg/mL and 1µg/mL for breadth-potency plots $IC_{50}$ and the $IC_{80}$ **(B, D, F, H)**. Each scFv is present in the combination at the titer indicated.

96% of viruses (**Figures 5F, H**). This indicated that triple combinations are able to reach nearly 100% neutralization at lower concentrations for both $IC_{50}$ and $IC_{80}$ (see **Supplementary Figure 4** for $IC_{50}$ in nM **(A)** and µg/mL **(B)** and $IC_{80}$ in nM **(C)** and µg/mL **(D)** titers of dual, and triple combinations predicted by the Bliss-Hill Independence model).

The predicted breadth of each combination was next determined at four concentrations: 0.1, 1, 10, and 50µg/mL in addition to the geometric mean for the combinations tested (with a cutoff at 50µg/mL). Combining these scFv improved the coverage at all concentrations for both $IC_{50}$ and $IC_{80}$ (**Figure 6**). Breadth for dual combinations ranged from 84% to 100% at $IC_{50}$ < 50µg/ml and 80% to 100% at $IC_{80}$ < 50µg/ml. For dual combinations, 100% breadth was reached for one combination at $IC_{50}$ < 1µg/mL, and for four combinations at $IC_{50}$ < 50µg/mL. For the $IC_{80}$, 98% breadth was obtained at 10µg/mL for the same combinations. Most combinations of three scFv had 100% breadth at $IC_{50}$ < 50 µg/ml, except for PGT121+3BNC117+8ANC195 and CAP256.25+PGT121 +8ANC195, which had a breadth of 96% and 93% respectively. Breadth was especially improved for lower concentrations at $IC_{80}$. For example, breadth for single scFv ranged from 0 to 44% for $IC_{50}$ < 0.1µg/ml and 0 to 24% for $IC_{80}$ < 0.1µg/ml, whereas dual combinations ranged from 22 to 62% for $IC_{50}$ and 2 to 29% for $IC_{80}$. At the same cutoff, the breadth for combinations of 3 antibodies ranged from 47% to 82% for $IC_{50}$ and 16 to 40% for $IC_{80}$. Geometric mean potency for the panel also improved from 0.2-4.95 µg/mL for single scFv to 0.27-2.08µg/mL for dual combinations and 0.09-0.61µg/mL for triple combinations at $IC_{80}$. This was expected as the titers were calculated as containing the same amount of each scFv at that concentration.

Since PGT121, 3BNC117, and CAP256.25 all had good potencies as scFv, using these together with 10E8v4 resulted in improved potency of the combination. Moreover, scFv such as CAP256.25 and PGT121 and/or 3BNC117 have complementary profiles, with 3BNC117, for example, being especially potent against subtype B viruses and CAP256.25 being potent against subtype C viruses (see **Supplementary Data 1** for the $IC_{50}$ and $IC_{80}$ of single scFv) (38). 10E8v4 is the broadest scFv and that resulted in the combinations containing 10E8v4 having the highest breadth. As a result, four of the five triple combinations with the best geometric mean titers included 10E8v4. Conversely, introducing less potent or less broad antibodies such as 8ANC195 resulted in less favorable antibody combinations, where 5 out of 6 combinations with the lowest potency and breadth contained 8ANC195, consistent with the relatively lower potency and breadth of this antibody. Of the top five, three combinations, CAP256.25+PGT121+10E8v4

| | $IC_{50}$ in µg/mL | | | | | $IC_{80}$ in µg/mL | | | | |
|---|---|---|---|---|---|---|---|---|---|---|
| | 0.1 | 1 | 10 | 50 | geomean | 0.1 | 1 | 10 | 50 | geomean |
| CAP256.25 | 20% | 47% | 62% | 62% | 0.20 | 11% | 16% | 29% | 49% | 1.82 |
| PGT121 | 44% | 56% | 62% | 71% | 0.12 | 24% | 44% | 51% | 56% | 0.20 |
| 3BNC117 | 29% | 47% | 69% | 78% | 0.39 | 13% | 31% | 62% | 69% | 0.98 |
| 10E8v4 | 27% | 96% | 98% | 100% | 0.21 | 2% | 49% | 98% | 98% | 0.82 |
| 8ANC195 | 0% | 20% | 51% | 69% | 2.94 | 0% | 7% | 24% | 40% | 4.95 |
| CAP256.25+10E8v4 | 53% | 100% | 100% | 100% | 0.07 | 18% | 73% | 98% | 100% | 0.36 |
| PGT121+10E8v4 | 69% | 98% | 98% | 100% | 0.05 | 36% | 80% | 98% | 98% | 0.19 |
| 3BNC117+10E8v4 | 60% | 96% | 98% | 100% | 0.08 | 20% | 93% | 98% | 98% | 0.27 |
| 10E8v4+8ANC195 | 40% | 96% | 98% | 100% | 0.16 | 2% | 64% | 98% | 98% | 0.57 |
| PGT121+3BNC117 | 64% | 78% | 91% | 96% | 0.08 | 38% | 67% | 82% | 91% | 0.28 |
| CAP256.25+3BNC117 | 51% | 71% | 93% | 98% | 0.13 | 27% | 51% | 71% | 89% | 0.58 |
| CAP256.25+8ANC195 | 27% | 60% | 82% | 91% | 0.36 | 11% | 20% | 58% | 80% | 2.08 |
| PGT121+8ANC195 | 44% | 60% | 80% | 87% | 0.16 | 24% | 47% | 67% | 82% | 0.62 |
| 3BNC117+8ANC195 | 33% | 60% | 78% | 87% | 0.36 | 13% | 40% | 67% | 80% | 1.00 |
| CAP256.25+PGT121 | 64% | 71% | 80% | 84% | 0.04 | 36% | 58% | 69% | 82% | 0.29 |
| CAP256.25+3BNC117+10E8v4 | 76% | 100% | 100% | 100% | 0.03 | 42% | 96% | 98% | 100% | 0.15 |
| CAP256.25+PGT121+10E8v4 | 78% | 100% | 100% | 100% | 0.02 | 47% | 89% | 98% | 100% | 0.11 |
| CAP256.25+10E8v4+8ANC195 | 60% | 100% | 100% | 100% | 0.06 | 20% | 82% | 98% | 100% | 0.28 |
| PGT121+3BNC117+10E8v4 | 87% | 98% | 98% | 100% | 0.03 | 58% | 96% | 98% | 98% | 0.09 |
| PGT121+10E8v4+8ANC195 | 76% | 98% | 98% | 100% | 0.05 | 42% | 84% | 98% | 98% | 0.16 |
| 3BNC117+10E8v4+8ANC195 | 62% | 96% | 98% | 100% | 0.07 | 22% | 93% | 98% | 98% | 0.23 |
| CAP256.25+PGT121+3BNC117 | 78% | 87% | 100% | 100% | 0.03 | 53% | 76% | 89% | 100% | 0.18 |
| CAP256.25+3BNC117+8ANC195 | 58% | 78% | 96% | 100% | 0.11 | 29% | 53% | 82% | 98% | 0.61 |
| PGT121+3BNC117+8ANC195 | 67% | 80% | 91% | 96% | 0.07 | 40% | 69% | 84% | 93% | 0.25 |
| CAP256.25+PGT121+8ANC195 | 64% | 78% | 93% | 93% | 0.05 | 38% | 58% | 80% | 93% | 0.34 |

**FIGURE 6** | Neutralization breadth for single and combinations of scFv against a 45-virus panel at four concentrations. Percentage neutralization at 0.1, 1, 10, and 50µg/mL was calculated from single scFv titers and from predicted scFv dual and triple combination titers for the $IC_{50}$ and $IC_{80}$. Colors indicate percentage neutralization with 1-19% in green, 20-49% yellow, 50-79% yellow-orange, 80-89% orange, 90-99% red and 100% dark red. Geometric mean at 50µg/mL is also given. Each scFv is present in the combinations at the titers indicated.

and CAP256.25+3BNC117+10E8v4 and CAP256.25+8ANC195 +10E8v4 neutralized all viruses below 1μg/mL and 98% of viruses at $IC_{80}$ below 10μg/mL. The best ranked PGT121 +3BNC117+10E8v4 combination neutralized 96% of viruses below 1μg/mL and 98% of viruses below 10μg/mL at the $IC_{80}$ value. This analysis indicated a significant gain of potency and neutralization breadth at lower concentrations than single scFv at both $IC_{50}$ and $IC_{80}$. This indicated that combinations of scFv were able to increase the coverage at lower concentrations, which will be vital in clinical settings.

## Predicting the Efficacy of scFv Combinations

The AMP trial showed that viral isolates that were sensitive to VRC01 with an $IC_{80}$<1μg/mL were prevented from establishing infection in 75% of cases. As indicated in **Figures 5** and **6**, scFv combinations can reach significant coverage by a single antibody at this potency with the best scFv combination potentially reaching a 96% protection level. However, other antibody classes may need higher levels of potency to provide similar protection as VRC01 and viral isolates which are neutralized close to this cut-off may allow for breakthrough. Dual coverage will be able to overcome these issues by neutralizing breakthrough viruses at higher potencies and providing a back-up in case antibody levels drop. Therefore, using this cut-off, we calculated the predicted dual coverage (i.e. by at least two scFv) of the combinations using the thresholds of single scFv $IC_{80}$ < 1μg/ml and < 10μg/mL. We found for dual combinations, the dual active coverage at 1μg/mL ranged from 20% with improvement at 10μg/mL to 51% for PGT121+10E8v4 (**Figures 7A, B**), This ranged from 0-20% at 1μg/mL and 9-62% for other combinations of two antibodies (See **Supplementary Figure 5**).

This was somewhat improved for triple combinations where we observed up to 58-80% dual active coverage at an $IC_{80}$ of

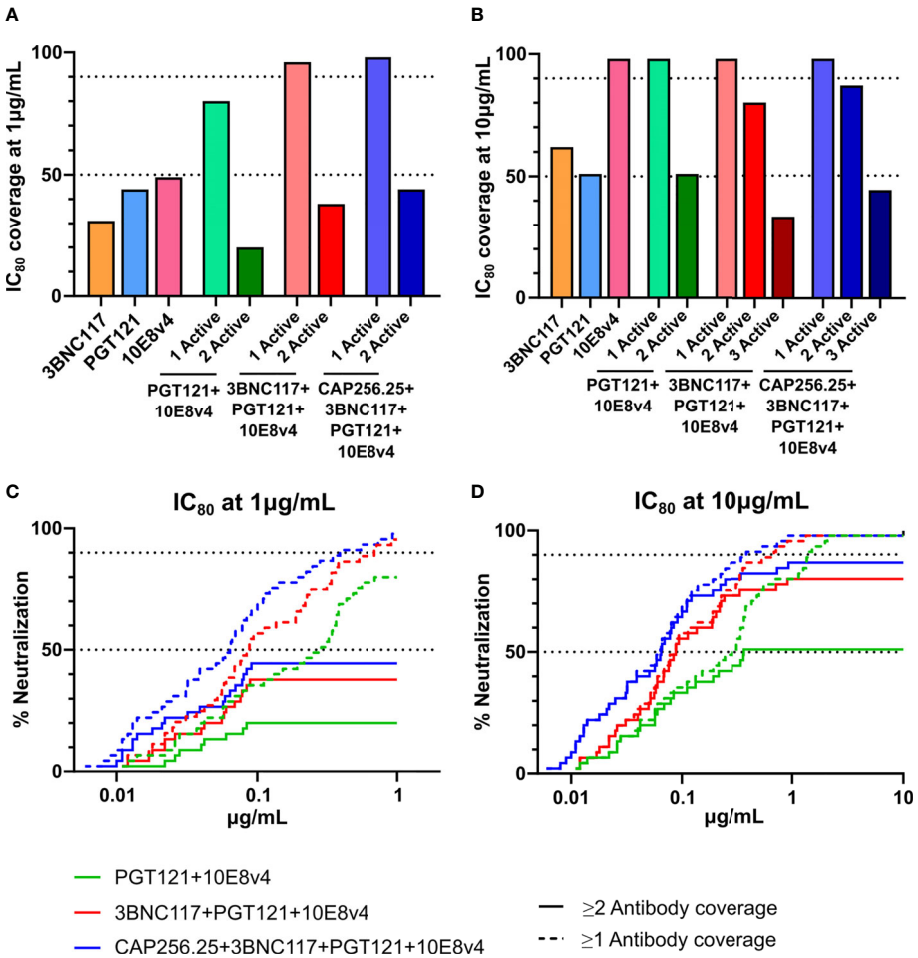


**FIGURE 7** | Predicted coverage and estimated efficacy of best scFv combinations. **(A, B)** Active coverage by one, two, three or four scFv was calculated at 2 concentrations (1μg/mL **(A)** and 10μg/mL **(B)** at $IC_{80}$ based on the predicted titers according to the Bliss-Hill Independence model. The broadest triple and quadruple combinations are shown. **(C, D)** Breadth Potency curves of active coverage of 1 and 2 scFv are given for the best combinations (3BNC17+10E8v4 and 3BNC17+10E8v4+PGT121, and CAP256.25+3BNC17+10E8v4+PGT121) at 1 μg/mL **(C)** and 10μg/mL **(D)**. 50% and 90% breadth are indicated by the dotted lines in **(C, D)**.

10μg/mL. The best 3-combinations,3BNC117+PGT121+10E8v4 showing the highest active coverage at 10μg/mL of 80%. Generally, triple combinations showed higher levels of active coverage by 2 antibodies and often included both 10E8v4 and 3BNC117. Similar to the dual combinations, low dual coverage was observed at 1μg/mL up to 38% (See **Figure 7A**, **Supplementary Figure 5**. This could not be significantly improved for quadruple combinations which showed 44% and 87% dual coverage respectively at 1 and 10μg/mL. This loss of active coverage by multiple antibodies is also demonstrated in the breadth potency curves (**Figures 7C, D**). These curves clearly show that although at 10μg/mL most of the dual coverage is maintained there is a significant drop off at 1μg/mL. This was mainly due to antibodies such as 3BNC117, PGT121, and 10E8v4 showing only 31-49% breadth at 1μg/mL and the CAP256.25 scFv losing significant potency compared to the IgG (38). IgG combinations including this antibody could show slightly better active coverage by 2 antibodies, up to 53% at an $IC_{80}$ of 1μg/mL and up to 91% at 10μg/mL (**Supplementary Data 6A** for predictions of IgG combinations titers in μg/mL and **6B** for neutralization breadth at 4 concentrations and dual coverage by IgG) (38). The other IgG and scFv showed similar levels of potency with specifically the 10E8v4 scFv retaining all of its potency explaining why the IgG combinations did not show higher levels of dual active coverage at 1μg/mL (**Figure 7**, **Supplementary Figure 6B**). This indicated that potency of single IgG and scFv needs to be improved to obtain higher levels of active coverage by 2 antibodies at lower antibody levels. The combination data demonstrate that the benefits of combinations of IgG targeting different HIV epitopes apply also to the smaller and more versatile scFv fragments.

## DISCUSSION

Combinations of scFv antibodies were able to enhance the breadth and potency of HIV-1 neutralization compared to a single scFv. Specifically, several triple combinations reached 100% coverage at $IC_{50}$ and $IC_{80}$ due to complementary neutralization profiles. Dual and triple combinations of scFv demonstrated broad coverage in the potency range that correlated with prevention in the AMP trials ($IC_{80}$<1μg/mL) and would therefore be expected to be highly effective in combating HIV transmission in high incidence areas.

Generally, dual scFv combinations followed an independent action model rather than a synergistic model of potency. The potency of the combination was usually similar to the potency of the most potent scFv in that mix. Although scFv may show less steric interference between antibodies this did not result in scFv showing significant potency improvements when used in combination. The close positioning of certain epitopes may prevent dual binding such as between V3 and CD4bs targeting scFv indicating that steric hindrance may have still impacted the scFv. Given the distinct MPER epitope located on the gp41 subunit instead of the gp120 subunit, we also expected independent effects for antibodies combined with 10E8v4, which was somewhat indicated in comparing experimental results with the most potent scFv. However, besides a few outliers, this was not apparent using the Bliss-Hill model. It is likely that binding of the MPER antibody confers conformational changes upon binding to its epitope precluding neutralization by other antibodies (47–50). scFv may be especially advantageous in bispecific constructs as their smaller size allows for easier expression. Bispecific products will also increase the local concentration of the second antibody and with the appropriate linker may in such cases allow for synergy. Similarly, minor losses of potency compared to the most potent scFv were overall a rare occurrence and were negated with the addition of a third antibody (in a triple combination with e.g. 10E8v4). The few cases of antagonism noted for scFv combinations may also be due to conformational changes rather than steric hindrance, which would occur after antibody binding. To explore these aspects, scFv-trimer complex crystallization studies would have to be done.

The Loewe model tended to underestimate the potency at $IC_{80}$ particularly of triple combinations. It also often predicted low-level synergy for combinations containing the MPER antibody 10E8v4 and the V2 antibody CAP256.25. The Bliss-Hill model did not indicate significant antagonism and/or synergy for any combination at either $IC_{50}$ or $IC_{80}$. We did observe a few individual outliers where for example the combination showed some improvement in $IC_{50}$ and $IC_{80}$ (CAP256.25+3BNC117+10E8v4) or similarly (3BNC117 +PGT121) showed loss of potency against individual viruses but no specific viral signature could be identified. Some of these may be limitations of the model itself as these tended to occur more often with viruses where the neutralization curves were not sigmoidal or with a low slope (18). The Bliss-Hill model tended to be better at predicting the $IC_{80}$ titers and both models were matched for the $IC_{50}$ titers. This finding is similar to IgG combinations where the Bliss-Hill model was also more accurate at predicting combination titers compared to the Loewe model, therefore the Bliss-Hill model was the preferred model for analyses of larger scFv datasets.

From a clinical perspective, the use of antibody combinations may mitigate the impact of suboptimal antibody levels. Overlapping neutralization can enhance coverage against single viruses, which ensures that complete viral neutralization is achieved at lower concentrations of antibody. The selection of antibody combinations with high potency ($IC_{80}$) can more effectively counter declining antibody levels associated with passive administration. Although combinations of two scFv neutralized 100% of viruses at the highest concentration tested, the coverage was much reduced at lower concentrations, whereas triple antibody combinations demonstrated much higher coverage at lower concentrations by combining broad antibodies with very potent antibodies. For example, at an $IC_{50}$ of 1μg/mL, 100% of viruses were neutralized and at an $IC_{80}$ of 1μg/mL, 96% of viruses were neutralized. This demonstrates that complementary neutralization of the same virus is extremely advantageous, which was previously demonstrated for combinations of IgG (20).

Besides improved coverage, we also observed improved active coverage by 2 antibodies for triple combinations compared to dual combinations (19). In experimental combinations, neutralization slopes were also improved by combinations of antibodies, especially $IC_{80}$ titers and neutralization plateaus (less than 100% neutralization of a virus) were also less common with antibody combinations (data not shown) (18). It may also be beneficial to use antibodies or scFv that bind trimers in different states; for example, CAP256.25 binds early, whereas 10E8v4 likely binds trimers that are in an intermediate state allowing for complementarity in virus neutralization (51–53). Clinically, active coverage by multiple antibodies will prevent antibody escape when the serum titers drop to close to the neutralization range. The AMP trial demonstrated that if the VRC01 antibody levels dropped, protection against less sensitive viruses ($IC_{80}$> 1μg/mL) was lost (17). This may differ for other antibodies or for antibodies targeting different epitopes and combinations may also provide dual active coverage of the viral quasispecies further improving this level of protection (54, 55). This highlights the need to use more potent antibodies but also to improve individual antibody potency. In the future, bNAbs and scFv may also need to be assessed in PBMC neutralization assays which may more accurately resemble *in vivo* neutralization, and could more accurately predict potency (17, 55). We observed that although overall coverage was improved, active coverage by multiple antibodies was low for both IgG and scFv using this set of antibodies. There are multiple efforts ongoing to improve antibody potency and bioavailability. Titers are likely to improve if newer scFv are developed which retain better potency compared to the IgG. Moreover, the selection of antibodies with optimal potency to cover geographically relevant viruses will ensure efficacy in the region.

For long-term antibody-mediated protection, adherence, and maintaining sufficient plasma levels in a wider population is critically important. At lower concentrations, scFv and IgG lose coverage especially in the ability to fully neutralize the virus (concentrations below $IC_{80}$ titers). This is also observed for IgG, indicating that all the antibodies in the combination must be kept at optimal levels. For IgG, one way to achieve this has been to introduce mutations in the Fc portion of the antibody to increase the half-life by up to 6 months (56, 57). A second option is to introduce them into the body *via* a stable expression system through a vectored immunoprophylaxis (VIP) approach. Some bNAbs were recently expressed using AAV, showing modest levels *in vivo* (58, 59). However, due to the space constraints on vectors, constructs with multi-specific modalities would prove difficult. Bispecific products, which would partially overcome this, are also limited by space constraints. scFv in comparison with their much smaller size may be more readily expressed on AAV, allowing for the expression of multiple scFv continuously. scFv have a genetic size approximately 2.6-times smaller than IgG allowing for the expression of minimally three scFv per AAV, and improved expression levels (9, 29, 60–66). AAV based scFv expression can help overcome the short half-life of scFv due to their lack of an Fc region. Some studies have shown success in the use of AAV based scFv for Alzheimer's disease, and Amyotrophic Lateral Sclerosis amongst others (61, 67, 68). *In vivo* data will be required to determine the antigenicity and bioavailability of scFv. However, scFv conjugated to short amino acid peptides or linked to targeting molecules were shown to have significant increases in bioavailability and stability (69–72). These strategies mitigate some of the challenges facing scFv.

The scFv studied here demonstrated high breadth and potency when used in combination. Although only a limited number of scFv were tested on a small panel of viruses, we demonstrated their potential against a larger panel of viruses through modeling. By selecting bNAbs that target all five epitopes we also showed the potential for complementary effects. These scFv showed little to no antagonism. As more potent scFv are engineered combinations with even better efficacy may be found. In addition, as scFv are more readily expressed on vectors, this could in future provide, an alternative avenue for the use of bNAbs in passive immunization. The encouraging results of the AMP trials are expected to fast-track the need to consider long-term delivery approaches for those antibodies with clinical benefit.

## DATA AVAILABILITY STATEMENT

The original contributions presented in the study are included in the article/**Supplementary Material**. Further inquiries can be directed to the corresponding author.

## ETHICS STATEMENT

Ethics approval was obtained as per local regulations (M160341). Antibody sequences were obtained from publicly available databases.

## AUTHOR CONTRIBUTIONS

RD performed all experiments, data interpretation, figures and manuscript generation, and literature review. KW performed data analysis and advised on statistical analysis. PM and LM supervised the project and assisted with data interpretation and manuscript writing. All authors contributed to the article and approved the submitted version.

## FUNDING

We acknowledge research funding from the South African Medical Research Council (SAMRC) Flagship Project, the NIH through a U01 grant (U01AI116086), the Poliomyelitis Research Fund (PRF) through a PRF research grant (17/15), and the Centre for the AIDS

Program of Research (CAPRISA). CAPRISA is funded by the South African HIV/AIDS Research and Innovation Platform of the South African Department of Science and Technology and was initially supported by the U.S. NIAID, NIH, U.S. Department of Health and Human Services grant U19 AI51794. R.T.V.D. is supported by a Poliomyelitis Research Foundation Ph.D. bursary (W 16/72). PM is supported by the South African Research Chairs Initiative of the Department of Science and Innovation and National Research Foundation of South Africa (grant no. 98341). KW is supported by the Bill and Melinda Gates Foundation Collaboration for AIDS Vaccine Discovery grant OPP1032144 (Comprehensive Antibody Vaccine Immune Monitoring Consortium CAVIMC) (https://www.cavd.org/Pages/default.aspx). The funders had no role in study design, data collection, and analysis, decision to publish, or preparation of the manuscript.

## ACKNOWLEDGMENTS

We thank H. Marcotte (Karolinska Institute) for the donation of the CAP256 VH-VL L1 scFv. We thank the AIDS Reagent Program, Division of AIDS, NIAID, NIH, for the use of the pCMVR vector and the pBR322-based IG-lambda expression vector. We also thank J. Mascola, the VRC, USA, for the donation of the PGT121 heavy- and light-chain plasmids.

## SUPPLEMENTARY MATERIAL

The Supplementary Material for this article can be found online at: https://www.frontiersin.org/articles/10.3389/fimmu.2021.734110/full#supplementary-material

## REFERENCES

1. Julg B, Liu P-T, Wagh K, Fischer WM, Abbink P, Mercado NB, et al. Protection Against a Mixed SHIV Challenge by a Broadly Neutralizing Antibody Cocktail. *Sci Transl Med* (2017) 9:eaao4235. doi: 10.1126/scitranslmed.aao4235
2. Saunders KO, Wang L, Joyce MG, Yang Z-YY, Balazs AB, Cheng C, et al. Broadly Neutralizing Human Immunodeficiency Virus Type 1 Antibody Gene Transfer Protects Nonhuman Primates From Mucosal Simian-Human Immunodeficiency Virus Infection. *J Virol* (2015) 89:8334–45. doi: 10.1128/jvi.00908-15
3. Martinez-Navio JM, Fuchs SP, Pantry SN, Lauer WA, Duggan NN, Keele BF, et al. Adeno-Associated Virus Delivery of Anti-HIV Monoclonal Antibodies Can Drive Long-Term Virologic Suppression. *Immunity* (2019) 50:567–575.e5. doi: 10.1016/j.immuni.2019.02.005
4. Parren PW, Marx PA, Hessell AJ, Luckay A, Harouse J, Cheng-Mayer C, et al. Antibody Protects Macaques Against Vaginal Challenge With a Pathogenic R5 Simian/Human Immunodeficiency Virus at Serum Levels Giving Complete Neutralization *In Vitro*. *J Virol* (2001) 75:8340–7. doi: 10.1128/JVI.75.17.8340-8347.2001
5. Klein F, Mouquet H, Dosenovic P, Scheid JF, Scharf L, Nussenzweig MC. Antibodies in HIV-1 Vaccine Development and Therapy. *Science (80-)* (2013) 341:1199–204. doi: 10.1126/science.1241144
6. Bekker L-G, Moodie Z, Grunenberg N, Laher F, Tomaras GD, Cohen KW, et al. Subtype C ALVAC-HIV and Bivalent Subtype C Gp120/MF59 HIV-1 Vaccine in Low-Risk, HIV-Uninfected, South African Adults: A Phase 1/2 Trial. *Lancet HIV* (2018) 5:e366–78. doi: 10.1016/S2352-3018(18)30071-7
7. Karasavvas N, Billings E, Rao M, Williams C, Zolla-Pazner S, Bailer RT, et al. The Thai Phase III HIV Type 1 Vaccine Trial (RV144) Regimen Induces Antibodies That Target Conserved Regions Within the V2 Loop of Gp120. *AIDS Res Hum Retroviruses* (2012) 28:1444–57. doi: 10.1089/aid.2012.0103
8. Rerks-Ngarm S, Pitisuttithum P, Nitayaphan S, Kaewkungwal J, Chiu J, Paris R, et al. Vaccination With ALVAC and AIDSVAX to Prevent HIV-1 Infection in Thailand. *N Engl J Med* (2009) 361:2209–20. doi: 10.1056/NEJMoa0908492
9. Lin A, Balazs AB. Adeno-Associated Virus Gene Delivery of Broadly Neutralizing Antibodies as Prevention and Therapy Against HIV-1 11 Medical and Health Sciences 1103 Clinical Sciences 11 Medical and Health Sciences 1108 Medical Microbiology Marit Van Gils, M.J.Vangils@Amc. *Retrovirology* (2018) 15:66. doi: 10.1186/s12977-018-0449-7
10. Marcotte H, Hammarström L. Passive Immunization. In: *Mucosal Immunology*. Elsevier: Cambridge, Massachusetts, United States (2015). 2:1403–34. doi: 10.1016/B978-0-12-415847-4.00071-9
11. Burton DR, Hangartner L. Broadly Neutralizing Antibodies to HIV and Their Role in Vaccine Design. *Annu Rev Immunol* (2016) 34:635–59. doi: 10.1146/annurev-immunol-041015-055515
12. Bhiman JN, Lynch RM. Broadly Neutralizing Antibodies as Treatment: Effects on Virus and Immune System. *Curr HIV/AIDS Rep* (2017) 14:54–62. doi: 10.1007/s11904-017-0352-1
13. Crowell TA, Colby DJ, Pinyakorn S, Sacdalan C, Pagliuzza A, Intasan J, et al. Safety and Efficacy of VRC01 Broadly Neutralising Antibodies in Adults With Acutely(RV397): A Phase 2, Randomised, Double-Blind, Placebo-Controlled Trial. *Lancet HIV* (2019) 6:e297–306. doi: 10.1016/S2352-3018(19)30053-0
14. Huang Y, Naidoo L, Zhang L, Carpp LN, Rudnicki E, Randhawa A, et al. Pharmacokinetics and Predicted Neutralisation Coverage of VRC01 in HIV-Uninfected Participants of the Antibody Mediated Prevention (AMP) Trials. *EBioMedicine* (2021) 64:103203. doi: 10.1016/j.ebiom.2020.103203
15. Edupuganti S, Mgodi N, Karuna ST, Andrew P, Rudnicki E, Kochar N, et al. Feasibility and Successful Enrollment in a Proof-Of-Concept HIV Prevention Trial of VRC01, a Broadly Neutralizing HIV-1 Monoclonal Antibody. *J Acquir Immune Defic Syndr* (2021) 87:671–9. doi: 10.1097/QAI.0000000000002639
16. Mgodi NM, Takuva S, Edupuganti S, Karuna S, Andrew P, Lazarus E, et al. A Phase 2b Study to Evaluate the Safety and Efficacy of VRC01 Broadly Neutralizing Monoclonal Antibody in Reducing Acquisition of HIV-1 Infection in Women in Sub-Saharan Africa. *JAIDS J Acquir Immune Defic Syndr* (2021) 87:680–7. doi: 10.1097/QAI.0000000000002649
17. Corey L, Gilbert PB, Juraska M, Montefiori DC, Morris L, Karuna ST, et al. Two Randomized Trials of Neutralizing Antibodies to Prevent HIV-1 Acquisition. *N Engl J Med* (2021) 384:1003–14. doi: 10.1056/nejmoa2031738
18. Wagh K, Bhattacharya T, Williamson C, Robles A, Bayne MG, Garrity J, et al. Optimal Combinations of Broadly Neutralizing Antibodies for Prevention and Treatment of HIV-1 Clade C Infection. *PloS Pathog* (2016) 12:e1005520. doi: 10.1371/journal.ppat.1005520
19. Kong R, Louder MK, Wagh K, Bailer RT, DeCamp A, Greene KM, et al. Improving Neutralization Potency and Breadth by Combining Broadly Reactive HIV-1 Antibodies Targeting Major Neutralization Epitopes. *J Virol* (2015) 89:2659–71. doi: 10.1128/JVI.03136-14
20. Wagh K, Seaman MS, Zingg M, Fitzsimons T, Barouch DH, Burton DR, et al. Potential of Conventional & Bispecific Broadly Neutralizing Antibodies for Prevention of HIV-1 Subtype A, C & D Infections. *PloS Pathog* (2018) 14:e1006860. doi: 10.1371/journal.ppat.1006860
21. CAPRISA. *CAPRISA Studies | CAPRISA* (2020). Available at: https://www.caprisa.org/Pages/CAPRISAStudies (Accessed September 3, 2020).
22. Mahomed S, Garrett N, Karim QA, Yende-Zuma N, Capparelli E, Baxter C, et al. Assessing the Safety and Pharmacokinetics of the Anti-HIV Monoclonal Antibody CAP256V2LS Alone and in Combination With VRC07-523LS and PGT121 in South African Women: Study Protocol for the First-in-Human CAPRISA 012B Phase I Clinical Trial. *BMJ Open* (2020) 10:e042247. doi: 10.1136/bmjopen-2020-042247
23. Karuna ST. Phase 1 Broadly Neutralizing Antibody Efforts(2021). Available at: https://www.hvtn.org/en/community/community-compass/vol20-issue1/phase-1-broadly-neutralizing-antibody-efforts.html (Accessed April 2, 2021).
24. Karuna ST, Corey L. Broadly Neutralizing Antibodies for HIV Prevention. *Annu Rev Med* (2020) 71:329–46. doi: 10.1146/annurev-med-110118-045506
25. Foucquier J, Guedj M. Analysis of Drug Combinations: Current Methodological Landscape. *Pharmacol Res Perspect* (2015) 3:e00149. doi: 10.1002/prp2.149

26. Davis-Gardner ME, Alfant B, Weber JA, Gardner MR, Farzan M. A Bispecific Antibody That Simultaneously Recognizes the V2-And V3-Glycan Epitopes of the Hiv-1 Envelope Glycoprotein is Broader and More Potent Than Its Parental Antibodies. *MBio* (2020) 11(1):e03080–19. doi: 10.1128/mBio.03080-19
27. Huang Y, Yu J, Lanzi A, Yao X, Andrews CD, Tsai L, et al. Engineered Bispecific Antibodies With Exquisite HIV-1-Neutralizing Activity. *Cell* (2016) 165:1621–31. doi: 10.1016/j.cell.2016.05.024
28. Khan SN, Sok D, Tran K, Movsesyan A, Dubrovskaya V, Burton DR, et al. Targeting the HIV-1 Spike and Coreceptor With Bi- and Trispecific Antibodies for Single-Component Broad Inhibition of Entry. *J Virol* (2018) 92(18):e00384–18. doi: 10.1128/jvi.00384-18
29. West AP, Galimidi RP, Gnanapragasam PNP, Bjorkman PJ. Single-Chain Fv-Based Anti-HIV Proteins: Potential and Limitations. *J Virol* (2012) 86:195–202. doi: 10.1128/JVI.05848-11
30. Song R, Pace C, Seaman MS, Fang Q, Sun M, Andrews CD, et al. Distinct HIV-1 Neutralization Potency Profiles of Ibalizumab-Based Bispecific Antibodies. *J Acquir Immune Defic Syndr* (2016) 73:365–73. doi: 10.1097/QAI.0000000000001119
31. Moshoette T, Ali SA, Papathanasopoulos MA, Killick MA. Engineering and Characterising a Novel, Highly Potent Bispecific Antibody Imab-CAP256 That Targets HIV-1. *Retrovirology* (2019) 16:1–12. doi: 10.1186/s12977-019-0493-y
32. Colcher D, Pavlinkova G, Beresford G, Booth BJ, Choudhury A, Batra SK. Pharmacokinetics and Biodistribution of Genetically-Engineered Antibodies (1998). Available at: https://search.proquest.com/openview/aad96f811b8e44830fd2f5817ff5b54b/1?pq-origsite=gscholar&cbl=27900 (Accessed August 14, 2018).
33. Unverdorben F, Richter F, Hutt M, Seifert O, Malinge P, Fischer N, et al. Pharmacokinetic Properties of IgG and Various Fc Fusion Proteins in Mice. *MAbs* (2016) 8:120–8. doi: 10.1080/19420862.2015.1113360
34. Yokota T, Milenic DE, Whitlow M, Schlom J. Rapid Tumor Penetration of a Single-Chain Fv and Comparison With Other Immunoglobulin Forms. *Cancer Res* (1992) 52:3402–8. doi: 10.1007/s00429-013-0597-4
35. Unverdorben F, Färber-Schwarz A, Richter F, Hutt M, Kontermann RE. Half-Life Extension of a Single-Chain Diabody by Fusion to Domain B of Staphylococcal Protein A. *Protein Eng Des Sel* (2012) 25:81–8. doi: 10.1093/protein/gzr061
36. Kumar S, Kumar R, Khan L, Makhdoomi MA, Thiruvengadam R, Mohata M, et al. CD4-Binding Site Directed Cross-Neutralizing scFv Monoclonals From HIV-1 Subtype C Infected Indian Children. *Front Immunol* (2017) 8:1568. doi: 10.3389/fimmu.2017.01568
37. Alam MMM, Kuwata T, Tanaka K, Alam MMM, Takahama S, Shimura K, et al. Synergistic Inhibition of Cell-to-Cell HIV-1 Infection by Combinations of Single Chain Variable Fragments and Fusion Inhibitors. *Biochem Biophys Rep* (2019) 20:100687. doi: 10.1016/j.bbrep.2019.100687
38. van Dorsten RT, Lambson BE, Wibmer CK, Weinberg MS, Moore PL, Morris L. Neutralization Breadth and Potency of Single-Chain Variable Fragments Derived From Broadly Neutralizing Antibodies Targeting Multiple Epitopes on the HIV-1 Envelope. *J Virol* (2020) 94(2):e01533–19. doi: 10.1128/JVI.01533-19
39. Portolano N, Watson PJ, Fairall L, Millard CJ, Milano CP, Song Y, et al. Recombinant Protein Expression for Structural Biology in HEK 293F Suspension Cells: A Novel and Accessible Approach. *J Vis Exp* (2014) 92: e51897. doi: 10.3791/51897
40. Gasteiger E, Hoogland C, Gattiker A, Duvaud S, Wilkins MR, Appel RD, et al. Protein Identification and Analysis Tools on the ExPASy Server. In: *The Proteomics Protocols Handbook*. Totowa, NJ: Humana Press (2005). 571–607. doi: 10.1385/1-59259-890-0:571
41. Gray ES, Madiga MC, Hermanus T, Moore PL, Wibmer CK, Tumba NL, et al. The Neutralization Breadth of HIV-1 Develops Incrementally Over Four Years and Is Associated With CD4+ T Cell Decline and High Viral Load During Acute Infection. *J Virol* (2011) 85:4828–40. doi: 10.1128/JVI.00198-11
42. Doria-Rose NA, Schramm CA, Gorman J, Moore PL, Bhiman JN, DeKosky BJ, et al. Developmental Pathway for Potent V1V2-Directed HIV-Neutralizing Antibodies. *Nature* (2014) 509:55–62. doi: 10.1038/nature13036
43. Moore PL, Sheward DJ, Nonyane M, Ranchobe N, Hermanus T, Gray ES, et al. Multiple Pathways of Escape From HIV Broadly Cross-Neutralizing V2-Dependent Antibodies. *J Virol* (2013) 87:4882–94. doi: 10.1128/JVI.03424-12
44. Todd CA, Greene KM, Yu X, Ozaki DA, Gao H, Huang Y, et al. Development and Implementation of an International Proficiency Testing Program for a Neutralizing Antibody Assay for HIV-1 in TZM-Bl Cells. *J Immunol Methods* (2012) 375:57–67. doi: 10.1016/j.jim.2011.09.007
45. Sarzotti-Kelsoe M, Bailer RT, Turk E, li LC, Bilska M, Greene KM, et al. Optimization and Validation of the TZM-Bl Assay for Standardized Assessments of Neutralizing Antibodies Against HIV-1. *J Immunol Methods* (2014) 409:131–46. doi: 10.1016/j.jim.2013.11.022
46. Mascola JR, D'Souza P, Gilbert P, Hahn BH, Haigwood NL, Morris L, et al. Recommendations for the Design and Use of Standard Virus Panels To Assess Neutralizing Antibody Responses Elicited by Candidate Human Immunodeficiency Virus Type 1 Vaccines. *J Virol* (2005) 79:10103–7. doi: 10.1128/jvi.79.16.10103-10107.2005
47. Rujas E, Caaveiro JMM, Partida-Hanon A, Gulzar N, Morante K, Apellániz B, et al. Structural Basis for Broad Neutralization of HIV-1 Through the Molecular Recognition of 10E8 Helical Epitope at the Membrane Interface. *Sci Rep* (2016) 6:1–13. doi: 10.1038/srep38177
48. Wang Y, Kaur P, Sun Z-YJ, Elbahnasawy MA, Hayati Z, Qiao Z-S, et al. Topological Analysis of the Gp41 MPER on Lipid Bilayers Relevant to the Metastable HIV-1 Envelope Prefusion State. *Proc Natl Acad Sci* (2019) 116:22556–66. doi: 10.1073/PNAS.1912427116
49. Fu Q, Shaik MM, Cai Y, Ghantous F, Piai A, Peng H, et al. Structure of the Membrane Proximal External Region of HIV-1 Envelope Glycoprotein. *Proc Natl Acad Sci* (2018) 115:E8892–9. doi: 10.1073/pnas.1807259115
50. Kim AS, Leaman DP, Zwick MB. Antibody to Gp41 MPER Alters Functional Properties of HIV-1 Env Without Complete Neutralization. *PloS Pathog* (2014) 10:e1004271. doi: 10.1371/JOURNAL.PPAT.1004271
51. Pinto D, Fenwick C, Caillat C, Silacci C, Guseva S, Dehez F, et al. Structural Basis for Broad HIV-1 Neutralization by the MPER-Specific Human Broadly Neutralizing Antibody Ln01. *Cell Host Microbe* (2019) 26:623–37.e8. doi: 10.1016/j.chom.2019.09.016
52. Zhou T, Doria-Rose NA, Cheng C, Stewart-Jones GBE, Chuang G-Y, Chambers M, et al. Quantification of the Impact of the HIV-1-Glycan Shield on Antibody Elicitation. *Cell Rep* (2017) 19:719–32. doi: 10.1016/j.celrep.2017.04.013
53. Doria-Rose NA, Bhiman JN, Roark RS, Schramm CA, Gorman J, Chuang GY, et al. New Member of the V1V2-Directed CAP256-VRC26 Lineage That Shows Increased Breadth and Exceptional Potency. *J Virol* (2015) 90:76–91. doi: 10.1128/JVI.01791-15
54. Lorenzi JCC, Mendoza P, Cohen YZ, Nogueira L, Lavine C, Sapiente J, et al. Neutralizing Activity of Broadly Neutralizing Anti-HIV-1 Antibodies Against Primary African Isolates. *J Virol* (2021) 95(5):e01909–20. doi: 10.1128/jvi.01909-20
55. Cohen YZ, Lorenzi JCC, Seaman MS, Nogueira L, Schoofs T, Krassnig L, et al. Neutralizing Activity of Broadly Neutralizing Anti-HIV-1 Antibodies Against Clade B Clinical Isolates Produced in Peripheral Blood Mononuclear Cells. *J Virol* (2017) 92:e01883–17. doi: 10.1128/JVI.01883-17
56. Liu Q, Lai YT, Zhang P, Louder MK, Pegu A, Rawi R, et al. Improvement of Antibody Functionality by Structure-Guided Paratope Engraftment. *Nat Commun* (2019) 10:741. doi: 10.1038/s41467-019-08658-4
57. Rosenberg YJ, Lewis GK, Montefiori DC, LaBranche CC, Lewis MG, Urban LA, et al. Introduction of the YTE Mutation Into the Non-Immunogenic HIV bnAb PGT121 Induces Anti-Drug Antibodies in Macaques. *PloS One* (2019) 14:e0212649. doi: 10.1371/journal.pone.0212649
58. van den Berg FT, Makoah NA, Ali SA, Scott TA, Mapengo RE, Mutsvunguma LZ, et al. AAV-Mediated Expression of Broadly Neutralizing and Vaccine-Like Antibodies Targeting the HIV-1 Envelope V2 Region. *Mol Ther - Methods Clin Dev* (2019) 14:100–12. doi: 10.1016/j.omtm.2019.06.002
59. Brady JM, Baltimore D, Balazs AB. Antibody Gene Transfer With Adeno-Associated Viral Vectors as a Method for HIV Prevention. *Immunol Rev* (2017) 275:324–33. doi: 10.1111/imr.12478
60. Monnier P, Vigouroux R, Tassew N. *In Vivo* Applications of Single Chain Fv (Variable Domain) (scFv) Fragments. *Antibodies* (2013) 2:193–208. doi: 10.3390/antib2020193

61. Hay CE, Gonzalez GA, Ewing LE, Reichard EE, Hambuchen MD, Nanaware-Kharade N, et al. Development and Testing of AAV-Delivered Single-Chain Variable Fragments for the Treatment of Methamphetamine Abuse. *PloS One* (2018) 13:e0200060. doi: 10.1371/journal.pone.0200060
62. Gruenert AK, Czugala M, Mueller C, Schmeer M, Schleef M, Kruse FE, et al. Self-Complementary Adeno-Associated Virus Vectors Improve Transduction Efficiency of Corneal Endothelial Cells. *PloS One* (2016) 11:e0152589. doi: 10.1371/journal.pone.0152589
63. Dong J-Y, Fan P-D, Frizzell RA. Quantitative Analysis of the Packaging Capacity of Recombinant Adeno-Associated Virus. *Hum Gene Ther* (2008) 7:2101–12. doi: 10.1089/hum.1996.7.17-2101
64. Wu Z, Yang H, Colosi P. Effect of Genome Size on AAV Vector Packaging. *Mol Ther* (2010) 18:80–6. doi: 10.1038/mt.2009.255
65. Liu Z, Chen O, Wall JBJ, Zheng M, Zhou Y, Wang L, et al. Systematic Comparison of 2A Peptides for Cloning Multi-Genes in a Polycistronic Vector. *Sci Rep* (2017) 7:2193. doi: 10.1038/s41598-017-02460-2
66. Raj D, Davidoff AM, Nathwani AC. Self-Complementary Adeno-Associated Viral Vectors for Gene Therapy of Hemophilia B: Progress and Challenges. *Expert Rev Hematol* (2011) 4:539–49. doi: 10.1586/ehm.11.48
67. Patel P, Kriz J, Gravel M, Soucy G, Bareil C, Gravel C, et al. Adeno-Associated Virus-Mediated Delivery of a Recombinant Single-Chain Antibody Against Misfolded Superoxide Dismutase for Treatment of Amyotrophic Lateral Sclerosis. *Mol Ther* (2014) 22:498–510. doi: 10.1038/mt.2013.239
68. Krishnaswamy S, Huang HW, Marchal IS, Ryoo HD, Sigurdsson EM. Neuronally Expressed Anti-Tau scFv Prevents Tauopathy-Induced Phenotypes in Drosophila Models. *Neurobiol Dis* (2020) 137:104770. doi: 10.1016/j.nbd.2020.104770
69. Morita S, Noguchi H, Horii T, Nakabayashi K, Kimura M, Okamura K, et al. Targeted DNA Demethylation *In Vivo* Using Dcas9-Peptide Repeat and scFv-TET1 Catalytic Domain Fusions. *Nat Biotechnol* (2016) 34:1060–5. doi: 10.1038/nbt.3658
70. Phoolcharoen W, Banyard AC, Prehaud C, Selden D, Wu G, Birch CPD, et al. *In Vitro* and *In Vivo* Evaluation of a Single Chain Antibody Fragment Generated in Planta With Potent Rabies Neutralisation Activity. *Vaccine* (2019) 37:4673–80. doi: 10.1016/j.vaccine.2018.02.057
71. Greineder CF, Villa CH, Walsh LR, Kiseleva RY, Hood ED, Khoshnejad M, et al. Site-Specific Modification of Single-Chain Antibody Fragments for Bioconjugation and Vascular Immunotargeting. *Bioconjug Chem* (2018) 29:56–66. doi: 10.1021/acs.bioconjchem.7b00592
72. Rafiq S, Yeku OO, Jackson HJ, Purdon TJ, van Leeuwen DG, Drakes DJ, et al. Targeted Delivery of a PD-1-Blocking scFV by CAR-T Cells Enhances Anti-Tumor Efficacy *In Vivo*. *Nat Biotechnol* (2018) 36:847–58. doi: 10.1038/nbt.4195

**Conflict of Interest:** The authors declare that the research was conducted in the absence of any commercial or financial relationships that could be construed as a potential conflict of interest.

**Publisher's Note:** All claims expressed in this article are solely those of the authors and do not necessarily represent those of their affiliated organizations, or those of the publisher, the editors and the reviewers. Any product that may be evaluated in this article, or claim that may be made by its manufacturer, is not guaranteed or endorsed by the publisher.

frontiers in Immunology

REVIEW
published: 19 October 2021
doi: 10.3389/fimmu.2021.708227

# To bnAb or Not to bnAb: Defining Broadly Neutralising Antibodies Against HIV-1

*Sarah A. Griffith and Laura E. McCoy**

*Division of Infection and Immunity, Institute of Immunity and Transplantation, University College London, London, United Kingdom*

Since their discovery, antibodies capable of broad neutralisation have been at the forefront of HIV-1 research and are of particular interest due to *in vivo* passive transfer studies demonstrating their potential to provide protection. Currently an exact definition of what is required for a monoclonal antibody to be classed as a broadly neutralising antibody (bnAb) has not yet been established. This has led to hundreds of antibodies with varying neutralisation breadth being studied and has given insight into antibody maturation pathways and epitopes targeted. However, even with this knowledge, immunisation studies and vaccination trials to date have had limited success in eliciting antibodies with neutralisation breadth. For this reason there is a growing need to identify factors specifically associated with bnAb development, yet to do this a set of criteria is necessary to distinguish bnAbs from non-bnAbs. This review aims to define what it means to be a HIV-1 bnAb by comparing neutralisation breadth, genetic features and epitopes of bnAbs, and in the process highlights the challenges of comparing the array of antibodies that have been isolated over the years.

**Keywords: HIV-1, broadly neutralising antibody, somatic hypermutation, complementary determining region, epitope**

OPEN ACCESS

***Edited by:***
*Philipp Schommers, University of Cologne, Germany*

***Reviewed by:***
*Srijayaprakash Babu Uppada, University of Alabama, United States*
*Nirianne Querijero Palacpac, Osaka University, Japan*

***Correspondence:**
*Laura E. McCoy*
*l.mccoy@ucl.ac.uk*

***Specialty section:***
*This article was submitted to Vaccines and Molecular Therapeutics, a section of the journal Frontiers in Immunology*

***Received:*** *11 May 2021*
***Accepted:*** *30 September 2021*
***Published:*** *19 October 2021*

***Citation:***
*Griffith SA and McCoy LE (2021) To bnAb or Not to bnAb: Defining Broadly Neutralising Antibodies Against HIV-1. Front. Immunol. 12:708227. doi: 10.3389/fimmu.2021.708227*

## INTRODUCTION

The only antigen exposed on the surface of human immunodeficiency virus (HIV)-1 is the envelope glycoprotein (Env), a trimer comprised of cleaved gp120-gp41 heterodimers, and is located on the surface of HIV to mediate entry into cells (1, 2). Neutralising antibodies (nAbs) directed towards Env can block viral entry and prevent infection by interfering with engagement of host cell receptors (CD4) or co-receptors (CCR5 or CXCR4), by stabilising pre-fusion Env to prevent membrane fusion or by increasing Env decay (3–9). Initial strain-specific nAbs, produced by the majority of HIV-1 infected individuals, can constrict infection and thus exert selection pressure on the virus (10, 11). However, viruses that have already entered cells integrate their genome into the host genome using a viral-encoded reverse transcriptase that is highly error-prone, with a mutation rate of 3.4 x $10^{-5}$ per base during a single round of replication (12). Random mutations introduced into the envelope gene (*env*) during replication may remove or hinder access to the epitopes targeted by nAbs, leading to neutralisation resistant variants that are able to persist and continue to infect new cells (13). High mutation rates combined with a short replication cycle and a tendency for

recombination consequently results in increasing quasispecies and viral diversity within an individual over the course of HIV-1 infection (14). After a few years some individuals infected with HIV-1 (10-30% adults) can develop nAbs capable of cross-neutralisation, and an even smaller subset (1-10%) termed elite neutralisers are able to produce broadly neutralising antibodies (bnAbs) (15). Infants on the other hand have a distinct immune response and often develop broadly neutralising plasma after as early as one year post-infection (16). This has been attributed to multivariant infection as opposed to diversity driven by viral escape due to the finding that circulating viruses in elite neutralisers are still sensitive to autologous nAbs in the plasma (17). Individual bnAbs isolated from HIV-infected individuals are currently of particular interest because passively transferred bnAbs can provide *in vivo* protection in animal models (18–22) and suppression of viral rebound in humans (23). This suggests a key role for bnAbs in the control of new and pre-existing HIV-1 infections. Moreover, these findings give support to the idea that a vaccine capable of eliciting bnAbs could provide the immune system with the head start required to prevent HIV-1 infection.

The first bnAbs were discovered in the early 1990's, and since then over 300 antibodies described as bnAbs and their lineage members have been isolated (24). These have been extensively studied to investigate their development, structural and genetic features, as well as the epitopes that they target. Poly-reactivity and auto-reactivity are common features among some bnAbs and have shown association with the ability to neutralise HIV (25, 26). Extreme somatic hypermutation (SHM) is a trait that has also been observed among the majority of bnAbs isolated from adults (27), and in some cases antibodies feature large insertions and/or deletions too, suggesting that complex affinity maturation pathways drive their development. Another characteristic trait is the length of time required for bnAbs to develop in infected adults, usually taking up to 2-3 years after original HIV-1 exposure, but in some cases can take up to 5 years to develop (28–33). The acquisition of high levels of SHM and slow development of these antibodies can be explained by the evolutionary arms race between the humoral immune response and HIV. Initial nAbs exert selection pressure on the virus that leads to viral variants capable of escaping neutralisation, this in turn selects for affinity-matured antibodies that again exert pressure on the virus and thus results in an ongoing cycle regarded as an evolutionary arms race (34). Ultimately, breadth of neutralisation is achieved by nAbs targeting conserved sites on the functional trimeric Env such as the CD4 binding site, trimer apex, high-mannose patch, gp120-gp41 interface (including the fusion peptide), membrane proximal region (MPER) and the more recently identified epitope referred to as the 'silent face' (35). The main bnAb epitopes, their location on the Env trimer and the mechanism of neutralisation by bnAbs have been brilliantly illustrated in existing reviews (36, 37). As mentioned in these reviews, the Env trimer is a glycoprotein covered by a high density of glycans that are added by the host post-translation according to the N-linked glycosylation sites encoded in the viral sequence (N-X-S/T). These N-linked glycans on Env consist of ~50% of the gp120 mass (38) and are generally less immunogenic than the protein itself. Although the presence of glycans lead to sites on Env being shielded from nAb access (39), the majority of bnAbs are in fact able to accommodate or even incorporate glycans in their epitopes (36). Furthermore, many bnAbs utilise infrequent genetic features such as long heavy chain complementary determining regions (CDRs) (40, 41), that are favourable to access recessed epitopes on Env. Overall, the genetic and structural features of bnAbs are unusual for antibodies, and have been suggested to be a result of perturbations in the regulation of immune tolerance mechanisms during chronic infection and inflammation (42–44).

As described above, individuals with sera that demonstrate very broad neutralising activity are termed elite neutralisers. This can be defined by the ability to neutralise a minimum of one Env pseudotyped virus (PV) with an $IC_{50}$ titre of 300, across four clades (45). The authors who defined this criterion also proposed a system by which a neutralisation score can be calculated to rank and characterise sera (average log-transformed titres for a PV panel), with scores ≥ 2.5 indicating elite neutralisers capable of producing bnAbs (45). Furthermore, this scoring system has proven successful with follow up studies confirming that bnAbs can be isolated from donors identified as elite neutralisers (46, 47). Currently HIV bnAbs are described as antibodies which; are highly effective against most circulating strains, neutralise a wide range of genetically diverse HIV-1 subtypes, potently neutralise a substantial percentage of primary isolates or exhibit some capacity to reach across clades and harder to neutralise tier 2 and 3 viruses (34, 36, 48, 49). Whilst these descriptions highlight the broad reactivity and potency of bnAbs, they are also vague and do not define a set of criteria to distinguish between an antibody that is cross-neutralising to a degree or a true bnAb. This raises the question: what specific requirements need to be met for an antibody to be classed as a bnAb? This could be answered by defining a certain percentage of strains that need to be neutralised by a bnAb, however the challenge lies in determining where the threshold should be. Over the years the neutralising activities of many HIV antibodies have been tested against different PVs in different studies. A major caveat is that these studies vary not only in the number of viruses tested but also in the types of viruses included in panels, making it very hard to compare neutralisation breadth. However the development of a tiering system which characterises the sensitivity of a virus to antibody neutralisation and establishment of reference viruses has greatly improved the systematic screening of nAb responses (50). Another factor that could be considered to define what is or isn't a bnAb is neutralisation potency. This characteristic reflects how effective an antibody is at inhibiting viral infection and has previously been used to show differences between the first and second generations of bnAbs (37). An alternative criteria to define a bnAb could plausibly be found among the unusual structural or genetic features of HIV bnAbs. However, these features appear to vary depending on the epitope targeted, again making a precise definition difficult. Until now, that the field has not converged on a conclusive set of criteria for what constitutes a bnAb has arguably been beneficial. Hundreds of antibodies have been isolated that have given insight into the exact epitopes targeted by different bnAb classes and the developmental pathways of bnAbs have been investigated by

studying lineage members. Many of these antibodies may have been missed or excluded if there had been a strict bnAb cut-off point. Nevertheless with most attempts to elicit a bnAb response in immunisation studies and vaccine trials being unsuccessful (51, 52), there is an increasing need to define what constitutes a bnAb in order to investigate the host immune responses associated with bnAb development (53–56). Studies to date have only made distinctions between bnAb and non-nAb responses at the level of serum neutralisation (28, 54, 57–59), a caveat being that this is a polyclonal response. It would therefore be valuable to have a clear division at the monoclonal antibody level to categorise bnAbs from non-bnAbs, which can only be achieved by defining what it means to be a bnAb.

This review will focus on a subset of monoclonal antibodies isolated from HIV-1 infected adults that have been previously tested for neutralisation and subsequently referred to as bnAbs. The Los Alamos National Lab (LANL) HIV database (24) was used to select a range of these antibodies from different donors and lineages. In addition, a literature search for HIV-1 broadly neutralising antibodies, restricted to papers published from 2018-2021, was also conducted to include more recently isolated antibodies not yet listed on the LANL HIV database.

## CAN WE DEFINE HIV bnAbs BY COMPARING THEIR NEUTRALISATION PROFILES?

The first generation of antibodies against HIV-1 termed as bnAbs were isolated prior to 2009 using phage display and hybridoma technology, since then advances in methods to generate and assess monoclonal antibodies (mAbs) led to a second generation of more potent bnAbs being isolated *via* single B cell cloning following either single B cell culture or antigen-specific sorting [reviewed in (36)]. More recently, a novel technique utilising a matched genomic and proteomic approach has been used to deconvolute polyclonal plasma and successfully isolate bnAb lineages (30). Following isolation, antibodies are screened against PVs in assays to determine their neutralisation capacity (60, 61). However, due to the diversity of HIV-1 there is a vast array of *env* variants that can be pseudotyped for use in these assays. Therefore it is no surprise that the author-defined neutralisation breadth highlighted in **Supplementary Table 1** has been assessed using different virus panels. This makes the comparison of antibody breadth problematic, and to add complexity to this matter, the number of viruses within each panel vary as do the clades and tiers of viruses included.

## THE IMPACT OF VIRAL TIERS AND CLADES ON NEUTRALISATION PROFILES OF ANTIBODIES

The tier of a virus is important because this defines the sensitivity to antibody neutralisation (50), and has been associated with the conformational state of the Env trimer due to differences in epitope exposure (62, 63), as illustrated in **Figure 1**. For example, viruses that are more neutralisation resistant have a higher proportion of Env in a closed conformation. Yet viruses with high sensitivity to antibody neutralisation, such as laboratory-adapted viruses, are referred to as tier 1A/B viruses and exhibit a predominantly open/intermediate conformation respectively. Most primary isolates however are classed as tier 2 viruses that have moderate sensitivity to neutralisation, while tier 3 viruses have low sensitivity and are therefore the most resistant to neutralisation. Consequently, a panel containing a high proportion of tier 1 viruses would likely make an antibody appear to have a broader neutralisation capacity than if tested against a panel containing a high proportion of tier 2/3 viruses.

The clade of the virus is also an important factor to consider, although there is limited data on clade-based differences in neutralisation sensitivity (64). However, it has been shown in serum studies that neutralising activity is generally higher when the clade of the PV matches that of the individual's own virus (45, 50, 65). Conflicting evidence suggests that whilst this is the case for plasma from clade C infections, it is not for clade B plasma (64, 66). The effect of virus clade on the neutralising response has also been observed with mAbs produced during natural infection or elicited by vaccination, where viruses from the same clade that stimulated the response were preferentially neutralised (67). Moreover, it has been identified that structural features characteristic of viral clades such as the presence or absence of specific residues can affect the sensitivity of neutralisation by bnAbs, but this is highly dependent on the epitope targeted (68). Therefore, a panel of viruses originating from only a single clade or circulating recombinant form (CRF) could arguably bias the neutralisation breadth achieved by the antibody tested. On the other hand, it might be informative to know if an antibody can neutralise heterologous viruses within a clade, as this level of cross-reactivity could be of benefit within certain communities. Whilst it is well-known that virus clades and CRFs are predominately found in specific geographic regions (69), it is necessary to take into account that there is often more than one clade or CRF within each region and that distributions are dynamic (70). For instance, analysis of regional distribution across Africa identified that whilst the south was almost exclusively clade C, the east was predominantly clade A, C or D yet in west and central Africa all clades and many CRFs were present, with proportions changing over time (71). Considering that Sub-Saharan Africa has the highest cases of HIV-1 in the world, this is particularly relevant and thus suggests that it would be appropriate to evaluate neutralisation breadth using viruses that reflect the diversity of HIV-1 clades/CRFs and not use virus panels that are specific for a single clade/CRF.

## STANDARD VIRUS PANELS FOR ASSESSING NEUTRALISATION BREADTH

The establishment of standard PV panels that take the viral tier and clade into account has provided a consistent way to

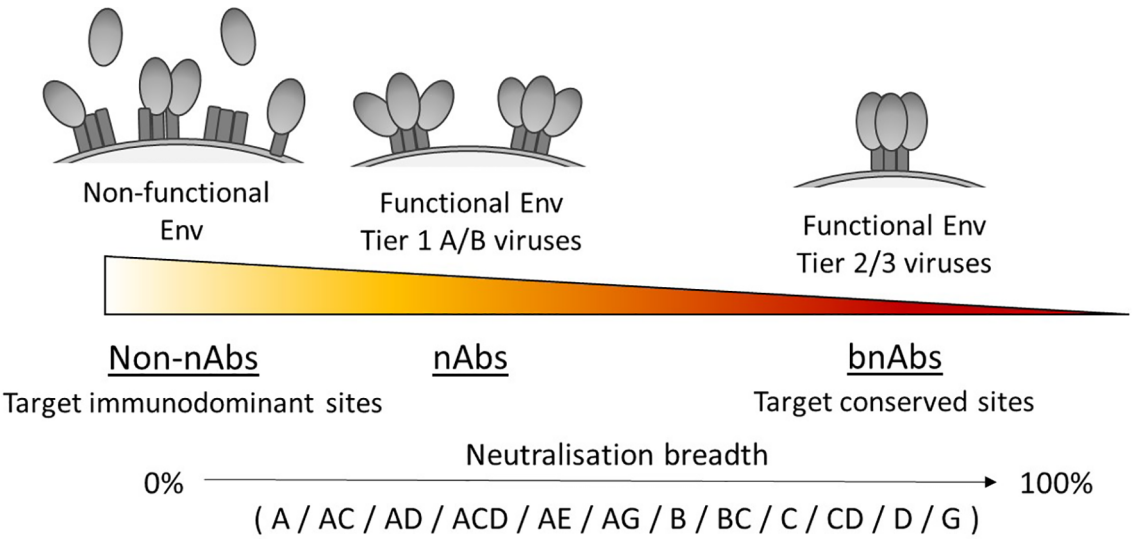


**FIGURE 1** | Neutralisation breadth corresponds with the ability to target functional Env trimers in a closed conformation. Tier 1A, tier 1B and tier 2/3 viruses have a predominantly open, intermediate and closed Env trimer conformation respectively and relates to their susceptibility to neutralisation, with tier 2/3 viruses being harder to neutralise. Antibodies that can neutralise tier 2/3 viruses from multiple clades (listed here in alphabetical order) have increased breadth by targeting conserved sites on the Env trimer.

screen for broadly neutralising antibody responses and also offers a way to compare antibody neutralisation breadth. The 6 PV standard panel and 12 PV global panel consist almost entirely of tier 2 viruses from multiple clades that were shown to be representative of larger panels of viruses from the global epidemic (45, 72), thus allowing the breadth of an antibody to be assessed using only a small number of viruses. Another widely used standard panel is the 118 multi-clade PV panel which is comprised primarily of the 109 virus panel (50) and represents diverse isolates of HIV-1 from different regions of the world. It should be noted that viruses from clade F, H, J and K are not present in this panel, however even when these are combined they result in <1% of infections worldwide (71).

Even with these standard virus panels available it is clear that not all reported bnAbs have been tested against them and that the panels used to define neutralisation breadth by HIV researchers continue to vary (**Supplementary Table 1**). However, it is apparent that one virus panel has been used more frequently than others to assess bnAbs, and that is the 118 multi-clade panel. This is arguably the most appropriate standard panel for comparing bnAb neutralisation profiles as it contains more viruses than the 6 or 12 PV panels and also utilises viruses from all major clades, both of which increase confidence in the breadth achieved. Although panels containing a larger number of viruses have also been used to characterise the neutralisation profile of individual bnAbs (**Supplementary Table 1**), these are not standard PV panels that are currently recognised on the LANL HIV database CATNAP tool (24) and have not been as widely used. For these reasons the breadth and potency of neutralisation by bnAbs against the 118 multi-clade panel was chosen for analysis in this review. In total it was feasible to include 41 bnAbs for direct comparison and this has been highlighted in **Table 1**. Regrettably nAbs with limited breadth such as 447-52D and b6 (77), that are not referred to as bnAbs were not included in the comparison because these have not been tested against the 118 PV panel.

Evaluation of bnAbs based on their neutralisation of the 118 multi-clade PV panel (**Table 1**) revealed that a minimum of 7 out of the 15 clades/CRFs in the panel are neutralised by all bnAbs. This is similar to the criterion for broad neutralisation by serum, in which elite activity is defined by the ability to neutralise a minimum of 4 clades/CRFs (45). In addition, the neutralisation breadth of bnAbs ranges from 21-100% with a geometric mean $IC_{50}$ of 0.02-4.3 μg/ml (**Table 1**). However by taking only second generation bnAbs from **Table 1** into consideration, the thresholds of >30% neutralisation breadth and potency ≤3.6 μg/ml against the 118 PV panel (**Figure 2A**) could be used to define the minimum criterion a bnAb needs to meet. Furthermore, second generation bnAbs had an average neutralisation capacity of 68% breadth with a geometric mean $IC_{50}$ of 0.6 μg/ml. Elite bnAbs with above average neutralisation breadth and potency could therefore be categorised as having >68% neutralisation breadth and potency of <0.6 μg/ml against the 118 PV panel (**Figure 2B**). However, this could be too strict of a cut off as 10-1074 does not fall into the category of an 'elite' bnAb, yet has been tested in human clinical trials and was capable of delaying viral rebound (78).

**TABLE 1** | Comparison of bnAb breadth against the 118 multi-clade standard PV panel.

| HIV bnAb | Neutralisation breadth | Viruses tested | Potency (μg/ml) | Clades/CRFs neutralised | Reference |
|---|---|---|---|---|---|
| N49P7 | 100% | 117 | 0.44 | 15 | (30) |
| 10E8 | 98% | 118 | 0.36 | 14 | (24) |
| 4E10* | 98% | 118 | 1.81 | 15 | (24) |
| 1-18 | 97% | 116 | 0.05 | 15 | (73) |
| 12A12 | 93% | 117 | 0.22 | 15 | (24) |
| LN01 | 92% | 118 | 0.96 | 15 | (74) |
| VRC01 | 91% | 118 | 0.38 | 15 | (24) |
| 3BNC117 | 89% | 118 | 0.12 | 15 | (24) |
| PG9 | 87% | 118 | 0.15 | 14 | (24) |
| NIH45-46 | 86% | 117 | 0.11 | 15 | (24) |
| VRC13 | 86% | 113 | 0.27 | 14 | (24) |
| VRC-CH31 | 84% | 115 | 0.32 | 15 | (24) |
| PG16 | 83% | 118 | 0.08 | 15 | (24) |
| PGDM1400 | 83% | 118 | 0.02 | 15 | (24) |
| PGV04 | 81% | 116 | 0.32 | 15 | (24) |
| PGT145 | 78% | 118 | 0.13 | 15 | (24) |
| PGT151 | 73% | 118 | 0.04 | 15 | (24) |
| 1B2530 | 72% | 113 | 3.62 | 14 | (24) |
| PGT128 | 68% | 118 | 0.06 | 13 | (24) |
| 8ANC195 | 68% | 118 | 1.23 | 15 | (24) |
| CH103 | 67% | 113 | 2.28 | 14 | (24) |
| PGT121 | 66% | 118 | 0.07 | 13 | (24) |
| 10-1074 | 63% | 118 | 0.06 | 13 | (24) |
| SF12 | 63% | 118 | 0.21 | 10 | (75) |
| PGT130 | 61% | 117 | 0.20 | 14 | (24) |
| BG18 | 61% | 116 | 0.03 | 14 | (24) |
| 2F5* | 58% | 118 | 2.83 | 13 | (24) |
| VRC26.08 | 57% | 116 | 0.02 | 13 | (24) |
| CH01 | 54% | 115 | 1.38 | 12 | (24) |
| VRC03 | 53% | 115 | 0.80 | 14 | (24) |
| 35O22 | 51% | 118 | 0.26 | 10 | (24) |
| IOMA | 49% | 116 | 2.33 | 12 | (24) |
| PCDN-33A | 46% | 113 | 0.50 | 11 | (24) |
| b12* | 44% | 118 | 4.32 | 10 | (24) |
| HJ16 | 38% | 118 | 1.17 | 12 | (24) |
| M4008_N1 | 36% | 115 | 0.95 | 12 | (76) |
| BG1 | 35% | 116 | 0.61 | 11 | (24) |
| PGT135 | 33% | 118 | 0.61 | 13 | (24) |
| 179NC75 | 31% | 116 | 0.16 | 10 | (24) |
| VRC-PG05 | 31% | 113 | 2.33 | 8 | (24) |
| 2G12* | 21% | 118 | 3.75 | 7 | (24) |

*The neutralisation breadth (percentage of viruses neutralised) and the number of clades/CRFs neutralised in the 118 PV panel was captured from the antibody isolation paper or LANL HIV CATNAP tool (24), bnAbs with data for >95% of PVs in the 118 PV panel were included. Potency is given as the geometric mean $IC_{50}$ of viruses neutralised. The total number of virus clades/CRFs in the 118 PV panel is 15, categorised according to the LANL HIV CATNAP tool. *First generation bnAbs isolated prior to 2009 are marked by an asterisk.*

*Higher neutralisation breadth, number of viruses tested and potency are indicated by a darker shade of green, yellow and red respectively.*

Therefore it may be appropriate to instead consider that more potent bnAbs could compromise for lower breadth of neutralisation, and vice versa, as demonstrated in **Figure 2C**. The different thresholds for defining HIV-1 bnAbs based on neutralisation breadth and potency have been summarised in **Figure 2D**.

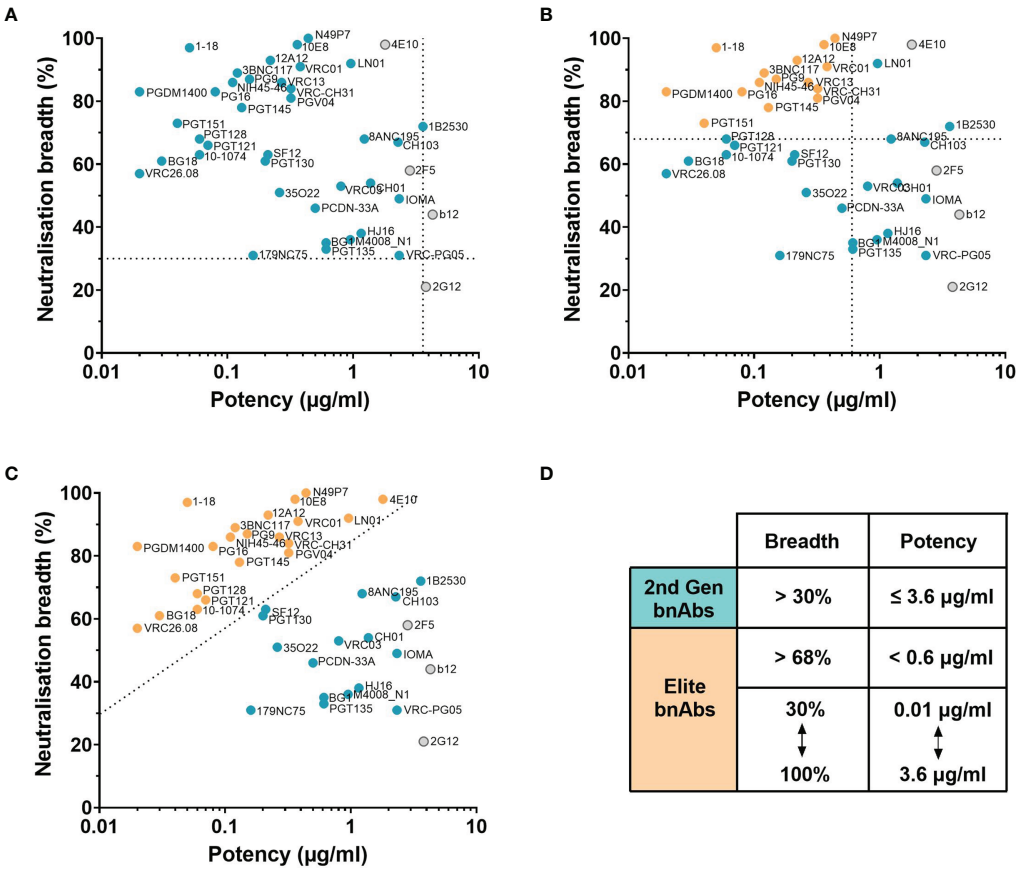


**FIGURE 2** | Neutralisation breadth and potency of HIV bnAbs against the 118 multi-clade PV panel. **(A–C)** First generation bnAbs isolated prior to 2009 are shown in grey and second generation bnAbs isolated after 2009 are shown in blue. **(A)** Dashed lines at 30% neutralisation breadth and potency (geometric mean $IC_{50}$) of 3.6 μg/ml define the minimum bnAb thresholds for second generation bnAbs (blue circles). **(B)** Dashed lines at 68% neutralisation breadth and potency (geometric mean $IC_{50}$) of 0.6 μg/ml define elite bnAbs (orange circles). **(C)** The diagonal dashed line ranging from 30% to 100% neutralisation breadth and 0.01 μg/ml to 3.6 μg/ml potency (geometric mean $IC_{50}$) compensates lower neutralisation breadth with lower potency to define elite bnAbs (orange circles). **(D)** Summary of the criteria that categorises second generation ($2^{nd}$ Gen) bnAbs in **(A)** and elite bnAbs in **(B, C)**.

## THERAPEUTIC POTENTIAL OF BROADLY NEUTRALISING ANTIBODIES

Analysing bnAbs based on their ability to neutralise the 118 multi-clade PV panel offers an unbiased way to compare antibody breadth and potency that could be a vital tool to identify the 'best' bnAbs, which are desirable for therapeutic use. However there may be instances where neutralisation breadth within a specific clade may be more beneficial than breadth against multiple clades. Nevertheless, it is hard to determine exactly how broad and potent a bnAb needs to be for successful prevention or suppression of HIV-1, although logically the closer to 100% coverage and the lower the potency the better. It is also worth considering that whilst PVs are a vital tool to characterise antibody activity *in vitro* these are not circulating viruses, and it has been shown that primary isolates derived from PBMCs can be less sensitive to bnAbs (79). In a recent press release the highly anticipated results of Phase 2b trials from the Antibody-Mediated Prevention (AMP) studies revealed that administration of the bnAb VRC01 was 75% effective at preventing acquisition of HIV strains susceptible to VRC01, however in the regions where this trial was conducted only 30% of circulating strains were VRC01-sensitive (80). This demonstrates the potential that bnAbs could have in providing protection against HIV in humans, but also highlights the prevalence of circulating strains with bnAb resistance. The use of bnAbs for the suppression of HIV-1 during interruption of antiretroviral therapy is also of high interest. In human clinical trials, administration of single bnAbs have shown that two doses of 3BNC117 suppressed viral rebound for an average of 6.7 weeks and three doses of VRC01 supressed viral rebound for a median of 4 weeks (81, 82). Although these bnAbs were evaluated in different trials the results suggest that 3BNC117 is more effective than VRC01. Interestingly, the neutralisation breadth of these two CD4bs bnAbs is similar, yet 3BNC117 is more potent than VRC01 (**Table 1**), indicating that bnAb potency is likely associated with the length of viral suppression. Findings from passive transfer studies in non-human primate models have led

to the proposal that only the most potent bnAbs, with a geometric mean $IC_{50}$ ≤0.1 μg/ml, would be capable of providing protection as viral coverage reduces with lower concentrations (47). Consistent with this, a highly potent CD4bs bnAb (1-18) with a geometric mean $IC_{50}$ of 0.05 μg/ml was able to maintain viral suppression in HIV-1 infected humanised mice, whereas viral rebound occurred with less potent and broad CD4bs bnAbs (3BNC117 and VRC01) (73). Although these preliminary findings imply that a single bnAb could maintain suppression if broad and potent enough, this has not yet been tested in humans and there may still be risk of viral escape. The most successful human clinical trial documented so far instead used a combination of bnAbs (3BNC117 and 10-1074) targeting different sites on the HIV-1 Env and was able to maintain viral suppression for a median of 21 weeks (23). This approach is similar to the switch from monotherapy to combination antiretroviral therapy, where the administration of multiple drugs with different inhibitory mechanisms is more effective at reducing viral load and diminishing the development of drug resistance (83). In the case of bnAb therapeutics, this combination strategy or use of bi-specifics could be implemented to help prevent the emergence of HIV-1 variants capable of neutralisation escape (84, 85). Ongoing trials with modified bnAbs, bi-specific bnAbs or novel bnAb combinations [reviewed in (86–88)] will hopefully shed more light on the requirements to achieve durable as opposed to transient suppression of HIV-1. Finally, an alternative to passively transferred bnAbs could be to instead engineer B cells to express bnAbs. This approach arguably has an advantage in that a durable response could be maintained through memory cell formation and that bnAbs could undergo SHM in response to viral escape (89), although this requires further investigation.

## CAN WE DEFINE HIV bnAbs BY COMPARING THEIR LEVELS OF SHM?

During affinity maturation the introduction of SHM into immunoglobulin genes by activation-induced cytidine deaminase (AID) is random and only B cells with improved antigen binding are selected to receive signals for survival (90). Thus, rounds of mutation and selection in germinal centres generate antibodies with increased levels of SHM and higher affinity for antigen. Antigen-experienced IgG antibodies from healthy adults have been shown to possess on average 7% mutation in the variable heavy chain (VH) (91). Interestingly HIV-1 Env specific antibodies from infected individuals (reactive to gp140) have been found to have a significantly higher number of VH mutations than non-reactive antibodies, which was proposed to be a result of chronic infection (92). In agreement with this, antibodies from chronic but not acute infections in general have been found to have higher SHM (93). It has also been found that HIV bnAbs have even higher levels of mutation compared to HIV antibodies with only limited neutralisation capacity (94), and germline reversion of bnAbs to unmutated common ancestors has suggested that SHM acquired during development is essential for neutralising activity (74, 94). Longitudinal studies have also indicated that antibodies accumulate mutations in response to emerging HIV-1 Env variants and that this results in increased neutralisation breadth over time (29, 32, 33, 95). However, there are exceptions where higher VH mutation doesn't improve breadth for antibodies from the same lineage (e.g. PGT128 vs PGT130 and PG9 vs PG16 in **Supplementary Table 1**) (46, 47). It is plausible that although antibodies from the same lineage have a common ancestor these may have diverged early during development and mutated separately, therefore the mutations acquired are likely to differ and thus affect antigen binding and breadth of neutralisation. Additionally nucleotide mutations can be silent and not impact antibody neutralisation. For example it has been suggested from the analysis of minimally mutated VRC01 that some of the mutated residues might not be required for breadth (96).

Whilst it is known that favourable mutations are selected during affinity maturation as they enhance binding to the specific antigen, determining the effect of SHM on the breadth of an antibody against heterologous viruses is not so simple. To try and address this, the VH mutation frequency and percentage of viruses neutralised have been compared here for bnAbs tested against the 118 PV standard panel. Interestingly, the neutralisation breadth of all HIV bnAbs did not have a significant correlation with higher SHM in the VH (p=0.099, **Figure 3A**), nor when they were grouped by the epitopes targeted (**Figure 3B**). Instead only a negative correlation between VH mutation and neutralisation breadth for gp120-gp41 interface bnAbs was observed (p=0.027, **Figure 3B**). Nevertheless, this did highlight that a VH mutation frequency of ≥ 9% was exhibited by all bnAbs (**Figure 3E**). Although this might be the case for bnAbs from adults, it has been demonstrated that HIV-1 infected infants can produce bnAbs without higher levels of SHM (27, 97). Indeed infant-derived bnAbs BF520.1 and AIIMS-P01 that target the Env high mannose patch have only a 7% VH mutation and both achieved 58% breadth against the 12 global PV panel (24, 27, 97). For comparison the adult-derived bnAb VRC29.03, targeting the same epitope, also achieved 58% breadth against this panel but has more than double the VH mutation (**Supplementary Table 1**). Unfortunately it is not possible to compare the breadth of VRC29.03 to the breadth of other bnAbs in **Table 1** because this bnAb has not been tested against the same panel of PVs. The humoral response of infants could have an advantage over adults by developing in the presence of maternal HIV-1 specific antibodies that may enhance the *de novo* response (16). This would be unsurprising considering that neutralisation breadth can be driven by the cooperation of antibody lineages (98–100). Conversely far fewer bnAbs from infants have been isolated than adults and so the neutralisation breadth of BF520.1 and AIIMS-P01 achieved without extreme SHM may be outliers. Furthermore, the immune system of infants differs substantially from adults [as reviewed in (101)], which raises the question whether their antibodies can be fairly compared to those of adults.

Another aspect to consider is that antibody variable regions are comprised of CDRs and framework regions (FWRs) with

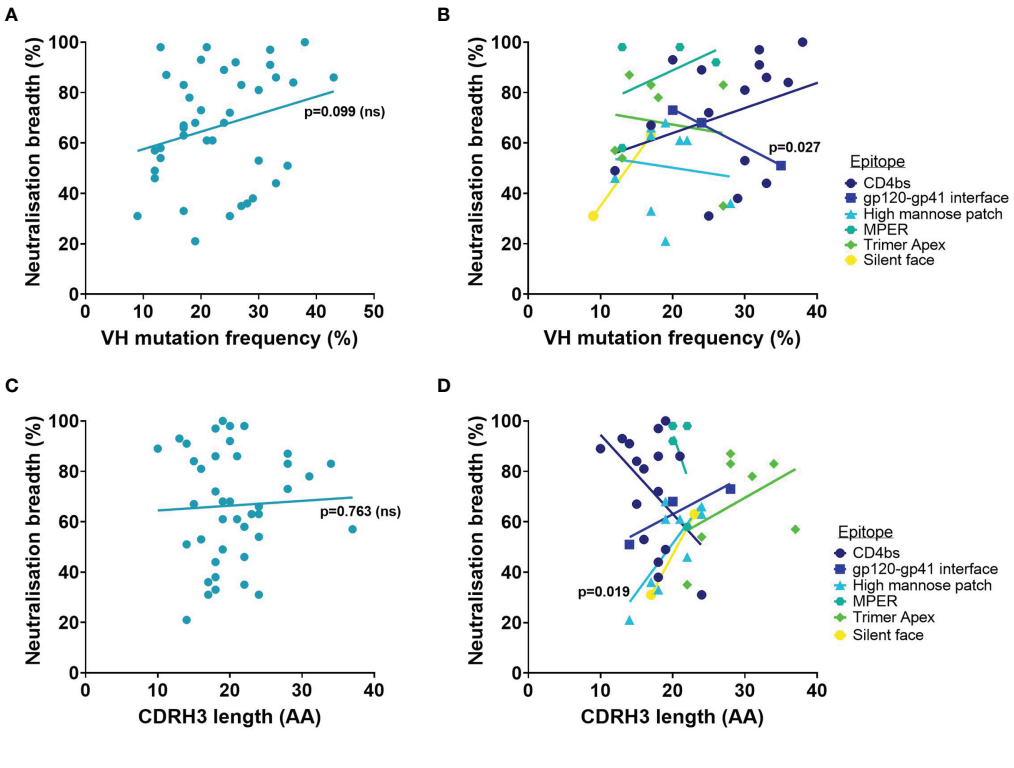


E

| | Range | Neutralisation breadth |
|---|---|---|
| VH mutation frequency | 9 - 43 % | Positive trend (ns): $R_2$=0.068, P value=0.099 |
| CD4bs | 12 - 43% | Positive trend (ns): $R_2$=0.122, P value=0.184 |
| Gp120-gp41 interface | 20 - 35% | Negative correlation: $R_2$=0.998, P value=0.027 |
| High mannose patch | 12 - 28% | No correlation: $R_2$=0.013, P value=0.773 |
| MPER | 13 - 26% | Positive trend (ns): $R_2$=0.197, P value=0.557 |
| Trimer apex | 12 - 27% | No correlation: $R_2$=0.025, P value=0.736 |
| Silent face | 9 - 17% | Analysis not able to be performed |
| CDRH3 length | 10 - 37 AAs | No association: $R_2$=0.002, P value=0.763 |
| CD4bs | 10 - 24 AAs | Negative trend (ns): $R_2$=0.208, P value=0.076 |
| Gp120-gp41 interface | 14 - 28 AAs | Positive trend (ns): $R_2$=0.857, P value=0.247 |
| High mannose patch | 14 - 24 AAs | Positive correlation: $R_2$=0.57, P value=0.019 |
| MPER | 20 - 22 AAs | No correlation: $R_2$=0.261, P value=0.489 |
| Trimer apex | 22 - 37 AAs | Positive trend (ns): $R_2$=0.192, P value=0.326 |
| Silent face | 17 - 23 AAs | Analysis not able to be performed |

**FIGURE 3** | VH mutation frequency, CDRH3 length and neutralisation breadth of HIV bnAbs against the 118 multi-clade PV panel. Mutation frequency was determined from VH nucleotide sequences. Correlations were determined by linear regression analysis, with $p<0.05$. **(A)** VH mutation frequency and neutralisation breadth of bnAbs had no association ($p=0.099$). **(B)** VH mutation frequency and neutralisation breadth of bnAbs grouped by epitope was associated for gp120-gp41 interface bnAbs ($p=0.027$). **(C)** CDRH3 length and neutralisation breadth of bnAbs had no association ($p=0.763$). **(D)** CDRH3 length and neutralisation breadth of bnAbs grouped by epitope was associated for high mannose patch bnAbs ($p=0.019$). **(E)** Summary of VH mutation frequency and CDRH3 length associations with neutralisation breadth. ns, Not significant.

SHM typically accumulating in CDR loops for improved interaction with antigen. Mutations are less tolerated in the FWRs, which support the three CDR loops per antibody chain, as changes in these regions are more likely to adversely affect the overall structure of the antibody. However, unlike most antibodies some HIV-1 bnAbs have a high number of FWR mutations that appear to be essential for their broad and potent neutralisation, by increasing flexibility of binding or through contacts with the antigen (94, 102). On the other hand, analysis of engineered variants for two bnAbs (VRC01 and 10E8) has instead implied that broad neutralisation can be achieved even when framework regions are reverted considerably (103). This suggests that only minimal framework mutations are required for these particular bnAbs and that additional mutations serve merely to improve the neutralisation potency.

## CAN WE DEFINE HIV bnAbs BY COMPARING THEIR CDRH3 LENGTH?

The length of the CDR loops can also affect antigen binding, and the heavy chain CDR3 (CDRH3) in particular is important for determining antigen specificity because it contains the most sequence diversity due to VDJ gene recombination in the pre-B cell (104). During development B cells undergo selection processes that leads to a relatively low frequency of B cell clones with long (>20 AAs) CDRH3 sequences (105–107), meaning these are infrequent genetic features in antibody repertoires, often being removed due to being auto-reactive (108). Remarkably many HIV-1 bnAbs have long CDRH3 loops that exceed the most frequent length of 14 amino acids and mean length of 15-16 amino acids (107, 109, 110). It is perhaps unsurprising that this genetic feature is present in HIV bnAbs given that longer CDRH3s have more opportunity for sequence variation and the potential to access recessed epitopes on antigens. Curiously CDRH3 sequences as long as that of the bnAb PG9 (28 AA) were revealed to be present in B cell repertoires from HIV-1 naïve individuals (111), suggesting that this feature, while relatively rare, is not unique to HIV bnAbs.

Considering that other CDR loops on the antibody heavy and light chains also contribute to antigen binding it is unlikely that the CDRH3 alone accounts for the neutralisation breadth of bnAbs. In agreement with this, there was no association of neutralisation breadth for bnAbs from **Table 1** with the length of their CDRH3 (p=0.763, **Figure 3C**). Yet when bnAbs were grouped by the epitopes targeted (**Figure 3D**) this revealed that a longer CDRH3 correlated with increased neutralisation breadth for bnAbs targeting the high mannose patch (p=0.019). Structural analysis has demonstrated that bnAbs against this epitope require extended CDRH3 loops to penetrate through the glycan shield and contact the more conserved envelope protein residues below (32, 112), offering a possible explanation for the association of CDRH3 length with breadth. Trimer apex bnAbs all had CDRH3 lengths of ≥22 AAs, highlighting the known requirement for a long CDRH3 to be able to access this epitope (113). However the trend between increased CDRH3 length with increased neutralisation breadth of apex bnAbs was not significant (**Figures 3D, E**). For the MPER epitope a long CDRH3 of 20-22 AAs appeared to be characteristic for all bnAbs but showed no correlation with breadth (**Figures 3D, E**). And while an increase in neutralisation breadth was observed for bnAbs with longer CDRH3s that target the gp120-gp41 interface and silent face, only a limited number of bnAbs were able to be included in this analysis and the association was not found to be significant (**Figures 3D, E**). In contrast for CD4bs bnAbs the length of the CDRH3 had a negative trend with neutralisation breadth, although this was not significant (p=0.076, **Figure 3E**). Considering that the majority of CD4bs bnAbs are VH gene restricted and bind predominantly *via* their CDRH2 (114, 115), rather than their CDRH3 loop, this is perhaps unsurprising.

Overall the level of SHM and the CDRH3 length of bnAbs required for neutralisation breadth (against the 118 PV panel) differ depending on the site being targeted on the HIV-1 Env and their mode of binding. Although HIV bnAbs have a high VH mutation and/or a long CDRH3, an increase in VH mutation did not correlate with increased breadth for any bnAbs and only an increase in CDRH3 length correlated with increased neutralisation breadth for those targeting the high mannose patch.

## CAN WE DEFINE BREADTH BY COMPARING EPITOPES OF bnAbs WITH NON-bnAbs?

The limited number of properly folded, functional Env trimers present on the surface of each virion is thought to be one of the many ways HIV is able to evade the immune system (1). Unprocessed Env protein that is not cleaved into gp120-gp41 heterodimers is non-functional, and as a result exposes non-neutralising epitopes (116). In addition, the instability of the Env trimer results in various forms such as non-functional gp41 stumps (depleted of gp120) and gp120-gp41 monomers being presented on the virion surface. These forms of Env are widely thought to act as decoys to the immune system by displaying epitopes (cluster I and II) on gp41 that are usually occluded by the trimer and so antibodies elicited to these sites that are able to bind but not neutralise HIV (117). Moreover, the shedding of gp120 from Env leads to the presence of circulating gp120 monomers that expose immunodominant sites and elicit non-neutralising antibodies (non-nAbs). Whilst some non-nAbs directed towards gp120 bind overlapping epitopes to nAbs, such as those in the CD4bs, V2 and V3 loop, their means of approach are not possible when gp120 is packed into a functional trimer (118–122). In agreement with this, immunisation studies using subunits of Env have had little success in eliciting desirable nAbs in comparison to native-like trimers [as reviewed in (123)]. It is therefore relatively easy to identify non-nAbs based on epitope alone due to their manner of binding and inability to target functional Env trimers, however distinguishing between nAbs and bnAbs based on their epitope is somewhat more complicated.

## NEUTRALISING ANTIBODIES TARGETING THE CD4bs

HIV initially requires interactions with CD4 on the host cell to gain entry, this is mediated by the CD4 receptor binding site (CD4bs) on the Env trimer and is therefore a functionally conserved region and a site of vulnerability. The CD4bs is situated on the gp120 subunit in a recessed hydrophobic pocket at the interface of the outer and inner domains (124), and is less accessible on the Env trimer compared to monomeric gp120 (125). Despite this, neutralising antibodies can be elicited against the CD4bs, although access has been demonstrated to be dependent on the angle of approach (126, 127). This helps to explain why some CD4bs antibodies are only capable of neutralising tier 1 viruses that exhibit a more open Env trimer

with fewer conformational constraints than tier 2/3 viruses (62, 128). CD4bs bnAbs however can neutralise tier 2/3 viruses through distinct approaches of binding, predominantly using their CDRH2 (for antibodies with VH1-2 or VH1-46) or their CDRH3.

The majority of CD4bs nAbs and bnAbs contact the highly conserved residue D368 on the CD4 binding loop (115), with only a few exceptions that instead are glycan dependant (129–131). As glycans do not substantially mask the CD4bs they are not often incorporated into CD4bs antibody epitopes. Nevertheless, glycans surrounding the binding site (e.g. N276 and N462) limit antibody access but can be accommodated or even bound by bnAbs with short, compact light chain CDR (CDRL) loops to prevent clashing which likely contributes to their neutralisation breadth (40, 130, 132). In addition, structural analysis of the VH1-2 restricted, VRC01-class bnAbs identified that a short or flexible CDRL1 is necessary to avoid steric clashes with Loop D (114). Recognition of the CD4bs by bnAbs has also been found to differ from non-bnAbs in clustering analysis due to their ability to contact residues further into the binding site (133). Similarly, longitudinal analysis of the CH235 antibody lineage revealed that progression towards the bnAb CH235.12 was driven by SHM, resulting in more specific contacts within the CD4 binding loop yet reduced contact with variable regions in close proximity such as the V5 loop (95). Indeed in a different study the limited neutralisation breadth displayed by the CD4bs nAb CAP257-RH1 was a consequence of its binding angle, which was incompatible with glycosylated V5 loops (129). Furthermore the most effective CD4bs bnAbs isolated to date (N6 that demonstrated 98% neutralisation breadth against a panel of 181 PVs and N49P7 with 100% neutralisation breadth against 117 of the 118 PV panel) have acquired extensive mutations to bury their CDRH2 into gp120 and engage conserved residues in the CD4 binding loop (30, 134). This mimics CD4 binding, which is common of many bnAbs in the VRC01-class and contributes to their neutralisation breadth (114, 135, 136).

## NEUTRALISING ANTIBODIES TARGETING THE V3

Another conserved region of Env is the V3 loop, which consists of three main structural regions: the base and the tip (also referred to as a crown), which are involved in co-receptor binding, and the more variable stem (137). However the V3 loop is buried beneath the V1/2 domain and not accessible until conformational changes cause the trimer to open upon CD4 engagement (138, 139). Most antibodies that target the V3 loop are therefore only capable of neutralising tier 1 viruses with a predominantly open conformation (similar to the CD4-bound state), this along with the high sequence variability of the V3 stem often leads to these antibodies being strain-specific (128). Conversely it has been demonstrated that V3 specific nAbs that target the V3 tip/crown, such as 447-52D, have the potential to neutralise some tier 2 viruses, although only weak/incomplete neutralisation has been observed which implies poor or transient accessibility to the epitope (67, 140). Recent analysis of strain-specific neutralising responses (from immunised rabbits) revealed an overlapping footprint at the base of the V3 with that of high mannose patch bnAbs, yet the specific epitope of these autologous antibodies and binding mechanism differed by contacting peptide residues in the V1 loop and not V3 glycans (141). In agreement with this, a longitudinal study has suggested that affinity for V3 glycans acquired during antibody evolution subsequently widens the breadth of neutralisation (32). Interestingly, V3 antibody neutralisation also correlates with the Env V1 loop length whereby breadth is achieved as longer loops are accommodated, although this often reduces antibody potency (33). These findings correspond with the fact that the conserved ($^{324}$GDIR$^{327}$) linear sequence at the base of the V3 loop is masked by the V1/V2 domain as well as the N-linked glycan supersite (N295, N301, N332, N339, N385 and N392) in the closed (pre-fusion) conformation of Env, typical of most circulating tier 2 viruses (142, 143). It has been demonstrated that bnAbs to this epitope are able to incorporate glycans into their epitope, in particular the N332 glycan, as well as use long CDR loops to reach past them to contact the conserved peptide residues (112, 144). The only exception being bnAb 2G12 which relies solely on contacting glycans (145). Often multiple V3 glycans or glycans close to this site, such as those protruding from the V1 loop, can also be utilised by high mannose patch bnAbs and consequently allows a degree of flexibility in their epitope and different angles of approach (33, 146–150). The breadth of neutralisation achieved by bnAbs against the high mannose patch is therefore aided by the ability to accommodate different glycans, due to changes in N-linked glycosylation sites often being a way that HIV is able to escape from neutralisation (10, 146).

## NEUTRALISING ANTIBODIES TARGETING THE V1/V2

Finally, the V1/V2 domain is another site on the gp120 subunit of Env that is targeted by the humoral response, and although this site itself is not directly involved in viral entry the V1/V2 loops are necessary to shield the region involved in co-receptor binding until it is required (151, 152). Neutralising antibodies directed to the hypervariable V1/V2 domain can therefore prevent opening of the trimer and exposure of the host cell co-receptor required for viral engagement. In the native Env trimer, the V1/V2 domain is located at the apex and is comprised of a five-stranded β-barrel, with conserved residues being located in the strands and more variable residues in the loops connecting these strands (153). However, it has also been revealed that residues in the V2 domain can adopt a coil or helical conformation in CD4-bound open trimers that result in the exposure of (short linear peptide) epitopes in tier 1A viruses that can be bound by nAbs (122, 154). Analysis of 'tier 1A' nAbs have revealed similarities with bnAbs in the residues contacted on Env, such as those at position 160 and 168-171 in the positively-

charged V2 site (113, 122, 155, 156), however the secondary structure of V2 in different Env conformations results in distinct epitopes. Furthermore, bnAbs targeting the trimer apex have been shown to preferentially recognise the quaternary structure of Env (exhibiting a β-conformation of V2) (157), and thus bind intermediate and/or closed conformations of the Env trimer exhibited by tier 1B and tier 2/3 viruses, rather than open conformations characteristic of tier 1A viruses (62, 158). Antibodies that exhibit strain-specific neutralisation have also been identified against the Env quaternary structure, however in the case of the nAb 2909 this can be explained by the reliance on K160 for neutralisation rather than the highly conserved N160 and thus has limited breadth (159, 160). In contrast bnAbs are dependent on glycans at the trimer apex, interacting with or requiring the presence of the N156 and N160 glycan protruding from the V2 strand B, with the latter being essential in bnAb epitopes as demonstrated by mutant viruses lacking N160 becoming partially or completely resistant to neutralisation (9, 113, 161–165). These glycans mask both the hole at the trimer apex and the positively-charged lysine-rich site on the V2 strand C which form epitopes that can be accessed by bnAbs using a long, negatively charged CDRH3 often containing a YYD motif with sulphated tyrosines (166). An exception to this being VRC38.01 which has a CDRH3 length of 16 AAs that may restrict its neutralisation breadth to 30% against the 208 PV panel, **Supplementary Table 1** (163). Furthermore V2 nAbs with more limited neutralisation capacity have been found to possess shorter CDRH3s than most apex bnAbs, and are often restricted by viruses with long V2 loops (46, 167). However, simply possessing a long CDRH3 is not enough to confer breadth, as demonstrated by the CAP256 antibody lineages, this loop must also protrude out and away from the rest of the antibody with an appropriate orientation (164). Nevertheless, a different binding approach has recently been displayed by bnAb BG1, where a protruding CDRH2 rather than CDRH3 contacts the protein residues beneath glycans, however these interactions appear to be more easily disrupted by changes in Env residues and may account for its lower neutralisation breadth compared to other apex bnAbs (9).

Overall, although the binding footprint of HIV bnAbs and nAbs are often similar, the angle of approach or specific residues contacted differ to enable bnAbs to neutralise a broad spectrum of viruses. In addition, bnAbs are able to accommodate glycans or even incorporate them into their epitope through the acquisition of beneficial mutations to allow a degree of flexibility in their binding. However even bnAbs against the same region on Env can vary in the residues that they engage, and whilst the epitopes of bnAbs have been well characterised the epitopes of nAbs have been studied less, thus making it challenging to predict the neutralisation breadth of an antibody based on epitope alone.

## SUMMARY

HIV bnAbs are of particular interest in HIV-1 research due to many studies demonstrating their potential to provide protection, and thus have been extensively studied. However, despite the vast amount of knowledge acquired about these antibodies there is no set of criteria to determine or define what it means to be a bnAb. This question has been addressed here by comparing bnAbs based on their neutralisation breadth and potency, their mutational frequencies and CDRH3 lengths and the epitopes targeted. The majority of bnAbs previously tested against the 118 multi-clade PV panel can neutralise ≥7 clades/CRFs and achieve >30% neutralisation breadth with a geomean $IC_{50}$ ≤3.6 μg/ml. In addition, bnAbs have a wide range of VH mutation (9-43%) and CDRH3 length (10-37AAs) but overall these features did not correlate with an increase in neutralisation breadth. Finally, it is hard to distinguish bnAbs solely on the epitope targeted because their footprints can, to a degree, overlap with those of nAbs.

In conclusion, while some traits are common to many bnAbs (high SHM, long CDRH3s or epitope specificity) it would not have been possible to identify current HIV-1 bnAbs based on these alone. Without prior knowledge of their neutralisation breadth these bnAbs are not distinctive enough from those of nAbs with limited neutralisation breadth. Regrettably this prevents new bnAbs from being discovered directly from repertoire sequencing (168) or from antibody binding footprints determined by competition binding experiments or epitope mapping of polyclonal serum (169), posing a challenge for defining immune profiles associated with bnAb development. Therefore individual bnAbs must continue to be characterised initially by functional screening to identify neutralisation breadth comparable to those that have already been isolated.

## AUTHOR CONTRIBUTIONS

SAG performed the literature searches, data collection and wrote the manuscript. LEM revised the final version of the manuscript. All authors contributed to the article and approved the submitted version.

## FUNDING

LEM is supported by an MRC Career Development Award MR/R008698/1 and receives funding from the European Research Council (ERC) under the European Union's Horizon 2020 research and innovation programme (Grant Agreement No. 757601).

## SUPPLEMENTARY MATERIAL

The Supplementary Material for this article can be found online at: https://www.frontiersin.org/articles/10.3389/fimmu.2021.708227/full#supplementary-material

## REFERENCES


1. Zhu P, Chertova E, Bess JJr., Lifson JD, Arthur LO, Liu J, et al. Electron Tomography Analysis of Envelope Glycoprotein Trimers on HIV and Simian Immunodeficiency Virus Virions. *Proc Natl Acad Sci USA* (2003) 100 (26):15812–7. doi: 10.1073/pnas.2634931100
2. McCune JM, Rabin LB, Feinberg MB, Lieberman M, Kosek JC, Reyes GR, et al. Endoproteolytic Cleavage of Gp160 is Required for the Activation of Human Immunodeficiency Virus. *Cell* (1988) 53(1):55–67. doi: 10.1016/0092-8674(88)90487-4
3. Ugolini S, Mondor I, Parren PW, Burton DR, Tilley SA, Klasse PJ, et al. Inhibition of Virus Attachment to CD4+ Target Cells is a Major Mechanism of T Cell Line-Adapted HIV-1 Neutralization. *J Exp Med* (1997) 186(8):1287–98. doi: 10.1084/jem.186.8.1287
4. Julien JP, Sok D, Khayat R, Lee JH, Doores KJ, Walker LM, et al. Broadly Neutralizing Antibody PGT121 Allosterically Modulates CD4 Binding *via* Recognition of the HIV-1 Gp120 V3 Base and Multiple Surrounding Glycans. *PloS Pathog* (2013) 9(5):e1003342. doi: 10.1371/journal.ppat.1003342
5. Platt EJ, Gomes MM, Kabat D. Kinetic Mechanism for HIV-1 Neutralization by Antibody 2G12 Entails Reversible Glycan Binding That Slows Cell Entry. *Proc Natl Acad Sci USA* (2012) 109(20):7829–34. doi: 10.1073/pnas.1109728109
6. Ruprecht CR, Krarup A, Reynell L, Mann AM, Brandenberg OF, Berlinger L, et al. MPER-Specific Antibodies Induce Gp120 Shedding and Irreversibly Neutralize HIV-1. *J Exp Med* (2011) 208(3):439–54. doi: 10.1084/jem.20101907
7. Kim AS, Leaman DP, Zwick MB. Antibody to Gp41 MPER Alters Functional Properties of HIV-1 Env Without Complete Neutralization. *PloS Pathog* (2014) 10(7):e1004271. doi: 10.1371/journal.ppat.1004271
8. Blattner C, Lee JH, Sliepen K, Derking R, Falkowska E, de la Peña AT, et al. Structural Delineation of a Quaternary, Cleavage-Dependent Epitope at the Gp41-Gp120 Interface on Intact HIV-1 Env Trimers. *Immunity* (2014) 40 (5):669–80. doi: 10.1016/j.immuni.2014.04.008
9. Wang H, Gristick HB, Scharf L, West AP, Galimidi RP, Seaman MS, et al. Asymmetric Recognition of HIV-1 Envelope Trimer by V1V2 Loop-Targeting Antibodies. *Elife* (2017) 6:e27389. doi: 10.7554/eLife.27389
10. Wei X, Decker JM, Wang S, Hui H, Kappes JC, Wu X, et al. Antibody Neutralization and Escape by HIV-1. *Nature* (2003) 422(6929):307–12. doi: 10.1038/nature01470
11. Richman DD, Wrin T, Little SJ, Petropoulos CJ. Rapid Evolution of the Neutralizing Antibody Response to HIV Type 1 Infection. *Proc Natl Acad Sci USA* (2003) 100(7):4144–9. doi: 10.1073/pnas.0630530100
12. Mansky LM, Temin HM. Lower *In Vivo* Mutation Rate of Human Immunodeficiency Virus Type 1 Than That Predicted From the Fidelity of Purified Reverse Transcriptase. *J Virol* (1995) 69(8):5087–94. doi: 10.1128/jvi.69.8.5087-5094.1995
13. Bar KJ, Tsao CY, Iyer SS, Decker JM, Yang Y, Bonsignori M, et al. Early Low-Titer Neutralizing Antibodies Impede HIV-1 Replication and Select for Virus Escape. *PloS Pathog* (2012) 8(5):e1002721. doi: 10.1371/journal.ppat.1002721
14. Hemelaar J. The Origin and Diversity of the HIV-1 Pandemic. *Trends Mol Med* (2012) 18(3):182–92. doi: 10.1016/j.molmed.2011.12.001
15. McCoy LE, McKnight Á. Lessons Learned From Humoral Responses of HIV Patients. *Curr Opin HIV AIDS* (2017) 12(3):195–202. doi: 10.1097/COH.0000000000000361
16. Goo L, Chohan V, Nduati R, Overbaugh J. Early Development of Broadly Neutralizing Antibodies in HIV-1-Infected Infants. *Nat Med* (2014) 20 (6):655–8. doi: 10.1038/nm.3565
17. Mishra N, Sharma S, Dobhal A, Kumar S, Chawla H, Singh R, et al. Broadly Neutralizing Plasma Antibodies Effective Against Autologous Circulating Viruses in Infants With Multivariant HIV-1 Infection. *Nat Commun* (2020) 11(1):4409. doi: 10.1038/s41467-020-18225-x
18. Klein F, Halper-Stromberg A, Horwitz JA, Gruell H, Scheid JF, Bournazos S, et al. HIV Therapy by a Combination of Broadly Neutralizing Antibodies in Humanized Mice. *Nature* (2012) 492(7427):118–22. doi: 10.1038/nature11604
19. Hessell AJ, Haigwood NL. Animal Models in HIV-1 Protection and Therapy. *Curr Opin HIV AIDS* (2015) 10(3):170–6. doi: 10.1097/COH.0000000000000152
20. Barouch DH, Whitney JB, Moldt B, Klein F, Oliveira TY, Liu J, et al. Therapeutic Efficacy of Potent Neutralizing HIV-1-Specific Monoclonal Antibodies in SHIV-Infected Rhesus Monkeys. *Nature* (2013) 503 (7475):224–8. doi: 10.1038/nature12744
21. Julg B, Liu PT, Wagh K, Fischer WM, Abbink P, Mercado NB, et al. Protection Against a Mixed SHIV Challenge by a Broadly Neutralizing Antibody Cocktail. *Sci Transl Med* (2017) 9(408):aao4235. doi: 10.1126/scitranslmed.aao4235
22. Garber DA, Adams DR, Guenthner P, Mitchell J, Kelley K, Schoofs T, et al. Durable Protection Against Repeated Penile Exposures to Simian-Human Immunodeficiency Virus by Broadly Neutralizing Antibodies. *Nat Commun* (2020) 11(1):3195. doi: 10.1038/s41467-020-16928-9
23. Mendoza P, Gruell H, Nogueira L, Pai JA, Butler AL, Millard K, et al. Combination Therapy With Anti-HIV-1 Antibodies Maintains Viral Suppression. *Nature* (2018) 561(7724):479–84. doi: 10.1038/s41586-018-0531-2
24. Yoon H, Macke J, West APJr., Foley B, Bjorkman PJ, Korber B, et al. CATNAP: A Tool to Compile, Analyze and Tally Neutralizing Antibody Panels. *Nucleic Acids Res* (2015) 43(W1):W213–9. doi: 10.1093/nar/gkv404
25. Liu M, Yang G, Wiehe K, Nicely NI, Vandergrift NA, Rountree W, et al. Polyreactivity and Autoreactivity Among HIV-1 Antibodies. *J Virol* (2015) 89 (1):784–98. doi: 10.1128/JVI.02378-14
26. Prigent J, Jarossay A, Planchais C, Eden C, Dufloo J, Kök A, et al. Conformational Plasticity in Broadly Neutralizing HIV-1 Antibodies Triggers Polyreactivity. *Cell Rep* (2018) 23(9):2568–81. doi: 10.1016/j.celrep.2018.04.101
27. Simonich CA, Williams KL, Verkerke HP, Williams JA, Nduati R, Lee KK, et al. HIV-1 Neutralizing Antibodies With Limited Hypermutation From an Infant. *Cell* (2016) 166(1):77–87. doi: 10.1016/j.cell.2016.05.055
28. Gray ES, Madiga MC, Hermanus T, Moore PL, Wibmer CK, Tumba NL, et al. The Neutralization Breadth of HIV-1 Develops Incrementally Over Four Years and is Associated With CD4+ T Cell Decline and High Viral Load During Acute Infection. *J Virol* (2011) 85(10):4828–40. doi: 10.1128/JVI.00198-11
29. Liao HX, Lynch R, Zhou T, Gao F, Alam SM, Boyd SD, et al. Co-Evolution of a Broadly Neutralizing HIV-1 Antibody and Founder Virus. *Nature* (2013) 496 (7446):469–76. doi: 10.1038/nature12053
30. Sajadi MM, Dashti A, Rikhtegaran Tehrani Z, Tolbert WD, Seaman MS, Ouyang X, et al. Identification of Near-Pan-Neutralizing Antibodies Against HIV-1 by Deconvolution of Plasma Humoral Responses. *Cell* (2018) 173 (7):1783–95.e14. doi: 10.1016/j.cell.2018.03.061
31. Doria-Rose NA, Schramm CA, Gorman J, Moore PL, Bhiman JN, DeKosky BJ, et al. Developmental Pathway for Potent V1V2-Directed HIV-Neutralizing Antibodies. *Nature* (2014) 509(7498):55–62. doi: 10.1038/nature13036
32. MacLeod DT, Choi NM, Briney B, Garces F, Ver LS, Landais E, et al. Early Antibody Lineage Diversification and Independent Limb Maturation Lead to Broad HIV-1 Neutralization Targeting the Env High-Mannose Patch. *Immunity* (2016) 44(5):1215–26. doi: 10.1016/j.immuni.2016.04.016
33. Bonsignori M, Kreider EF, Fera D, Meyerhoff RR, Bradley T, Wiehe K, et al. Staged Induction of HIV-1 Glycan-Dependent Broadly Neutralizing Antibodies. *Sci Transl Med* (2017) 9(381):eaai7514. doi: 10.1126/scitranslmed.aai7514
34. Bonsignori M, Liao HX, Gao F, Williams WB, Alam SM, Montefiori DC, et al. Antibody-Virus Co-Evolution in HIV Infection: Paths for HIV Vaccine Development. *Immunol Rev* (2017) 275(1):145–60. doi: 10.1111/imr.12509
35. McCoy LE. The Expanding Array of HIV Broadly Neutralizing Antibodies. *Retrovirology* (2018) 15(1):70. doi: 10.1186/s12977-018-0453-y
36. McCoy LE, Burton DR. Identification and Specificity of Broadly Neutralizing Antibodies Against HIV. *Immunol Rev* (2017) 275(1):11–20. doi: 10.1111/imr.12484
37. Burton DR, Hangartner L. Broadly Neutralizing Antibodies to HIV and Their Role in Vaccine Design. *Annu Rev Immunol* (2016) 34:635–59. doi: 10.1146/annurev-immunol-041015-055515
38. Doores KJ, Bonomelli C, Harvey DJ, Vasiljevic S, Dwek RA, Burton DR, et al. Envelope Glycans of Immunodeficiency Virions are Almost Entirely Oligomannose Antigens. *Proc Natl Acad Sci USA* (2010) 107(31):13800–5. doi: 10.1073/pnas.1006498107
39. Berndsen ZT, Chakraborty S, Wang X, Cottrell CA, Torres JL, Diedrich JK, et al. Visualization of the HIV-1 Env Glycan Shield Across Scales. *Proc Natl Acad Sci* (2020) 117(45):28014–25. doi: 10.1073/pnas.2000260117

40. West APJr., Scharf L, Scheid JF, Klein F, Bjorkman PJ, Nussenzweig MC. Structural Insights on the Role of Antibodies in HIV-1 Vaccine and Therapy. *Cell* (2014) 156(4):633–48. doi: 10.1016/j.cell.2014.01.052
41. Borrow P, Moody MA. Immunologic Characteristics of HIV-Infected Individuals Who Make Broadly Neutralizing Antibodies. *Immunol Rev* (2017) 275(1):62–78. doi: 10.1111/imr.12504
42. Verkoczy L, Kelsoe G, Moody MA, Haynes BF. Role of Immune Mechanisms in Induction of HIV-1 Broadly Neutralizing Antibodies. *Curr Opin Immunol* (2011) 23(3):383–90. doi: 10.1016/j.coi.2011.04.003
43. Soldemo M, Karlsson Hedestam GB. Env-Specific Antibodies in Chronic Infection Versus in Vaccination. *Front Immunol* (2017) 8:1057. doi: 10.3389/fimmu.2017.01057
44. Schroeder KM, Agazio A, Torres RM. Immunological Tolerance as a Barrier to Protective HIV Humoral Immunity. *Curr Opin Immunol* (2017) 47:26–34. doi: 10.1016/j.coi.2017.06.004
45. Simek MD, Rida W, Priddy FH, Pung P, Carrow E, Laufer DS, et al. Human Immunodeficiency Virus Type 1 Elite Neutralizers: Individuals With Broad and Potent Neutralizing Activity Identified by Using a High-Throughput Neutralization Assay Together With an Analytical Selection Algorithm. *J Virol* (2009) 83(14):7337–48. doi: 10.1128/JVI.00110-09
46. Walker LM, Phogat SK, Chan-Hui PY, Wagner D, Phung P, Goss JL, et al. Broad and Potent Neutralizing Antibodies From an African Donor Reveal a New HIV-1 Vaccine Target. *Science* (2009) 326(5950):285–9. doi: 10.1126/science.1178746
47. Walker LM, Huber M, Doores KJ, Falkowska E, Pejchal R, Julien JP, et al. Broad Neutralization Coverage of HIV by Multiple Highly Potent Antibodies. *Nature* (2011) 477(7365):466–70. doi: 10.1038/nature10373
48. Kumar R, Qureshi H, Deshpande S, Bhattacharya J. Broadly Neutralizing Antibodies in HIV-1 Treatment and Prevention. *Ther Adv Vaccines Immunother* (2018) 6(4):61–8. doi: 10.1177/2515135518800689
49. Dashti A, DeVico AL, Lewis GK, Sajadi MM. Broadly Neutralizing Antibodies Against HIV: Back to Blood. *Trends Mol Med* (2019) 25(3):228–40. doi: 10.1016/j.molmed.2019.01.007
50. Seaman MS, Janes H, Hawkins N, Grandpre LE, Devoy C, Giri A, et al. Tiered Categorization of a Diverse Panel of HIV-1 Env Pseudoviruses for Assessment of Neutralizing Antibodies. *J Virol* (2010) 84(3):1439–52. doi: 10.1128/JVI.02108-09
51. van Schooten J, van Gils MJ. HIV-1 Immunogens and Strategies to Drive Antibody Responses Towards Neutralization Breadth. *Retrovirology* (2018) 15(1):74. doi: 10.1186/s12977-018-0457-7
52. Pollara J, Easterhoff D, Fouda GG. Lessons Learned From Human HIV Vaccine Trials. *Curr Opin HIV AIDS* (2017) 12(3):216–21. doi: 10.1097/COH.0000000000000362
53. Locci M, Havenar-Daughton C, Landais E, Wu J, Kroenke MA, Arlehamn CL, et al. Human Circulating PD-1+CXCR3-CXCR5+ Memory Tfh Cells are Highly Functional and Correlate With Broadly Neutralizing HIV Antibody Responses. *Immunity* (2013) 39(4):758–69. doi: 10.1016/j.immuni.2013.08.031
54. Moody MA, Pedroza-Pacheco I, Vandergrift NA, Chui C, Lloyd KE, Parks R, et al. Immune Perturbations in HIV-1-Infected Individuals Who Make Broadly Neutralizing Antibodies. *Sci Immunol* (2016) 1(1):aag0851. doi: 10.1126/sciimmunol.aag0851
55. Kouyos RD, Rusert P, Kadelka C, Huber M, Marzel A, Ebner H, et al. Tracing HIV-1 Strains That Imprint Broadly Neutralizing Antibody Responses. *Nature* (2018) 561(7723):406–10. doi: 10.1038/s41586-018-0517-0
56. Martin-Gayo E, Gao C, Chen HR, Ouyang Z, Kim D, Kolb KE, et al. Immunological Fingerprints of Controllers Developing Neutralizing HIV-1 Antibodies. *Cell Rep* (2020) 30(4):984–96.e4. doi: 10.1016/j.celrep.2019.12.087
57. Bradley T, Peppa D, Pedroza-Pacheco I, Li D, Cain DW, Henao R, et al. RAB11FIP5 Expression and Altered Natural Killer Cell Function Are Associated With Induction of HIV Broadly Neutralizing Antibody Responses. *Cell* (2018) 175(2):387–99.e17. doi: 10.1016/j.cell.2018.08.064
58. Rusert P, Kouyos RD, Kadelka C, Ebner H, Schanz M, Huber M, et al. Determinants of HIV-1 Broadly Neutralizing Antibody Induction. *Nat Med* (2016) 22(11):1260–7. doi: 10.1038/nm.4187
59. Landais E, Huang X, Havenar-Daughton C, Murrell B, Price MA, Wickramasinghe L, et al. Broadly Neutralizing Antibody Responses in a Large Longitudinal Sub-Saharan HIV Primary Infection Cohort. *PloS Pathog* (2016) 12(1):e1005369. doi: 10.1371/journal.ppat.1005369
60. Hanson CV, Crawford-Miksza L, Sheppard HW. Application of a Rapid Microplaque Assay for Determination of Human Immunodeficiency Virus Neutralizing Antibody Titers. *J Clin Microbiol* (1990) 28(9):2030–4. doi: 10.1128/jcm.28.9.2030-2034.1990
61. Montefiori DC. Measuring HIV Neutralization in a Luciferase Reporter Gene Assay. *Methods Mol Biol* (2009) 485:395–405. doi: 10.1007/978-1-59745-170-3_26
62. Montefiori DC, Roederer M, Morris L, Seaman MS. Neutralization Tiers of HIV-1. *Curr Opin HIV AIDS* (2018) 13(2):128–36. doi: 10.1097/COH.0000000000000442
63. Munro JB, Gorman J, Ma X, Zhou Z, Arthos J, Burton DR, et al. Conformational Dynamics of Single HIV-1 Envelope Trimers on the Surface of Native Virions. *Science* (2014) 346(6210):759–63. doi: 10.1126/science.1254426
64. Dreja H, O'Sullivan E, Pade C, Greene KM, Gao H, Aubin K, et al. Neutralization Activity in a Geographically Diverse East London Cohort of Human Immunodeficiency Virus Type 1-Infected Patients: Clade C Infection Results in a Stronger and Broader Humoral Immune Response Than Clade B Infection. *J Gen Virol* (2010) 91(Pt 11):2794–803. doi: 10.1099/vir.0.024224-0
65. Hraber P, Korber BT, Lapedes AS, Bailer RT, Seaman MS, Gao H, et al. Impact of Clade, Geography, and Age of the Epidemic on HIV-1 Neutralization by Antibodies. *J Virol* (2014) 88(21):12623–43. doi: 10.1128/JVI.01705-14
66. Cavacini LA, Duval M, Patil A, Wood C, Mayer KH, Ruprecht RM, et al. Dichotomy in Cross-Clade Reactivity and Neutralization by HIV-1 Sera: Implications for Active and Passive Immunotherapy. *J Med Virol* (2005) 76(2):146–52. doi: 10.1002/jmv.20339
67. Han Q, Jones JA, Nicely NI, Reed RK, Shen X, Mansouri K, et al. Difficult-To-Neutralize Global HIV-1 Isolates are Neutralized by Antibodies Targeting Open Envelope Conformations. *Nat Commun* (2019) 10(1):2898. doi: 10.1038/s41467-019-10899-2
68. Stephenson KE, Wagh K, Korber B, Barouch DH. Vaccines and Broadly Neutralizing Antibodies for HIV-1 Prevention. *Annu Rev Immunol* (2020) 38:673–703. doi: 10.1146/annurev-immunol-080219-023629
69. Buonaguro L, Tornesello ML, Buonaguro FM. Human Immunodeficiency Virus Type 1 Subtype Distribution in the Worldwide Epidemic: Pathogenetic and Therapeutic Implications. *J Virol* (2007) 81(19):10209–19. doi: 10.1128/JVI.00872-07
70. Bbosa N, Kaleebu P, Ssemwanga D. HIV Subtype Diversity Worldwide. *Curr Opin HIV AIDS* (2019) 14(3):153–60. doi: 10.1097/COH.0000000000000534
71. Hemelaar J, Gouws E, Ghys PD, Osmanov S. Global Trends in Molecular Epidemiology of HIV-1 During 2000-2007. *Aids* (2011) 25(5):679–89. doi: 10.1097/QAD.0b013e328342ff93
72. deCamp A, Hraber P, Bailer RT, Seaman MS, Ochsenbauer C, Kappes J, et al. Global Panel of HIV-1 Env Reference Strains for Standardized Assessments of Vaccine-Elicited Neutralizing Antibodies. *J Virol* (2014) 88(5):2489–507. doi: 10.1128/JVI.02853-13
73. Schommers P, Gruell H, Abernathy ME, Tran MK, Dingens AS, Gristick HB, et al. Restriction of HIV-1 Escape by a Highly Broad and Potent Neutralizing Antibody. *Cell* (2020) 180(3):471–89.e22. doi: 10.1016/j.cell.2020.01.010
74. Pinto D, Fenwick C, Caillat C, Silacci C, Guseva S, Dehez F, et al. Structural Basis for Broad HIV-1 Neutralization by the MPER-Specific Human Broadly Neutralizing Antibody Ln01. *Cell Host Microbe* (2019) 26(5):623–37.e8. doi: 10.1016/j.chom.2019.09.016
75. Schoofs T, Barnes CO, Suh-Toma N, Golijanin J, Schommers P, Gruell H, et al. Broad and Potent Neutralizing Antibodies Recognize the Silent Face of the HIV Envelope. *Immunity* (2019) 50(6):1513–29.e9. doi: 10.1016/j.immuni.2019.04.014
76. Jia M, Liberatore RA, Guo Y, Chan KW, Pan R, Lu H, et al. VSV-Displayed HIV-1 Envelope Identifies Broadly Neutralizing Antibodies Class-Switched to IgG and IgA. *Cell Host Microbe* (2020) 27(6):963–75.e5. doi: 10.1016/j.chom.2020.03.024
77. Binley JM, Wrin T, Korber B, Zwick MB, Wang M, Chappey C, et al. Comprehensive Cross-Clade Neutralization Analysis of a Panel of Anti-Human Immunodeficiency Virus Type 1 Monoclonal Antibodies. *J Virol* (2004) 78(23):13232–52. doi: 10.1128/JVI.78.23.13232-13252.2004

78. Caskey M, Schoofs T, Gruell H, Settler A, Karagounis T, Kreider EF, et al. Antibody 10-1074 Suppresses Viremia in HIV-1-Infected Individuals. *Nat Med* (2017) 23(2):185–91. doi: 10.1038/nm.4268
79. Lorenzi JCC, Mendoza P, Cohen YZ, Nogueira L, Lavine C, Sapiente J, et al. Neutralizing Activity of Broadly Neutralizing Anti-HIV-1 Antibodies Against Primary African Isolates. *J Virol* (2021) 95(5):e01909–20. doi: 10.1128/JVI.01909-20
80. *Antibody Infusions Prevent Acquisition of Some HIV Strains, NIH Studies Find: National Institutes of Health* (2021). Available at: https://www.nih.gov/news-events/news-releases/antibody-infusions-prevent-acquisition-some-hiv-strains-nih-studies-find.
81. Scheid JF, Horwitz JA, Bar-On Y, Kreider EF, Lu CL, Lorenzi JC, et al. HIV-1 Antibody 3BNC117 Suppresses Viral Rebound in Humans During Treatment Interruption. *Nature* (2016) 535(7613):556–60. doi: 10.1038/nature18929
82. Bar KJ, Sneller MC, Harrison LJ, Justement JS, Overton ET, Petrone ME, et al. Effect of HIV Antibody VRC01 on Viral Rebound After Treatment Interruption. *N Engl J Med* (2016) 375(21):2037–50. doi: 10.1056/NEJMoa1608243
83. Arts EJ, Hazuda DJ. HIV-1 Antiretroviral Drug Therapy. *Cold Spring Harb Perspect Med* (2012) 2(4):a007161. doi: 10.1101/cshperspect.a007161
84. Kong R, Louder MK, Wagh K, Bailer RT, deCamp A, Greene K, et al. Improving Neutralization Potency and Breadth by Combining Broadly Reactive HIV-1 Antibodies Targeting Major Neutralization Epitopes. *J Virol* (2015) 89(5):2659–71. doi: 10.1128/JVI.03136-14
85. Wagh K, Seaman MS, Zingg M, Fitzsimons T, Barouch DH, Burton DR, et al. Potential of Conventional & Bispecific Broadly Neutralizing Antibodies for Prevention of HIV-1 Subtype A, C & D Infections. *PloS Pathog* (2018) 14(3):e1006860. doi: 10.1371/journal.ppat.1006860
86. Caskey M, Klein F, Nussenzweig MC. Broadly Neutralizing Anti-HIV-1 Monoclonal Antibodies in the Clinic. *Nat Med* (2019) 25(4):547–53. doi: 10.1038/s41591-019-0412-8
87. Liu Y, Cao W, Sun M, Li T. Broadly Neutralizing Antibodies for HIV-1: Efficacies, Challenges and Opportunities. *Emerg Microbes Infect* (2020) 9(1):194–206. doi: 10.1080/22221751.2020.1713707
88. Julg B, Barouch DH. Neutralizing Antibodies for HIV-1 Prevention. *Curr Opin HIV AIDS* (2019) 14(4):318–24. doi: 10.1097/COH.0000000000000556
89. Huang D, Tran JT, Olson A, Vollbrecht T, Tenuta M, Guryleva MV, et al. Vaccine Elicitation of HIV Broadly Neutralizing Antibodies From Engineered B Cells. *Nat Commun* (2020) 11(1):5850. doi: 10.1101/2020.03.17.989699
90. Victora GD, Nussenzweig MC. Germinal Centers. *Annu Rev Immunol* (2012) 30:429–57. doi: 10.1146/annurev-immunol-020711-075032
91. IJ H, van Schouwenburg PA, van Zessen D, Pico-Knijnenburg I, Driessen GJ, Stubbs AP, et al. Evaluation of the Antigen-Experienced B-Cell Receptor Repertoire in Healthy Children and Adults. *Front Immunol* (2016) 7:410. doi: 10.3389/fimmu.2016.00410
92. Scheid JF, Mouquet H, Feldhahn N, Seaman MS, Velinzon K, Pietzsch J, et al. Broad Diversity of Neutralizing Antibodies Isolated From Memory B Cells in HIV-Infected Individuals. *Nature* (2009) 458(7238):636–40. doi: 10.1038/nature07930
93. Breden F, Lepik C, Longo NS, Montero M, Lipsky PE, Scott JK. Comparison of Antibody Repertoires Produced by HIV-1 Infection, Other Chronic and Acute Infections, and Systemic Autoimmune Disease. *PloS One* (2011) 6(3):e16857. doi: 10.1371/journal.pone.0016857
94. Klein F, Diskin R, Scheid JF, Gaebler C, Mouquet H, Georgiev IS, et al. Somatic Mutations of the Immunoglobulin Framework are Generally Required for Broad and Potent HIV-1 Neutralization. *Cell* (2013) 153(1):126–38. doi: 10.1016/j.cell.2013.03.018
95. Bonsignori M, Zhou T, Sheng Z, Chen L, Gao F, Joyce MG, et al. Maturation Pathway From Germline to Broad HIV-1 Neutralizer of a CD4-Mimic Antibody. *Cell* (2016) 165(2):449–63. doi: 10.1016/j.cell.2016.02.022
96. Jardine JG, Sok D, Julien JP, Briney B, Sarkar A, Liang CH, et al. Minimally Mutated HIV-1 Broadly Neutralizing Antibodies to Guide Reductionist Vaccine Design. *PloS Pathog* (2016) 12(8):e1005815. doi: 10.1371/journal.ppat.1005815
97. Kumar S, Panda H, Makhdoomi MA, Mishra N, Safdari HA, Chawla H, et al. An HIV-1 Broadly Neutralizing Antibody From a Clade C-Infected Pediatric Elite Neutralizer Potently Neutralizes the Contemporaneous and Autologous Evolving Viruses. *J Virol* (2019) 93(4):e01495–18. doi: 10.1128/JVI.01495-18
98. Ng CT, Jaworski JP, Jayaraman P, Sutton WF, Delio P, Kuller L, et al. Passive Neutralizing Antibody Controls SHIV Viremia and Enhances B Cell Responses in Infant Macaques. *Nat Med* (2010) 16(10):1117–9. doi: 10.1038/nm.2233
99. Gao F, Bonsignori M, Liao HX, Kumar A, Xia SM, Lu X, et al. Cooperation of B Cell Lineages in Induction of HIV-1-Broadly Neutralizing Antibodies. *Cell* (2014) 158(3):481–91. doi: 10.1016/j.cell.2014.06.022
100. Anthony C, York T, Bekker V, Matten D, Selhorst P, Ferreria RC, et al. Cooperation Between Strain-Specific and Broadly Neutralizing Responses Limited Viral Escape and Prolonged the Exposure of the Broadly Neutralizing Epitope. *J Virol* (2017) 91(18):e00828–17. doi: 10.1128/JVI.00828-17
101. Martinez DR, Permar SR, Fouda GG. Contrasting Adult and Infant Immune Responses to HIV Infection and Vaccination. *Clin Vaccine Immunol* (2016) 23(2):84–94. doi: 10.1128/CVI.00565-15
102. Kondo HX, Kiribayashi R, Kuroda D, Kohda J, Kugimiya A, Nakano Y, et al. Effects of a Remote Mutation From the Contact Paratope on the Structure of CDR-H3 in the Anti-HIV Neutralizing Antibody PG16. *Sci Rep* (2019) 9(1):19840. doi: 10.1038/s41598-019-56154-y
103. Georgiev IS, Rudicell RS, Saunders KO, Shi W, Kirys T, McKee K, et al. Antibodies VRC01 and 10E8 Neutralize HIV-1 With High Breadth and Potency Even With Ig-Framework Regions Substantially Reverted to Germline. *J Immunol* (2014) 192(3):1100–6. doi: 10.4049/jimmunol.1302515
104. Xu JL, Davis MM. Diversity in the CDR3 Region of V(H) is Sufficient for Most Antibody Specificities. *Immunity* (2000) 13(1):37–45. doi: 10.1016/S1074-7613(00)00006-6
105. Wardemann H, Yurasov S, Schaefer A, Young JW, Meffre E, Nussenzweig MC. Predominant Autoantibody Production by Early Human B Cell Precursors. *Science* (2003) 301(5638):1374–7. doi: 10.1126/science.1086907
106. Larimore K, McCormick MW, Robins HS, Greenberg PD. Shaping of Human Germline IgH Repertoires Revealed by Deep Sequencing. *J Immunol* (2012) 189(6):3221–30. doi: 10.4049/jimmunol.1201303
107. DeKosky BJ, Lungu OI, Park D, Johnson EL, Charab W, Chrysostomou C, et al. Large-Scale Sequence and Structural Comparisons of Human Naive and Antigen-Experienced Antibody Repertoires. *Proc Natl Acad Sci USA* (2016) 113(19):E2636–45. doi: 10.1073/pnas.1525510113
108. Yu L, Guan Y. Immunologic Basis for Long HCDR3s in Broadly Neutralizing Antibodies Against HIV-1. *Front Immunol* (2014) 5:250. doi: 10.3389/fimmu.2014.00250
109. Tiller T, Tsuiji M, Yurasov S, Velinzon K, Nussenzweig MC, Wardemann H. Autoreactivity in Human IgG+ Memory B Cells. *Immunity* (2007) 26(2):205–13. doi: 10.1016/j.immuni.2007.01.009
110. Shi B, Ma L, He X, Wang X, Wang P, Zhou L, et al. Comparative Analysis of Human and Mouse Immunoglobulin Variable Heavy Regions From IMGT/LIGM-DB With IMGT/HighV-QUEST. *Theor Biol Med Model* (2014) 11:30. doi: 10.1186/1742-4682-11-30
111. Willis JR, Finn JA, Briney B, Sapparapu G, Singh V, King H, et al. Long Antibody HCDR3s From HIV-Naïve Donors Presented on a PG9 Neutralizing Antibody Background Mediate HIV Neutralization. *Proc Natl Acad Sci USA* (2016) 113(16):4446–51. doi: 10.1073/pnas.1518405113
112. Sok D, Pauthner M, Briney B, Lee JH, Saye-Francisco KL, Hsueh J, et al. A Prominent Site of Antibody Vulnerability on HIV Envelope Incorporates a Motif Associated With CCR5 Binding and Its Camouflaging Glycans. *Immunity* (2016) 45(1):31–45. doi: 10.1016/j.immuni.2016.06.026
113. Andrabi R, Voss JE, Liang CH, Briney B, McCoy LE, Wu CY, et al. Identification of Common Features in Prototype Broadly Neutralizing Antibodies to HIV Envelope V2 Apex to Facilitate Vaccine Design. *Immunity* (2015) 43(5):959–73. doi: 10.1016/j.immuni.2015.10.014
114. Zhou T, Zhu J, Wu X, Moquin S, Zhang B, Acharya P, et al. Multidonor Analysis Reveals Structural Elements, Genetic Determinants, and Maturation Pathway for HIV-1 Neutralization by VRC01-Class Antibodies. *Immunity* (2013) 39(2):245–58. doi: 10.1016/j.immuni.2013.04.012
115. Zhou T, Lynch RM, Chen L, Acharya P, Wu X, Doria-Rose NA, et al. Structural Repertoire of HIV-1-Neutralizing Antibodies Targeting the CD4 Supersite in 14 Donors. *Cell* (2015) 161(6):1280–92. doi: 10.1016/j.cell.2015.05.007

116. Haim H, Salas I, Sodroski J. Proteolytic Processing of the Human Immunodeficiency Virus Envelope Glycoprotein Precursor Decreases Conformational Flexibility. *J Virol* (2013) 87(3):1884–9. doi: 10.1128/JVI.02765-12
117. Moore PL, Crooks ET, Porter L, Zhu P, Cayanan CS, Grise H, et al. Nature of Nonfunctional Envelope Proteins on the Surface of Human Immunodeficiency Virus Type 1. *J Virol* (2006) 80(5):2515–28. doi: 10.1128/JVI.80.5.2515-2528.2006
118. Poignard P, Moulard M, Golez E, Vivona V, Franti M, Venturini S, et al. Heterogeneity of Envelope Molecules Expressed on Primary Human Immunodeficiency Virus Type 1 Particles as Probed by the Binding of Neutralizing and Nonneutralizing Antibodies. *J Virol* (2003) 77(1):353–65. doi: 10.1128/JVI.77.1.353-365.2003
119. Moore JP, Trkola A, Korber B, Boots LJ, Kessler JA2nd, McCutchan FE, et al. A Human Monoclonal Antibody to a Complex Epitope in the V3 Region of Gp120 of Human Immunodeficiency Virus Type 1 has Broad Reactivity Within and Outside Clade B. *J Virol* (1995) 69(1):122–30. doi: 10.1128/jvi.69.1.122-130.1995
120. de Taeye SW, Ozorowski G, Torrents de la Peña A, Guttman M, Julien JP, van den Kerkhof TL, et al. Immunogenicity of Stabilized HIV-1 Envelope Trimers With Reduced Exposure of Non-Neutralizing Epitopes. *Cell* (2015) 163(7):1702–15. doi: 10.1016/j.cell.2015.11.056
121. Spurrier B, Sampson J, Gorny MK, Zolla-Pazner S, Kong XP. Functional Implications of the Binding Mode of a Human Conformation-Dependent V2 Monoclonal Antibody Against HIV. *J Virol* (2014) 88(8):4100–12. doi: 10.1128/JVI.03153-13
122. Liao HX, Bonsignori M, Alam SM, McLellan JS, Tomaras GD, Moody MA, et al. Vaccine Induction of Antibodies Against a Structurally Heterogeneous Site of Immune Pressure Within HIV-1 Envelope Protein Variable Regions 1 and 2. *Immunity* (2013) 38(1):176–86. doi: 10.1016/j.immuni.2012.11.011
123. Medina-Ramírez M, Sanders RW, Sattentau QJ. Stabilized HIV-1 Envelope Glycoprotein Trimers for Vaccine Use. *Curr Opin HIV AIDS* (2017) 12 (3):241–9. doi: 10.1097/COH.0000000000000363
124. Kwong PD, Wyatt R, Robinson J, Sweet RW, Sodroski J, Hendrickson WA. Structure of an HIV Gp120 Envelope Glycoprotein in Complex With the CD4 Receptor and a Neutralizing Human Antibody. *Nature* (1998) 393 (6686):648–59. doi: 10.1038/31405
125. Lyumkis D, Julien J-P, de Val N, Cupo A, Potter CS, Klasse P-J, et al. Cryo-EM Structure of a Fully Glycosylated Soluble Cleaved HIV-1 Envelope Trimer. *Science* (2013) 342(6165):1484–90. doi: 10.1126/science.1245627
126. Tran K, Poulsen C, Guenaga J, de Val N, Wilson R, Sundling C, et al. Vaccine-Elicited Primate Antibodies Use a Distinct Approach to the HIV-1 Primary Receptor Binding Site Informing Vaccine Redesign. *Proc Natl Acad Sci USA* (2014) 111(7):E738–47. doi: 10.1073/pnas.1319512111
127. Chen L, Kwon YD, Zhou T, Wu X, O'Dell S, Cavacini L, et al. Structural Basis of Immune Evasion at the Site of CD4 Attachment on HIV-1 Gp120. *Science* (2009) 326(5956):1123–7. doi: 10.1126/science.1175868
128. Moody MA, Gao F, Gurley TC, Amos JD, Kumar A, Hora B, et al. Strain-Specific V3 and CD4 Binding Site Autologous HIV-1 Neutralizing Antibodies Select Neutralization-Resistant Viruses. *Cell Host Microbe* (2015) 18(3):354–62. doi: 10.1016/j.chom.2015.08.006
129. Wibmer CK, Gorman J, Anthony CS, Mkhize NN, Druz A, York T, et al. Structure of an N276-Dependent HIV-1 Neutralizing Antibody Targeting a Rare V5 Glycan Hole Adjacent to the CD4 Binding Site. *J Virol* (2016) 90 (22):10220–35. doi: 10.1128/JVI.01357-16
130. Balla-Jhagjhoorsingh SS, Corti D, Heyndrickx L, Willems E, Vereecken K, Davis D, et al. The N276 Glycosylation Site is Required for HIV-1 Neutralization by the CD4 Binding Site Specific HJ16 Monoclonal Antibody. *PloS One* (2013) 8(7):e68863. doi: 10.1371/journal.pone.0068863
131. Freund NT, Horwitz JA, Nogueira L, Sievers SA, Scharf L, Scheid JF, et al. A New Glycan-Dependent CD4-Binding Site Neutralizing Antibody Exerts Pressure on HIV-1 In Vivo. *PloS Pathog* (2015) 11(10):e1005238. doi: 10.1371/journal.ppat.1005238
132. Pancera M, Zhou T, Druz A, Georgiev IS, Soto C, Gorman J, et al. Structure and Immune Recognition of Trimeric Pre-Fusion HIV-1 Env. *Nature* (2014) 514(7523):455–61. doi: 10.1038/nature13808
133. Cheng HD, Grimm SK, Gilman MS, Gwom LC, Sok D, Sundling C, et al. Fine Epitope Signature of Antibody Neutralization Breadth at the HIV-1 Envelope CD4-Binding Site. *JCI Insight* (2018) 3(5):e97018. doi: 10.1172/jci.insight.97018
134. Huang J, Kang BH, Ishida E, Zhou T, Griesman T, Sheng Z, et al. Identification of a CD4-Binding-Site Antibody to HIV That Evolved Near-Pan Neutralization Breadth. *Immunity* (2016) 45(5):1108–21. doi: 10.1016/j.immuni.2016.10.027
135. Wu X, Yang ZY, Li Y, Hogerkorp CM, Schief WR, Seaman MS, et al. Rational Design of Envelope Identifies Broadly Neutralizing Human Monoclonal Antibodies to HIV-1. *Science* (2010) 329(5993):856–61. doi: 10.1126/science.1187659
136. Scheid JF, Mouquet H, Ueberheide B, Diskin R, Klein F, Oliveira TY, et al. Sequence and Structural Convergence of Broad and Potent HIV Antibodies That Mimic CD4 Binding. *Science* (2011) 333(6049):1633–7. doi: 10.1126/science.1207227
137. Huang CC, Tang M, Zhang MY, Majeed S, Montabana E, Stanfield RL, et al. Structure of a V3-Containing HIV-1 Gp120 Core. *Science* (2005) 310 (5750):1025–8. doi: 10.1126/science.1118398
138. Mbah HA, Burda S, Gorny MK, Williams C, Revesz K, Zolla-Pazner S, et al. Effect of Soluble CD4 on Exposure of Epitopes on Primary, Intact, Native Human Immunodeficiency Virus Type 1 Virions of Different Genetic Clades. *J Virol* (2001) 75(16):7785–8. doi: 10.1128/JVI.75.16.7785-7788.2001
139. Julien JP, Cupo A, Sok D, Stanfield RL, Lyumkis D, Deller MC, et al. Crystal Structure of a Soluble Cleaved HIV-1 Envelope Trimer. *Science* (2013) 342 (6165):1477–83. doi: 10.1126/science.1245625
140. Hioe CE, Wrin T, Seaman MS, Yu X, Wood B, Self S, et al. Anti-V3 Monoclonal Antibodies Display Broad Neutralizing Activities Against Multiple HIV-1 Subtypes. *PloS One* (2010) 5(4):e10254. doi: 10.1371/journal.pone.0010254
141. Nogal B, McCoy LE, van Gils MJ, Cottrell CA, Voss JE, Andrabi R, et al. HIV Envelope Trimer-Elicited Autologous Neutralizing Antibodies Bind a Region Overlapping the N332 Glycan Supersite. *Sci Adv* (2020) 6(23):eaba0512. doi: 10.1126/sciadv.aba0512
142. Krachmarov CP, Honnen WJ, Kayman SC, Gorny MK, Zolla-Pazner S, Pinter A. Factors Determining the Breadth and Potency of Neutralization by V3-Specific Human Monoclonal Antibodies Derived From Subjects Infected With Clade A or Clade B Strains of Human Immunodeficiency Virus Type 1. *J Virol* (2006) 80(14):7127–35. doi: 10.1128/JVI.02619-05
143. Behrens AJ, Vasiljevic S, Pritchard LK, Harvey DJ, Andev RS, Krumm SA, et al. Composition and Antigenic Effects of Individual Glycan Sites of a Trimeric HIV-1 Envelope Glycoprotein. *Cell Rep* (2016) 14(11):2695–706. doi: 10.1016/j.celrep.2016.02.058
144. Mouquet H, Scharf L, Euler Z, Liu Y, Eden C, Scheid JF, et al. Complex-Type N-Glycan Recognition by Potent Broadly Neutralizing HIV Antibodies. *Proc Natl Acad Sci USA* (2012) 109(47):E3268–77. doi: 10.1073/pnas.1217207109
145. Sanders RW, Venturi M, Schiffner L, Kalyanaraman R, Katinger H, Lloyd KO, et al. The Mannose-Dependent Epitope for Neutralizing Antibody 2G12 on Human Immunodeficiency Virus Type 1 Glycoprotein Gp120. *J Virol* (2002) 76(14):7293–305. doi: 10.1128/JVI.76.14.7293-7305.2002
146. Sok D, Doores KJ, Briney B, Le KM, Saye-Francisco KL, Ramos A, et al. Promiscuous Glycan Site Recognition by Antibodies to the High-Mannose Patch of Gp120 Broadens Neutralization of HIV. *Sci Transl Med* (2014) 6 (236):236ra63. doi: 10.1126/scitranslmed.3008104
147. Pejchal R, Doores KJ, Walker LM, Khayat R, Huang PS, Wang SK, et al. A Potent and Broad Neutralizing Antibody Recognizes and Penetrates the HIV Glycan Shield. *Science* (2011) 334(6059):1097–103. doi: 10.1126/science.1213256
148. Doores KJ, Kong L, Krumm SA, Le KM, Sok D, Laserson U, et al. Two Classes of Broadly Neutralizing Antibodies Within a Single Lineage Directed to the High-Mannose Patch of HIV Envelope. *J Virol* (2015) 89(2):1105–18. doi: 10.1128/JVI.02905-14
149. Kong L, Lee JH, Doores KJ, Murin CD, Julien JP, McBride R, et al. Supersite of Immune Vulnerability on the Glycosylated Face of HIV-1 Envelope Glycoprotein Gp120. *Nat Struct Mol Biol* (2013) 20(7):796–803. doi: 10.1038/nsmb.2594
150. Barnes CO, Gristick HB, Freund NT, Escolano A, Lyubimov AY, Hartweger H, et al. Structural Characterization of a Highly-Potent V3-Glycan Broadly

Neutralizing Antibody Bound to Natively-Glycosylated HIV-1 Envelope. *Nat Commun* (2018) 9(1):1251. doi: 10.1038/s41467-018-03632-y
151. Wang H, Barnes CO, Yang Z, Nussenzweig MC, Bjorkman PJ. Partially Open HIV-1 Envelope Structures Exhibit Conformational Changes Relevant for Coreceptor Binding and Fusion. *Cell Host Microbe* (2018) 24(4):579–92.e4. doi: 10.1016/j.chom.2018.09.003
152. Ozorowski G, Pallesen J, de Val N, Lyumkis D, Cottrell CA, Torres JL, et al. Open and Closed Structures Reveal Allostery and Pliability in the HIV-1 Envelope Spike. *Nature* (2017) 547(7663):360–3. doi: 10.1038/nature23010
153. Pan R, Gorny MK, Zolla-Pazner S, Kong XP. The V1V2 Region of HIV-1 Gp120 Forms a Five-Stranded Beta Barrel. *J Virol* (2015) 89(15):8003–10. doi: 10.1128/JVI.00754-15
154. Wibmer CK, Richardson SI, Yolitz J, Cicala C, Arthos J, Moore PL, et al. Common Helical V1V2 Conformations of HIV-1 Envelope Expose the α4β7 Binding Site on Intact Virions. *Nat Commun* (2018) 9(1):4489. doi: 10.1038/s41467-018-06794-x
155. van Eeden C, Wibmer CK, Scheepers C, Richardson SI, Nonyane M, Lambson B, et al. V2-Directed Vaccine-Like Antibodies From HIV-1 Infection Identify an Additional K169-Binding Light Chain Motif With Broad ADCC Activity. *Cell Rep* (2018) 25(11):3123–35.e6. doi: 10.1016/j.celrep.2018.11.058
156. Pinter A, Honnen WJ, D'Agostino P, Gorny MK, Zolla-Pazner S, Kayman SC. The C108g Epitope in the V2 Domain of Gp120 Functions as a Potent Neutralization Target When Introduced Into Envelope Proteins Derived From Human Immunodeficiency Virus Type 1 Primary Isolates. *J Virol* (2005) 79(11):6909–17. doi: 10.1128/JVI.79.11.6909-6917.2005
157. McLellan JS, Pancera M, Carrico C, Gorman J, Julien J-P, Khayat R, et al. Structure of HIV-1 Gp120 V1/V2 Domain With Broadly Neutralizing Antibody PG9. *Nature* (2011) 480(7377):336–43. doi: 10.1038/nature10696
158. Ivan B, Sun Z, Subbaraman H, Friedrich N, Trkola A. CD4 Occupancy Triggers Sequential Pre-Fusion Conformational States of the HIV-1 Envelope Trimer With Relevance for Broadly Neutralizing Antibody Activity. *PloS Biol* (2019) 17(1):e3000114. doi: 10.1371/journal.pbio.3000114
159. Changela A, Wu X, Yang Y, Zhang B, Zhu J, Nardone GA, et al. Crystal Structure of Human Antibody 2909 Reveals Conserved Features of Quaternary Structure-Specific Antibodies That Potently Neutralize HIV-1. *J Virol* (2011) 85(6):2524–35. doi: 10.1128/JVI.02335-10
160. Tian J, López CA, Derdeyn CA, Jones MS, Pinter A, Korber B, et al. Effect of Glycosylation on an Immunodominant Region in the V1V2 Variable Domain of the HIV-1 Envelope Gp120 Protein. *PloS Comput Biol* (2016) 12(10):e1005094. doi: 10.1371/journal.pcbi.1005094
161. Pancera M, Shahzad-Ul-Hussan S, Doria-Rose NA, McLellan JS, Bailer RT, Dai K, et al. Structural Basis for Diverse N-Glycan Recognition by HIV-1-Neutralizing V1-V2-Directed Antibody PG16. *Nat Struct Mol Biol* (2013) 20(7):804–13. doi: 10.1038/nsmb.2600
162. Sok D, van Gils MJ, Pauthner M, Julien JP, Saye-Francisco KL, Hsueh J, et al. Recombinant HIV Envelope Trimer Selects for Quaternary-Dependent Antibodies Targeting the Trimer Apex. *Proc Natl Acad Sci USA* (2014) 111(49):17624–9. doi: 10.1073/pnas.1415789111
163. Cale EM, Gorman J, Radakovich NA, Crooks ET, Osawa K, Tong T, et al. Virus-Like Particles Identify an HIV V1V2 Apex-Binding Neutralizing Antibody That Lacks a Protruding Loop. *Immunity* (2017) 46(5):777–91.e10. doi: 10.1016/j.immuni.2017.04.011
164. Doria-Rose NA, Bhiman JN, Roark RS, Schramm CA, Gorman J, Chuang GY, et al. New Member of the V1V2-Directed CAP256-VRC26 Lineage That Shows Increased Breadth and Exceptional Potency. *J Virol* (2016) 90(1):76–91. doi: 10.1128/JVI.01791-15
165. Landais E, Murrell B, Briney B, Murrell S, Rantalainen K, Berndsen ZT, et al. HIV Envelope Glycoform Heterogeneity and Localized Diversity Govern the Initiation and Maturation of a V2 Apex Broadly Neutralizing Antibody Lineage. *Immunity* (2017) 47(5):990–1003.e9. doi: 10.1016/j.immuni.2017.11.002
166. Gorman J, Chuang GY, Lai YT, Shen CH, Boyington JC, Druz A, et al. Structure of Super-Potent Antibody CAP256-VRC26.25 in Complex With HIV-1 Envelope Reveals a Combined Mode of Trimer-Apex Recognition. *Cell Rep* (2020) 31(1):107488. doi: 10.1016/j.celrep.2020.03.052
167. Gorny MK, Pan R, Williams C, Wang XH, Volsky B, O'Neal T, et al. Functional and Immunochemical Cross-Reactivity of V2-Specific Monoclonal Antibodies From HIV-1-Infected Individuals. *Virology* (2012) 427(2):198–207. doi: 10.1016/j.virol.2012.02.003
168. Zhu J, Wu X, Zhang B, McKee K, O'Dell S, Soto C, et al. *De Novo* Identification of VRC01 Class HIV-1-Neutralizing Antibodies by Next-Generation Sequencing of B-Cell Transcripts. *Proc Natl Acad Sci USA* (2013) 110(43):E4088–97. doi: 10.1073/pnas.1306262110
169. Bianchi M, Turner HL, Nogal B, Cottrell CA, Oyen D, Pauthner M, et al. Electron-Microscopy-Based Epitope Mapping Defines Specificities of Polyclonal Antibodies Elicited During HIV-1 BG505 Envelope Trimer Immunization. *Immunity* (2018) 49(2):288–300.e8. doi: 10.1016/j.immuni.2018.07.009

**Conflict of Interest:** The authors declare that the research was conducted in the absence of any commercial or financial relationships that could be construed as a potential conflict of interest.

**Publisher's Note:** All claims expressed in this article are solely those of the authors and do not necessarily represent those of their affiliated organizations, or those of the publisher, the editors and the reviewers. Any product that may be evaluated in this article, or claim that may be made by its manufacturer, is not guaranteed or endorsed by the publisher.

frontiers in Immunology

ORIGINAL RESEARCH
published: 11 November 2021
doi: 10.3389/fimmu.2021.749891

# Anti-Drug Antibodies in Pigtailed Macaques Receiving HIV Broadly Neutralising Antibody PGT121

*Wen Shi Lee*[1], *Arnold Reynaldi*[2], *Thakshila Amarasena*[1], *Miles P. Davenport*[2], *Matthew S. Parsons*[1,3,4] *and Stephen J. Kent*[1,5*]

[1] Department of Microbiology and Immunology, The Peter Doherty Institute for Infection and Immunity, University of Melbourne, Melbourne, VIC, Australia, [2] Kirby Institute, University of New South Wales, Kensington, NSW, Australia, [3] Department of Pathology and Laboratory Medicine, School of Medicine, Emory University, Atlanta, GA, United States, [4] Yerkes National Primate Research Center, Emory University, Atlanta, GA, United States, [5] Melbourne Sexual Health Centre and Department of Infectious Diseases, Central Clinical School, Monash University, Melbourne, VIC, Australia

Broadly neutralising antibodies (bNAbs) may play an important role in future strategies for HIV control. The development of anti-drug antibody (ADA) responses can reduce the efficacy of passively transferred bNAbs but the impact of ADA is imperfectly understood. We previously showed that therapeutic administration of the anti-HIV bNAb PGT121 (either WT or LALA version) controlled viraemia in pigtailed macaques with ongoing SHIV infection. We now report on 23 macaques that had multiple treatments with PGT121. We found that an increasing number of intravenous doses of PGT121 or human IgG1 isotype control antibodies (2-4 doses) results in anti-PGT121 ADA induction and low plasma concentrations of PGT121. ADA was associated with poor or absent suppression of SHIV viremia. Notably, ADA within macaque plasma recognised another human bNAb 10E8 but did not bind to the variable domains of PGT121, suggesting that ADA were primarily directed against the constant regions of the human antibodies. These findings have implications for the development of preclinical studies examining multiple infusions of human bNAbs.

**Keywords: HIV, broadly neutralizing antibodies (bNAb), PGT121, anti-drug antibodies (ADA), pigtailed macaque**

OPEN ACCESS

***Edited by:***
*Kshitij Wagh,*
*Los Alamos National Laboratory (DOE), United States*

***Reviewed by:***
*Frederic Bibollet-Ruche, University of Pennsylvania, United States*
*Kelly Seaton, Duke University, United States*

***Correspondence:**
*Stephen J. Kent*
*skent@unimelb.edu.au*

***Specialty section:***
*This article was submitted to Vaccines and Molecular Therapeutics, a section of the journal Frontiers in Immunology*

***Received:*** *30 July 2021*
***Accepted:*** *26 October 2021*
***Published:*** *11 November 2021*

***Citation:***
*Lee WS, Reynaldi A, Amarasena T, Davenport MP, Parsons MS and Kent SJ (2021) Anti-Drug Antibodies in Pigtailed Macaques Receiving HIV Broadly Neutralising Antibody PGT121. Front. Immunol. 12:749891. doi: 10.3389/fimmu.2021.749891*

## INTRODUCTION

Monoclonal antibodies to prevent or treat HIV infection are of increasing interest. Passive infusion of bNAbs effectively controls viremia in HIV-infected subjects and SHIV-infected macaques when the strain is sensitive to the bNAb (1–4). Control of HIV with bNAbs will require multiple treatments since the half-life of standard IgG antibodies is commonly 2-3 weeks and the half-life of IgG antibodies with mutations that extend half-lives is commonly 8-12 weeks (5). Repeated treatment of humans with monoclonal antibodies can lead to anti-drug (anti-antibody) antibodies (commonly termed ADA) (6, 7). Anti-HIV bNAbs are commonly heavily mutated away from the germline in the Fab region of the antibody (8), which could result in immunogenic epitopes. A disadvantage of macaque/SHIV studies of bNAbs is the foreign nature of the entire human bNAb (both the Fab and the Fc). Previous work has illustrated that ADA is common when

human bNAbs are delivered to rhesus macaques since the entire antibody is foreign and ADA to both the Fab and Fc can occur (9–12).

Although ADA is an important issue in macaque studies of human bNAbs, several knowledge gaps remain. The number of human mAb treatments needed to induce ADA is not well studied. ADA is presumably effectively primed with a limited number of bNAb administrations, then when boosted to high levels by another administration, results in rapid clearance of the bNAb and consequent reduced antiviral efficacy. However, these precise relationships have not been widely studied.

PGT121 is a potent bNAb that binds to V3 glycans of HIV-1 Env and is effective against a majority of HIV-1 strains. PGT121 has been of great interest in cure-related HIV trials, particularly in combination with a TLR7 agonist where partial control of SHIV in the absence of ART was observed (13). HIV cure studies are likely to need multiple bNAb administrations and robust evaluation in macaque pre-clinical models to delineate a precise role. However, PGT121 has been reported to induce ADA in rhesus macaques (*Macaca mulatta*) by both subcutaneous administration and through delivery *via* an adeno-associated vector (10, 14). Although SIV- or SHIV-infected pigtailed macaques (*Macaca nemestrina*) are an important and useful model of HIV-1, ADA to bNAbs in pigtailed macaques has not previously been studied. We analyzed ADA to the bNAb PGT121 in 23 SHIV-infected pigtailed macaques, assessing the frequency and specificity of ADA generated to PGT121 and the relationship of ADA to loss of potency in controlling viremia. This work will help inform future studies of bNAbs in pigtailed macaques.

# MATERIALS AND METHODS

## Non-Human Primates

Juvenile pigtailed macaques were sourced from the Monash University Animal Research Platform, the Australian National macaque breeding facility. The Monash University and Australian Commonwealth Scientific and Industrial Research Organization Animal Health Animal Ethics Committees approved all macaque studies. The macaques described here were from three separate studies to assess (i) the efficacy of PGT121 in preventing cell-free or cell-associated $SHIV_{SF162P3}$ infection (3), (ii) the efficacy of WT or LALA PGT121 in preventing cell-associated $SHIV_{SF162P3}$ infection and treating ongoing $SHIV_{SF162P3}$ infection (15) and (iii) the efficacy of PGT121 (16) or eCD4-Ig (unpublished) in preventing intrarectal $SHIV_{SF162P3}$ infection in the presence of seminal plasma. The number and type of human antibody exposures for all macaques in this study are listed in **Supplementary Table 1**.

PGT121 WT, PGT121 LALA, eCD4-Ig and the human IgG1 isotype control antibody were all administered intravenously at 1mg/kg one hour prior to challenge with $SHIV_{SF162P3}$. Both PGT121 WT and LALA were purchased from the Center for Antibody Development and Production (Scripps Research Institute) while the human IgG1 isotype control antibody (clone 52H5/TT1204) was provided by Keith Reimann (NIH Nonhuman Primate Reagent Resource). eCD4-Ig was kindly provided by Stuart Turville (Kirby Institute, University of New South Wales) and Michael Farzan (Scripps Research Institute). A pool of human seminal plasma was generated using samples obtained from the Opposites Attract cohort study (17).

## Viral Load Quantification

Viral RNA in the plasma of $SHIV_{SF162P3}$-infected macaques was measured by digital droplet PCR (ddPCR) as described previously (15). The decay rates of plasma viral loads were estimated using an ordinary linear regression method on the log-transformed values of the measurements using GraphPad Prism software.

## ELISA to Measure ADA in Macaque Plasma

ELISAs were performed to measure the level of anti-drug antibodies against full-length PGT121, PGT121 scFv (Creative Biolabs) and 10E8 (NIH AIDS Reagent Program) in macaque plasma. 96-well Maxisorp plates (Thermo Fisher) were coated overnight at 4°C with 1μg/ml of PGT121, PGT121 scFv or 10E8 in PBS. After blocking with PBS containing 4% bovine serum albumin (BSA) and 0.1% Tween-20, duplicate wells of macaque plasma (1:100 dilution in PBS with 0.2% Tween-20, 0.1% BSA and 0.5% NP-40) were added and incubated for 1.5 hrs at 37°C. Next, plates were incubated with a HRP-conjugated secondary antibody specific for macaque IgG (clone 1B3, Kerafast; 1:16,000 dilution) for 1 hr at 37°C. Plates were then developed with TMB substrate (Sigma), stopped with 0.16M sulphuric acid and read at 450nm using the FLUOstar Omega microplate reader. The absorbance values ($OD_{450}$) of macaque plasma samples were background subtracted with wells containing only PBS and normalised to a positive plasma control for ADA (sample from macaque NM08) by dividing the OD values of test samples with the OD values of the positive control. To validate the ELISA, we measured plasma endpoint titres for ADA and found that ADA measured at a 1:100 plasma dilution (normalised $OD_{450}$) correlated strongly with ADA measured by endpoint titre ($r = 0.91$, $p = 0.0001$; spearman correlation).

## ELISA to Measure Plasma Concentration of PGT121

96-well Maxisorp plates (Thermo Fisher) were coated overnight at 4°C with 1μg/ml of $HIV_{BaL}$ gp120 (NIH AIDS Reagent Program). After blocking with PBS containing 4% BSA and 0.1% Tween-20, macaque plasma (1:50 and 1:250 dilutions in PBS with 0.2% Tween-20, 0.1% BSA and 0.5% NP-40) was added and incubated for 1.5 hrs at 37°C. Next, plates were incubated with a HRP-conjugated anti-human IgG secondary antibody that does not cross-react with macaque IgG (#2049-05, Southern Biotech; 1:8,000 dilution) for 1 hr at 37°C. Plates were then developed with TMB substrate (Sigma), stopped with 0.16M sulphuric acid and read at 450nm using the FLUOstar Omega microplate reader. Serial dilutions of PGT121 were included on each plate to construct a standard curve, from which the concentration of PGT121 within macaque plasma was

calculated using non-linear regression analysis (using the "Hyperbola (X is concentration)" option in GraphPad Prism).

### Statistics

Statistical analyses were performed with Graphpad Prism 8. The correlation of ADA and viral load decay rate was assessed using the non-parametric Spearman test.

## RESULTS

### Induction of Anti-PGT121 Antibodies in Macaques Following Exposure to Human Antibodies

As part of two previous studies (3, 15), a subset of pigtailed macaques were administered either 1mg/kg of PGT121 (with WT Fc) or a human IgG1 isotype control intravenously prior to challenge with cell-free or cell-associated simian HIV (SHIV). Animals receiving PGT121 were protected from viral challenge while animals receiving isotype control developed high levels of viraemia (**Figure 1** and **Supplementary Figure 1**). For a separate study, two animals (NM04 and NM05) were rectally challenged with SHIV following exposure to human seminal plasma and subsequently developed high levels of viraemia (16). The viraemic animals were then used to examine the therapeutic efficacy of PGT121 with either WT Fc or a LALA mutation to abrogate Fcγ receptor engagement (15). While the first therapeutic infusion of PGT121 WT and LALA successfully suppressed viraemia in three of five macaques, two animals (NM01 and NM04) did not exhibit a corresponding decline in plasma viral loads. Viral loads for NM02 and NM03 were suppressed following the first infusion of PGT121 but not after the second infusion. The lack of therapeutic efficacy for PGT121 WT and LALA in certain cases led us to examine whether these five macaques developed anti-PGT121 anti-drug IgG antibodies (ADA) following multiple exposures to antibodies of human origin. As shown in **Figure 1**, all four macaques that failed PGT121 therapy (NM01, NM02, NM03 and NM04) had high levels of PGT121-specific ADA at the time of failed PGT121 therapy (indicated by red text). Most animals developed PGT121 ADA only after 2-3 exposures to either PGT121 or the human IgG1 isotype control antibody. NM03 developed low levels of ADA 3 weeks after the first infusion of PGT121, which waned over time and were boosted to high levels two weeks after the third exposure to a human antibody. Interestingly, while macaque NM04 did not have any ADA following two intravenous infusions of PGT121, ADA were likely primed by the two infusions of human mAbs and the animal developed ADA 4 weeks following two subsequent intrarectal administrations of human seminal plasma (which contains IgG antibodies). PGT121 ADA began to wane in NM01 5 weeks after the last PGT121 exposure but remained high in all other animals.

### Lack of PGT121 Therapeutic Efficacy Due to PGT121-Specific ADA

To examine the impact of ADA on the therapeutic efficacy of PGT121 more clearly, we measured the plasma concentration of PGT121 in three macaques that failed PGT121 therapy following the second infusion (**Figure 2**). After the first intravenous infusion, plasma PGT121 levels reached 11.2μg/ml, 3μg/ml and 6μg/ml in NM02, NM03 and NM08 respectively, resulting in a sharp decline in viral loads that eventually rebounded after plasma PGT121 dropped to undetectable levels. In all three animals, PGT121 ADA rose to high levels 2-4 weeks following first infusion of PGT121. ADA remained high at the time of second infusion, resulting in low plasma concentrations of PGT121 and no corresponding decline in plasma viraemia (**Supplementary Figure 2**). These results confirm that the lack of PGT121 therapeutic efficacy was caused by the low levels of bioavailable PGT121 in plasma, likely due to blocking or rapid clearance by PGT121-specific ADA.

An important measure of the potency of bNAbs and other HIV therapeutics is the rate at which virus decays in the days after administration. With the large number of animals studied, we were able to analyse whether ADA was associated with slower viral decay. We found that the level of PGT121 ADA at the time of infusion negatively correlated with the decay rate of viral loads within 72 hours of PGT121 infusion ($r = -0.41$, $p<0.05$; **Figure 3**). A stronger negative correlation between ADA and viral load decay rate is observed if animals without ADA at the time of infusion are excluded ($r = -0.62$, $p<0.05$).

### PGT121-Specific ADA Increase With the Number of Exposures to Human Antibodies

To examine the number of exposures to human antibodies required for the induction of ADA within pigtailed macaques, we measured anti-PGT121 ADA in macaques pre- and 3-4 weeks post-exposure to all sources of human antibodies (**Figure 4A**). Some macaques received two administrations of human seminal plasma (either intrarectally or both intrarectally and intravaginally) two weeks apart (**Supplementary Table 1**), in which case anti-PGT121 ADA was only measured pre- and post-second administration. 23 macaques had been exposed to human antibodies at least twice, with 2 macaques developing very low levels of ADA after first exposure and 4 of 23 macaques developing ADA after second exposure. Following the third exposure, out of 10 macaques that had not seroconverted, a further 7 macaques developed ADA. Interestingly, 7 macaques did not develop ADA following four exposures to human antibodies, while all macaques that had five exposures developed high levels of ADA after the fifth exposure.

We then examined whether the different sources of human antibodies resulted in differential induction of ADA (**Figure 4B**). Intravenous infusions of PGT121 (WT and LALA) and the human IgG1 isotype control antibody all elicited high levels of ADA against PGT121 following 2-5 exposures. Only one animal developed low levels of ADA following intrarectal exposure to human seminal plasma (which contains IgG antibodies) on its fourth exposure to human antibodies. These results show that the elicitation of ADA depends more on the number of exposures to human antibodies rather than the type of antibody exposure.

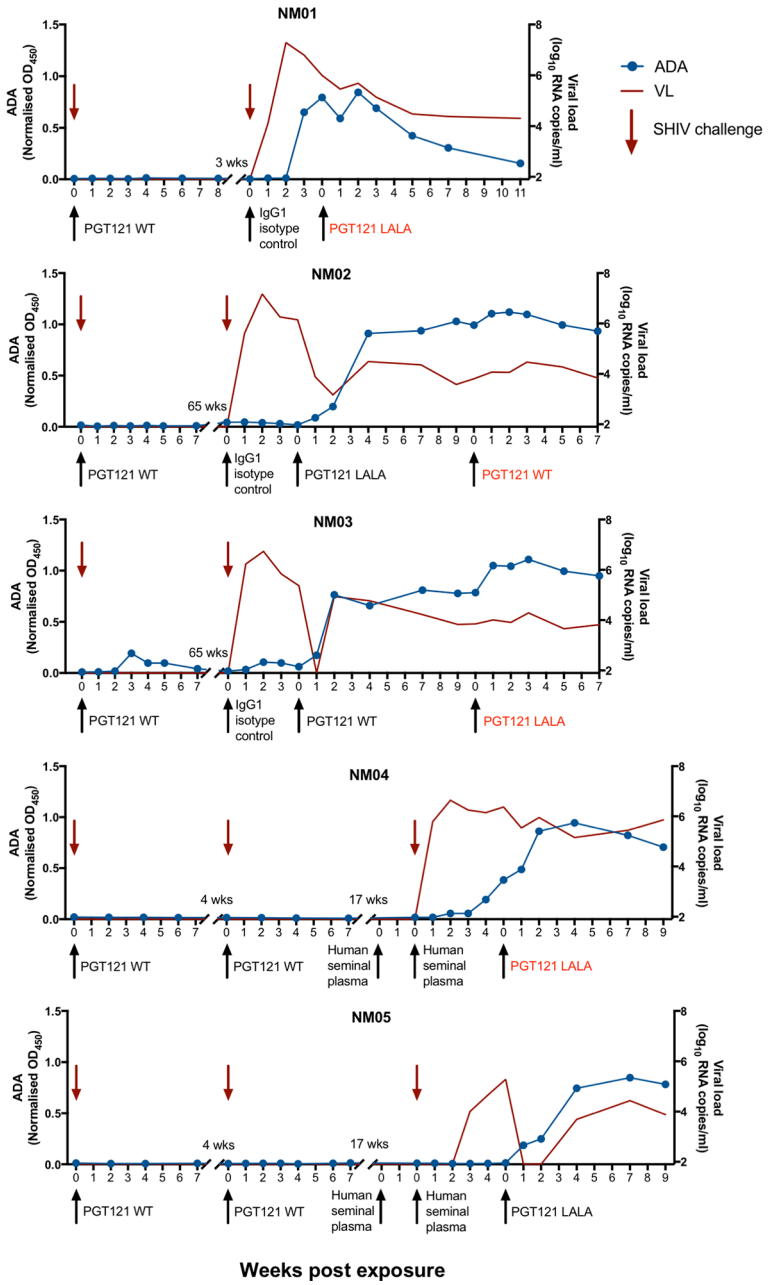


**FIGURE 1** | Anti-PGT121 antibodies develop in pigtailed macaques following exposure to human antibodies. Five pigtailed macaques were administered PGT121 or a human IgG1 isotype control antibody intravenously (1mg/kg) prior to challenge with cell-free or cell-associated SHIV. Macaques NM04 and NM05 were administered human seminal plasma either intrarectally or both intravaginally and intrarectally prior to intrarectal challenge with SHIV. Viraemic animals were then infused with PGT121 with either WT or LALA Fc. Macaque anti-PGT121 ADA are shown in the blue line (left y-axis) while SHIV viral loads are shown in the red line (right y-axis). Black arrows indicate antibody administration while red arrows indicate SHIV challenge. The red text indicates failed therapy with PGT121 WT or LALA.

## ADA Are Specific for the Constant but Not Variable Domains of PGT121

To interrogate the specificity of ADA within macaque plasma, we next measured the level of antibodies against PGT121 and the gp41-specific bNAb 10E8, which also uses a λ light chain. NM02 and NM03 both had antibodies against PGT121 and 10E8 (**Figure 5A**), implying that the ADA developed from exposure to PGT121 and the isotype control antibody were recognising the constant regions of IgG1 as they were not exclusively specific for PGT121. To confirm these results, we then examined whether

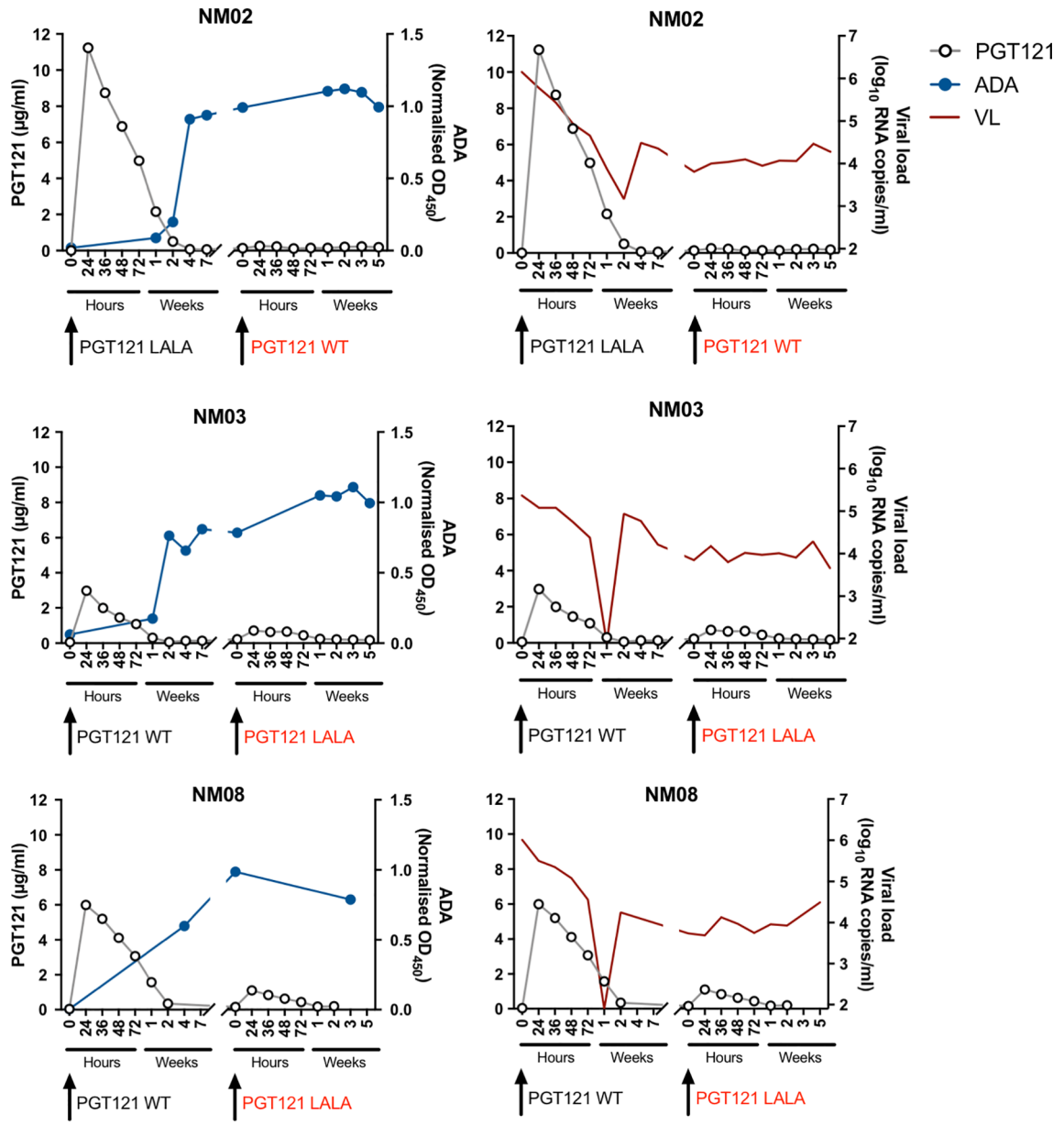


**FIGURE 2** | Anti-PGT121 antibodies limit the plasma concentration of PGT121 and diminish the therapeutic efficacy of PGT121 against SHIV. The plasma concentration of PGT121 WT or LALA post-infusion (open circles, left y-axis) is plotted with the level of anti-PGT121 ADA (blue line, right y-axis) or SHIV viral loads (red line, right y-axis). Black arrows indicate antibody administration. The red text indicates failed therapy with PGT121 WT or LALA.

macaque ADA could recognise the single chain variable fragment (scFv) of PGT121, which contains only the variable domains of both heavy and light chains ($V_H$ and $V_L$) without the constant domains ($C_H1$, $C_H2$, $C_H3$ and $C_L$). The three macaques tested (NM01, NM02 and NM03) did not have any antibodies recognising the scFv of PGT121 (**Figure 5B**), but had high levels of antibodies recognising full-length PGT121, confirming that the ADA were indeed recognising the constant but not variable domains of PGT121.

## DISCUSSION

The macaque SHIV challenge model of HIV exposure and infection has long been used to examine the protective and therapeutic efficacy of HIV-1 bNAbs isolated from people living with HIV (3, 12, 15, 18–20). bNAbs will generally need to be administered multiple times or delivered continuously *via* viral vectors to maintain efficacy but this poses risks of developing ADA. We describe herein that intravenous administration of human

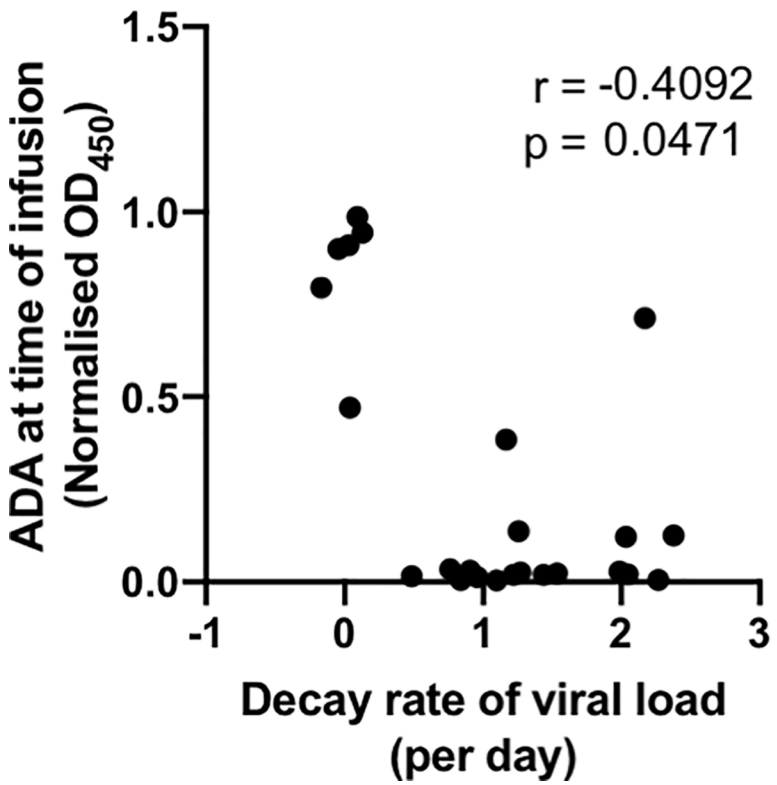


**FIGURE 3** | ADA at time of infusion negatively correlates with viral suppression by PGT121. Macaques with active SHIV infection were administered PGT121 WT or LALA. Plasma viral loads were measured by digital droplet PCR at 0, 24, 36, 48 and 72 hours after PGT121 infusion and the decay rate within 72 hours was calculated using linear regression. The correlation was performed using a non-parametric spearman test.

antibodies (1mg/kg) to macaques can lead to the development of anti-PGT121 ADA responses, rising after 2-4 exposures with human antibodies. Interestingly, in an animal that had received two prior infusions of PGT121, anti-PGT121 ADA were detected following two subsequent intrarectal exposures to human seminal plasma (which contains IgG antibodies), showing that mucosal exposure to human antibodies can also lead to the development of ADA. The high levels of anti-PGT121 ADA in these animals resulted in low plasma concentrations of PGT121 following intravenous infusion, impacting the therapeutic efficacy of PGT121 in suppressing SHIV viraemia. The ADA responses did not recognise the variable domains of PGT121 and were therefore not anti-idiotypic, but were directed against the constant domains of PGT121, cross-reacting with a different bNAb, 10E8. While some macaques remained ADA-naïve even after 4 exposures to human antibodies, we recommend that future studies limit the number of infusions of human antibodies to reduce the likelihood of ADA impairing the efficacy of infused antibodies.

The ADA we measured were directed against the constant domains of PGT121 instead of the variable domains. This presumably reflects dominant epitopes in the human IgG1 Fc recognized by the pigtailed macaques, but may also have been exacerbated in our studies as the macaques were exposed to multiple sources of human antibodies (PGT121, human IgG1 isotype control and/or human seminal plasma). The repeated exposures to human IgG1 could have focussed the ADA response to the conserved constant regions instead of the variable domains. A previous study detected PGT121 anti-idiotypic responses in rhesus macaques following two homologous subcutaneous infusions at a higher dose (5mg/kg) (9, 10). A potential way to overcome the elicitation of anti-human ADA in macaques is to "simianise" the bNAbs by grafting the complementarity-determining regions (CDR) of bNAbs onto homologous macaque germline genes with macaque IgG constant regions. While this approach does remove a large portion of immunogenic human antibody epitopes, repeated passive transfer of simianised VRC01 and AAV-delivery of simianised VRC07 still resulted in the development of anti-idiotypic antibodies in macaques (21, 22), reducing the utility of the macaque model in testing repeated or sustained deliveries of HIV bNAbs.

Dosing interval may affect the induction of bNAb-specific ADA, similar to that observed for some human mAbs in use such as TNF inhibitors where longer spaced episodic treatment results in higher induction of ADA compared to regular shorter intervals (23). For our PGT121 studies, we dosed our pigtailed macaques at widely spaced intervals (average 13 weeks, range 2-124) to allow for sufficient drug washout and for SHIV to recrudesce between antibody doses. This wide interval almost

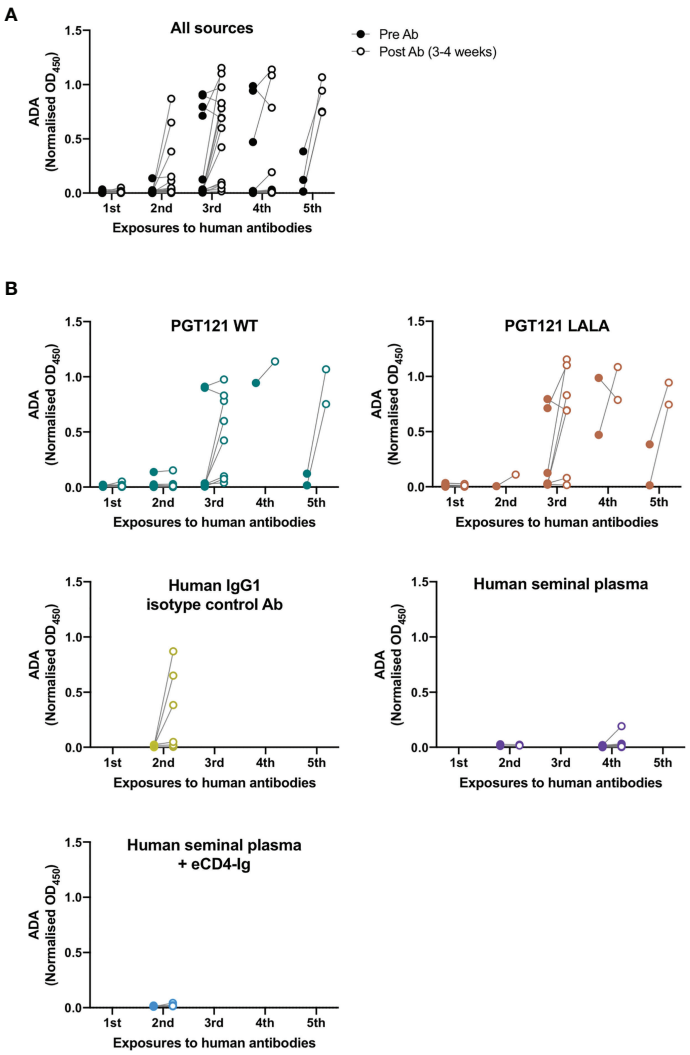


**FIGURE 4** | Anti-PGT121 ADA increases with the number of exposures to human antibodies. **(A)** The level of anti-PGT121 ADA in macaques before (closed circles) and 3-4 weeks after (open circles) exposure to human antibodies. **(B)** The level of anti-PGT121 ADA before and after exposure to different sources of human antibodies (intravenous administration of PGT121 WT, PGT121 LALA, eCD4-Ig and human IgG1 isotype control antibody or intrarectal/intravaginal administration of human seminal plasma).

uniformly generated ADA after 2-4 doses and thus it was not possible for us to dissect the relative roles of dosing interval or number of doses. One study in rhesus macaques dosed PGT121 at 2 weekly intervals, maintaining control of SHIV, and did not report ADA (13). Future studies of ADA to HIV bNAbs could consider designs to directly assess the role of interval in induction of ADA. Refinement of dosing intervals could be important to limit the generation of ADA responses.

While the elicitation of ADA in non-human primates due to species differences does not translate to humans, bNAbs are typically highly somatically mutated from germline sequences and could potentially be immunogenic. A phase 1 trial of VRC01 administration in humans did not detect anti-VRC01 ADA even after 6 intravenous infusions at 20mg/kg (24). Another phase 1 trial of 3BNC117 and 10-1074 infusion detected ADA in 4 of 18 participants, with one participant having treatment-induced ADA to 3BNC117, one having treatment-induced ADA to 10-1074 and two having anti-3BNC117 ADA at baseline (25). During the study, ADA were not at high enough concentrations to inhibit 3BNC117 or 10-1074 neutralisation of HIV although the ADA, if boosted by further doses of the bNAb, could ultimately limit the effectiveness of the bNAb. Thus, passive infusions of certain bNAbs can result in the generation of ADA responses in humans and should be monitored carefully in future clinical trials.

There is growing interest in utilising bNAbs to prevent or treat HIV infection. Macaque challenge models with SHIV have been a crucial model to test the efficacy of bNAbs preclinically, though the elicitation of ADA responses hampers the ability to

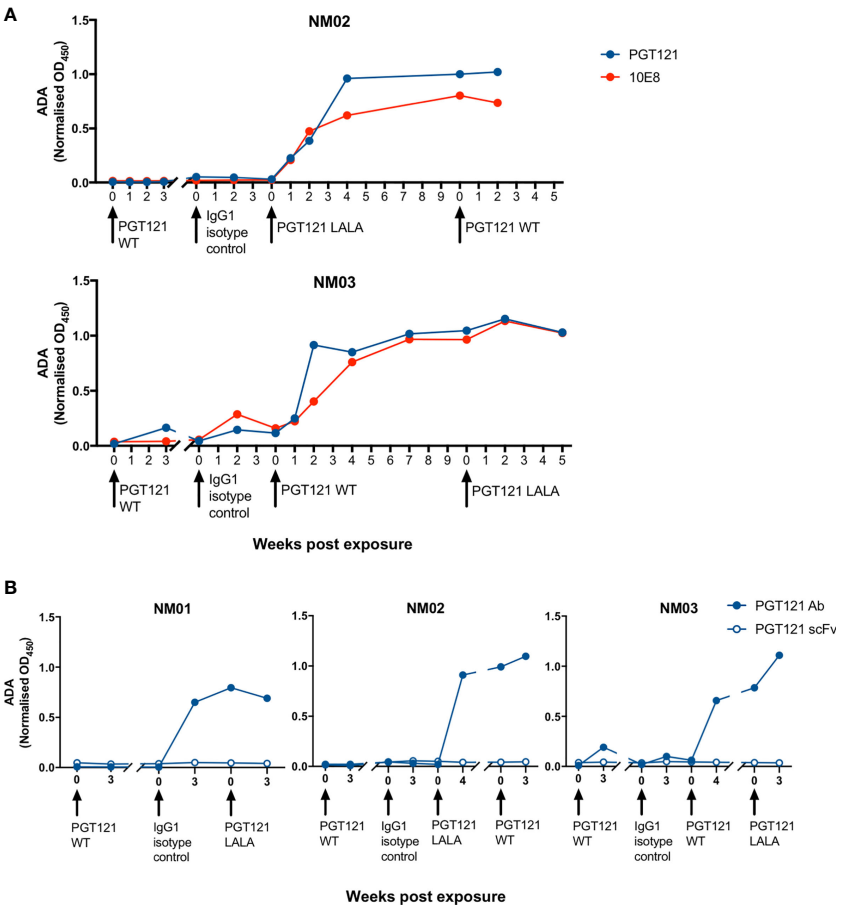


**FIGURE 5** | The specificity of ADA responses in pigtailed macaques following multiple infusions of human antibodies. **(A)** Macaque anti-PGT121 and anti-10E8 ADA are shown in blue and red respectively. **(B)** The level of macaque ADA against full length PGT121 (closed circles) and PGT121 scFv (open circles). Black arrows indicate antibody administration.

examine repeated or sustained deliveries of human antibodies. Our findings suggest that future preclinical studies of human antibodies in pigtailed macaques, similar to rhesus macaques, should limit the number of infusions to avoid generating ADA that can diminish the efficacy of the mAbs of interest.

## DATA AVAILABILITY STATEMENT

The raw data supporting the conclusions of this article will be made available by the authors, without undue reservation.

## ETHICS STATEMENT

The animal study was reviewed and approved by the Monash University and Australian Commonwealth Scientific and Industrial Research Organisation Animal Health Animal Ethics Committees.

## AUTHOR CONTRIBUTIONS

Conceived and designed experiments: WL, MP, and SK. Performed experiments: WL and TA. Analysed the data: WL, AR, TA, and MP. Wrote the paper: WL and SK. Revised the paper: AR, TA, MP, and MD. All authors contributed to the article and approved the submitted version.

## FUNDING

This work was supported by a National Health and Medical Research Council Program Grant to SK. This work was also supported by the National Institutes of Health's Office of the Director, Office of Research Infrastructure Programs (P51OD011132). The funders had no role in study design, data collection and analysis, decision to publish, or preparation of the manuscript.

## SUPPLEMENTARY MATERIAL

The Supplementary Material for this article can be found online at: https://www.frontiersin.org/articles/10.3389/fimmu.2021.749891/full#supplementary-material

**Supplementary Figure 1 |** The development of anti-PGT121 ADA following multiple exposures to human antibodies in individual macaques. Macaque anti-PGT121 ADA are shown in the blue line (left y-axis) while SHIV viral loads are shown in the red line (right y-axis). Black arrows indicate antibody administration while red arrows indicate SHIV challenge. The numbers in red indicate the viral load decay rate (per day) within 72 hours of therapeutic PGT121 WT or PGT121 LALA administration.

**Supplementary Figure 2 |** Mean levels of anti-PGT121 ADA, plasma concentration of PGT121 and corresponding SHIV viral loads in macaques NM02, NM03 and NM08. The mean plasma concentrations of PGT121 WT or LALA post-infusion (open circles, left y-axis) are plotted with the mean levels of anti-PGT121 ADA (blue line, right y-axis) and mean SHIV viral loads (red line, right y-axis). Black arrows indicate antibody administration. The red text indicates failed therapy with PGT121 WT or LALA. The data are depicted as the mean and standard error of the mean.

## REFERENCES


1. Caskey M, Schoofs T, Gruell H, Settler A, Karagounis T, Kreider EF, et al. Antibody 10-1074 Suppresses Viremia in HIV-1-Infected Individuals. *Nat Med* (2017) 23(2):185–91. doi: 10.1038/nm.4268
2. Caskey M, Klein F, Lorenzi JC, Seaman MS, West APJr., Buckley N, et al. Viraemia Suppressed in HIV-1-Infected Humans by Broadly Neutralizing Antibody 3BNC117. *Nature* (2015) 522(7557):487–91. doi: 10.1038/nature14411
3. Parsons MS, Lloyd SB, Lee WS, Kristensen AB, Amarasena T, Center RJ, et al. Partial Efficacy of a Broadly Neutralizing Antibody Against Cell-Associated SHIV Infection. *Sci Transl Med* (2017) 9(402):eaaf1483. doi: 10.1126/scitranslmed.aaf1483
4. Barouch DH, Whitney JB, Moldt B, Klein F, Oliveira TY, Liu J, et al. Therapeutic Efficacy of Potent Neutralizing HIV-1-Specific Monoclonal Antibodies in SHIV-Infected Rhesus Monkeys. *Nature* (2013) 503 (7475):224–8. doi: 10.1038/nature12744
5. Gaudinski MR, Coates EE, Houser KV, Chen GL, Yamshchikov G, Saunders JG, et al. Safety and Pharmacokinetics of the Fc-Modified HIV-1 Human Monoclonal Antibody VRC01LS: A Phase 1 Open-Label Clinical Trial in Healthy Adults. *PloS Med* (2018) 15(1):e1002493. doi: 10.1371/journal.pmed.1002493
6. van Schouwenburg PA, Krieckaert CL, Nurmohamed M, Hart M, Rispens T, Aarden L, et al. IgG4 Production Against Adalimumab During Long Term Treatment of RA Patients. *J Clin Immunol* (2012) 32(5):1000–6. doi: 10.1007/s10875-012-9705-0
7. Vultaggio A, Matucci A, Nencini F, Pratesi S, Parronchi P, Rossi O, et al. Anti-Infliximab IgE and non-IgE Antibodies and Induction of Infusion-Related Severe Anaphylactic Reactions. *Allergy* (2010) 65(5):657–61. doi: 10.1111/j.1398-9995.2009.02280.x
8. Klein F, Diskin R, Scheid JF, Gaebler C, Mouquet H, Georgiev IS, et al. Somatic Mutations of the Immunoglobulin Framework are Generally Required for Broad and Potent HIV-1 Neutralization. *Cell* (2013) 153 (1):126–38. doi: 10.1016/j.cell.2013.03.018
9. Bolton DL, Pegu A, Wang K, McGinnis K, Nason M, Foulds K, et al. Human Immunodeficiency Virus Type 1 Monoclonal Antibodies Suppress Acute Simian-Human Immunodeficiency Virus Viremia and Limit Seeding of Cell-Associated Viral Reservoirs. *J Virol* (2016) 901321–32. doi: 10.1371/journal.pone.0212649
10. Rosenberg YJ, Lewis GK, Montefiori DC, LaBranche CC, Lewis MG, Urban LA, et al. Introduction of the YTE Mutation Into the non-Immunogenic HIV bNAb PGT121 Induces Anti-Drug Antibodies in Macaques. *PloS One* (2019) 14(2):e0212649. doi: 10.1371/journal.pone.0212649
11. Martinez-Navio JM, Fuchs SP, Pedreno-Lopez S, Rakasz EG, Gao G, Desrosiers RC. Host Anti-Antibody Responses Following Adeno-Associated Virus-Mediated Delivery of Antibodies Against HIV and SIV in Rhesus Monkeys. *Mol Ther* (2016) 24(1):76–86. doi: 10.1038/mt.2015.191
12. Shapiro MB, Cheever T, Malherbe DC, Pandey S, Reed J, Yang ES, et al. Single-Dose bNAb Cocktail or Abbreviated ART Post-Exposure Regimens Achieve Tight SHIV Control Without Adaptive Immunity. *Nat Commun* (2020) 11(1):70. doi: 10.1038/s41467-019-13972-y
13. Borducchi EN, Liu J, Nkolola JP, Cadena AM, Yu WH, Fischinger S, et al. Antibody and TLR7 Agonist Delay Viral Rebound in SHIV-Infected Monkeys. *Nature* (2018) 563(7731):360–4. doi: 10.1038/s41586-018-0600-6
14. Gardner MR, Fetzer I, Kattenhorn LM, Davis-Gardner ME, Zhou AS, Alfant B, et al. Anti-Drug Antibody Responses Impair Prophylaxis Mediated by AAV-Delivered HIV-1 Broadly Neutralizing Antibodies. *Mol Ther* (2019) 27 (3):650–60. doi: 10.1016/j.ymthe.2019.01.004
15. Parsons MS, Lee WS, Kristensen AB, Amarasena T, Khoury G, Wheatley AK, et al. Fc-Dependent Functions are Redundant to Efficacy of Anti-HIV Antibody PGT121 in Macaques. *J Clin Invest* (2018) 129(1):182–91. doi: 10.1172/JCI122466
16. Parsons MS, Kristensen AB, Selva KJ, Lee WS, Amarasena T, Esterbauer R, et al. Protective Efficacy of the Anti-HIV Broadly Neutralizing Antibody PGT121 in the Context of Semen Exposure. *EBioMedicine* (2021) 70:103518. doi: 10.1016/j.ebiom.2021.103518
17. Bavinton BR, Pinto AN, Phanuphak N, Grinsztejn B, Prestage GP, Zablotska-Manos IB, et al. Viral Suppression and HIV Transmission in Serodiscordant Male Couples: An International, Prospective, Observational, Cohort Study. *Lancet HIV* (2018) 5(8):e438–47. doi: 10.1016/S2352-3018(18)30132-2
18. Hessell AJ, Hangartner L, Hunter M, Havenith CE, Beurskens FJ, Bakker JM, et al. Fc Receptor But Not Complement Binding is Important in Antibody Protection Against HIV. *Nature* (2007) 449(7158):101–4. doi: 10.1038/nature06106
19. Hessell AJ, Poignard P, Hunter M, Hangartner L, Tehrani DM, Bleeker WK, et al. Effective, Low-Titer Antibody Protection Against Low-Dose Repeated Mucosal SHIV Challenge in Macaques. *Nat Med* (2009) 15(8):951–4. doi: 10.1038/nm.1974
20. Hangartner L, Beauparlant D, Rakasz E, Nedellec R, Hoze N, McKenney K, et al. Effector Function Does Not Contribute to Protection From Virus Challenge by a Highly Potent HIV Broadly Neutralizing Antibody in Nonhuman Primates. *Sci Transl Med* (2021) 13(585). doi: 10.1126/scitranslmed.abe3349
21. Saunders KO, Wang L, Joyce MG, Yang ZY, Balazs AB, Cheng C, et al. Broadly Neutralizing Human Immunodeficiency Virus Type 1 Antibody Gene Transfer Protects Nonhuman Primates From Mucosal Simian-Human Immunodeficiency Virus Infection. *J Virol* (2015) 89(16):8334–45. doi: 10.1128/JVI.00908-15
22. Saunders KO, Pegu A, Georgiev IS, Zeng M, Joyce MG, Yang ZY, et al. Sustained Delivery of a Broadly Neutralizing Antibody in Nonhuman Primates Confers Long-Term Protection Against Simian/Human Immunodeficiency Virus Infection. *J Virol* (2015) 89(11):5895–903. doi: 10.1128/JVI.00210-15
23. Atiqi S, Hooijberg F, Loeff FC, Rispens T, Wolbink GJ. Immunogenicity of TNF-Inhibitors. *Front Immunol* (2020) 11:312. doi: 10.3389/fimmu.2020.00312
24. Mayer KH, Seaton KE, Huang Y, Grunenberg N, Isaacs A, Allen M, et al. Safety, Pharmacokinetics, and Immunological Activities of Multiple Intravenous or Subcutaneous Doses of an Anti-HIV Monoclonal Antibody, VRC01, Administered to HIV-Uninfected Adults: Results of a Phase 1 Randomized Trial. *PloS Med* (2017) 14(11):e1002435. doi: 10.1371/journal.pmed.1002435
25. Cohen YZ, Butler AL, Millard K, Witmer-Pack M, Levin R, Unson-O'Brien C, et al. Safety, Pharmacokinetics, and Immunogenicity of the Combination of the Broadly Neutralizing Anti-HIV-1 Antibodies 3BNC117 and 10-1074 in Healthy Adults: A Randomized, Phase 1 Study. *PloS One* (2019) 14(8): e0219142. doi: 10.1371/journal.pone.0219142


**Conflict of Interest:** The authors declare that the research was conducted in the absence of any commercial or financial relationships that could be construed as a potential conflict of interest.

this article, or claim that may be made by its manufacturer, is not guaranteed or endorsed by the publisher.

# Advantages of publishing in Frontiers

**OPEN ACCESS**
Articles are free to read for greatest visibility and readership

**FAST PUBLICATION**
Around 90 days from submission to decision

**HIGH QUALITY PEER-REVIEW**
Rigorous, collaborative, and constructive peer-review

**TRANSPARENT PEER-REVIEW**
Editors and reviewers acknowledged by name on published articles

**Frontiers**
Avenue du Tribunal-Fédéral 34
1005 Lausanne | Switzerland

**Visit us:** www.frontiersin.org
**Contact us:** frontiersin.org/about/contact

**REPRODUCIBILITY OF RESEARCH**
Support open data and methods to enhance research reproducibility

**DIGITAL PUBLISHING**
Articles designed for optimal readership across devices

**FOLLOW US**
@frontiersin

**IMPACT METRICS**
Advanced article metrics track visibility across digital media

**EXTENSIVE PROMOTION**
Marketing and promotion of impactful research

**LOOP RESEARCH NETWORK**
Our network increases your article's readership